

VOL. 692 NOS. 1 + 2 10 FEBRUARY 1995

COMPLETE IN ONE ISSUE

**18th International Symposium
on Column Liquid Chromatography
Minneapolis, MN, 8-13 May 1994
Part II**

JOURNAL OF

CHROMATOGRAPHY A

INCLUDING ELECTROPHORESIS AND OTHER SEPARATION METHODS

EDITORS

U.A.Th. Brinkman (Amsterdam)
R.W. Giese (Boston, MA)
J.K. Haken (Kensington, N.S.W.)
C.F. Poole (London)
L.R. Snyder (Orinda, CA)
S. Terabe (Hyogo)

EDITORS, SYMPOSIUM VOLUMES,

E. Heftmann (Orinda, CA), Z. Deyl (Prague)

EDITORIAL BOARD

D.W. Armstrong (Rolla, MO)
W.A. Aue (Härlifax)
P. Boček (Brno)
P.W. Carr (Minneapolis, MN)
J. Crommen (Liège)
V.A. Davankov (Moscow)
G.J. de Jong (Weesp)
Z. Deyl (Prague)
S. Dilli (Kensington, N.S.W.)
Z. El Rassi (Stillwater, OK)
H. Engelhardt (Saarbrücken)
M.B. Evans (Hatfield)
S. Fanali (Rome)
G.A. Guiochon (Knoxville, TN)
P.R. Haddad (Hobart, Tasmania)
I.M. Hais (Hradec Králové)
W.S. Hancock (Palo Alto, CA)
S. Hjertén (Uppsala)
S. Honda (Higashi-Osaka)
Cs. Horváth (New Haven, CT)
J.F.K. Huber (Vienna)
J. Janák (Brno)
P. Jandera (Pardubice)
B.L. Karger (Boston, MA)
J.J. Kirkland (Newport, DE)
E. sz. Kováts (Lausanne)
C.S. Lee (Ames, IA)
K. Macek (Prague)
A.J.P. Martin (Cambridge)
E.D. Morgan (Keele)
H. Poppe (Amsterdam)
P.G. Righetti (Milan)
P. Schoenmakers (Amsterdam)
R. Schwarzenbach (Dübendorf)
R.E. Shoup (West Lafayette, IN)
R.P. Singhal (Wichita, KS)
A.M. Siouffi (Marseille)
D.J. Strydom (Boston, MA)
T. Takagi (Osaka)
N. Tanaka (Kyoto)
K.K. Unger (Mainz)
P. van Zoonen (Bilthoven)
R. Verpoorte (Leiden)
Gy. Vigh (College Station, TX)
J.T. Watson (East Lansing, MI)
B.D. Westerlund (Uppsala)

EDITORS, BIBLIOGRAPHY SECTION

Z. Deyl (Prague), J. Janák (Brno), V. Schwarz (Prague)

ELSEVIER

JOURNAL OF CHROMATOGRAPHY A

INCLUDING ELECTROPHORESIS AND OTHER SEPARATION METHODS

Scope. The *Journal of Chromatography A* publishes papers on all aspects of **chromatography, electrophoresis** and related methods. Contributions consist mainly of research papers dealing with chromatographic theory, instrumental developments and their applications. In the *Symposium volumes*, which are under separate editorship, proceedings of symposia on chromatography, electrophoresis and related methods are published. *Journal of Chromatography B: Biomedical Applications*—This journal, which is under separate editorship, deals with the following aspects: developments in and applications of chromatographic and electrophoretic techniques related to clinical diagnosis or alterations during medical treatment; screening and profiling of body fluids or tissues related to the analysis of active substances and to metabolic disorders; drug level monitoring and pharmacokinetic studies; clinical toxicology; forensic medicine; veterinary medicine; occupational medicine; results from basic medical research with direct consequences in clinical practice.

Submission of Papers. The preferred medium of submission is on disk with accompanying manuscript (see *Electronic manuscripts* in the Instructions to Authors, which can be obtained from the publisher, Elsevier Science B.V., P.O. Box 330, 1000 AH Amsterdam, Netherlands). Manuscripts (in English; *four* copies are required) should be submitted to: Editorial Office of *Journal of Chromatography A*, P.O. Box 681, 1000 AR Amsterdam, Netherlands, Telefax (+31-20) 485 2304, or to: The Editor of *Journal of Chromatography B: Biomedical Applications*, P.O. Box 681, 1000 AR Amsterdam, Netherlands. Review articles are invited or proposed in writing to the Editors who welcome suggestions for subjects. An outline of the proposed review should first be forwarded to the Editors for preliminary discussion prior to preparation. Submission of an article is understood to imply that the article is original and unpublished and is not being considered for publication elsewhere. For copyright regulations, see below.

Publication information. *Journal of Chromatography A* (ISSN 0021-9673): for 1995 Vols. 683–714 are scheduled for publication. *Journal of Chromatography B: Biomedical Applications* (ISSN 0378-4347): for 1995 Vols. 663–674 are scheduled for publication. Subscription prices for *Journal of Chromatography A*, *Journal of Chromatography B: Biomedical Applications* or a combined subscription are available upon request from the publisher. Subscriptions are accepted on a prepaid basis only and are entered on a calendar year basis. Issues are sent by surface mail except to the following countries where air delivery via SAL is ensured: Argentina, Australia, Brazil, Canada, China, Hong Kong, India, Israel, Japan, Malaysia, Mexico, New Zealand, Pakistan, Singapore, South Africa, South Korea, Taiwan, Thailand, USA. For all other countries airmail rates are available upon request. Claims for missing issues must be made within six months of our publication (mailing) date. Please address all your requests regarding orders and subscription queries to: Elsevier Science B.V., Journal Department, P.O. Box 211, 1000 AE Amsterdam, Netherlands. Tel.: (+31-20) 485 3642; Fax: (+31-20) 485 3598. Customers in the USA and Canada wishing information on this and other Elsevier journals, please contact Journal Information Center, Elsevier Science Inc., 655 Avenue of the Americas, New York, NY 10010, USA, Tel. (+1-212) 633 3750, Telefax (+1-212) 633 3764.

Abstracts/Contents Lists published in Analytical Abstracts, Biochemical Abstracts, Biological Abstracts, Chemical Abstracts, Chemical Titles, Chromatography Abstracts, Current Awareness in Biological Sciences (CABS), Current Contents/Life Sciences, Current Contents/Physical, Chemical & Earth Sciences, Deep-Sea Research/Part B: Oceanographic Literature Review, Excerpta Medica, Index Medicus, Mass Spectrometry Bulletin, PASCAL-CNRS, Referativnyi Zhurnal, Research Alert and Science Citation Index.

US Mailing Notice. *Journal of Chromatography A* (ISSN 0021-9673) is published weekly (total 52 issues) by Elsevier Science B.V., (Sara Burgerhartstraat 25, P.O. Box 211, 1000 AE Amsterdam, Netherlands). Annual subscription price in the USA US\$ 5389.00 (US\$ price valid in North, Central and South America only) including air speed delivery. Second class postage paid at Jamaica, NY 11431. **USA POSTMASTERS:** Send address changes to *Journal of Chromatography A*, Publications Expediting, Inc., 200 Meacham Avenue, Elmont, NY 11003. Airfreight and mailing in the USA by Publications Expediting.

See inside back cover for Publication Schedule, Information for Authors and information on Advertisements.

© 1995 ELSEVIER SCIENCE B.V. All rights reserved.

0021-9673/95/\$09.50

No part of this publication may be reproduced, stored in a retrieval system or transmitted in any form or by any means, electronic, mechanical, photocopying, recording or otherwise, without the prior written permission of the publisher, Elsevier Science B.V., Copyright and Permissions Department, P.O. Box 521, 1000 AM Amsterdam, Netherlands.

Upon acceptance of an article by the journal, the author(s) will be asked to transfer copyright of the article to the publisher. The transfer will ensure the widest possible dissemination of information.

Special regulations for readers in the USA—This journal has been registered with the Copyright Clearance Center, Inc. Consent is given for copying of articles for personal or internal use, or for the personal use of specific clients. This consent is given on the condition that the copier pays through the Center the per-copy fee stated in the code on the first page of each article for copying beyond that permitted by Sections 107 or 108 of the US Copyright Law. The appropriate fee should be forwarded with a copy of the first page of the article to the Copyright Clearance Center, Inc., 222 Rosewood Drive, Danvers, MA 01923, USA. If no code appears in an article, the author has not given broad consent to copy and permission to copy must be obtained directly from the author. The fee indicated on the first page of an article in this issue will apply retroactively to all articles published in the journal, regardless of the year of publication. This consent does not extend to other kinds of copying, such as for general distribution, resale, advertising and promotion purposes, or for creating new collective works. Special written permission must be obtained from the publisher for such copying.

No responsibility is assumed by the Publisher for any injury and/or damage to persons or property as a matter of products liability, negligence or otherwise, or from any use or operation of any methods, products, instructions or ideas contained in the materials herein. Because of rapid advances in the medical sciences, the Publisher recommends that independent verification of diagnoses and drug dosages should be made.

Although all advertising material is expected to conform to ethical (medical) standards, inclusion in this publication does not constitute a guarantee or endorsement of the quality or value of such product or of the claims made of it by its manufacturer.

⊗ The paper used in this publication meets the requirements of ANSI/NISO Z39.48-1992 (Permanence of Paper).

Printed in the Netherlands

For Contents see p. VII.

JOURNAL OF CHROMATOGRAPHY A

VOL. 692 (1995)

JOURNAL OF CHROMATOGRAPHY A

INCLUDING ELECTROPHORESIS AND OTHER SEPARATION METHODS

EDITORS

U.A.Th. BRINKMAN (Amsterdam), R.W. GIESE (Boston, MA), J.K. HAKEN (Kensington, N.S.W.),
C.F. POOLE (London), L.R. SNYDER (Orinda, CA), S. TERABE (Hyogo)

EDITORS, SYMPOSIUM VOLUMES

E. HEFTMANN (Orinda, CA), Z. DEYL (Prague)

EDITORIAL BOARD

D.W. Armstrong (Rolla, MO), W.A. Aue (Halifax), P. Boček (Brno), P.W. Carr (Minneapolis, MN), J. Crommen (Liège), V.A. Davankov (Moscow), G.J. de Jong (Weesp), Z. Deyl (Prague), S. Dilli (Kensington, N.S.W.), Z. El Rassi (Stillwater, OK), H. Engelhardt (Saarbrücken), M.B. Evans (Hatfield), S. Fanali (Rome), G.A. Guiochon (Knoxville, TN), P.R. Haddad (Hobart, Tasmania), I.M. Hais (Hradec Králové), W.S. Hancock (Palo Alto, CA), S. Hjertén (Uppsala), S. Honda (Higashi-Osaka), Cs. Horváth (New Haven, CT), J.F.K. Huber (Vienna), J. Janák (Brno), P. Jandera (Pardubice), B.L. Karger (Boston, MA), J.J. Kirkland (Newport, DE), E. sz. Kováts (Lausanne), C.S. Lee (Ames, IA), K. Macek (Prague), A.J.P. Martin (Cambridge), E.D. Morgan (Keele), H. Poppe (Amsterdam), P.G. Righetti (Milan), P. Schoenmakers (Amsterdam), R. Schwarzenbach (Dübendorf), R.E. Shoup (West Lafayette, IN), R.P. Singhal (Wichita, KS), A.M. Siouffi (Marseille), D.J. Strydom (Boston, MA), T. Takagi (Osaka), N. Tanaka (Kyoto), K.K. Unger (Mainz), P. van Zoonen (Bilthoven), R. Verpoorte (Leiden), Gy. Vigh (College Station, TX), J.T. Watson (East Lansing, MI), B.D. Westerlund (Uppsala)

EDITORS, BIBLIOGRAPHY SECTION

Z. Deyl (Prague), J. Janák (Brno), V. Schwarz (Prague)



ELSEVIER

Amsterdam – Lausanne – New York – Oxford – Shannon – Tokyo

J. Chromatogr. A, Vol. 692 (1995)

© 1995 ELSEVIER SCIENCE B.V. All rights reserved.

0021-9673/95/\$09.50

No part of this publication may be reproduced, stored in a retrieval system or transmitted in any form or by any means, electronic, mechanical, photocopying, recording or otherwise, without the prior written permission of the publisher, Elsevier Science B.V., Copyright and Permissions Department, P.O. Box 521, 1000 AM Amsterdam, Netherlands.

Upon acceptance of an article by the journal, the author(s) will be asked to transfer copyright of the article to the publisher. The transfer will ensure the widest possible dissemination of information.

Special regulations for readers in the USA – This journal has been registered with the Copyright Clearance Center, Inc. Consent is given for copying of articles for personal or internal use, or for the personal use of specific clients. This consent is given on the condition that the copier pays through the Center the per-copy fee stated in the code on the first page of each article for copying beyond that permitted by Sections 107 or 108 of the US Copyright Law. The appropriate fee should be forwarded with a copy of the first page of the article to the Copyright Clearance Center, Inc., 222 Rosewood Drive, Danvers, MA 01923, USA. If no code appears in an article, the author has not given broad consent to copy and permission to copy must be obtained directly from the author. The fee indicated on the first page of an article in this issue will apply retroactively to all articles published in the journal, regardless of the year of publication. This consent does not extend to other kinds of copying, such as for general distribution, resale, advertising and promotion purposes, or for creating new collective works. Special written permission must be obtained from the publisher for such copying.

No responsibility is assumed by the Publisher for any injury and/or damage to persons or property as a matter of products liability, negligence or otherwise, or from any use or operation of any methods, products, instructions or ideas contained in the materials herein. Because of rapid advances in the medical sciences, the Publisher recommends that independent verification of diagnoses and drug dosages should be made.

Although all advertising material is expected to conform to ethical (medical) standards, inclusion in this publication does not constitute a guarantee or endorsement of the quality or value of such product or of the claims made of it by its manufacturer.

♻️ The paper used in this publication meets the requirements of ANSI/NISO Z39.48-1992 (Permanence of Paper).

Printed in the Netherlands

SYMPOSIUM VOLUME



**18TH INTERNATIONAL SYMPOSIUM
ON
COLUMN LIQUID CHROMATOGRAPHY**

PART II

Minneapolis, MN (USA), 8-13 May 1994

Guest Editor

L.D. BOWERS
(Indianapolis, IN, USA)

The papers submitted for the Symposium Volumes on the *18th International Symposium on Column Liquid Chromatography* are published in two consecutive Volumes of the *Journal of Chromatog-*

raphy A, Vols. 691 and 692 (1995). The Foreword only appears in Vol. 691. A combined Author Index to both Vols. 691 and 692 only appears in Vol. 692.

CONTENTS

(Abstracts/Contents Lists published in Analytical Abstracts, Biochemical Abstracts, Biological Abstracts, Chemical Abstracts, Chemical Titles, Chromatography Abstracts, Current Awareness in Biological Sciences (CABS), Current Contents/Life Sciences, Current Contents/Physical, Chemical & Earth Sciences, Deep-Sea Research/Part B: Oceanographic Literature Review, Excerpta Medica, Index Medicus, Mass Spectrometry Bulletin, PASCAL-CNRS, Referativnyi Zhurnal, Research Alert and Science Citation Index)

18TH INTERNATIONAL SYMPOSIUM ON COLUMN LIQUID CHROMATOGRAPHY, MINNEAPOLIS, MN, USA, 8-13 MAY 1994, PART II

ENVIRONMENTAL APPLICATIONS

- Automated procedure for determination of trace amounts of aldehydes in drinking water
by R. Wu and L.B. White (Fremont, CA, USA) 1
- Automated precolumn concentration and high-performance liquid chromatographic analysis of polynuclear aromatic hydrocarbons in water using a single pump and a single valve
by F. Lai and L. White (Fremont, CA, USA) 11
- Optimization of automated solid-phase extraction for quantitation of polycyclic aromatic hydrocarbons in aqueous media by high-performance liquid chromatography-UV detection
by N.C. Fladung (Johnston, IA, USA) 21
- High-performance liquid chromatographic determination of sulfonylureas in soil and water
by G.C. Galletti (Gallina, Italy) and A. Bonetti and G. Dinelli (Bologna, Italy) 27
- Liquid chromatographic determination of the mycotoxin fumonisin B₂ in physiological samples
by G.S. Shephard, P.G. Thiel and E.W. Sydenham (Tygerberg, South Africa) 39

PHARMACEUTICALS, DRUGS, BIOMEDICAL APPLICATIONS

- Determination of L-735 524, an human immunodeficiency virus protease inhibitor, in human plasma and urine via high-performance liquid chromatography with column switching
by E. Woolf, T. Au, H. Haddix and B. Matuszewski (West Point, PA, USA) 45
- Comparison of high-performance liquid chromatographic methods for the determination of 1,2-dibromo-2,4-dicyanobutane in cosmetic products
by S.C. Rastogi and S.S. Johansen (Roskilde, Denmark) 53
- Alkylsulphonic acid ion pairing with radial compression columns for determining plasma or cerebrospinal fluid 1- β -D-arabinofuranosylcytosine in pediatric pharmacokinetic analysis
by M.L. Stout and Y. Ravindranath (Detroit, MI, USA) 59
- High-performance liquid chromatographic method for potency determination of cephalexin in commercial preparations and for stability studies
by M.-C. Hsu (Taoyuan, Taiwan) and Y.-S. Lin and H.-C. Chung (Taipei, Taiwan) 67
- Rapid liquid chromatographic-mass spectrometric assay for oxymetazoline in whole rat blood
by F.J. Hayes, T.R. Baker, R.L.M. Dobson and M.S. Tsueda (Cincinnati, OH, USA) 73
- Hydrophobicity parameter from high-performance liquid chromatography on an immobilized artificial membrane column and its relationship to bioactivity
by A. Nasal, M. Sznitowska, A. Bucirski and R. Kaliszan (Gdańsk, Poland) 83
- Unusual examples of the liquid chromatographic resolution of racemates. Resolution of π -donor analytes on a π -donor chiral stationary phase
by M.H. Hyun, J.-J. Ryoo, Y.J. Cho and J.S. Jin (Pusan, South Korea) 91
- High-performance liquid chromatographic determination of (4-[¹¹C]methoxyphenyl)-(5-fluoro-2-hydroxyphenyl)-methyl-eneaminobutyric acid and its benzophenone metabolite
by F. De Vos and G. Slegers (Ghent, Belgium) 97
- Use of high-performance liquid chromatography-diode array detection in forensic toxicology
by E.M. Koves (Toronto, Canada) 103

Qualitative and quantitative determination of illicit heroin street samples by reversed-phase high-performance liquid chromatography: method development by CARTAGO-S by K. Grogg-Sulser, H.-J. Helmlin and J.-T. Clerc (Berne, Switzerland)	121
Determination of aflatoxins in medicinal herbs and plant extracts by K. Reif and W. Metzger (Verstenbergsgreuth, Germany)	131
Determination of liquiritin, glycyrrhizin, hesperidin, cinnamic acid, cinnamaldehyde, honokiol and magnolol in the traditional Chinese medicinal preparation Wu-Ji-San by high-performance liquid chromatography by Y.-C. Lee, C.-Y. Huang, K.-C. Wen and T.-T. Suen (Taipei, Taiwan)	137
Chemometric categorization of octadecylsilyl bonded-phase silica columns using test mixtures and confirmation of results with pharmaceutical compound separations by B.A. Olsen and G.R. Sullivan (Lafayette, IN, USA)	147
Liquid chromatographic determination of the macrolide antibiotics roxithromycin and clarithromycin in plasma by automated solid-phase extraction and electrochemical detection by M. Hedenmo and B.-M. Eriksson (Mölnådal, Sweden)	161
Analysis of mycolic acids by high-performance liquid chromatography and fluorimetric detection. Implications for the identification of mycobacteria in clinical samples by S.R. Hagen and J.D. Thompson (Hamilton, MT, USA)	167
Resolution of promethazine, ethopropazine, trimeprazine and trimipramine enantiomers on selected chiral stationary phases using high-performance liquid chromatography by G.W. Ponder (Athens, GA, USA), S.L. Butram (Dahlonga, GA, USA), A.G. Adams (Marietta, GA, USA) and C.S. Ramanathan and J.T. Stewart (Athens, GA, USA)	173
Comparison of theory-based and empirical modeling for the prediction of chromatographic behavior in the ion-pairing separation of benzodiazepine-derived pharmaceutical compounds by L.A. Larew, B.A. Olsen, J.D. Stafford and M.V. Wilhelm (Lafayette, IN, USA)	183
Simultaneous determination of granisetron and its 7-hydroxy metabolite in human plasma by reversed-phase high-performance liquid chromatography utilizing fluorescence and electrochemical detection by V.K. Boppana (King of Prussia, PA, USA)	195
Determination of citrate, inositol and gentisic acid in a pharmaceutical diagnostic formulation by ion-moderated partition chromatography (Short communication) by R.W. Chong and B.J. Moore (St. Louis, MO, USA)	203
Use of overlapping resolution mapping scheme for optimization of the high-performance liquid chromatographic separation of pharmaceuticals by C.P. Ong, K.K. Chow, C.L. Ng, F.M. Ong, H.K. Lee and S.F.Y. Li (Singapore, Singapore)	207
APPLICATIONS, OTHERS	
Preparative high-performance liquid chromatography for the purification of natural anthocyanins by M. Fiorini (Bologna, Italy)	213
Compositional distribution characterization of poly(methyl methacrylate)-graft-polydimethylsiloxane copolymers by T.C. Schunk (Rochester, NY, USA) and T.E. Long (Kingsport, TN, USA)	221
Rapid scaleable chromatographic purification of nucleic acids from proteinaceous mixtures (Short communication) by Y.L. Hofman (Wilmington, DE, USA), K.L. Petrillo (Newark, DE, USA), H.C. Greenblatt and R. Lehrer (Wilmington, DE, USA) and M.S. Payne (Newark, DE, USA)	233
Separation of photosynthetic pigments and their precursors by reversed-phase high-performance liquid chromatography using a photodiode-array detector by B. Schoefs (Villeneuve d'Ascq, France), M. Bertrand (Tourlaville, France) and Y. Lemoine (Villeneuve d'Ascq, France)	239
Analysis of nerve agent degradation products using capillary ion electrophoresis (Short communication) by S.A. Oehrle (Milford, MA, USA) and P.C. Bossle (Aberdeen Proving Ground, MD, USA)	247
Extending the scope of chiral separation of basic compounds by cyclodextrin-mediated capillary zone electrophoresis by C. Quang and M.G. Khaledi (Raleigh, NC, USA)	253

CONTENTS

IX

Determination of polycarboxylic acids by capillary electrophoresis with copper complexation by J.P. Wiley (Edgewater, NJ, USA)	267
Mass spectrometric detectors for samples separated by planar electrophoresis (Review) by K.L. Busch (Atlanta, GA, USA)	275
Selectivity control in micellar electrokinetic chromatography of small peptides using mixed fluorocarbon-hydrocarbon ~ anionic surfactants by B. Ye, M. Hadjmohammadi and M.G. Khaledi (Raleigh, NC, USA)	291
Linear solvation energy relationships in micellar liquid chromatography and micellar electrokinetic capillary chromatography by S. Yang and M.G. Khaledi (Raleigh, NC, USA)	301
Micellar liquid chromatographic separation of sulfonamides in physiological samples using direct on-column injection by S. Yang and M.G. Khaledi (Raleigh, NC, USA)	311
Experimental evidence for the existence of duoselective (Type III) enantiomer separations in the capillary electrophoretic analysis of chiral weak acids by M.E. Biggin, R.L. Williams and G. Vigh (College Station, TX, USA)	319
AUTHOR INDEX VOLS. 691 AND 692	327

Automated procedure for determination of trace amounts of aldehydes in drinking water

Ran Wu*, Landy B. White

Thermo Separation Products, P.O. Box 5116, Fremont, CA 94537, USA

Abstract

According to method 8315 of the US Environmental Protection Agency, the analysis of aldehydes in drinking water includes manual derivatization, solid-phase extraction and HPLC separation. The procedure is time consuming and labor intensive. A new column-switching technique has been developed to automate the formaldehyde analysis with a standard HPLC system. This method replaces the sample loop on the injection valve of the autosampler with a precolumn where sample cleanup and preconcentration occur. Acetonitrile was used to dissolve the derivatizing reagent and as a system flush to reduce the blank contamination. The method is evaluated for reproducibilities, linearities, spike recoveries and minimum detection limits for two aldehydes.

1. Introduction

Formaldehyde is a natural oxidation product of many organic compounds [1]. It is also formed by incomplete combustion of many organic substances and is widely present in the atmosphere [2]. The major sources of formaldehyde found in drinking water are from the discharge of industrial wastes and oxidative water treatment processes [3]. Formaldehyde is a potential mutagen and carcinogen in laboratory animal tests [4,5]. Because of its adverse effect on human health, routine testing for formaldehyde and acetaldehyde in drinking water is required by the US Environmental Protection Agency (EPA) in some areas [6].

The current EPA method 8315 for the determination of aldehydes in drinking water involves derivatization with 2,4-dinitrophenylhydrazine (DNPH), manual solid-phase extraction

and preconcentration, followed by HPLC separation [7-10]. The procedure is tedious, labor intensive and time consuming. To automate the procedure would normally require an expensive and complex robotic system. Presented here is a newly developed automated method utilizing a personal computer (PC)-controlled sample processing workstation that performs the derivatization and accomplishes the sample cleanup and preconcentration with a conventional HPLC system. The only modification of this HPLC system is the replacement of the sample loop with a precolumn on the injection valve of the autosampler. Through the customized PC-controlled sample processing workstation, the sample was derivatized by adding DNPH and mixing in the autosampler. Then the derivatized sample was metered into the precolumn (typically 500 to 1500 μ l) and washed using an on-board prep syringe drive. Later, the sample was on-line eluted to the analytical column for HPLC separation. The common high blank response prob-

* Corresponding author.

lem for formaldehyde analysis [3,11] was improved by dissolving DNPH in acetonitrile instead of ethanol [9], and a system flush with acetonitrile at the end of each injection.

Compared to the traditional on-line column-switching technique which requires an extra washing pump and an external switching valve, this column-switching technique requires a rather simple HPLC system. The automated method is simple, efficient and the amount of waste generated by this method is reduced significantly.

2. Experimental

2.1. Equipment

A TSP SpectraSYSTEM liquid chromatograph (Thermo Separation Products, Fremont, CA, USA) consisting of a P4000 pump coupled with SCM400 solvent conditioning module, an AS3000 autosampler with sample preparation option, a UV2000 detector, PC1000 software and a PC-controlled sample processing workstation loaded with HyperAccess modem software (Hilgraeve, Monroe, MI, USA) was used.

Mega Bond Elut C₁₈ cartridges (2 g) and the Vac-Elut vacuum manifold from Varian Sample Prep Products (Varian, Harbor City, CA, USA) were used for manual solid-phase extraction.

2.2. Chemicals

DNPH (70%, w/w, purity) and acetaldehyde (99% purity) were obtained from Aldrich (Milwaukee, WI, USA). Formaldehyde (37% formalin solution) was purchased from Sigma (St. Louis, MO, USA). DNPH-derivatized formaldehyde and DNPH-derivatized acetaldehyde standard mixture (1000 mg/l each in methanol) was obtained from Accustandard (New Haven, CT, USA). Glacial acetic acid and HPLC-grade acetonitrile were obtained from J.T. Baker (Phillipsburg, NJ, USA). Sodium hydroxide pellets were purchased from Mallinckrodt (Paris, KY, USA).

2.3. Preparation of standard solutions, spiked samples and reagent solutions

The working standard was made by diluting 10 μ l of the DNPH-formaldehyde and DNPH-acetaldehyde standard mixture to 1 ml with deionized water (10 mg/l). Serial dilutions were made from the working standard to different concentrations for the calibration curves.

A manually spiked sample was made by spiking formaldehyde and acetaldehyde solutions into 100 ml of deionized water in a Nalgene bottle for determination of the method linearity, reproducibility and spike recovery.

To make 500 mg/l of DNPH derivatizing reagent, 7.15 mg of DNPH (70%, w/w) was dissolved in 10 ml of acetonitrile. The 5 M sodium acetate buffer was prepared by adjusting 28.5 ml of glacial acetic acid to pH 5 with 5 M sodium hydroxide, then diluting the solution to 100 ml with deionized water.

2.4. Experimental conditions

A 1.5 cm \times 3.2 mm RP-18 Newguard column (7 μ m particle size, silica-based C₁₈ guard column) was used for the precolumn (Applied Biosystems, San Jose, CA, USA) on the injection valve. The samples in the sample vials were preserved at 4°C in the autosampler before the analyses. The separation was carried out at room temperature on a 15 cm \times 4.6 mm Keystone Deltabond AK column (5 μ m silica particles bonded with a polymeric stationary phase) equipped with an integral guard column (Keystone Scientific, Bellefonte, PA, USA). The mobile phase was isocratic acetonitrile–water (35:65) at a flow-rate of 1 ml/min. Detection was by UV absorption at 360 nm.

2.5. Experimental procedures

Sample preparation

In accordance with EPA method 8315, 4 ml of acetate buffer were manually pipetted into 100 ml of the spiked sample, then the sample was adjusted to pH 5 with sodium hydroxide. A 1-ml

volume of this sample was transferred into a sample vial and placed in the autosampler. Through the RS232 communication with the autosampler, the customized sample processing workstation manipulated the autosampler's syringe movements, injection valve, flush valve and solvent valve. Fig. 1 shows the autosampler configuration for sample preparation.

A 60- μ l volume of DNPH was added into the sample vial by the autosampler's sample syringe. Then the sample vial was transferred to the built-in heater/mixer to vortex mix the sample for 10 min at room temperature for the derivatization reaction. Using the column-switching technique (described next), 500 μ l of the derivatized sample were loaded on the precolumn for sample cleanup and preconcentration, followed by on-line HPLC separation.

Column-switching mechanism

Fig. 2 illustrates the column-switching mechanism which consists of the following steps:

Step 1: The precolumn was preconditioned with water. Then the pump flow was stopped, and the injection valve was moved to "inject" position. The prep syringe drew a large volume

of sample into the solvent holding loop (see Fig. 2a).

Step 2: The injection valve was moved to "load" position, and the prep syringe pushed the sample onto the precolumn for trace enrichment (see Fig. 2b).

Step 3: The pump flow was restarted, as the prep syringe flushed 5 ml of water through the precolumn to perform sample cleanup (see Fig. 2c).

Step 4: The injection valve was moved to "inject" position, and the mobile phase back flushed the sample out of the precolumn and completed the injection onto the analytical column for HPLC separation (see Fig. 2d).

Step 5: While the sample was analyzed on the HPLC system, the prep syringe rinsed and conditioned the precolumn with water and started to process the next sample (see Fig. 2e).

Another set of the manually spiked samples was processed according to the original EPA method 8315 as a control group to compare to the automated method. The procedures included manual derivatization, C₁₈ solid-phase extraction and conventional HPLC separation with 20- μ l injection on the sample loop.

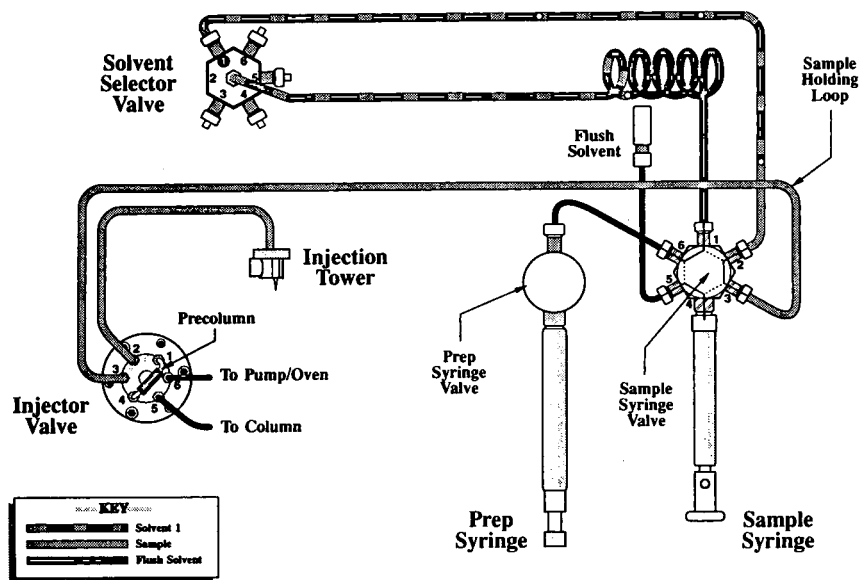


Fig. 1. Autosampler configuration for customized column-switching mechanism.

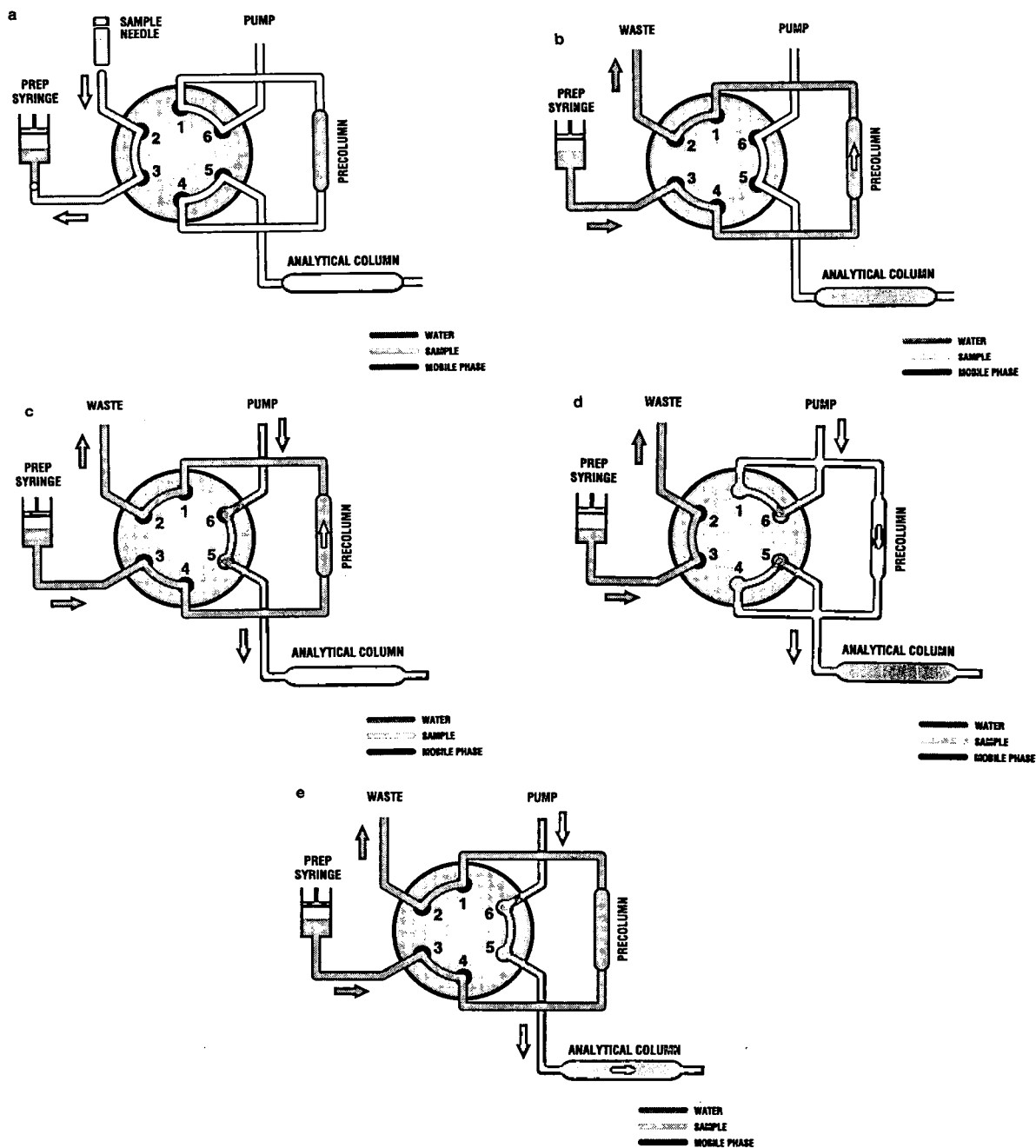


Fig. 2. Detailed illustrations of the column-switching mechanism on a conventional HPLC system. See text.

3. Results

Fig. 3 shows a typical chromatogram for the DNPH-derivatized formaldehyde and DNPH-de-

rivatized acetaldehyde from the column-switching system. Fig. 4 shows a chromatogram of 1 $\mu\text{g/l}$ for both prederivatized aldehydes using a 500- μl sample on the column-switching system.

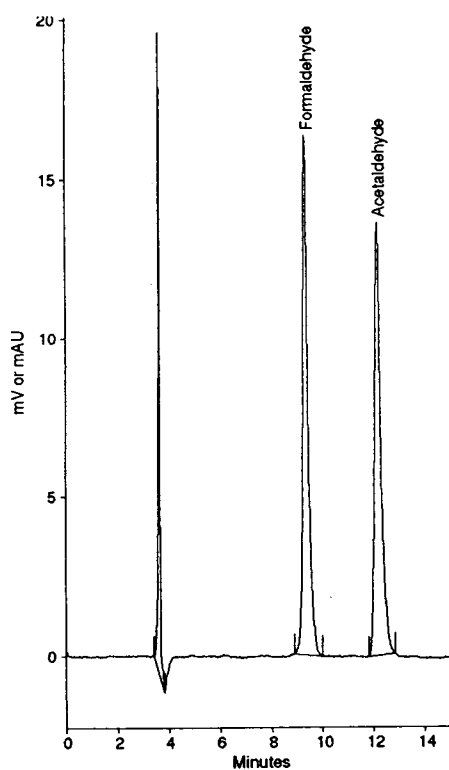


Fig. 3. Chromatogram of DNPH-derivatized formaldehyde and DNPH-derivatized acetaldehyde on the column-switching system. The injection volume was 500 μ l, and the concentration was 100 μ g/l in water each.

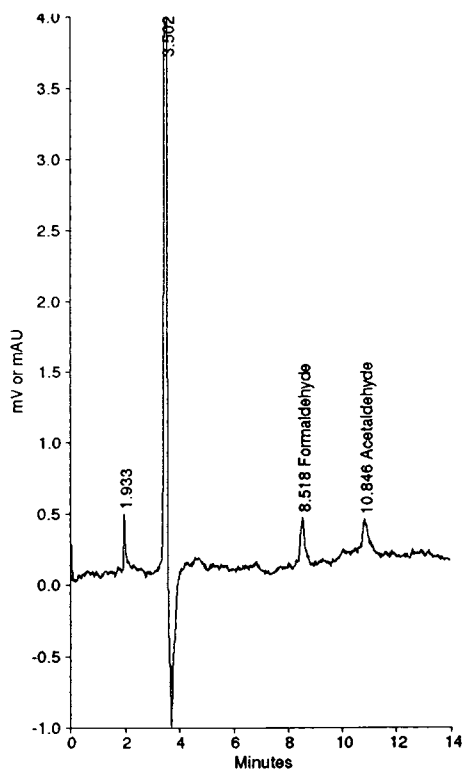


Fig. 4. DNPH-derivatized formaldehyde (1 μ g/l) and 1 μ g/l of DNPH-derivatized acetaldehyde on the column-switching HPLC system. The injection volume was 500 μ l.

The detection limits for both aldehydes on the conventional HPLC system, using a 20- μ l injection were about 25 μ g/l (see Fig. 5), based on a S/N ratio of 3. The detection limits for both aldehydes on the column-switching system therefore have improved significantly over the conventional HPLC system because of the ability to load a large volume of sample on the precolumn. The sample loading volumes on the precolumn were linear to the signal responses. Fig. 6 shows the linear relations for different loading volumes (between 200 and 1000 μ l) and the corresponding signal responses at 2 mg/l level for both aldehydes. Tables 1 and 2 summarize the performance of the automated column-switching method for formaldehyde analysis in comparison with the original EPA method 8315. The injection reproducibilities on the column-switching

system; using prederivatized standards; were calculated based on seven consecutive 500- μ l samplings from seven individual vials at the concentrations between 0.1 and 1 mg/l. The R.S.D. for the conventional HPLC system for both aldehydes was calculated from seven consecutive injections of 20 μ l from the same vial at the concentrations between 0.1 and 1 mg/l. Therefore, the injection reproducibilities for the column-switching system (0.8–2.9%) were comparable with the conventional HPLC system (0.4–4.2%). The automated method was defined as automatically adding 60 μ l of DNPH into 1 ml of manually spiked samples, vortex mixing the sample in the heater/mixer, followed by column-switching technique and on-line HPLC separation. Based on the same statistical calculation described above, the automated method reproducibilities were 1.3–1.9% versus 0.6–1.3% for

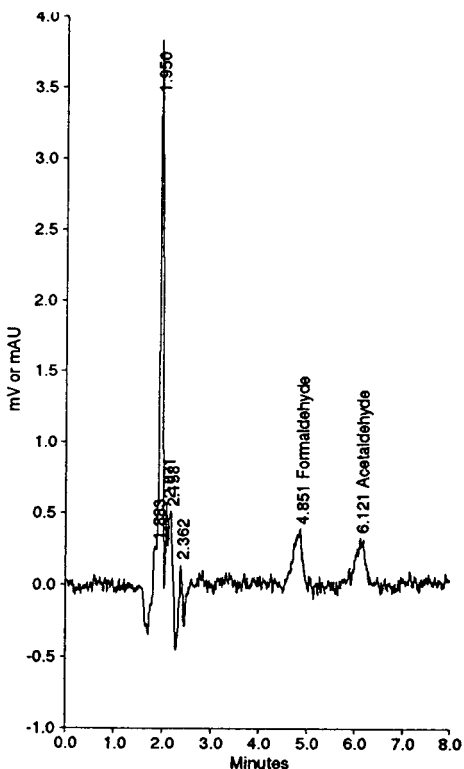


Fig. 5. DNP-derivatized formaldehyde (25 $\mu\text{g}/\text{l}$) and 25 $\mu\text{g}/\text{l}$ of DNP-derivatized acetaldehyde on the conventional HPLC system. The injection volume was 20 μl .

the manual EPA method. The study of the efficiency of vortex mixing for formaldehyde analysis indicates the derivatization reaches a plateau in 10–20 min. The spike recoveries were calculated according to the calibration curve generated from the commercially prederivatized aldehyde standard. The data were obtained from spiking 0.1 to 0.5 mg/l of formaldehyde and acetaldehyde standard solutions into two batches of deionized water samples. In comparing the spike recoveries of the automated method (90–105%) to 86% recovery reported by the EPA for organic free water, the performance of the automated method was very comparable.

The formaldehyde linearity on the column-switching system was obtained by running the prederivatized formaldehyde standard between the concentrations of 0.05 and 1 mg/l. The five points on the calibration curve represented the average of seven peak area measurements at each concentration. All the peak area measurements had R.S.D.s of less than 3%. The standard error for each point was less than 2%. When peak area measurements were linearly correlated with concentrations using the equation $\text{peak area} = \text{concentration} \cdot 6\,995\,347 + 108\,551$, the correlation coefficient was 0.9991. For manually spiked formaldehyde samples,

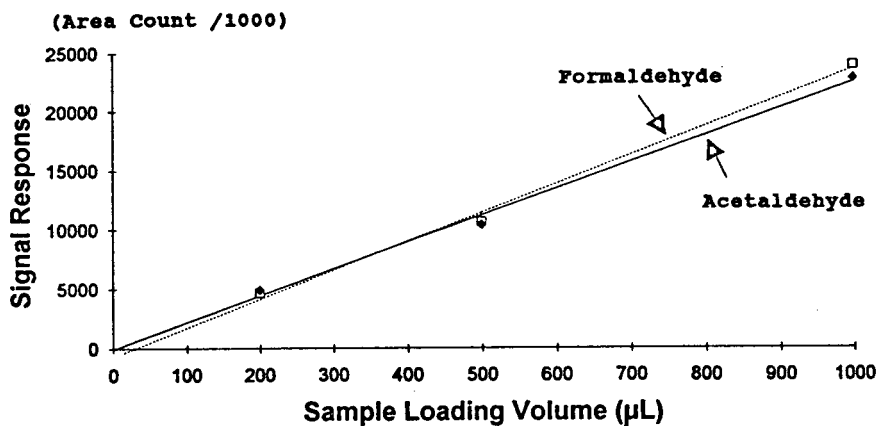


Fig. 6. Linear plots of the sample loading volume on the precolumn versus signal response for formaldehyde and acetaldehyde at a concentration of 2 mg/l level. The correlation coefficient for formaldehyde (\square , dotted line) was 0.9975. The correlation coefficient for acetaldehyde (\diamond , solid line) was 0.9971.

Table 1
System performance

	Column-switching HPLC system	Conventional HPLC system
<i>Formaldehyde</i>		
Reproducibility (R.S.D., %)	0.8-2.9	0.5-4.2
Detection limit ($\mu\text{g/l}$)	< 1	< 25
<i>Acetaldehyde</i>		
Reproducibility (R.S.D., %)	0.9-2.6	0.4-4.2
Detection limit ($\mu\text{g/l}$)	< 1	< 25

A comparison between column-switching and conventional HPLC systems using the commercially derivatized formaldehyde and acetaldehyde standards. The experimental conditions were described in the *Column-switching mechanism* section under Experimental.

using the equation $\text{peak area} = \text{concentration} \cdot 6595335 + 393258$, the correlation coefficient was 0.9999 based on the same statistical calculation described above.

The common problem of a high blank response for formaldehyde analysis can be improved by substituting acetonitrile for ethanol (on EPA method 8315) to dissolve DNPH, in addition to flushing the system with acetonitrile at the end of each analysis. Using these procedures, the formaldehyde readings in blank samples were reduced by 10 to 25 $\mu\text{g/l}$. The blank acetaldehyde reading was minimized to zero.

Drinking water samples were collected from six different local areas and analyzed with the

previously described automated method. All but one of the formaldehyde concentrations found were below the limit of detection of the EPA method (see Table 3). No problems were encountered with the sample cleanup as stated.

4. Discussion

The current EPA method 8315 for the determination of aldehydes in drinking water requires manual derivatization, solid-phase extraction and HPLC separation. This study shows that the entire procedure can be fully automated with a conventional HPLC system.

The traditional on-line column-switching sys-

Table 2
Method performance

	Fully automated method	Manual extraction and HPLC separation
<i>Formaldehyde</i>		
Reproducibility (R.S.D., %)	1.3-1.4	0.6-0.9
Spike recovery (%)	90-105	86
<i>Acetaldehyde</i>		
Reproducibility (R.S.D., %)	1.4-1.9	1.0-1.3
Spike recovery (%)	90-104	93-98

A comparison between the fully automated method (automated derivatization, column switching and on-line HPLC separation) and the EPA manual extraction method using the manually spiked water samples. The experimental conditions were described in the *Experimental procedures* section under Experimental.

Table 3
Real sample analyses

Local area	Formaldehyde ($\mu\text{g/l}$) ^a	Acetaldehyde ($\mu\text{g/l}$)
1	11.0	ND
2	8.9	ND
3	5.7	ND
4	7.4	ND
5	6.6	ND
6	6.9	ND

The analysis results of drinking water samples collected from six local areas. The sample preparation procedures and column-switching technique were described in the *Experimental procedures* section under Experimental. ND = Not detected.

^a The EPA reported method detection limit for formaldehyde is $7.2 \mu\text{g/l}$. These values include reagent blank concentration of approximately $2 \mu\text{g/l}$ formaldehyde.

tem requires an extra pump and an external switching valve in addition to the conventional HPLC system. The column-switching mechanism described here, however, replaces the sample loop with a precolumn and completes the same procedure without additional HPLC equipment. The data show the performance of the automated column-switching system for formaldehyde analysis is either comparable to or better than the original EPA method.

One of the most significant advantages of this automated method is its efficiency compared to the original EPA method. The sample preparation feature of the autosampler enables the automation of the derivatization reaction by the prep syringe and the heater/mixer. The prep syringe adds the derivatizing reagent to the sample vial. The heater/mixer vortex mixes the sample to ensure a homogeneous reaction. The column-switching technique replaces the manual solid-phase extraction for sample cleanup and trace enrichment, followed by on-line HPLC separation. The overall sample preparation and analysis time for each sample is less than 30 min and can be performed simultaneously with the previous analysis. Furthermore, the organic solvent wastes generated by this automated method

have been reduced to less than 10 ml for each sample.

The ubiquitous occurrence of formaldehyde in the environment makes the detection of low levels of formaldehyde almost impossible. One way to avoid the high blank response problem is to rigorously purify each chemical used in the method so that chemicals are aldehyde-free. However, the EPA specifies the use of ethanol to dissolve DNPH. The EPA reported detection limit for acetaldehyde was $171 \mu\text{g/l}$ which included $130 \mu\text{g/l}$ acetaldehyde reading from blank samples. The high background reading of acetaldehyde in the EPA method results from the oxidation of ethanol. Using acetonitrile as a substitute for ethanol to dissolve DNPH will avoid this source of acetaldehyde contamination. Another advantage of using acetonitrile is that DNPH is more soluble in acetonitrile than in ethanol. To reduce formaldehyde contamination, a system flush with acetonitrile will eliminate the majority of the formaldehyde residues remaining in the system, thus minimizing the system background reading for the next injection.

This is a simple and reliable method for automating the aldehydes analysis in drinking water. Although the method was developed in the laboratory in a clean and controlled environment, expanding the methodology to other sample matrices will require studies of the lifespan and selectivity of the precolumn. Obviously, more complicated sample matrices will have a more pronounced effect upon the precolumn selectivity and useful life. Through the sample processing workstation, the automated derivatization capability of the autosampler and the column-switching technique described in this paper are potentially applicable to automate many other HPLC analyses in the future.

Acknowledgements

The authors appreciate the valuable suggestions from Vance Nau and Fran Lai, and also acknowledge support from Lenore Kelly and Marty Hartigan.

References

- [1] *Investigation of Selected Potential Environmental Contaminants: Formaldehyde*, US Environmental Protection Agency, Office of Toxic Substances, Washington, DC, 1976.
- [2] J. de Andrade and R. Tanner, *Atmos. Environ., Part A*, 26A (1992) 819.
- [3] E. Cotsaris and B. Nicholson, *Analyst (Cambridge, U.K.)*, 118 (1993) 265
- [4] B. Tomkins, J. McMahon and W. Caldwell, *J. Assoc. Off. Anal. Chem.*, 72 (1989) 835.
- [5] R.C. Craftstorm, A.J. Jr. Fornace, H. Autrup, J.F. Lechner and C.C. Harris, *Science*, 220 (1983) 216.
- [6] *Preliminary Assessment of Suspected Carcinogens in Drinking Water*, US Environmental Protection Agency, Office of Toxic Substances, Washington, DC, 1985.
- [7] P. Whittle and P. Rennie, *Analyst (London)*, 113 (1988) 665.
- [8] M. Bicking, W. Cooke, F. Kawahara and J. Longbottom, *J. Chromatogr.*, 455 (1988) 310
- [9] *EPA Method 8315; Fed. Reg.*, Vol. 1, Section B, Revision 2 (1990) (CFR260.11 and CFR270.6 for SW846).
- [10] G. Chiavari, G. Torsi and A. Asmundsdottir, *Ann. Chim. (Rome)*, 82 (1992) 349.
- [11] X. Zhou and K. Mopper, *Environ. Sci. Technol.*, 24 (1990) 1482.



ELSEVIER

Journal of Chromatography A, 692 (1995) 11–20

JOURNAL OF
CHROMATOGRAPHY A

Automated precolumn concentration and high-performance liquid chromatographic analysis of polynuclear aromatic hydrocarbons in water using a single pump and a single valve

Fran Lai*, Landy White

Thermo Separation Products, 45757 Northport Loop West, Fremont, CA 94537, USA

Abstract

The analysis of polynuclear aromatic hydrocarbons (PAHs) has been widely practiced using liquid–liquid extraction as a method of sample clean-up and sample enrichment. For the analysis of PAHs by HPLC, alternative sample preparation methods using solid-phase extraction or precolumn concentration have been reported. These methods normally required a switching valve and/or pump in addition to the HPLC system. This study reports a precolumn concentration method using no additional valve or pump to the HPLC system. The method is evaluated for recoveries, reproducibilities, linearity and minimum detection limits.

1. Introduction

A major current environmental concern is the presence of polynuclear aromatic hydrocarbons in soil, water, petroleum products, seafood etc. Polynuclear aromatic hydrocarbons (PAHs) are ubiquitous pollutants introduced into the environment by the pyrolysis or combustion of organic material. The presence of these compounds in the environment is a health concern due to their carcinogenicity. The US Environmental Protection Agency (EPA) has classified sixteen PAHs as priority pollutants and is requiring monitoring of drinking water, industrial waste water and groundwater from waste disposal sites.

Methods for PAH analyses have been developed using HPLC with UV–Vis and fluorescence detection [1–6].

The current EPA Method 550 for determination of PAHs in drinking water uses liquid–liquid extraction for sample preparation. Liquid–liquid extraction is tedious, time-consuming and produces large amounts of waste organic solvent.

As an alternative or improved method over liquid–liquid extraction for sample clean-up and enrichment, solid-phase extraction (SPE) has been developed over the last fifteen years. Manual off-line SPE has been demonstrated in the analysis of PAHs in drinking water [3,7] and in seafood [8]. Further, SPE performed on-line with HPLC has been reported in the analysis of biological fluids [9,10]. The precolumn used for SPE was placed on-line between the autosampler and the analytical column. It was controlled by a switching valve and swept by one or more external pumps [3,7–10]. Another simplified (and less expensive) configuration was reported [11] where the autosampler, switching valve and external pump were replaced by a manual sy-

* Corresponding author.

ringe-loading injector. On-line precolumn concentration has also been reported in the analysis of drinking water [12] in which an autosampler specially adapted for precolumn switching was used.

In this study, we describe a new automated method of precolumn concentration for the analysis of drinking water. This method uses an autosampler controlled by a customized "Method Development Language" and a precolumn which replaces the sample loop in the autosampler. The only switching valve used is the one in the autosampler and the only pump used is the HPLC pump. No extra switching valve or external pump is required. A small aliquot of the sample (typically 1.5 ml or multiples of it) is concentrated or enriched on a precolumn using the technique of SPE, and then eluted on-line onto the HPLC system. In the HPLC analysis, the sensitivity for the different PAHs was optimized by using a variable-wavelength program for both fluorescence and UV detection.

This precolumn concentration process is fast and simultaneous with the HPLC analysis of the previous sample. Compared to liquid-liquid extraction, it saves time and reduces solvent waste significantly. The system configuration is the same as a regular HPLC system except for the unique autosampler.

2. Experimental

2.1. Instrumentation

The HPLC system, consisting of P4000 pump with solvent-conditioning module, AS3000 autosampler, FL2000 fluorescence detector, FOCUS UV-Vis detector, PC1000 software and Method Development Language software, was from Thermo Separation Products (Fremont, CA, USA). The PAH column, 15 cm × 4.6 mm with built-in guard column was from Keystone Scientific (Bellefonte, PA, USA). The precolumn used was an Aquapore RP-18 cartridge, 1 cm × 3.2 mm from Perkin-Elmer, Applied Biosystems Division (Foster City, CA, USA).

2.2. Materials

PAH standard mixture was obtained from Supelco (Bellefonte, PA, USA). Acetone, HPLC grade, and acetonitrile, HPLC grade were from J.T. Baker (Phillipsburg, NJ, USA).

2.3. Methods

An automated precolumn concentration (PCC) system was set up as follows: the sample loop in the injection valve of the AS3000 was replaced with an Aquapore precolumn. The AS3000 was controlled by a customized "Method Development Language" which manipulated the syringe movements, injection valve, flush valve and solvent valve. For conditioning of the precolumn, four different solvents could be selected to pass through the precolumn in increments of up to 1.5 ml (preparative syringe capacity in the autosampler), with coordination of the syringe and the valve positions. The system also picked up sample from a vial, up to 1.5 ml each time (autosampler vial capacity) and loaded it onto the precolumn, thus concentrating the sample on the precolumn. Finally a rinse step was performed using the same mechanism as the conditioning step. The waste in each PCC step went directly to a waste line in the autosampler. The injection valve was then switched and the mobile phase eluted the precolumn concentrated analytes onto the analytical column. While the HPLC was analyzing a sample, the precolumn concentration of the next sample was performed simultaneously.

The PCC method used in this study consists of the following steps: (1) the precolumn was conditioned with 1.5 ml methanol, followed by 1.3 ml water (Fig. 1a); (2) 1.5 ml sample was loaded on the precolumn (Fig. 1b and c); (3) the precolumn was rinsed with 1 ml water (Fig. 1a); (4) the concentrated sample was injected onto the HPLC system (Fig. 1d).

HPLC conditions are shown in Table 1.

Calibration standard was prepared by diluting the standard mixture (concentrations shown in Table 2) 1:100 with acetone. A 5- μ l volume was injected (using Push Loop) for calibration.

Table 1
HPLC conditions

Column	Keystone PAH, 15 cm × 4.6 mm with built-in guard column		
Mobile phase	Time (min)	Acetonitrile (%)	Water (%)
	0.00	50	50
	3.00	50	50
	23.00	95	5
	30.00	95	5
	30.01	50	50
	33.00	50	50
Mobile phase	Time (min)	Acetonitrile (%)	Water (%)
modification	0.00	51	49
for 577- μ l	0.10	51	49
loop	0.11	50	50
injection	3.00	50	50
	Remainder of gradient same as above		
Flow-rate	1.5 ml/min		
Detection:	Fluorescence with timed wavelength program:		
	Time (min)	Excitation (nm)	Emission (nm)
	0.00	220	340
	8.50	266	324
	10.70	250	380
	13.60	230	420
	17.00	270	388
	22.00	250	420
	27.50	290	420
	31.00	300	482
	33.00	300	482
	UV with timed wavelength program:		
	Time (min)	Wavelength (nm)	
	0.00	270	Auto zero
	10.80	254	Auto zero
	13.60	240	Auto zero
	17.50	260	Auto zero
	21.50	254	Auto zero
	27.50	300	Auto zero
	33.00	300	Auto zero

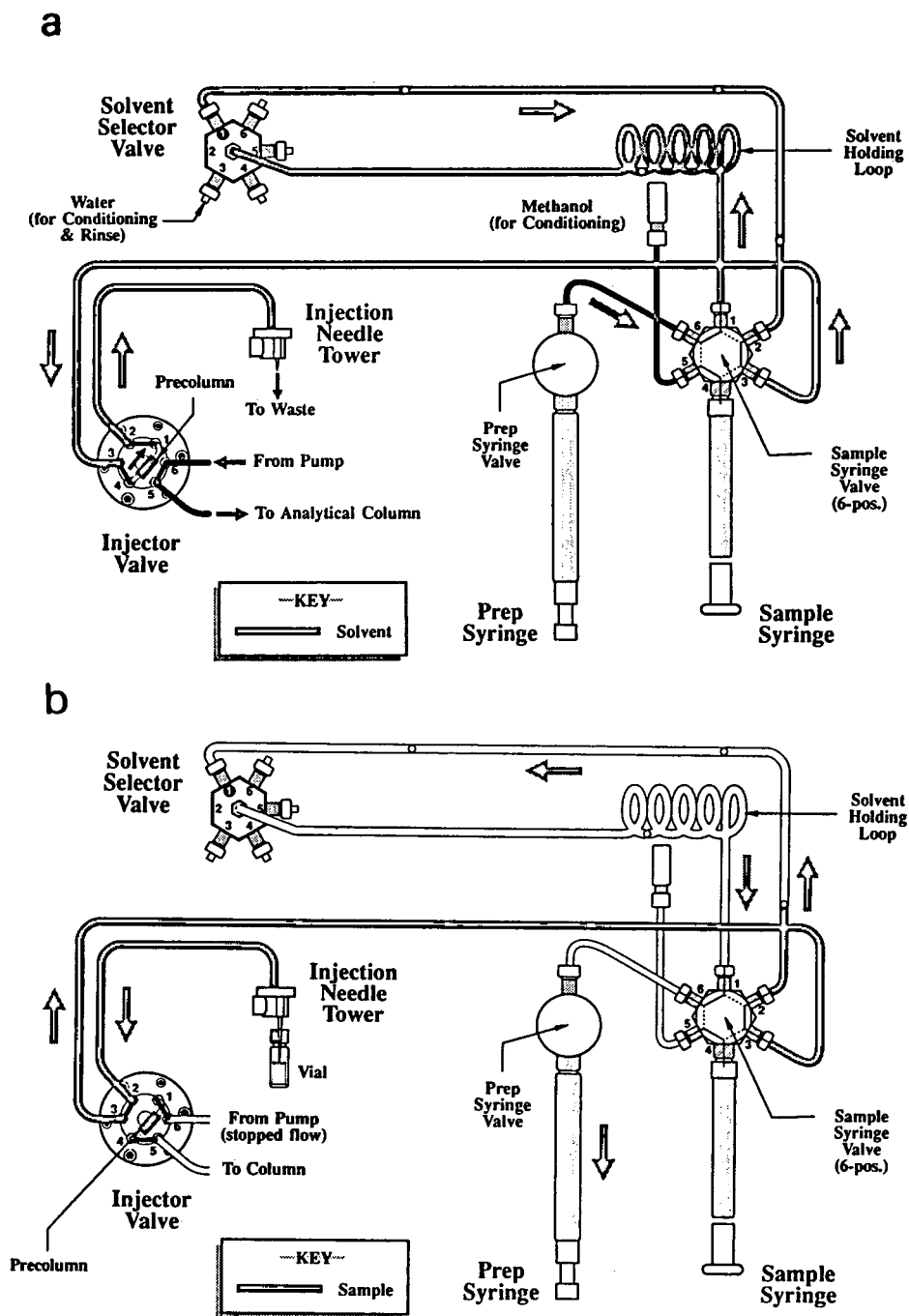


Fig. 1. (a) Precolumn conditioning and rinsing flow path (methanol passes through solvent holding loop and precolumn to waste). (b) Sampling flow path (sample drawn from sample vial to holding loop). (c) Precolumn loading flow path (sample pushed from holding loop through precolumn to waste). (d) Injection flow path (mobile phase flows through precolumn, eluting sample onto HPLC column). Prep = Preparative.

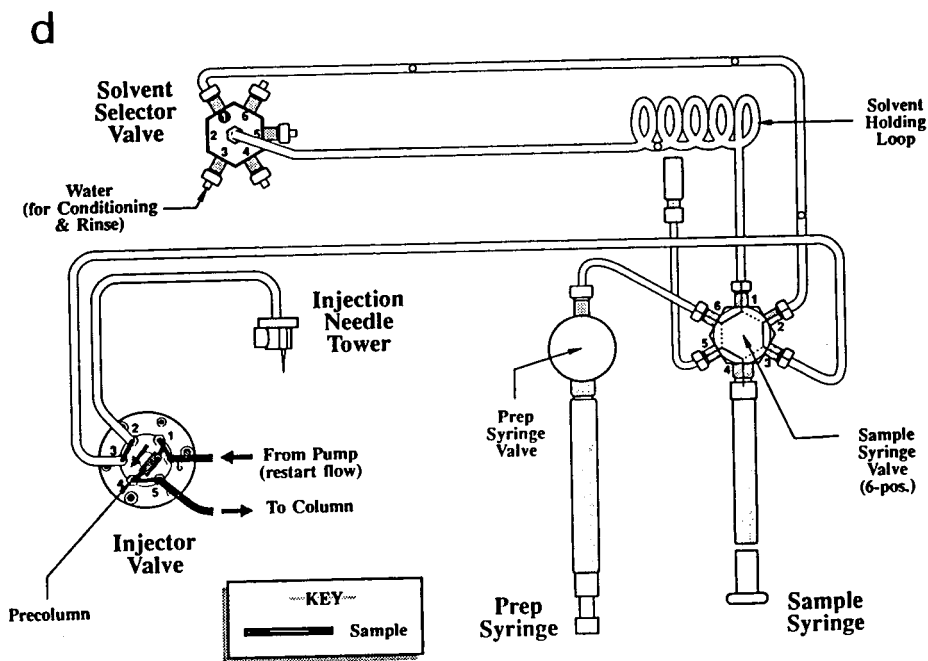
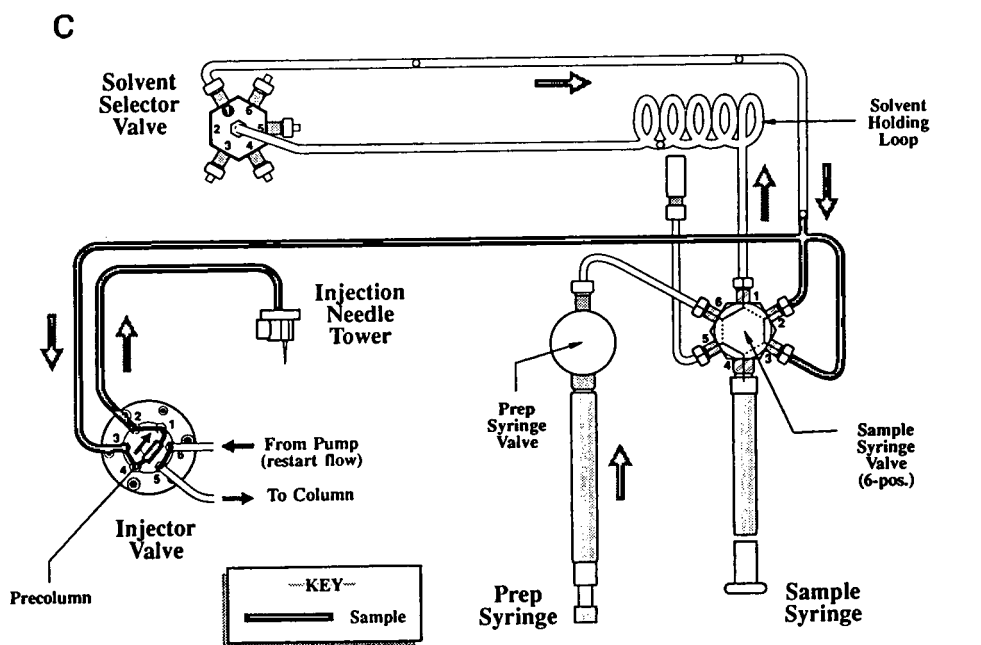


Fig. 1 (Continued).

Table 2
Concentrations of PAH standard mixture from Supelco

Component	$\mu\text{g/ml}$
(1) Naphthalene	1000
(2) Acenaphthylene	2000
(3) Acenaphthene	1000
(4) Fluorene	200
(5) Phenanthrene	100
(6) Anthracene	100
(7) Fluoranthene	200
(8) Pyrene	100
(9) Benz[<i>a</i>]anthracene	100
(10) Chrysene	100
(11) Benzo[<i>b</i>]fluoranthene	200
(12) Benzo[<i>k</i>]fluoranthene	100
(13) Benzo[<i>a</i>]pyrene	100
(14) Dibenz[<i>a,h</i>]anthracene	200
(15) Benzo[<i>ghi</i>]perylene	200
(16) Indeno[1,2,3- <i>cd</i>]pyrene	100

Spiked blank was prepared by spiking 1 l of HPLC-grade water with 1 ml of the calibration standard and used to determine recovery, reproducibility and linearity of the PCC method.

To determine recovery, a full-loop injection of the spiked blank was injected as the *reference standard*. The loop was pre-calibrated to be 577 μl . To compensate for the retention time shifting effect of the large volume of weak solvent injected, the gradient was modified by using an initial mobile phase of acetonitrile–water (51:49) for 0.1 min. The concentration of this reference standard was calculated using the calibration standard above. Then 1500 μl of the spiked blank were analyzed using the PCC method.

To determine reproducibility of multiple analyses of the same spiked blank, six consecutive PCC–HPLC runs of 1500 μl of the spiked blank were performed. To determine reproducibility of recoveries among different spiked blanks, 3 l of water in three different flasks were spiked, and the recoveries of six samples from each spiked blank were averaged. The relative standard deviation of the results of the three spiked blanks were calculated.

To determine linearity (of this method, not of the calibration standard) a 1500- μl blank was run, followed by 300, 600, 900, 1200, 1500 and

1800 μl of spiked blank. Due to the volume limitation of the sample vial, the 1800- μl spiked blank was composed of two consecutive samplings, 900 μl each, from two consecutive vials.

To determine the minimum detection limits, 50, 30 and 20 μl of the spiked blank were run. The detection limit is defined as the amount of sample which yields a peak at a signal-to-noise ratio equal to 3.

3. Results

The chromatogram of 1.5 ml of spiked blank using UV detection shows 16 peaks at a very low signal-to-noise level (Fig. 2a). The chromatogram using simultaneous fluorescence detection shows 14 peaks with significantly higher sensitivity compared to UV while acenaphthylene and indeno[1,2,3-*cd*]pyrene are undetected (Fig. 2b). In this study, UV data are used for the calculations for acenaphthalene, but are too close to the detection limit for the other peaks. Therefore only fluorescence data are used for the calculations for the other peaks, except indeno[1,2,3-*cd*]pyrene, for which neither fluorescence nor UV has sufficient sensitivity for this application.

3.1. Recovery

Normally, recoveries are calculated based on the calibration standard. However, in this study, the reference standard was found to have a significant loss in concentration from the theoretical values based on dilution of the calibration standard. The experimental and theoretical values of the reference standard are compared in Table 3. The recoveries of the spiked blank based on the reference standard (assumed to be 100%) are also shown in Table 3.

3.2. Reproducibility

Reproducibility of retention times (Table 4) and areas (Table 5) of six consecutive PCC-injection sequences of 1500 μl of a spiked blank is shown as relative standard deviation (R.S.D.)

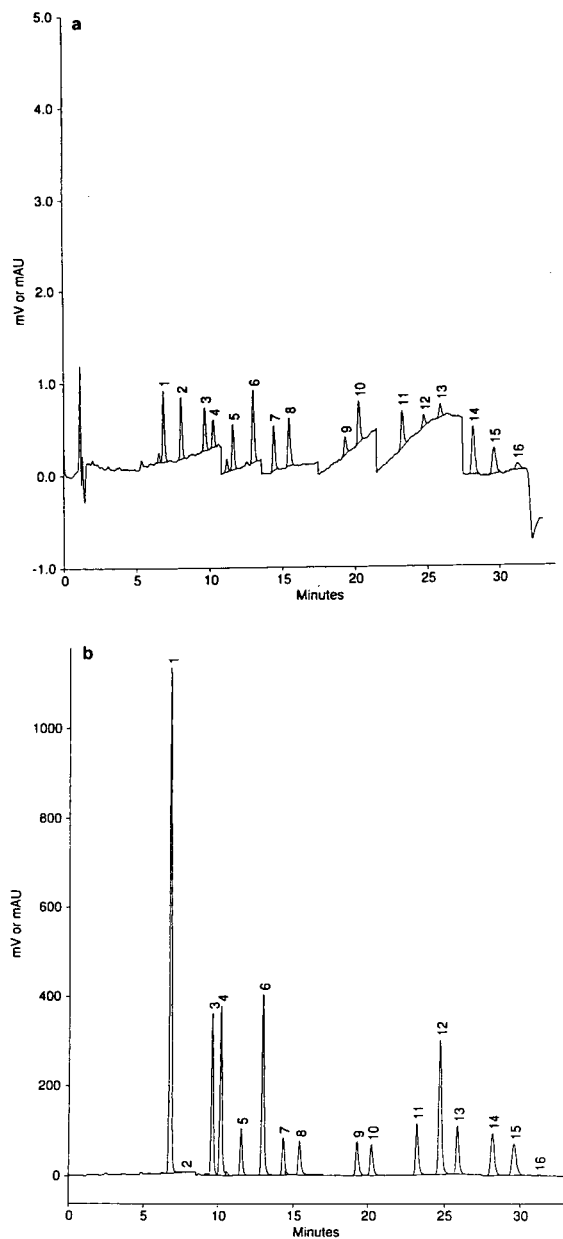


Fig. 2. Chromatograms of PAH priority pollutants in 1.5 ml of spiked blank using PCC–HPLC and (a) UV detection or (b) fluorescence detection. Peaks: 1 = naphthalene; 2 = acenaphthylene; 3 = acenaphthene; 4 = fluorene; 5 = phenanthrene; 6 = anthracene; 7 = fluoranthene; 8 = pyrene; 9 = benz[a]anthracene; 10 = chrysene; 11 = benzo[b]fluoranthene; 12 = benzo[k]fluoranthene; 13 = benzo[a]pyrene; 14 = dibenz[a,h]anthracene; 15 = benzo[ghi]perylene; 16 = indeno[1,2,3-cd]pyrene.

for each peak as automatically calculated using the PC1000 software.

Reproducibilities of recoveries of three different spiked blanks are also shown in Table 5.

3.3. Linearity

A six-point calibration was obtained for peaks 1 and 3–15 using fluorescence. A five-point calibration was obtained for peak 2 using UV since the 300- μ l data point fell below the detection limit.

The correlation coefficients determined by fluorescence for these 14 peaks range from 0.9733 to 0.9991. The correlation coefficient determined for acenaphthylene by UV was 0.9965 (Table 6).

3.4. Minimum detection limits

The minimum detection limits for the 15 PAHs in μ g/l (of the spiked sample) with a signal-to-noise ratio of 3 are reported in Table 6. Of the 15 compounds, 14 meet the minimum detection limit spiking level in EPA Method 550 with the exception of fluoranthene. Doubling the load volume lowered the detection limit for fluoranthene to 0.025 μ g/l, which meets the minimum detection limit spiking level.

4. Discussion

The most significant advantage of the PCC method presented is its efficiency compared to liquid–liquid extraction. The PCC process takes only 10 to 15 min (vs. hours in liquid–liquid extraction) and can be performed simultaneously with the previous HPLC analysis. The amount of organic waste per sample is reduced by approximately 200 ml per extraction, or several liters per week for the average environmental laboratory.

While off-line SPE has the advantage of using a new cartridge for each sample and allows a large volume of sample to pass through, the PCC method here has shown clean blanks between samples.

A major difference between this method and

Table 3
Concentration of reference standard and recoveries of spiked blank (fluorescence detection, except peak 2, UV detection)

Peak	Theoretical concentration ($\mu\text{g/l}$)	% Of theoretical concentration found in reference standard	Recovery (%) with PCC based on reference standard
(1) Naphthalene	10	117	85
(2) Acenaphthylene	20	94	81
(3) Acenaphthene	10	97	81
(4) Fluorene	2	99	75
(5) Phenanthrene	1	97	65
(6) Anthracene	1	100	59
(7) Fluoranthene	2	92	58
(8) Pyrene	1	89	61
(9) Benz[<i>a</i>]anthracene	1	58	35
(10) Chrysene	1	60	39
(11) Benzo[<i>b</i>]fluoranthene	2	53	32
(12) Benzo[<i>k</i>]fluoranthene	1	65	38
(13) Benzo[<i>a</i>]pyrene	1	49	36
(14) Dibenz[<i>a,h</i>]anthracene	2	128	59
(15) Benzo[<i>ghi</i>]perylene	2	94	65
(16) Indeno[1,2,3- <i>cd</i>]pyrene	1	–	–

EPA Method 550 is that an aliquot (1.5 ml) of the spiked blank is analyzed here while the whole spiked blank (1 l) is analyzed in the EPA method. In this study, the spiked blank was

Table 4
Reproducibility of retention times for precolumn concentrated PAH priority pollutants

Peak	R.S.D. of retention time ($n = 6$)
(1) Naphthalene	0.84
(2) Acenaphthylene ^a	0.78
(3) Acenaphthene	0.65
(4) Fluorene	0.68
(5) Phenanthrene	0.69
(6) Anthracene	0.69
(7) Fluoranthene	0.64
(8) Pyrene	0.60
(9) Benz[<i>a</i>]anthracene	0.54
(10) Chrysene	0.56
(11) Benzo[<i>b</i>]fluoranthene	0.53
(12) Benzo[<i>k</i>]fluoranthene	0.53
(13) Benzo[<i>a</i>]pyrene	0.52
(14) Dibenz[<i>a,h</i>]anthracene	0.63
(15) Benzo[<i>ghi</i>]perylene	0.67

^a By UV detection. All other peaks by fluorescence detection.

found, by direct loop injection, to have a significantly lower concentration than the theoretical value assuming complete solution. For that reason, relative (rather than absolute) recoveries were calculated based on the reference standard.

By using the technique of precolumn concentration and fluorescence detection, this method is able to meet the spiking-level requirement for 14 of the 16 PAHs analyzed when only 1.5 ml (from one autosampler vial) was loaded. When two vials of the sample are loaded, increasing the sample size to 3 ml, the detection sensitivity for fluoranthene can be increased to meet the EPA-required spiking level. The detection limit study was not performed by actual dilution to the EPA-required spiking level and analyzing 1500 μl because of the non-linearity of the dilution of the spike. For the same reason, linearity was not performed by analyzing 1500 μl of different dilutions, but rather by different volumes of the same dilution.

This PCC method produced good results for linearity. Peak area R.S.D.s are less than 10% in 40 out of the 48 instances and recoveries are higher than 50% in 9 out of 15 analytes in Table 5. Calculations of recoveries were dependent on the peak areas of the reference standard, which

Table 5
Reproducibility of areas and recoveries for precolumn concentrated PAH priority pollutants for different spiked blanks

Peak	R.S.D. of peak areas (%)			Recoveries	
	Spiked blank 1 (n = 6)	Spiked blank 2 (n = 6)	Spiked blank 3 (n = 6)	Average recovery (%) (n = 3)	R.S.D. (%) (n = 3)
(1) Naphthalene	4.78	1.95	6.47	80.3	9.01
(2) Acenaphthylene ^a	1.35	3.48	2.84	72.0	11.0
(3) Acenaphthene	3.41	2.11	2.57	85.0	12.4
(4) Fluorene	3.25	2.29	5.34	71.7	6.9
(5) Phenanthrene	3.77	4.38	7.09	63.0	11.4
(6) Anthracene	3.25	5.20	4.02	56.3	11.4
(7) Fluoranthene	3.58	7.56	5.04	56.7	9.7
(8) Pyrene	5.44	7.60	7.47	61.2	16.2
(9) Benz[a]anthracene	4.17	11.11	5.60	34.3	14.7
(10) Chrysene	3.83	10.83	4.31	36.7	21.2
(11) Benzo[b]fluoranthene	22.13	18.92	2.05	26.0	25.2
(12) Benzo[k]fluoranthene	11.69	20.01	4.56	40.7	32.5
(13) Benzo[a]pyrene	10.86	3.90	5.15	30.3	18.6
(14) Dibenzo[a,h]anthracene	3.40	10.27	1.53	49.0	28.9
(15) Benzo[ghi]perylene	4.29	7.65	1.47	73.0	15.5

^a By UV detection. All other peaks by fluorescence detection.

was a 577- μ l injection. No doubt, that had a volume overloading effect causing a certain amount of peak broadening, but this reference

standard eliminates the variable of PAH solubility in the spike blank for the purpose of evaluating the PCC method.

Table 6
Correlation coefficients and minimum detection limits of precolumn concentrated PAH priority pollutants

Peak	Correlation coefficient	Minimum detection limit (μ g/l)
(1) Naphthalene	0.9950	0.29
(2) Acenaphthylene ^a	0.9965	4.44
(3) Acenaphthene	0.9994	0.25
(4) Fluorene	0.9908	0.05
(5) Phenanthrene	0.9987	0.025
(6) Anthracene	0.9962	0.026
(7) Fluoranthene ^b	0.9977	0.05
(8) Pyrene	0.9733	0.022
(9) Benz[a]anthracene	0.9816	0.007
(10) Chrysene	0.9841	0.012
(11) Benzo[b]fluoranthene	0.9841	0.01
(12) Benzo[k]fluoranthene	0.9845	0.009
(13) Benzo[a]pyrene	0.9889	0.01
(14) Dibenzo[a,h]anthracene	0.9854	0.02
(15) Benzo[ghi]perylene	0.9991	0.018

^a By UV detection. All other peaks by fluorescence detection.

^b Using twice the sample volume lowers the minimum detection limit to 0.025 μ g/l.

The above finding of a “loss” of PAHs when an aliquot of a spiked blank was analyzed is consistent with some reports on spike recovery studies of PAHs. PAHs are classified as hydrophobic organic compounds which are relatively insoluble in water and tend to adsorb onto other non-aqueous phases, either through hydrophobic interaction when the non-aqueous phase is a non-polar compound [13] or through conjugate π bonding when the non-aqueous phase is a polar compound [14,15]. It has been speculated that since spiked analytes may often be less retained on or in the environmental matrices than the native analytes, the use of spike recovery studies may overestimate the efficiencies of extraction methods [16,17]. The results in this study support this statement for extraction of the whole spiked sample. This raises the question as to whether spiked blanks are currently being treated properly using liquid–liquid extraction if the analytes of interest are not homogeneous in the matrix. Further study would be required to resolve this issue.

5. Conclusions

A new method of precolumn concentration has been presented using a single pump and a single valve controlled by a customized “Method Development Language”. Analysis of PAHs in water has been performed using this method with as little as 1.5 ml of sample resulting in good reproducibility, linearity and sensitivity. This method also addresses a difference in treatment (compared to the liquid–liquid extraction method) of PAH-spiked water samples which may have a problem of inhomogeneity in the spiking. This method is potentially useful for fast screening of drinking water samples.

Acknowledgements

The authors gratefully acknowledge the technical advice from Eileen Ferguson, Vance Nau,

Ran Wu and Lenore Kelly during the course of this study.

References

- [1] W.E. May and S.A. Wise, *Anal. Chem.*, 56 (1984) 225–232.
- [2] W.F. Kline, S.A. Wise and W.E. May, *J. Liq. Chromatogr.*, 8 (1985) 223–237.
- [3] H.G. Kicinski and A. Kettrup, *Vom Wasser*, 71 (1988) 245–254.
- [4] A.M. Krstulovic and P.R. Brown, *Anal. Chem.*, 48 (1976) 1383.
- [5] A.M. Krstulovic and D.M. Rosie, *Am. Lab.*, 7 (1977) 11.
- [6] H.G. Kicinski, S. Adamek and A. Kettrup, *Bestimmung von PAK's mittels HPLC in Wasser- und Bodenproben*, Van Acken Verlag, Krefeld, 1988, pp. 176–181.
- [7] H.G. Kicinski, S. Adamek and A. Kettrup, *Chromatographia*, 28 (1989) 203–208.
- [8] G.A. Perfetti, P.J. Nyman, S. Fisher, F.L. Joe, Jr. and G.W. Diachenko, *J. Assoc. Off. Anal. Chem. Int.*, 75 (1992) 872–877.
- [9] J.C. Kraft, C. Echhoff, W. Kuhn, B. Loeffberg and H. Nau, *J. Liq. Chromatogr.*, 11 (1988) 2051–2069.
- [10] K. Zech and R. Huber, *J. Chromatogr.*, 353 (1986) 351–360.
- [11] W. Voelter, T. Kronbach, K. Zech and R. Huber, *J. Chromatogr.*, 239 (1982) 475–482.
- [12] C.E. Goewie and E.A. Hogendoorn, *J. Chromatogr.*, 410 (1987) 211–216.
- [13] I. Tinoco, K. Sauer and J. Wang, *Physical Chemistry*, Prentice-Hall, Old Tappan, NJ, 2nd ed., 1978.
- [14] M.L. Lee, M.V. Novotny and K.D. Bartle, *Analytical Chemistry of Polynuclear Aromatic Compounds*, Academic Press, New York, 1981.
- [15] M.D. Burford, S.B. Hawthorne and D.J. Miller, *Anal. Chem.*, 65 (1993) 1497–1505.
- [16] N. Alexandrou and J. Pawliszyn, *Anal. Chem.*, 67 (1989) 2770.
- [17] H. Liu and G. Amy, *Environ. Sci. Technol.*, 27 (1993) 1553–1562.

Optimization of automated solid-phase extraction for quantitation of polycyclic aromatic hydrocarbons in aqueous media by high-performance liquid chromatography–UV detection

Nanette C. Fladung

Analytical Services Team Leader, Microbial Environmental Services, 7300 N.W. 62nd Avenue, Johnston, IA 50131-1004, USA

Abstract

A solid-phase extraction method for the quantitation of 16 regulated polycyclic aromatic hydrocarbons (PAHs) was developed and conditions were optimized to meet the recoveries stated in US Environmental Protection Agency Method 550.1. The best elution procedure soaked the extraction cartridge with acetonitrile followed by elution with methylene chloride. Rinsing the sample bottle with acetonitrile and combining the rinse with the sample extract was necessary to achieve the desired recoveries. The average recovery for a mixture of the sixteen regulated PAHs was 83%.

1. Introduction

One of the main concerns for the analysis of contaminants in an analytical support laboratory is how to accurately analyze samples without utilizing excessive amounts of time and laboratory space. Polycyclic aromatic hydrocarbons (PAHs) in ground water and other aqueous media are some of the contaminants which need to be analyzed for the regulatory testing and studies necessary for remediation work. To meet these needs, this analytical support laboratory chose to analyze PAHs in aqueous media by solid-phase extraction (SPE). We chose SPE since it is easily automated, uses less solvent, and uses less hood space than the more traditional liquid–liquid extraction methods. PAHs are potentially carcinogenic compounds 16 of which have been selected by the US Environmental

Protection Agency (EPA) as Constant Decree priority pollutants for regulatory purposes [1].

The purpose of this study was to see if the procedure described in EPA Method 550.1 [2] could be automated and if higher concentrations of PAHs could successfully be used. EPA Method 550.1 is approved for the analysis of PAHs in drinking water by liquid–solid extraction. The calibration range for this method is in the low $\mu\text{g/l}$ level. The concentration range need for our analyses ranged from this lower level up to the low mg/l levels.

Samples were initially analyzed according to the test procedures in Refs. [3] and [4]. These initial attempts to automate solid phase extraction of PAHs yielded recoveries of less than 50% for each compound. This led us to look at each step of the extraction process in order to get sample recoveries equivalent to those in ac-

cepted EPA procedures such as EPA Method 550.1.

2. Materials and methods

Samples were prepared using equipment from Zymark (Hopkinton, MA, USA). The Zymark AutoTrace SPE workstation was used to automate the SPE of water samples. The AutoTrace operates with positive pressure liquid flow instead of the traditional vacuum manifold techniques. EnvirElute/PAH SPE columns from Varian (Sugarland, TX, USA) with 1 g sorbent mass and 6 ml column volume were used for sample concentration. The Zymark TurboVap II concentration workstation with nitrogen gas was used to further concentrate the extract from the AutoTrace to a final volume of 1 ml.

All PAH extracts were analyzed using equipment from Perkin-Elmer (PE, Norwalk, CT, USA), which was run according to the Quick-Turnaround HPLC method [5,6]. The HPLC system consisted of a Model 250 binary LC pump, an ISS-200 autosampler, and an LC235C diode array UV detector. A PE Chromspher-3 PAH column packed with 3 μm d_p 120 Å polymeric C_{18} material (100 mm \times 4.6 mm with a 10-mm integral guard column) and a solvent gradient system with acetonitrile and water were used for separation of the PAHs. Turbochrom data acquisition program version 3.1 from PE Nelson (Cupertino, CA, USA) provided data acquisition and handling.

Optimization of the SPE procedure was carried out in three separate phases. The first phase was to set up the HPLC for analysis of PAHs. The second phase was to optimize the recovery of the concentration step. The final phase was to optimize the recovery of the automated SPE procedure.

The Zymark TurboVap II was used for concentrating the sample extract from the AutoTrace SPE workstation. To begin the second phase of the optimization procedure, the concentration step was optimized for operating conditions and physical handling techniques. A spiked solvent sample was initially concentrated on the Tur-

boVap II. Recoveries of the lower-molecular-mass PAHs were less than 50%. Recoveries for the heavier PAHs were acceptable. The initial conditions for evaporation set the water bath at temperatures below the boiling point of the solvents: 40°C for methylene chloride (MeCl) and 60°C for acetonitrile (ACN).

The following steps were involved in optimizing the TurboVap for standard recovery. Different pressures for the nitrogen gas were evaluated, the temperature of the water bath was varied, and the amount and type of solvent was varied. The recommended operating pressure for the TurboVap is between 8 and 15 p.s.i. (1 p.s.i. = 6894.76 Pa). Varying the pressure in this range did not have an effect on the recoveries of the PAHs. A pressure of 11 p.s.i. of nitrogen was used for all subsequent concentrations via the TurboVap.

To determine the optimal operating conditions to concentrate MeCl, 10 ml of MeCl were added to a concentrator tube. Next, 12.5 mg/analyte of the PAH standard were injected into the concentrator tube. The TurboVap was then turned on and the solvent was evaporated down to 0.75 ml. This end point is detected automatically by sensors in the TurboVap II. At this point ACN was added to the concentrator tube. The ACN was thoroughly mixed with the remaining MeCl solution and concentrated. Finally, 0.25 ml of ACN were added drop-wise into the tube and used to rinse the slanted portion of it. This experiment was continued while varying the temperature, volume of ACN, and physical handling techniques. The optimal temperature for the water bath was determined to be 35°C for the elimination of MeCl. The optimal operating temperature to eliminate ACN was 40°C. These experiments also indicated that the optimal volume of ACN during the solvent exchange is 15 ml. This volume insured MeCl was evaporated and did not interfere with HPLC analysis. If MeCl was present in the sample injected onto the HPLC column, poor peak shape was observed.

When greater amounts of ACN were added during the solvent exchange residence time of the extract in the sample concentrator increased.

Experimentation showed that the residence time of the extract in the concentrator tubes should not be longer than 45 min. If the residence time was too long the more volatile PAHs were carried away by the nitrogen. Because of this, a lower temperature in the water bath did not necessarily insure higher recoveries.

For the analysis of PAHs by HPLC–UV, the UV detector was programmed using the following settings: 280 nm (peaks 1–5), 335 nm (peaks 6–10) and 360 nm (peaks 11–16). (For peak identification, see Table 1.) Interference could be seen on some of the peaks. These included acenaphthylene and anthracene. The interference caused the concentration of these peaks to be artificially high. These interferences are not the same ones noted in EPA Method 550.1 and may be dependent on the sorbent material used in the extraction or the HPLC column used. There were no problems getting the HPLC operational by this method. The only precaution that needed to be taken was to ensure that the wavelength changes on the diode array detector occurred after the appropriate peaks.

The Zymark AutoTrace SPE workstation was used to process the liquid samples. The samples were automatically pumped from the sample containers through EnvirElut/PAH extraction columns. The sample cartridges were then dried for 5 min with nitrogen to dry the sample cartridge before sample elution with ACN and MeCl chloride.

Zymark literature recommended soaking the extraction cartridge with solvent before elution to increase analyte recoveries. This procedure was implemented and did increase analyte recovery. Table 2 shows the AutoTrace extraction procedure.

3. Results

Sample recoveries for the overall process were determined from spiked tap water samples that were processed by the AutoTrace and TurboVap II and analyzed by HPLC. Initial standards processed in this manner did not have adequate analyte recoveries. To determine where the

Table 1
PAH Recoveries

PAH	Recovery (%)				
	First elution	Sample bottle	Sample bottle, adjusted	Second elution	Second elution, adjusted
(1) Naphthalene	82.2	0.7	82.9	0.5	83.4
(2) Acenaphthylene	87.6	0.0	87.6	1.9	89.5
(3) Acenaphthene	83.3	0.0	83.3	3.5	86.8
(4) Fluorene	84.8	3.2	87.9	3.7	91.6
(5) Phenanthrene	78.0	8.5	86.6	5.7	92.3
(6) Anthracene	63.1	70.3	133.5	5.1	138.5
(7) Fluoranthene	63.8	20.9	84.6	6.3	90.9
(8) Pyrene	55.5	20.1	75.7	6.8	82.5
(9) Benz[<i>a</i>]anthracene	34.8	52.5	87.3	3.2	90.5
(10) Chrysene	31.7	67.4	99.1	4.0	103.1
(11) Benzo[<i>k</i>]fluoranthene	33.5	56.3	89.8	0.0	89.8
(12) Benzo[<i>a</i>]pyrene	30.0	53.0	83.0	0.9	83.9
(13) Dibenzo[<i>a,h</i>]anthracene	30.5	52.4	82.8	2.8	85.6
(14) Benzo[<i>b</i>]fluoranthene	36.5	58.9	95.4	24.9	120.3
(15) Benzo[<i>ghi</i>]perylene	31.8	55.3	87.2	1.2	88.4
(16) Ideno[1,2,3- <i>cd</i>]pyrene	28.7	55.9	84.6	3.2	87.7
Average recovery (%)	53.5		89.4		94.0

Table 2
AutoTrace extraction procedure

Step	Autotrace command
1	Process six samples using the following procedure
2	Wash syringe with 7 ml of MeCl
3	Wash syringe with 7 ml of methanol
4	Wash syringe with 7 ml of water
5	Wash syringe with 3 ml of methanol
6	Condition column with 5 ml of MeCl into solvent waste
7	Dry column with nitrogen for 1 min
8	Condition column with 10 ml of methanol into solvent waste
9	Condition column with 5 ml of water into aqueous waste
10	Load 1000 ml of sample onto column
11	Rinse column with 10 ml of water into aqueous waste
12	Dry column with nitrogen gas for 5 min
13	Soak and collect 4.0-ml fraction using ACN
14	Pause for 3 min
15	Soak and collect 3.5-ml fraction using MeCl
16	Pause for 3 min
17	Collect 3.5-ml fraction into sample tube using MeCl
18	End

The Zymark AutoTrace SPE workstation is used to extract and concentrate PAHs from aqueous media. Conditions for extraction: nitrogen pressure between 0.6 and 0.8 bar; solvents: acetonitrile, methanol, methylene chloride and water.

analytes were being lost in the sample preparation process, a number of experiments were performed. These experiments included elution of the extraction cartridge a second time, rinsing the sample bottle with ACN for concentration and analysis, and injecting the standard directly onto the SPE extraction cartridge instead of making an aqueous standard. Table 1 shows the results of these experiments. Fig. 1 shows the results when the standard was injected directly on to the SPE extraction column instead of loading an aqueous standard onto the SPE extraction cartridge. The recovery of PAHs from this experiment indicate that elution from the SPE extraction columns followed by concentration with the TurboVapII gives acceptable recoveries. Therefore, the only part of the extraction process that contributed to loss of analyte recovery was loading the sample onto the extraction cartridge and the loss of analyte in the sample bottle and the transfer process.

Table 1 shows that rinsing the sample bottle with ACN recovers a significant amount of the lost analyte. This indicates that much of the error in the SPE extraction process comes from making and loading the aqueous standard. To confirm this, a standard was placed directly on the SPE extraction cartridge. These cartridges were then eluted, concentrated and analyzed on

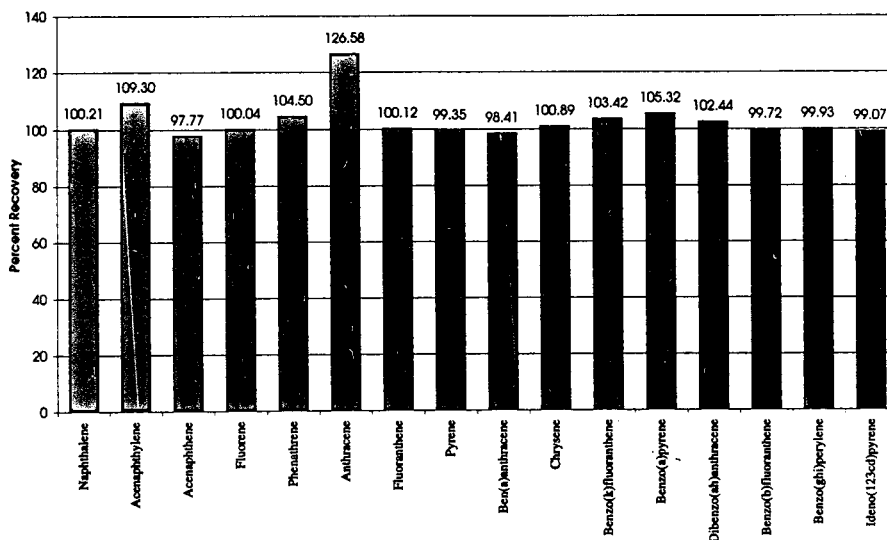


Fig. 1. Recovery with direct injection of standard onto SPE cartridge.

the HPLC. Fig. 1 shows excellent recoveries from this experiment.

Kerkdijk et al. [7] suggests rinsing the sample bottles with isopropanol (3×), 20% nitric acid and isopropanol respectively. The water sample is then to be diluted with isopropanol (3:1) to prevent PAH adsorption to the container wall. This process has not been tried in our laboratory, but looks promising.

A comparison of the variable-wavelength program and a program with a constant wavelength of 255 nm for the analysis of environmental samples was made. In addition to the variable-wavelength program used in the quick turn-around method, the second channel of the UV detector collected data at a constant wavelength of 255 nm. Fig. 2 shows a PAH standard run using the programmed UV detector, an extracted sample using the programmed UV detector, and the same extracted sample using the 255 nm wavelength only. These chromatograms show the

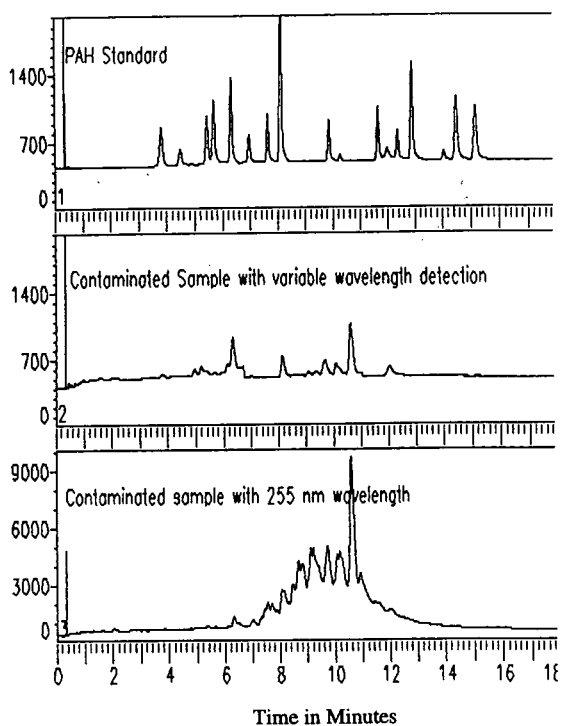


Fig. 2. PAH Standard run using programmed UV detection, an extracted sample using programmed UV detection, and the same extracted sample using detection at 255 nm only.

benefit of the variable-wavelength program. Each of the 16 regulated PAHs is easily detected with the variable-wavelength program, but the detection of other contaminants is greatly reduced.

4. Discussion

SPE cartridges can successfully be used for the analysis of PAHs in aqueous media. In addition to the relatively low concentration of PAHs addressed in EPA Method 550.1, SPE can be used with concentrations of PAHs an order of magnitude higher. These higher concentrations are normally found at heavily contaminated sites or in enrichment cultures often used in laboratory studies.

While the automation of SPE would appear to be straightforward, each step of the sample preparation process had to be optimized separately. The preparation of aqueous PAH standards is difficult due to their low solubilities. Rinsing the sample container with ACN and adding the rinse to the solvent extract gives recoveries for this method which are equal to or better than those described in EPA Method 550.1. Rinsing the sample container is also part of the procedure described in EPA Method 550.1. Automation of the extraction process allows for efficient use of chemist time without giving up accuracy of data. The Perkin-Elmer Quick Turnaround method allows for detection of all 16 regulated PAHs without excessive interference from other compounds with a variable-wavelength UV detector.

A comparison between this method and EPA 550.1 is discussed below. A 3- μm particle diameter column was used instead of a 5- μm particle diameter column in the HPLC. This allowed for faster elution times (18 min instead of 30 min) without the loss of separation. Liquid–solid extraction cartridges were used instead of Empore extraction disks. The main disadvantage of the extraction cartridges has been the length of time necessary to load the sample onto the cartridge; this time is not reduced by the automated method, but six samples can be extracted

at the same time with no operator supervision. Interferences can be seen in both methods. This method uses only a UV detector instead of UV and fluorescence detectors. The same quality of data can be obtained due to the wavelength programming used by this method and the LC235C diode array UV detector allows for spectral confirmation of the peaks detected.

References

- [1] Z.A. Grosser, J.F. Ryan and M.W. Dong, *J. Chromatogr.*, 642 (1993) 75.
- [2] J.W. Hodgeson, *Polynuclear Aromatic Hydrocarbons: EPA Method 550.1*, US Environmental Protection Agency, Cincinnati, OH, 1990, pp. 143–165.
- [3] *AutoTrace SPE Workstation Application Highlights*, Zymark, Hopkinton, MA, 1992.
- [4] B.A. Hale and A.M. Hanagan, *Automated Solid Phase Extraction Method Development/Validation at a Drinking Water Utility*, Denver Water Department, Denver, CO, 1992.
- [5] M.W. Dong, J.X. Duggan and S. Stefanou, *LC·GC*, 11 (1993) 802.
- [6] *Perkin-Elmer Cookbook: HPLC System for PAH Analysis; LC-292*, Perkin-Elmer, Norwalk, CT, 1993.
- [7] H. Kerkdijk, G. Haak and J.A. Ooms, presented at the 1994 Pittsburgh Conference, poster.



ELSEVIER

Journal of Chromatography A, 692 (1995) 27–37

JOURNAL OF
CHROMATOGRAPHY A

High-performance liquid chromatographic determination of sulfonylureas in soil and water

Guido C. Galletti^a, Alessandra Bonetti^b, Giovanni Dinelli^{b,*}

^a*Istituto di Microbiologia e Tecnologia Agraria e Forestale, Università di Reggio Calabria, P.zza S. Francesco 4, I-89061 Gallina, Reggio Calabria, Italy*

^b*Dipartimento di Agronomia, Università di Bologna, via F. Re 8, I-40126 Bologna, Italy*

Abstract

Isocratic and gradient conditions for the separation of four sulfonylurea herbicides, namely chlorsulfuron, metsulfuron, chlorimuron and thifensulfuron, by reversed-phase high-performance liquid chromatography (HPLC) on C₆ and C₁₈ columns were established. Liquid–liquid (LL) and solid-phase extraction (SPE) procedures for the extraction and concentration of the herbicides from water and soil samples were tested. LL and SPE recoveries, HPLC detection limits and repeatability and dependence of the capacity factor on mobile phase composition are discussed. Typical chromatograms are shown.

1. Introduction

Sulfonylureas are a class of herbicides characterized by low application rates (typically in the range 10–100 g ha⁻¹) and low toxicity to mammals. Such molecules are formed by three moieties, generally (i) a monosubstituted benzene ring, (ii) a diazinic or triazinic ring with various substituents and (iii) a sulfonylurea bridge (Fig. 1). In some instances, a disubstituted benzene, a thiophene, a pyridine or a non-aromatic moiety is present as moiety (i) (Fig. 1).

Various methods have been published for the determination of sulfonylureas. The most recent papers include bioassay [1], enzyme immunoassay [2], gas chromatography [3,4], capillary electrophoresis [5] and high-performance liquid

chromatography (HPLC) [6,7]. Each has its own advantages and disadvantages.

Bioassays reach very low detection limits (0.1 ppb), but are aspecific. Immunoassays show similar sensitivity and reduce sample work-up and analysis time, but are expensive and not yet commercially available. Two recent papers showed an elegant way to form stable N,N'-dimethyl derivatives of sulfonylureas in soil and water using diazomethane in ethyl acetate [3,4]. However, gas chromatographic analysis contrasts with the low volatility and thermal instability of underivatized and monomethylated sulfonylureas, and is uncommon for such a class of herbicides. Capillary electrophoresis has been used to determine chlorsulfuron and metsulfuron in tap water [5], but has yet to be applied to soil, its main problem being the low sample loadability.

HPLC is the most commonly adopted method

* Corresponding author.

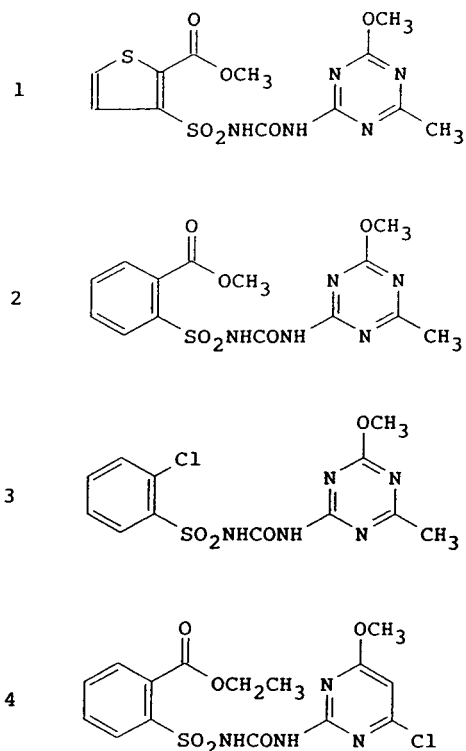


Fig. 1. Structures of sulfonylureas: 1 = thifensulfuron; 2 = metsulfuron; 3 = chlorsulfuron; 4 = chlorimuron.

for sulfonylurea determination in soil and water [6,7]. Chromatographic techniques, including HPLC, need preliminary enrichment steps when analyte concentrations in the sample are below the minimum injectable level. Minimum concentrations of sulfonylurea standard solutions for HPLC with UV detection are about 1 ppm. Photoconductivity detectors lower such detection limits by about one order of magnitude. Although sulfonylurea concentrations as low as 0.2 ppb have been determined in soil using HPLC with photoconductivity detection [7], careful control of various operating parameters is needed to optimize sensitivity and baseline stability [8–10]. In conclusion, photoconductivity detectors are not commonly adopted in HPLC.

Since 1982, when the first sulfonylurea herbicide, chlorsulfuron, became commercially available, at least sixteen different herbicide

products containing different sulfonylureic active ingredients have appeared on market. Surprisingly, most HPLC publications have dealt with the simultaneous determination of one or two sulfonylureas only, aimed at improving the detection limit rather than increasing the number of detected molecules.

Prior to research on sulfonylurea degradation in soil, we decided to test some extraction and HPLC conditions in an attempt to increase the number of sulfonylureas detectable in one run. Four sulfonylureas (Fig. 1) were selected among those commercially available. Three compounds, chlorsulfuron, metsulfuron and chlorimuron, are monosubstituted benzenic sulfonylureas. Thifensulfuron is characterized by a monosubstituted thiophene instead of a benzene ring. The former compounds are characterized by long residence times in soil. The latter is representative of a category of sulfonylureas more easily degraded in soil. Such molecules are of less environmental impact, but are more elusive, because they decompose faster.

2. Experimental

2.1. Reagents

Reagents for HPLC separations and extraction were pesticide-free and supplied by Sigma (St. Louis, MO, USA). The sample concentration column for solid-phase extraction consisted in a Bakerbond (Phillipsburg, NJ, USA) C₁₈ (1 g, 40- μ m silica particles). Sulfonylurea commercial products were kindly provided by Professor P. Catizone and Dr. A. Vicari, Department of Agronomy, University of Bologna.

2.2. Sulfonylurea samples

Chlorsulfuron, metsulfuron, chlorimuron and thifensulfuron were extracted from commercial formulates with freshly redistilled dichloromethane in a Soxhlet extractor for 3 h. After dehydration with anhydrous sodium sulfate, dichloromethane was distilled off in a rotary evaporator. The residual sulfonylureas were sub-

jected to nuclear magnetic resonance, infrared and mass spectral analyses to confirm their identity and used for subsequent experiments without further purification. Sulfonylurea yields from the commercial formulatates ranged from 24 to 71% (Table 1).

2.3. Standard solutions

A stock standard solution at a concentration of 100 ppm was prepared by dissolving 10 mg each of the four sulfonylureas in 100 ml of methanol–water (40:60). Appropriate dilutions of this stock standard solution were made with methanol–water (40:60) to obtain working standard solutions of 0.25, 0.5, 1, 2, 4, 5 and 10 ppm.

A similar procedure was adopted for (a) thifensulfuron, metsulfuron and chlorsulfuron in one stock solution and (b) chlorimuron in a separate stock solution, in order to run “isocratic 2 and 3” respectively (see Section 2.7).

2.4. Water sample fortification and extraction

Water (100 ml) containing the four sulfonylureas (4 ppb each) was passed through a disposable C_{18} column previously conditioned with methanol (5 ml) and water (5 ml). Adsorbed sulfonylureas were eluted with methanol (5 ml). Excess of solvent was removed in a rotary evaporator. The residue was dissolved in 0.01% $HClO_4$ –methanol (1:1, 100 μ l). An aliquot of this solution was injected into the HPLC system. The whole procedure was done in triplicate.

Table 1
Sulfonylurea yield (%) after duplicate Soxhlet extraction from commercial formulations

Compound	Declared	Found	
		Sample 1	Sample 2
Chlorsulfuron	75	71	73
Metsulfuron	20	24	24
Chlorimuron	Not declared	27	26
Thifensulfuron	Not declared	66	66

2.5. Soil sample fortification

The soil used for the trials was a sandy loam soil (58% sand, 15% silt, 27% clay, 1.3% organic matter, pH 6.5) from Cadriano, Bologna, sieved to 3 mm.

A stock standard solution containing 1 ppm of the four sulfonylureas was obtained by dissolving 10 mg of each compound in 10 l of doubly distilled water. A 500-g amount of soil (on an oven-dry basis) was treated by uniform spraying of 25 ml of the stock standard solution to obtain a final concentration of 50 ppb. The same procedure was effected for the soil samples at 20 and 10 ppb, spraying 10 and 5 ml of the stock standard solution on 500 g of soil (on an oven-dry basis). After the fortification, the soil samples were mixed for 5 min in a blender and frozen at $-20^{\circ}C$.

2.6. Soil extraction

A liquid–liquid and a solid-phase extraction were employed and compared.

Liquid–liquid extraction (in duplicate) of the fortified soil samples was performed according to Zahnow [11]. Briefly, the buffer for extraction was methanol–0.1 M NaOH (1:1, v/v) (pH 11). Purification of extract was performed using methylene chloride. The solvent was discarded and the aqueous phase was adjusted to pH 3–4 by adding 10% HCl dropwise. Again, methylene chloride was added, shaken, separated from the aqueous phase and evaporated to dryness in a Rotavapor at $45^{\circ}C$. A 50-g amount of soil (on an oven-dry basis) for the 50 and 20 ppb levels and 100 g for the 10 ppb level were used. The dry residues after all extraction steps were dissolved in 1 ml of methanol–water (60:40). In this way, an enrichment of 50-fold was obtained for the samples at 50 and 20 ppb and 100-fold for the sample at 10 ppb.

Solid-phase extraction was performed in duplicate according to Dinelli et al. [5]. Briefly, 100 ml of sodium hydrogencarbonate solution (0.1 M, pH 7.8) was added to 50 g of soil (50 and 20 ppb fortifications) and to 100 g of soil for the 10 ppb level. The suspension was shaken for 1 h.

The slurry was centrifuged at 12 000 rpm for 5 min. The extraction procedure was repeated twice and the liquid extracts were combined. The extracts were adjusted to pH 2.5 with 0.1 M HCl and passed through the solid-phase extraction column. The dry residues were reconstituted with 1 ml of methanol–water (60:40), thus obtaining an enrichment of 50-fold for the 50 and 20 ppb samples and 100-fold for the 10 ppb sample.

2.7. High-performance liquid chromatography

The HPLC system was a Beckman (Palo Alto, CA, USA) System Gold 126 with two pumps and a Rheodyne Model 7725-i valve (20- μ l loop). A Beckman Model 168 diode array detector was used.

Reversed-phase C_6 and C_{18} columns were tested using both isocratic and gradient elution modes. The dependence of the capacity factors on the mobile phase composition was checked for both columns. Response and retention time repeatabilities were checked for the C_{18} column, which was used more generally.

The C_6 column was a Viospher (5 μ m, 120 \times 4.6 mm I.D.) (Violet, Rome, Italy). The mobile phase was (A) 0.01% HClO₄ in water and (B) methanol at a flow-rate of 1 ml/min. The A:B ratio was 55:45 (v/v) for isocratic elution (hereafter called “isocratic 1”). For gradient elution, the A:B ratio was varied from 60:40 to 40:60 (v/v) in 20 min, holding the final conditions for 5 min (hereafter called “gradient 1”).

The C_{18} column was a Beckman C_{18} Ultrasphere (25 cm \times 4.6 mm I.D., 5 μ m particle size). Analyses were performed in isocratic and gradient modes. For the first isocratic separation (hereafter called “isocratic 2”) the mobile phase was (A) water (pH 2.5, adjusted phosphoric acid) and (B) methanol in the ratio 60:40 (v/v) at 1 a flow-rate of ml/min. For the second isocratic condition (“isocratic 3”) the mobile phase was the same as above but in ratio 40:60. For the gradient separation, the gradient was performed by maintaining initial conditions at water (pH 2.5, adjusted with 85% phosphoric acid)–methanol (60:40) for 5 min, then increas-

ing the B content linearly to reach a final water:methanol ratio of 30:70, which was maintained for 5 min before resetting. The injections volume was 20 μ l and detection was performed at 224 and 234 nm.

3. Results and discussion

3.1. Reversed-phase C_6 column

This column was tested first because it was expected that the analysis times would be faster than those with C_{18} columns. Actually, separations of standard mixtures of the four sulfonylureas were completed in about 25 min adopting both isocratic 1 and gradient 1 conditions (Fig. 2a and c). Responses (data not shown) were linear in the 0.1–2 ppm range ($R^2 > 0.999$).

The retention time of chlorimuron was much longer than those of the other three compounds. This observation can be explained by considering that its structure bears a chlorine-substituted diazinic ring instead of the relatively more polar methoxy-substituted triazinic ring of the other sulfonylureas, the other features not differing substantially.

Both isocratic and gradient conditions were chosen as the best compromise between rapidity of analysis and separation efficiency. This consideration is better explained in Fig. 3a, in which the capacity factors of the four sulfonylureas are plotted against mobile phase composition. The efficiency of the C_6 column used did not allow the separation of the four sulfonylureas with organic modifier contents in the mobile phase higher than 50%. Under such circumstances, the C_6 column was applied to the analysis of water samples only, as explained in the following section.

3.2. Reversed-phase C_{18} column

As expected, the sulfonylurea retention times were much longer using a C_{18} column, the analysis of the three earlier eluting compounds requiring about 35 min. Under such conditions,

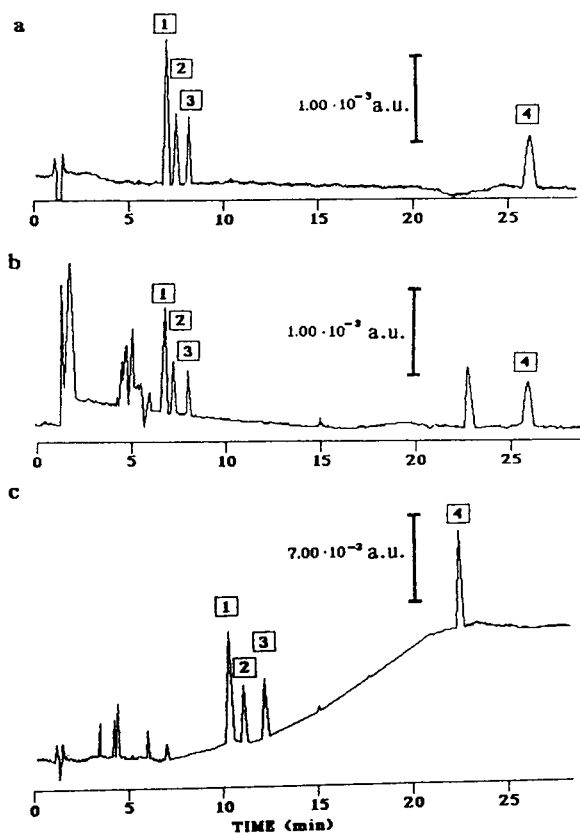


Fig. 2. Separation of sulfonylureas on a C_6 column using isocratic 1 conditions for (a) the standard mixture and (b) a spiked water extract and gradient 1 conditions for (c) the standard mixture. Detection at 234 nm. Peak numbers: compounds as in Fig. 1.

the retention time of chlorimuron was very delayed and useless for practical applications. This problem was overcome by (a) determining chlorimuron separately from the other three molecules and (b) using gradient conditions. Fig. 4a–c shows the separation of sulfonylurea standard mixtures under isocratic and gradient eluting conditions, namely (a) isocratic 2, (b) isocratic 3 and (c) gradient 2.

Isocratic conditions 2 and 3 were those adopted for the determination of sulfonylureas in soil in this work, as discussed in the next section. However, the capacity factors were linear and the compounds were well resolved in a range of mobile phase compositions wider than that with the C_6 column (Fig. 3b), allowing the possibility

of further separations, depending on the sample nature, the sulfonylurea and the interferent concentrations.

Given the more general application of the reversed-phase C_{18} column, the retention time and peak area repeatabilities and response linearity were checked. With regard to retention time repeatability, Table 2 shows the results obtained after ten replicate injections on the same day (intra-day) and during 1 month (inter-day). The retention time fluctuations were within a maximum of 2.8% (R.S.D.) and did not appear much larger in 1 month than in 1 day.

Peak-area variability (Table 3) measured in the same way as above showed R.S.D.s in the range 3.7–8.4%, which did not differ at two detection wavelengths. Finally, the responses of all sulfonylureas were highly linear in the range 0.25–10 ppm injected (Table 4).

3.3. Sample clean-up, sulfonylurea enrichment and analysis

Water, C_6 HPLC column

Table 5 shows the recoveries of sulfonylureas after triplicate solid-phase extractions of aqueous solutions at the 5 ppb level, obtaining a 10^3 -fold enrichment. At such concentrations, i.e., 5 ppm, sulfonylureas were well above the detection limits and typical chromatograms appeared were obtained such as that shown in Fig. 2b, in which the four sulfonylureas are well separated and free from water interferences.

Soil, C_{18} HPLC column

Two different soil clean-ups were tested, one based on liquid–liquid sulfonylurea partitioning and the other on a solid-phase extraction. Sulfonylurea recoveries as determined after duplicate extractions of soil samples spiked in the range 10–50 ppb are given in Tables 6 and 7.

The method based on liquid–liquid partitioning seemed unsatisfactory (Table 6), in that the extraction recoveries were low when the sulfonylurea concentrations in the sample were lower than 50 ppb. The thifensulfuron recoveries were particularly low at all concentrations tested. This observation is consistent with the reported

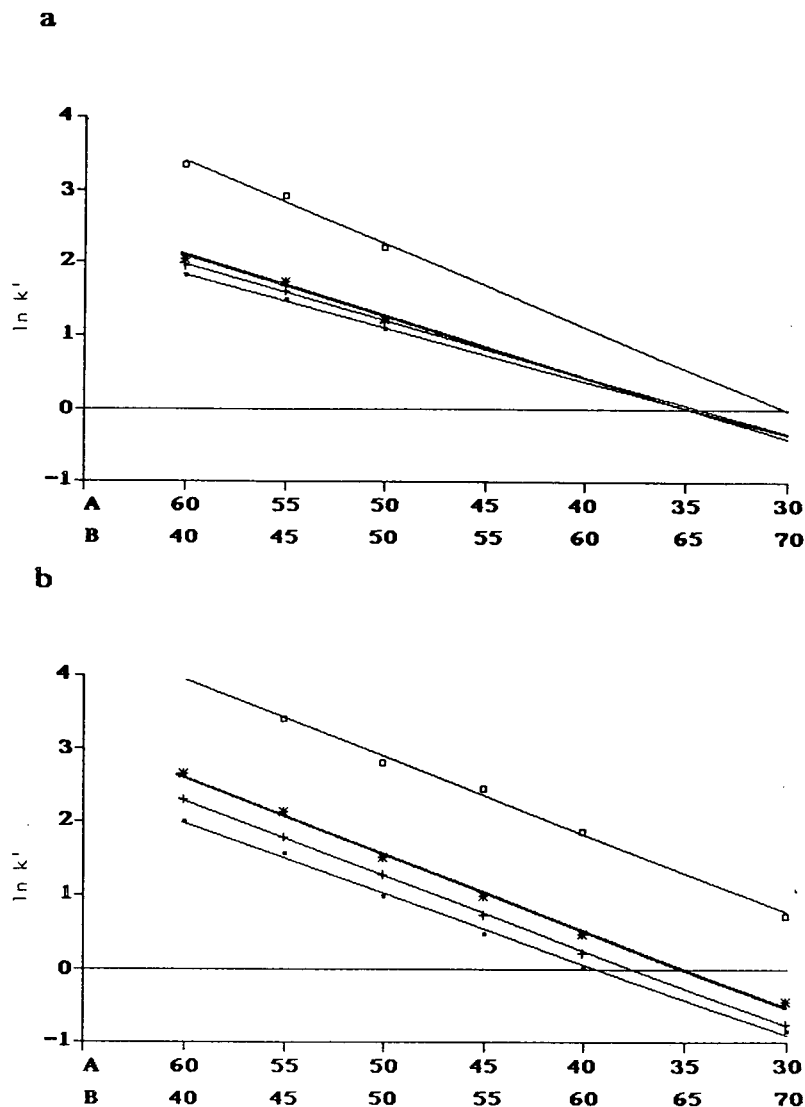


Fig. 3. Dependence of capacity factors on mobile phase composition for (a) C_6 column and (b) C_{18} column. \square = Thifensulfuron; * = metsulfuron; + = chlorsulfuron; \blacksquare = chlorimuron.

relatively labile nature of thifensulfuron compared with the other three molecules and with the very fast degradation of sulfonylureas at low and high pH in aqueous systems [12–15].

Solid-phase extraction (Table 7), more rapid than the previous one, improved the recovery of thifensulfuron, owing to the milder pH conditions. The recoveries of all sulfonylureas did not seem to be affected by sample concentration.

Fig. 5 shows the separations under isocratic 2 and 3 conditions of sulfonylureas from soils spiked at 10 ppb levels after solid-phase extraction and 100-fold enrichment. The early-eluting and large soil interferences corroborate the previous statement about the need to use a C_{18} instead of a C_6 column, in order to separate sulfonylureas properly from interferences. While gradient elution was effective in separating all

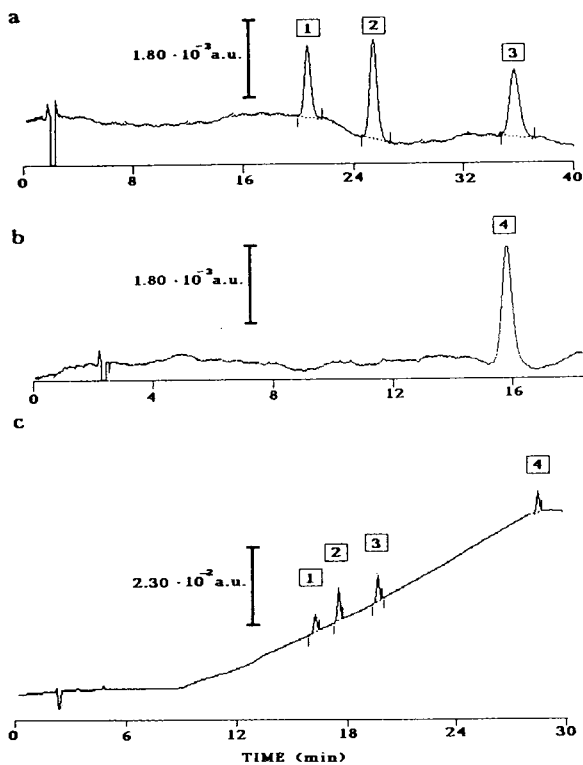


Fig. 4. Separation of standard sulfonylureas on a C_{18} column using various elution conditions: (a) isocratic 2, (b) isocratic 3 and (c) gradient 2. Detection at 234 nm. Peak numbers: compounds as in Fig. 1.

sulfonylureas in about 30 min (Fig. 4c), some soil interferences co-eluted with peaks of thifensulfuron and metsulfuron, suggesting that the use of two isocratic conditions was safer. In fact, the

high correlation coefficients between the UV spectra scanned over the sulfonylurea peaks from soil and standard mixtures (lower and upper curve, respectively, in Fig. 6) suggest that little if any interference was from the soil matrix.

3.4. Method sensitivity

Table 8 compares the minimum concentrations at which sulfonylureas were detected in this work with the detection limits reported by other workers in different substrates and using different chromatographic techniques. The orders of magnitude only are reported for such detection limits, given the variable concept of definition of detection limit used by different workers.

The overall method sensitivity appears to be governed by essentially two factors: (i) sensitivity inherent to the analytical technique and (ii) enrichment coefficient applicable to a particular substrate.

Concerning sensitivity, a final concentration of 1–5 ppm is the lower limit for solutions to be analyzed by gas chromatography and HPLC with UV detection. Such techniques are therefore substantially equivalent to this respect. A tenfold improvement to 0.1 ppm (order of magnitude) can be achieved by capillary electrophoresis and by HPLC with photoconductivity detection. Detection limits of 0.01 ppm have been reported for the latter after accurate optimization of the chromatographic conditions.

Concerning sample effects, limits may differ

Table 2

Intra-day and inter-day retention time (t_R) and repeatability [standard deviation (in parentheses) and relative standard deviation (R.S.D.)]

Compound	Intra-day		Inter-day	
	t_R (min)	R.S.D. (%)	t_R (min)	R.S.D. (%)
Thifensulfuron ^a	21.3 (0.4)	1.9	21.0 (0.5)	2.5
Metsulfuron ^a	25.4 (1.1)	2.1	24.9 (0.7)	2.7
Chlorsulfuron ^a	35.7 (0.8)	2.2	35.5 (1.0)	2.8
Chlorimuron ^b	16.5 (0.3)	1.6	16.3 (0.3)	2.0

Average of ten injections of 1 ppm sulfonylurea solutions on the same day (intra-day) and on ten different days during 1 month (inter-day). Detection at 234 nm.

^a Analysis according to isocratic 2 conditions.

^b Separate analysis to the other three compounds, according to isocratic 3 conditions.

Table 3

Intra-day and inter-day peak area (arbitrary units) and repeatability [standard deviation (in parentheses) and R.S.D.]

Compound	Detection wavelength (nm)	Intra-day		Inter-day	
		Area	R.S.D. (%)	Area	R.S.D. (%)
Thifensulfuron ^a	234	0.58 (0.03)	4.7	0.59 (0.04)	6.1
	224	0.93 (0.04)	4.6	0.96 (0.06)	6.5
Metsulfuron ^a	234	1.11 (0.04)	3.7	1.06 (0.04)	3.8
	224	1.59 (0.06)	3.7	1.48 (0.07)	4.5
Chlorsulfuron ^a	234	0.75 (0.05)	6.1	0.75 (0.06)	8.4
	224	1.12 (0.07)	6.1	1.13 (0.09)	7.9
Chlorimuron ^b	234	1.15 (0.04)	3.7	1.14 (0.06)	5.5
	224	0.95 (0.04)	3.9	0.94 (0.05)	5.6

Average of ten injections of 1 ppm sulfonylurea solutions on the same day (intra-day) and on ten different days during 1 month (inter-day). Detection at 234 and 224 nm.

^{a,b} See Table 2.

Table 4

Calibration graphs for the four sulfonylureas in the range 0.25–10 ppm [injected solutions 0.25, 0.5, 1, 2, 4, 5 and 10 ppm; y = ppm; x = area (arbitrary units)]

Compound	Detection at 224 nm		Detection at 234 nm	
	y	R^2	y	R^2
Thifensulfuron ^a	$1.027x + 0.045$	0.991	$1.750x - 0.062$	0.990
Metsulfuron ^a	$0.671x + 0.057$	0.999	$1.010x - 0.058$	0.999
Chlorsulfuron ^a	$0.795x - 0.138$	0.999	$1.221x - 0.068$	0.999
Chlorimuron ^b	$1.094x - 0.056$	0.994	$0.947x - 0.069$	0.997

^{a,b} See Table 2.

by up to a factor of 10^3 depending on (i) whether the sample extracts can be concentrated without the risk of concentrating impurities that may

Table 5

Sulfonylurea recoveries with standard deviations (in parentheses) after triplicate solid-phase extraction from a water sample at 5 ppb

Compound	Recovery (%)
Chlorsulfuron	84.0 (4.5)
Metsulfuron	82.0 (4.2)
Chlorimuron	90.0 (3.8)
Thifensulfuron	90.0 (8.5)

interfere with the analytes and (ii) which sample size is easier to manipulate. Water samples in the litre range can be enriched by a factor 10^3 – 10^4 , whereas enrichments of 10–50-fold are more common for 10–100-g samples of soil and plant materials. Gas chromatography allows enrichments from soil extracts of 10^3 -fold, possibly owing to the “filter effect” of both derivatization and volatility. Consequently, while the determination of sulfonylureas at sub-ppb levels in water is relatively straightforward, soil samples are more commonly analysed in the 1–10 ppb range.

In conclusion, detection limits of 1 ppb and even 0.2 ppb have been reported but, as stated by Beyer et al. [13], “conducting routine analysis at these levels is very difficult”.

Table 6

Sulfonylurea recoveries with standard deviations (in parentheses) after duplicate liquid–liquid extraction from soil samples at different herbicide concentrations (detection at 224 nm)

Concentration (ppb)	Recovery (%)			
	Thifensulfuron	Metsulfuron	Chlorsulfuron	Chlorimuron
50	56.4 (6.6)	94.5 (6.5)	95.5 (1.3)	87.4 (3.1)
20	40.6 (4.4)	65.2 (4.9)	64.4 (1.5)	60.1 (3.4)
10	41.7 (3.5)	47.0 (4.0)	70.6 (16.4)	63.4 (4.9)

Table 7

Sulfonylurea recoveries with standard deviations (in parentheses) after duplicate solid-phase extraction from soil samples at different herbicide concentrations (detection at 224 nm)

Concentration (ppb)	Recovery (%)			
	Thifensulfuron	Metsulfuron	Chlorsulfuron	Chlorimuron
50	75.8 (8.4)	90.4 (0.5)	91.3 (5.7)	97.3 (11.1)
20	83.4 (3.3)	108.4 (1.2)	91.9 (20.8)	75.8 (2.4)
10	71.1 (1.5)	95.6 (3.4)	88.4 (7.6)	97.8 (4.6)

4. Conclusions

Sulfonylurea application rates of 10–100 g ha⁻¹ correspond to initial nominal soil concentrations of 0.1–1 ppm. Sulfonylurea concentrations of 10–50 ppb in soil and above 1 ppb in

water were adopted in this work as more suitable limits for setting up a rapid, simple and routine method to screen several sulfonylureas in tests about their degradation rate in soil, where the expected residue levels will be above the detection limit. Although no attempt was made to lower the detection limits reported in the literature, improved recovery of sulfonylureas from soil was demonstrated with solid-phase extraction, and isocratic HPLC with diode-array detection performed satisfactorily for our intended purposes. We believe we have demonstrated the validity of solid-phase extraction and the applicability of various HPLC conditions to the determination of four sulfonylureas.

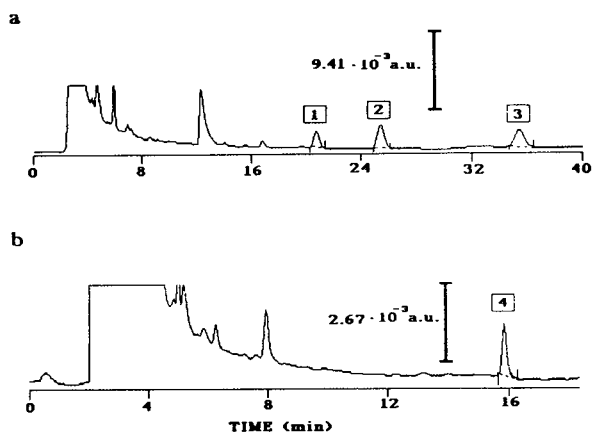


Fig. 5. Separation of sulfonylureas from a soil spiked at 10 ppb using (a) isocratic 2 and (b) isocratic 3 conditions and a C₁₈ column. Peak numbers: compounds in Fig. 1.

Acknowledgement

This work was financed by the European Economic Community within the project “Application and Evaluation of a New Method for the Monitoring of Pesticide Pollution in Water”, contract AIR3-ST92-002.

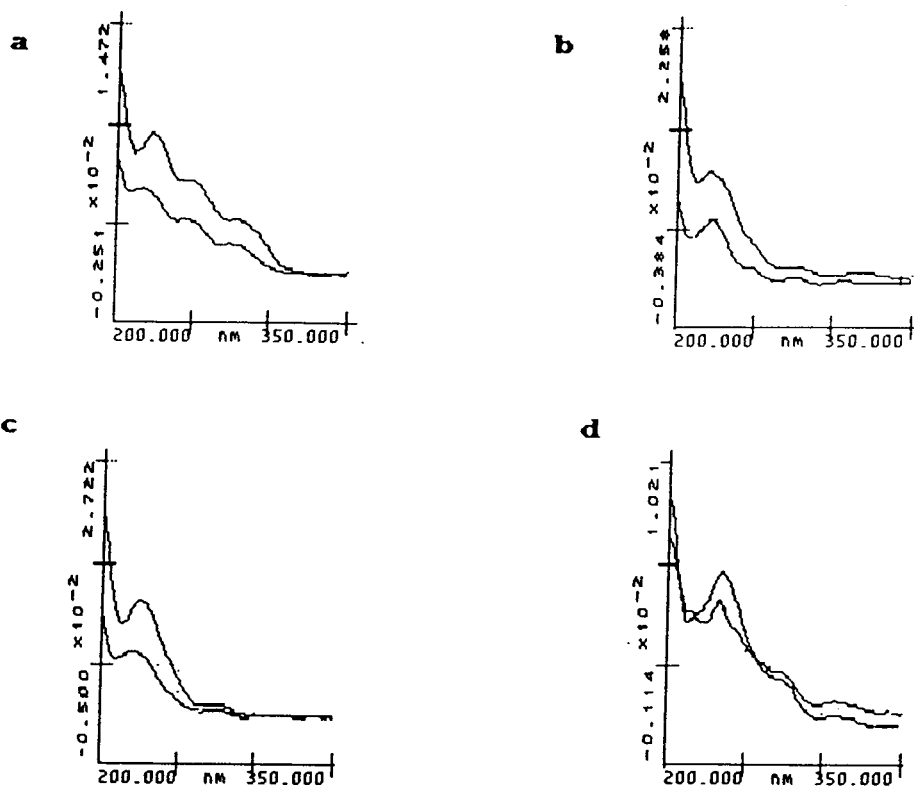


Fig. 6. UV spectral scans for (a) thifensulfuron, (b) metsulfuron, (c) chlorsulfuron and (d) chlorimuron. Upper curves, standard; lower curves, soil extract.

Table 8

Selected examples of minimum sulfonylurea concentrations (order of magnitude) as reported in literature compared with the levels used in this work

Sample	Sample amount	Initial concentration (ppb)	Enrichment factor	Final concentration (ppm)	Analytical method ^a	Ref.
Water	1 l	0.1	10 ⁴	1	CE-UV	[5]
Water	1 l	0.1	10 ⁴	1	GC-ECD	[4]
Water	100 ml	5	10 ³	5	HPLC-UV	This work
Soil	50 g	0.2	50	0.01	HPLC-PID	[7]
Soil	100 g	1	10 ³	1	GC-ECD	[4]
Soil	100 g	10	100	1	HPLC-UV	This work
Soil	50 g	50	50	2.5	HPLC-UV	[16]
Plant	10 g	10	10	0.1	HPLC-PID	[17]

^aCE-UV = capillary electrophoresis with ultraviolet detection; GC-ECD = gas chromatography with electron-capture detection; HPLC-UV = high-performance liquid chromatography with ultraviolet detection; HPLC-PID = high-performance liquid chromatography with photoionization detection.

References

- [1] S.L. Sunderland, P.W. Santelmann and T.A. Baughmann, *Weed Sci.*, 39 (1991) 296.
- [2] M. Nord-Christerson and L. Bergstrom, in *Proceedings of Brighton Crop Protection Conference on Weeds*, Vol. 3, The British Crop Protection Council, Surrey, 1989, p. 1127.
- [3] P. Klaffenbach, P.T. Holland and D.R. Lauren, *J. Agric. Food Chem.*, 41 (1993) 388.
- [4] P. Klaffenbach and P.T. Holland, *J. Agric. Food Chem.*, 41 (1993) 396.
- [5] G. Dinelli, A. Vicari and P. Catizone, *J. Agric. Food Chem.*, 41 (1993) 742.
- [6] D. Molins, C.K. Wong, D.M. Cohen and K.P. Munnelly, *J. Pharm. Sci.*, 64 (1975) 123.
- [7] E.W. Zahnaw, *J. Agric. Food Chem.*, 33 (1985) 479.
- [8] D.J. Popovich, J.B. Nixon and B.J. Ehrlich, *J. Chromatogr. Sci.*, 17 (1979) 643.
- [9] P. Ciccioioli, R. Tappa and A. Guiducci, *Anal. Chem.*, 53 (1981) 1309.
- [10] D.C. Locke, B.S. Dhingra and A.D. Baker, *Anal. Chem.* 54 (1982) 447.
- [11] E.C. Zahnaw, *J. Agric. Food Chem.*, 30 (1982) 854.
- [12] J. Sabadie, *Weed Res.*, 30 (1990) 413.
- [13] E.M. Beyer, M.J. Duffy, J.V. Hay, D.D. Schluter, in P.C. Kearney and D.D. Kaufmann (Editors), *Herbicides: Chemistry, Degradation, and Mode of Action*, Vol. 3, Marcel Dekker, New York, pp. 117–189.
- [14] G. Dinelli, A. Vicari, A. Bonetti, P. Catizone, in A.M. Del Re, E. Capri, S.P. Evans, P. Natali and M. Trevisan (Editors), *Proceedings of the IX Symposium on Pesticide Chemistry, Degradation and Mobility of Xenobiotics, Piacenza, 11–13 October 1993*, Edizioni Biagini, Lucca, 1994, pp. 411–420.
- [15] C. Smith, *Sulfonylurea Herbicides*, PJB Publications, Richmond, Surrey, 1991.
- [16] M. Businelli, C. Marucchini, P. Patumi and P.L. Giusquiani, in *Current Perspective in Environmental Biogeochemistry*, INPRA–CNR, 1987, pp. 47–56.
- [17] J.L. Prince and R.A. Guinivan, *J. Agric. Food Chem.*, 36 (1988) 63.

Liquid chromatographic determination of the mycotoxin fumonisin B₂ in physiological samples

G.S. Shephard*, P.G. Thiel, E.W. Sydenham

Programme on Mycotoxins and Experimental Carcinogenesis, Medical Research Council, P.O. Box 19070, Tygerberg 7505, South Africa

Abstract

The fungus *Fusarium moniliforme* produces a group of mycotoxins, the fumonisins, of which the most abundant are fumonisins B₁ (FB₁) and B₂ (FB₂). Previously developed analytical methods for the determination of FB₁ in physiological samples have been modified for the determination of FB₂ by the use of less polar extraction solvents. Plasma and urine extracts were purified on strong anion-exchange solid-phase extraction cartridges and fecal extracts on reversed-phase (C₁₈) cartridges. FB₂ in purified extracts was determined by reversed-phase HPLC with fluorescence detection using preformed *o*-phthalaldehyde derivatives. These methods were reproducible (R.S.D. of less than 6%) with recoveries greater than 85%. In a short preliminary study, they have been applied to the determination of the fate of FB₂ dosed to rats by gavage. Of the dose given to the animals, over 90% was recovered unmetabolised in the feces within 48 h.

1. Introduction

The fumonisin mycotoxins are a group of structurally related secondary metabolites produced by the fungus *Fusarium moniliforme* Sheldon, a common contaminant of corn worldwide [1]. Of the fumonisins currently identified, fumonisin B₁ (FB₁) and fumonisin B₂ (FB₂) are the major compounds produced in culture and found in contaminated feed and foodstuffs [2,3]. Both toxins are diesters of propane-1,2,3-tricarboxylic acid and similar long-chain polyhydroxyamines [1] (Fig. 1).

FB₁ has been shown to cause equine leukoencephalomalacia [4] and porcine pulmonary edema [5]. It is also hepatocarcinogenic and

hepatotoxic in rats [1,6] and has been statistically associated with an increased risk of esophageal cancer in man [7]. As FB₂ is generally found at significant levels together with FB₁ in contaminated food [3,8], and since it possesses similar cancer initiating and cytotoxic properties to FB₁

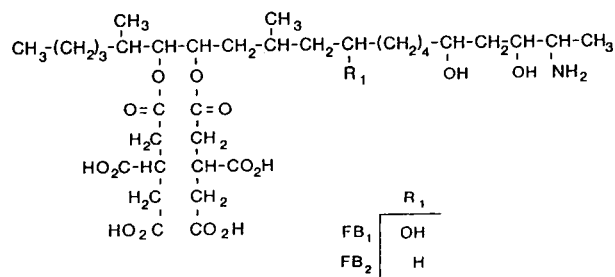


Fig. 1. Structures of fumonisin B₁ (FB₁) and fumonisin B₂ (FB₂).

* Corresponding author.

[9], it may also be expected to have importance to human health. Toxicokinetic studies have been undertaken with FB₁ in laboratory animals [10–15]. In order to extend these studies to FB₂, analytical methods, developed for FB₁ [14,16], have been modified and validated for the determination of FB₂ in plasma, urine and feces. This paper reports the development and validation of these methods and their application to a short preliminary study on the excretion of FB₂ by experimental rats.

2. Experimental

2.1. Reagents

Bond-Elut strong anion-exchange (SAX) and reversed-phase (C₁₈) solid-phase extraction cartridges (3 ml capacity containing 500 mg sorbent) were purchased from Varian (Harbor City, CA, USA). FB₂ was isolated from *F. moniliforme* MRC 826 cultures [17]. ¹⁴C-labelled FB₂ (¹⁴C]FB₂; 64 μCi mmol⁻¹) was prepared by spiking a growing corn culture of *F. moniliforme* MRC 826 with L-[methyl-¹⁴C]methionine (> 50 mCi mmol⁻¹; Amersham, UK) [18]. The radiochemical purity of the [¹⁴C]FB₂ was assessed by TLC [17]. The FB₂ spot on the TLC plate contained 92% of the applied radioactivity. All other reagents and solvents were analytical grade from Merck (Darmstadt, Germany).

2.2. Sample collection

Physiological samples (blood, urine and feces) were obtained from rats and monkeys bred in the animal unit of the Medical Research Council (Tygerberg, South Africa). Blood samples were collected in tubes containing tripotassium EDTA as anticoagulant. Plasma was obtained by centrifugation at 1200 g for 10 min at 4°C. In a short preliminary study on the excretion of [¹⁴C]FB₂ by rats, two male Wistar rats (approximately 100 g body mass) were each dosed by gavage with 0.12 mg FB₂ in a water solution and confined in

a single metabolic cage for the collection of urine and feces daily over a 2-day period.

Samples for method development were obtained by spiking plasma, urine, and fecal extracts with FB₂ standard to a level of between 3 and 5 μg ml⁻¹. Fecal samples obtained from the preliminary study on excretion were used to investigate the extraction of FB₂ from rat feces. The radioactivity present in samples was determined by liquid scintillation counting after solubilization [14].

2.3. Determination of FB₂ in plasma

A 500-μl aliquot of plasma was diluted with 1 ml of water and deproteinised with 1.5 ml of acetonitrile. After centrifugation at 1200 g for 10 min at 10°C, a 2-ml aliquot of the supernatant was purified on a SAX cartridge which had been conditioned with 5 ml of acetonitrile and 5 ml of acetonitrile–water (1:1, v/v). The sorbent was immediately washed with 5 ml of acetonitrile–water (1:1, v/v) and 5 ml of methanol. FB₂ was eluted with 10 ml of 5% acetic acid in methanol. The flow-rate through the cartridge was maintained at around 1–1.5 ml min⁻¹. The eluate was dried under a stream of nitrogen at 60°C and the residue was redissolved in 200 μl of 0.1 M sodium borate prior to derivatization and HPLC analysis.

2.4. Determination of FB₂ in urine

A 250-μl aliquot of rat urine was diluted with 750 μl of water and 3 ml of methanol. This diluted sample was purified on a SAX cartridge, conditioned with 5 ml of methanol and 5 ml of methanol–water (3:1, v/v). After washing the sorbent with 5 ml of methanol–water (3:1, v/v) and 5 ml of methanol, the FB₂ was eluted and dried as described above for plasma extracts. The residue was dissolved in 200 μl of methanol prior to HPLC analysis.

2.5. Determination of FB₂ in feces

Feces were freeze-dried after collection and then ground to a powder. A subsample (1.5–2.5

g) was extracted by vortexing for 1 min in a capped tube with 15 ml 0.1 M EDTA (pH 5.2)–methanol (4:1, v/v). The mixture was centrifuged at 2000 g for 10 min at 4°C, the supernatant removed and the extraction repeated a further 9 times. The supernatants were combined, centrifuged at 4000 g for 10 min. and then an aliquot was acidified with 5 M hydrochloric acid to pH 3.1–3.2. Immediately thereafter a 3-ml aliquot was applied to a Bond-Elut C₁₈ cartridge which had been conditioned with 5 ml of methanol and 5 ml of water. The sorbent was washed with 5 ml of water, 5 ml of methanol–water (1:3, v/v) and 3 ml of methanol–water (1:1, v/v). FB₂ was eluted with 15 ml of methanol and the solvent evaporated under a stream of nitrogen at 60°C. The residue was dissolved in 0.5 ml of methanol prior to HPLC analysis.

2.6. Chromatographic analysis

FB₂ in the purified extracts was quantified by HPLC of preformed *o*-phthaldialdehyde (OPA) derivatives on a Phenomenex (Rancho Palos Verdes, CA, USA) C₁₈ reversed-phase IB-SIL column (50 × 4.6 mm I.D.) packed with material of 3 μm particle size and eluted at 1 ml min⁻¹ with methanol–0.1 M sodium dihydrogenphosphate (72:28, v/v) adjusted to pH 3.4 with orthophosphoric acid. The remainder of the HPLC system and the preparation of OPA derivatives were as previously described [16].

3. Results and discussion

The analytical methods described here for the determination of FB₂ in physiological samples were developed by modification of previously published methodology for FB₁ [14,16]. Since FB₂ is less polar than FB₁, consideration was given to the use of less polar extraction solvents. In the extraction of FB₂ from plasma, use of methanol for deproteinisation resulted in recoveries of 80.4% ± 4.5% R.S.D. (*n* = 5). Substitution of acetonitrile for methanol resulted in an increase in recovery to 90.3% ± 2.5% R.S.D. (*n* = 8) at the 4.3 μg ml⁻¹ level. Six replicate

analyses of a single sample of plasma gave precision of 2.1% R.S.D. at this level.

The analytical method developed for the determination of FB₁ in urine was found to be equally valid for FB₂. Analytical recovery of FB₂ was 101.5% ± 2.2% R.S.D. (*n* = 6) at the 5.0 μg ml⁻¹ level and replicate analyses of a single urine sample gave a precision of 2.9% R.S.D. (*n* = 6).

It has previously been shown that FB₁ is strongly retained within the fecal matrix of rats and, to a lesser extent, also of monkeys [14]. Similarly, FB₂ was found to be strongly bound within this matrix and repeated extractions were required to achieve adequate analytical recovery of the toxin. Methanol was again inadequate as an extraction solvent. The efficiency of 0.1 M EDTA (pH 5.2), previously used for fecal extractions, was slightly improved by the addition of 20% methanol, although nine extractions were required to achieve extraction efficiencies greater than 90% (Fig. 2). The fecal extracts were combined and the pH was adjusted to 3.2 prior to clean-up on C₁₈ solid-phase extraction cartridges. At pH values below 3.1 considerable precipitation of EDTA occurred and the recovery of FB₂ was deleteriously affected. Analytical recovery from the fecal extract deter-

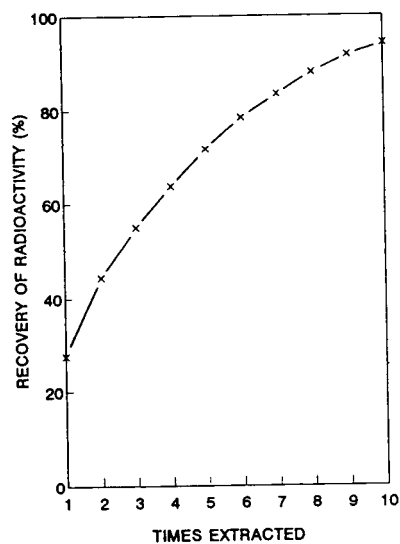


Fig. 2. Cumulative extraction recovery of [¹⁴C]FB₂ from rat feces as a percentage of the radioactivity in the sample.

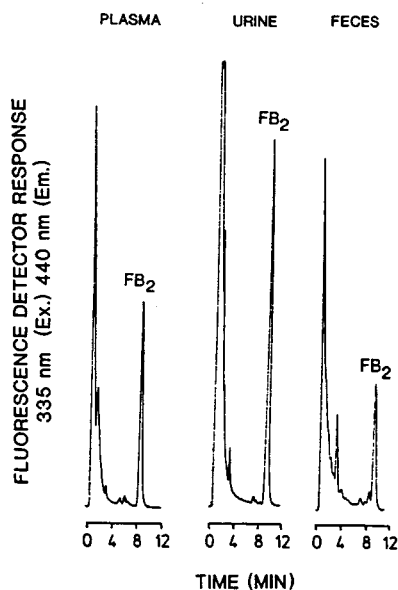


Fig. 3. Chromatograms of OPA-derivatised plasma, urine and fecal samples. The amount of FB_2 injected ranged from 20 to 45 ng.

mined at the $3.1 \mu\text{g ml}^{-1}$ level was $86.4\% \pm 4.6\%$ R.S.D. ($n=6$) and the precision of FB_2 determination from a single extract was 4.6% R.S.D. ($n=6$).

Fig. 3 shows chromatograms obtained from each of the three physiological samples. In all analyses, FB_2 was separated from other com-

ponents which mainly elute near the front-end of the chromatogram. The absence of co-eluting impurities was demonstrated in all cases by analysis of blank samples.

Table 1 shows the results of a preliminary study of excretion of $[^{14}\text{C}]\text{FB}_2$ by two rats dosed by gavage. Most of the dosed toxin was recovered unmetabolised in a 48-h period, mainly from the feces with trace amounts in urine. The levels of FB_2 were corrected for extraction and analytical recoveries and show a close correspondence to the radioactivity levels determined in the samples.

The methods reported here for the determination of FB_2 have been shown to be reproducible with good recoveries. As in the case of FB_1 , FB_2 was strongly retained in feces and required multiple extraction steps to achieve acceptable recoveries. The preliminary study of the excretion of FB_2 by rats has indicated that the methods described here will yield further insights into the toxicokinetics of the fumonisins in experimental animals.

Acknowledgements

The authors wish to thank J.V. Seier, P.W. De Lange and H.J.B. Joubert for technical assistance in the handling of laboratory animals.

Table 1
Excretion of $[^{14}\text{C}]\text{FB}_2$ by rats

Day	Urine		Feces	
	FB_2^a (% of dose)	$^{14}\text{C}^b$ (% of dose)	FB_2^a (% of dose)	$^{14}\text{C}^b$ (% of dose)
1	0.2	0.7	72.9 ^c	68.4
2	<0.1	0.3	23.1 ^c	30.5
Total	0.2	1.0	96.0	98.9

^a Determined by HPLC.

^b Determined by liquid scintillation counting.

^c Corrected for extraction and analytical recovery.

References

- [1] W.C.A. Gelderblom, K. Jaskiewicz, W.F.O. Marasas, P.G. Thiel, R.M. Horak, R. Vleggaar and N.P.J. Kriek, *Appl. Environ. Microbiol.*, 54 (1988) 1806.
- [2] P.G. Thiel, W.F.O. Marasas, E.W. Sydenham, G.S. Shephard, W.C.A. Gelderblom and J.J. Nieuwenhuis, *Appl. Environ. Microbiol.*, 57 (1991) 1089.
- [3] E.W. Sydenham, G.S. Shephard, P.G. Thiel, W.F.O. Marasas and S. Stockenström, *J. Agric. Food Chem.*, 39 (1991) 2014.
- [4] T.S. Kellerman, W.F.O. Marasas, P.G. Thiel, W.C.A. Gelderblom, M. Cawood and J.A.W. Coetzer, *Onderstepoort J. Vet. Res.*, 57 (1990) 269.
- [5] L.R. Harrison, B.M. Colvin, J.T. Greene, L.E. Newman and J.R. Cole, *J. Vet. Diagn. Invest.*, 2 (1990) 217.
- [6] W.C.A. Gelderblom, N.P.J. Kriek, W.F.O. Marasas and P.G. Thiel, *Carcinogenesis*, 12 (1991) 1247.
- [7] E.W. Sydenham, P.G. Thiel, W.F.O. Marasas, G.S. Shephard, D.J. Van Schalkwyk and K.R. Koch, *J. Agric. Food Chem.*, 38 (1990) 1900.
- [8] P.F. Ross, L.G. Rice, G.D. Osweiler, P.E. Nelson, J.L. Richard and T.M. Wilson, *Mycopathologia*, 117 (1992) 109.
- [9] W.C.A. Gelderblom, M.E. Cawood, S.D. Snyman, R. Vleggaar and W.F.O. Marasas, *Food Chem. Toxicol.*, 31 (1993) 407.
- [10] G.S. Shephard, P.G. Thiel and E.W. Sydenham, *Food Chem. Toxicol.*, 30 (1992) 277.
- [11] G.S. Shephard, P.G. Thiel, E.W. Sydenham, J.F. Alberts and W.C.A. Gelderblom, *Toxicon*, 30 (1992) 768.
- [12] G.S. Shephard, P.G. Thiel, E.W. Sydenham and J.F. Alberts, *Food Chem. Toxicol.*, 32 (1994) 489.
- [13] W.P. Norred, R.D. Plattner and W.J. Chamberlain, *Nat. Toxins*, 1 (1993) 341.
- [14] G.S. Shephard, P.G. Thiel, E.W. Sydenham, R. Vleggaar and J.F. Alberts, *Food Chem. Toxicol.*, 32 (1994) 23.
- [15] G.S. Shephard, P.G. Thiel, E.W. Sydenham, J.F. Alberts and M.E. Cawood, *Toxicon*, in press.
- [16] G.S. Shephard, P.G. Thiel and E.W. Sydenham, *J. Chromatogr.*, 574 (1992) 299.
- [17] M.E. Cawood, W.C.A. Gelderblom, R. Vleggaar, Y. Behrend, P.G. Thiel and W.F.O. Marasas, *J. Agric. Food Chem.*, 39 (1991) 1958.
- [18] J.F. Alberts, W.C.A. Gelderblom, R. Vleggaar, W.F.O. Marasas and J.P. Rheeder, *Appl. Environ. Microbiol.*, 59 (1993) 2673.

Determination of L-735 524, an human immunodeficiency virus protease inhibitor, in human plasma and urine via high-performance liquid chromatography with column switching

E. Woolf*, T. Au, H. Haddix, B. Matuszewski

Merck Research Laboratories, Department of Drug Metabolism, West Point, PA 19486, USA

Abstract

A method for the determination of an HIV protease inhibitor, L-735 524, in human plasma and urine is described. Isolation of the analyte and the internal standard from the matrices was achieved via multiple liquid–liquid extractions with methyl *tert.*-butyl ether. The analyte lacks significant UV absorption at wavelengths greater than 220 nm, hence a column switching system using a cyano and C₁₈ column was used to further purify the extracts prior to UV detection at 210 nm. The assay has been found to be linear and has been validated over the concentration range of 5 to 500 ng/ml, when 1-ml aliquots of plasma or urine were extracted. The assay has been utilized to support human pharmacokinetic studies.

1. Introduction

Compound I, N-[2(R)-hydroxy-1(S)-indanyl]-5-[[[2(S)-*tert.*-butylaminocarbonyl]-4-(3-pyridylmethyl)piperazino]-4(S)-hydroxy-2(R)-phenylmethyl-pentanamide (L-735 524, Fig. 1) is

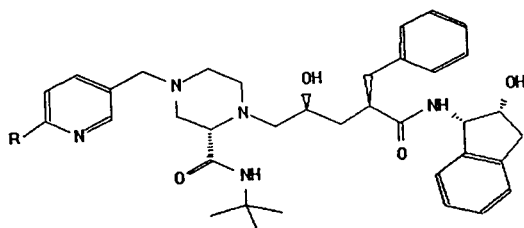


Fig. 1. Chemical structures of compound I (L-735 524) (R = H) and internal standard II (R = CH₃).

* Corresponding author.

a potent and specific *in vitro* inhibitor of the human immunodeficiency virus Type 1 (HIV-1)-encoded protease [1–3]. HIV has been identified as the causative agent of acquired immune deficiency syndrome (AIDS) [4–7]. HIV-1 protease is utilized during the viral replication cycle to cleave a polyprotein into individual functional proteins, and thus transform the virus into an infectious form [8–10]. Inhibition of HIV-1 protease *in vivo* would be expected to prevent virus maturation, and therefore might be effective in the treatment of HIV-infected individuals [11,12]. An assay to determine the plasma and urine concentrations of I after oral dosing was needed to support human pharmacokinetic, safety and tolerability clinical studies. The development of a high-performance liquid chromatographic (HPLC) method using column switching [13,14] for the quantitation of I in plasma and urine is the subject of this paper.

2. Experimental

2.1. Materials

Compound I was obtained from the chemical data department of Merck Research Labs. (Rahway, NJ, USA). Compound II (Fig. 1), the internal standard, was prepared in the Medicinal Chemistry Department of Merck Research Labs. (West Point, PA, USA). Acetonitrile and methyl *tert.*-butyl ether (MTBE) (Omnisolve HPLC grade) were from EM Science (Gibbstown, NJ, USA). Drug-free human plasma was purchased from Sera-Tech Biologicals (New Brunswick, NJ, USA). Control urine was provided by volunteers in the Department of Drug Metabolism of Merck Research Labs.

2.2. Instrumentation

The HPLC system (Fig. 2) consisted of a Perkin-Elmer (Norwalk, CT, USA) Model 410 pump (pump 1, P₁), a Perkin-Elmer Model 250 pump (pump 2, P₂), a Waters (Milford, MA, USA) WISP 715 automatic injector, a Valco (Houston, TX, USA) ten-port electrically actuated valve, and an Applied Biosystems (Foster City, CA, USA) 785 absorbance detector. The valve was controlled from the "timed events" output of pump 1. The analog output from the detector was connected to a PE-Nelson (Cupertino, CA, USA) Access-Chrom data system via a PE-Nelson 941 analog-to-digital interface.

2.3. Chromatographic conditions

The mobile phase for pump 1 consisted of a mixture of acetonitrile–water (34:66, v/v). The mobile phase for pump 2 was a mixture of acetonitrile–water (38:62, v/v). Each mobile phase was made 10 mM in orthophosphoric acid by the addition of 690 μ l of 85% orthophosphoric acid per liter of mobile phase. The pH (apparent) of each of the mobile phases was adjusted to 7.5 with 10 M sodium hydroxide. The mobile phases were filtered through a nylon

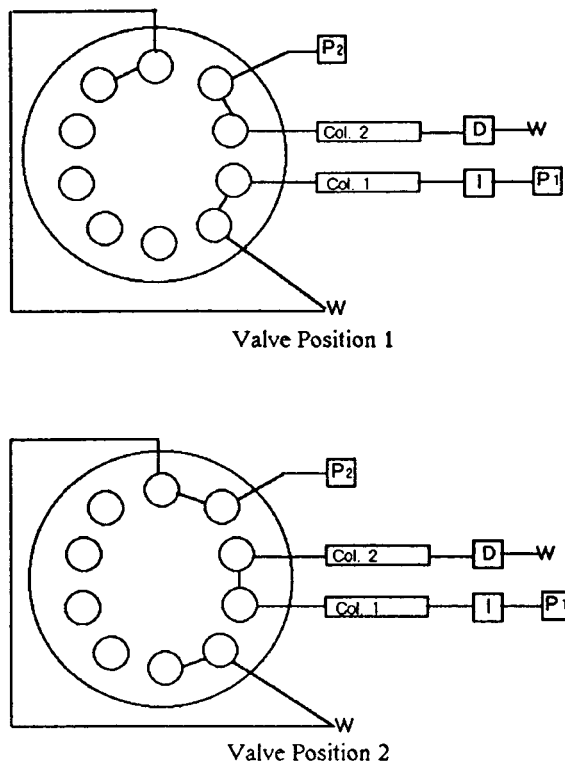


Fig. 2. Block diagram of HPLC column-switching system. I = Injector; P = pump; Col. = column; D = detector; W = waste.

filter (0.20 μ m) prior to use. Each mobile phase was delivered at a flow-rate of 1.2 ml/min.

Column 1 (Fig. 2) was a Zorbax SB-CN (5- μ m particles with a pore diameter of 80 \AA) cartridge column (80 \times 4 mm) from Mac-Mod Analytical (Chadds Ford, PA, USA). Column 2 (Fig. 2) was an Inertsil ODS-2 (5- μ m particles with a pore diameter of 150 \AA) column (150 \times 4.6 mm) packed by Keystone Scientific (State College, PA, USA). Column 1 was replaced after 150–200 injections, while the lifetime of column 2 was greater than 750 injections. The columns were used at ambient temperature (approximately 22°C).

The sample injection volume was 125 μ l. Ultraviolet absorbance at 210 nm was used for detection.

2.4. Switching valve programming

The times at which the events on pump 1 were set to trigger the valve were determined daily using the following procedure. The valve was placed in position 2, as shown in Fig. 2. A piece of 0.007-in. I.D. tubing (1 in. = 2.54 cm) was connected in place of column 2.

A “window check” sample was prepared by pipetting 50 μl of a 10 $\mu\text{g}/\text{ml}$ solution of **I** in acetonitrile and 25 μl of a 10 $\mu\text{g}/\text{ml}$ solution of **II** in acetonitrile into a disposable glass culture tube, evaporating the solvent under a stream of nitrogen and reconstituting the residue in 200 μl of pump 1 mobile phase.

A 125- μl volume of the “window check” sample was then injected into the modified system. The time, t_1 , at which the compound **I** peak began to elute (approximately 3.8 min), and the time, t_2 , at which the compound **II** peak returned to baseline (approximately 5.2 min) were determined. The timed events were then set to place the valve in position 1 at the beginning of the run, switch the valve to position 2 at t_1 , and return the valve to position 1 at t_2 . Following this procedure, column 2 was reconnected, and the system was ready for use.

2.5. Preparation of standards

A 20 $\mu\text{g}/\text{ml}$ stock solution of **I** was prepared by weighing 1.0 mg of reference material into a 50-ml volumetric flask, dissolving the compound in 25 ml of acetonitrile, and filling the flask to volume with water. A 2.0 $\mu\text{g}/\text{ml}$ stock solution was prepared by diluting 5 ml of the 20 $\mu\text{g}/\text{ml}$ solution to 50 ml with acetonitrile–water (50:50, v/v).

Working standards of 10, 8, 4 and 2 $\mu\text{g}/\text{ml}$ were prepared by dilution of the 20 $\mu\text{g}/\text{ml}$ stock with acetonitrile–water (50:50, v/v). Working standards of 1, 0.4, 0.2 and 0.1 $\mu\text{g}/\text{ml}$ were prepared by dilution of the 2.0 $\mu\text{g}/\text{ml}$ stock with acetonitrile–water (50:50, v/v). Working standard solutions were found to be stable for at least 1 month at room temperature.

Analysis standards were prepared by adding

50 μl of each working standard to 1 ml of drug-free plasma or urine. The resulting standards ranged in concentration from 5 to 500 ng/ml.

2.6. Sample extraction procedure

A 1-ml aliquot of plasma or urine (sample or standard) was pipetted into a 15-ml disposable glass centrifuge tube (Kimble, Vineland, NJ, USA). A 25- μl volume of a 10 $\mu\text{g}/\text{ml}$ solution of internal standard (compound **II**) in acetonitrile was added and the contents of the tube were vortex mixed. A 1-ml volume of 0.1 M pH 9.5 borate buffer was added, the tube contents were vortexed, and 8.0 ml of MTBE were added. The tube was sealed with a PTFE-lined screw cap (Qorpak 5201; Fisher Scientific, Springfield, NJ, USA), tumble mixed on a Glas Col (Terre Haute, IN, USA) RD350 rotator for 5 min, and centrifuged at 1500 g for 5 min. The tube was then placed in a dry ice–acetone bath, the lower aqueous layer was frozen, and the entire upper organic layer was transferred to a clean centrifuge tube. A 1-ml volume of 10 mM HCl was added to the tube containing the organic layer. Following tumble mixing and centrifugation (as described above), the upper organic layer was aspirated to waste. The acid layer that remained was neutralized by the addition of 10 μl of 1 M sodium hydroxide, after which it was buffered to pH 9.5 by the addition of 1.0 ml of 0.1 M borate buffer. MTBE (8 ml) was added to the tube. After tumble mixing and centrifugation using the conditions described above, the lower aqueous layer was frozen in a dry ice–acetone bath, and the organic layer was transferred to a 100 \times 16 mm glass culture tube. The tube was placed in a Turbo-Vap evaporator (Zymark, Hopkinton, MA, USA) set at 42°C and the solvent was evaporated under a stream of nitrogen. The resulting residue was reconstituted in 200 μl of pump 1 mobile phase and the sample was transferred to a polymethylpentene limited-volume insert contained in an autosampler vial. The vial was capped and placed in an autosampler tray

prior to injection into the column switching system.

3. Results

3.1. Assay specificity

Fig. 3 shows chromatograms of extracted control plasma, a plasma standard containing **I** (10 ng/ml) and **II** (250 ng/ml) and a plasma sample

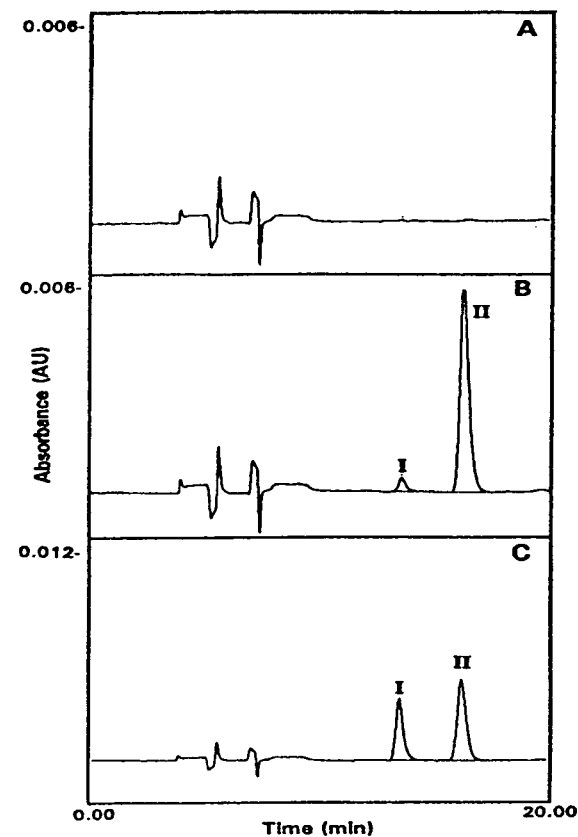


Fig. 3. Representative chromatograms of plasma. (A) Control human plasma, (B) plasma spiked with 10 ng/ml **I** and internal standard **II** (250 ng/ml), (C) plasma sample from human subject 1.5 h after administration of 200 mg **I**. Internal standard **II** added at 250 ng/ml. The concentration of **I** is equivalent to 120.8 ng/ml.

taken from a subject after receiving a 200-mg dose of **I**. Fig. 4 shows chromatograms of extracted control urine, a urine standard containing **I** (500 ng/ml) and **II** (250 ng/ml) and a urine sample collected between 0 and 3 h following the administration of 200 mg **I**. A comparison of Fig. 3A with Fig. 3B and Fig. 4A with Fig. 4B illustrates that no endogenous peaks co-elute with any of the analytes. The specificity of the method is further illustrated by the fact that all pre-dose plasma and urine samples from subjects

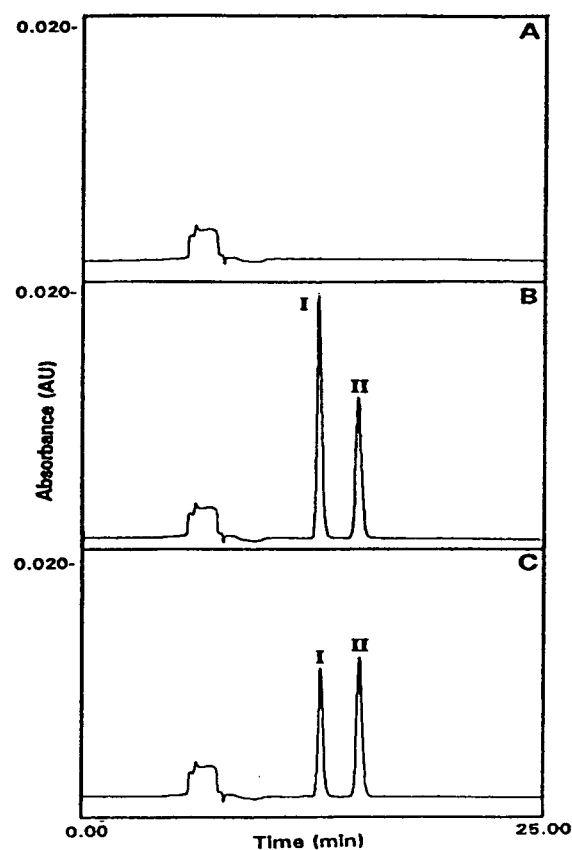


Fig. 4. Representative chromatograms of urine. (A) Control human urine, (B) urine spiked with 500 ng/ml **I** and internal standard **II** (250 ng/ml), (C) 0–3-h urine collection from a human subject obtained after the administration of 200 mg **I**. Sample diluted 1:200 prior to the addition of internal standard **II** at a concentration of 250 ng/ml. The concentration of **I** is equivalent to 52.05 μ g/ml.

Table 1
Extraction recovery of I from human plasma and urine

Concentration (ng/ml)	Mean ($n = 5$) recovery (%) ^a	
	Plasma	Urine
5.0	84.7 (2.2)	68.1 (7.3)
10.0	81.2 (2.9)	70.0 (3.6)
20.0	79.5 (1.0)	69.0 (7.1)
50.0	82.0 (0.7)	66.0 (8.3)
100.0	78.3 (2.9)	66.0 (4.9)
200.0	84.3 (6.5)	69.0 (5.6)
400.0	81.4 (3.2)	71.0 (5.0)
500.0	78.3 (5.0)	67.0 (13.3)

^a Values in parentheses are R.S.D.s.

involved in clinical trials were free of interfering peaks.

3.2. Linearity

Weighted (weighting factor = $1/y$ where y = peak height ratio) least-squares regression calibration curves, constructed by plotting the peak height ratio of I/II vs. standard concentration yielded coefficients of regression typically greater than 0.999 over the concentration range of 5 to 500 ng/ml of I. The use of the weighted least-

squares regression resulted in less than a 10% deviation between the nominal standard concentrations and the experimentally determined standard concentrations calculated from the regression equation.

3.3. Extraction recovery

The recovery of the extraction procedure was determined by comparing the responses of the working standards of I injected directly into the HPLC system with those of extracted plasma and urine standards. The results (Table 1) indicate that the mean recovery of the extraction procedure over the concentration range of 5–500 ng/ml I is 81.2% for plasma and 68.3% for urine.

3.4. Assay precision and accuracy

Replicate standards ($n = 5$) were analyzed to assess the within-day variability of the assay. The mean assayed concentrations as well as the mean accuracy and relative standard deviations (R.S.D.s) of the analyses are shown in Table 2.

Quality control samples containing concentrations of 15 and 350 ng/ml I in plasma and urine

Table 2
Intraday precision and accuracy of the assay as assessed by the replicate ($n = 5$) analysis of standards

Nominal standard concentration (ng/ml)	Plasma			Urine		
	Mean ($n = 5$) analyzed standard concentration (ng/ml)	Accuracy (%) ^a	R.S.D. (%)	Mean ($n = 5$) analyzed standard concentration (ng/ml)	Accuracy (%) ^a	R.S.D. (%)
5.0	5.4	108.0	3.7	5.5	110.0	4.4
10.0	10.5	105.0	6.4	10.6	106.0	3.5
20.0	20.6	103.0	3.3	19.7	98.5	4.4
50.0	48.6	97.2	2.1	47.7	95.4	3.7
100.0	98.9	98.9	4.8	98.6	98.6	5.3
200.0	202.4	101.2	3.1	197.8	98.9	2.3
400.0	399.8	100.0	1.1	407.4	101.9	1.6
500.0	504.7	100.9	1.2	514.7	102.9	1.6

^a Calculated as (mean analyzed concentration/nominal concentration) · 100.

Table 3
Inter-day variability of the assay as assessed by R.S.D.s of low- and high-concentration quality control samples

Nominal concentration (ng/ml)	Plasma ^a		Urine ^b	
	Mean (<i>n</i> = 46) analyzed concentration (ng/ml)	R.S.D. (%)	Mean (<i>n</i> = 17) analyzed concentration (ng/ml)	R.S.D. (%)
15.0	14.8	5.8	15.2	2.7
350.0	342.5	3.2	336.3	2.4

^a Over a period of 42 days.

^b Over a period of 17 days.

were prepared and frozen (-20°C) in 1-ml aliquots. These quality controls were analyzed over periods of 42 days (plasma) and 19 days (urine) to assess the inter-day variability of the assay. The results (Table 3) indicate that the inter-day variability of the assay, as measured by the R.S.D. is less than 6%. The results also indicate that frozen plasma samples containing **I** appear stable for at least 6 weeks, while urine samples are stable for at least 2 weeks.

3.5. Limit of quantification

The limit of quantification of the assay, defined as the lowest concentration that yielded an within-day R.S.D. of less than 10% and an within-day accuracy between 90 and 110% of nominal concentration, was 5 ng/ml in plasma or urine.

4. Discussion

In vitro experiments have demonstrated that a concentration of less than 100 nM (61.4 ng/ml) **I** was required to inhibit the spread of HIV-1 in cell culture by at least 95%. Hence, an assay with low ng/ml sensitivity was needed to support human pharmacokinetic studies.

The ultraviolet-visible spectrum of **I** obtained in a solution of acetonitrile–10 mM phosphate buffer (pH 7) (50:50, v/v) exhibited maxima at 262 nm and <200 nm. The molar extinction coefficient of the 262-nm band was 3060 M^{-1}

cm^{-1} . The spectrum was found to be unaffected by pH changes. The compound was not found to exhibit fluorescence.

The relatively low molar absorptivity at 262 nm indicated that an assay with low nanogram sensitivity using this wavelength for detection was not likely. Since the UV spectrum of **I** revealed that the molar extinction coefficient of the molecule at 210 nm was approximately $29\,000\text{ M}^{-1}\text{ cm}^{-1}$, it was decided to develop an assay with UV detection at this low wavelength. In order to develop an assay at 210 nm, a relatively non-specific wavelength for detection, an extensive sample clean-up was required prior to injection into the HPLC system.

Development of a suitable extraction scheme began with a study of the extractability of **I** from buffers over a pH range of between 1 and 12. The pyridine ring in the molecule has a $\text{p}K_{\text{a}}$ estimated to be between 5 and 6. It was found that **I** was quantitatively extracted with MTBE from solutions with a pH greater than 7, where the pyridine moiety would be un-ionized, and no recovery was observed from solutions whose pH was less than 3, where the pyridine ring would be expected to be fully ionized. Based on this finding, plasma and urine samples spiked with **I** and buffered at pH values between 7 and 12 were extracted and chromatographed under reversed-phase conditions on a C_{18} column. The resulting chromatograms contained endogenous peaks that co-eluted with the analyte of interest. These peaks could not be separated from the peak of interest through mobile phase or column

manipulations. The addition of a back extraction step into acid, with a subsequent re-extraction into MTBE significantly reduced the interference from plasma and urine components, but low-level, co-eluting endogenous peaks were still present in the extracts of samples when detection at 210 nm was used.

An observation was made that the pattern of the endogenous peaks appeared different on a cyano column operated in the reversed-phase mode, as compared to that on a C₁₈ column. The peaks which interfered with the detection of **I** on the cyano column apparently were different than those that interfered on the C₁₈ column.

In order to take advantage of the different selectivity of the cyano and C₁₈ columns, a column switching system [13,14] was employed. The system (Fig. 2), configured around a ten-port valve, was designed to operate as follows. The system was initially set such that the output of the cyano column (column 1) was directed toward waste (valve position 1). The extracted sample was injected into the system. As **I** began to elute from the cyano column, the valve was switched to position 2. Compounds **I** and **II**, which was only partially resolved from **I** on the cyano column, were transferred by means of the switching valve to the C₁₈ column (column 2). After **II** eluted from the cyano column, the valve was returned to position 1. Compounds **I** and **II** were resolved from each other and endogenous interferences on the C₁₈ column while other endogenous components from the cyano column were directed toward waste. By combining the different selectivities provided by the cyano and C₁₈ columns, **I** and **II** could be detected under

interference free conditions at 210 nm. Additionally, band broadening was minimized in the present configuration, as the mobile phase used with the cyano column was weaker than that used with the C₁₈ column. The lack of band broadening contributed to the fact that a limit of quantification of 5 ng/ml could be achieved with the column-switching system. Similar methods employing column switching to enable short-wavelength UV detection of analytes extracted from biological matrices have been previously reported [15,16].

Although the recovery of the extraction procedure was slightly less for urine as compared to plasma, it was constant over the range of the standard curve. Additionally, the precision and accuracy of the urine assay were found to be comparable to those of the plasma assay, indicating that the lower recovery did not adversely affect the overall performance of the assay with urine as the matrix.

The described assay has been used to analyze clinical samples obtained after oral administration of **I**. The plasma levels of **I** that resulted after the administration of 200 mg of **I** to three volunteers are presented in Table 4. The corresponding urinary recoveries of unchanged **I** are shown in Table 5.

5. Conclusions

An HPLC assay using column switching has been developed for the determination of **I** in human plasma and urine. The method has been found to be precise, accurate and suitable for the

Table 4
Plasma concentrations (ng/ml) of **I** following single-dose administration of 200 mg to selected healthy volunteers

Subject	Time (h)					
	0	0.5	1.0	2.0	4.0	8.0
1	nd	1251.0	870.9	205.2	70.7	10.7
2	nd	1142.3	1340.6	433.0	152.0	22.1
3	nd	785.4	622.0	193.5	67.7	8.3

nd = Not detected.

Table 5
Urinary recovery of I following single-dose administration of 200 mg to selected healthy volunteers

Subject	Urinary recovery (mg) over time interval					Total recovery	
	0–3 h	3–6 h	6–12 h	12–24 h	24–48 h	mg	% Dose
1	12.49	1.03	0.42	0.16	0.02	14.12	7.02
2	12.26	0.37	0.59	0.16	0.04	13.42	6.67
3	12.05	0.79	0.75	0.14	0.04	13.77	6.84

analysis of plasma and urine samples. The assay has been successfully applied for the analysis of over 3000 clinical samples from human pharmacokinetic studies.

Acknowledgements

The human plasma and urine samples were obtained from clinical studies directed by Dr. P. Deutsch, Department of Clinical Pharmacology, Merck Research Labs. The authors would like to thank Rhonda Levin, Department of Medicinal Chemistry, Merck Research Labs. for the synthesis of the internal standard.

References

- [1] B.D. Dorsey, R.B. Levin, S.L. McDaniel, J.P. Vacca, P.L. Drake, J.A. Zugay, E.A. Emini, W.A. Schlieff, J.C. Quintero, J.H. Lin, I.W. Chen, D. Ostovic, P.M.D. Fitzgerald, M.K. Holloway, P.S. Anderson and J.R. Huff, presented at the 206th National Meeting of the American Chemical Society, Chicago, IL, 22–27 August, 1993, Abstract Medi-6.
- [2] D. Askin, K. Eng, K. Rossen, R. Purick, K. Wells, R. Volante and P. Reider, *Tetrahedron Lett.*, 35 (1994) 673.
- [3] J.P. Vacca, B.D. Dorsey, W.A. Schlieff, R.B. Levin, S.L. McDaniel, P.L. Darke, J. Zugay, J.C. Quintero, O.M. Blahy, E. Roth, V.V. Sardana, A.J. Schlabach, P.I. Graham, J.H. Condra, L. Gotlib, M.K. Holloway, J. Lin, I.W. Chen, K. Vastag, D. Ostovic, P.S. Anderson, E.A. Emini and J.R. Huff, *Proc. Natl. Acad. Sci. U.S.A.*, 91 (1994) 4096.
- [4] M. Popovic, M.G. Sarngadharan, E. Read and R.C. Gallo, *Science*, 224 (1984) 497.
- [5] R.C. Gallo, S.Z. Salahuddin, M. Popovic, G.M. Shearer, M. Kaplan, B.F. Haynes, T.J. Palker, R. Redfield, J. Oleske, B. Safai, G. White, P. Foster and P.D. Markham, *Science*, 224 (1984) 500.
- [6] J. Schupbach, M. Popovic, R.V. Gilden, M.A. Gonda, M.G. Sarngadharan and R.C. Gallo, *Science*, 224 (1984) 503.
- [7] M.G. Sarngadharan, M. Popovic, L. Bruch, J. Schupbach and R.C. Gallo, *Science*, 224 (1984) 506.
- [8] L.H. Pearl and W.R. Taylor, *Nature*, 329 (1987) 351.
- [9] S. Seelmeier, H. Schmidt, V. Turk and K. von der Helm, *Proc. Natl. Acad. Sci. U.S.A.*, 85 (1988) 6612.
- [10] N.E. Kohl, E.A. Emini, W.A. Schlieff, L.J. Davis, J.C. Heimbach, R.A.F. Dixon, E.M. Scolnick and I.S. Sigal, *Proc. Natl. Acad. Sci. U.S.A.*, 85 (1988) 4686.
- [11] M.I. Johnston, H.S. Allaudeen and N. Sarver, *Trends Pharmacol. Sci.*, 10 (1989) 305.
- [12] B.M. Dunn and J. Kay, *Antiviral Chem. Chemother.*, 1 (1990) 3.
- [13] H.J. Cortes, *J. Chromatogr.*, 626 (1992) 3.
- [14] P. Campins-Falco, R. Herraez-Hernandez and A. Sevilano-Cabeza, *J. Chromatogr.*, 619 (1993) 177.
- [15] K. Yamashita, M. Motohashi and T. Yashiki, *J. Chromatogr.*, 487 (1989) 357.
- [16] K. Yamashita, M. Motohashi and T. Yashiki, *J. Chromatogr.*, 527 (1990) 103.



ELSEVIER

Journal of Chromatography A, 692 (1995) 53–57

JOURNAL OF
CHROMATOGRAPHY A

Comparison of high-performance liquid chromatographic methods for the determination of 1,2-dibromo-2,4-dicyanobutane in cosmetic products

Suresh C. Rastogi*, Sys S. Johansen

Department of Environmental Chemistry, National Environmental Research Institute, Ministry of Environment, Frederiksborgvej 399, P.O.Box 358, DK-4000 Roskilde, Denmark

Abstract

Three known HPLC methods for the analysis of 1,2-dibromo-2,4-dicyanobutane (BCB) were compared to evaluate the strength of the methods for the routine analysis of BCB in cosmetic products. Reversed- and normal-phase HPLC with UV detection were not suitable for routine analysis of BCB in cosmetics. Reversed-phase HPLC with electrochemical detection fulfilled the requirements of a method to be used on a routine basis.

1. Introduction

1,2-Dibromo-2,4-dicyanobutane (BCB), also known as methyl-dibromo glutaronitrile, is a biocide which is used as a preservative in cosmetic products, food packaging materials, paints, glues, etc. BCB is commercially marketed under the trade names Euxyl K400 and Mergaurd 1200, both being a mixture of 20% BCB and 80% phenoxy ethanol. The use of BCB as a preservative in cosmetics is regulated by the European Union's (EU) Cosmetic Directive 76/768/EEC [1]. The maximum allowed concentration of BCB in cosmetic products is 0.1%. Sun-care products, however, should not contain >0.025% BCB. Since the introduction of BCB in the European Market, about 10 years ago, a number of cases of contact dermatitis due to the use of BCB-containing cosmetics have been described (see Ref. [2]).

To monitor that the cosmetic products comply with the EU's Cosmetic Directive, a method for routine analysis of BCB in cosmetics was required. A literature survey revealed that BCB in cosmetics could be analysed by gas chromatography (GC) using nitrogen–phosphorus detection [3], reversed-phase high-performance liquid chromatography (HPLC) with UV detection [4], normal-phase HPLC with UV detection [5] and reversed-phase HPLC with electrochemical detection [6]. Our efforts to adapt the GC method [3] revealed that the method was not reproducible (data not shown) because of uncontrolled decomposition of BCB in the GC injector at temperatures > 150°C. Analysis of BCB by GC–mass spectrometry employing cold on-column injection also revealed that the (decomposed) BCB was eluted when the GC column temperature was > 150°C. Therefore, HPLC was preferred for BCB analysis. However, the λ_{\max} of BCB (220 nm) is a problem for HPLC analysis of BCB with UV detection, because many cosmetic

* Corresponding author.

ingredients as well as HPLC mobile phase(s) may also show significant absorbance at this wavelength. On the other hand, analysis of BCB by HPLC–electrochemical detection, which involves reductive electrochemical detection of bromine [6], may not be suitable for routine analysis because such systems are very sensitive to the presence of oxygen (air) in the HPLC system, and they are not very stable. Therefore, the known HPLC methods were compared for their applicability for the analysis of BCB in cosmetic products.

2. Experimental

2.1. Chemicals

BCB reference substance was obtained from Bureau Community References (BCR, Brussels, Belgium). HPLC-grade acetone was from Fluka (Buchs, Switzerland) and HPLC-grade methanol, acetonitrile, isopropanol and hexane were from Rathburn (Walkerburn, UK). All other chemicals of analytical grade were from E. Merck (Darmstadt, Germany).

2.2. HPLC equipment

HPLC pump Model 510, autosampler Wisp 712 and UV detector 490 were from Waters Chromatography, Millipore (Milford, MA, USA). The electrochemical detector (LC-4B amperometric detector) was from Bioanalytical Systems (West Lafayette, IN, USA). Chromatographic data were collected using a D-2000 Chromato-integrator from Hitachi (Tokyo, Japan).

2.3. Samples

Three cosmetic samples, a shampoo, a cream and a lotion were used for the comparison of HPLC methods. Thirty cosmetic products (17 hair and body shampoos and 13 creams and lotions including one sun-care product) were analysed for BCB by the selected HPLC method.

2.4. Sample preparation and analysis of BCB

Previously described sample preparation methods [4–6] prior to HPLC analysis of BCB were adapted with the exception that the filtration of sample extract in one of the methods [6] was substituted by centrifugation. The known HPLC methods [4,5] were optimized, using different HPLC columns and mobile phases, as described elsewhere [7]. For the optimization of reversed-phase HPLC [4], efficiencies of Spherisorb S 5 ODS and Hypersil 5 ODS (both 5 μm particle size) columns were compared; and the four-solvent (methanol, acetonitrile, tetrahydrofuran and water) optimization method [7] was used for the mobile phase. Efficiencies of Hibar LiChrosorb, Hypersil CN and Nucleosil CN columns were compared for the optimization of normal-phase HPLC [5]; and the mobile phase composition was optimized by varying the ratio of hexane–isopropanol. For the electrochemical detection of BCB separated by HPLC [6], the detector parameters were optimized for the analysis of 20 ppm (w/w) BCB solution. In brief, the optimized methods for the analysis of BCB in cosmetics were as follows.

(1) Approximately 1 g cosmetic product was suspended in 10 ml methanol, followed by ultrasonic treatment and filtration through a 0.45- μm membrane filter. HPLC of BCB in the filtrate was performed employing a 250 mm \times 4.6 mm I.D. Spherisorb 5 ODS column and acetonitrile–tetrahydrofuran–water (20:10:70) as mobile phase. The flow-rate of mobile phase was 2 ml/min and UV detection was performed at 220 nm.

(2) Approximately 1 g sample suspended in isopropanol was heated at 60°C followed by filtration through a 0.2- μm membrane filter. HPLC of BCB was performed employing a 250 mm \times 4.6 mm I.D. Hibar LiChrosorb, particle size 7 μm , column and hexane–isopropanol (87:13) as mobile phase. The flow-rate of the mobile phase was 1 ml/min and UV detection was performed at 230 nm [5].

(3) Approximately 1 g sample suspended in 80% aqueous methanol was heated at 60°C followed by centrifugation at 600 g for 5 min.

BCB analysis in the filtrate was performed by HPLC employing a 250 mm × 4.6 mm I.D. Zorbax C₈ column and 40% aqueous acetone containing 0.02 M sodium sulphate and 0.002 M sodium chloride as mobile phase. Reductive electrochemical detection was performed using a gold electrode. An Ag/AgCl electrode was used as the reference electrode [6]. The flow-rate of the mobile phase was 1 ml/min and the detector settings were: range 500 nA and measuring potential –0.6 V.

3. Results and discussion

The three available HPLC methods for the analysis of BCB in cosmetics were compared to

evaluate their applicability for routine analysis of BCB in cosmetic products. The HPLC methods were optimized and then applied for the analysis of BCB in three samples (a shampoo, a lotion and a cream). Various aspects of the methods, technical, economical and physical resources, and work environment were compared (Table 1). Chromatograms of BCB in a shampoo, spiked with 0.1% BCB, by the optimized HPLC methods are shown in Fig. 1.

The analytical method employing reversed-phase HPLC and UV detection at 220 nm is the simplest and very stable. However, the recovery of BCB from the samples was very low (< 30%). This could probably be increased by modifying the sample preparation method, but the method has other problems as well: not a

Table 1
Comparison of the three HPLC methods for BCB analysis in cosmetics

Parameters	Reversed-phase HPLC–UV detection	Normal-phase HPLC–UV detection	Reversed-phase HPLC–electrochemical detection	Method of choice
Detection limit (ppm) ($S/N > 3$)	50	50	0.5	3
Linearity of calibration curve (ppm)	25–250	10–300	0.5–40	3
Selectivity of BCB detection	*	*/**	SD	3
Column efficiency (number of plates)	4900	9800	25 000	3
Capacity factor, k' BCB	5.6	2.8	3.9	2/3
Stability of eluent	**/**	*	*/**	1
HPLC analysis time per sample (min)	25–90	15	20	2
Recovery of BCB (%)	15–30	75–115	96–102	3
Repeatability of:				3
standard BCB (%)	3	11	1	
sample extract (%)	–	6	1	
Simplicity of sample preparation	*	*	*	–
Physical and mental strain	*/**	*	**	3
Resources	**/**	**	*/**	1
Work environment	**	*	**/**	3

Qualitative evaluation: *** = good; ** = acceptable; * = less good. SD = Selective detection. – = could not be evaluated. Repeatability was determined for the 10-replicate analysis of 10 ppm solution of standard BCB by electrochemical detection (150 ppm of standard-BCB by UV detection) and for the 10-replicate analysis of a shampoo spiked to contain 0.1% BCB. Physical and mental strain refer to the efforts needed for the optimal functioning of a method on routine basis.

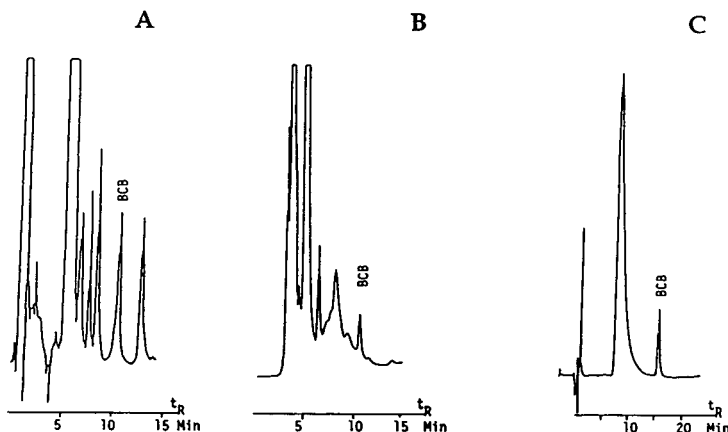


Fig. 1. Analysis of BCB (0.1%) in a shampoo by reversed-phase HPLC with UV detection (A), normal-phase HPLC with UV detection (B) and reversed-phase HPLC with electrochemical detection (C). See Experimental for details.

proper separation of BCB from other components in cosmetic products, non-specific detection of BCB at 220 nm where many cosmetic ingredients as well as HPLC mobile phase also show significant absorbance, and long analysis times because some of the cosmetic ingredients (especially in creams and lotions) elute very late (elution time > 60 min). Although the method worked well for the analysis of a shampoo (Fig. 1A), analysis of BCB in a cream and a lotion by this method was not satisfactory, because the BCB peak was not properly resolved from the neighbouring peaks (results not shown). Changing the HPLC column to a Hypersil ODS column or changing the mobile phase composition [7] to optimize the method did not affect the resolution factor (< 0.9) of BCB peak significantly. Thus, this method may only be suitable for the analysis of BCB in simple mixtures, for example, raw materials for cosmetics.

Analysis of BCB by normal-phase HPLC [5] showed a reasonable recovery (> 75%) of BCB from the cosmetic products, a reasonably good separation of BCB from other cosmetic ingredients (Fig. 1B) and short analysis times as well. The method, however, is not practical for routine analysis because a very long time (6–12 h) is required for the HPLC system to be stabilized and the UV detection at 230 nm,

though better than that at 220 nm, is unspecific. Furthermore, the use of hexane is not considered to be safe.

The third method of BCB analysis by reversed-phase HPLC with reductive electrochemical detection of bromine, fulfilled the technical requirement for a routine method except that the baseline of the chromatogram was rather unstable and the retention time (t_R) of BCB was unstable (because of relatively quick evaporation of acetone from the constantly degassed mobile phase). Under the following conditions —replacement of PTFE tubings with steel tubings to stop the diffusion of air/oxygen into the HPLC system [6], column temperature at $40 \pm 0.2^\circ\text{C}$ [6] and room temperature at $20 \pm 0.2^\circ\text{C}$ — the baseline was stable (Fig. 1C). The major peak in Fig. 1C is a ghost peak of the HPLC system and that has nothing to do with the sample or standard BCB. The ghost peak does not interfere with the determination of BCB. Attempts to identify the cause of the ghost peak indicated that the ghost peak may have an association with the injection process, because a peak with the same t_R also appeared when the helium degassed mobile phase was injected. One of the possible reasons may thus be that a small portion of pressurized air, which is used for the injection process by autosampler, is introduced together

with the sample in the analytical column followed by the reductive electrochemical detection of the air/oxygen.

The HPLC system takes about 2 h to stabilize. The HPLC mobile phase which is recirculated, may be changed every 24 h. An internal standard, for example, bronidox or bronopol which are also used as preservatives in cosmetics, can be used in this method to ascertain the identification of BCB on the basis of its relative retention time (Fig. 2). This method is being used for the

routine analysis of BCB in cosmetics in our laboratory without any problem.

Acknowledgements

We thank Professor Steen Honoré Hansen for the fruitful discussions during the progress of the present work. Skillful technical assistance was provided by Mrs. Gitte H. Jensen.

References

- [1] Council Directive 76/768/EEC of 27 July 1976 on the approximation of the laws of the Member States relating to cosmetic products, *Off. J. Eur. Communities*, L262 (1976) 169.
- [2] B.M. Hausen, *Contact Dermatitis*, 28 (1993) 149.
- [3] K.D. Schweiter and K. Stanzl, *Seifen-Oele-Fette-Wachse*, 114 (1988) 537.
- [4] N. de Kruijf, M.A.H. Rijk and A. Schouten, *TNO Report A 87.286/261300*, CIVO-TNO, Zeist, Netherlands, 1987.
- [5] N. de Kruijf, A. Schouten, L.A. Prantoto-Soetardhi and M.A.H. Rijk, *TNO Report A 89.375/290148*, TNO-CIVO, Zeist, Netherlands, 1988.
- [6] J.W. Weijland, A. Stern and J. Rooslaar, *Cosmetica-report 54*, Regional Inspectorate for Health Protection, Enschede, Netherlands, 1993.
- [7] L.R. Snyder, J.L. Glajch and J.L. Kirkland, *Practical HPLC Method Development*, Wiley, New York, 1988.

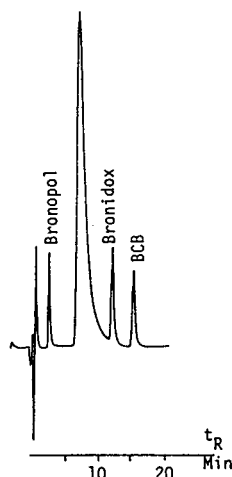


Fig. 2. Analysis of a solution of brominated preservative standards by reversed-phase HPLC with electrochemical detection. Concentrations of preservatives in the solution were Bronopol 220 ppm, Bronidox 57 ppm and BCB 10 ppm.

Alkylsulphonic acid ion pairing with radial compression columns for determining plasma or cerebrospinal fluid 1- β -D-arabinofuranosylcytosine in pediatric pharmacokinetic analysis

M.L. Stout*, Y. Ravindranath

Departments of Pediatrics and Pharmacology, Wayne State University, and Divisions of Clinical Pharmacology/Toxicology and Hematology/Oncology, Children's Hospital of Michigan, 3901 Beaubien Boulevard, Detroit, MI 48201, USA

Abstract

In order to accurately and precisely measure plasma and cerebrospinal fluid (CSF) 1- β -D-arabinofuranosylcytosine (Ara-C) in pediatric samples with adequate sensitivity and without interference, we have developed a reversed-phase ion-pairing technique utilizing the free amino group of the pyrimidine ring of Ara-C. Optimum resolution and separation was achieved utilizing a 4 μ m C₁₈ radial compression column. Ara-C and the internal standard 8-bromo-cyclic-AMP eluted at 6.5 and 4.6 min, respectively, with complete resolution. The minimum detectable amount is 2.5 pmol in a 50- μ l volume. The assay was linear in both plasma and CSF. Intra- and inter-day assay precision were less than 4% and 9%, respectively, for plasma with similar results obtained for CSF. Neither endogenous compounds nor commonly co-administered drugs interfere. Validity for our method was supported by the successful assay of over 400 pediatric plasma and 50 CSF samples for pharmacokinetic analysis. The method offers accuracy, precision, sensitivity and efficiency for plasma or CSF Ara-C determination.

1. Introduction

Several high-performance liquid chromatographic (HPLC) methods have been developed within the last fifteen years to determine both plasma and cerebrospinal fluid (CSF) levels of the antileukemic drug 1- β -D-arabinofuranosylcytosine (Ara-C). Many were developed for adult studies that utilize short-duration (1–3 h) intravenous (i.v.) high-dose infusions. The ensuing infusion, and post-infusion levels, remain elevated well above the sensitivity limit of standard HPLC detection equipment. Also, adequate plasma and CSF samples can be obtained in adults so that sensitivity limits for most HPLC

methods are not a serious concern. On the other hand, analysis of plasma and CSF Ara-C in pediatric patients presents special problems, especially when patients are treated on long-duration (2–4 days) i.v. high-dose regimens [1,2]. While adequate concentrations are present within plasma during infusion, these levels may be 5–50 times lower than that seen in the short-duration i.v. high-dose adult regimens [3–9]. In addition, post-infusion determinations are required for up to 4 h for proper calculation of biexponential elimination kinetics [10]. Many HPLC methods available today lack the required sensitivity due to several factors: inadequate extraction recovery techniques [11–14], poor separation of drug from endogenous plasma constituents or from drug metabolites and poor

* Corresponding author.

baseline resolution and detection at low concentrations [11,12,15–21]. Several methods have been developed and tested on only pure aqueous or buffered samples rather than plasma or CSF extracts [22,23]. A large proportion of these methods extract the drug from plasma but do not utilize an internal standard [4,11,14,15,17–19,21,24], or directly inject plasma or plasma ultrafiltrates, which may shorten column life [3,13,20,25]. Many methods have relatively long chromatographic analysis times (20–50 min) or utilize multiple columns, extractions or gradient systems [4,7,11,12,15,20,21,24].

While these problems are easily addressed and solved in assay systems utilizing adult samples, the same cannot be said for pediatric samples. Because of small sample sizes encountered ($\leq 200 \mu\text{l}$ plasma), increased sensitivity needs due to low post-infusion concentrations, interferences due to combination or adjuvant drug therapy and/or tumor lysis products, and need for rapid analysis to avoid concentrations associated with toxicity, we have developed a reversed-phase ion-pairing method that utilizes the free amino group of the pyrimidine ring of Ara-C and the ion-pairing alkylsulphonic acid, 1-pentanesulphonic acid (PSA). Using our method, and a Radial-Pak column, the required sensitivity, specificity and speed of analysis can be obtained for accurate and precise analysis of this drug in pediatric infusion and post-infusion plasma and CSF.

2. Experimental

2.1. Chemicals

Ara-C (Sigma, St. Louis, MO, USA) was utilized as the free base. Tetrahydrouridine (THU) was purchased from Calbiochem (San Diego, CA, USA). Uracil arabinoside (Ara-U), uracil, uridine, cytosine, cytidine, adenosine, adenine and 8-bromo-cyclic adenosine monophosphate (8-Br-cAMP) were all purchased from Sigma. A variety of other drugs were tested for possible interference with Ara-C (see Table 3). Of these compounds only ketorolac (Syntex

Labs., Palo Alto, CA, USA) and metoclopramide (A.H. Robins Co., Richmond, VA, USA) were obtained directly from the pharmaceutical manufacturer. All other drug compounds were obtained from Sigma. Potassium phosphate buffer, sodium hydroxide and trichloroacetic acid (TCA) were purchased from Mallinckrodt (Paris, KY, USA). All ion-pairing agents and tri-N-octylamine were obtained from Sigma. Hydrochloric acid was obtained from J.T. Baker (Phillipsburg, NJ, USA). Acetonitrile, methanol, dichloromethane and 1,1,2-trichlorotrifluoroethane were purchased from Burdick & Jackson (Muskegon, MI, USA).

2.2. Chromatography

The HPLC system consisted of a Beckman (Berkeley, CA, USA) Model 110B single-piston isocratic solvent-delivery module, a Rheodyne Model 7125 injection valve equipped with a 100- μl loop, a 4- μm C₁₈ Nova-Pak (150 \times 3.9 mm I.D.) radial compression column and a Nova-Pak C₁₈ Guard-Pak precolumn (Waters Millipore, Milford, MA, USA). Radial compression was achieved by a Waters Z module. In order to reduce band broadening and decrease dead space, microbore tubing (0.18–0.23 mm I.D.) was used throughout the system. A Waters Model 441 fixed-wavelength UV-Vis detector (280 nm) was utilized for all detections. All HPLC assays were carried out at ambient temperature with a flow-rate of 1.8 ml/min. Mobile phase consisted of 10 mM potassium phosphate buffer and 27.5 mM PSA as ion-pairing agent with acetonitrile and methanol (96:3:1, v/v/v). The pH was adjusted to 4.00 with KOH. Both peak area and height were measured using a LCI-100 laboratory computing integrator (Perkin-Elmer, Norwalk, CT, USA).

2.3. Assay procedure

In order to accurately determine extremely low levels of Ara-C in plasma, all background noise should be reduced to a minimum so as to obtain the highest possible signal-to-noise ratio. Therefore, both dichloromethane, and 1,1,2-tri-

chlorotrifluoroethane solvents used in the extraction procedure were further purified of possible UV absorbing impurities by acid/base washes. Using a separation funnel, equal volumes of the solvent and 1 M NaOH were shaken together, allowed to separate, and the base removed. This was followed by a wash in distilled deionized water and by a wash in an equal volume of 1 M HCl. After removal of the acid, two further washes in distilled deionized water removed all traces of acid. Further purification of these organic solvents was accomplished by adsorption with activated charcoal followed by filtration to remove all charcoal fines. The NaOH and HCl solutions were made in pure distilled deionized water, slurried overnight in activated charcoal, and filtered as above. All organic solvents were stored at -20°C . Enough purified solvent can be prepared at one time for several hundred assays. In order to monitor the purification process, blank plasma extractions were carried out and assayed before and after these procedures. Baseline noise was reduced significantly so that the signal-to-noise ratio increased at least twofold. This allowed detection of Ara-C in plasma at the 10^{-8} M level.

Blood (ca. 1 ml) was collected in heparinized tubes containing THU, a deaminase inhibitor (final concentration $100\ \mu\text{M}$). Whole blood was centrifuged in a microfuge (14 000 g) for 5 min at $0-4^{\circ}\text{C}$ and plasma was collected and stored at -70°C until analysis. CSF (1–2 ml) was also collected in the presence of THU, centrifuged, and stored at -70°C until analysis.

Extraction and centrifugation were performed at $0-4^{\circ}\text{C}$ at all times. After the addition of $10\ \mu\text{l}$ of the I.S., 8-Br-cAMP ($5\ \mu\text{M}$ final concentration) to $190\ \mu\text{l}$ of Ara-C containing plasma, $200\ \mu\text{l}$ of cold $0.6\ \text{M}$ TCA was added dropwise with continual vortex mixing. Samples were left on ice for 10 min with occasional vortex mixing throughout that period. Precipitated plasma or CSF samples were microfuged 5 min at 14 000 g, supernatant was removed to a new 1.5-ml microfuge tube and the volume recorded. To the acidified supernatant was added 1.1 volumes of $0.5\ \text{M}$ tri-N-octylamine in 1,1,2-trichlorotrifluoroethane and the mixture vortex mixed vig-

orously (30–45 s) several times and microfuged for 5 min. The lower organic phase was removed and the remaining aqueous extract was again microfuged for three minutes. The aqueous phase was carefully removed to a new 1.5-ml microfuge tube and approximately 1.1 ml of dichloromethane was added, the mixture vortexed for 1–2 min, centrifuged as above and the lower organic phase carefully removed. The remaining aqueous phase was again microfuged for 2–3 min to remove all traces of organic solvent. The final aqueous extract was removed to a new 1.5-ml microfuge tube and dried at 50°C under nitrogen atmosphere. Aqueous extracts were stored at -70°C until chromatography.

At analysis, all aqueous extracts were reconstituted in $100\ \mu\text{l}$ of mobile phase and $50\ \mu\text{l}$ were injected. Plasma standard curves were prepared from healthy pooled plasma of volunteers. Standards ranged from 50 to $0\ \mu\text{M}$. CSF standard curves were prepared in artificial CSF (Elliotts B solution) and ranged in concentration from 50 to $0\ \mu\text{M}$. After extraction and analysis, data were analyzed by linear regression methods.

3. Results and discussion

In order to determine the optimal ion-pairing agent and pH for separation, 1-hexanesulphonic acid, 1-heptanesulphonic acid and 1-octanesulphonic acid were also tested in addition to PSA. All tests were performed at $5\ \mu\text{M}$ Ara-C in extracted pooled volunteer plasma. Use of these ion-pairing agents at constant pH (5.0) caused retention times for Ara-C and the internal standard to increase greatly (≥ 10 min). Reduction of the concentration of these agents reduced retention times but with loss of resolution of drug from normal plasma constituents. The PSA ion-pairing agent gave optimal separation of drug and internal standard from normal plasma constituents within a reasonable analysis time (≤ 8.0 min). The pH was altered between 3.0 and 7.0 for the PSA ion-pairing agent and optimal separation and analysis time was obtained at pH 4.0. Since this ion-pairing agent is better than 97% ionized (anion) and the amino

function of Ara-C is essentially 100% charged (cation) at pH 4.0, it is not surprising that optimal ion-pairing chromatography is attained at this pH. Decrease in pH would result in reduction of charged ion-pairing anion while increase in pH would reduce the effective cationic drug species. In either case, alterations in pH from 4.0 ultimately reduced chromatographic resolution. The other ion-pairing agents were also examined at pH 4.0 but the same relative changes seen at pH 5.0 were retained at this new pH.

Initial chromatograms of blank plasma revealed a few unknown plasma constituents that were highly retained on this column. Washing the aqueous extracts with dichloromethane removed these late-eluting plasma constituents from all samples. Although these late-eluting constituents were not found in blank CSF, these samples

were also treated with dichloromethane. Chromatography and recovery of pure standards in Elliotts B solution or with patient CSF samples was not affected by dichloromethane washes.

Fig. 1a illustrates a typical chromatogram of blank plasma from a pediatric patient prior to chemotherapy with Ara-C. As can be seen there is a resolvable baseline at the retention time for Ara-C (ca. 6.5 min). The internal standard has a retention time of 4.8 min. Overall chromatographic time is under 10 min. Fig. 1b is a chromatogram of the same patient receiving 100 mg/m²/h for 48 h. This sample was taken before the infusion was terminated and represents a plasma steady state level (hour 47). As seen from this figure both Ara-C and the internal standard resolve from one another and no post-peak shoulders or severe tailing occurs. Peak shape is uniformly symmetrical. Fig. 1c repre-

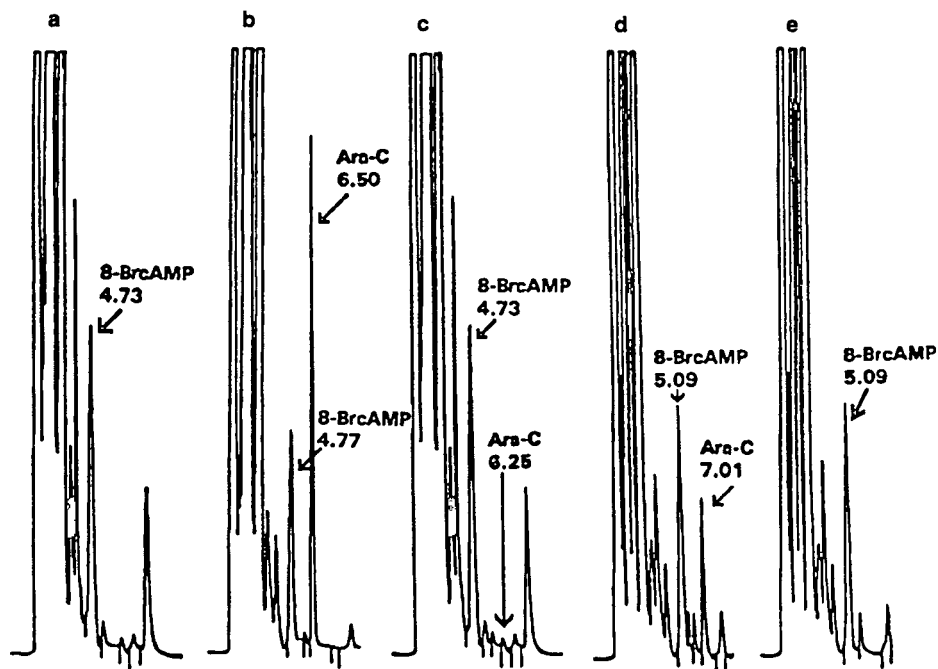


Fig. 1. HPLC of Ara-C in plasma and CSF of a pediatric patient receiving 100 mg/m²/h Ara-C for two days. (a) Blank preinjection plasma; (b) steady state plasma level (sampled at hour 47 of infusion); (c) 4-h post-infusion Ara-C plasma level; (d) steady state Ara-C CSF level (sampled at hour 47 of infusion); (e) sample of drug-free CSF (taken from diagnostic CSF). This sample is not the same as that seen in (d). Retention times for Ara-C in plasma were 6.25–6.50 min and in CSF 7.01 min. Internal standard retention times were approximately 4.73 min in plasma and 5.09 min in CSF. In order to compensate for an increase in ambient temperature during this assay for CSF, and to keep all pertinent peaks within their window tolerances, flow-rates were decreased to 1.7 ml/min. This caused a slight increase in the retention times for internal standard and Ara-C.

sents a 4-h post-infusion plasma determination. The peak representing Ara-C is easily quantitated even though plasma levels have fallen over 10-fold. Patients also had CSF levels drawn simultaneously with their steady state plasma levels. As seen in Fig. 1d, Ara-C appears in easily detected concentrations in the CSF. Fig. 1e is a chromatogram of CSF in which Ara-C is absent (blank). These results indicate that high-dose long-duration i.v. infusions in children attain detectable CSF levels, and Ara-C can cross the blood brain barrier from plasma. There appear to be no interfering peaks for either Ara-C or the internal standard within CSF. The major plasma metabolite for Ara-C, Ara-U, coeluted within the solvent front and did not interfere with the chromatography of the parent drug or I.S.

The following analytical procedures were followed to validate our chromatographic method for both plasma and CSF. Standard curves for both plasma and CSF were linear ($r^2 \geq 0.998$) and intersected true zero within 1% (relative to the full scale curve). The regression equation for plasma [$y = 1.0043 (\pm 0.0068 \text{ S.E.M.})x + 0.0386 (\pm 0.1297)$] indicated that analytically HPLC determined concentrations for these standards varied in a direct linear 1:1 proportion with respect to the actual prepared concentrations. Also, the validity of these curves can be further verified by the accuracy of blind samples prepared in an independent laboratory. Plasma samples were prepared in a blind fashion in concentrations ranging from 50 to 0.0 μM . The maximum relative percent error for these determinations never exceeded 5.5% and the value determined for a blank sample was zero. (Table 1). Minimum detectable amount in plasma is 0.1 μM and in CSF, 0.08 μM . Standard curves for both plasma and CSF are linear over at least a 2.5 log range. The regression equation for CSF was similar to that seen for plasma [$y = 0.968 (\pm 0.00965)x + 0.1856 (\pm 0.1834)$]. Accuracy results for CSF in artificial CSF (Elliotts B solution) were not performed since it was felt this media would have little effect on drug determination and, results would vary minimally from a repeat of the standard curve.

Table 1
Ara-C assay validation data for plasma and CSF analysis

Concentration (μM)	R.S.D. (%)	
	Plasma	CSF
<i>Intra-day</i>		
10	1.33	—
2	—	3.21
1	4.16	5.30
<i>Inter-day</i>		
10	3.69	—
2	—	6.53
1	8.71	7.74
Accuracy for plasma ^a		
Known concentration (μM)	Analytically determined (μM)	Error (%)
0.0	0.0	0.0
9.0	8.82	2.00
16.0	16.17	1.06
25.0	23.66	5.36
40.0	39.38	1.55

^a Samples were prepared in a blind fashion in the laboratory of Dr. G. Dombi, Childrens Hospital of Michigan.

At least six to eight samples at both low (1 μM plasma, 1.0 μM CSF) and high (10 μM plasma, 2.0 μM CSF) concentrations were analyzed during one experiment (intra-day precision assay) and at least one sample was analyzed at each concentration over at least six to eight different assay days (inter-day precision assay). Inter- and intra-day precisions were determined from quantitative data of both peak area and peak height. Table 1 indicates that both intra- and inter-day assay relative standard deviations (R.S.D.s) for plasma at each concentration were excellent. At lower concentrations peak height proved to be the better measure in determining the precision of this method. This may be related to either peak tailing or baseline noise during determination. The intra- and inter-day assay R.S.D.s for artificial CSF (Elliotts B solution) were excellent regardless of the method of peak

quantitation utilized. It must be remembered that this solution is not a true CSF since many constituents within actual CSF are not present (enzymes, carbohydrates, lipids, amino acids, neurotransmitters, certain ions, vitamins, etc.). This would undoubtedly contribute to an increase in the actual determined coefficients.

Recovery of sample was determined by spiking plasma or Elliotts B solution with a known amount of Ara-C, extracting and analyzing the sample repetitively, and comparing this to a pure aqueous sample of equivalent concentration that has not been extracted. Percent recovery is defined as the concentration ratio of extracted spiked plasma or CSF to pure aqueous sample $\times 100$. As can be seen from Table 2, recovery of drug from pooled plasma or from artificial CSF was essentially quantitative at both low and high concentrations. Extraction from lipemic or hemolyzed patient samples did not alter extraction efficiency.

The radial compression columns used for our assay were superior in resolution and decreased overall chromatographic time by 2–3-fold from standard steel columns. Well over 600 assays could be performed on a single column without serious loss of resolution, peak symmetry, or increase in baseline noise.

A variety of other pure compounds were assayed to determine if interference occurs with either the internal standard or drug itself. Table 3 list many agents commonly co-administered with Ara-C during antileukemic therapy. Al-

Table 2
Ara-C assay validation data for plasma and CSF analysis

	Extraction efficiency (%) ^a
Plasma: 5 μM	96.20 (R.S.D. = 8.37%, $n = 6$)
Plasma: 1 μM	96.88 (R.S.D. = 6.56%, $n = 6$)
CSF: 2 μM	98.2 (R.S.D. = 2.43%, $n = 6$)
CSF: 1 μM	97.8 (R.S.D. = 4.56%, $n = 6$)

^a Extraction efficiency was determined by comparing extracted "spiked" plasma and CSF samples against pure unextracted samples in water. The ratio of the HPLC-determined spiked plasma vs. water values $\times 100$ equaled the percent extraction efficiency.

Table 3
Ara-C assay validation data for plasma and CSF analysis

Interference analysis	
<i>Drugs</i>	<i>Plasma drug metabolite</i>
Thorazine	Uracil arabinoside
Chlorpromazine	
Promazine	<i>Natural metabolite</i>
Metoclopramide	Cytosine
Diazepam	Uracil
Oxazepam	Adenosine
Chlordiazepoxide	Cytidine
Phenobarbital	Adenine
Diphenhydramine	Adenosine monophosphate
Cimetidine	Cyclic adenosine monophosphate
Codeine	Uridine
Ibuprofen	
Ceftazidime	
Chloramphenicol	
Penicillin	
Ampicillin	
Gentamycin	
Tobramycin	
Kanamycin	
Dexamethasone	
Acetaminophen	
Hydrocortisone	
Methotrexate	
Daunorubicin	
Cyclophosphamide	
Vinblastine	
Vincristine	
Etoposide	
Teniposide	
Actinomycin D	
Asparaginase	

though many of these compounds possess a free amino group, a substituted amino group, or a ring containing hetero nitrogen, there was no interference produced. Interference was determined by assay of the pure compound in the presence of Ara-C and internal standard. If the retention time of the interfering compound was within ± 0.5 min of either the internal standard or Ara-C, the compound was spiked into plasma and extracted. Of all the compounds tested, only the metabolites of Ara-C and other nucleosides chromatographed close to the retention times of the standard and Ara-C. The antibiotics, antiemetics, antipyretics, sedative agents and other antineoplastics drugs did not interfere. These

compounds either were non-retained, or had excessively long retention times. Also, many of these agents had their maximum UV absorbance well above or below that of the optimal absorbance for Ara-C (280 nm) and could not be detected at clinical plasma levels. The various drug and natural metabolites mentioned in Table 3 were all spiked into plasma or artificial CSF, extracted and assayed in the presence of the internal standard and Ara-C. The major plasma drug metabolite of Ara-C, Ara-U, and cytidine, the naturally occurring 1- α isomer of Ara-C, did not interfere with our assay. Adenosine monophosphate, cyclic adenosine monophosphate (cAMP), adenine, uridine and adenosine did not interfere with the internal standard.

Comparison of our method with other HPLC methods analyzing this drug in similar populations and at similar dose and infusion durations, indicate equivalent or better precision than pre-

viously published assays. Table 4 lists both intra- and inter-day assay R.S.D.s for Ara-C in several different HPLC assay systems. Coefficients for these assays range from 2.0 to 15.2% (intra) and from 2.7 to 12.3% (inter) over a wide concentration range for plasma. Our method attained intra- and inter-day assay R.S.D.s for plasma ranging between 1.33 and 4.16% (intra) and between 3.69 and 8.71% (inter).

We have successfully used our method to analyze Ara-C steady state plasma and CSF levels and post-infusional elimination pharmacokinetics in pediatric patients receiving high-dose long-duration i.v. infusions. Well over 400 plasma and 50 CSF samples have been measured. Our results [27,28] correlate well in many respects with other HPLC methods used to determine Ara-C plasma pharmacokinetics. Ara-C steady state plasma, CSF, CSF to plasma ratios, and biexponential pharmacokinetic con-

Table 4
Ara-C HPLC plasma assays: precision comparisons

Ref.	Concentration range (μM)	Within R.S.D. (%)	Between R.S.D. (%)
[3]	0.2–492 (within) 0.82 and 4.92 (between)	≤ 5.0 –	9.3 and 7.0
[12]	8.2–410 (within)	6–12%	–
[22]	Unknown pure aqueous sample		1.0
[30] ^a	0.001–0.025	≤ 10.0	5.2–13.0
[16]	82 (within) 328 (between)	2.0 2.7	4.3 2.7
[25]	0.41–410 (within) 0.41 (between)	3.1–7.4	– 5.6
[21]	82 205	5.2 2.3	6.8 3.2
[17]	2 8	9.1 15.2	12.3 12.0
Present paper	10 1	1.33 4.16	3.69 8.71

All samples were prepared in plasma or serum.

^a Radioimmunoassay for comparison.

stants that we have determined for pediatric long-duration high-dose infusions are all within reasonable values of the current literature for this drug [1,2,19,26,29]. This assay fulfilled all the necessary criteria of specificity, sensitivity, efficiency, accuracy and precision required to monitor this potent antineoplastic agent in pediatric plasma and CSF samples.

Acknowledgements

This work was funded by a grant from Leukemia Research Life Inc., Detroit, MI, USA. The authors gratefully acknowledge the assistance of Ms. Ginni Cosgrove in the preparation of this manuscript.

References

- [1] J. Ochs, J.A. Sinkule, M.K. Danks, A.T. Look, W.P. Bowman and G. Rivera, *J. Clin. Oncol.*, 2 (1984) 1092.
- [2] V.I. Avramis, K.I. Weinberg, J.K. Sato, C. Lenarsky, M.L. Willoughby, T.D. Coates, M.F. Ozkaynak and R. Parkman, *Cancer Res.*, 49 (1989) 241.
- [3] H. Breithaupt, H. Pralle, T. Eckhardt, M. VonHatteningberg, J. Schick and H. Loffler, *Cancer*, 50 (1982) 1257.
- [4] A.P. Early, H.D. Preisler, H. Slocum and Y.M. Rustum, *Cancer Res.*, 42 (1982) 1587.
- [5] Y. Pommier, L. Pochat, J.P. Marie and R.A. Zittoun, *Cancer Treat. Rep.*, 67 (1983) 371.
- [6] M.L. Slevin, E.M. Piall, G.W. Aherne, V.J. Harvey, A. Johnston and T.A. Lister, *J. Clin. Oncol.*, 1 (1983) 546.
- [7] R.L. Capizzi, J.L. Yang, E. Cheng, T. Bjornsson, D. Sahasrabudhe, R.S. Tan and Y.C. Cheng, *J. Clin. Oncol.*, 1 (1983) 763.
- [8] J.O. Lillemark, W. Plunkett and D.O. Dixon, *Cancer Res.*, 45 (1985) 5952.
- [9] L.E. Damon, W. Plunkett and C.A. Linker, *Cancer Res.*, 51 (1991) 4141.
- [10] W.A. Ritschel (Editor), *Handbook of Basic Pharmacokinetics*, Drug Intelligence Publications, Hamilton, IL, 3rd ed., 1986, pp. 442–454.
- [11] Y.M. Rustum, *Anal. Biochem.*, 90 (1978) 289.
- [12] P. Lissen, A. Drenthe-Schonk, H. Wessels and C. Haanen, *J. Chromatogr.*, 223 (1981) 371.
- [13] H. Breithaupt and J. Schick, *J. Chromatogr.*, 225 (1981) 99.
- [14] R.C. Donehower, J.E. Karp and P.J. Burke, *Cancer Treat. Rep.*, 70 (1986) 1059.
- [15] M.G. Pallavicini and J.A. Mazrimas, *J. Chromatogr.*, 183 (1980) 449.
- [16] J.R. Wermeling, J.M. Pruemmer, F.M. Hassan, A. Warner and A.J. Pesce, *Clin. Chem.*, 35 (1989) 1011.
- [17] D.K. Lloyd, A.M. Cypess and I.W. Wainer, *J. Chromatogr.*, 568 (1991) 117.
- [18] J.C. Scott-Moncrieff, T.C.K. Chan, M.L. Samuels, J.R. Cook, G.L. Coppoc, D.B. DeNicola and R.C. Richardson, *Cancer Chemother. Rep.*, 29 (1991) 13.
- [19] S. Zimm, J.M. Collins, J. Miser, D. Chatterji and D.G. Poplack, *Clin. Pharmacol. Ther.*, 35 (1984) 826.
- [20] J.A. Lopez, G.P. Beardsley, J.G. Krikorian, R.W. Mortara and R.P. Agarwal, *Cancer Res.*, 43 (1983) 5190.
- [21] S.V. Galushko and I.P. Shishkina, *J. Pharm. Biomed. Anal.*, 10 (1992) 1093.
- [22] L.D. Kissinger and N.L. Stemm, *J. Chromatogr.*, 353 (1986) 309.
- [23] A.M. Pimenov, Y.V. Tikhonov and P.T. Toguzov, *J. Liq. Chromatogr.*, 9 (1986) 1003.
- [24] R.L. Schilsky and F.S. Ordway, *J. Chromatogr.*, 337 (1985) 63.
- [25] A. Riccardi, T. Servidei, A. Lasorella and R. Riccardi, *J. Chromatogr.*, 497 (1989) 302.
- [26] Y. Takashima and K. Matsuyama, *J. Clin. Pharmacol.*, 27 (1987) 330.
- [27] M.L. Stout, Y. Ravindranath, J. Kurtzberg, M. Schwenn, M. Amylon and J. Katz, *Proc. Am. Soc. Clin. Oncol.*, 12 (1993) 318.
- [28] Y. Ravindranath, M.L. Stout, J. Kurtzberg, M. Schwenn, M. Amylon and J. Katz, *Med. Ped. Oncol.*, 21 (1993) 537.
- [29] V.I. Avramis, R. Biener, M. Krailo, J. Finklestein, L. Ettlinger, M. Willoughby, S.E. Siegel and J.S. Holcenberg, *Cancer Res.*, 47 (1987) 6786.
- [30] T. Sato, M. Morozumi, K. Kodama, A. Kuninaka and H. Yoshino, *Cancer Treat. Rep.*, 68 (1984) 1357.

High-performance liquid chromatographic method for potency determination of cephalexin in commercial preparations and for stability studies

Mei-Chich Hsu^{a,*}, Yu-Shan Lin^b, Hsiou-Chuan Chung^b

^aGraduate Institute of Sports Sciences, National College of Physical Education and Sports, 250 Wen-Hwa 1st Road, Kweishan, Taoyuan 33333, Taiwan

^bNational Laboratories of Foods and Drugs, Department of Health, Executive Yuan, 161-2, Kuen-Yang Street, Nankang, Taipei 11513, Taiwan

Abstract

A reversed-phase column liquid chromatographic method was developed for the assay of cephalexin in bulk drugs and pharmaceutical preparations. An equation was derived showing a linear relationship between peak-area ratio of cephalexin to acetaminophen (internal standard) and the cephalexin concentration over a range of 0.2–1.75 mg/ml ($r = 0.9999$). Standard addition recoveries were generally greater than 99.5%. The relative standard deviations were between 0.38 and 0.63% in the within-day assay, and 1.05% in the between-day assay. The column liquid chromatographic assay results were compared with those obtained from a microbiological assay, which indicated that the proposed method is a suitable substitute for the microbiological method for potency assays and stability studies of cephalexin preparations.

1. Introduction

The present official assay method of the *British Pharmacopoeia* [1] for the analysis of potency of cephalexin oral preparations is an iodometric titration. The *US Code of Federal Regulations* [2] described two official methods for potency assay of cephalexin: a microbiological method and iodometric titration. The regulations state that the results obtained from the microbiological method shall be conclusive. The Minimum Requirement for Antibiotic Products [3] for the analysis of potency of cephalexin in bulk drug substance and its preparations indicates mi-

crobiological and turbidimetric methods. The greatest disadvantage of the microbiological and chemical methods in current use is their lack of specificity. This deficiency has prompted the search for an alternative method which is fast, simple and selective, e.g. column liquid chromatography (LC). Several LC methods have been applied for separation of cephalexin and other cephalosporins or penicillins [4–10]. Few methods for the determination of cephalexin in pharmaceutical samples have been reported [11–16]. However, the drawback of these procedures is either the tedious sample preparation procedure or lack of comparison with the results of a microbiological method.

In order to establish whether an HPLC meth-

* Corresponding author.

od would be acceptable, it is important to determine whether it is robust enough for assaying samples kept under extreme conditions. Degradation in the sample should be equally reflected by microbiological and HPLC assays. This paper describes a comparison of a proposed HPLC method with a microbiological assay for the determination of cephalexin in commercial formulations. Further, cephalexin was kept at elevated temperatures as part of an accelerated degradation experiment and assayed by microbiological and HPLC methods.

2. Experimental

2.1. Instruments

A Model 576 LC pump (Gasukuro Kogyo, Tokyo, Japan), a Gasukuro Kogyo Model 502U Spectrodetector and a Gasukuro Kogyo Model 12 Chromatocorder were employed during the study. The mobile phase was pumped through a reversed-phase column (μ Bondapak C₁₈; 30 cm \times 3.9 mm I.D.; particle size, 10 μ m; Waters) with an isocratic flow-rate of 1.0 ml/min. The detector was set at 254 nm. Chromatography was performed at room temperature. Injections of 20 μ l of all solutions to be analysed were made.

2.2. Reagents and materials

Methanol (LC grade) was supplied by ALPS Chemical Co. (Taipei, Taiwan). Glacial acetic acid (reagent grade) was supplied by E. Merck (Darmstadt, Germany). 7-Aminodesacetoxycephalosporanic acid was purchased from Sigma (St. Louis, MO, USA). Acetaminophen was a gift of Winthrop Labs. Taiwan Branch Office (Sterling Products International, Taipei, Taiwan). Cephalexin monohydrate was USP reference standard (Rockville, MD, USA). Cephalexin bulk drug was supplied by Eli Lilly (Taipei, Taiwan). Capsules, granules and powder for oral solutions were obtained from commercial sources.

2.3. Mobile phase

The mobile phase was methanol–1.25% glacial acetic acid (25:75, v/v). The mobile phase was filtered (0.45- μ m pore size Millipore filter) and degassed with an ultrasonic bath prior to use.

2.4. Internal standard solution

Internal standard (acetaminophen, 63.0 mg) was dissolved in 5.0 ml of methanol and diluted to 25.0 ml with water to form the internal standard solution.

2.5. Cephalexin standard solution

To form cephalexin standard solution, 1.0 ml of internal standard solution was added to an accurately weighed amount of cephalexin standard equivalent to a 25.0-mg potency of cephalexin and the volume was brought up to 50.0 ml.

2.6. Sample preparations

To form sample preparations, 1.0 ml of internal standard solution was added to an accurately weighed amount of bulk drugs, homogeneous capsule contents, granule or powder for oral solution formulations equivalent to a 25.0-mg potency of cephalexin and the volume was brought up to 50.0 ml with water.

2.7. Solution for linearity response

Eight concentrations of cephalexin (0.2, 0.3, 0.5, 0.75, 1.0, 1.25, 1.5 and 1.75 mg/ml) were prepared. Each concentration was chromatographed six times.

2.8. Solution for recovery studies

To an accurately weighed 25.0-mg potency of sample composites of commercial preparations were added different amounts of cephalexin standard and 1.0 ml of internal standard solution. Each solution was made up to 50.0 ml with water and was chromatographed in triplicate.

2.9. Microbiological assay procedure

The protocol of analysis was basically that described in Minimum Requirements for Antibiotics Products of Japan [3]. *Bacillus subtilis* (Culture Collection and Research Center, Hsinchu, Taiwan) was used in the microbiological assay. According to the cup plate method, standards and test drugs were diluted to 1.0 mg/ml (potency) concentrated solution with 1% phosphate buffer solution (pH 6.0) and then diluted to 20.0 and 5.0 $\mu\text{g/ml}$ with 1% phosphate buffer solution (pH 6.0) on the day of analysis. Five petri dishes of 9.0 cm inside diameter were used for each sample. After incubation for 16 to 18 h, the inhibition zone diameter was measured by a zone analyzer (ZA-F; Toyo, Tokyo, Japan).

3. Results and discussion

The linearity of the peak-area ratio (cephalexin versus internal standard) was verified by injection of eight solutions containing cephalexin in a concentration range of 0.2 to 1.75 mg/ml. A straight line with a correlation coefficient of 0.9999 ($y = 5.5536x + 0.0178$) was obtained when the ratios of the area counts of the cephalexin divided by the area counts of the internal standard were plotted against concentration of cephalexin.

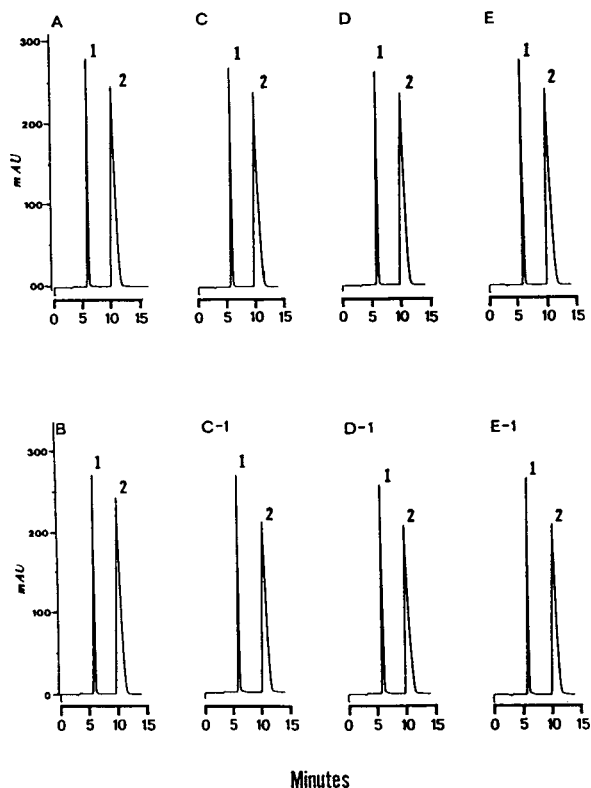


Fig. 1. Chromatograms of cephalexin preparations. (A) USP standard; (B) bulk drug substance; (C) 500-mg capsule; (C-1) degraded 500-mg capsule; (D) 500 mg/g granule; (D-1) degraded 500 mg/g granule; (E) 500 mg/g powder for oral solution; (E-1) degraded 500 mg/g powder for oral solution. Peaks: 1 = acetaminophen; 2 = cephalexin.

Table 1
Recovery of cephalexin from various commercial composites

Formulation	Added (mg)	Found (mg)	Recovered (%)	Average recovered (%)	
Capsule	250 mg	10.0	9.95	99.5	99.6
		15.0	14.97	99.8	
		20.0	19.90	99.5	
500 mg	10.0	10.01	100.1	100.2	
	15.0	15.02	100.1		
	20.0	20.09	100.4		
Granule, 500 mg/g	10.0	9.96	99.6	99.7	
	15.0	14.98	99.9		
	20.0	19.94	99.7		

Reproducibilities for both the within-day assay and the between-day assay were evaluated. The relative standard deviations (R.S.D.s), on the basis of peak-area ratios for six replicate injections in the within-day assay, were between 0.38 and 0.63% at the concentration of 0.5 mg/ml. The R.S.D. in the between-day assay ($n = 6$) was 1.05% at the same amount.

The results of standard addition recovery studies of cephalexin from sample composites of commercial preparations are shown in Table 1. The average recovery was greater than 99.6%.

Typical chromatograms of the cephalexin commercial dosage forms are shown in Fig. 1. The retention time was about 6.0 min for the internal standard and 11.3 min for cephalexin. Excipients from commercial formulations did not interfere. Furthermore, the HPLC method can detect a compound related to the cephalexin, i.e., 7-aminodesacetoxycephalosporanic acid, which was eluted prior to cephalexin (Fig. 2).

When sample solutions of capsule, granule and powder for oral solution were heat degraded, the resulting mixtures yielded chromatograms containing additional peaks, none of which interfered with the interpretation and measurement of the chromatographic peaks for cephalexin and acetaminophen. Chromatograms of 2-, 3- and 5-h degraded solutions of granule samples at 100°C showed cephalexin disappearance and degradation product accumulation with increasing incubation time (Fig. 3). Several additional peaks were found when the detection sensitivity was increased. It is obvious that decomposition products elute before the intact drug. Same results were found when samples decomposed by using 0.1 M sodium hydroxide. To examine the purity of the cephalexin peak in the heat-degraded samples, a UV photodiode array detector was used. The evaluation of chromatographic peak homogeneity was performed by absorbance ratios and a three-dimensional spectrochromatogram. The results presented good confirmation of the cephalexin peak identity (data not shown).

Studies were initiated to ascertain the suitability of the proposed method for stability studies.

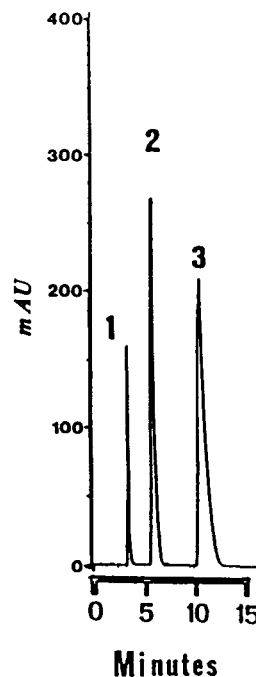


Fig. 2. Chromatogram of a mixture preparation. Peaks: 1 = 7-aminodesacetoxycephalosporanic acid; 2 = acetaminophen; 3 = cephalexin.

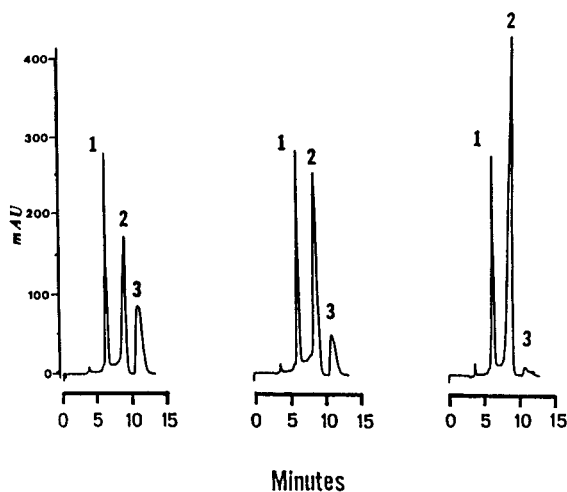


Fig. 3. Chromatograms of 2-, 3- and 5-h degraded solutions (from left to right) of granule samples at 100°C showing cephalexin (peak 3) disappearance and degradation product (peak 2) accumulation with increasing incubation time. Peak 1 is acetaminophen.

For the degraded solutions, the solutions of capsule, granule and powder for oral solution formulations containing 1.0 mg/ml cephalexin were prepared by water. The solutions were degraded at 100°C. For the degraded powdered composites, the capsule, granule and powder for oral solution formulations were directly stored in temperature-controlled cabinets (100°C). Degraded solutions and degraded powdered composites were taken from the cabinets periodically for microbiological and HPLC assays. The assay values, expressed as a percentage of the level claim, are given in Tables 2 and 3. The nine paired values in Table 2 have a correlation coefficient of 0.9934. The 21 paired values in Table 3 have a correlation coefficient of 0.9364. Hence, no significant difference in the assay values obtained by the two analytical methods was found for degraded or non-degraded samples. A number of samples of bulk drug substance and commercial preparations of eight brands were analyzed for cephalexin content by HPLC. These samples were also assayed by the microbiological method. The results are shown

Table 3

Comparison of percent potency of cephalexin and its degraded powdered composites in capsule, granule and powder for oral solution formulations as determined by microbiological and HPLC methods

Formulation	Degradation time (h)	% of declared concentration by	
		Microbiological method	HPLC method
Capsule	0	113.5	110.5
	3	108.6	104.2
	5	103.5	102.8
	7	99.6	101.6
	9	98.4	101.1
	11	96.9	101.0
Granule	42	86.6	84.8
	0	111.1	108.5
	3	104.4	102.0
	5	102.8	101.2
	7	101.0	102.2
	9	100.4	98.4
Powder for oral solution	11	95.8	98.1
	42	85.2	84.3
	0	110.8	107.7
	3	96.7	100.8
	5	94.4	98.0
	7	93.1	98.4
Powder for oral solution	9	94.3	97.3
	11	92.6	97.1
	42	83.7	86.0

Table 2

Comparison of percent potency of cephalexin and its degraded solutions in capsule, granule and powder for oral solution formulations as determined by microbiological and HPLC methods

Formulation	Degradation time (h)	% of declared concentration by	
		Microbiological method	HPLC method
Capsule	0	110.6	111.6
	1	92.7	94.4
	2	50.5	48.5
Granule	0	111.3	109.5
	1	98.5	96.1
	2	49.7	48.4
Powder for oral solution	0	106.3	108.6
	1	94.1	92.9
	2	21.0	31.8

in Table 4. A *t*-test was applied to the data; analysis showed no significant difference at the 95% confidence level for any of the preparations when assayed by the microbiological or HPLC methods.

This study demonstrates the applicability of the proposed HPLC method for the potency determination of cephalexin in bulk drug and capsule and granule formulations. The method can be successfully used for routine quality control and stability assays and offers advantages in speed, simplicity and reliability.

Table 4
Comparison of microbiological and HPLC assays for cephalixin

Sample	Potency ^a by	
	Microbiological method	HPLC method
<i>Bulk drug</i>		
USP standard	950.0	950.0
Brand A	939.2	936.8
<i>Dosage form, declared</i>		
Brand A, 250 mg/capsule	105.8	104.6
Brand A, 500 mg/capsule	109.8	107.0
Brand B, 250 mg/capsule	106.4	104.4
Brand C, 500 mg/capsule	106.5	103.1
Brand D, 250 mg/capsule	105.3	108.2
Brand D, 500 mg/g granules	105.7	107.8
Brand E, 500 mg/capsule	103.5	104.2
Brand F, 500 mg/capsule	107.7	106.5
Brand G, 250 mg/capsule	106.2	101.5
Brand H, 500 mg/g powder for oral solution	106.5	104.5

^a The potency was determined as $\mu\text{g}/\text{mg}$ for bulk drug and as a percentage of the declared amount for dosage forms. Values for the microbiological assay are averages of five determinations; values for HPLC are averages of triplicate determinations.

Acknowledgements

We thank Winthrop Laboratories Taiwan Branch Office, Sterling Products International, Taipei, Taiwan, for their generous gifts of acetaminophen for the study.

This work was supported by grant DOH 82-22 from the Department of Health, Executive Yuan, Taipei, Taiwan.

References

- [1] *British Pharmacopoeia*, Her Majesty's Stationary Office, London, 1988.
- [2] *Code of Federal Regulations*, Title 21, Part 440, US Government Printing Office, Washington, DC, 1990.
- [3] *Minimum Requirements for Antibiotic Products of Japan*, English version, Japan Antibiotics Research Association, Tokyo, 1986.
- [4] E.R. White, M.A. Carroll, J.E. Zarembo and A.D. Bender, *J. Antibiot.*, 38 (1975) 205.
- [5] M.A. Carroll, E.R. White, Z. Jancsik and J.E. Zarembo, *J. Antibiot.*, 30 (1977) 397.
- [6] E. Crombez, G.A. Bens, G. Van der Weken, W. Van den Bossche and P. De Moerloose, *Chromatographia*, 11 (1978) 653.
- [7] F. Salto, *J. Chromatogr.*, 161 (1978) 379.
- [8] A. Brunetta, L. Mosconi, S. Pongiluppi, U. Scagnolari and G. Zambonin, *Boll. Chim. Farm.*, 120 (1981) 335.
- [9] M.C. Nahata, *J. Chromatogr.*, 228 (1982) 429.
- [10] N. Kovacic-Bosnjak, Z. Mandic and M. Kovacevic, *Chromatographia*, 23 (1987) 350.
- [11] L.J. Lorenz, F.N. Bashore and B.A. Olsen, *J. Chromatogr. Sci.*, 30 (1992) 211.
- [12] V. Das Gupta and J. Parasrampur, *Drug Dev. Ind. Pharm.*, 13 (1987) 2231.
- [13] J. Marincel, N. Bosnjak and M. Lamut, *Acta Pharm. Jugosl.*, 38 (1988) 35.
- [14] *United States Pharmacopoeia XXII, National Formulary XVII*, United States Pharmacopoeial Convention, Rockville, MD, 1990.
- [15] D.P. Wang and M.K. Yeh, *Chin. Pharm. J. (Chunh-Hua Yao Hsueh Tsa Chih)*, 42 (1990) 349.
- [16] Y. Zhao, X. Qian and Z. Li, *Sepu*, 10 (1992) 183.



ELSEVIER

Journal of Chromatography A, 692 (1995) 73–81

JOURNAL OF
CHROMATOGRAPHY A

Rapid liquid chromatographic–mass spectrometric assay for oxymetazoline in whole rat blood

Fred J. Hayes*, Timothy R. Baker, Roy L.M. Dobson, Michael S. Tsueda

Miami Valley Laboratories, OTC-Health Care Technology Division, The Procter and Gamble Company, Cincinnati, OH 45239-8707, USA

Abstract

A rapid HPLC–electrospray mass spectrometric assay for the quantitation of oxymetazoline in whole rat blood has been developed. Sample preparation was a single liquid–liquid extraction after addition of a deuterated internal standard (IS) and pH adjustment. An aliquot of reconstituted extract was injected onto a narrow-bore octadecyl reversed-phase column at a flow-rate of 400 $\mu\text{l}/\text{min}$. Using a 20:1 post-column split, 5% of the eluent was introduced into the mass spectrometer interface. Elution of the analyte and IS occurred in less than 2 min. This rapid separation was made possible because of the sample cleanup and the selectivity of the mass spectrometric detection. The $[\text{M} + \text{H}]^+$ ions for oxymetazoline (m/z 261) and $[\text{}^2\text{H}_6]\text{oxymetazoline}$ (m/z 270) were detected using selected ion monitoring. The linear range of the assay was 0.67–167 ng/g of blood and the limit of quantitation with a 0.30-g sample was 1.0 ng/g. The assay permitted the analysis of nine samples per hour with the requisite sensitivity and selectivity and was used to determine the blood pharmacokinetics of oxymetazoline in rats dosed via intravenous and intranasal routes.

1. Introduction

In recent years, there has been a growing awareness of the potential of intranasal (i.n.) drug administration [1]. Several advantages can be achieved from delivering drugs intranasally [2]. Losses of drug due to degradation in the gastrointestinal tract, gut wall metabolism, and/or hepatic “first-pass” metabolism and elimination can be avoided. Additionally, the existence of a rich vasculature and a highly permeable structure in the nasal membranes can enhance absorption giving plasma concentration vs. time profiles that are comparable to those obtained by intravenous (i.v.) administration.

Various animal models have been evaluated for studying intranasal drug administration; the most common is the rat model [1]. We are using the rat model to study the intranasal absorption of oxymetazoline. This drug has been used safely and effectively as a nasal decongestant for almost thirty years [3]. Practical advantages of this model include ease of handling and cost effectiveness. A disadvantage of using rats is their small blood volumes. Typically, sample volumes are limited to 0.50 ml if serial sampling is performed from the same animal. This can create significant analytical obstacles in an attempt to fully characterize absorption and the pharmacokinetic (PHK) profile of a drug.

We sought to develop a sensitive, non-radioisotopic assay that could be used to accurately

* Corresponding author.

determine the blood pharmacokinetics of i.n.- and i.v.-dosed oxymetazoline. A liquid chromatographic method for the determination of radiolabeled oxymetazoline in rabbit urine, using fraction collection–liquid scintillation counting detection following sample cleanup and preconcentration, has been reported [4]. A method for the determination of unlabeled oxymetazoline in biological fluids has not been reported to date.

Initial efforts were directed toward method development using GC–MS and GC–MS–MS with chemical derivatization and electron ionization. The value of GC–MS-based techniques for the trace-level determination of drugs and their metabolites in biological fluids is well established, particularly when used in conjunction with stable-isotope-labeled internal standards [5]. In addition, recent reports of quantitative GC–MS–MS methodology demonstrate that added selectivity provided by a second stage of mass analysis can result in lower limits of quantitation and shorter analysis times [6,7] than are possible using standard GC–MS. However, the quantitation range required for our application could not be reliably achieved by GC–MS or GC–MS–MS, using electron ionization of trimethylsilylated oxymetazoline because of unacceptable interactions between the derivative and active GC sites.

Because of the difficulties encountered with the GC-based approaches, we evaluated the utility of HPLC–MS for low-level quantitation of oxymetazoline. MS has become widely utilized as a selective and sensitive detector for HPLC [8]. Several interfacing technologies have been used to couple the advantages of HPLC separation with the power of MS detection including the moving belt [9], thermospray [10,11], and particle beam [12,13]. The more recent combination of HPLC with MS using electrospray (ES) interfacing [14,15] has led to the use of this technique for new qualitative purposes and routine quantitation. A pneumatically assisted version of ES, called ionspray [16], has demonstrated the instrumental ruggedness required for routine quantitation of pharmaceuticals in biological matrices [17].

Many HPLC–ES–MS features make this tech-

nology attractive for use as a bioanalytical technique. For example, although widely varying across compound classes, the sensitivity is excellent in many cases. The ES interface offers mild conditions for the introduction of polar compounds to the gas phase, thereby eliminating the need for derivatization required in many GC-based methods and allowing the analysis of analytes not amenable to GC. The high selectivity of MS detection (especially MS–MS) generally allows for simple sample cleanup and minimizes chromatographic separation requirements. These features can afford significantly shorter sample preparation and analysis times, compared to other bioanalytical methods.

We have developed and describe here a rapid HPLC–ES–MS assay for quantitation of low levels of oxymetazoline in whole rat blood. The assay was applied to studies comparing the blood pharmacokinetics of oxymetazoline in rats dosed via i.v. and i.n. routes. To the best of our knowledge, this is the first reported non-radioisotopic method for the determination of this widely used drug in a biological matrix.

2. Experimental

2.1. Chemicals and reagents

Oxymetazoline [6-*tert.*-butyl-3-(2-imidazolin-2-ylmethyl)-2,4-dimethylphenol] hydrochloride USP Reference Standard was acquired from the United States Pharmacopeial Convention, Rockville, MD, USA. [²H₉]Oxymetazoline (IS-d₉) internal standard (free base form) was synthesized at Procter and Gamble's Miami Valley Laboratories, Cincinnati, OH, USA. The chemical structures for oxymetazoline and IS-d₉ are shown in Fig. 1. [2-¹⁴C]Oxymetazoline hydrochloride (specific activity 31 mCi/mmol) was custom synthesized by Amersham, Arlington Heights, IL, USA. Ammonium acetate, acetonitrile and methanol were HPLC grade (Fisher Scientific, Cincinnati, OH, USA). Unless otherwise specified, all other reagents were ACS grade and obtained from standard suppliers. Solutions were made with water obtained from a Barnstead

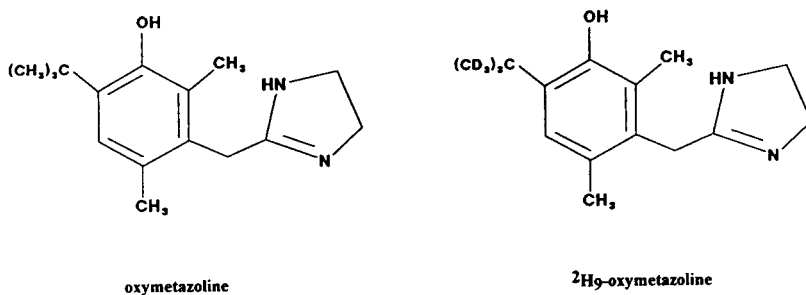


Fig. 1. The chemical structures of oxymetazoline and [²H₉]oxymetazoline.

Nanopure cartridge system (Boston, MA, USA). Heparinized whole rat blood samples were taken from control, i.n.-dosed and i.v.-dosed Sprague-Dawley rats (200–300 g) obtained from Charles River Labs. (Plymouth, MI, USA).

2.2. Extraction recovery experiments

Aliquots of a [¹⁴C]oxymetazoline solution in methanol were added with or without IS-d₉ as carrier to 100 × 16 mm borosilicate glass extraction tubes. The solvent was evaporated and 0.30 g of freshly thawed blank whole rat blood was added. The samples were vortexed and allowed to equilibrate for 30 min. The blood samples were then buffered with Na₂CO₃ and extracted once with 4.0 ml of anhydrous diethyl ether. The organic extracts were transferred to clean 100 × 16 mm borosilicate glass culture tubes and evaporated to dryness under nitrogen at 35°C. Dried extracts were reconstituted with 0.20 ml of acetonitrile–5 mM ammonium acetate buffer (50:50), transferred to liquid scintillation vials, and analyzed for total counts (Model 2200CA liquid scintillation analyzer; Packard, Meriden, CT, USA). Percent recoveries, based on dpm, were calculated versus aliquots of the [¹⁴C]oxymetazoline stock solution.

2.3. Validation and quality control (QC) sample preparation

To evaluate method accuracy and precision, various amounts of the oxymetazoline reference standard (0.56, 2.17, 10.84 or 51.90 ng) were

spiked, along with 50 ng IS-d₉, into 0.30 g of freshly thawed blank whole rat blood in 100 × 16 mm borosilicate glass culture tubes. The samples were vortexed, allowed to equilibrate for 30 min, buffered with 0.90 ml of 0.10 M Na₂CO₃, and extracted once with 3.0 ml of anhydrous diethyl ether. The volume of ether was reduced to 3.0 ml to minimize solvent usage and losses of the analyte due to absorption to the glass surface. The organic extracts were transferred to clean 100 × 16 mm borosilicate glass culture tubes, evaporated to dryness under nitrogen at 35°C, and stored at –20°C until analysis. On the day of analysis the dried extracts were thawed, reconstituted in 100 μl of acetonitrile–5 mM ammonium acetate (50:50), and transferred to autosampler vials. In this way, spiked validation samples were prepared at four levels (*n* = 5) on two separate days except for a 2.17-ng spike that was prepared on three separate days. Similarly, spiked QC samples were prepared at three levels (*n* = 3 each) on days coinciding with PHK sample preparation.

2.4. PHK study sample preparation

Prewighed blood samples (0.10 to 0.50 g) were received frozen in 1.5-ml polypropylene microcentrifuge tubes. These were thawed to room temperature, spiked with 50 ng IS-d₉, vortexed, and allowed to equilibrate for 30 min. The samples were then transferred to 100 × 16 mm borosilicate glass extraction tubes with three separate volumes of 0.10 M Na₂CO₃ (each buffer volume was equal to sample volume to

assure the same mequiv. buffer/g blood ratio for each sample) and extracted once with 3.0 ml of anhydrous diethyl ether. The organic extracts were transferred to clean 100 × 16 mm borosilicate glass culture tubes, evaporated to dryness under nitrogen at 35°C, and stored at –20°C until analysis. On the day of analysis the dried extracts were thawed, reconstituted in 100 µl of acetonitrile–5 mM ammonium acetate (50:50), and transferred to autosampler vials.

2.5. Preparation of HPLC–ES-MS standards

Non-matrix working standards were prepared in acetonitrile–5 mM ammonium acetate (50:50) and analyzed for daily method calibration. Quantitative transfers were made from stock solutions of oxymetazoline hydrochloride (based on mass of the free base form) and IS-d₉ using Wiretrol calibrated micropipettes (Drummond, Broomall, PA, USA) and a P-1000 Gilson Pipetman continuously adjustable pipette (Rainin, Woburn, MA, USA). Working standards ranged from 0.2–50 ng/100 µl with each containing 50 ng/100 µl of IS-d₉ and were stored at 2°C. Based on the reconstitution volume of 100 µl for an extract from 0.30 g blood, this range of standards is equivalent to 0.67–167 ng/g blood. Aliquots were transferred to autosampler vials prior to analysis.

2.6. HPLC–ES-MS conditions

Liquid chromatography was conducted using a Waters 600MS pump in conjunction with a Waters 715 Ultrawisp autosampler (Milford, MA, USA). The column was a 15 cm × 2.1 mm, 5 µm particle diameter, 8 nm pore size, Zorbax Rx-C₁₈ (MacMod Analytical, Chadds Ford, PA, USA). The mobile phase consisted of a filtered (0.20 µm) and degassed solution of acetonitrile–5 mM ammonium acetate pH 6.5 (60:40), which was pumped at a flow-rate of 400 µl/min at room temperature. Using a 20:1 post-column split, 5% of the flow was directed into the mass spectrometer interface. In all cases, 20 µl of the standards and sample extracts were injected.

All experiments were conducted using a PE-

Sciex (Thornhill, Ontario, Canada) API III tandem quadrupole mass spectrometer with the articulated ionspray interface. For quantitation, the instrument was operated with the third quadrupole in the selected ion monitoring (SIM) mode. The collision cell (Q2) used in this work was the original open cell design. Ions at m/z 261 and 270 were monitored (0.7 s cycle time) to detect the $[M + H]^+$ of oxymetazoline and IS-d₉, respectively. A nebulizer gas (air) pressure of 42 p.s.i. (1 p.s.i. = 6894.76 Pa) and a curtain gas (nitrogen) flow of 1.2 l/min were used, as well as an indicated orifice voltage of 70 V. The mass spectrometer was calibrated daily using a 10^{–4} M solution of polypropyleneglycols (PPGs) that was directly infused with a Harvard Apparatus 22 (South Natick, MA, USA) syringe pump at 10 µl/min.

2.7. Quantitation

Calibration curves were generated from the non-matrix working standards run on each day of analysis. Oxymetazoline levels in QC and unknown samples were determined from weighted (1/ x) curves derived from the peak area ratios of standard to IS-d₉. All peak areas were selected using the PE-Sciex MacQuan program. The calibrations (eight data points, $n = 1$ each point) were linear over the range of standards used (0.2–50 ng/100 µl). Typical regression data for a daily standard curve generated for analyses of samples (e.g., 40 µg i.n. dose described later) were: slope 0.0465; intercept 0.00429; correlation coefficient 0.99983; standard error of regression for y estimate 0.00920. The standard deviations for the slope and intercept from six daily standard curves were 0.00332 and 0.00131, respectively.

3. Results

3.1. Extraction recovery experiments

[¹⁴C]Oxymetazoline was used to develop and optimize the extraction procedure for recovery of the drug. Results from preliminary in vitro

Table 1
Effect of Na₂CO₃ amount on recovery of 50 ng [¹⁴C]oxymetazoline from rat blood

Na ₂ CO ₃ Concentration (M)	mequiv. buffer/g blood	Percent recovery (± S.D.)
0.00	0.00	12 (± 0.74)
0.01	0.06	32 (± 1.6)
0.02	0.12	67 (± 3.4)
0.04	0.24	77 (± 3.6)
0.06	0.36	78 (± 5.1)
0.08	0.48	82 (± 1.6)
0.10	0.60	83 (± 3.2)
0.15	0.90	83 (± 3.8)
0.20	1.20	87 (± 3.9)

A 0.90-ml volume of buffer was used at each concentration, 0.30 g blood (*n* = 3) at each concentration.

studies indicated that oxymetazoline partitions between plasma and red blood cells in a concentration-dependent manner with higher proportions partitioning into the cells at low ng/g levels. Based on these data (not shown), whole blood was chosen as the target matrix from which to isolate the analyte. Compounds of similar structure [e.g., 2-(2-hydroxyphenyl)imidazoline] have reported *pK_a* values of approximately 7 and 11 [18]. Therefore, a liquid–liquid extraction with diethyl ether following pH adjustment with aqueous Na₂CO₃ appeared to be the most promising approach to sample preparation.

Results of an experiment to determine the optimum amount of Na₂CO₃ buffer (mequiv./g blood) required for optimal recovery of oxy-

metazoline from 0.30 g of blood using one extraction with diethyl ether are given in Table 1. Based on these data, 0.90 ml of 0.10 M Na₂CO₃ added to 0.30 g of blood (0.60 mequiv./g) gives good recovery due to adequate pH adjustment without addition of excess reagent that could result in significant salt carryover into the ether extract. Table 2 illustrates the carrier effect of 50 ng IS-d₉ on the recovery of [¹⁴C]oxymetazoline from blood using a single extraction over the concentration range of 1.67–333 ng/g. Recoveries with addition of the internal standard were significantly improved for the lower concentrations. This is due to a shift in the total level of oxymetazoline to concentrations where partitioning into red blood cells is essentially constant.

3.2. HPLC–ES–MS results

The electrospray mass spectra of oxymetazoline and IS-d₉ are shown in Fig. 2. The base peak in each spectrum results from the [M + H]⁺ at *m/z* 261 and 270, respectively. The presence of a d₈ analogue (*m/z* 269), a d₇ analogue (*m/z* 268), and so on, can be seen in the spectrum of the labeled compound, indicating that the *tert.*-butyl group is not fully incorporated with deuterium. This has no effect on the use of this material as an internal standard since no oxymetazoline-d₀ could be detected in this material. For the purposes of this work the d₉ analogue was monitored and the other analogues (d₈–d₅) were ignored. Other peaks seen in the spectra (<25% relative intensity) are believed

Table 2
Extraction efficiency for [¹⁴C]oxymetazoline from blood without and with 50 ng IS-d₉

[¹⁴ C]Oxymetazoline spike (ng/g)	Recovery (%)	
	Without IS-d ₉ (± S.D.)	With IS-d ₉ (± S.D.)
1.67	68 (± 6.7)	82 (± 3.4)
10.4	77 (± 2.7)	81 (± 4.4)
41.7	83 (± 5.8)	85 (± 2.4)
167	89 (± 3.5)	82 (± 3.0)
333	88 (± 3.6)	86 (± 3.0)

A 0.90-ml volume of 0.10 M Na₂CO₃ was used for pH adjustment, 0.30 g blood (*n* = 3) at each concentration.

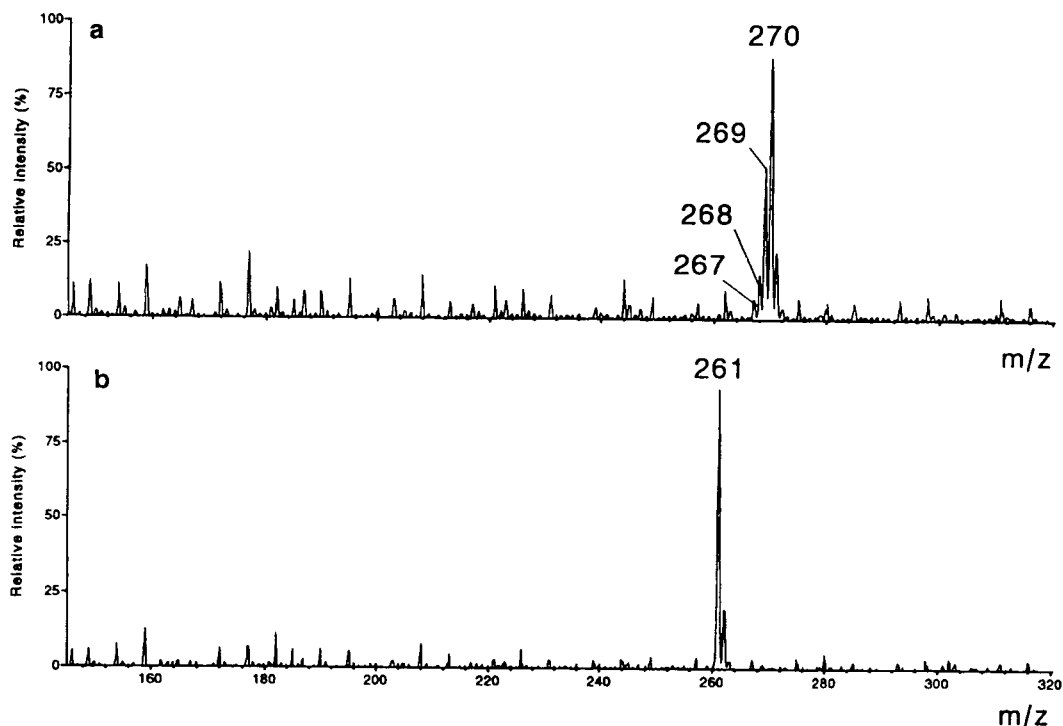


Fig. 2. Electro spray mass spectra of oxymetazoline (b) and its labeled analogue, $[^2\text{H}_9]$ oxymetazoline (a). Flow injection analysis with acetonitrile–2 mM ammonium acetate (50:50) at 40 $\mu\text{l}/\text{min}$.

to be primarily chemical noise from the mobile phase. No evidence of fragmentation of $[\text{M} + \text{H}]^+$, using these conditions, was noted.

Since the original intent of this work was to detect the analyte using selected reaction monitoring (SRM) MS–MS techniques, daughter ion spectra using these $[\text{M} + \text{H}]^+$ ions as parents were next obtained (Fig. 3). Unfortunately, daughter ions found in these MS–MS spectra could not be abundantly formed. No experimental conditions, using the open collision cell (Q2), could be found for this highly conjugated compound that would create daughter ions with high enough efficiency to allow sensitive detection using an SRM scheme.

Since MS–MS detection was not feasible, single MS detection (SIM) was utilized. This detection mode, with the described sample preparation, still allowed rapid sample elution and detection. An example of this is illustrated in Fig. 4 where HPLC–ES–MS chromatogram SIM traces for a 2.17 ng/g spike of oxymetazoline

with 50 ng IS- d_9 in rat blood are displayed. For comparison, a SIM trace (m/z 261) for a blank sample spiked with 50 ng IS- d_9 is superimposed on the 2.17 ng/g spiked sample trace. Although there is noticeable peak tailing (asymmetry factor 2.0, calculated by method of Foley and Dorsey [19]), likely due to interaction of the nitrogen containing ring with residual silanols on the silica packing, use of the Zorbax Rx column permits elution of this basic compound without the use of additional mobile phase modifiers (e.g., triethylamine) that would decrease sensitivity of the $[\text{M} + \text{H}]^+$ signal.

Table 3 summarizes the results of all validation and QC analyses. The limit of quantitation of the method, with a 0.30-g sample, was 1.0 ng/g.

3.3. Pharmacokinetic results

Typical blood PHK profiles of oxymetazoline in rats generated from i.v. and i.n. dosings of the drug in saline solution are shown in Fig. 5 (40

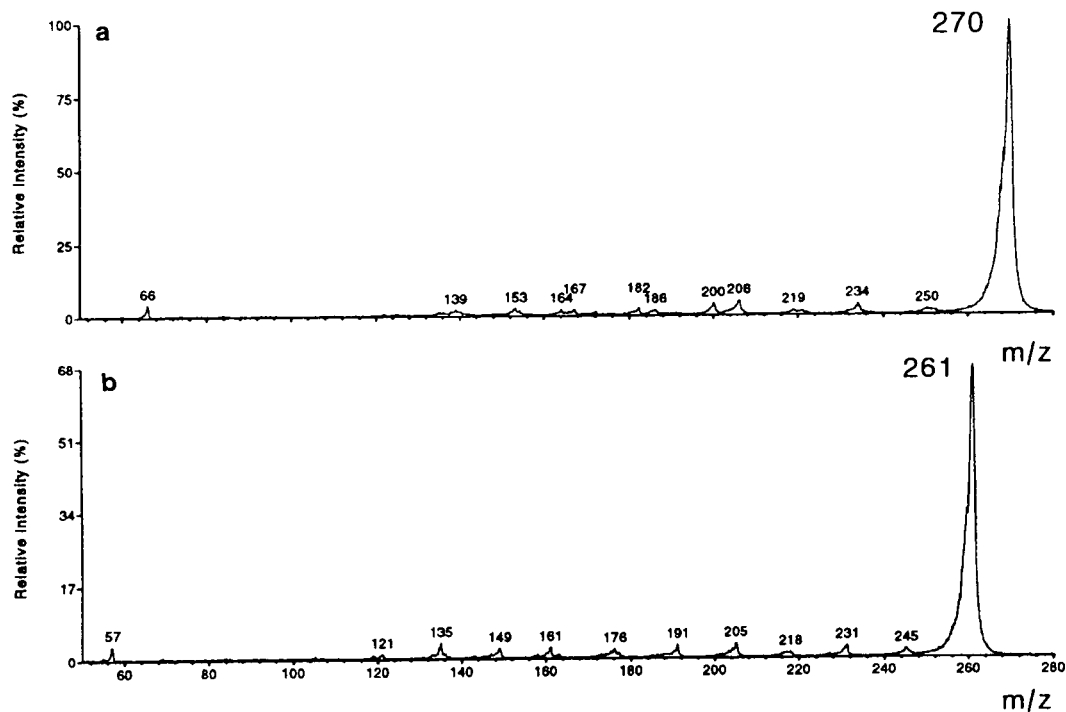


Fig. 3. Electrospray tandem mass spectra (daughters of MH^+) of oxymetazoline (b) and its labeled analogue, $[^2H_9]$ oxymetazoline (a). Flow injection analysis with acetonitrile–2 mM ammonium acetate (50:50) at 40 μ l/min.

μ g/dose). Blood samples (typically less than 300 μ l) were taken serially following administration of the drug. Fig. 5 illustrates the dramatic differences in blood levels delivered by the two administration routes. The results show that oxymetazoline is not extensively absorbed into the systemic circulation of rats from the intranasally dosed saline solution. The bioavailability of oxymetazoline delivered by the i.n. dosing ($n = 4$) was 6.8%. This was calculated using areas under the curves (0–90 min time points) for the i.n. and i.v. administrations.

4. Discussion

Although it is not particularly thermally labile, oxymetazoline must be derivatized prior to GC analysis because of its polar characteristics. Even then, the trimethylsilylated derivative (TMS₂-oxymetazoline) will interact with the active sites in the heated chromatographic system, thereby

becoming a limiting factor for trace-level determinations (data not shown). However, oxymetazoline can be subjected to HPLC separation using column packings that contain less acidic residual silanols (e.g., Zorbax Rx) and introduced to the mass spectrometer via the ES interface in its free-base (underivatized) form.

Although low level detection of oxymetazoline by HPLC–MS–MS using the open collision cell was not feasible, MS detection with SIM permitted development of an assay with the limit of quantitation (1 ng/g in whole blood) necessary for this application. This detection mode, even with the single liquid–liquid extraction, still allowed rapid sample elution and detection without the need for chemical derivatization.

Subsequent to the PHK study described above, additional sample preparation experiments led to a significant improvement in the level of analyte that could be accurately quantitated if larger samples were available. Briefly, a solid-phase extraction with Bakerbond C₁₈ solid-

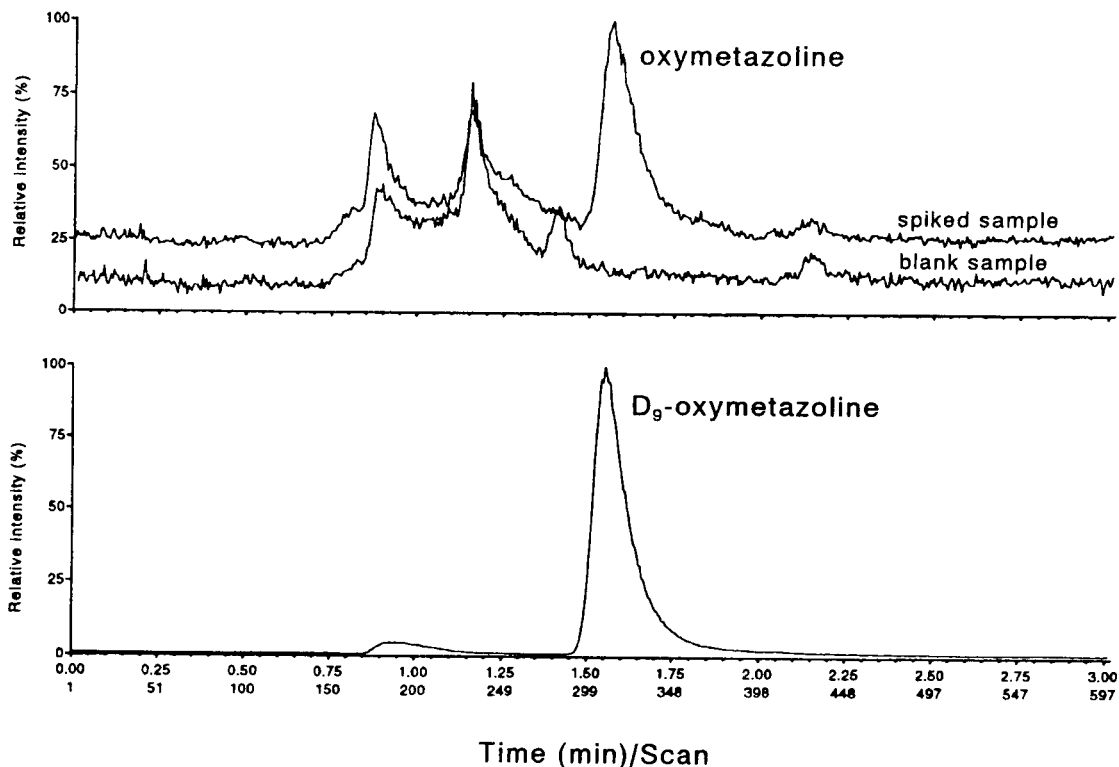


Fig. 4. HPLC-ES-MS chromatogram traces using selected ion monitoring of extracts for 2.17 ng/g oxymetazoline (top, m/z 261) with 50 ng/g [$^2\text{H}_9$]oxymetazoline (bottom, m/z 270) spiked into 0.30 g rat blood. The relative intensity signal for the superimposed blank extract trace (top, m/z 261) is offset 12.5% for comparison.

phase extraction cartridges (J.T. Baker, Pittsburgh, PA, USA) was performed following the initial liquid-liquid extraction. Feasibility studies using 2.0-ml samples of human serum (Sigma, St. Louis, MO, USA) showed that 200 pg/ml oxymetazoline could be readily quantitated.

The collision cell (Q2) used in this work was

Table 3

Accuracy and precision for validation and QC matrix spikes by HPLC-ES-MS

Spiked (ng)	n	Recovered (ng)	Accuracy (%)	R.S.D. (%)
Blank	13	0.053		
0.56	28	0.62	111	19.2
2.17	33	2.30	106	11.9
10.84	28	11.09	102	6.59
51.90	10	51.39	99	3.54

the original open cell design. An improved, closed cell has since become available for the PE-Sciex instrumentation. The possibility of an

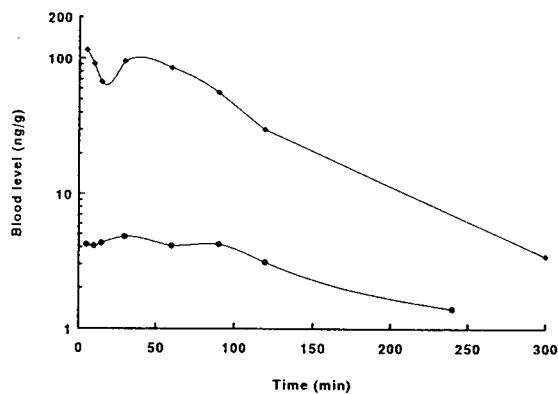


Fig. 5. Pharmacokinetic profiles of oxymetazoline generated from 40 μg i.v. (upper trace) and i.n. (lower trace) solutions administered to rats ($n = 4$).

MS–MS detection scheme for this analyte using the new enclosed collision cell has not been fully explored. However, this improved collision cell does provide enhanced production of product ions. It is reasonable to believe that greater sensitivity could be achieved with an SRM scheme using the new collision cell through better discrimination against matrix interferences.

5. Conclusions

The results of the work described here illustrate the potential of HPLC–ES–MS-based technology for quantitative determination of polar drugs, such as oxymetazoline, in biological matrices. The HPLC–MS approach with ES interfacing permitted the development of a rapid assay without the need for derivatization. The assay provided the requisite sensitivity to accurately define the blood pharmacokinetic profiles of oxymetazoline in rats dosed intravenously and intranasally with the drug. This was especially critical for the i.n. administration route in saline solution because of low sample volumes (typically less than 300 μ l) due to serial blood sampling from the same animal and the poor nasal absorption of oxymetazoline in this model.

Acknowledgements

The authors gratefully acknowledge Stanislaw Pikul and Greg A. Switzer for synthesis of the deuterated oxymetazoline internal standard used in this work.

References

- [1] S. Gizurarson, *Acta Pharm. Nord.*, 2 (1990) 105.
- [2] Y.W. Chien, K.S.E. Su and S. Chang, in J. Swarbrick (Editor), *Nasal Systemic Drug Delivery*, Marcel Dekker, New York, 1989, Ch. 1, p. 1.
- [3] D.E. Cowen, *Ear Nose Throat J.*, 45 (1966) 58.
- [4] E. Duzman, J. Anderson, J.B. Vita, J.C. Lue, C. Chen and I.H. Leopold, *Arch. Ophthalmol.*, 101 (1983) 1122.
- [5] A.P. De Leenheer and L.M. Thienpont, *Mass Spectrom. Rev.*, 11 (1992) 249.
- [6] R.L.M. Dobson, D.M. Neal, B.R. DeMark and S.R. Ward, *Anal. Chem.*, 62 (1990) 1819.
- [7] R.L.M. Dobson, G.R. Kelm and D.M. Neal, *Biol. Mass Spectrom.*, 23 (1994) 75.
- [8] K.B. Tomo and C.E. Parker, *J. Chromatogr.*, 492 (1989) 189.
- [9] P. Arpino, *Mass Spectrom. Rev.*, 8 (1989) 35.
- [10] C.R. Blakely and M.L. Vestal, *Anal. Chem.*, 55 (1983) 750.
- [11] P. Arpino, *Mass Spectrom. Rev.*, 9 (1990) 631.
- [12] R.C. Willoughby and R.R. Browner, *Anal. Chem.*, 56 (1984) 2626.
- [13] P.C. Winkler, D.D. Perkins, W.K. Williams and R.F. Browner, *Anal. Chem.*, 60 (1988) 489.
- [14] C.M. Whitehouse, R.N. Drego, M. Yamashita and J.B. Fenn, *Anal. Chem.*, 57 (1985) 675.
- [15] J.B. Fenn, M. Mann, C.K. Meng, S.F. Wong and C.M. Whitehouse, *Mass Spectrom. Rev.*, 9 (1990) 37.
- [16] A.P. Bruins, T.R. Covey and J.D. Henion, *Anal. Chem.*, 59 (1987) 2642.
- [17] T.R. Covey, E.D. Lee and J.D. Henion, *Anal. Chem.*, 58 (1986) 2453.
- [18] G.D. Fasman (Editor), *CRC Handbook of Biochemistry and Molecular Biology*, Vol. 1, CRC Press, Boca Raton, 3rd ed., 1976, p. 334.
- [19] J.P. Foley and J.G. Dorsey, *Anal. Chem.*, 55 (1983) 730.

Hydrophobicity parameter from high-performance liquid chromatography on an immobilized artificial membrane column and its relationship to bioactivity

Antoni Nasal, Małgorzata Sznitowska, Adam Buciński, Roman Kaliszan*

Faculty of Pharmacy, Medical Academy of Gdańsk, Gen. J. Hallera 107, 80-416 Gdańsk, Poland

Abstract

There are numerous measures of hydrophobicity employed in the quantitative structure–bioactivity relationship studies. Individual bioactivity parameters may appear best predicted by the specific hydrophobicity parameters. Introduction of an original reversed-phase material, the immobilized artificial membranes (IAMs) opened new perspectives for bioactivity predictions in the case of the hydrophobicity-driven processes. Comparative studies of performance of the HPLC-derived hydrophobicity measures demonstrate the advantages of the IAM-derived hydrophobicity parameters in predicting the human skin permeation by non-ionizable agents as exemplified by steroid hormones. On the other hand, the skin permeation data of agents ionized at physiological pH appeared less dependent of the retention on IAMs. The IAM columns increase the means of characterization of various aspects of hydrophobicity. Their advantages over the slow equilibrium methods of hydrophobicity determination are the simplicity of operation and the suitability of the generated retention measures for predicting specific bioactivity parameters.

1. Introduction

The *n*-octanol–water liquid–liquid partition system is the common reference system providing the most popular scale of hydrophobicity, i.e., logarithm of partition coefficient, $\log P$ [1]. Although the *n*-octanol–water system cannot be assumed the best possible model for all biological permeation barriers and receptor binding sites, large compilations of $\log P$ data [2] form the basis for many satisfactory bioactivity predictions. On the other hand, tediousness and poor reproducibility of hydrophobicity determination

by the slow equilibration methods called the attention of researchers towards reversed-phase high-performance liquid chromatography (RP-HPLC) as a tool for a convenient assessment of relative hydrophobicities within a series of solutes.

The RP-HPLC systems commonly applied for hydrophobicity determination employ octanol-like or hydrocarbonaceous stationary phase materials [3]. Recently, a new RP-HPLC stationary phase material became available which models natural membranes, namely the so-called immobilized artificial membrane (IAM) [4]. The IAM phases form confluent monolayers of immobilized membrane lipids (lecithin), wherein each lipid molecule is covalently bound to propylamine-silica. Unreacted propylamine moieties

* Corresponding author.

can additionally be end-capped with methylglycolate. Membrane lipids possess polar headgroups and two non-polar chains. One of the alkyl chains is linked to the propylamine-silica surface. The immobilized lipid headgroups protrude away from the stationary phase surface and are the first contact site between solutes and IAM [5].

Preliminary studies have demonstrated a good correlation between retention data determined on IAMs and human skin permeation for short series of alcohols and steroids. The same biological data showed poor correlation with chromatographic retention parameters determined on a regular hydrocarbonaceous reversed-phase column [4,5]. Kaliszan et al. [6] demonstrated weak correlations ($R = 0.8$) between retention data determined on the IAM-type columns and the reference hydrophobicity measure, $\log P$, for a series of psychotropic and antihistamine drugs. There was also a very weak correlation between the logarithm of the capacity factor from the IAM column, $\log k'_{IAM}$, and the extrapolated to pure buffer eluent logarithm of capacity factor determined on a deactivated hydrocarbonaceous silica column [6]. Recently, Kaliszan et al. [7] reported high correlation between $\log k'_{IAM}$ determined with buffers of physiological pH and the ionization-corrected reference hydrophobicity parameter from the *n*-octanol–water system for a group of β -adrenolytics ($R = 0.962$) and a poorer correlation ($R = 0.839$) for a series of phenothiazines. Regression analysis of several pharmacokinetic and other bioactivity data for the agents under study in terms of hydrophobicity parameters demonstrated the performance of $\log k'_{IAM}$ to be as good as that of the reference hydrophobicity parameters in predicting of the activity of drugs within biophase.

In this report we further confirm the observation that retention data determined in a simple, fast and reproducible manner on IAM columns comprise information on properties of series of xenobiotics which are distinctive from those provided by the *n*-octanol–water systems. We compare the performance of different hydrophobicity scales in predicting a human skin permeability.

2. Experimental

2.1. Materials

Three test series of the compounds were analyzed: steroid hormones, phenolic derivatives and a group of agents known to permeate skin in an ionized form.

The following steroids were chromatographed: estradiol, estriol, estrone, hydrocortisone, pregnenolone, progesterone, testosterone (all from Sigma, St. Louis, MO, USA), aldosterone, cortisone and deoxycorticosterone (all from Koch-Light Labs., Colnbrook, UK).

The test group of phenolic compounds was made up of the following derivatives: *p*-bromophenol, chlorocresol, *p*-chlorophenol, *o*-cresol, *m*-cresol, *p*-cresol, *p*-ethylphenol, *m*-nitrophenol, *p*-nitrophenol (all from Aldrich, Steinheim, Germany), methylhydroxybenzoate (Unia Labs., Warsaw, Poland), β -naphthol, phenol, resorcinol, thymol (POCh, Gliwice, Poland).

The group of solutes ionizable at physiological conditions consisted of: baclofen (Polfa, Starogard, Poland), L-phenylalanine, L-tyrosine, L-tryptophan (all from Sigma), sodium salicylate (Polfa).

2.2. Human skin permeation data

Logarithms of permeability coefficient, $\log K_p$, had been chosen as measures of skin permeability by various solutes.

The human skin permeation data ($\log K_p$) of steroid hormones were taken from Scheuplein et al. [8]. The permeability data of phenolic compounds across human epidermis were taken from Roberts et al. [9]. The respective skin permeation data for the test series of ionizable agents were found in Ruland and Kreuter [10], Mazenga et al. [11] and Kurihara-Bergstrom et al. [12].

2.3. Reference partition coefficients

The human skin–water partition coefficient data ($\log P_m$) for a group of steroid hormones

were found in literature [8]. Reference *n*-octanol–water partition coefficients for the three series of test compounds were taken from Refs. [2], [13] and [14].

2.4. Determination of hydrophobicity by HPLC on an IAM column

The column used was formed by 1-myristoyl-2-[(13-carboxyl)-tridecoyl]-*sn*-3-glycerophosphocholine (lecithin-COOH) bonded to silica-propylamine with the unreacted propylamine moieties end-capped with methylglycolate. A commercially distributed IAM.PC.MG 150 × 4.6 mm I.D. column was purchased from Regis (Morton Grove, IL, USA). The column was characterized by particle diameter 12 μm and pore diameter 300 Å.

The chromatographic system consisted of a Model L-6200A pump, a Model L-4250 UV–VIS detector and a Model D-2500 chromato-integrator (all from Merck–Hitachi, Vienna, Austria). The experiments were carried out at ambient temperature using a flow-rate of 1 ml/min.

Test series of steroids and phenols were chromatographed with acetonitrile–0.1 M sodium phosphate buffer pH 6.0 (5:95, v/v) eluent. Detection wavelength varied for individual solutes. The compounds studied were injected into the column after dissolution in methanol. In case

of the test series of highly ionizable solutes the eluent was pure buffer without organic modifier.

Capacity factors, k'_{IAM} , were calculated assuming as the dead volume of the column a solvent disturbance signal given by methanol.

2.5. Statistical procedure

Quantitative relationships between human skin permeability coefficients and hydrophobicity parameters of the compounds analyzed were studied by a multiple regression analysis method. A standard, commercially available statistical package was employed using a personal computer. Requirements for meaningful regression analysis [15] were observed.

3. Results and discussion

The first set of solutes studied comprised a series of steroid hormones for which the reference hydrophobicity data: *n*-octanol–water partition coefficient ($\log P_{oct}$) and human skin–water partition coefficient ($\log P_m$) were found in the literature [8,13]. Respective data are collected in Table 1 along with the chromatographic hydrophobicity parameter obtained on the IAM column, $\log k'_{IAM}$, and the human skin permeation data, $\log K_p$.

Table 1
Human skin permeability coefficients ($\log K_p$, $\log P_m$) and hydrophobicity parameters ($\log k'_{IAM}$, $\log P_{oct}$) of a group of steroid hormones

No.	Compound	$\log K_p^a$	$\log P_m^a$	$\log k'_{IAM}$	$\log P_{oct}^b$
1	Aldosterone	−9.08	0.83	0.649	1.08
2	Cortisone	−8.56	0.93	0.772	1.42
3	Deoxycorticosterone	−6.90	1.57	1.730	2.88
4	Estradiol	−7.08	1.66	2.179	2.69
5	Estriol	−7.95	1.36	1.368	2.47
6	Estrone	−6.00	1.66	2.001	2.76
7	Hydrocortisone	−9.08	0.85	0.843	1.53
8	Pregnenolone	−6.38	1.70	2.124	3.13
9	Progesterone	−6.38	2.01	2.199	3.70
10	Testosterone	−6.95	1.36	1.693	3.31

^a K_p (cm s^{−1}) and P_m according to Scheuplein et al. [8].

^b According to El Tayar et al. [13].

The relationship between $\log K_p$ and $\log k'_{IAM}$ for the steroids is given by the equation:

$$\log K_p = -10.19(\pm 0.37) + 1.77(\pm 0.22) \log k'_{IAM}$$

$$n = 10, R = 0.942, p < 5 \cdot 10^{-5} \quad (1)$$

where n is the number of data points used to derive regression equation, R is the correlation coefficient, p is the significance level and numbers in parentheses denote the standard deviations of individual regression coefficients. Good quality of correlation provided by Eq. 1 is illustrated in Fig. 1a.

The corresponding equation which describes $\log K_p$ in terms of $\log P_{oct}$ has the form:

$$\log K_p = -10.39(\pm 0.53) + 1.18(\pm 0.20) \log P_{oct}$$

$$n = 10, R = 0.900, p < 4 \cdot 10^{-4} \quad (2)$$

Correlation between the observed $\log K_p$ data and the data calculated by Eq. 2 is illustrated in Fig. 1b. Good statistical quality of both Eqs. 1 and 2 can be explained by the fact that the hydrophobicity parameters, $\log k'_{IAM}$ and $\log P_{oct}$, are evidently intercorrelated ($R = 0.911$). However, as evident from Fig. 1 the $\log k'_{IAM}$ is a better predictor of skin permeation than $\log P_{oct}$.

For the group of hormones analyzed a highly significant correlation between the skin–water partition coefficient ($\log P_m$) and hydrophobicity parameter determined on the IAM column, $\log k'_{IAM}$, has also been observed:

$$\log P_m = 0.40(\pm 0.10) + 0.64(\pm 0.06) \log k'_{IAM}$$

$$n = 10, R = 0.966, p < 10^{-5} \quad (3)$$

The corresponding equation describing $\log P_m$ in terms of $\log P_{oct}$ has the form:

$$\log P_m = 0.33(\pm 0.17) + 0.42(\pm 0.06) \log P_{oct}$$

$$n = 10, R = 0.917, p < 2 \cdot 10^{-4} \quad (4)$$

Previously Raykar et al. [16] reported correlation between $\log P_{oct}$ and $\log P_m$. The high statistical quality of Eqs. 3 and 4 proves that both $\log k'_{IAM}$ and $\log P_{oct}$ can be used to evaluate the partitioning of steroids between the water and the stratum corneum. Again, the \log

k'_{IAM} seems to be more reliable for this purpose than $\log P_{oct}$.

The permeability data of 14 phenolic compounds across human epidermis and the reference hydrophobicity data taken from El Tayar et al. [13] are given in Table 2 along with the chromatographic hydrophobicity parameters obtained on the IAM column, $\log k'_{IAM}$.

Eq. 5 describes the parabolic relationship between an epidermis permeability coefficient, $\log K_p$, and the $\log P_{oct}$ proposed by the original authors:

$$\log K_p = -8.71(\pm 0.48) - 0.37(\pm 0.10)$$

$$\cdot (\log P_{oct})^2$$

$$+ 2.38(\pm 0.46) \log P_{oct}$$

$$n = 14, R = 0.943, s = 0.22 \quad (5)$$

A lower correlation was observed between $\log K_p$ and a chromatographically determined hydrophobicity parameter, $\log k'_{IAM}$:

$$\log K_p = -6.16(\pm 0.20) - 0.46(\pm 0.37)$$

$$\cdot (\log k'_{IAM})^2$$

$$+ 1.54(\pm 0.47) \log k'_{IAM}$$

$$n = 14, R = 0.797, s = 0.40 \quad (6)$$

The linear relationship between $\log K_p$ and the hydrophobicity measures $\log P_{oct}$ and $\log k'_{IAM}$, have the forms, respectively:

$$\log K_p = -7.20(\pm 0.29) + 0.81(\pm 0.13) \log P_{oct}$$

$$n = 14, R = 0.876, p < 4 \cdot 10^{-5} \quad (7)$$

$$\log K_p = -6.09(\pm 0.20) + 1.05(\pm 0.26) \log k'_{IAM}$$

$$n = 14, R = 0.765, p < 10^{-3} \quad (8)$$

In case of this data set $\log P_{oct}$ appears to be a better bioactivity predictor than $\log k'_{IAM}$. It has to be noted, however, that a difference between the two hydrophobicity measures is mostly due to the single solute, namely resorcinol. Its $\log K_p$ deviates evidently from the remaining solutes. $\log P_{oct}$ appears to better account for this deviation but it may be fortuitous.

The available skin permeation and reference hydrophobicity data for a series of agents known to permeate skin in an ionized forms are col-

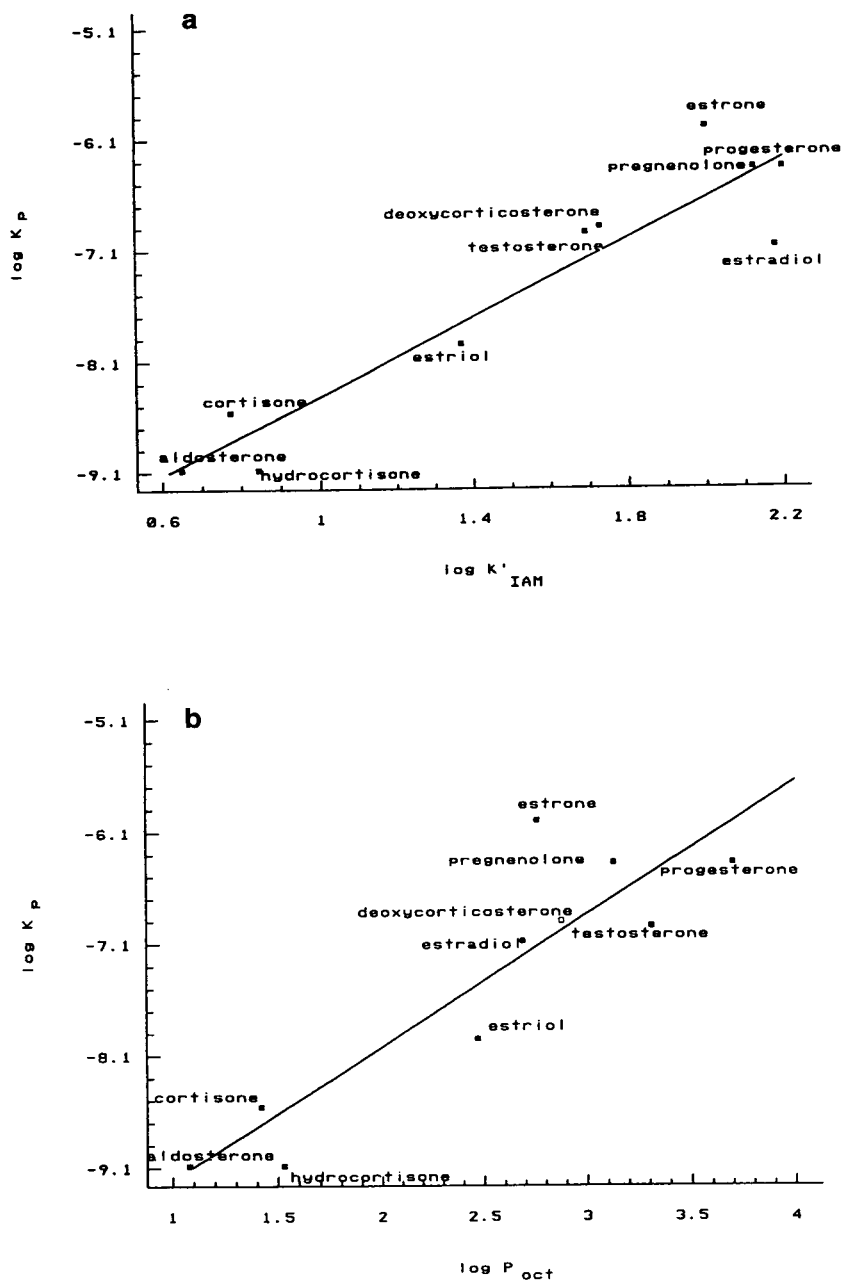


Fig. 1. Correlation between the human skin permeation data of steroid hormones observed by Scheuplein et al. [8], $\log K_p$, and (a) logarithm of chromatographic capacity factor determined on an immobilized artificial membrane column, $\log k'_{IAM}$ or (b) logarithm of *n*-octanol–water partition coefficient according to Craig [2], $\log P_{oct}$.

Table 2
Human skin permeability data ($\log K_p$) and hydrophobicity parameters ($\log k'_{IAM}$, $\log P_{oct}$) of phenolic compounds

No.	Compound	$\log K_p^a$	$\log k'_{IAM}$	$\log P_{oct}^b$
1	<i>p</i> -Bromophenol	-5.00	0.995	2.59
2	Chlorocresol	-4.82	1.183	3.10
3	<i>p</i> -Chlorophenol	-5.00	0.728	2.39
4	<i>o</i> -Cresol	-5.36	0.363	1.95
5	<i>m</i> -Cresol	-5.37	0.363	1.96
6	<i>p</i> -Cresol	-5.31	0.418	1.94
7	<i>p</i> -Ethylphenol	-5.01	0.761	2.37
8	Methylhydroxybenzoate	-5.60	0.520	1.96
9	β -Naphthol	-5.11	1.254	2.84
10	<i>m</i> -Nitrophenol	-5.81	0.598	2.00
11	<i>p</i> -Nitrophenol	-5.81	0.595	1.91
12	Phenol	-5.64	0	1.46
13	Resorcinol	-7.18	-0.141	0.78
14	Thymol	-4.83	1.342	3.30

^a K_p in cm s^{-1} according to Roberts et al. [9].

^b According to El Tayar et al. [13].

lected in Table 3. Correlation between $\log k'_{IAM}$ and $\log K_p$ is significant ($R = 0.903$) and that between $\log P$ and $\log K_p$ is meaningless ($R = 0.136$). Unfortunately, the number of the available data points is highly limited and the correlation observed may be fortuitous.

It is hypothesized that for ionized penetrants another mechanism of skin absorption operates. A porous pathway is supposed and aqueous solubility, not the hydrophobic–hydrophilic partition equilibrium, to determine the rate of skin permeation by ions [11,17].

Hydrophobicity is a complex property depending both on the molecular structure of the solute and on the environment in which it is actually

placed. There is no a single, universal hydrophobicity measuring system which could be recommended in every case of structure–bioactivity relationships. Perhaps particular properties of the IAM phases allow for some modeling of skin permeation. Contrary to the standard hydrophobic phases, the IAMs possess polar headgroups being the first site of contact with interacting solutes similarly to natural biomembranes. That first interaction would be of a polar (hydrophilic) nature. If it would be decisive for skin permeation of polar, water-soluble agents then the observed correlation between $\log k'_{IAM}$ and $\log K_p$ is not by chance but real. It is highly probable, however, that the IAM phase is unable to

Table 3
Human skin permeability data ($\log K_p$) and hydrophobicity parameters ($\log k'_{IAM}$, $\log P_{oct}$) of ionized agents

No.	Compound	$\log K_p^a$	$\log k'_{IAM}$	$\log P_{oct}^b$
1	Baclofen	-6.77	-0.725	-0.96
2	Phenylalanine	-8.08	-0.646	-1.35
3	Sodium salicylate	-7.82	-0.575	2.26 ^c
4	Tyrosine	-8.14	-0.545	-2.26
5	Tryptophan	-8.39	-0.412	-1.04

^a K_p in cm s^{-1} according to Ruland and Kreuter [10], Mazzenga et al. [11] and Kurihara-Bergstrom et al. [12].

^b According to Craig [2] and Hansch and Leo [14].

^c Value reported for salicylic acid.

account for the hydrophobicity differences among readily ionized compounds. Such compounds elute too close to the non-retained markers to make their relative retention data reliable. The correlations reported here will further be tested with the additional skin permeability data currently prepared by us.

In conclusion we would like to emphasize that the new IAM columns allow for a fast and convenient characterization of hydrophobicity of xenobiotics. Our results supply the evidence in support of the hypothesis that HPLC hydrophobicity measures determined on IAM columns may provide different (and more significant in individual cases) input to the description of individual hydrophobicity-affected bioactivity data than the standard hydrophobicity parameters [7]. This could be rationalized in terms of a closer similarity of the IAM structure to the biophase-forming species than in the case of an n-octanol–water system.

Certainly the hypothesis on the general advantage of the HPLC scale determined on IAM columns for molecular pharmacology and pharmacokinetics requires further testing. However, there is an unquestionable advantage of the approach recommended here: it is much easier to obtain precise and reproducible hydrophobicity measures by the means of an IAM column than by the standard shake-flask or by the octanol-like HPLC approaches.

Acknowledgement

Support for this research by the Komitet Badań Naukowych, Warsaw, Poland (Project No. 408319101) is acknowledged.

References

- [1] C. Hansch and T. Fujita, *J. Am. Chem. Soc.*, 86 (1964) 1616.
- [2] P.N. Craig, in C.J. Dayton (Editor), *Comprehensive Medicinal Chemistry*, Vol. 6, Pergamon Press, Oxford, 1992, pp. 237–991.
- [3] R. Kaliszan, *Quantitative Structure–Chromatographic Retention Relationships*, Wiley, New York, 1987.
- [4] H. Turnhofer, J. Schnabel, M. Betz, G. Lipka, C. Pidgeon and H. Hauser, *Biochim. Biophys. Acta*, 1064 (1991) 275.
- [5] C. Pidgeon, C. Marcus and F. Alvarez, in T.D. Baldwin and J.W. Kelly (Editors), *Applications of Enzyme Biotechnology*, Plenum Press, New York, 1992, pp. 201–220.
- [6] R. Kaliszan, A. Kaliszan and I.W. Wainer, *J. Pharm. Biomed. Anal.*, 11 (1993) 505.
- [7] R. Kaliszan, A. Nasal and A. Buciński, *Eur. J. Med. Chem.*, 29 (1994) 163.
- [8] R.J. Scheuplein, H. Blank, G.J. Brauner and D. MacFarlane, *J. Invest. Dermatol.*, 52 (1969) 63.
- [9] M.S. Roberts, R.A. Anderson and J. Swarbrick, *J. Pharm. Pharmacol.*, 29 (1977) 677.
- [10] A. Ruland and J. Kreuter, *Int. J. Pharm.*, 72 (1991) 149.
- [11] G.C. Mazzenga, B. Berner and F. Jordan, *J. Controlled Release*, 20 (1992) 163.
- [12] T. Kurihara-Bergstrom, K. Knutson, L.J. DeNoble and C.Y. Goates, *Pharm. Res.*, 7 (1990) 762.
- [13] N. El Tayar, R.-S. Tsai, B. Testa, P.-A. Carrupt, C. Hansch and A. Leo, *J. Pharm. Sci.*, 80 (1991) 744.
- [14] C. Hansch, A. Leo, *Substituent Constants for Correlation Analysis in Chemistry and Biology*, Wiley, New York, 1979.
- [15] M.S. Charton, S. Clementi, S. Ehrenson, O. Exner, J. Shorter and S. Wold, *Quant. Struct. Act. Relat.*, 4 (1985) 29.
- [16] P.V. Raykar, M.-C. Fung, B.D. Anderson, *Pharm. Res.*, 5 (1988) 140.
- [17] G. Flynn, in R.L. Bronaugh and H.I. Maibach (Editors), *Percutaneous Absorption: Mechanism — Methodology — Drug Delivery*, Marcel Dekker, New York, 1989, p. 27.



ELSEVIER

Journal of Chromatography A, 692 (1995) 91–96

JOURNAL OF
CHROMATOGRAPHY A

Unusual examples of the liquid chromatographic resolution of racemates

Resolution of π -donor analytes on a π -donor chiral stationary phase

Myung Ho Hyun*, Jae-Jeong Ryoo, Yoon Jae Cho, Jong Sung Jin

Department of Chemistry, Pusan National University, Pusan 609-735, South Korea

Abstract

A π -basic chiral stationary phase (CSP) derived from (*S*)-1-(6,7-dimethyl-1-naphthyl)isobutylamine was used for the resolution of the enantiomers of π -basic 3,5-dimethylanilide derivatives of non-steroidal anti-inflammatory drugs related to α -arylpropionic acids. The separation factors are large enough for analytical purposes, baseline resolution being obtained. From the resolution of 3,5-dimethylanilide, N-methyl-3,5-dimethylanilide, N-alkylamide and N,N-dialkylamide derivatives of naproxen, it was concluded that the π -basic aryl derivatizing group plays a role as a hydrogen bond acceptor in the chiral recognition process and the amide NH hydrogen of analytes is essential for chiral recognition.

1. Introduction

Pirkle-type chiral stationary phases (CSPs) typically resolve the enantiomers of racemic analytes through π -donor–acceptor interactions between the CSP and the analyte [1–3]. To utilize π -donor–acceptor interactions, Pirkle-type CSPs incorporate π -acidic and/or π -basic aryl functional groups to interact with complementary aryl groups in the analytes. Racemic analytes which lack π -acidic or π -basic aryl functional groups are commonly derivatized with achiral π -acidic or π -basic reagents. CSPs containing π -acidic aryl groups have been used for the resolution of the enantiomers of π -basic

analytes [4,5]. Similarly, CSPs containing π -basic aryl groups have been used for the resolution of the enantiomers of π -acidic analytes [6]. CSPs containing both of π -acidic and π -basic aryl groups have been utilized to resolve either π -basic or π -acidic analytes [7,8]. In each case, a π – π interaction between the CSP and the analyte is believed to play an important role in chiral recognition. In the absence of π – π interaction, the ability to separate enantiomers on Pirkle-type CSPs is expected to be greatly reduced. Accordingly, the resolution of π -acceptor racemates on π -acceptor CSPs or the resolution of π -donor racemates on π -donor CSPs is of some interest in that they are unexpected.

The resolution of π -acceptor racemates on π -acceptor CSPs has been reported. For exam-

* Corresponding author.

ple, Lienne et al. [9] reported that N-(3,5-dinitrobenzoyl) derivatives of α -aminoamides or α -amino esters (π -acceptor racemates) are resolved with reasonable separation factors on the π -acceptor CSP derived from N-(3,5-dinitrobenzoyl)-(*S*)-tyrosine. However, it should be noted that the π -basic aryl group present in Tambute's CSP may conceivably serve as a π -donor in the chiral recognition process. In contrast, the resolution of π -donor analytes on π -donor CSPs with more than marginal separation factors has not been reported except for the resolution of the enantiomers of arylhydantoin on N-aryl- α -amino acid CSPs described in a thesis [10]. The recent report by Oliveros et al. [11] of the resolution of some π -donor analytes on π -donor CSPs has been questioned by Pirkle et al. [12] and aroused our attention in this area.

In this paper, we report that CSP **1**, widely used for the resolution of a variety of π -acidic racemates [13–17], can be successfully used for the resolution of the enantiomers of the 3,5-dimethylanilide derivatives of non-steroidal anti-inflammatory drugs (NSAIDs) related to α -arylpropionic acids. This study may provide good examples for the unusual liquid chromatographic resolution of π -donor analytes on π -donor CSPs.

2. Experimental

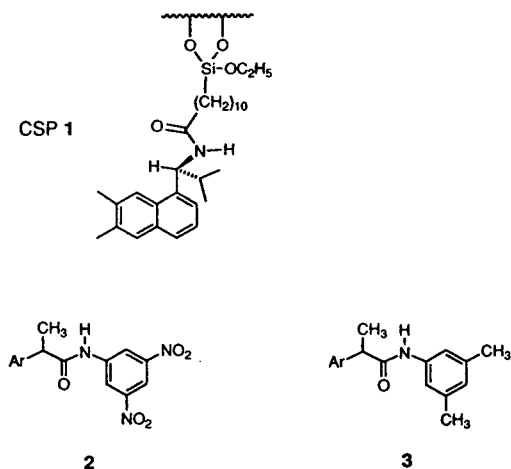
The HPLC system consisted of a Waters (Milford, MA, USA) Model 510 pump, a Rheodyne (Cotati, CA, USA) Model 7125 injector with a 20- μ l sample loop, a Youngin (Seoul, Korea) Model 710 absorbance detector with a 254-nm UV filter and a Youngin D520B computing integrator. All chromatographic data were obtained using 2-propanol–hexane (90:10) as the mobile phase at a flow-rate of 2.0 ml/min. The column void volume was measured by injecting 1,3,5-tri-*tert*-butylbenzene obtained from Regis (Morton Grove, IL, USA) [18].

A stainless-steel chiral HPLC column (250 mm \times 4.6 mm I.D.) packed with CSP **1** (support, Spherisorb 5- μ m silica gel; loading level, 0.21 mmol of chiral selector per gram of stationary phase based on either C or N) was available

from previous studies [15] and was used unchanged. Analytes were also available from previous studies or were prepared by treating acid chlorides with arylamines or alkylamines as described previously [19,20].

3. Results and discussion

CSP **1** has been used for the resolution of the 3,5-dinitroanilide derivatives, **2**, of NSAIDs related to α -arylpropionic acids [21]. In these resolutions, a chiral recognition mechanism utilizing a face-to-face π -donor–acceptor interaction, a face-to-edge π – π interaction and a hydrogen-bonding interaction between the CSP and the analytes was proposed [20]. Based on the chiral recognition mechanism proposed, the 3,5-dimethylanilide derivatives, **3**, of NSAIDs are expected to show little or no resolution on CSP **1** because of the lack of a π -acidic group in the type **3** analytes. Surprisingly, we found that CSP **1** resolves the enantiomers of the type **3** analytes with reasonable separation factors.



The chromatographic data for the resolution of the enantiomers of 3,5-dimethylanilide and 3,5-dinitroanilide derivatives of α -phenylpropionic acid and NSAIDs on CSP **1** are compared in Table 1. Retention factors, k' , for the resolution of the 3,5-dimethylanilide derivatives, **3**, on CSP **1** are much smaller than those of the 3,5-dinitroanilide derivatives **2**, as shown in

Table 1
Resolution of 3,5-dinitroanilide derivatives **2** and 3,5-dimethylanilide derivatives **3** of α -phenylpropionic acid and NSAIDs on CSP **1**

NSAID	2			3		
	k'_1	α	Conf.	k'_1	α	Conf.
α -Phenylpropionic acid	13.36	1.84	R	2.86	1.27	R
Ibuprofen	7.76	2.12	R	1.59	1.28	R
Naproxen	20.17	1.42	R	4.14	1.31	R
Fenoprofen	10.83	1.61		3.02	1.29	
Flurbiprofen	11.93	1.64		3.88	1.31	
Ketoprofen	10.10	2.00		3.95	1.23	
Alminoprofen	4.47	3.01		3.66	1.25	

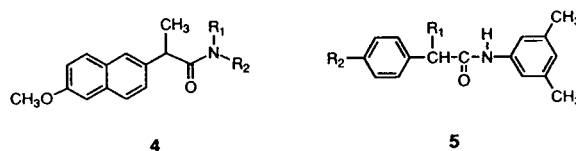
Conditions: mobile phase, 2-propanol–hexane (10:90); flow-rate, 2.0 ml/min; temperature, ambient. k'_1 = Retention factor for the first-eluted enantiomer; α = separation factor; Conf. = absolute configuration of the second-eluted enantiomer.

Table 1. The separation factors, α , are also lower when the derivatizing group is changed from the π -acidic 3,5-dinitroanilide to the π -basic 3,5-dimethylanilide. However, the separation factors for the 3,5-dimethylanilide derivatives, **3**, of NSAIDs on CSP **1** are large for CSP **1** to be used for analytical purposes. The elution orders shown in Table 1 were determined by comparing the chromatograms from racemic samples with those from optically active samples prepared from commercially available α -phenylpropionic acid, ibuprofen and naproxen. The elution orders for the 3,5-dimethylanilide derivatives, **3**, on CSP **1** determined in this way are in accord with those for the 3,5-dinitroanilide derivatives, **2**, as shown in Table 1.

To see the effect of the aryl derivatizing group on the resolution trends, various anilide derivatives of α -phenylpropionic acid, ibuprofen, naproxen and simple N-alkyl- and N,N-dialkylamide derivatives of naproxen were prepared and resolved on CSP **1**. The results from the chromatography of various anilide derivatives of α -phenylpropionic acid, ibuprofen and naproxen on CSP **1** are summarized in Table 2. One example is shown in Fig. 1. The results obtained by chromatographing simple N-alkyl- and N,N-dialkylamide derivatives, **4**, of naproxen on CSP **1** are given in Table 3. It is noted from Table 2

and Fig. 1 that the retention of both enantiomers decreases drastically as the derivatizing aryl group is changed from 3,5-dinitrophenyl to 3-nitrophenyl to phenyl itself. In contrast, the retention decreases only slightly as the aryl derivatizing group is changed from phenyl to 3-methylphenyl to 3,5-dimethylphenyl. In addition, the retention of a simple ethyl- or propylamide derivative of naproxen is comparable to that of a π -basic aryl derivative of naproxen, as noted from Tables 2 and 3. From these observations, it is presumed that the face-to-face π - π interaction between the π -basic aryl group of the CSP and the π -acidic aryl group such as 3,5-dinitrophenyl or 3-nitrophenyl of the analyte is the major component of the interactions leading to retention of the enantiomers. However, π -basic aryl derivatizing groups such as phenyl, 3-methylphenyl and 3,5-dimethylphenyl do not seem to contribute to a face-to-face π - π interaction between the CSP and the analyte. The slight decrease in retention as the aryl derivatizing group is changed from phenyl to 3-methylphenyl to 3,5-dimethylphenyl may come from the increased lipophilicity of the analyte.

The separation factors, α , also vary according to the aryl derivatizing group, as shown in Table 2. In general, the analytes containing a π -acidic aryl derivatizing group have larger separation factors than those containing a π -basic aryl derivatizing group. However, the analytes containing a π -basic aryl derivatizing group show baseline resolution with reasonably good separation factors, as shown in Fig. 1. It is interesting to note in Table 2 that changing the π -basic aryl derivatizing group does not have any notable effect on the separation factors of the enantiomers, indicating that the π -basicity or the bulkiness of the aryl derivatizing group plays no significant role in the chiral recognition.



Simple N-alkylamide derivatives of naproxen are also resolved on CSP **1** even though the

Table 2

Resolution of various anilide derivatives of (A) α -phenylpropionic acid, (B) ibuprofen and (C) naproxen on CSP 1

Parent	Ar	k'_1	k'_2	α	Conf.
A	3,5-Dimethylphenyl	2.86	3.62	1.27	R
	3-Methylphenyl	3.02	3.74	1.24	R
	Phenyl	3.46	4.22	1.22	R
	3-Nitrophenyl	5.58	8.00	1.43	R
	3,5-Dinitrophenyl	13.36	24.56	1.84	R
B	3,5-Dimethylphenyl	1.59	2.04	1.28	R
	3-Methylphenyl	1.64	2.11	1.29	R
	Phenyl	1.87	2.34	1.25	R
	3-Nitrophenyl	3.15	4.83	1.53	R
	3,5-Dinitrophenyl	7.76	16.45	2.12	R
C	3,5-Dimethylphenyl	4.14	5.43	1.31	R
	3-Methylphenyl	5.55	7.29	1.31	R
	Phenyl	6.43	8.41	1.31	R
	3-Nitrophenyl	10.53	15.21	1.44	R
	3,5-Dinitrophenyl	20.17	28.64	1.42	R

Conditions: mobile phase, 2-propanol–hexane (10:90); flow-rate, 2.0 ml/min; temperature, ambient. k'_1 = Retention factor for the first-eluted enantiomer; k'_2 = retention factor for the second-eluted enantiomer; α = separation factor; Conf. = absolute configuration of the second-eluted enantiomer.

separation factors, α , are small, as shown in Table 3. However, N,N-dialkylamide derivatives of naproxen are not resolved at all on CSP 1. Similarly, the N-methyl-3,5-dimethylanilide of naproxen is not resolved on CSP 1. It is also noted from Table 3 that variation in the length or the bulkiness of the N-alkyl substituent of an

N-alkylamide derivative of naproxen does not produce a marked effect on the separation factors.

From these results, it is presumed that the π -basic aryl derivatizing group does play a role

Table 3
Resolution of N-alkyl- and N,N-dialkylamide derivatives 4 and N-methyl-3,5-dimethylanilide of naproxen on CSP 1

4		k'_1	k'_2	α
R ₁	R ₂			
H	CH ₂ CH ₃	6.72	7.33	1.09
H	CH ₂ CH ₂ CH ₃	4.59	5.08	1.11
H	(CH ₂) ₆ CH ₃	2.42	2.71	1.12
H	C(CH ₃) ₃	2.20	2.46	1.12
CH ₂ CH ₃	CH ₂ CH ₃	1.98	1.98	1.00
CH(CH ₃) ₂	CH(CH ₃) ₃	0.88	0.88	1.00
CH ₃	3,5-Dimethylphenyl	0.88	0.88	1.00

Conditions: mobile phase, 2-propanol–hexane (10:90); flow-rate, 2.0 ml/min; temperature, ambient. k'_1 = Retention factor for the first-eluted enantiomer; k'_2 = retention factor for the second-eluted enantiomer; α = separation factor.

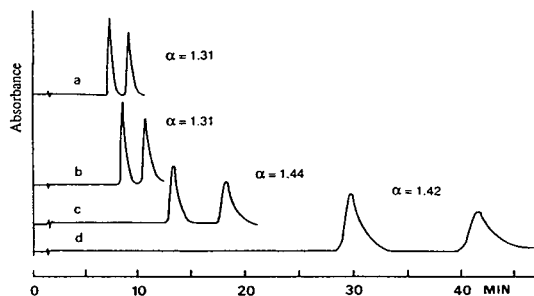


Fig. 1. Resolution of (a) 3,5-dimethylanilide, (b) anilide, (c) 3-nitroanilide and (d) 3,5-dinitroanilide derivatives of racemic naproxen on CSP 1. For chromatographic conditions, see Experimental.

in the chiral recognition of the NSAID derivatives on π -basic CSP 1. The role does not seem to be simply steric since π -basic aryl or N-alkyl groups of different size do not notably affect separation factors. However, hydrogen bonding interactions which utilize the π -basic aryl group as a hydrogen-bonding acceptor [22] could play a role in chiral recognition. It does seem that the amide NH is essential for chiral recognition of the analytes, as none of the tertiary amides of naproxen are resolved on CSP 1, as shown in Table 3. However, a definitive statement concerning the mechanism by which these enantiomers are separated on π -basic CSP 1 must await further study.

In order to obtain more information about the chiral recognition mechanism, the 3,5-dimethylanilides, **5**, a homologous series of α -(*p*-alkylphenyl) alkanolic acids, were prepared and resolved on CSP 1. In a previous study [20], we were able to provide a mechanistic rationale for the resolution of the 3,5-dinitroanilide derivatives of NSAIDs on CSP 1 by studying the chromatographic resolution of the enantiomers of 3,5-dinitroanilide derivatives of α -(*p*-alkylphenyl) alkanolic acids. Similarly, we thought that by variation of the length of the *p*-alkyl and α -alkyl substituents of the type **5** compounds, we might determine whether intercalation processes play a significant role in the chiral recognition of these analytes. However, variation of the lengths of these substituents has only a small effect on the separation factors for the enantiomers of the members of this series of analytes. These data are summarized in Table 4. Lengthening the α -alkyl group of **5** slightly diminishes the separation factors whereas lengthening the *p*-alkyl group of **5** slightly enhances the separation factors. Hence intercalation processes play no significant role in the chiral recognition of these analytes by CSP 1.

In conclusion, we have shown that 3,5-dimethylanilide derivatives of NSAIDs can be resolved on CSP 1 with reasonably useful separation factors. These resolutions are unusual examples of the resolution of π -donor analytes on a π -basic chiral stationary phase. These resolutions are practically important in terms of

Table 4
Resolution of 3,5-dimethylanilide derivatives **5** of α -(*p*-alkylphenyl)alkanoic acids on CSP 1

5		k'_1	k'_2	α
α -Alkyl (R_1)	<i>p</i> -Alkyl (R_2)			
CH ₃	H	2.86	3.62	1.27
CH ₂ CH ₃	H	2.96	3.64	1.23
(CH ₂) ₂ CH ₃	H	2.84	3.62	1.27
(CH ₂) ₄ CH ₃	H	2.61	3.19	1.22
(CH ₂) ₆ CH ₃	H	2.38	2.90	1.22
(CH ₂) ₉ CH ₃	H	2.04	2.45	1.20
CH ₃	CH ₃	2.56	3.16	1.23
CH ₃	(CH ₂) ₂ CH ₃	2.11	2.80	1.33
CH ₃	(CH ₂) ₅ CH ₃	1.67	2.24	1.34
CH ₃	(CH ₂) ₇ CH ₃	1.51	2.06	1.36
CH ₃	(CH ₂) ₉ CH ₃	1.38	1.90	1.38

Conditions: mobile phase, 2-propanol–hexane (90:10); flow rate, 2.0 ml/min; temperature, ambient. k'_1 = Retention factor for the first-eluted enantiomer; k'_2 = retention factor for the second-eluted enantiomer; α = separation factor.

saving analytical time and, in consequence, saving eluting solvent. For example, the resolution of the 3,5-dimethylanilide derivative of naproxen can be accomplished within 12 min whereas that of the 3,5-dinitroanilide derivative of naproxen requires almost 45 min for complete resolution, as shown in Fig. 1. The details of the chiral recognition mechanism employed by CSP 1 for the resolution of π -donor analytes is not yet clear and efforts to elucidate the chiral recognition mode are in progress.

Acknowledgement

This work was supported by grants from the Organic Chemistry Research Centre sponsored by the Korea Science and Engineering Foundation.

References

- [1] W.H. Pirkle and T.C. Pochapsky, *Chem. Rev.*, 89 (1989) 347.

- [2] P. Macaudiere, M. Lienne and M. Caude, in A.M. Krstulovic (Editor), *Chiral Separations by HPLC: Application to Pharmaceutical Compounds*, Ellis Horwood, Chichester, 1989, Ch. 14, p. 399.
- [3] W.H. Pirkle and T.C. Pochapsky, *Adv. Chromatogr.*, 27 (1987) 73.
- [4] W.H. Pirkle and J.E. McCune, *J. Chromatogr.*, 471 (1989) 271.
- [5] W.H. Pirkle, J.M. Finn, J.L. Schreiner and B.C. Hamper, *J. Am. Chem. Soc.*, 103 (1981) 3964.
- [6] W.H. Pirkle, T.C. Pochapsky, G.S. Mahler, D.E. Corey and D.S. Reno, *J. Org. Chem.*, 51 (1986) 4991.
- [7] M.H. Hyun and W.H. Pirkle, *J. Chromatogr.*, 393 (1987) 357.
- [8] A. Tambute, L. Siret, M. Caude, A. Begos and R. Rosset, *Chirality*, 2 (1990) 106.
- [9] M. Lienne, P. Macaudiere, M. Caude, R. Rosset and A. Tambute, *Chirality*, 1 (1989) 45.
- [10] T.C. Pochapsky, *Ph.D. Thesis*, University of Illinois, Urbana, IL, 1986.
- [11] L. Oliveros, C. Minguillon, B. Desmazieres and Desbene, *J. Chromatogr.*, 589 (1992) 53.
- [12] W.H. Pirkle, C.J. Welch and Q. Yang, *J. Chromatogr.*, 639 (1993) 329.
- [13] W.H. Pirkle, M.H. Hyun and B. Bank, *J. Chromatogr.*, 316 (1984) 585.
- [14] W.H. Pirkle, G.S. Mahler and M.H. Hyun, *J. Liq. Chromatogr.*, 9 (1986) 443.
- [15] M.H. Hyun, I.-K. Baik and W.H. Pirkle, *J. Liq. Chromatogr.*, 11 (1988) 1249.
- [16] M.H. Hyun, Y.-W. Park and I.-K. Baik, *Tetrahedron Lett.*, 29 (1988) 4735.
- [17] M.H. Hyun and M.S. Kim, *Bull. Korean Chem. Soc.*, 12 (1991) 104.
- [18] W.H. Pirkle and C.J. Welch, *J. Liq. Chromatogr.*, 14 (1991) 1.
- [19] M.H. Hyun and W.H. Pirkle, *Bull. Korean Chem. Soc.*, 8 (1988) 45.
- [20] M.H. Hyun, S.M. Cho, J.-J. Ryoo and M.S. Kim, *J. Liq. Chromatogr.*, 17 (1994) 317.
- [21] M.H. Hyun, M.S. Kim and J.-J. Ryoo, *Bull. Korean Chem. Soc.*, 14 (1993) 9.
- [22] K.B. Whetsel and J.H. Lady, *J. Phys. Chem.*, 69 (1965) 1596.



ELSEVIER

Journal of Chromatography A, 692 (1995) 97–102

JOURNAL OF
CHROMATOGRAPHY A

High-performance liquid chromatographic determination of (4-[¹¹C]methoxyphenyl)-(5-fluoro-2-hydroxyphenyl)-methyleaminobutyric acid and its benzophenone metabolite

Filip De Vos*, Guido Slegers

Department of Radiopharmacy, University of Ghent, Harelbekestraat 72, B-9000 Ghent, Belgium

Abstract

The high-performance liquid chromatographic determination of [¹¹C]MPGA {(4-[¹¹C]methoxyphenyl)-(5-fluoro-2-hydroxyphenyl)methyleaminobutyric acid} and [¹¹C]MBENZ (5-fluoro-2-hydroxy-4'-[¹¹C]methoxybenzophenone) is described. The method was successfully applied to the quality control of [¹¹C]MPGA radiopharmaceutical preparations and for plasma analysis after i.v. injection of [¹¹C]MPGA into mice. For determination in plasma, rapid extraction with dichloromethane from buffered plasma (pH 4.5), prior to chromatography, is necessary. Separation is effected on an RP-C₁₈ column, using a mixture of 0.05 M potassium phosphate–0.025 M citric acid (pH 6.5) and methanol (42:58, v/v) as the mobile phase. Detection is achieved using an ultraviolet absorption detector set at 255 nm in combination with an NaI (Tl) detector. Quantitative measurements of radioactivity are performed on a one-channel γ -ray spectrometer. The linearity, precision and accuracy for the method are also provided.

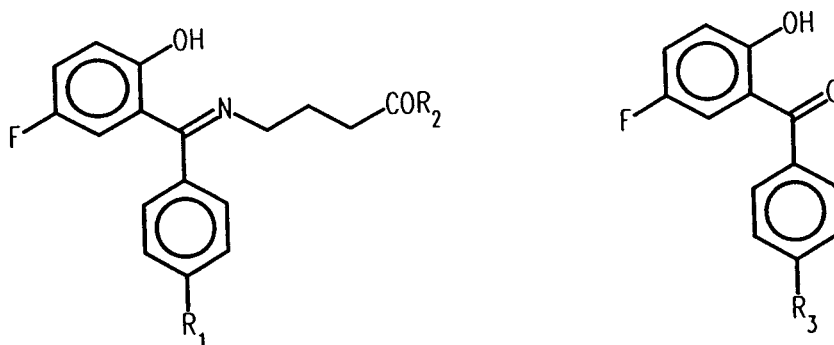
1. Introduction

γ -Aminobutyric acid (GABA) is an important neurotransmitter in the central nervous system (CNS) [1]. However, GABA is too hydrophilic to pass the blood–brain barrier readily. To solve this problem, lipophilic derivatives of GABA, e.g., progabide [III, (4-chlorophenyl)-(5-fluoro-2-hydroxyphenyl)methyleaminobutyramide] (Fig. 1), are applied [2–4]. Visualization of the GABA receptor by positron emission tomography (PET) could be an important diagnostic method in the recognition of neurological diseases. [¹¹C]MPGA {I, (4-[¹¹C]methoxyphenyl)-

(5-fluoro-2-hydroxyphenyl)methyleaminobutyric acid} (Fig. 1) is a derivative of III and a potent radioligand for the study of the GABA receptor in mammalian brain by PET.

[¹¹C]MPGA (I) is synthesized in a two-step reaction and purified by semi-preparative HPLC. The synthesis involves O-methylation of HBENZ (V, 5-fluoro-2-hydroxy-4'-hydroxybenzophenone) (Fig. 1) with [¹¹C]iodomethane to form [¹¹C]MBENZ (VI, 5-fluoro-2-hydroxy-4'-[¹¹C]methoxybenzophenone) (Fig. 1). A subsequent Schiff reaction with γ -aminobutyric acid yields I [5]. After synthesis, the chemical and radiochemical purity of the I preparation has to be determined. Moreover, for receptor studies in the brain, the specific activity of the radiopharmaceutical preparation is also an important parameter.

* Corresponding author.



(I)	[¹¹ C]MPGA	R ₁ =O ¹¹ CH ₃	R ₂ =OH	(V)	HBENZ	R ₃ =OH
(II)	MPGA	R ₁ =OCH ₃	R ₂ =OH	(VI)	[¹¹ C]MBENZ	R ₃ = ¹¹ CH ₃
(III)	progabide	R ₁ =Cl	R ₂ =NH ₂	(VII)	MBENZ	R ₃ =OCH ₃
(IV)	progabidic acid	R ₁ =Cl	R ₂ =OH			

Fig. 1. Structures of [¹¹C]MPGA (I), MPGA (II), progabide (III), progabidic acid (IV), HBENZ (V), [¹¹C]MBENZ (VI) and MBENZ (VII).

Once administered, radiopharmaceuticals, like any other compound, may be liable to rapid metabolism [6]. When, however, quantitative PET data regarding receptor density and affinity are needed, information on the fraction of unchanged radiopharmaceutical in the body must be available. The imine link of [¹¹C]MPGA can, analogously to progabidic acid [IV, (4-chlorophenyl)-(5-fluoro-2-hydroxyphenyl)methyleneaminobutyric acid] (Fig. 1), be broken down *in vivo* to release GABA and VI.

Considering the short half-life of ¹¹C ($t_{1/2}$ = 20.4 min, β -ionization), a fast and reproducible specific assay for the simultaneous determination of I and VI in radiopharmaceutical preparations and plasma is required.

Many methods have been proposed for the determination of III and IV, including GC with electron-capture detection and HPLC with UV or electrochemical detection [7-10]. These analyses were unable to detect the benzophenone metabolite. Only two methods for the simultaneous

determination of progabide, progabidic acid and benzophenone have been described [11,12].

This paper describes a rapid HPLC procedure for the separation of I and VI in combination with UV and NaI(Tl) detection. The developed method was successfully applied to the quality control of radiopharmaceutical preparations and to plasma analysis for I and VI after *i.v.* administration to mice.

2. Experimental

2.1. Chemicals

MPGA (II), MBENZ (VII) and HBENZ (V) were synthesized in our laboratory and identified by ¹H NMR and mass spectrometry [5]. [¹¹C]MPGA (I) was synthesized according to a procedure described elsewhere [5]. Citric acid, methanol and dichloromethane were obtained from Janssen Chimica (Beerse, Belgium). Mono-

potassium phosphate and sodium hydroxide were obtained from UCB (Leuven, Belgium).

2.2. Equipment

The isocratic HPLC equipment consisted of a Waters Model 590 pump (Millipore, Waters Chromatography Division, Milford, MA, USA), a UV detector (Pye Unicam, Cambridge, UK), a syringe injector equipped with a 20- μ l loop (Valco Instruments, Eke, Belgium), a CR5-A automatic integrator (Shimadzu, Tokyo, Japan) and an NaI(Tl) detector (Mini Instruments, Essex, UK). The eluate was collected in fractions with a Redifrac fraction collector (Pharmacia Biotech, Brussels, Belgium). Radioactivity counting was done with a one-channel γ -ray spectrometer equipped with an NaI(Tl) detector (Canberra, Meriden, CO, USA).

2.3. Chromatographic conditions

A LiChrospher 5- μ m RP-C₁₈ column (150 \times 4.0 mm I.D.) (Merck, Darmstadt, Germany) was used. The mobile phase consisted of a mixture of 0.050 M monobasic potassium phosphate–0.025 M citric acid buffer (adjusted to pH 6.5 with sodium hydroxide) and methanol (42:58, v/v). The flow-rate was set at 1.0 ml/min. UV detection was achieved at 255 nm. The sensitivity of the UV detector was set at 0.08 AUFS. The radiochromatogram was plotted as log(cpm) versus time. Analyses were performed at ambient temperature.

For quality control of the [¹¹C]MPGA (I) radiopharmaceutical preparations, 20 μ l were injected into the HPLC system immediately after synthesis. For the determination of the amount of carrier MPGA (II), the peak area was compared with a calibration graph.

A stock standard solution of II was prepared in methanol and stored at 2–6°C. Working standard solutions were prepared freshly by diluting the stock standard solution with mobile phase. A linear calibration graph of peak area versus concentration of II (2–40 μ g/ml) was constructed according to the least-squares method.

2.4. Plasma analysis of [¹¹C]MPGA (I)

A 250- μ l plasma sample was pipetted into a conical glass tube and 25 μ l of standard solutions of II (20 μ g/ml in methanol) and VII (20 μ g/ml in methanol) and 250 μ l extraction buffer (0.25 M citric acid in water adjusted to pH 4.5 with sodium hydroxide) were added. The mixture was gently mixed for 1 min and extracted with 1 ml of dichloromethane by vigorous shaking on a vortex mixer for 2 min. After centrifugation (3 min, 1000 g) the organic phase was separated and evaporated under a gentle stream of nitrogen. The residue was reconstituted in 50 μ l of mobile phase and 20 μ l were injected immediately into the HPLC system. The eluate was collected with a fraction collector at time intervals of 0.5 min. The collected fractions were counted for radioactivity on a one-channel γ -ray spectrometer.

3. Results and discussion

3.1. Chromatographic conditions

For our purposes a good separation of II and VII is necessary. Fig. 2 shows the chromatogram of a mixture of the mentioned compounds. The retention times of II and VII were 3.52 and 10.7 min, respectively (k' = 2.63 and 10.0, respectively; the hold-up time was determined with water). The chromatographic conditions provide a good resolution of both peaks and allow the identification and determination of II. Moreover, I and VI can be isolated for radioactivity counting in a γ -ray spectrometer.

As previously reported, the imine binding in GABA derivatives is unstable in aqueous media [13], undergoing hydrolysis to benzophenone derivatives and GABA. Maximum hydrolytic stability is reached at pH 7. The stability of an aqueous standard solution of II was controlled by injecting 20 μ l every 15 min for 1 h. No change in peak height or peak area was observed during storage at 2–6°C.

A linear correlation for II was found between the peak area and the amount of product in-

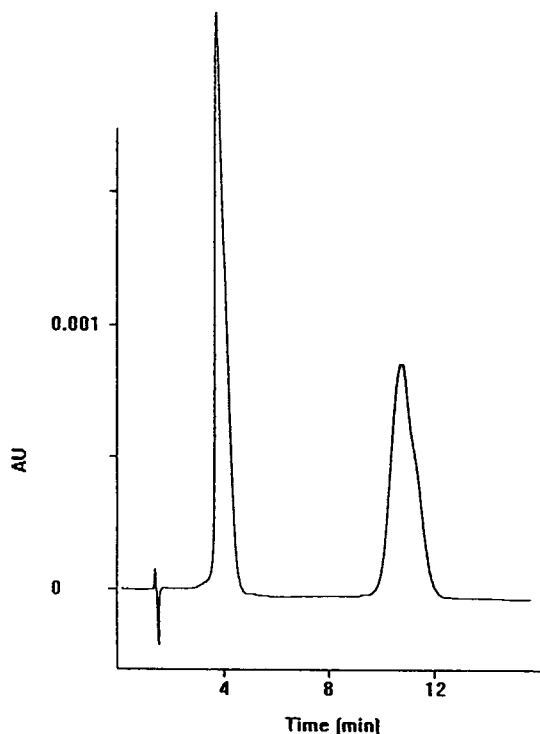


Fig. 2. Chromatogram with UV detection obtained after injection of 20 μ l of a mixture containing MPGA (II) (20 μ g/ml) and MBENZ (VII) (20 μ g/ml).

jected in the range 2–40 μ g/ml [regression equation expressed as area = slope \times concentration (μ g/ml) + intercept; slope = 3636, intercept = -3110, $r = 0.9996$].

The accuracy of the method was tested by an intra-assay precision test and the reproducibility by an inter-assay precision test. The choice of the concentrations used was based on the minimum and maximum levels of carrier II that could be found in a radiopharmaceutical preparation. The results are given in Tables 1 and 2. The recovery for II lies between 98.8 and 100.8% and the mean relative standard deviation is 2.01%.

It was found that 1.74 GBq (S.D. 0.218 GBq, $n = 3$) of I could be produced with a specific activity of 7.77 GBq/ μ mol (S.D. 3.19 GBq/ μ mol, $n = 3$). None of the products showed impurities in the UV trace or radiochromatogram. A typical radiochromatogram is shown in Fig. 3.

Table 1

Accuracy for the determination of MPGA (II) in radiopharmaceutical preparations ($n = 3$)

Amount added (μ g/ml)	Amount found (μ g/ml)	S.D. (μ g/ml)	Recovery (%)
9.61	9.50	0.25	98.8
19.2	19.4	0.41	101.0
39.4	38.8	0.90	100.8
Mean			100.2

Table 2

Precision of the determination of MPGA (II) in radiopharmaceutical preparations ($n = 3$)

Amount added (μ g/ml)	Amount found (μ g/ml)	S.D. (μ g/ml)	R.S.D. (%)
9.61	9.70	0.19	1.95
19.2	19.5	0.36	1.84
38.4	38.0	0.85	2.24
Mean			2.01

3.2. Plasma analyses for [11 C]MPGA (I)

The extraction of [11 C]MPGA (I) from plasma obtained from mice injected with 3.7 MBq, corresponding to approximately 130 ng of car-

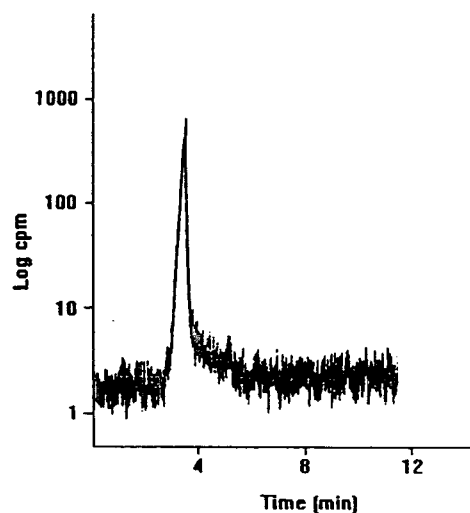


Fig. 3. Typical radiochromatogram obtained after injection of 20 μ l of a [11 C]MPGA preparation.

rier, was not reproducible. Therefore, 500 ng of both standard **II** and **VII** were added to the plasma before extraction. The recovery was determined by comparing the peak areas of **II** and **VII** in the chromatogram with the peak areas of the respective standard solutions. Recoveries of **II** and **VII** of 90 and 91%, respectively, were obtained.

The stability of **I** during the extraction was controlled by HPLC. The radiochromatogram of a blank plasma spiked with 37 kBq of **I** and treated as described under Experimental showed only one peak with the same retention time as **II**, indicating that no hydrolysis at the imine binding took place during the extraction procedure.

The radiochromatogram of a typical mouse plasma sample extract is shown in Fig. 4. All radioactivity corresponding to **I** is present in the fractions collected between 2.5 and 4.5 min and is well separated from **VI**. The fraction of unchanged **I** in plasma samples was determined by measuring the ratio of the radioactivity corre-

sponding to **I** to the total radioactivity present in all collected fractions.

A 3.7-MBq amount of **I** was administered i.v. to white male mice (strain NMRI) and blood samples were taken at 5, 10 and 30 min post-injection. Plasma was obtained by centrifugation of the collected blood at 3000 g for 5 min. The plasma samples were treated as described under Experimental. The fraction of unchanged **I** was 95, 97 and 94% at 5, 10 and 30 min after injection, respectively. These values indicate that up to 30 min after administration no metabolization of importance occurred. No blood samples were taken at longer times post-injection because the amount of radioactivity present in the collected HPLC fractions was too low to perform adequate radioactivity counting.

4. Conclusions

An HPLC method for the separation of MPGA (**II**) and MBENZ (**VII**) has been developed. The method was successfully applied to the quality control of [^{11}C]MPGA (**I**) radiopharmaceutical preparations and for plasma analyses for **I** and [^{11}C]MBENZ (**VI**) after i.v. administration of **I** to mice.

Acknowledgements

This work was supported by a grant from the IWONL, NFWO and the Onderzoeksraad of the University of Ghent.

References

- [1] P. Krogsgaard-Larsen, *J. Med. Chem.*, 24 (1981) 1377.
- [2] J.P. Kaplan and B.M. Raizon, *J. Med. Chem.*, 23 (1980) 702.
- [3] K.G. Lloyd, S. Arbilla, K. Beaumont, M. Briley, G. De Montis, B. Scatton, S.Z. Langer and G. Bartholini, *J. Pharmacol. Exp. Ther.*, 220 (1980) 672.
- [4] N.G. Bowery, D.R. Hill, A.L. Hudson and G.W. Price, in G. Bartholini (Editor), *I.E.R.S.*, Vol. 3, Raven Press, New York, 1988, p. 63.

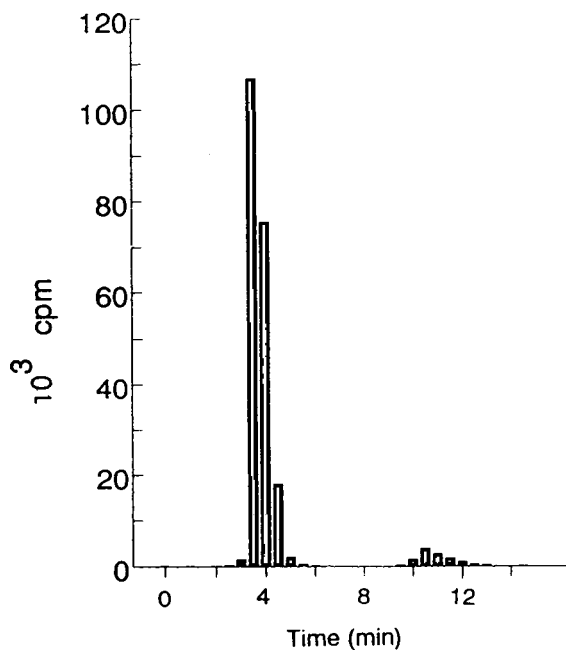


Fig. 4. Distribution of the radioactivity versus time for a mice plasma sample 30 min after administration of [^{11}C]MPGA (**I**).

- [5] F. De Vos and G. Slegers, *J. Labelled Compd.*, 34 (1994) 643.
- [6] B. Mazière, R. Cantineau, H.H. Coenen, M. Guillaume, C. Halldin, A. Luxen, C. Loc'h and S.K. Luthra, in G. Stöcklin and V.W. Pike (Editors), *Radiopharmaceuticals for Positron Emission Tomography*, Kluwer, Dordrecht, 1993, Ch. 4, p. 151.
- [7] G. Gillet, J. Fraisse-André, C.R. Lee, L.G. Dring and P.L. Morselli, *J. Chromatogr.*, 230 (1982) 154.
- [8] W. Yonekawa, H.J. Kupferberg and T. Lambert, *J. Chromatogr.*, 273 (1983) 103.
- [9] V. Ascalone, P. Catalani and L. Dal Bo', *J. Chromatogr.*, 344 (1985) 231.
- [10] J.P. Decourt, P. Mura, Y. Papet, A. Piriou and D. Reiss, *J. Chromatogr.*, 527 (1990) 214.
- [11] P. Padovani, C. Deves, G. Bianchetti, J.P. Thenot and P.L. Morselli, *J. Chromatogr.*, 308 (1984) 229.
- [12] N.F. Farraj, S.S. Davis, G.D. Parr and H.N.E. Stevens, *Pharm. Res.*, 4 (1987) 28.
- [13] N.F. Farraj, S.S. Davis, G.D. Parr and H.N.E. Stevens, *Pharm. Res.*, 5 (1988) 226.

Use of high-performance liquid chromatography–diode array detection in forensic toxicology

Eva M. Koves

Center of Forensic Sciences, 25 Grosvenor St, Toronto, Ontario M7A 2G8, Canada

Abstract

A comprehensive approach to the analysis for many drugs in postmortem blood and biological fluids using high-performance liquid chromatography and diode array detection has been developed. To reduce the likelihood of co-eluting interference components of postmortem blood or other drugs, selective back-extraction was also used to screen and quantitate drugs in blood and biofluids. An isocratic mobile phase (acetonitrile, phosphoric acid and triethylamine buffer, pH 3.4) was developed and found stable, reliable and convenient for general drug screening and quantitation. A library of drug spectra in the ultraviolet wavelength range (210–367 nm) was established for 272 drugs on two reversed-phase columns: Supelcosil (biphenyl) and LiChrospher RP-8.

The application of several methods to whole blood, the analysis of complex cases and the use of multicomponent analysis for qualitative and quantitative analysis is discussed.

1. Introduction

High-performance liquid chromatography (HPLC) has developed into one of the most useful and widely used analytical techniques in the last two decades. The range and variety of compounds that can be analysed by HPLC has led to its application in environmental, clinical and forensic laboratories. In the early days, HPLC was primarily a quantitative technique, retention times being the only criteria for identification. With the advent of diode array detection (DAD) for HPLC, the ultraviolet (UV) spectrum becomes accessible as a three-dimensional data matrix. Data are available not only for retention time and peak height, but also for wavelength, thus, allowing identification from UV spectral properties in addition to retention behaviour.

DAD dramatically improves the selectivity of HPLC and offers many capabilities, previously enjoyed only by gas chromatography–mass spectrometry. HPLC–DAD has proven itself for screening anabolics [1], neuroleptics [2], diuretics [3], basic drugs [4] and many other compounds [5–12]. A survey of the literature showed however, that a great variety of HPLC columns and mobile phases were required. In view of the wide range of conditions reported for the chromatographic analysis of drugs, the goal of this work was to establish standard chromatographic conditions that could be used both for basic and acidic drugs. In this paper, four years of experience with HPLC–DAD systems is presented. The application of several methods to whole blood, the analysis of complex cases and the use of multicomponent analysis for qualitative and quantitative analysis is also illustrated.

2. Experimental

2.1. Liquid chromatography system

The components of an LC system have been described previously [13]. The system includes a Model 9010 pump, a Model 9095 autosampler, a Model 9065 photodiode array detector, a Compaq 386 computer with the LC Star 9020 workstation and with the PolyView (version 2.02) software, all from Varian, Georgetown, Canada. The LC Star 9020 workstation software is used for system control and chromatographic data handling and the PolyView software is used for automated post-run spectral evaluation and for multicomponent analysis.

Chromatographic separation was achieved isocratically at ambient temperature on reversed-phase columns. The detailed analytical conditions are listed in Table 1. Mobile phase was

continuously degassed with helium during use. After the system was equilibrated (approximately 60 min), the mobile phase was recycled back to the reservoir. Drugs were monitored at 229 nm and, if required, were quantitated at their UV maxima. Injection was 25 μ l out of a final volume of 300 μ l.

2.2. Chemicals and reagents

Drug standards were of the highest possible purity and obtained from pharmaceutical manufacturing companies. Stock solutions containing 0.4 mg/ml of free base/acid of each drug in methanol were stored at -20°C . Acetonitrile and methanol were distilled-in-glass quality (spectra analysed) and supplied by Caledon Labs. (Georgetown, Canada). Triethylamine (TEA) was purchased from Sigma (St. Louis, MO, USA). All other chemicals were of analytical-

Table 1
Chromatographic conditions for drugs on reversed-phase HPLC columns

Column type and conditions	Comment
(I) Supelcosil LC-DP, 5 μ m, 250 mm \times 4.6 mm I.D. (Supelco Canada, Oakville, Canada) Mobile phase CH_3CN -0.025% (v/v) H_3PO_4 -TEA buffer, pH 3.4 (25:10:5, v/v/v) Flow-rate 0.6 ml/min	Used for quantitation and confirmation of drugs and for screening acidic drugs
(II) LiChrospher 100 RP-8, 5 μ m, 250 mm \times 4.0 mm I.D. (Hewlett-Packard, Mississauga, Canada) Mobile phase CH_3CN -0.025% (v/v) H_3PO_4 -TEA buffer, pH 3.4 (60:25:15, v/v/v) Flow-rate 0.6 ml/min	Used for quantitation of drugs (mostly phenothiazines) and for screening basic and acidic drugs
(III) APEX ODS, 5 μ m, 250 mm \times 4.6 mm I.D. (Mandel Scientific, Guelph, Canada) Mobile phase methanol-water (50:50, v/v) ^a or (40:60, v/v) ^b Flow-rate 1.0 ml/min ^a or 0.4 ml/min ^b	Used for quantitation of barbiturates, phenytoin, salicylic acid, acetaminophen and theophylline
(IV) Nova-Pak Phenyl, 5 μ m, 150 mm \times 3.9 mm I.D. (Waters, Division of Millipore, Mississauga, Canada) Mobile phase methanol-water (60:40, v/v) ^c or CH_3CN -0.025% (v/v) H_3PO_4 (50:50, v/v) Flow-rate 0.7 ml/min ^c or 0.6 ml/min	Used for quantitation of some benzodiazepines and for the confirmation of some drugs

^a Barbiturate and phenytoin analysis.

^b Salicylic acid, acetaminophen and theophylline analysis.

^c Benzodiazepines.

reagent grade and solvents distilled-in-glass quality. Water was purified using a Millipore Milli-Q Plus water-purification system (Millipore, Mississauga, Canada).

TEA buffer was prepared by adding 9 ml of concentrated phosphoric acid and 10 ml of TEA to 900 ml of water. After the pH was adjusted to 3.4 with diluted phosphoric acid, the volume was made up to 1 l with water and stored at 4°C. Before it was used to make up the mobile phase, it was kept at room temperature overnight and filtered through a Millipore 0.45- μ m HA filter.

2.3. Methods

Extraction of acidic drugs

Extraction and chromatographic conditions have been developed in this laboratory and reported elsewhere [14,15]. The method is outlined in Fig. 1. Blood samples were rotated with Amberlite XAD-2 resin-slurry, then the mixture

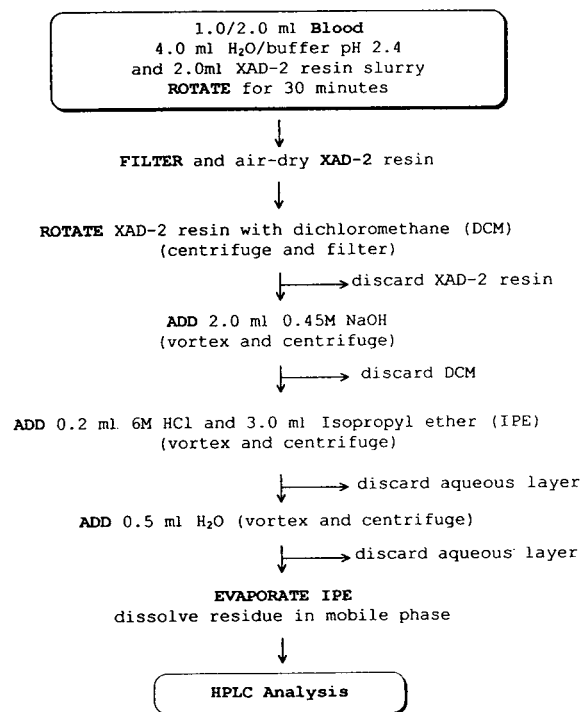


Fig. 1. Flow diagram of method for acidic drug extraction from blood.

was transferred into an empty Brinkmann column (containing a small plug of cotton), filtered and washed. The air-dried resin was rotated with dichloromethane and filtered. Acidic drugs were back-extracted into 0.45 M NaOH, acidified with 6 M HCl and re-extracted with isopropyl ether. The final extract was washed, evaporated and reconstituted with mobile phase.

Extraction of basic drugs

In 1992 we reported on a method for the detection and quantitation of basic drugs in postmortem blood using HPLC–DAD [13]. The method is based on selective extraction of basic and weakly basic drugs, by back-extraction into 0.1 M sulphuric acid and 6 M hydrochloric acid after the initial extraction from 2.0 ml of blood with toluene under basic conditions. The extraction procedure is outlined in Fig. 2, fractions B and C. Only minor modification of the method was necessary for the quantitation of acid- or alkaline-sensitive drugs such as diltiazem: instead of 0.1 M H₂SO₄, back-extracted into 0.01 M H₂SO₄ and the acid fraction was made alkaline with 0.5 M K₂CO₃ before it was re-extracted with toluene.

A specific extraction procedure has been developed for the quantitation of some benzodiazepines such as nitrazepam, oxazepam, clonazepam, demoxepam and lorazepam [16]. These drugs were separated from the other basic drugs by using diluted NaOH solution for back-extraction after the initial extraction with toluene (Fig. 2, fraction A).

Spectral libraries

Dilutions of the stock solutions with the mobile phase (1:100) were used to establish retention times and create a library of spectra in the ultraviolet range (210–367 nm). The spectra were acquired under the same conditions as for sample analysis and were stored with the absolute retention times. Eight group standards were also prepared in methanol at a concentration of 0.4 mg/ml for each drug. They covered a variety of basic, acidic and amphoteric drugs (a total of 60 drugs). These group standards were stored at –20°C and were diluted with mobile phase

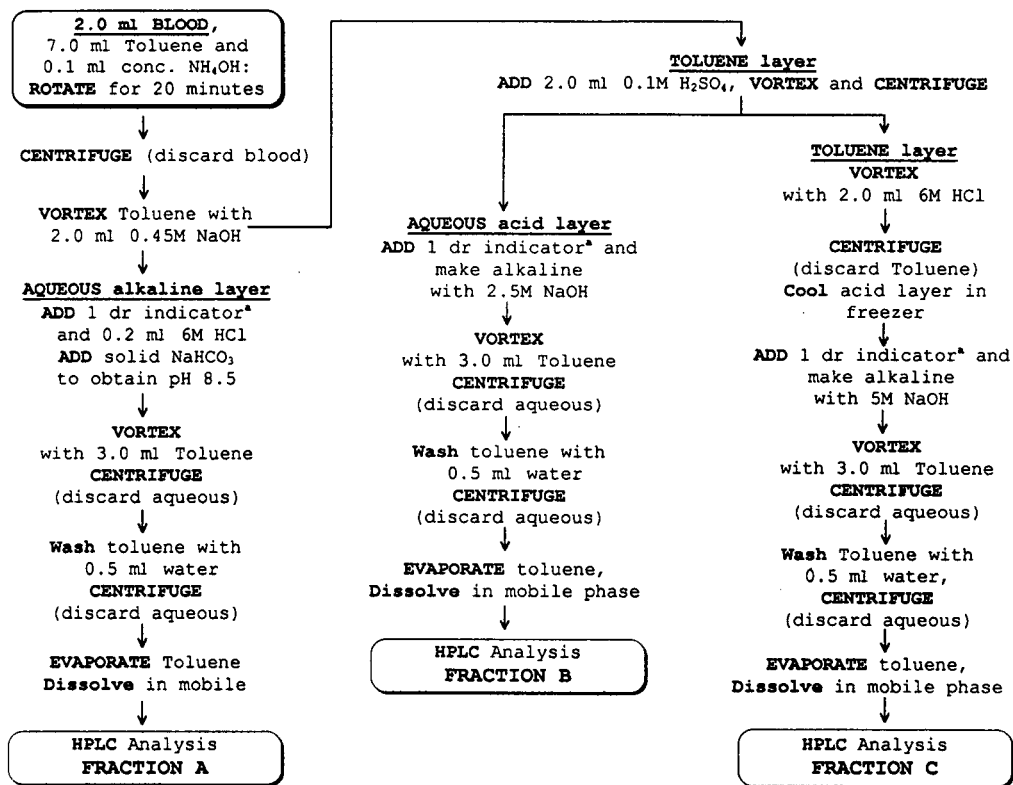


Fig. 2. Flow diagram of method for basic drug extraction from blood. *1% Bromothymol blue (w/v) in methanol–water (1:1, v/v). dr = drop.

(1:100) to monitor column performance and the validity of identifications based on the library data. The complete directory of the library's contents on two reversed-phase columns is listed in Table 2.

A separate library was created for multicomponent analysis. Group standards were prepared at a concentration of 0.8 mg/ml. These group standards were diluted with mobile phase (1:100) and injected on the LiChrospher column. The area spectrum obtained for each drug (a total of 245 drugs), in addition to identification, retention time and the amount of the injected drug, made up the library.

Data analysis

The PolyView spectral processing software and library search employed in this work have been described by Sheenan et al. [17]. The data

libraries included five data files, containing 272 and 280 drugs on the Supelcosil and LiChrospher columns, respectively (Table 2). The PolyView Report included: (a) a continuous plot of UV absorbance as a function of time from 0 to 20 min at 229 nm, (b) a continuous plot of purity parameter (PUP) from 0 to 20 min over a wavelength range of 210 to 367 nm and (c) a library search report with overlay graphic. A retention time window of $\pm 5\%$ and a PUP of ± 1 nm were set as primary search criteria. A dissimilarity value of 0.06 was set to the confirm peak identity and peak homogeneity.

Multicomponent analysis

Twelve group standards, containing 76 drugs were prepared to evaluate the applicability of the PolyView multicomponent analysis (MCA) software to the quantitation

Table 2
Retention times (t_R) for drugs on reversed-phase HPLC columns

Drug	t_R^a (min)	t_R^b (min)	Drug	t_R^a (min)	t_R^b (min)
Acebutolol	6.51	3.72	Cisapride	10.90	5.81
Acebutolol metabolite 1	5.71	3.41	Clobazam	7.20	7.11
Acebutolol metabolite 2	6.08	—	Clomipramine	17.90	8.53
Acepromazine	12.10	5.81	Clonazepam	6.45	6.02
Acetaminophen	4.75	3.68	Clonidine	7.97	4.25
Acetanilide	5.47	4.90	Clopendixol	14.10	6.81
Acetazoleamide	4.77	3.68	Clozapine	10.90	5.15
Acetophenazine	9.83	4.89	Cocaine	10.00	4.99
Albuterol	5.57	3.27	Codeine	6.09	3.42
Alprazolam	6.40	6.44	Colchicine	5.09	4.15
Aminochlorobenzophenone	9.48	13.10	Coumarine	6.27	6.09
Aminopromazine	17.20	8.10	Creatinine	5.15	3.11
Amitriptyline	15.80	7.27	Cyclizine	12.40	5.78
Amobarbital	5.94	5.59	Cyclobenzaprine	15.50	7.05
Amoxapine	11.40	5.55	Dantrolene	6.04	5.23
Anileridine	11.70	5.92	Demoxepam	5.75	5.05
Antazoline	11.50	5.91	Desacetyldiltiazem	9.28	4.59
Antipyrine	5.39	4.54	Desalkylflurazepam	6.51	6.56
Atenolol	5.33	3.11	Desalkylhydroxyflurazepam	5.91	5.42
Atropine	6.95	3.75	Desipramine	13.00	6.26
Azacyclonal	8.70	4.52	Desmethylchloridiazepoxide	5.75	4.69
Azatadine	10.70	4.55	Desmethylchloridiazepoxide ^c	6.30	5.05
Baclofen	5.71	3.47	Diazepam	7.71	8.83
Benzocaine	6.25	6.23	Dichloroisoproterenol	8.43	4.84
Bromazepam	5.79	5.06	Diclofenac	8.68	9.97
Bromocriptine	10.80	6.21	Diethazine	15.10	7.38
Bromodiphenhydramine	14.70	7.48	Diffunisal	5.91	5.95
Brompheniramine	11.10	5.44	Dihydroxybenzoic acid	4.28	3.46
Brotizolam	7.43	7.90	Diltiazem	11.10	5.42
Bupivacaine	10.60	5.79	Diltiazem metabolite 1	10.60	5.09
Buspirone	9.07	4.98	Diltiazem metabolite 3	8.74	4.37
Butabarbital	5.60	4.92	Diltiazem metabolite 4	8.13	7.49
Butalbital	5.77	5.12	Dinitro- <i>o</i> -cresol	7.09	7.49
Caffeine	4.79	3.84	Diphenhydramine	12.20	6.01
Carbamazepine	6.15	5.49	Diphenidol	12.10	6.05
Carbamazepine metabolite	—	10.30	Diphenoxylate	dne	14.10
Cetirizine	8.89	5.29	Dipyridamol	8.58	4.79
Chlophendianol	10.60	5.33	Disopyramide	9.56	4.89
Chlorcyclizine	14.70	6.89	Dobutamine	6.58	3.80
Chlordiazepoxide	6.85	5.26	Doxapram	8.67	4.64
Chlormezanone	6.03	5.33	Doxepine	12.90	6.06
Chloroquine	12.70	3.55	Doxepine ^c	13.40	—
Chlorpheniramine	10.80	5.25	Droperidol	8.63	4.71
Chlorpromazine	17.00	7.75	Encainide	9.42	4.91
Chlorpromazine sulfoxide	8.37	4.26	Ethopropazine	16.60	8.25
Chlorpropamide	6.40	6.34	Ethylidiazepam	8.40	10.50
Chlorprothixene	17.60	8.29	Ethylmorphine	6.74	3.63
Chlorthalidone	5.14	4.03	Fenethazine	12.50	5.98
Chlorzoxazone	6.01	5.87	Fenopropfen	8.00	8.87
Cimetidine	5.47	3.16	Fenoterol	5.74	3.38

(Continued on p. 108)

Table 2 (continued)

Drug	t_R^a (min)	t_R^b (min)	Drug	t_R^a (min)	t_R^b (min)
Fentanyl	11.40	6.03	Mephentoin	5.99	5.40
Flavoxate	11.30	5.94	Mepivacaine	7.71	4.20
Floctafenine	6.57	5.84	Mepyramine	12.95	6.06
Fluoxetine	12.20	7.07	Mesoridazine	10.12	5.02
Flupenthixol	13.70	7.53	Metaproterenol	5.41	3.18
Flupenthixol ^c	14.20	7.68	Metformine	5.68	3.25
Fluphenazine	13.60	7.22	Methadone	16.58	8.43
Fluphenazine sulfoxide	7.51	4.07	Methaqualone	6.82	7.44
Flurazepam	10.50	5.53	Methdilazine	15.16	6.66
Flurbiprofen	8.01	8.91	Methocarbamol	5.02	3.94
Fluspirilene	18.30	9.79	Methotrexate	4.72	2.93
Fluvoxamine	9.97	5.94	Methotrimeprazine	15.23	7.19
Fonazine	12.50	6.02	Methoxamine	6.41	3.62
Frusemide	5.78	5.03	Methoxypromazine	14.36	6.54
Glutethimide	6.60	6.24	Methyldopa	4.05	2.82
Glyburide	8.51	9.83	Methylenedioxyamphetamine	6.89	3.83
Guaifenesine	4.94	3.93	Methylphenidate	8.61	4.65
Haloperidol	11.10	6.17	Metoclopramide	7.92	4.26
Heroin	7.90	4.11	Metolazone	6.05	5.16
Homidium Bromide	13.70	6.28	Metoprolol	7.12	4.19
Homotropine	6.77	3.63	Metronidazole	4.83	3.86
Hydralazine	6.46	3.49	Midazolam	10.21	6.30
Hydralazine ^c	—	5.16	Moclobemide	6.86	3.85
Hydrochlorothiazide	5.09	3.98	Morphine	5.60	3.20
Hydrocodone	6.93	3.71	Nadolol	5.64	3.39
Hydromorphone	5.84	3.42	Nalbuphine	6.56	3.61
Hydroxychloroquine	9.60	3.23	Naloxone	6.16	3.51
Hydroxyethylflurazepam	6.21	5.94	Naphazoline	9.13	4.77
Hydroxyzine	11.40	6.27	Naproxen	6.97	7.18
Ibuprofen	8.12	10.50	Nifedepine	7.42	7.91
Imipramine	14.70	6.78	Nifedepine ^c	7.66	8.28
Indomethacin	8.45	9.22	Nitrazepam	6.27	5.97
Indoxyl	3.82	3.19	Nizatidine	5.57	3.13
Isopromethazine	13.60	6.65	Nordiazepam	6.70	6.81
Ketazolam	7.72	9.23	Norepinephrine	4.90	—
Ketazolam ^c	8.32	8.85	Norfluoxetine	10.78	6.43
Ketoconazole	11.30	5.92	Normeperidine	8.29	4.46
Ketoprofen	7.02	7.04	Nortriptyline	13.70	6.75
Ketorolac	6.32	5.55	Oxazepam	6.00	4.52
Labetalol	7.68	4.22	Oxprenolol	8.27	3.69
Levorphanol	—	4.26	Oxycodone	6.51	5.82
Lidocaine	8.04	4.50	Oxymetazoline	10.42	5.82
Loratadine	10.90	13.25	Parathion	11.15	16.34
Lorazepam	6.14	5.78	Paroxetine	11.06	5.77
Lovastatine	10.49	14.79	Pemoline	4.91	3.84
Loxapine	13.78	6.26	Pentazocine	9.91	5.47
Mazindol	9.71	5.06	Pentobarbital	5.92	5.58
Mefenamic acid	9.77	13.08	Pentoxifylline	5.01	4.15
Mepazine	15.28	7.04	Pericyazine	10.24	5.13
Meperidine	9.21	4.83	Perphenazine	13.16	6.33
Mephenesine	5.34	4.55	Phenacetin	5.63	5.24

Table 2 (continued)

Drug	t_R^a (min)	t_R^b (min)	Drug	t_R^a (min)	t_R^b (min)
Pheniramine	9.49	4.49	Sotalol	5.96	3.41
Phenobarbital	5.61	4.74	Spirolactone	8.50	9.12
Phenol	5.85	5.29	Strychnine	7.49	3.88
Phenolphthalein	6.05	5.66	Sulfinpyrazone	5.71	5.33
Phentolamine	9.05	4.79	Sulindac	6.17	5.99
Phenylbutazone	10.15	12.11	Temazepam	8.86	6.70
Phenyltoloxamine	13.20	6.31	Terbutaline	5.62	3.27
Phenytoin	6.11	5.26	Terfenadine	dne	12.24
Pimozide	14.36	7.96	Tetrabenazine	—	4.08
Pindolol	7.02	4.07	Tetrabenazine ^c	—	6.00
Pipamazine	11.22	5.63	Tetracaine	10.81	5.44
Pipotiazine	10.94	5.66	Theophylline	4.52	3.45
Piroxicam	6.84	6.67	Thiethylperazine	dne	9.45
Pizotyline	15.78	6.84	Thiopental	7.04	7.33
Pramoxine	11.16	6.25	Thiopropazine	15.39	6.34
Prazepam	10.49	12.77	Thiopropazate	16.64	8.49
Prazosine	7.38	4.21	Thioridazine	dne	9.82
Probenecid	7.49	—	Thiothixene	16.49	6.57
Procaineamide	6.32	3.52	Thymol	7.93	10.45
Procaine	7.25	4.03	Tiaprofenic acid	6.84	6.65
Prochlorperazine	dne	8.18	Timolol	7.04	3.94
Procyclidine	dne	4.65	Tocainide	6.28	3.60
Promazine	14.24	6.34	Tolbutamide	6.74	6.94
Promethazine	13.20	6.40	Tolmetine	6.45	6.29
Promethazine sulfoxide	—	4.50	Trazodone	8.37	4.58
Propafenone	12.20	6.37	Triamterene	6.73	3.90
Propantheline	7.08	—	Triazolam	6.43	6.65
Propantheline ^c	8.03	—	Trifluoperazine	dne	9.32
Propiomazine	14.08	7.10	Trifluoperazine sulfoxide	9.08	4.45
Propofol	10.07	15.24	Triflupromazine	17.28	8.93
Propranolol	9.19	4.91	Triiodothyroacetic acid	8.15	8.40
Protriptyline	13.20	6.33	Trimebutine	12.21	6.21
Quazepam	11.94	17.69	Trimeprazine	14.91	7.07
Quinidine	8.72	4.55	Trimethoprim	6.67	3.65
Quinidine ^c	9.29	4.83	Trimipramine	15.49	7.66
Quinine	8.34	4.47	Verapamil	13.28	6.96
Quinine ^c	8.90	4.75	Verapamil metabolite 1	12.60	6.66
Racemethorphan	11.47	5.92	Verapamil metabolite 2	11.10	5.88
Ranitidine	5.88	3.27	Verapamil metabolite 3	8.63	4.68
Remoxipride	8.84	4.64	Verapamil metabolite 4	7.92	4.41
Risperidone	9.12	4.63	Warfarin	8.01	8.29
Salicylic acid	5.20	4.35	Xylometazoline	12.68	7.16
Scopolamine	6.95	3.70	Yohimbine	8.15	4.37
Secobarbital	6.19	5.91	Zomepirac	6.96	7.02
Sertraline	14.50	7.68	Zopiclone	7.50	3.79
SKF	19.27	10.72			

dne = Did not elute on this column within 20 min.

^a Supelcosil LC-DP, particle size 5 μ m, 25 cm \times 4.6 mm I.D.

^b LiChrospher 100 RP-8, particle size 5 μ m, 25 cm \times 4.0 mm I.D.

^c Secondary peak.

of unresolved peaks. Within the twelve groups, the three sub-groups contained the same set of drugs in three combinations. In general, the ratios for the three drugs under the same retention time were 0.5:1.0:2.5, 1.0:0.5:2.5 and 2.5:1.0:0.5. This experiment was performed with a resolution factor of $R_s = 0.0$ (completely fused).

2.4. Analysis of forensic samples

Quantitation

Calibration standards were prepared by spiking outdated Red Cross blood which was artificially aged at room temperature for approximately 3–4 weeks. The blood was preserved with 1 g/100 ml of sodium fluoride. Quantitation of a drug (basic, acidic or others) was based on the peak areas, representing concentrations likely to be encountered at the high end of therapeutic use. A standard curve was constructed using duplicate samples at each concentrations. Drug-free blood was included in the assay to produce blank chromatogram. The efficiency of the extraction was calculated by comparing the peak areas at each point on the blood standard curve with those of standards prepared for spiking and diluted to the appropriate concentrations with mobile phase. Chromatographic conditions, final volume and peak areas of blood and straight standards were documented for each assay, which allowed the variability of recovery for each drugs to be followed.

Screening

Assays for screening postmortem blood and urine samples were performed as outlined in Fig. 1 and 2. A procedure for extraction of gastric contents has also been developed in this laboratory [18]. A portion of the gastric content was mixed with ethanol and kept on a water bath for 15 min. After filtration, the ethanol was evaporated, the residue was dissolved in 10 ml of water and filtered. A 1-ml volume was extracted to obtain three fractions: amphoteric/neutral, basic and acidic. The final extract was evaporated and reconstituted with 0.5 ml of mobile

phase. An aliquot of 25 μ l was injected onto the column.

3. Results and discussion

3.1. HPLC columns and libraries

The APEX ODS column has been used for the chromatographic analysis of salicylic acid, acetaminophen, theophylline and barbiturates for ten years. The reproducibility of the retention times using different batches of columns of the same brand was very good. Experience has shown that this column is suitable for the analysis of barbiturates using a methanol–water mobile phase. The chromatogram of an extract of blood containing six barbiturates, including sigmodal as an internal standard and phenytoin is shown in Fig. 3. In addition, retention times obtained for the same set of barbiturates (except the internal standard sigmodal) in 1984 are listed. Originally, the barbiturate assay was carried out on an SP8100 chromatography system, later it was transferred to the LC Star system,

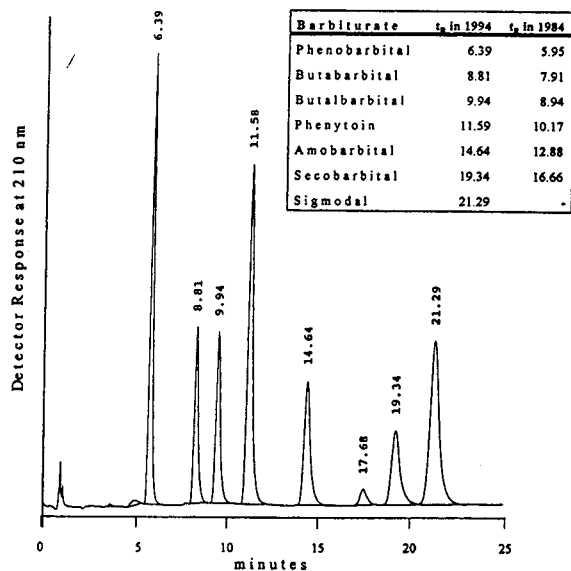


Fig. 3. Chromatogram obtained from extract of spiked blood sample on APEX ODS column. Concentration of each barbiturate was 5.0 μ g/ml of blood. t_R = retention time in min.

thus accounting for the difference of approximate 10% in the retention times between 1984 and 1994.

In the previous study [13] it was demonstrated that the APEX ODS column has been successfully used for the chromatographic analysis of basic and other drugs for two years. Reproducibility, however, between two columns of the same brand but different batches was unsatisfactory when the mobile phase was a mixture consisting of acetonitrile and buffer. The problems included tailing peaks, poor reproducibility of retention times and change in elution order for basic drugs. To replace the APEX ODS column, two other columns were investigated. The LiChrospher column was previously used for the analysis of phenothiazine and the Supelcosil column (diphenyl), was chosen for better selectivity. The long-term reproducibility of the retention time on both columns was very good. The selectivity and elution patterns of a second set of the columns (LiChrospher and Supelcosil) of different batches were nearly identical when tested with seven group standards. The retention times in the data base had to be slightly cor-

rected for routine use, but this can be completed within a week. There was no difficulty using the same libraries for two LC systems; the detectors were calibrated, the same columns and mobile phase were used and the length of the stainless-steel tubing on the two instruments was identical. The HPLC system was verified at the beginning of the analysis using group standards. The two test groups are illustrated in Fig. 4.

The multicomponent analysis employed in this work was described by Excoffier et al. [19] and reviewed by Keller et al. [20]. Since 1986, the performance of the system has been continuously monitored and it was found that the UV absorbance of a drug remained within $\pm 10\%$ for the same column, mobile phase and instrument used. Therefore an MCA library containing 245 drugs was created to investigate the long-term use of a permanent library to determine the identity and concentration of drugs in co-eluting peaks. The MCA software is limited in its ability to determine the individual drugs from the spectrum of a mixture if it is composed of more than six drugs at the same retention time. Therefore small sub-libraries containing approximate

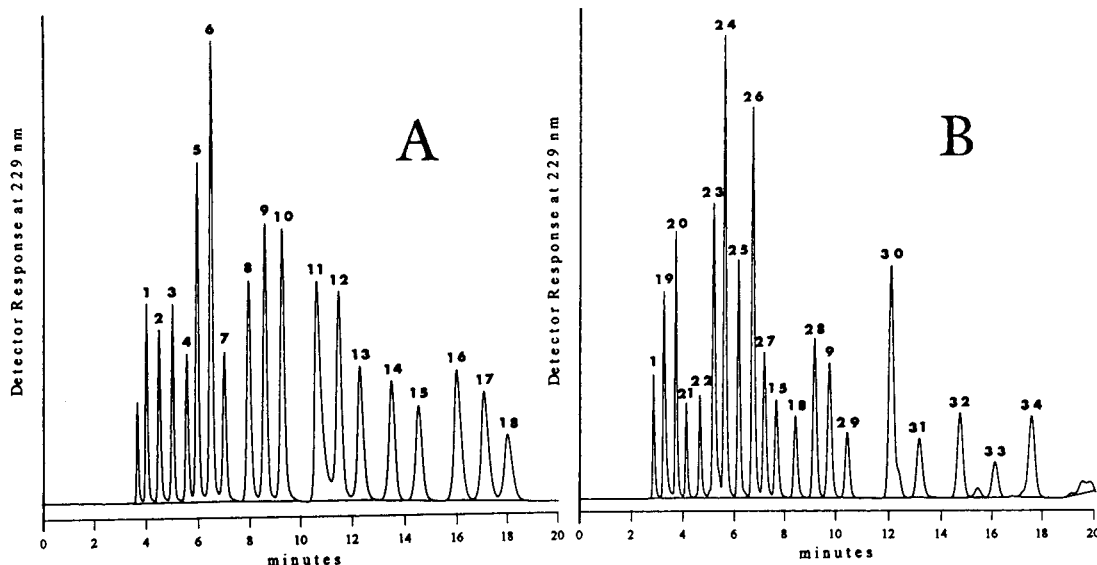


Fig. 4. Chromatograms obtained on Supelcosil (A) and LiChrospher (B) columns with standard solutions containing a mixture of drugs. Peaks: 1 = methyldopa; 2 = theophylline; 3 = methocarbamol; 4 = nizatidine; 5 = sotalol; 6 = acebutolol; 7 = ketoprofen; 8 = flurbiprofen; 9 = glyburide; 10 = propranolol; 11 = midazolam; 12 = diltiazem; 13 = fluoxetine; 14 = verapamil; 15 = sertraline; 16 = amitriptyline; 17 = chlorpromazine; 18 = clomipramine; 19 = hydroxychloroquine; 20 = acetaminophen; 21 = metoprolol; 22 = trazodone; 23 = clozapine; 24 = lorazepam; 25 = chlorpropamide; 26 = temazepam; 27 = trimeprazine; 28 = indomethacin; 29 = ibuprofen; 30 = phenylbutazone; 31 = diphenoxylate; 32 = propofol; 33 = parathion; 34 = quazepam.

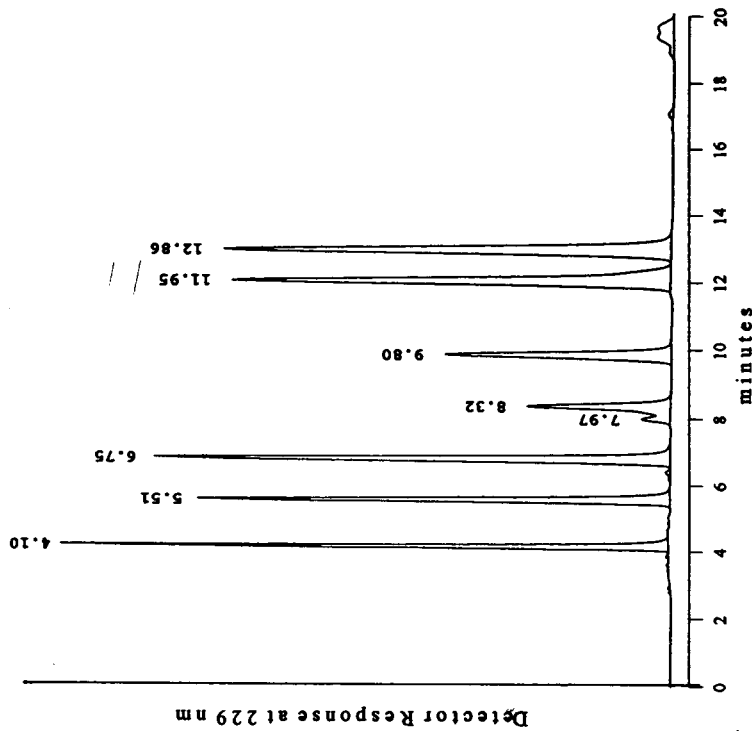
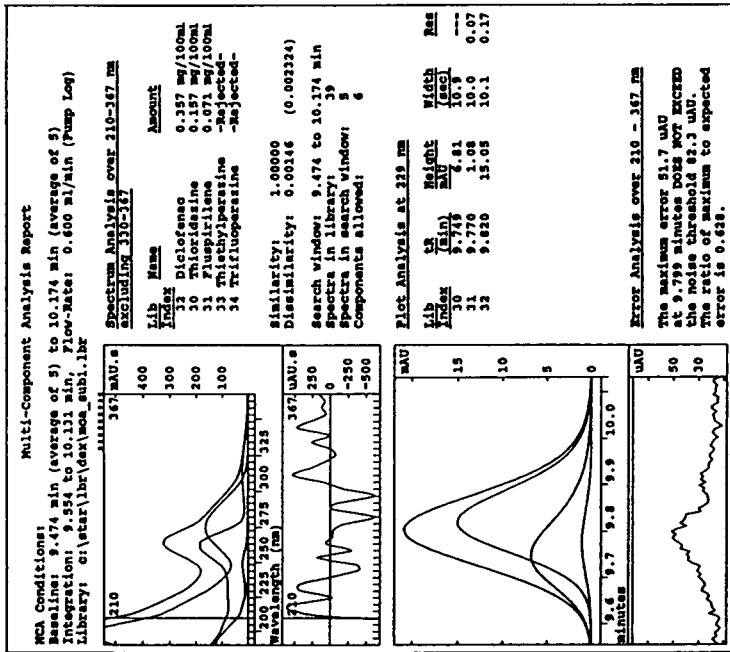


Fig. 5. Multicomponent analysis of a mixture of 20 drugs. Target concentration of diclofenac, thioridazine and fluspirilene were 0.360, 0.159 and 0.072 mg/100 ml, respectively, at $t_R = 9.80$ min.

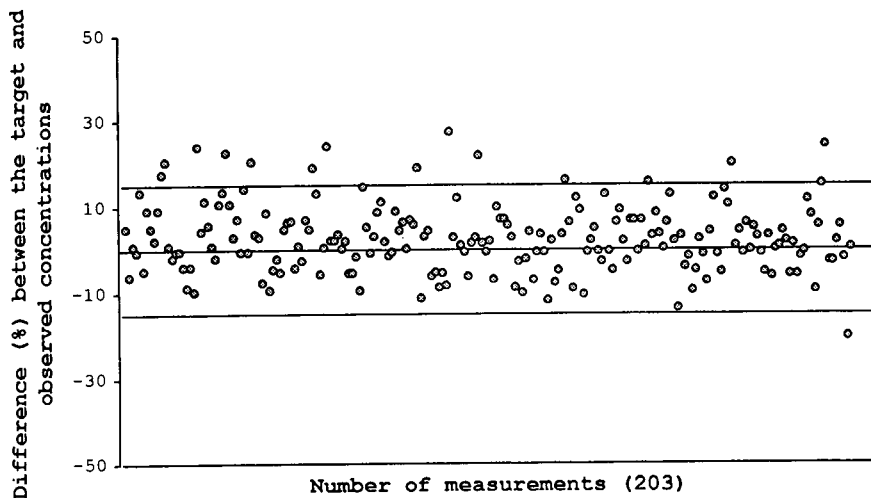


Fig. 6. Accuracy of multicomponent analysis for the quantitation of co-eluting drugs.

40 drugs were created from the main library and the number of drugs with similar or identical retention time in those sub-libraries was six. The chromatogram in Fig. 5 represents one of the mixtures containing 20 drugs. Fig. 6 shows that 93% of the drugs, totally or partially fused into the chromatographic peak of another drug, could be quantitatively isolated with $\pm 15\%$ accuracy. This study has confirmed the potential usefulness of MCA but more work has to be completed before it can be used on a routine basis. At present, the following guidelines are used: (a) previous information on the probable co-eluting drugs in quantitative MCA is required. This information can be obtained from GC–nitrogen–phosphorus detection screening, case history or the types of drugs submitted with the case, (b) limit the number of candidates by using selective extraction i.e. excluding the presence of acidic, amphoteric and neutral drugs from a basic extract, (c) obtain qualitative information by manually inspecting the eluted peak and (d) establish fit criteria based on error analysis and inject a standard of known concentration concurrently with the MCA analysis.

3.2. Extraction of acidic drugs

Direct acidic extracts of biological specimens prepared for drug screening purposes often con-

tain other substances which interfere with HPLC analysis. The XAD-2 procedure has been in use over ten years in this laboratory for the quantitation of barbiturates and phenytoin. It has been extended to the screening and quantitation of other acidic drugs such as naproxen, ibuprofen, ketorolac, piroxicam, flurbiprofen, warfarin etc. The addition of a back-extraction step into 0.45 M NaOH increased selectivity of the procedure and provided an extract with no background peaks.

Salicylic acid, acetaminophen and theophylline were extracted with ethyl acetate. Because of the lyophilic properties of acetaminophen and theophylline, purification using back-extraction was not feasible. However, the high therapeutic concentrations of these drugs allowed the direct extraction of whole blood with ethyl acetate using 0.5 ml of blood and a final volume of 2.0 ml. Interference from blood impurities had no effect on the identification and quantitation. Evaluation of solid-phase extraction instead of direct extraction with ethyl acetate is in progress.

3.3. Extraction of basic drugs

One of the most demanding problems in forensic toxicology is the analysis of complex cases when a variety of drugs and metabolites are present which interfere with each other in the chromatographic analysis. The method de-

scribed eliminates some of the problems encountered in the analysis of "multiple drug overdose" cases. The benefit of selective extraction is illustrated in Fig. 7. A 2-ml volume of blood was spiked with 10 drugs at a concentration of 0.1 mg/100 ml each; after the initial extraction with toluene under basic conditions, it was extracted with 0.45 M NaOH, 0.1 M H₂SO₄ and 6 M HCl. As shown in Fig. 7A, the poorly resolved or totally fused peaks obstruct the accurate quantitation of these drugs. By contrast, using the method outlined in Fig. 2, all drugs can be easily quantitated and identified in the three fractions (Fig. 7B, C and D). Figs. 8 and 9 show chro-

matograms of basic extracts of forensic case blood samples with multiple drugs findings.

3.4. Analysis of forensic samples

Two cases (Fig. 8A and B) were analysed for diltiazem and a third case (Fig. 8C) for verapamil. In each case, unexpected drugs (bromazepam, acebutolol and trimethoprim, respectively) were identified by the library search. The first case had a limited amount of blood sample and could not be re-extracted to determine the concentration of bromazepam. A quantitative bromazepam standard was injected

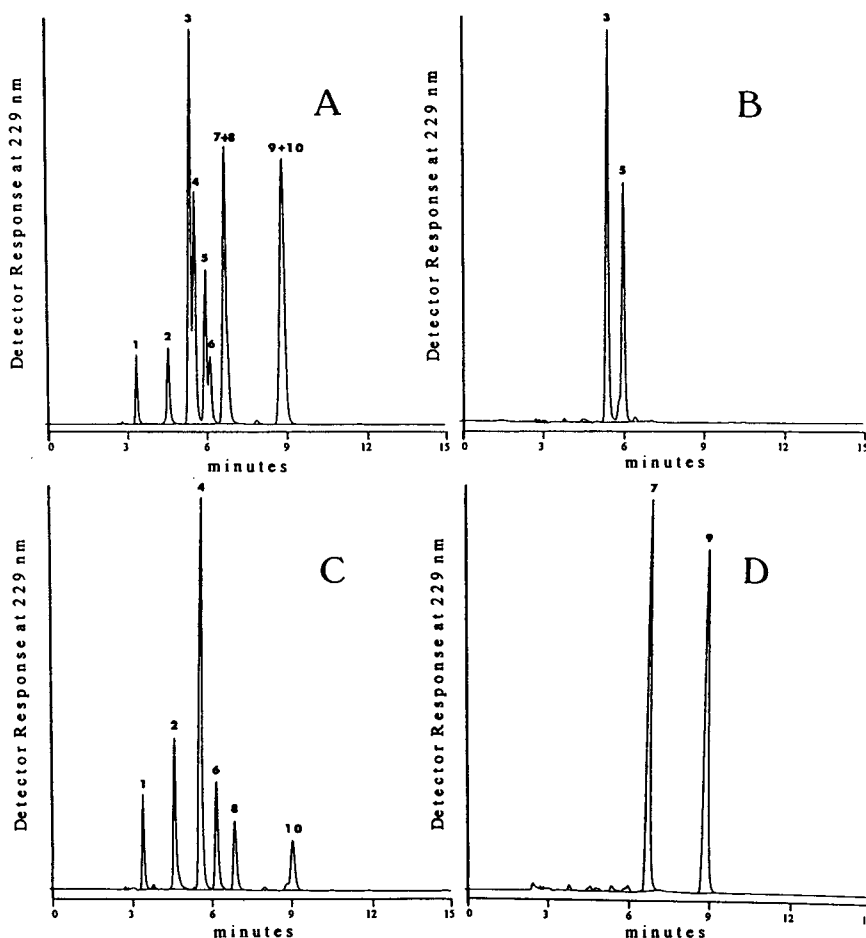


Fig. 7. Chromatograms obtained of the basic extracts of a spiked blood sample: (A) spiking standard, (B) fraction A, (C) fraction B and (D) fraction C. Peaks: 1 = codeine; 2 = trazodone; 3 = oxazepam; 4 = flurazepam; 5 = clonazepam; 6 = haloperidol; 7 = temazepam; 8 = imipramine; 9 = diazepam; 10 = trifluopromazine.

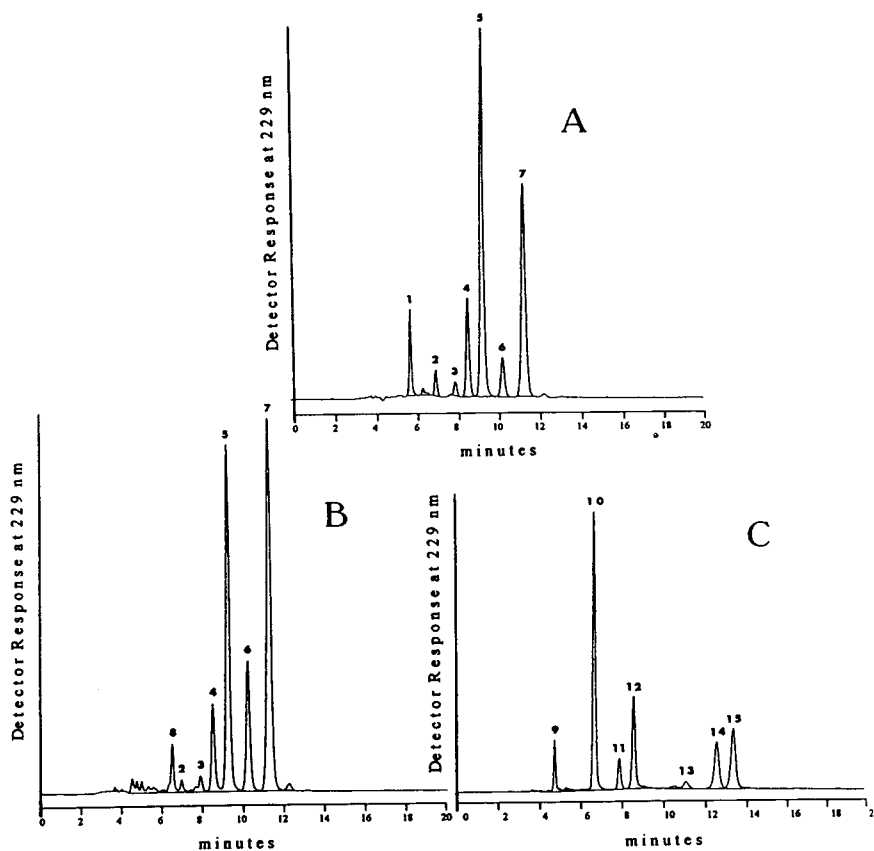


Fig. 8. Chromatograms obtained from the basic extracts of three forensic blood samples (A, B and C). Peaks: 1 = bromazepam; 2–4, 6 = diltiazem metabolites; 5 = desacetyldiltiazem; 7 = diltiazem; 8 = acebutolol; 9 = caffeine; 10 = trimethoprim; 11–14 = verapamil metabolites; 15 = verapamil.

and the peak area obtained was compared with the peak area of the equivalent standard in a previous bromazepam assay; it was within 10%. Using an average factor for the recovery of bromazepam from blood (based on long-term statistical data), the concentration of bromazepam was calculated.

Chlorpromazine, trifluoperazine and their metabolites were identified in another case blood (Fig. 9A). Manual inspection of peak number 4 indicated the presence of a benzodiazepine and phenothiazine. Using the qualitative MCA method, the peak was identified as bromazepam and a phenothiazine metabolite. In spite of the presence of several drugs and their metabolites, the concentration of temazepam was determined accurately using selective extraction (Fig. 9B).

Fig. 10 shows a chromatogram obtained from the XAD-2 extract of a forensic case blood sample in which naproxen was expected. In addition to naproxen, ibuprofen and ketorolac were found. Due to the negligible absorption of ketorolac at 229 nm, there was no observable peak in the chromatogram at $t_R = 6.2$ min. The automatic library search, however, provided a positive identification of ketorolac. Two extraneous peaks occurred at retention times of 4.03 and 5.35 min. The similarity of spectral properties of peak number 2 and ibuprofen indicated that the peak at $t_R = 5.35$ min is the metabolite of ibuprofen. Peak number 1 was not identified.

The screening of two gastric content samples in forensic cases is illustrated in Fig. 11A and B. Zopiclone, mesoridazine, perphenazine and

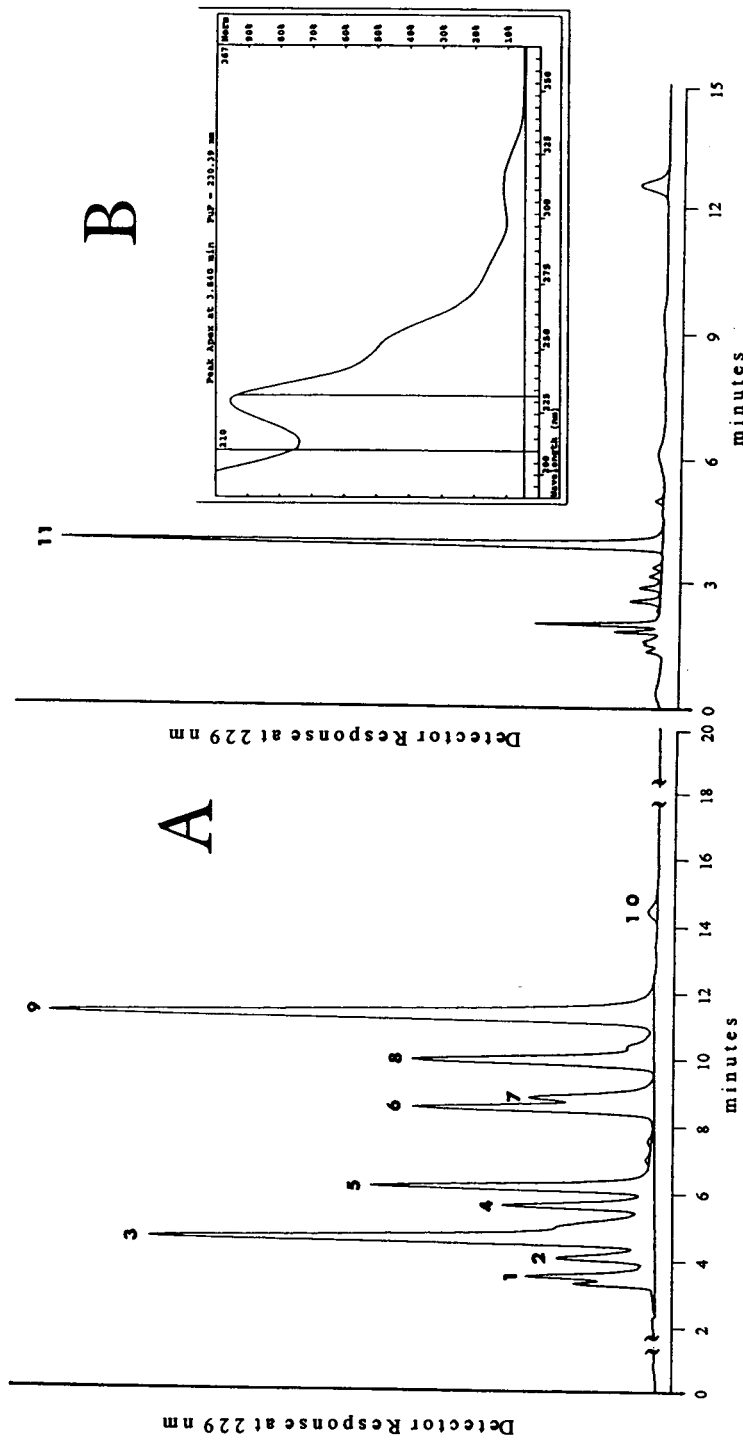


Fig. 9. Chromatograms obtained from the basic extracts of a forensic blood sample: (A) 0.1 M H₂SO₄ acid fraction and (B) 6 M HCl acid fraction. Peaks: 1 = caffeine; 2 = chlorpromazine sulfoxide; 3 = trifluoperazine sulfoxide; 4 = coelution of bromazepam and phenothiazine metabolite; 5, 7, 8 = phenothiazine metabolites; 6 = not identified; 9 = chlorpromazine; 10 = trifluoperazine; 11 = temazepam.

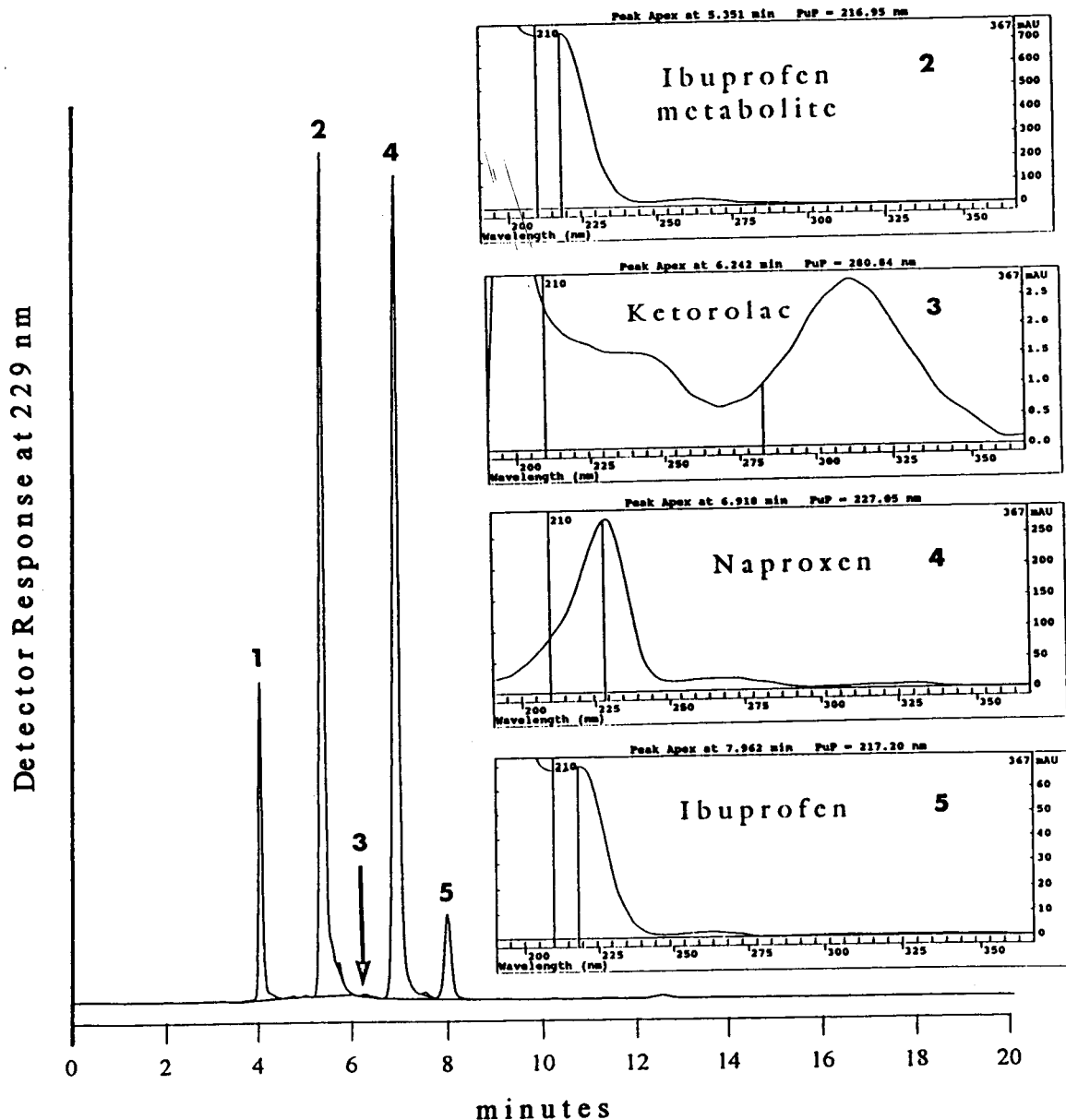


Fig. 10. Chromatogram obtained from the XAD-2 extract of a forensic blood sample and UV spectra of peaks 2, 3, 4 and 5. Peaks: 1 = not identified; 2 = ibuprofen metabolite; 3 = ketorolac; 4 = naproxen; 5 = ibuprofen.

thioridazine were identified in case 1. It should be noted that the peak eluted at about 9.9 min represents an enormous amount of thioridazine. Over 150 gastric content samples were screened in the last year and no carryover was observed during analysis. The mobile phase was re-routed

to the waste during the assay to prevent contamination of the mobile phase in the reservoir due to the high concentration of drugs in the gastric contents. By contrast with case 1, the chromatogram of the extract of gastric content in case 2 revealed only one chromatographic peak. No

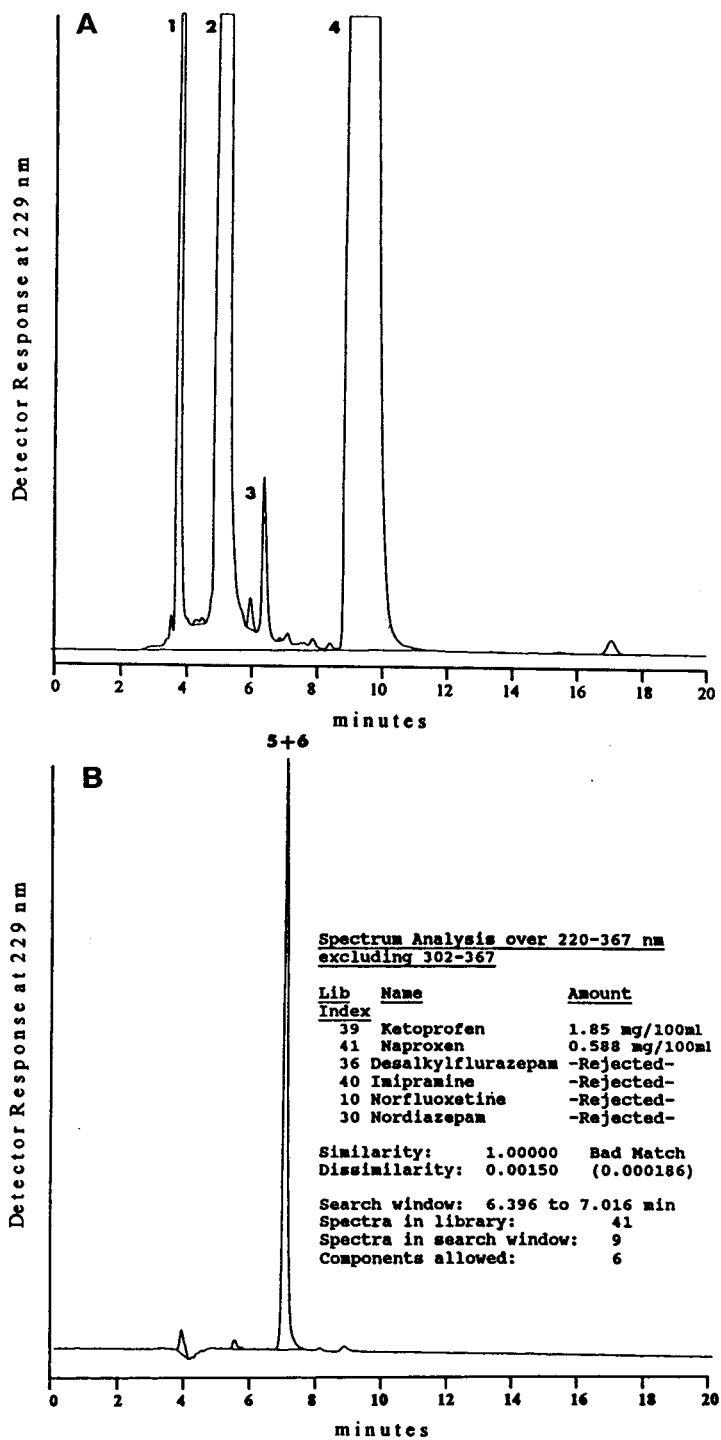


Fig. 11. Chromatograms obtained from extracts of two gastric contents (A and B). Peaks: 1 = zopiclone; 2 = mesoridazine; 3 = perphenazine; 4 = thioridazine; 5, 6 = co-elution of ketoprofen and naproxen.

match was made with the library search but the PUP indicated that it was not a homogeneous peak. Using MCA, the presence of ketoprofen and naproxen was confirmed.

4. Conclusions

The suitability of an isocratic HPLC–DAD system with computer-aided drug identification for toxicological screening and quantitation has been described. Extracts of postmortem blood samples as clean as possible were prepared, thus preventing co-elution of endogenous compounds with any drugs that may be present. It has been demonstrated that the back-extraction procedure resulted in clean extracts allowing identification of drugs based on spectra obtained by DAD. The use of the extraction characteristics of drugs together with the library search, allows more confidence in determining the identity of a drug. MCA presents to HPLC a major advance in the identification and quantitation of co-eluting chromatographic peaks. The results of this work have successfully demonstrated the application of PolyView-MCA software to the quantitation of 76 drugs. It was concluded that DAD together with MCA, offers a valuable tool for the HPLC analysis of forensic case samples involving multiple drugs. Using a library with candidate spectra, MCA can be employed to determine which drugs are present in a fused chromatographic peak.

Acknowledgements

Thanks are due to K. Lawrence for his skilful technical assistance. Special gratitude is due to D. Bilkic who conducted the numerous tests required for evaluation of the MCA. The author

is indebted to the following co-workers who contributed to this work during the past ten years: I.P. Casaseca, B. Mailvaganam, D. Mammoliti, A.H. Nagahara, D. Riley, S. Rimek and B. Walker.

References

- [1] E.J.M. Jansen, L.A. van Ginkel, R.H. van den Berg and R.W. Stephany, *J. Chromatogr.*, 580 (1992) 111.
- [2] A. Tracqui, P. Knitz, P. Kreissig and P. Mangin, *J. Liq. Chromatogr.*, 15 (1992) 1381.
- [3] S.F. Cooper, R. Massé and R. Dugal, *J. Chromatogr.*, 489 (1989) 65.
- [4] B.K. Logan, D.T. Stafford, I.R. Tebbett and C.M. Moore, *J. Anal. Toxicol.*, 14 (1990) 154.
- [5] P.M. Kabra, B.E. Stafford and L.J. Marton, *J. Anal. Toxicol.*, 5 (1981) 177.
- [6] D.W. Hill and K.J. Langner, *J. Liq. Chromatogr.*, 10 (1987) 377.
- [7] T.V. Alfredson, A.H. Maki, M.E. Adaskaveg, J.-L. Excoffier and M.J. Waring, *J. Chromatogr.*, 507 (1990) 277.
- [8] M. Bogusz and M. Wu, *J. Anal. Toxicol.*, 15 (1991) 188.
- [9] A. Turcant, A. Premel-Cabic, A. Cailleux and P. Allain, *Clin. Chem.*, 37 (1991) 1210.
- [10] M. Bogusz, J.P. Franke, R.A. de Zeeuw and M. Erkens, *Fresenius' J. Anal. Chem.*, 347 (1993) 73.
- [11] O.H. Drammer, A. Kotsos and I.M. McIntyre, *J. Anal. Toxicol.*, 17 (1993) 225.
- [12] T.W. Ryan, *J. Liq. Chromatogr.*, 16 (1993) 315.
- [13] E.M. Koves and J. Wells, *J. Forensic Sci.*, 37 (1992) 42.
- [14] E.M. Koves and W.-C. Sun, in M.H. Ho (Editor), *Analytical Methods in Forensic Chemistry*, London, 1990, Ch. 23. p. 342.
- [15] D.A. Riley and E.M. Koves, *Can. Soc. Forens. Sci. J.*, 25 (1992) 191.
- [16] E.M. Koves and K. Lawrence, in preparation.
- [17] T.L. Sheenan, M. Adaskaveg and J.L. Excoffier, *Am. Lab.*, 21 (1989) 66.
- [18] W.C. Sun, personal communication.
- [19] J.L. Excoffier, M. Joseph, J.J. Robinson and T.L. Sheehan, *J. Chromatogr.*, 631 (1993) 15.
- [20] H.R. Keller, P. Kiechle, F. Erni, D.L. Massart and J.L. Excoffier, *J. Chromatogr.*, 641 (1993) 1.



ELSEVIER

Journal of Chromatography A, 692 (1995) 121–129

JOURNAL OF
CHROMATOGRAPHY A

Qualitative and quantitative determination of illicit heroin street samples by reversed-phase high-performance liquid chromatography: method development by CARTAGO-S

Kathrin Grogg-Sulser, Hans-Jörg Helmlin, Jean-Thomas Clerc*

Institute of Pharmacy, University of Berne, Baltzerstrasse 5, CH-3012 Berne, Switzerland

Abstract

The development of a method involving reversed-phase HPLC using CARTAGO-S, a spreadsheet computer program as a method development tool is described for the simultaneous qualitative and quantitative determination of heroin in illicitly manufactured street samples containing by-products originating from opium and also commonly occurring adulterants that have been found in Switzerland. The method utilizes simple sample dissolution followed by reversed-phase HPLC on a 3- μ m ODS-1 column with acetonitrile–water–phosphoric acid–hexylamine as the mobile phase. UV detection and quantification were carried out at 210 nm. The optimum linear gradient elution consisted of four steps with a total duration of 36 min. Excellent agreement between predicted and measured retention times with differences ranging from 0.45% to 6.8% was found. For calibration, all compounds showed a good linear relationship between peak area and concentration. The low UV cut-off of this mobile phase allows the detection of heroin and related compounds at its major UV absorption at 210 nm. With this method, the limits of detection absolute ranged from 10 ng for noscapine, corresponding to 0.09% of the sample mass, in the best case to 100 ng for cocaine in the worst case, depending on molar absorptivities.

1. Introduction

In recent years in Switzerland, there has been a strong increase in illicit drug consumption and in the number of overdoses and deaths related to drugs, especially heroin. The subject of this study was to analyse heroin street samples by HPLC and to study both qualitative and quantitative aspects.

Heroin is produced by acetylation of morphine originating from opium. In clandestine laboratories the purification of morphine and also of heroin is seldom efficient. The heroin produced contains significant amounts of the opium al-

kaloids and their acetylated products. In addition, most illicit heroin street samples are adulterated and/or diluted several times before reaching the user. Adulterants such as analgesics, local anaesthetics and caffeine are pharmacologically active substances that mimic the bitter taste of heroin, whereas carbohydrates such as lactose, mannitol and sucrose are inactive and are often used for dilution purposes.

Various methods for the analysis of heroin described in the literature encompass a diversity of chromatographic techniques such as GC with flame ionization detection [1–5], GLC [6] and GC–MS [7]. HPLC overcomes the problems associated with GC such as adsorption, heat instability, transesterification and solubility [8–

* Corresponding author.

10], which result in poor precision and accuracy. The successful separation of opiates in illicit heroin by HPLC has been described by several workers [1,11–17].

This paper reports a fast and accurate HPLC procedure for the simultaneous determination of heroin, cocaine, acetylcodeine, noscapine, papaverine, 6-monoacetylmorphine, morphine, paracetamol, caffeine, benzocaine, lidocaine and procaine in illicitly manufactured heroin street samples using UV detection. The qualitative determination of codeine and 3-monoacetylmorphine is also reported.

Method development for the gradient separation of thirteen components found in illicit heroin street samples was performed with CARTAGO-S [18], a spreadsheet-based computer program, which is under development in our laboratory.

Because no single chromatographic procedure can overcome the co-elution of compounds, each sample was subjected to both HPLC and GC-MS. In addition, TLC screening was performed for sugars according to a routine method of the laboratory [19].

2. Experimental

2.1. Instrumentation

The HPLC system consisted of a chromatograph with two M 6000-A pumps and of a Model 660 solvent programmer (Waters, Milford, MA, USA), a Model 7125 injector (Rheodyne, Cotati, CA, USA) fitted with a 20- μ l sample loop, an LC 55 spectrophotometer (Perking-Elmer, Künsnacht, Switzerland), and a Shimadzu Chromatopac C-R1 B data processor (Burkhard Instrumente, Zurich, Switzerland). Separations were performed at 25°C on a 125 \times 4 mm I.D. column packed with 3- μ m Spherisorb ODS-1 (Phase Separations, Deeside, UK), filled by Macherey-Nagel (Oensingen, Switzerland), with a 4 \times 4 mm I.D. precolumn, packed with 5- μ m LiChrospher 100 (Merck, Darmstadt, Germany). The mobile phases were (A) water containing 5.0 ml (8.5 g) of orthophosphoric acid

(85%) and 0.56 ml (0.44 g) of hexylamine per 1000 ml and (B) acetonitrile–water (9:1; v/v) containing 5.0 ml (8.5 g) of orthophosphoric acid (85%) and 0.56 ml (0.44 g) of hexylamine per 1000 ml. The flow-rate was 0.7 ml/min. The eluents were filtered through a membrane filter (regenerated cellulose, 0.45 μ m; Schleicher and Schuell, Dassel, Germany) and degassed by sonication. Methanol was used for washing the column. The detection wavelength was set at 210 nm.

2.2. Chemicals and reagents

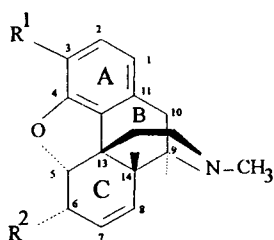
Hexylamine (99%, purum) was provided by Fluka (Buchs, Switzerland). Water used for HPLC was doubly distilled. All other chemicals and solvents were of analytical-reagent or HPLC grade, purchased from Merck. Morphine \cdot HCl (1), cocaine \cdot HCl (11), codeine (4), papaverine \cdot HCl (13), procaine \cdot HCl (2), lidocaine \cdot HCl (6), paracetamol (3) and benzocaine (8), all of Pharmacopoeia Eur II grade, were obtained from Siegfried (Zofingen, Switzerland). Caffeine (7), pure, was obtained from Merck and noscapine (12) from Mepha Pharma (Aesch, Switzerland). Heroin (10), 6-monoacetylmorphine (5) and acetylcodeine (9) were prepared by the method of Wright [20] and 3-monoacetylmorphine (14) by the method of Welsh [21]; their purities were established by GC-MS. The structures of 1, 4, 5, 9, 10 and 14 are shown in Fig. 1.

2.3. Heroin street samples

Heroin street samples (ca. 30 mg) were collected by assistants of Contact (a governmental subsidized socio-medical institution for the support of drug addicts) in Berne directly from the users.

2.4. Gradient elution optimization

CARTAGO-S exploits the fact that the logarithm of the capacity factor varies approximately linearly with the concentration of the organic modifier. The parameters of this linear relationship are determined for each compound



	R ¹	R ²
Morphine (1)	OH	OH
Heroin (10)	COOCH ₃	COOCH ₃
6-Monoacetylmorphine (5)	OH	COOCH ₃
3-Monoacetylmorphine (14)	COOCH ₃	OH
Codeine (4)	OCH ₃	OH
Acetylcodeine (9)	OCH ₃	COOCH ₃

Fig. 1. Structures of heroin and related compounds.

using at least two isocratic runs. These are then used to predict the retention behaviour in piecewise linear gradients. The program is implemented in a spreadsheet and can be used for chromatogram simulation and for optimization.

2.5. Chromatographic conditions

The optimum elution profile consisted of four steps with a total duration of 36 min: first a gradient from 9% to 14% B in 4 min, followed by an isocratic step with 14% B for 13 min; the third step was a gradient from 14% to 45% B in 11 min and the fourth step was isocratic conditions at 45% B for 8 min (see also Fig. 2). The times given are corrected for the gradient delay time (i.e., the time lag between initiation of the gradient at the pumps and its onset at the sample inlet). The absorbance of the column effluent was monitored at 210 nm. The re-equilibration time after each run was 20 min.

2.6. Calibration

Quantitative determinations of heroin and selected adulterants were performed on the basis

of the peak areas using the external standard method.

Calibration graphs were constructed from aqueous solutions (10 mmol ortho-phosphoric acid; pH 2.5) of pure standard substances at known concentrations selected to correspond to those in illicit heroin street samples. The concentrations for calibration range with a linear response are shown in Table 2. Each calibration graph was constructed from triplicate determinations of at least four concentration levels. The injection volume was 15 μ l. The average value of the area for each calibration point was used to study the linearity of the response.

2.7. Sample preparation

Homogenized heroin street samples were accurately weighed (ca. 15 mg) into a 20-ml volumetric flask and dissolved in aqueous acid (10 mmol orthophosphoric acid; pH 2.5) using an ultrasonic bath for 10 min. Samples containing more than 30% heroin have to be diluted before analysis. Filtration prior to injection was necessary (Spartan 13/30, 0.2 μ m; Schleicher and Schuell).

2.8. Precision and reproducibility

For checking the precision and accuracy of the method, a heroin sample was prepared by grinding together known amounts of heroin, cocaine·HCl, morphine·HCl, 6-monoacetylmorphine, acetylcodeine, noscapine·HCl, papaverine·HCl, caffeine, paracetamol, lidocaine, procaine·HCl and benzocaine. Five accurately weighed amounts of this control sample were then treated as described and each sample was analysed in duplicate.

Aliquots of a calibration mixture were partitioned and frozen at -18°C . The stability of the calibration was determined by injection a control mixture at the beginning of each week or at other times as required in order to check calibration and efficiency of the chromatographic system.

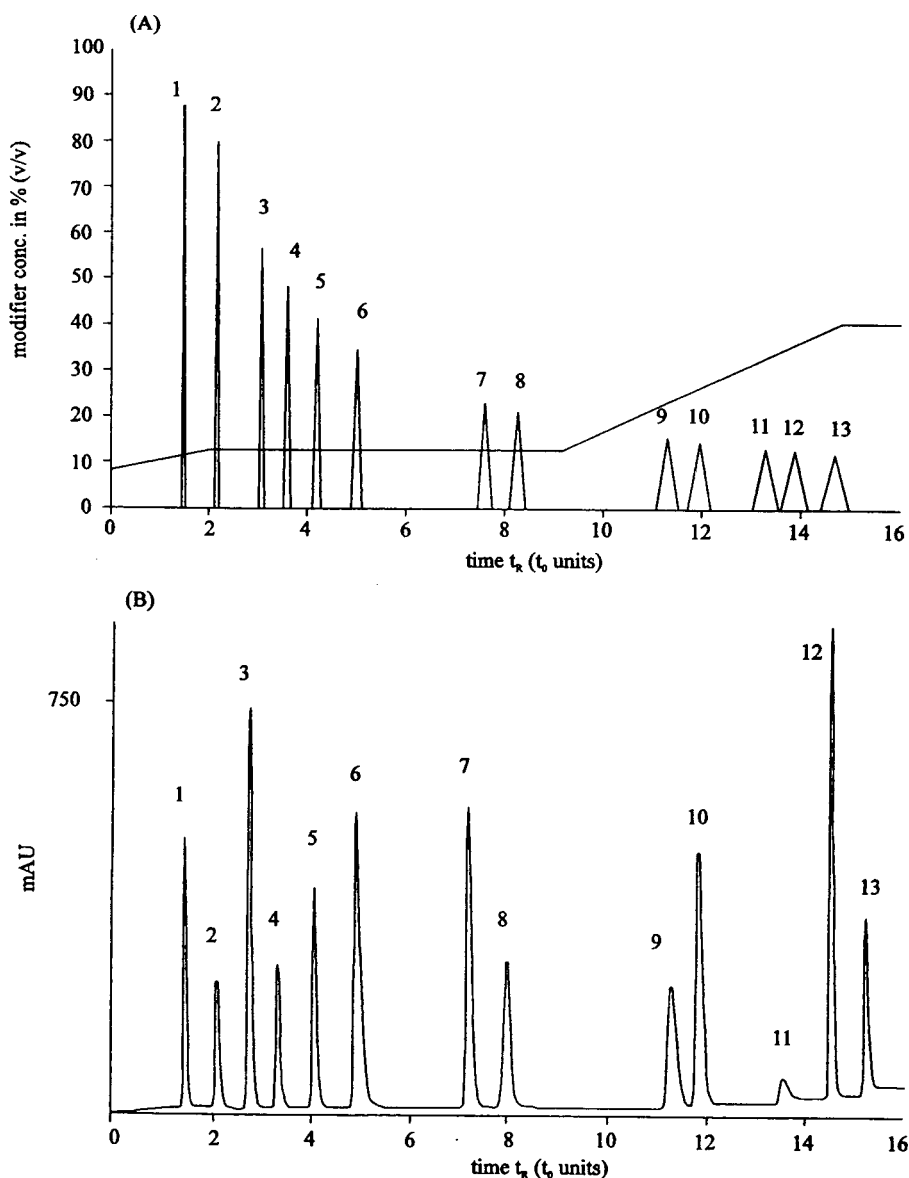


Fig. 2. (A) Chromatogram predicted by CARTAGO-S and (B) chromatogram of reference substances. Peaks: 1 = morphine; 2 = procaine; 3 = paracetamol; 4 = codeine; 5 = 6-monoacetylmorphine; 6 = lidocaine; 7 = caffeine; 8 = benzocaine; 9 = acetylcodeine; 10 = heroin; 11 = cocaine; 12 = noscapine; 13 = papaverine.

3. Results and discussion

3.1. HPLC system

By using CARTAGO-S, time-consuming experimental evaluation of optimum piecewise linear gradient elution was prevented and op-

timum chromatographic conditions were achieved within a reasonable time for thirteen components with a wide range of polarities. Table 1 shows the results of predicted retention times, t_R (t_0 units = t_R/t_0), by CARTAGO-S, measured t_R , elution time (minutes), precision of t_R within-day and week-to-week and resolution

Table 1
Results of t_R predicted by CARTAGO-S, measured t_R , elution time, precision of t_R within-day and week-to-week and resolution

Substance	Predicted t_R (t_0 units)	Measured t_R (t_0 units)	Elution time (min)	R.S.D. of t_R (%) ($n = 5$)		R_s
				Within-day	Week-to-week	
Morphine (1)	1.5	1.5	2.9	0.77	7.7	
Procaine (2)	2.2	2.2	4.3	0.46	2.0	4.5
Paracetamol (3)	3.1	2.9	5.7	0.92	3.8	4.7
Codeine (4)	3.6	3.4	6.7	0.45	2.5	3.1
6-Monoacetylmorphine (5)	4.2	4.1	8.0	0.51	2.4	4.0
Lidocaine (6)	5.0	4.8	9.4	0.36	2.1	3.5
Caffeine (7)	7.6	7.3	14.3	0.42	4.0	9.1
Benzocaine (8)	8.3	8.1	15.9	0.18	2.1	3.2
Acetylcodeine (9)	11.3	11.2	21.9	0.42	3.0	7.2
Heroin (10)	11.8	11.8	23.1	0.22	2.3	1.4
Cocaine (11)	13.0	13.4	26.3	0.15	1.3	5.0
Noscapine (12)	13.6	14.5	28.4	0.12	1.2	3.9
Papaverine (13)	14.3	15.1	29.6	0.07	1.2	2.5

Chromatographic conditions as described in Experimental.

between selected substances. Excellent agreement between predicted and measured t_R with differences ranging from 0.45% for benzocaine to 6.8% for paracetamol was found. For within-day determinations, the relative standard deviations (R.S.D.s) for t_R ranged from 0.07 to 0.92% and for week-to-week precision the R.S.D.s ranged from 1.17 to 4%. However, small errors in concentration of one or more compounds of the organic or aqueous phase are propagated to errors in t_R , so care should be taken when preparing the mobile phase. The notoriously difficult separation of 3- from 6-monoacetylmorphine was adequate for qualitative separation, the experimental retention times being 7.66 and 8.04 min, respectively.

With this system, more than 300 analyses have now been performed without significant changes in t_R and resolution power, proving that no column degradation had occurred due to the organic mobile phase as reported [16].

It is well known that basic compounds may show a pronounced tailing effect on certain reversed-phase columns owing to interactions with the residual polar silanol groups of the stationary phase [22,23]. The addition of an amine modifier to the mobile phase as a masking agent for the silanol groups improves the peak shape and changes the capacity factor (k'). With

the addition of orthophosphoric acid to the mobile phase, an acidic eluent with a pH of ca. 2.5 is obtained, so that the components of interest, such as heroin and other basic substances, are protonated [24].

A chromatogram predicted by CARTAGO-S and the corresponding real chromatogram are shown in Fig. 2 and a chromatogram for an illicit heroin sample is shown in Fig. 3. All compounds are sufficiently separated and have symmetrical, sharp, non-tailing peaks.

With some samples, small peaks eluting just after 6-monoacetylmorphine, heroin, papaverine and noscapine were observed. It is well known that noscapine and also thebaine, codeine and morphine give degradation and rearrangement products due to heat and acetylation [25–27]. Injection of a concentrated solution of noscapine that had been acetylated at 100°C for 2 h showed peaks at the same t_R , indicating that these substances originate from noscapine. Further investigations need to be carried out to prove this assumption.

3.2. Calibration

Working in the linear range of the detector, the calibration graph was linear from 68 to 306 $\mu\text{g/ml}$ for heroin (Table 2). As the concen-

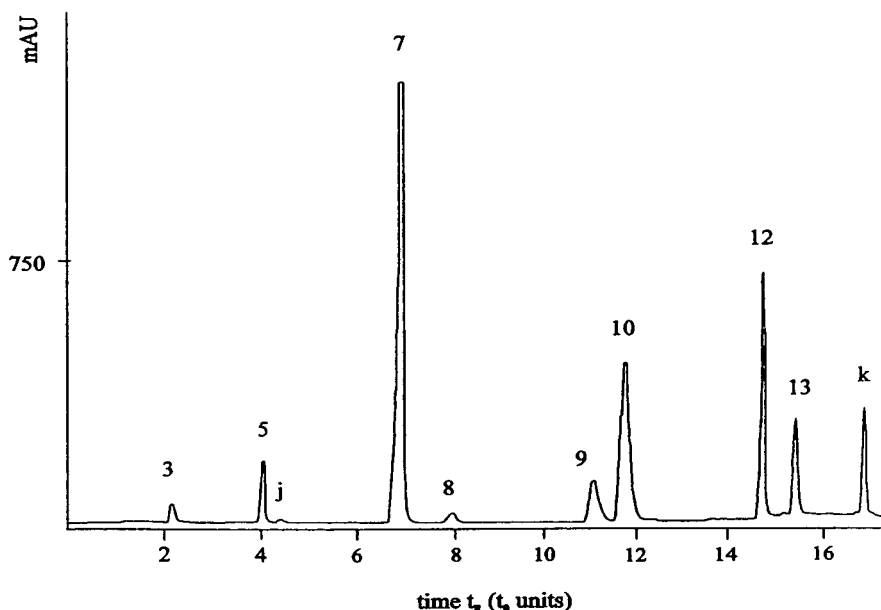


Fig. 3. Chromatogram of a heroin street sample. Peaks: 3 = procaine; 5 = 6-monoacetylmorphine; 7 = caffeine; 8 = benzocaine; 9 = acetylcodeine; 10 = heroin; 12 = noscapine; 13 = papaverine; j and k, unidentified, but probably due to noscapine degradation or rearrangement products.

trations of papaverine and acetylcodeine in actual samples vary from 0 to 6.5% from 0 to 14% [28], respectively, in relation to heroin, calibration for these substances was set in the

concentration range expected in illicit heroin. In contrast, the concentration of noscapine can vary from 0 to 200% and that of 6-monoacetylmorphine from 0 to 223% [19] in relation to heroin,

Table 2
Regression data for selected compounds and linear range

Substance	Calibration range ($\mu\text{g/ml}$)	Slope	Intercept	S_y	S_x	n	r^2
Morphine (1)	3.7–36.7	4382	5538	2130	59	11	0.9984
6-Monoacetylmorphine (5)	4.7–46.8	3197	3735	1668	36	11	0.9988
Heroin (10)	68–306	4021	–84893	9335	4021	6	0.9995
Acetylcodeine (9)	4.1–41	4139	–6959	767	21	9	0.9998
Noscapine (12)	2.9–43.2	7329	358	2608	56	12	0.9994
Papaverine (13)	4.9–49	2992	2677	1463	30	11	0.9990
Cocaine (11)	21.7–260	482	–2163	839	3.6	7	0.9996
Benzocaine (8)	50–150	1554	6728	1121	15	5	0.9997
Procaine (2)	43–134	982	399	1521	21	5	0.9986
Lidocaine (6)	43–134	3433	4870	2231	31	5	0.9975
Caffeine (7)	12.6–101	8326	–45993	21287	277	6	0.9956
Paracetamol (3)	34.3–147	4126	–51395	9303	111	4	0.9985

Experimental conditions as described in Experimental.

S = Standard deviation; n = number of measurements; r = correlation coefficient.

which often makes further dilution of the sample solution necessary in order to determine noscapine and 6-monoacetylmorphine. For all compounds an excellent linear relationship between peak area and concentration was observed (Table 2).

Another advantage of this separation system is the low UV cut-off range of the mobile phase, which allows the detection of heroin and related compounds at its major UV absorption maximum of 210 nm. At this wavelength heroin and related compounds show up to a ten-fold increased sensitivity in comparison with detection at 280, 284, 279 and 228 nm as applied by other workers [1,11,12,15,17]. The limits of detection absolute on-column ranged from 10 ng for noscapine, corresponding to 0.09% of the sample mass, to 100 ng for cocaine, which shows poor absorption at 210 nm. Papaverine also shows less absorption at 210 nm. Using diode-array or multiple-wavelength detection would overcome this problem by quantifying each compound at its optimum wavelength. In addition, using a diode-array detector for checking purity or carry-

ing out detection at different wavelengths would increase the separation power significantly [15]. Fig. 4 shows the overlaid UV spectra of heroin, noscapine and cocaine, measured in the mobile phase.

3.3. Precision, reproducibility and recovery

A control solution was injected at the beginning of each week or at other times to determine the reproducibility of calibration. To investigate the precision and recovery of sampling, five aliquots of a heroin sample that was made up in this laboratory were analysed. The results are given in Table 3. Calibration proved to be stable over a long period, making this method extremely valuable for long-term routine analyses of illicit heroin samples. Good results for precision and recovery were also obtained with this method. Analysing a pure standard solution containing heroin after 2 and 4 h, no 6-monoacetylmorphine could be detected, proving that heroin has a sufficient short-term stability in the chosen solvent [29].

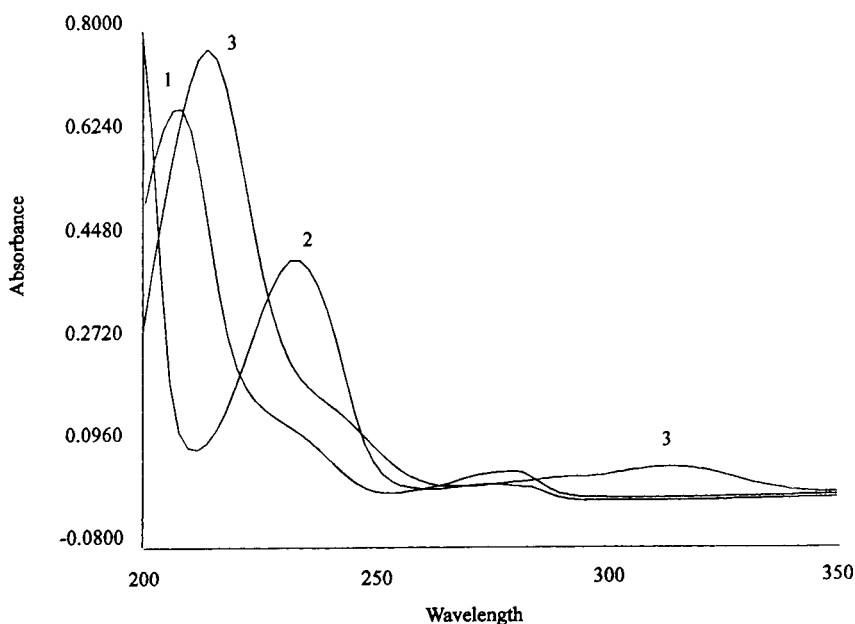


Fig. 4. UV absorption of (1) heroin, (2) cocaine and (3) noscapine, measured in the mobile phase. Wavelength in nm; absorbance in mAU.

Table 3
Results of precision and recovery of sampling

Substance	Reproducibility of calibration (n = 8) (8 weeks)			Replicate sampling (n = 5)			Recovery (%) (n = 5)
	Mean ($\mu\text{g/ml}$)	S.D. ($\mu\text{g/ml}$)	R.S.D. (%)	Mean ($\mu\text{g/ml}$)	S.D. ($\mu\text{g/ml}$)	R.S.D. (%)	
Cocaine (11)	63.15	1.2	1.9	68.15	1.1	1.6	97.9
Heroin (10)	83.27	1.6	1.9	245.00	4.6	1.9	101.6
Caffeine (7)	37.84	1.1	2.9	31.91	0.7	2.2	100.2
Paracetamol (3)	69.81	1.9	2.7	85.36	1.5	1.7	96.3
Procaine (2)	86.16	2.4	2.8	78.53	1.6	2.1	102.3
Benzocaine (8)	100.72	2.2	2.2	88.52	2.6	3.0	97.6
Lidocaine (6)	87.53	2.3	2.7	81.29	1.6	1.8	97.5
Morphine (1)	28.94	0.9	3.1	7.78	0.25	3.2	103.7
Noscapine (12)	35.32	0.9	2.5	26.89	0.98	3.6	99.4
Papaverine (13)	39.65	1.3	3.3	8.12	0.33	4.0	96.1
Acetylcodeine (9)	40.19	0.8	2.0	19.02	0.38	2.0	103.5
6-Monoacetylmorphine (5)	35.71	0.8	2.2	7.57	0.37	4.9	102.9

Experimental conditions as described in Experimental.

4. Conclusions

An excellent separation of heroin and selected basic impurities and adulterants was obtained via reversed-phase liquid chromatography. Inexpensive methodology suitable for small laboratories was developed which allowed the simultaneous determination of heroin, morphine, 6-monoacetylmorphine, papaverine, acetylcodeine, noscapine and cocaine and also various adulterants such as paracetamol, caffeine, procaine, benzocaine and lidocaine over a wide concentration range. Simple sample pretreatment minimizes the time required and variations due to the extraction technique.

References

- [1] E. Kaa, *J. Forensic Sci.*, 36 (1991) 866–879.
- [2] C. Barnfield, S. Burns, D.L. Byrom and A.V. Kemmenoe, *Forensic Sci. Int.*, 39 (1988) 107–117.
- [3] I. Barni Comparini, F. Centini and A. Pariali, *J. Chromatogr.*, 279 (1983) 609.
- [4] A. Sperling, *J. Chromatogr.*, 538 (1991) 269.
- [5] E. Bertol, F. Mari and M.G. Di Milia, *J. Chromatogr.*, 466 (1989) 384.
- [6] T.A. Gough and P.B. Baker, *J. Chromatogr. Sci.*, 19 (1981) 227–234.
- [7] M. Chiarotti, N. Fucci and C. Furnari, *Forensic Sci. Int.*, 50 (1991) 47.
- [8] T.A. Gough and P.B. Baker, *J. Chromatogr. Sci.*, 19 (1981) 227.
- [9] E. Brochmann-Hanssen, *J. Pharm. Sci.*, 51 (1962) 1095.
- [10] H. Huizer, *Analytical Studies on Illicit Heroin*, University of Leiden, Leiden, 1988.
- [11] T.A. Gough and P.B. Baker, *J. Chromatogr. Sci.*, 19 (1981) 483.
- [12] P.C. White, I. Jane, A. Scott and B. Connett, *J. Chromatogr.*, 265 (1983) 293.
- [13] Billiet, R. Wolters, L. de Galan and H. Huizer, *J. Chromatogr.*, 368 (1986) 351.
- [14] P.C. White, A. Etherington and T. Catterick, *Forensic Sci. Int.*, 37 (1988) 55.
- [15] I.S. Lurie and S.M. Carr, *J. Liq. Chromatogr.*, 9 (1986) 2485.
- [16] I.S. Lurie and K. McGuinness, *J. Liq. Chromatogr.*, 10 (1987) 2189.
- [17] D. Bernhauer and E.F. Fuchs, *Arch. Kriminol.*, 169 (1982) 73.
- [18] H.J. Helmlin and J.T. Clerc, presented at the 16th International Symposium on Column Liquid Chromatography, Baltimore, MD, 1992, abstracts, p. 49.
- [19] K. Grogg, in preparation.
- [20] J. Wright, *J. Pharmacol. Exp. Ther.*, 71 (1941) 164.
- [21] L.H. Welsh, *J. Org. Chem.* 19 (1954) 1409.
- [22] D. Chan Leach, *LC·GC Int.*, 1 (1988) 22.

- [23] H. Engelhardt, *Chromatographia*, 29 (1990) 59.
- [24] A.C. Moffat (Editor), *Clarke's Isolation and Identification of Drugs in Pharmaceuticals, Body Fluids, and Post-Mortem Material*, Pharmaceutical Press, London, 1986.
- [25] A.C. Allen, D.A. Cooper, J.M. Moore and Ch.B. Teer, *J. Org. Chem.*, 49 (1984) 3462.
- [26] A.C. Allen, D.A. Cooper, J.M. Moore, M. Gloger and H. Neumann, *Anal. Chem.*, 56 (1984) 2940.
- [27] H. Neumann and M. Gloger, *Chromatographia*, 16 (1982) 261.
- [28] E. Kaa, *Z. Rechtsmed.*, 99 (1987) 87.
- [29] D. Bernhauer, E.F. Fuchs and H. Neumann, *Fresenius' Z. Anal. Chem.*, 316 (1983) 501.



ELSEVIER

Journal of Chromatography A, 692 (1995) 131–136

JOURNAL OF
CHROMATOGRAPHY A

Determination of aflatoxins in medicinal herbs and plant extracts

Klaus Reif*, Wolfgang Metzger

PhytoLab GmbH & Co. KG, Dutendorfer Strasse 5–7, 91487 Verstenbergsgreuth, Germany

Abstract

The occurrence of the aflatoxins B₁, B₂, G₁ and G₂ in common medicinal herbs and plant extracts was examined. The aflatoxins are toxic metabolites of the fungal strains *Aspergillus flavus* and *Aspergillus parasiticus*. The method involves the implementation of high-performance liquid chromatography (HPLC) together with fluorescence detection. Aflatoxins B₁ and G₁ are determined as their bromine derivatives, produced in an on-line, postcolumn electrochemical cell (KOBRA cell). The aflatoxins are extracted using a mixture of methanol and water and isolated and concentrated by means of immunoaffinity column chromatography. The aflatoxins are separated and detected by HPLC using an RP-18 column and a scanning fluorescence detector. The method permits the detection of aflatoxins with a detection limit of 0.05 ppb and recoveries in a range 70–100% for a variety of medicinal herbs. The method was tested on capsicum, potatoes, stinging nettles, birch leaves, senna leaves, etc.

1. Introduction

Aflatoxins are toxic metabolites of fungal origin (*Aspergillus flavus* and *Aspergillus parasiticus*). These mycotoxins are known to be highly toxic and carcinogenic. Therefore, the contamination of foods and animal feed with these mycotoxins is controlled by legal limits worldwide. In Germany these limits are 4 ppb (w/w) for the sum of aflatoxins B₁, B₂, G₁ and G₂ and 2 ppb for aflatoxin B₁. For human dietary products, such as infant nutriment, there are stronger legal limits: 0.05 ppb for aflatoxin B₁ and the sum of all aflatoxins.

Much has been published about the occurrence of aflatoxins in nuts (peanuts), nut-like

products, corn and other natural products [1–3]. Only a few papers have described the contamination of spice (e.g., capsicum) [4] and dried fruit [5]. In this study, we examined the occurrence of aflatoxins in medicinal herbs, plant extracts and herbal remedies using HPLC with fluorescence detection after electrochemical derivatization in a KOBRA cell [6]. Especially birch leaves, senna fruits, *Rauwolfia serpentina*, etc., could be naturally contaminated. Previously, most determinations of aflatoxins have involved two dimensional high-performance thin-layer chromatography (HPTLC) with fluorescence detection by means of a TLC scanner. Enzyme-linked immunosorbent assay (ELISA) tests and most often HPLC methods have been described.

Fluorescence detection with iodine postcolumn derivatization has two distinct disadvantages:

* Corresponding author.

first it requires the use of two HPLC pumps and second there is the problem of the instability of the iodine solution. The method using trifluoroacetic acid (TFA) as derivatizing agent has poor reproducibility and is difficult to automate.

The official methods in Germany [9] using two-dimensional TLC is time consuming and cannot be used for every matrix. For example, the medicinal herb *Rauwolfia serpentina* is known to give wrong results using TFA derivatization or TLC techniques because of its content of fluorescent alkaloids such as reserpine and rescinnamine.

2. Experimental

This method was employed for tests on a variety of medicinal herbs and their extracts: capsicum, stinging nettles, ginger, cardamom, hawthorn (*Crataegi folium cum flore*), mistletoe (*Visci herba*), cone flower (*Echinaceae angustifoliae radix*), deadly nightshade (*Belladonnae folium*), birch leaves, senna leaves, potatoes, beans, ivy leaves (*Hedera folium*), horse chestnut (*Hippocastani semen*), fennel seed (*Foeniculi fructus*), valerian (*Valerianae radix*), gourd seed (*Cucurbitae semen*), melissa (*Melissae folium*), cress (*Nasturtii herba*), passion flowers, etc.

2.1. Principle

The aflatoxins are extracted using a mixture of methanol and water by sonification and isolated and concentrated by the means of immunoaffinity column chromatography. The aflatoxins are separated and detected by HPLC using an RP-18 column and a scanning fluorescence detector.

2.2. Reagents

All reagents used were of analytical-reagent grade. No interference with the aflatoxins was observed. The extraction solvent was a mixture of methanol (LC grade; Baker, Gross-Gerau, Germany) with water (70:30, v/v). The mobile phase was water–methanol (58:42, v/v) with addition of 119 mg/l of potassium bromide

(Merck, Darmstadt, Germany) and nitric acid (65%, 100 μ l/l) (Merck).

The aflatoxin working standard solutions were prepared by dilution of a stock standard solution (Mix Kit-M; Supelco, Bellefonte, PA, USA) with methanol (1:100, v/v). The resulting absolute concentration was determined by comparison of the HPLC signals with standard solutions of single aflatoxins. For this purpose pure aflatoxins were dissolved in methanol and determined by means of UV spectrophotometry, the UV absorption of the standard solutions being measured at 362 nm against pure methanol. The aflatoxin concentration was calculated using the following equation.

$$c = A \cdot 1000 \cdot F \quad (1)$$

where c = concentration (ng/ml), A = absorption and F = 14.31 for aflatoxin B₁, 13.08 for aflatoxin B₂, 15.53 for aflatoxin G₁ and 15.53 for aflatoxin G₂.

This solution was further diluted with water (1:20, v/v). The resulting concentrations were 0.15 ng/ml for aflatoxin B₂ and G₂ and 0.50 ng/ml for aflatoxin B₁ and G₁. The solutions can be stored at -18°C in the dark.

All work was carried out in the absence of daylight. All glassware was cleaned with dilute hydrochloric acid and water. Used glassware was decontaminated using sodium hypochlorite solution (4% active chlorine; Rühl-Chemie, Germany).

2.3. Apparatus

A sonification bath was used for the extraction of the aflatoxins. As a clean-up step immunoaffinity column chromatography (Aflaprep columns; Coring System, Darmstadt, Germany) was applied. The HPLC system was purchased from Waters (Eschborn, Germany). The HPLC equipment consists of a system interface module (SIM box, Waters), an HPLC pump (W510; Waters), an injection valve (Rheodyne Model 7125 or W717 autosampler; Waters), a precolumn (Nova-Pak C₁₈; Waters), the analytical column (Radial-Pak cartridge packed with RP-18 Type 8

NVC, 4 μm , 100 \times 8 mm I.D.; Waters), the KOBRA cell and a scanning fluorescence detector (W470; Waters). The KOBRA cell was purchased from Coring System.

2.4. Extraction

A 5-g amount of a homogenous sample, which was collected by official methods [7], was mixed and homogenized in a mill (<0.5 mm, Retschmill). To this sample 20 ml methanol–water (70:30, v/v) was added and extracted by sonification for 30 min. After centrifugation an aliquot of the supernatant (5 ml) was diluted with water to 25 ml and thoroughly mixed.

2.5. Immunoaffinity column chromatography

The solution obtained was passed through the Aflaprep immunoaffinity column, which was conditioned with 10 ml of water. After washing with 20 ml of water, the aflatoxins were eluted in six successive steps with 0.5 ml of methanol, with a stop of 30 s after each step, under reduced pressure using a Vac-Elut system. The solution obtained was diluted with water to 10 ml and was used directly for injection after membrane filtration.

2.6. HPLC conditions

The HPLC analysis was carried out as follows. The isocratic HPLC system consisted of a pump (W510; Waters), an injection valve (Rheodyne Model 7125) with a 200- μl sample loop or an autosampler (W717; Waters). Separation was carried out on a Radial-Pak cartridge, Type 8 NVC C-18 (4 μm , 100 \times 8 mm I.D. (Waters) with a precolumn (Nova-Pak C₁₈; Waters). The eluent was water–methanol (58:42, v/v) with the addition of 119 mg potassium bromide and 100 μl of nitric acid (65%) per litre at a flow-rate of 0.8 ml/min (isocratic). The aflatoxins were detected using a scanning fluorescence detector ($\lambda_{\text{ex}} = 360 \text{ nm}$, $\lambda_{\text{em}} = 440 \text{ nm}$; filter, 1.5 s; attenuation, 8; gain, $\times 100$; emission band width, 30 nm). Aflatoxins B₁ and G₁ were derivatized using a KOBRA cell with a current of 100 μA

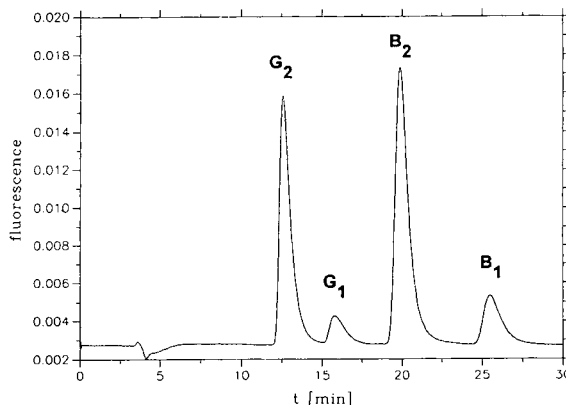


Fig. 1. Chromatogram of a standard pool without KOBRA cell.

and a length of the reaction coil of 28.2 cm. The chromatograms were evaluated using a chromatography workstation (Waters) with Maxima or Millennium software. A system interface module (SIM box) served to control the pump and to digitize the signals of the fluorescence detector.

3. Results and discussion

Fig. 1 shows a chromatogram of a standard solution of the four aflatoxins without the KOBRA cell (current 0 μA) and Fig. 2 one with the KOBRA cell (current 100 μA).

The signals represent an amount of 35–57 pg

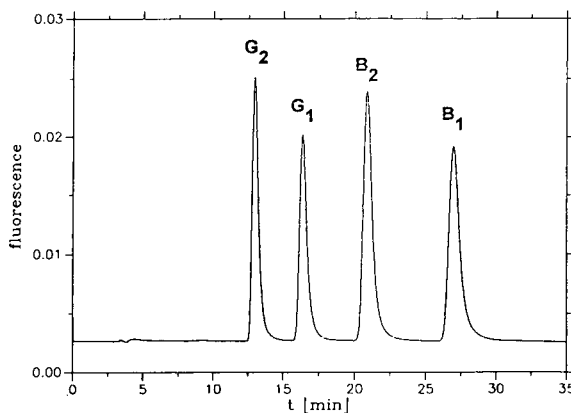


Fig. 2. Chromatogram of a standard pool with KOBRA cell.

of each aflatoxin. Using the KOBRA cell, the sensitivity for the detection of aflatoxin B₁ and G₁ is drastically increased. The developed method can be used for determination of aflatoxins in complex plant materials (medicinal herbs, plant extracts) and in herbal remedies, such as tinctures and coated and uncoated tablets. Also herbs containing fluorescent components, such as citrus pulps, *Rauwolfia serpentina* and licorice (*Liquiritiae radix*) could be successfully examined.

The method was validated corresponding to the EC guideline "Analytical Validation" and the Tripartite ICH Text on Validation of Analytical Procedures by the CPMP working party on Quality of Medicinal Products [8]. This document is concerned with the discussion of the characteristics that must be considered during the validation of analytical procedures included as part of registration applications submitted within the EC, Japan and USA. Typical validation characteristics for impurity tests are specificity, precision (repeatability), accuracy, linearity and detection limit of the method.

3.1. Specificity

The specificity of the analysis is given, on the one hand, by the comparison of the retention times of the signals in the sample and the standard pool, and on the other, by the excitation and emission spectra of the signals. Fig. 3 shows as an example the excitation spectrum of

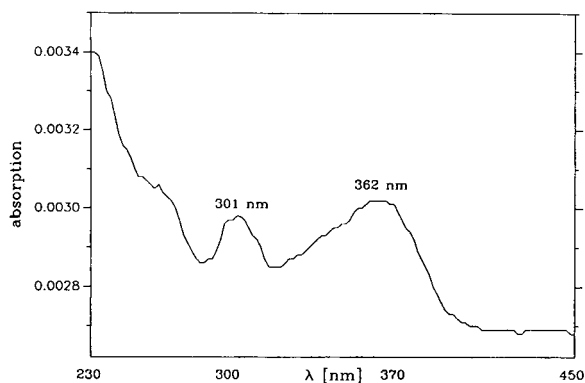


Fig. 3. Excitation spectrum of aflatoxin B₁.

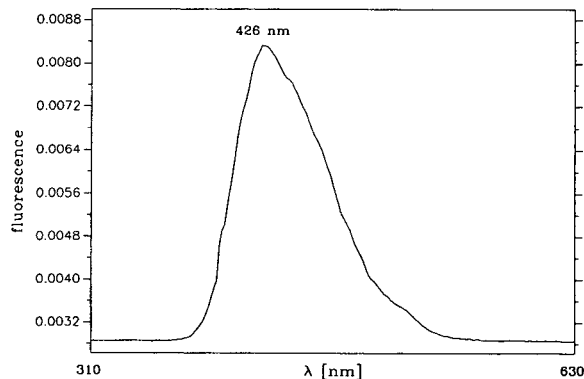


Fig. 4. Emission spectrum of aflatoxin B₁.

aflatoxin B₁ and Fig. 4 the corresponding emission spectrum.

In addition, samples that were not contaminated by aflatoxins were measured without the

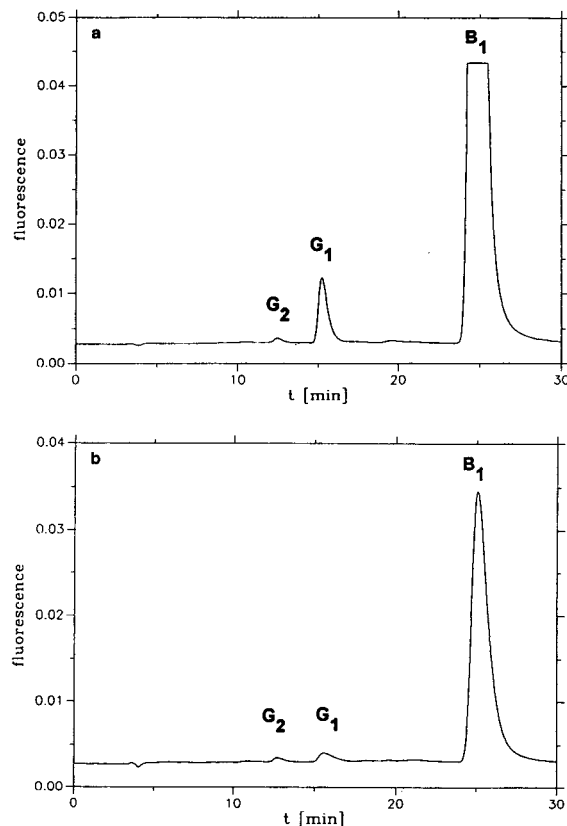


Fig. 5. Chromatograms of a natural contaminated extract of *Rauwolfia serpentina* (a) with and (b) without KOBRA cell.

Table 1
Reproducibility of the analytical procedure ($n = 6$; $P = 95\%$)

Aflatoxin	R.S.D. (%)	C.I. (ppb)
B ₁	5.15	0.0962
B ₂	2.43	0.0340
G ₁	2.43	0.0368
G ₂	3.20	0.0221

KOBRA cell. In the case of natural contamination the signals for aflatoxin B₁ and G₁ will be decreased.

Fig. 5a and b show chromatograms of a natural contaminated extract of *Rauwolfia serpentina* with and without the KOBRA cell. The signals of the aflatoxin B₁ and G₁ are decreased without the KOBRA cell. This is indirect proof of the specificity of the method.

3.2. Precision

The precision was determined by a multiple analysis of a spiked sample (capsicum). The precision is expressed by the relative standard deviation (R.S.D.) and the confidence interval of the mean value (C.I.; $n = 6$; $P = 95\%$; Table 1). The level of contamination was 1.780 ppb for aflatoxin B₁, 1.333 ppb for aflatoxin B₂, 1.444 ppb for aflatoxin G₁ and 0.659 ppb for aflatoxin G₂.

3.3. Accuracy

The accuracy of the method was examined by

the determination of the recoveries of the aflatoxins (Table 2). The recoveries of different matrices were determined by the addition of an aflatoxin pool to the sample (0.24 ng/ml aflatoxin G₂, 0.29 ng/ml aflatoxin G₁, 0.18 ng/ml aflatoxin B₂, 0.26 ng/ml aflatoxin B₁).

3.4. Linearity

The linearity of the measurements was checked for a standard solution containing aflatoxins in a range from the limit of detection up to a concentration of 10 ng/ml. The calibration graphs can be described by the following equations:

$$\text{aflatoxin B}_1: y = 0.843x \quad (R^2 = 0.999)$$

$$\text{aflatoxin B}_2: y = 0.897x \quad (R^2 = 1.000)$$

$$\text{aflatoxin G}_1: y = 0.843x \quad (R^2 = 1.000)$$

$$\text{aflatoxin G}_2: y = 0.843x \quad (R^2 = 1.000)$$

where y = fluorescence intensity and x = concentration (ng/ml).

4. Conclusions

A postcolumn procedure using a KOBRA cell to generate bromine electrochemically has been described. The sensitivity of the method is substantially increased with the use of the cell. The method can be applied to various plant materials and herbal remedies and with high selectivity for all aflatoxins; no matrix effects are observed.

Table 2
Recoveries of aflatoxins in different medicinal herbs

Sample	Recovery (%)			
	Aflatoxin B ₁	Aflatoxin B ₂	Aflatoxin G ₁	Aflatoxin G ₂
Potatoes	96.1	92.6	97.1	88.7
Valerian	78.6	84.7	82.0	57.8
Fennel seed	78.6	79.6	87.8	68.5
Coriander	66.4	70.9	78.2	59.1
Gourd seed	99.4	93.5	97.1	78.7

The procedure offers several advantages over other methods: high reproducibility, good recoveries for a variety of plant materials, easy automation, no need to use aggressive or unstable reagents, such as TFA or iodine, and inexpensive equipment (only one HPLC pump is used).

References

- [1] R. Knutti, *Chromatographia*, 12 (1979) 349.
- [2] W.A. Pons, *J. Assoc. Off. Anal. Chem.*, 62 (1979) 586.
- [3] A. Simonella, *J. High Resolut. Chromatogr. Chromatogr. Commun.*, 10 (1987) 626.
- [4] S. El-Dessouki, *Dtsch. Lebens.-Rundsch.*, 3 (1992) 78.
- [5] G. Niedwetzki, *J. Chromatogr. A*, 661 (1994) 175.
- [6] W.Th. Kok, *Anal. Chim. Acta*, 162 (1984) 19.
- [7] *German Pharmacopoeia*, Vol. 1, Deutscher Apotheker Verlag, Stuttgart, 10th ed., 1991, method V.4.N7.
- [8] CPMP Working Party on Quality of Medicinal Products, *Tripartite ICH Text: Validation of Analytical Procedures, Draft No. 3 (III/5626/93-EN)*, Directorate-General III/E-3, Commission of the European Communities, Brussels, 1993.
- [9] Bundesgesundheitsamt, *LMBG §35, 5. Lieferung, 00-00-2*, Beuth Verlag, Berlin, 1981.



ELSEVIER

Journal of Chromatography A, 692 (1995) 137-145

JOURNAL OF
CHROMATOGRAPHY A

Determination of liquiritin, glycyrrhizin, hesperidin, cinnamic acid, cinnamaldehyde, honokiol and magnolol in the traditional Chinese medicinal preparation Wu-Ji-San by high-performance liquid chromatography

Yuh-Chuang Lee, Cheng-Yu Huang, Kuo-Ching Wen*, Tsi-Tee Suen

National Laboratories of Foods and Drugs, Department of Health, Executive Yuan, 161-2 Kuen-Yang Street, Nankang, Taipei, Taiwan

Abstract

A high-performance liquid chromatographic method for the determination of liquiritin, glycyrrhizin, hesperidin, cinnamic acid, cinnamaldehyde, honokiol and magnolol in a traditional Chinese medicinal preparation, Wu-Ji-San, which contains *Glycyrrhizae Radix*, *Citri Leiocarpae Exocarpium*, *Aurantii Fructus*, *Cinnamomi Ramulus* and *Magnoliae Cortex*, was established. The samples were separated with a Cosmosil 5C₁₈-AR column by linear gradient elution using 0.03% (v/v) phosphoric acid-acetonitrile (0 min, 95:5; 52 min, 30:70) as the mobile phase at a flow-rate of 1.0 ml/min and the eluate was detected at 254 nm. *n*-Propyl benzoate was used as the internal standard and seven regression equations showing linear relationships between the peak-area ratios of each marker to *n*-propyl benzoate and concentration were obtained. The recoveries of the markers listed above were 84.77, 87.07, 79.81, 72.71, 72.72, 77.15 and 73.74%, respectively. The relative standard deviations were less than 5% ($n = 5$). Very satisfactory and reproducible results were obtained within 52 min for the simultaneous determination of the seven markers. Different processes such as concentration by reduced-pressure evaporation, freeze-drying and spray-drying were studied with regard to their effects on the marker contents. There were only minor effects on most of the markers except cinnamic acid and cinnamaldehyde. Three commercial concentrated products of Wu-Ji-San were also analysed. The contents of the marker substances in the commercial preparations were different from those in a standard decoction.

1. Introduction

Quantitative studies on the constituents of Chinese medicinal preparations generally started from the examination of a single herb component and then proceeded with the analysis of traditional prescriptions containing that specific constituent. As a result, most analytical work on Chinese medicine is confined to a single herb,

e.g., the determination of glycyrrhizin and liquiritin in *Glycyrrhizae Radix* [1-3], hesperidin in *Citrus Pericarpium* [4,5] and magnolol and honokiol in *Magnoliae Cortex* [6].

In Taiwan, the Department of Health will request that all concentrated herbal preparations submitted for registration should include the determination of at least two chemical constituents as markers after 1995. Further, in order to promote the Good Manufacture Practice (GMP) of Chinese medicinal preparations, our

* Corresponding author.

aim was to develop simple and expedient analytical methods for routine quality control.

In recent years, we have established many analytical methods for Chinese medicinal preparations, some of which have been published in this journal [7–9]. In this study, we selected a Chinese medicinal preparation, Wu-Ji-San, and employed HPLC to determine simultaneously the contents of seven marker substances. During the search for the optimum conditions, we found that using an aqueous acid–acetonitrile eluent is a feasible way to perform the analysis. *n*-Propyl benzoate was used as the internal standard and there was no interference at the same retention time.

2. Experimental

2.1. Materials

According to Ref. [10], the materials used to prepare Wu-Ji-San are *Poria*, *Atractylodis Rhizoma*, *Pinelliae Tuber*, *Citri Leiocarpae Exocarpium* and *Atractylodis Lanceae Rhizoma* (2.0 g each) and *Paeoniae Radix*, *Cnidii Rhizoma*, *Angelicae Radix*, *Magnoliae Cortex*, *Angelicae Dahuricae Radix*, *Aurantii Fructus*, *Platycodi Radix*, *Cinnamomi Ramulus*, *Zingiberis Siccatum Rhizoma*, *Ephedrae Herba*, *Zizyphi Fructus*, *Glycyrrhizae Radix* and *Zingiberis Rhizoma* (1.2 g each). Each material was obtained from the market and pulverized (8 mesh). For concentrated commercial products of Wu-Ji-San, three different brands were purchased from the market.

2.2. Chemicals and reagents

The structures of the marker substances are shown in Fig. 1. Glycyrrhizin, cinnamic acid, cinnamaldehyde, honokiol and hesperidin were purchased from Nacalai Tesque (Kyoto, Japan), liquiritin, magnolol and the internal standard *n*-propyl benzoate from Wako (Osaka, Japan), acetonitrile and methanol (HPLC grade) from Labscan (Dublin, Ireland) and phosphoric acid

(analytical-reagent grade) from Kanto (Tokyo, Japan). Ultrapure distilled water with a resistivity greater than 18 M Ω was used.

2.3. Instrumentation

HPLC was conducted with a Waters Model 625 system equipped with a Waters Model 486 UV detector and a Rheodyne Model 9125-080 injector (Millipore, Boston, MA, USA). Peak areas were calculated with a Shiunn Haw computing integrator. A Cosmosil 5C₁₈-AR (5 μ m) reversed-phase column (150 \times 4.6 mm I.D.) (Nacalai Tesque) was used.

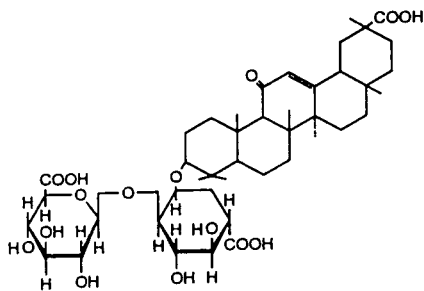
Concentration by reduced-pressure evaporation, freeze-drying and spray-drying of a standard decoction were carried out with a Rotavapor (R110/RE120/EL-13; Büchi, Flawil, Switzerland), freeze drier (Freeze Mobile 3; Virtis, Gardiner, NY, USA) and a mini spray dryer (Büchi Model 190), respectively.

2.4. Liquid chromatography

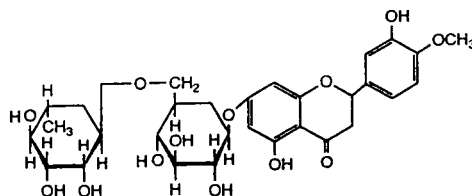
The mobile phase was a gradient of 0.03% (v/v) phosphoric acid–acetonitrile (0 min, 95:5; 52 min, 30:70), filtered through a 0.45- μ m Millipore filter and degassed prior to use. The analyses were carried out at a flow-rate of 1.0 ml/min with UV detection at 254 nm.

2.5. Preparation of standard solution

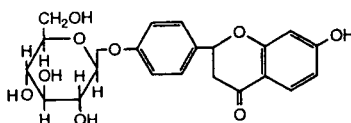
To prepare a standard solution containing liquiritin, hesperidin, cinnamic acid, cinnamaldehyde, glycyrrhizin, honokiol and magnolol, accurately weighed amounts of each compound were dissolved in 70% methanol to give serial concentrations with the ranges 8.1–36.5, 15.36–122.88, 0.476–2.14, 0.011–0.050, 10.6–47.9, 0.667–3.00 and 1.78–8.00 μ g/ml, respectively. An appropriate volume of internal standard solution was then added. Calibration graphs were plotted after linear regression of the peak-area ratios with concentrations.



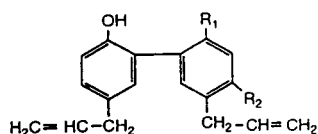
Glycyrrhizin



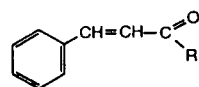
Hesperidin



Liquiritin



	R ₁	R ₂
Magnolol	OH	H
Honokiol	H	OH



	R
Cinnamic Acid	OH
Cinnamaldehyde	H

Fig. 1. Structures of marker substances.

2.6. Preparation of sample solutions

Standard decoction

Amounts of crude drugs equivalent to a daily dose of Wu-Ji-San were weighed and pulverized, a twentyfold mass of water was added and the mixture was boiled for more than 30 min to halve the original volume. After filtration while

hot, the filtrate was diluted with methanol to give a 70% methanol solution and then a suitable amount of internal standard was added to the solution to give a concentration of 0.15 $\mu\text{g}/\text{ml}$ of *n*-propyl benzoate.

Interference test

Amounts of crude drugs equivalent to a daily

Table 1

Inter- and intra-day relative standard deviations ($n = 5$) for liquiritin, glycyrrhizin, hesperidin, cinnamic acid, cinnamaldehyde, magnolol and honokiol in Wu-Ji-San

Marker substance	Concentration ($\mu\text{g/ml}$)	Peak area of marker substance/ peak area of <i>n</i> -propyl benzoate		R.S.D. (%) ^a	
		Inter-day	Intra-day	Inter-day	Intra-day
Liquiritin	8.1	0.154	0.154	0.81	0.72
Hesperidin	15.36	0.086	0.086	1.79	1.78
Cinnamic acid	0.47	0.081	0.081	3.53	2.01
Cinnamaldehyde	0.01	0.748	0.747	0.35	0.42
Glycyrrhizin	10.6	0.181	0.181	1.97	2.01
Honokiol	0.67	0.048	0.048	2.15	1.29
Magnolol	1.78	0.035	0.035	4.67	4.78

^a $n = 5$ with 95% confidence limits.

dose of Wu-Ji-San without, one at a time, Glycyrrhizae Radix, Citri Leiocarpae Exocarpium, Cinnamomi Ramulus, Magnoliae Cortex, Citri Leiocarpae Exocarpium and Aurantii Fruc-

tus were weighed and pulverized, a twentyfold mass of water was added and the mixture was boiled for more than 30 min to halve the original

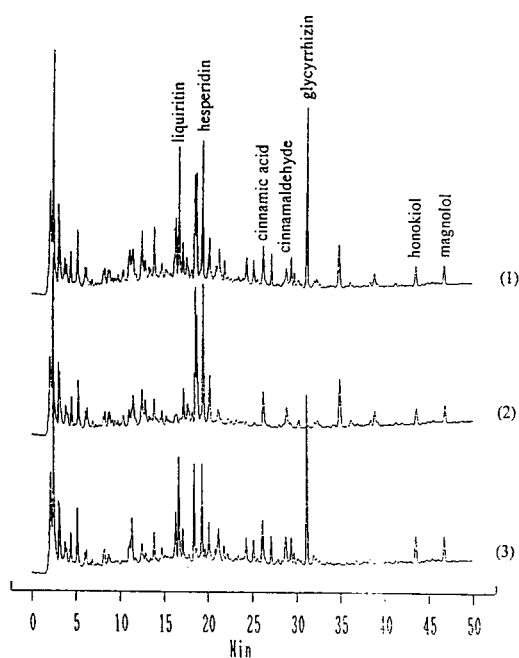


Fig. 2. Chromatograms of liquiritin, hesperidin, cinnamic acid, cinnamaldehyde, glycyrrhizin, honokiol and magnolol in Wu-Ji-San. (1) Standard decoction; (2) standard decoction without Glycyrrhizae Radix; (3) standard decoction without Citri Leiocarpae Exocarpium.

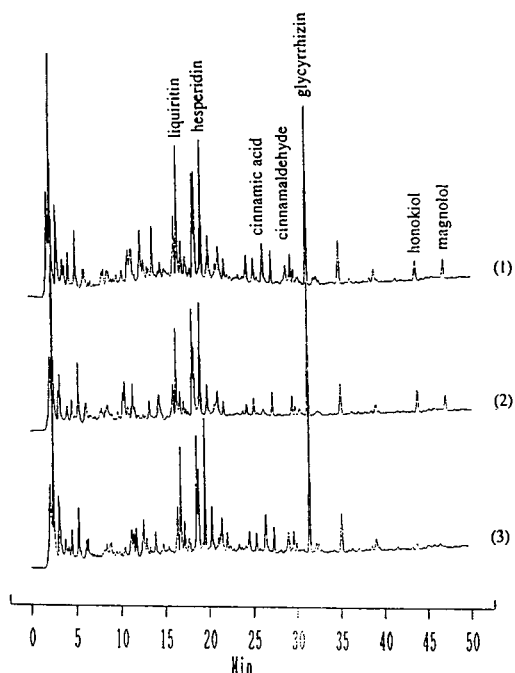


Fig. 3. Chromatograms of liquiritin, hesperidin, cinnamic acid, cinnamaldehyde, glycyrrhizin, honokiol and magnolol in Wu-Ji-San. (1) Standard decoction; (2) standard decoction without Cinnamomi Ramulus; (3) standard decoction without Magnoliae Cortex.

Table 2
Recovery of liquiritin, glycyrrhizin, hesperidin, cinnamic acid, cinnamaldehyde, magnolol and honokiol in Wu-Ji-San

Marker substance	Added ($\mu\text{g/ml}$)	Found ($\mu\text{g/ml}$)	Recovery (%)	Mean \pm S.D. ^a (%)	R.S.D. (%)
Liquiritin	16.20	13.80	85.19	84.77 \pm 3.45	3.53
	12.15	10.60	87.24		
	8.10	7.10	87.65		
	4.05	3.20	79.01		
Glycyrrhizin	21.20	18.30	86.32	87.07 \pm 1.91	1.09
	15.90	13.90	87.42		
	10.60	9.10	85.85		
	5.30	4.70	88.68		
Hesperidin	15.36	12.30	80.08	79.81 \pm 0.41	0.45
	30.72	24.30	79.10		
	61.44	49.20	80.08		
	122.88	98.30	79.99		
Cinnamic acid	0.95	0.70	73.61	72.71 \pm 7.55	8.99
	0.71	0.50	70.13		
	0.48	0.30	63.08		
	0.24	0.19	84.03		
Cinnamaldehyde	0.022	0.015	68.18	72.72 \pm 3.21	3.83
	0.017	0.012	72.72		
	0.011	0.009	77.27		
	0.006	0.004	72.72		
Honokiol	1.33	1.07	80.21	77.15 \pm 2.98	3.35
	1.00	0.80	79.96		
	0.67	0.49	73.46		
	0.33	0.25	74.96		
Magnolol	3.56	2.70	75.84	73.74 \pm 4.15	4.88
	2.67	2.10	78.65		
	1.78	1.30	73.03		
	0.89	0.60	67.42		

^a $n = 5$ with 95% confidence limits.

volume. After filtration while hot, the filtrate was diluted with methanol to give a 70% methanol solution.

Contents of liquiritin, glycyrrhizin, hesperidin, cinnamic acid, cinnamaldehyde, honokiol and magnolol in crude drug

Amounts of individual crude drugs equivalent to a daily dose of Wu-Ji-San was weighed and pulverized, a twentyfold mass of water was added and the mixture was boiled for more than 30 min to halve the original volume. After filtration while hot, the filtrate was diluted with

methanol to give a 70% methanol solution and then a suitable amount of internal standard was added to the solution to give a concentration of 0.15 $\mu\text{g/ml}$ of *n*-propyl benzoate.

Concentrated products of standard decoction

Concentration of a standard decoction by reduced-pressure evaporation, freeze-drying and spray-drying was carried out. The residues obtained were dissolved in a suitable amount of 70% methanol and internal standard was then added to give a concentration of 0.15 $\mu\text{g/ml}$ of *n*-propyl benzoate.

Concentrated herbal preparations from market

An amount of the concentrated herbal preparation equivalent to a daily dose was weighed accurately and extracted with a twentyfold mass of water for 30 min in an ultrasonic bath. After extraction, the samples were filtered and diluted with methanol to give a 70% methanol solution and internal standard was then added to give a concentration of 0.15 $\mu\text{g}/\text{ml}$ of *n*-propyl benzoate.

2.7. Solutions for recovery study

An appropriate amount of the concentrated herbal preparation from the market was weighed accurately and extracted with 70% methanol for 20 min in an ultrasonic bath, the filtrate was divided into five portions (one as a control group), each portion (except the control) was spiked with different concentrations of standard

solution to add various concentrations of liquiritin (16.20, 12.15, 8.10, 4.05 $\mu\text{g}/\text{ml}$), glycyrrhizin (21.20, 15.90, 10.60, 5.30 $\mu\text{g}/\text{ml}$), hesperidin (15.36, 30.72, 61.44, 122.88 $\mu\text{g}/\text{ml}$), cinnamic acid (0.95, 0.71, 0.48, 0.24 $\mu\text{g}/\text{ml}$), cinnamaldehyde (0.022, 0.017, 0.011, 0.006 $\mu\text{g}/\text{ml}$), honokiol (1.33, 1.00, 0.67, 0.33 $\mu\text{g}/\text{ml}$) or magnolol (3.56, 2.67, 1.78, 0.89 $\mu\text{g}/\text{ml}$), and internal standard was then added to give a concentration of 0.15 $\mu\text{g}/\text{ml}$ of *n*-propyl benzoate. All samples were filtered through a 0.45- μm Millipore filter and were injected for HPLC analysis to calculate the recovery.

3. Results and discussion

To check the precision of this method, we injected standard solutions of liquiritin, glycyrrhizin, hesperidin, cinnamic acid, cin-

Table 3
Contents of seven marker substances in a standard decoction and three different commercial preparations of Wu-Ji-San

Sample	Liquiritin		Glycyrrhizin		Hesperidin	
	Mean \pm S.D. ^a (mg/g)	R.S.D. (%)	Mean \pm S.D. ^a (mg/g)	R.S.D. (%)	Mean \pm S.D. ^a (mg/g)	R.S.D. (%)
Standard decoction	13.71 \pm 0.57	3.78	21.14 \pm 0.08	0.34	3.75 \pm 0.16	4.02
Commercial preparation A	11.72 \pm 0.39	2.91	32.86 \pm 1.49	3.94	N.D. ^b	—
Commercial preparation B	N.D. ^b	—	11.59 \pm 0.43	3.22	11.15 \pm 0.46	3.63
Commercial preparation C	2.88 \pm 0.10	3.08	7.25 \pm 0.11	1.33	9.02 \pm 0.34	3.34

Sample	Cinnamaldehyde		Cinnamic acid		Magnolol		Honokiol	
	Mean \pm S.D. ^a (mg/g)	R.S.D. (%)	Mean \pm S.D. ^a (mg/g)	R.S.D. (%)	Mean \pm S.D. ^a (mg/g)	R.S.D. (%)	Mean \pm S.D. ^a (mg/g)	R.S.D. (%)
Standard decoction	0.89 \pm 0.05	5.24	0.69 \pm 0.04	5.56	3.58 \pm 0.26	6.33	0.80 \pm 0.04	5.30
Commercial preparation A	10.80 \pm 0.63	5.00	2.18 \pm 0.16	6.39	5.21 \pm 0.42	7.05	3.50 \pm 0.11	2.75
Commercial preparation B	0.96 \pm 0.07	6.94	0.32 \pm 0.02	5.97	1.39 \pm 0.11	7.31	0.31 \pm 0.02	7.70
Commercial preparation C	7.60 \pm 0.12	1.36	0.43 \pm 0.02	4.56	3.09 \pm 0.26	7.52	2.47 \pm 0.07	2.66

^a $n = 5$ with 95% confidence limits.

^b Not determined.

namaldehyde, honokiol and magnolol at the concentrations of 8.1, 15.36, 0.47, 0.01, 10.6, 0.67 and 1.78 $\mu\text{g}/\text{ml}$, respectively, five times on the same day. The intra-day relative standard deviations (R.S.D.s) were 0.72, 1.78, 2.01, 0.42, 2.01, 1.29 and 4.78%, respectively. The inter-day R.S.D.s obtained for a 5-day period were 0.81, 1.79, 3.53, 0.35, 1.97, 2.15 and 4.67%, respectively (Table 1). The recoveries of liquiritin, glycyrrhizin, hesperidin, cinnamic acid, cinnamaldehyde, honokiol and magnolol were 84.77, 87.07, 79.81, 72.71, 72.72, 77.15 and 73.74%, respectively (Table 2). For herbal analysis, the values mentioned above indicated acceptable precision and accuracy.

Calibration graphs for liquiritin, hesperidin, cinnamic acid, cinnamaldehyde, glycyrrhizin, honokiol and magnolol were obtained over the ranges 8.1–36.5, 15.36–122.88, 0.476–2.14, 0.011–0.050, 10.6–47.9, 0.667–3.00 and 1.78–8.00 $\mu\text{g}/\text{ml}$, respectively. The regression equations were $y = 5.165951 \cdot 10^{-2}x + 3.466 \cdot 10^{-4}$

($r = 0.9999$) for liquiritin, $y = 5.761677x + 6.605 \cdot 10^{-2}$ ($r = 0.9998$) for glycyrrhizin, $y = 1.816894 \cdot 10^{-3}x - 5.224 \cdot 10^{-4}$ ($r = 0.9991$) for hesperidin, $y = 6.281 \cdot 10^{-2}x + 5.866181$ ($r = 0.9989$) for cinnamic acid, $y = 3.15 \cdot 10^{-7}x + 0.1493414 \cdot 10^{-4}$ ($r = 0.9999$) for cinnamaldehyde, $y = 6.246814x + 2.059 \cdot 10^{-2}$ ($r = 0.9958$) for magnolol and $y = 14.28926x - 4.032 \cdot 10^{-2}$ ($r = 0.9994$) for honokiol in Wu-Ji-San, where y is the peak-area ratio of the marker to the internal standard and x is the concentration of the marker. These results showed good linear relationships between peak-area ratio and concentration.

To ensure the specificity and selectivity of the method, we prepared five blank decoctions for comparison. They were combinations excluding, one at a time, Glycyrrhizae Radix, Citri Leiocarpae Exocarpium, Cinnamomi Ramulus, Magnoliae Cortex, Citri Leiocarpae Exocarpium and Aurantii Fructus. The chromatograms are shown in Figs. 2–4. The retention times of the marker

Table 4
Contents of the seven marker substances in standard decoction and in products after concentration by various processes

Sample	Liquiritin		Glycyrrhizin		Hesperidin			
	Mean \pm S.D. ^a (mg/g)	R.S.D. (%)	Mean \pm S.D. ^a (mg/g)	R.S.D. (%)	Mean \pm S.D. ^a (mg/g)	R.S.D. (%)		
Standard decoction	13.71 \pm 0.57	3.78	21.14 \pm 0.08	0.34	3.57 \pm 0.16	4.02		
Concentration under reduced pressure	13.44 \pm 0.76	4.92	18.78 \pm 0.93	4.30	3.59 \pm 0.25	6.15		
Freeze-drying	13.41 \pm 0.82	5.30	18.32 \pm 0.77	3.68	3.59 \pm 0.27	6.64		
Spray-drying	13.79 \pm 0.62	3.92	19.16 \pm 0.88	4.00	3.56 \pm 0.19	4.54		
Sample	Cinnamaldehyde		Cinnamic acid		Magnolol		Honokiol	
	Mean \pm S.D. ^a ($\mu\text{g}/\text{g}$)	R.S.D. (%)	Mean \pm S.D. ^a (mg/g)	R.S.D. (%)	Mean \pm S.D. ^a ($\mu\text{g}/\text{g}$)	R.S.D. (%)	Mean \pm S.D. ^a (mg/g)	R.S.D. (%)
Standard decoction	0.89 \pm 0.05	5.24	0.69 \pm 0.04	5.56	3.58 \pm 0.26	6.33	0.80 \pm 0.04	5.30
Concentration under reduced pressure	N.D. ^b	–	N.D. ^b	–	3.25 \pm 0.32	8.58	0.48 \pm 0.03	6.88
Freeze-drying	N.D. ^b	–	N.D. ^b	–	3.01 \pm 0.27	5.85	0.62 \pm 0.04	5.85
Spray-drying	N.D. ^b	–	N.D. ^b	–	3.47 \pm 0.18	4.62	0.51 \pm 0.01	1.06

^a $n = 5$ with 95% confidence limits.

^b Not determined.

Table 5
Contents of marker substances in crude drug and turnover ratio in standard decoction of Wu-Ji-San

Crude drug	Daily dose (g)	Marker substance	Content of marker substance in crude drug (mg/g) ^a		R.S.D.	Theoretical content of marker substance in standard decoction (daily dose, A)	Content of marker substance in standard decoction (mg/g) (daily dose, B)	Turnover ratio [B/A (%)]
			Mean	± S.D.				
Glycyrrhizae Radix	1.2	Liquiritin	37.56	± 1.15	2.65	45.07	16.45	36.50
		Glycyrrhizin	89.21	± 1.65	1.60	107.05	25.37	23.70
		Hesperidin	24.03	± 1.04	3.77	76.90	11.42	14.85
Citri Leiocarpae Exocarpium Aurantii Fructus	2.0 1.2	Cinnamic acid	1.92	± 0.02	1.13	2.30	0.83	36.09
			Cinnamaldehyde ^b	1.45	± 0.02	1.41	1.74	1.07
Magnoliae Cortex	1.2	Magnolol	41.51	± 1.58	3.30	49.81	4.30	8.63
		Honokiol	5.82	± 0.41	6.07	6.98	0.96	13.75

^a n = 5 with 95% confidence limits.

^b µg/g.

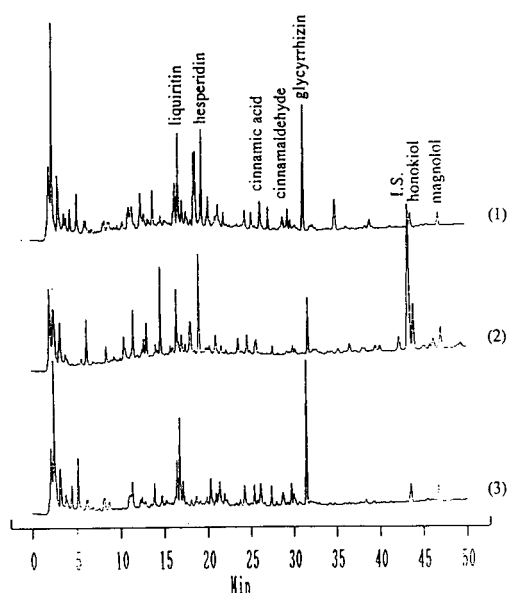


Fig. 4. Chromatograms of liquiritin, hesperidin, cinnamic acid, cinnamaldehyde, glycyrrhizin, honokiol and magnolol in Wu-Ji-San. (1) Standard decoction; (2) commercial preparation; (3) standard decoction without Citri Leiocarpae Exocarpium and Aurantii Fructus.

substances and internal standard, i.e., liquiritin, hesperidin, cinnamic acid, cinnamaldehyde, glycyrrhizin, *n*-propyl benzoate, honokiol and magnolol, were 16, 19, 26, 29, 31, 43, 44 and 47 min, respectively. On inspection of the three-dimensional chromatograms, these eight constituents all showed good purity. There was no peak found at their retention times in blank decoctions. The three commercial preparations also showed satisfactory separations.

The contents of marker substances in commercial preparations differ greatly among each other and from those in the standard decoction, as shown in Table 3. This is probably due to the different sources of the crude drugs and different manufacturing processes. The effects of different concentration processes were also investigated using reduced-pressure evaporation, spray-drying and freeze-drying, and the results are given

in Table 4. Neither cinnamaldehyde nor cinnamic acid was detected after these three kinds of concentration process. This may be due to the volatility of cinnamaldehyde and the low content of cinnamic acid. In addition, it showed only minor effects on the contents of the other five markers.

The turnover ratios of these constituents were defined as the percentage yields of these constituents detected in the Chinese medicinal preparations, calculated on the basis of their contents in the respective crude drugs. The turnover ratios of these markers vary greatly among each other (from 61.49% to 8.63%), as shown in Table 5. Wu-Ji-San contains eighteen kinds of crude drugs, and each crude drug has been known to contain many chemical constituents. In the process of preparing decoctions, whether the molecular interactions cause poor turnover ratios is a complicated problem and needs further study.

References

- [1] K. Sagara, Y. Ito, T. Oshima, H. Murayama and H. Itokawa, *Shoyakugaku Zasshi*, 40 (1986) 77.
- [2] K. Yoneda, E. Yamagata and M. Tsujimura, *Shoyakugaku Zasshi*, 44 (1990) 202.
- [3] K. Yoneda, E. Yamagata and M. Tsujimura, *Shoyakugaku Zasshi*, 45 (1991) 220.
- [4] S. Tosa, S. Ishihara, M. Toyota, S. Yosida, H. Nakazawa and T. Tomimatsu, *Shoyakugaku Zasshi* 42 (1988) 41.
- [5] S. Ishihara, S. Yoshida, S. Tosa, H. Nakazawa and T. Tomimatsu, *Shoyakugaku Zasshi*, 44 (1990) 127.
- [6] D.-C. Chen and J.-W. Liu, *Acta Pharm. Sin.*, 17 (1982) 360.
- [7] K.-C. Wen, C.-Y. Huang and F.-S. Liu, *J. Chromatogr.*, 593 (1992) 191.
- [8] K.-C. Wen, C.-Y. Huang and F.-L. Lu, *J. Chromatogr.*, 631 (1993) 241.
- [9] Y.-C. Lee, C.-Y. Huang, K.-C. Wen and T.-T. Suen, *J. Chromatogr. A*, 660 (1994) 299.
- [10] H.-Y. Hsu and C.-S. Hsu, *Commonly Used Chinese Herb Formulas with Illustrations*, Oriental Healing Arts Institute, Taiwan, 1980.



Chemometric categorization of octadecylsilyl bonded-phase silica columns using test mixtures and confirmation of results with pharmaceutical compound separations

B.A. Olsen*, G.R. Sullivan

Lilly Research Laboratories, Eli Lilly and Company, P.O. Box 685, Drop Code TL12, Lafayette, IN 47902, USA

Abstract

The chromatographic properties of seventeen commercial octadecylsilyl phases were characterized in order to determine column similarities and differences that would aid in column selection for method development, choice of an alternate column and method ruggedness testing. Chromatographic test mixtures from the literature were used to probe the hydrophobicity, free silanol interactions, trace metal activity, and shape selectivity of these columns. Principal components and cluster analysis methods were used to categorize the columns into groups that tended to display similar chromatographic properties. The validity of the groups was tested with mixtures of pharmaceutical compounds under a variety of mobile phase conditions. In general, columns that were categorized together from the test mixture analysis showed similar behavior for the analysis of the pharmaceutical compound mixtures.

1. Introduction

Octadecylsilyl (ODS) bonded-phase silica is arguably the most widely used stationary phase for reversed-phase high-performance liquid chromatography [1]. This has led to a proliferation of ODS phases from many manufacturers. One survey listed 117 suppliers of reversed-phase columns, so even allowing for duplication, a large number of ODS phases is available [2]. It is also well-recognized that all ODS phases do not exhibit similar separation behavior. Factors such as particle size, surface area, pore size, trace metal activity, bonded-phase surface density, bonding chemistry, silica deactivation, and bonded-phase stability can all influence retention,

selectivity, and peak shape properties of analytes. While some general rules can be applied, such as smaller particle sizes will provide higher efficiency, it is often difficult to predict the properties of a column based on stationary phase characteristics normally listed by manufacturers.

The large number of ODS phases available and the variability in their properties can make column choice for method development a difficult or somewhat arbitrary process. This choice is often made based on experience with given columns and compounds, advertising claims, or by trial and error. Choosing an ODS column could be more efficient if the choices were reduced by categorizing columns into groups that display similar behavior. If the initial column choice was not acceptable (and it is still deemed desirable to employ an ODS phase), a column

* Corresponding author.

from a different category would be more likely to show different behavior than one from the same category. Such a categorization would also be useful in selecting an alternative column that is likely to be similar to one specified in a literature or compendial method.

Investigation of method ruggedness toward changes in stationary phase characteristics can be valuable in method development to give an indication of whether the separation will be sensitive to these characteristics. Changes in chromatographic behavior from batch to batch or when a manufacturing change is implemented for a given stationary phase are often problematic for method performance over time. These difficulties may not be apparent in a manufacturer's quality control testing but can be manifested as selectivity, retention, or peak shape changes compared to previous columns in end-user applications. In testing method ruggedness with columns categorized into groups as mentioned above, similar results obtained with a column from a different group would suggest that the method will be quite rugged, while different behavior on a column from the same group would indicate the opposite. This approach may be more informative than performing the method with several columns of the same type to test ruggedness.

Classification of columns for improving the choice of alternate columns or evaluation of behavior for basic compounds have been goals addressed in the literature. Methods employing various test mixtures and data analysis techniques have been described. Several relatively simple test mixtures have been used to probe hydrophobic, silanophobic and polar interactions of solutes and stationary phases [3–11]. Other investigators have used more specialized compounds to characterize columns [12–15] or focused on specific interactions such as shape selectivity [16] or trace metal activity [17]. Data analysis techniques have included qualitative description of results [3,13,18], classification based on performance parameters or indices [4,5,7,9,10,14–17], and chemometric methods such as principal components and cluster analysis [6,8,12]. In earlier related work, Massart and

co-workers [19–23] described cluster analysis/numerical taxonomy techniques for the determination of optimal sets of gas chromatographic phases or thin-layer chromatographic systems.

In this work, test mixtures based on those described by Schmitz et al. [6], Sander and Wise [16] and Verzele and Dewaele [17] were used to characterize seventeen commercially available ODS columns. Principal components and cluster analysis methods were used to categorize the columns according to the similarity of their chromatographic behavior with the test mixtures. Furthermore, investigation of several columns was conducted using "real" analysis conditions for pharmaceutical compounds to check the validity of the categories derived from the test mixtures. This also tested the usefulness of the category groupings for determination of method ruggedness as described above.

2. Experimental

2.1. Reagents

HPLC-grade acetonitrile and methanol were obtained from EM Science (Gibbstown, NJ, USA). Buffers were prepared using appropriate concentrations of potassium phosphate, mono- and dibasic (EM Science), sodium acetate (EM Science), and orthophosphoric acid (85%, Fisher Scientific, Fair Lawn, NJ, USA). Water for mobile phases and sample solutions was purified with a Milli-Q system from Millipore (Milford, MA, USA).

Aniline, phenol, *o*-toluidine, *m*-toluidine, *p*-toluidine, methylbenzoate, N,N-dimethylaniline, 2,4-pentanedione (acetylacetone), naphthalene, 1-nitronaphthalene, amitriptyline hydrochloride and 4-acetamidophenol were obtained from Aldrich (Milwaukee, WI, USA). Toluene was from Mallinckrodt (Paris, KY, USA). Standard Reference Material 869–Column Selectivity Test Mixture for LC (polycyclic aromatic hydrocarbons, PAHs) was from the National Institute of Standards and Technology (Gaithersburg, MD, USA) The mixture was diluted with acetonitrile to the following concentrations: benzo[a]pyrene

(BaP, 0.4 $\mu\text{g/ml}$), tetrabenzonaphthalene (TBN, 0.6 $\mu\text{g/ml}$) and phenanthro[3,4-*c*]phenanthrene (PhPh, 2.2 $\mu\text{g/ml}$). Nortriptyline hydrochloride, dirithromycin, cephalexin, loracarbef and cefaclor were from Lilly Research Labs.

2.2. Apparatus

The chromatographic system consisted of a Model 600 pump with column heater (Waters, Bedford, MA, USA), a Model 728 autoinjector (Alcott, Norcross, GA, USA) with a fixed-loop injection valve (Valco, Houston, TX, USA), and a Model 787 variable-wavelength UV detector (Applied Biosystems, Ramsey, NJ, USA). Chromatograms were recorded using an in-house data acquisition system. The columns investigated are listed in Table 1.

2.3. Software

The principal components and cluster analyses were performed using the statistical analysis software JMP (for the Macintosh), version 3.0.2 from the SAS Institute, Cary, NC, USA. Some

cluster analysis was performed using the CLUSTER procedure in SAS software also from the SAS Institute.

3. Results and discussion

The test mixtures were chosen for their ability to show differences among columns based on various factors known to affect chromatographic performance. A mixture of basic and neutral compounds was used to probe hydrophobic and free silanol interactions [6]. Trace metal activity was tested using 2,4-pentanedione (acetylacetone), a strong metal chelator, with naphthalene and 1-nitronaphthalene to test silanol interactions [17]. Shape selectivity was determined using polynuclear aromatic hydrocarbons differing in degree of planarity [16]. Data obtained for these test mixtures on 17 different columns are given in Table 2. Data from three Zorbax Rx-C₁₈ columns with duplicate measurements taken on different days from one of these columns were included. Observations from each test mixture are summarized below.

Table 1
Columns investigated using test mixtures

Column	Supplier
Kromasil C ₁₈	Keystone Scientific, Bellefonte, PA, USA
Nucleosil C ₁₈	Keystone Scientific
LiChrosorb RP18	Keystone Scientific
ODS Hypersil	Keystone Scientific
BDS Hypersil C ₁₈	Keystone Scientific
Partisil 5 ODS-3	Whatman, Clifton, NJ, USA
Partisil 10 ODS-2 (10 μm)	Whatman
Zorbax Rx-C ₁₈	MacMod Analytical, Chadds Ford, PA, USA
Zorbax ODS	MacMod Analytical
Spherisorb ODS	Regis, Morton Grove, IL, USA
Spherisorb ODS-II	Regis
Inertsil 5 ODS (2)	MetaChem, Redondo Beach, CA, USA
YMC-Pack ODS-A	YMC, Wilmington, NC, USA
Supelcosil LC18	Supelco, Bellefonte, PA, USA
Supelcosil LC18-DB	Supelco
Ultrasphere ODS	Beckman, San Ramon, CA, USA
$\mu\text{Bondapak C}_{18}$ (10 μm , 300 \times 3.9 mm)	Waters, Milford, MA, USA

All columns were 250 \times 4.6 mm with 5- μm particles unless otherwise indicated.

Table 2
Data from analysis of test mixtures

Column	Aniline		Phenol, k'	<i>o</i> -Toluidine, k'	<i>m</i> -Toluidine, k'	<i>p</i> -Toluidine, k'	N,N-Dimethylamine		Methylbenzoate, k'
	k'	Peak width					k'	Peak width	
Kromasil C ₁₈	0.85	26	0.91	1.25	1.34	1.59	4.60	34	2.68
Nucleosil C ₁₈	0.82	16	0.72	1.16	1.30	1.80	3.70	48	2.25
Partisil 5 ODS-3	0.80	17	0.74	1.10	1.32	1.94	3.04	50	2.03
BDS Hypersil C ₁₈	6.58	179	0.56	6.18	13.27*	22.37*	23.88*	687*	1.51
Partisil 10 ODS-2	1.76	40	0.90	2.36	3.07	5.22	7.30	131	3.04
Inertsil 5 ODS (2)	0.66	15	0.68	1.03	1.03	1.03	3.73	23	2.37
Zorbax Rx-C ₁₈ -1, day 1	0.60	14	0.59	0.88	0.96	1.24	3.48	22	1.98
Zorbax Rx-C ₁₈ -1, day 2	0.59	13	0.59	0.88	0.94	1.19	3.48	22	1.98
Zorbax Rx-C ₁₈ -2	0.49	13	0.51	0.76	0.76	0.90	3.05	21	1.74
Zorbax Rx-C ₁₈ -3	0.55	17	0.54	0.81	0.87	1.22	3.26	24	1.81
Spherisorb ODS-II	3.62	125	0.56	3.82	6.81	11.68*	13.61*	470*	1.55
YMC ODS	0.62	11	0.77	0.96	0.96	0.96	3.48	22	2.21
Supelcosil LC18-DB	9.98*	341*	0.61	9.57*	20.26*	34.24*	35.54*	1340*	1.76
Ultrasphere ODS	1.15	48	0.62	1.39	2.00	4.06	4.43	80	1.95
μ Bondapak C ₁₈	0.56	13	0.56	0.77	0.84	1.09	2.17	24	1.51
Supelcosil LC18	10.38*	354	0.62	9.98*	21.07*	35.63*	36.93*	1390*	1.85
Zorbax ODS	1.64	89	0.79	1.94	2.80	5.79	8.32	366	2.87
Spherisorb ODS	2.99	141	0.34	3.14	5.72	9.94*	11.6*	534*	1.20
Hypersil ODS	4.06	206	0.57	4.14	8.64	13.5*	15.22*	796*	1.69
LiChrosorb RP18	0.61	13	0.63	0.96	0.96	1.10	3.36	46	2.00

Table 2 (continued)

Column	Toluene, k'	BaP, k'	PhPh, k'	TBN, k'	α TBN/BaP	Acetylacetone		Nitronaphthalene, k'	Naphthalene, k'	α naphthalene/ nitronaphthalene
						k'	Peak width			
Kromasil C ₁₈	6.54	8.47	7.88	13.44	1.59	0.53	20	3.89	7.00	1.80
Nucleosil C ₁₈	4.24	4.60	4.73	8.21	1.78	0.51	48	3.37	4.44	1.32
Partisil 5 ODS-3	3.25	2.81	3.31	5.12	1.82	1.25	208	2.32	2.88	1.24
BDS Hypersil C ₁₈	3.47	4.72	4.42	7.56	1.60	0.30	19	2.08	3.65	1.75
Partisil 10 ODS-2	5.61	8.27	6.93	11.86	1.43	5.22*	500*	4.39	6.00	1.37
Inertsil 5 ODS (2)	5.22	6.10	6.10	10.48	1.72	0.48	15	3.41	5.38	1.58
Zorbax Rx-C ₁₈ -1, day 1	4.85	6.40	5.47	9.47	1.48	0.39	15	2.80	5.20	1.86
Zorbax Rx-C ₁₈ -1, day 2	4.87	6.40	5.47	9.47	1.48	0.40	14	2.88	5.34	1.86
Zorbax Rx-C ₁₈ -2	4.44	6.40	5.47	9.47	1.48	0.36	21	2.46	4.74	1.93
Zorbax Rx-C ₁₈ -3	4.59	6.40	5.47	9.47	1.48	0.38	14	2.74	4.74	1.86
Spherisorb ODS-II	2.43	5.65	5.17	8.84	1.57	1.38	260	3.32	5.09	1.45
YMC ODS	4.90	5.50	6.10	10.58	1.92	0.44	13	3.15	5.05	1.61
Supelcosil LC18-DB	3.93	4.84	5.23	9.11	1.88	5.10*	500*	2.48	4.13	1.67
Ultrasphere ODS	4.74	5.44	5.72	10.05	1.85	0.43	97	2.99	5.33	1.78
μ Bondapak C ₁₈	2.49	2.51	2.90	4.59	1.83	0.47	124	1.73	2.18	1.26
Supelcosil LC18	4.16	4.93	5.28	9.23	1.87	0.39	70	2.53	4.22	1.67
Zorbax ODS	6.89	7.65	7.60	13.43	1.76	5.79*	500*	4.11	7.05	1.72
Spherisorb ODS	1.95	2.37	1.84	3.05	1.29	0.59	118	1.58	1.99	1.26
Hypersil ODS	3.71	3.85	4.40	7.50	1.95	0.35	31	2.31	3.71	1.61
LiChrosorb RP18	3.83	4.94	4.94	8.65	1.75	0.67	202	2.99	4.06	1.36

Peak widths at 10% of peak height are given in s for selected compounds. Entries with asterisks were obtained by regression from other peak data or were assigned as indicated in text. Capacity factors, peak widths and separation factors were used as raw data for principal components and cluster analysis.

3.1. Base/neutral test mixture

This test mixture was perhaps the most revealing of those investigated. Chromatograms from four columns representing the range of behavior for basic compounds are shown in Fig. 1. Large differences in retention and peak shape were apparent. All columns gave sharp peaks for toluene and methylbenzoate, with the retention of these peaks giving an indication of column hydrophobicity. The YMC ODS column gave sharp peaks for all components and the toluidine isomers were not separated, indicating minimal residual silanol activity [5]. Although the Zorbax Rx-C₁₈ column gave good peak shape for aniline and N,N-dimethylaniline (DMA), the toluidine isomers were partially separated. Complete separation of the toluidine isomers was obtained on some columns, such as the Nucleosil C₁₈. This column also exhibited tailing peaks for the basic compounds. Finally, for the Supelcosil, Hypersil and Spherisorb columns, the basic compounds were eluted very late as poorly shaped or almost indiscernible peaks or were not eluted at all during the run time of the experiments.

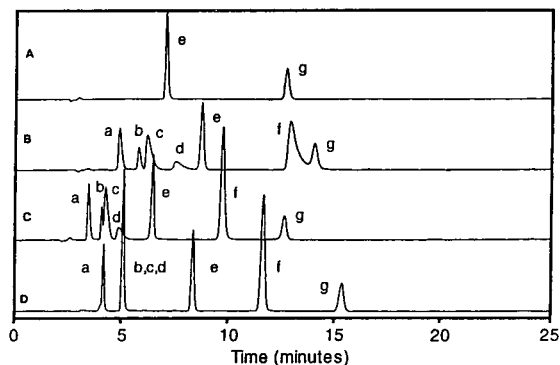


Fig. 1. Representative chromatograms for base/neutral test mixture. Columns: A = Supelcosil LC18; B = Nucleosil C₁₈; C = Zorbax Rx-C₁₈; D = YMC ODS. Peaks: a = aniline (10 $\mu\text{g/ml}$); b = *o*-toluidine (8.8 $\mu\text{g/ml}$); c = *m*-toluidine (16 $\mu\text{g/ml}$); d = *p*-toluidine (6 $\mu\text{g/ml}$); e = methylbenzoate (34 $\mu\text{g/ml}$); f = N,N-dimethylaniline (7.2 $\mu\text{g/ml}$); g = toluene (86 $\mu\text{g/ml}$). Phenol (18 $\mu\text{g/ml}$) was injected separately. Mobile phase: methanol–water (65:35). Flow-rate: 1.0 ml/min. Detection: absorbance at 254 nm. Injection volume: 20 μl .

The chemometric techniques used for analysis require that a specific data value be present for all potential clustering units. Otherwise, either the clustering unit—in this case, the column—or the measured variable must be eliminated from the analysis. In this study, some of the peaks had censored retention times; that is, the retention times were known to exceed a certain value, but the exact time could not be determined. To retain all clustering units and all variables in the analysis, the censored data were replaced by estimates obtained using regression analysis. Because strong correlations existed between variables with some censored data and variables with existing data, it was possible to obtain predictions for the censored observations. For example, DMA is highly correlated with aniline. The Spherisorb and Hypersil columns have observed data for aniline but censored data for DMA. A linear model based on complete data from other columns was used to predict the DMA value from the existing value for aniline. Other censored data were handled in a similar fashion.

The lack of a starting point (no observed retention time for aniline) for the Supelcosil columns was not a major issue. Because of the strong correlations between the Supelcosils for other variables, it is assumed the aniline retention times would be very close. Although the assignment of aniline retention times for the Supelcosils at greater than 25 min (the experimental run time) was somewhat arbitrary, this is not expected to influence the results of the subsequent analyses.

3.2. Chelator test mixture

The main difference among columns observed with this test mixture was the behavior of acetylacetone. As shown in Fig. 2, the elution behavior ranged from a sharp peak near the void volume of the column to a very broad or even completely retained peak. When an acetylacetone peak was not observed, the retention time was chosen to be the maximum run time of the experiment (15 min) and the peak width was assigned as about twice the maximum

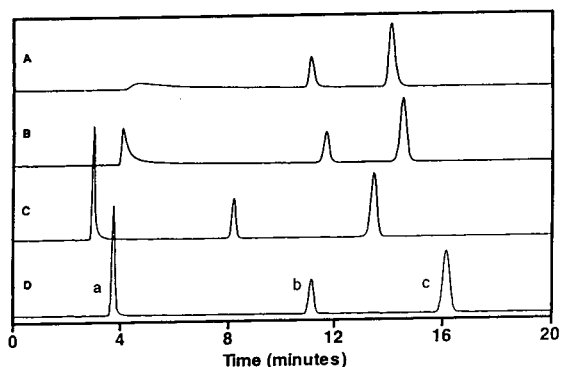


Fig. 2. Representative chromatograms for chelator test mixture. Columns: A = LiChrosorb RP18; B = Nucleosil C₁₈; C = Zorbax Rx-C₁₈; D = Inertsil C₁₈. Peaks: a = 2,4-pentanedione (0.2 μl/ml); b = 1-nitronaphthalene (54 μg/ml); c = naphthalene (300 μg/ml). Mobile phase: methanol–0.5% aqueous sodium acetate (70:30). Flow-rate: 1.0 ml/min. Detection: absorbance at 254 nm. Injection volume: 10 μl.

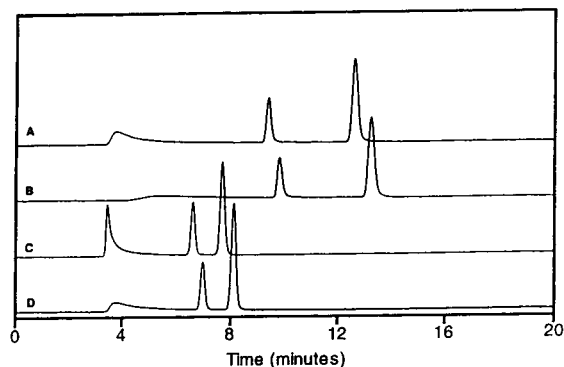


Fig. 3. Effect of column exposure to phosphate buffers (50 mM, pH 2.5 and 7.5) on response of chelator test mixture. A = Spherisorb ODS-II, used; B = Spherisorb ODS-II, new; C = μBondapak C₁₈, used; D = μBondapak C₁₈, new. Conditions as in Fig. 2.

observed value on other columns (500 s). The separation factor for naphthalene to 1-nitronaphthalene was included in Table 1 as an indication of silanophobic interactions [17].

Verzele and Dewaele [17] indicated that trace metal activity may change depending on mobile phase conditions to which the column has been exposed. In particular, mobile phases containing phosphoric acid, were reported to reduce trace metal activity. To check the effect of column history on acetylacetone elution, several columns were examined by running the chelator test mixture on a new column and on the same column after exposure to phosphate mobile phases. As shown in Fig. 3 for Spherisorb ODS-II and μBondapak C₁₈ columns, some changes were evident after exposure to phosphate mobile phases (see Figs. 6–8 for conditions), but in agreement with the observation by Verzele and Dewaele [17], the trace metal activity was not completely suppressed. The peak width of the acetylacetone peak decreased somewhat, but the values obtained before exposure to phosphate were used in Table 1. Over an extended period of time this effect could contribute to changes observed in column behavior attributed to column “aging” [24,25].

3.3. Shape selectivity test mixture

This test mixture was chromatographed using conditions given by Sander and Wise [16]. The separation factor for TBN and BaP has been shown to indicate the polymeric or monomeric nature of C₁₈ bonded phases, with factors less than or equal to 0.9 indicating a phase prepared with a polymeric surface modification process [16]. None of the columns used in this study were listed as polymeric and all gave shape selectivity factors greater than 1.0. The factors obtained were consistent with those reported previously and showed some columns to be monomeric in nature ($1.7 \leq \alpha \leq 2.2$) and the rest to have intermediate shape selectivity properties ($1.0 < \alpha < 1.7$) [16]. Data obtained for one of the Zorbax Rx-C₁₈ columns were used for the others since this test mixture was run on only one column.

3.4. Column categorization

Principal components analysis (PCA) was performed on the correlation matrix for all variables of the combined test mixture data set to reduce the dimensionality and better understand the variability structure of the data [26]. The correlation matrix was used to counter the influence the

variables with larger variances would have on a PCA of the covariance matrix. The first four PCs from this analysis had eigenvalues greater than 1 and account for greater than 95% of the variability (Table 3). In addition to the raw data, the standardized PC scores for the first four PCs were used for categorizing the columns with cluster analysis.

PCA of the retention and peak width data showed that results for the basic compounds were highly correlated. As expected, toluene and methylbenzoate results also had a high correlation. For additional analysis, the raw data set was reduced to include only aniline and toluene k' values along with aniline peak width. Ratios of aniline to phenol and p -toluidine to o -toluidine k' values were also included as indicators of column performance, particularly regarding activity of residual silanols [5]. The TBN/BaP ratio from the shape selectivity test mixture and the acetylacetone peak width and

naphthalene/nitronaphthalene ratio from the chelator test mixture were also included in this reduced data set.

Cluster analysis is another useful technique to give insight into patterns or structure that may be present in a data set. Results obtained from cluster analysis are dependent on which of several procedures is used. As recommended by Massart et al. [27], multiple clustering approaches were applied. Two similarity measures were examined; Euclidean distance and the Pearson product-moment correlation coefficient [28]. Columns that are proportionally or additively different in their retention properties, and that could be equalized by an adjustment of mobile phase strength, would be found to be different when using Euclidean distance as a measure of similarity. The correlation coefficient measure ignores proportional or additive differences which may not be critical in determining column similarity. Both measures were used to

Table 3

First four principal components of test mixture data including eigenvalues, eigenvectors, percent of variability accounted for by each PC and the cumulative percent variability accounted for by the PCs

	PC1	PC2	PC3	PC4
Eigenvalue	8.6478	6.1480	2.0829	1.2050
Percent	45.5150	32.3577	10.9626	6.3419
Cumulative percent	45.5150	77.8727	88.8352	95.1771
Eigenvectors				
Aniline, k'	-0.25816	0.25745	0.05321	0.01135
Aniline, peak width	-0.26205	0.24913	0.04267	0.00992
Phenol, k'	0.22365	0.18507	-0.23233	0.32766
o -Toluidine, k'	-0.25335	0.26442	0.03967	0.00571
m -Toluidine, k'	-0.26016	0.25448	0.06015	0.02210
p -Toluidine, k'	-0.25852	0.25796	0.05200	0.00441
DMA, k'	-0.25144	0.26666	0.06072	-0.00277
DMA, peak width	-0.26258	0.24886	0.02607	0.00497
Mebenzoate, k'	0.26909	0.18706	-0.19633	0.11437
Toluene, k'	0.26428	0.21157	0.11339	0.09650
BaP, k'	0.25685	0.21712	0.18031	-0.20624
PhPh, k'	0.24603	0.26175	0.13266	0.05642
TBN, k'	0.24038	0.26606	0.14529	0.04688
α TBN/BaP	-0.06875	0.09316	-0.15254	0.78525
Acetylacetone, peak width	0.00138	0.21824	-0.50038	-0.31263
α naphthalene/nitronaphthalene	0.08608	0.13937	0.57102	-0.08893
Acetylacetone, k'	0.04693	0.26484	-0.40809	-0.31274
Nitronaphthalene, k'	0.26774	0.20266	-0.12720	-0.00130
Naphthalene, k'	0.26688	0.22363	1.15506	-0.03809

cluster the standardized original data and scores from the first four PCs. Using the PCs for cluster analysis serves as a check on the categorization procedure using the raw data and can also determine whether PCA is an appropriate method for reducing the dimensionality of the data. Checking results using the reduced data set can add additional confidence in the final groupings.

Two commonly used clustering algorithms, average linkage and Ward's minimum variance method, were used to categorize the columns. Average linkage defines the similarity between clusters to be the average of the similarities among the objects in one cluster and the objects in the other. Ward's method combines, at each step, the two clusters that result in the smallest increase in the sums of squares within clusters. Ward's method in itself is sensitive to additive

and proportional differences so the use of the correlation coefficient as the measure of similarity was not necessary.

Results from the various clustering methods showed some differences but general trends in grouping were apparent. Four examples are shown in Fig. 4. As expected, the Zorbax Rx-C₁₈ columns always clustered together. Pairs of columns based on the same silica (Hypersil, Supelcosil, Spherisorb), treated and untreated for basic compounds, usually grouped together. Also, those that gave broad peaks (Hypersil, Supelcosil, Spherisorb) and those giving narrow peaks (YMC, Inertsil, Kromasil, Zorbax Rx) for basic compounds tended to cluster together. Intermediate columns (LiChrosorb, Nucleosil, μ Bondapak, Partisil 5 ODS-3) tended to move around, sometimes clustering with each other

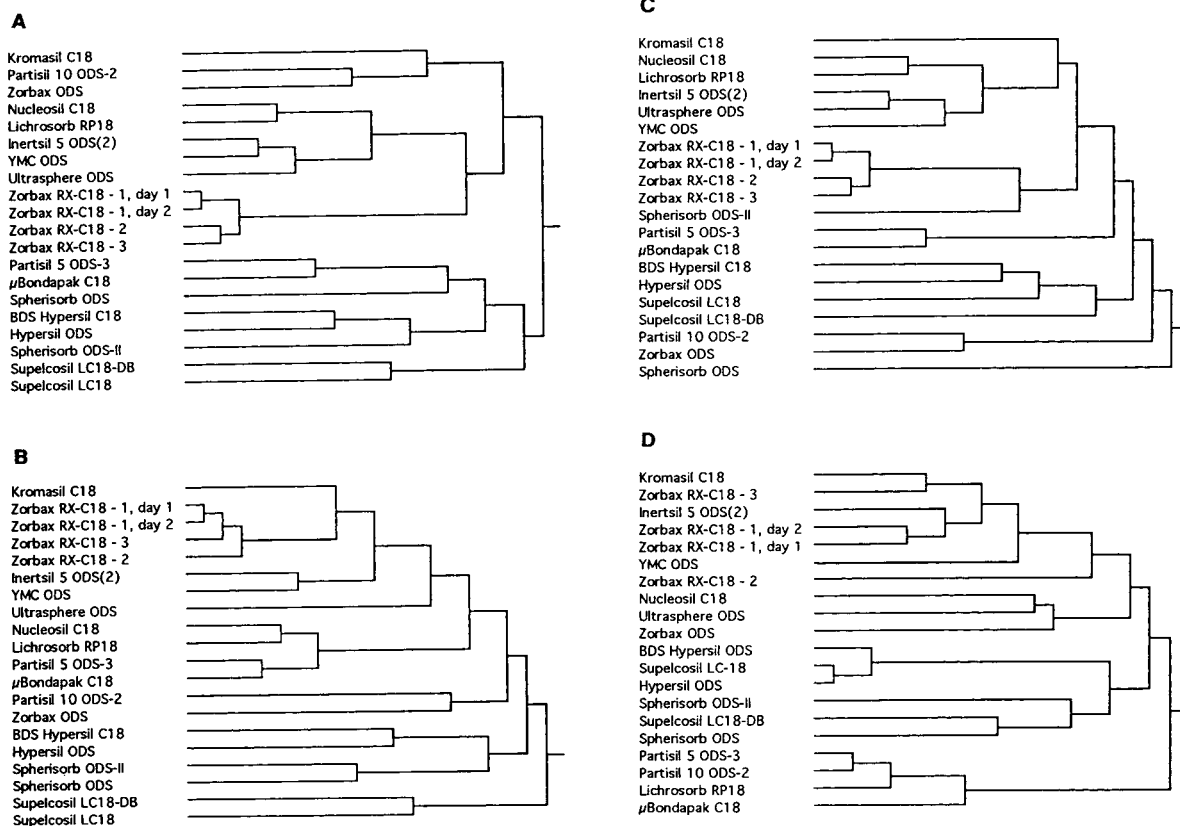


Fig. 4. Column clustering using different data sets and methods. (A) Raw data, Ward's method; (B) reduced data, average linkage; (C) first four principal components, average linkage; (D) raw data correlation matrix, average linkage.

and sometimes with other groups. In a few cases, unexpected or perhaps anomalous clustering results were obtained. For example, in Fig. 4A, Kromasil is grouped with Zorbax ODS and Partisil 10 ODS-2. This was not observed using other combinations of data set and clustering algorithm and underscores the need to use multiple methods for this type of analysis.

Relatively good consistency in clustering results was observed using the raw data, the PCs, and the reduced data. This provides an indication that the PCs and reduced data set each represent the raw data fairly well.

An important conclusion from this analysis is that a very rigid categorization of columns is not warranted. Some of the clusters were quite "loose" with relatively large distances between members of the group. However, it is possible to put the columns in small groups with quite similar behavior and in somewhat broader categories based on trends observed in the cluster analysis. Such a grouping is shown in Fig. 5. Columns within the same group would be expected to have a greater probability of giving similar results compared to columns in other groups. The consistency noted above among the data sets and clustering methods that were used adds confidence to these groupings. These categories are also generally consistent with visual comparison of chromatograms.

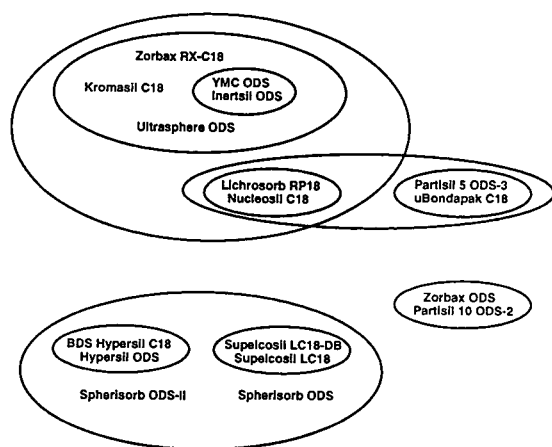


Fig. 5. Qualitative column groupings based on cluster analysis results.

3.5. Validation of column categories with pharmaceutical test mixtures

Test mixtures and mobile phase conditions used for column evaluation and categorization were chosen to accentuate differences between stationary phases. This is in contrast to methods for real applications in which mobile phases are usually developed to mask column differences. This is often accomplished by manipulation of pH, ionic strength, and the addition of silanol-masking reagents such as triethylamine. Additional confidence in the column categorization developed above can be obtained by comparison of results from different columns for analysis of mixtures representing real applications and much different mobile phase conditions than used for the original test mixture evaluation.

Pharmaceutical separations provide a good way of checking the column categorization. Three different applications were run on columns from similar and different clusters. If the clusters are valid, it would be expected that the separation behavior of columns within the same cluster will be very similar. Different behavior observed for columns from different clusters would also support the validity of the groupings. Similar behavior for different clusters could indicate that the clusters are not valid, but more likely would suggest that the method is not sensitive to column characteristics, i.e., the method is rugged.

Tricyclic antidepressants

The chromatographic behavior of the tricyclic antidepressants, amitriptyline and nortriptyline, using the *US Pharmacopeia* mobile phase conditions for amitriptyline hydrochloride injection [29] was examined. These compounds are amines and can be expected to give tailing peaks with some columns and mobile phases. Chromatograms obtained from several columns are shown in Fig. 6. The retention and peak shapes for amitriptyline and nortriptyline were similar for columns that would be expected to exhibit similar behavior based on the test mixture analysis. The YMC, Inertsil and Kromasil columns were grouped with each other and gave relatively

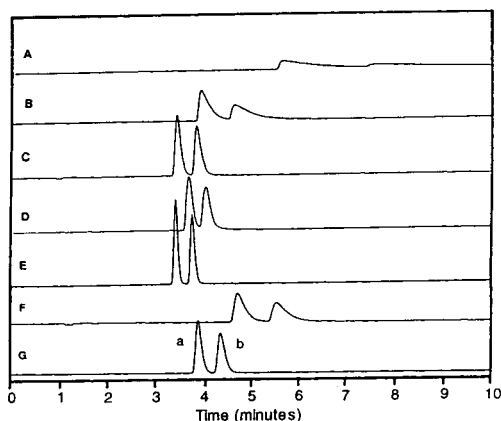


Fig. 6. Tricyclic antidepressant separation. Columns: A = Supelcosil LC18-DB; B = BDS Hypersil ODS; C = Kromasil C₁₈; D = Inertsil ODS; E = YMC ODS; F = Partisil 5 ODS (3); G = μ Bondapak C₁₈. Peaks: a = nortriptyline · HCl (0.2 mg/ml); b = amitriptyline · HCl (0.2 mg/ml). Mobile phase: acetonitrile–0.09 M aqueous sodium phosphate (pH adjusted to 2.5 with phosphoric acid) (58:42). Flow-rate: 2.0 ml/min. Detection: absorbance at 254 nm. Injection volume: 10 μ l.

sharp peaks that were eluted within about 4 min. Supelcosil LC18-DB and BDS Hypersil ODS columns were also grouped together and each gave longer retention with greater tailing compared to the other group of columns. The μ Bondapak C₁₈ and Partisil 5-ODS (3) columns were predicted to behave similarly. In this case, the Partisil 5-ODS (3) column was closer to the BDS Hypersil ODS column and the μ Bondapak C₁₈ was closer to the YMC group, especially in terms of peak shape. The μ Bondapak C₁₈ phase is recommended for this application [30]. It is apparent that the YMC group could provide equivalent separations that would probably not be obtained from columns in other groups. The column groupings appear to be fairly consistent for this application and the results show which groups of columns are likely to be acceptable for the method and which are not.

Dirithromycin

Dirithromycin is a macrolide antibiotic known to exhibit poor chromatography on several columns [31]. A mixture of dirithromycin, *epi*-dirithromycin and erythromyclamine is easily generated by allowing a sample solution to

degrade partially. This solution was analyzed using several columns with the results shown in Fig. 7. The Supelcosil LC18-DB and Hypersil ODS (column recommended for this method) columns which grouped together with test mixtures gave similar chromatography for this sample. Also grouped with these columns was Supelcosil LC18 which gave similar retention but significantly greater tailing. Columns from other groups provided separations that were quite similar (YMC ODS, Zorbax Rx-C₁₈) or drastically different (Spherisorb ODS-II, μ Bondapak C₁₈, Nucleosil C₁₈). In this case, the separation appears to be rugged over two different column groups, but not so for the columns outside these groups. Also, the secondary grouping of Hypersil columns with Supelcosil and Spherisorb was valid for Supelcosil, but not for Spherisorb. This

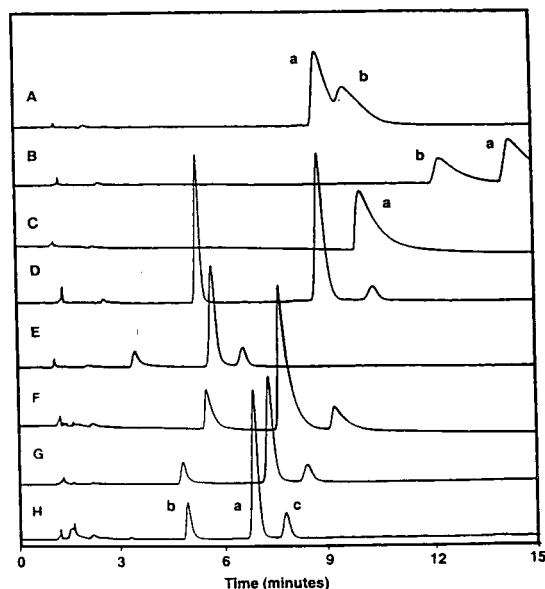


Fig. 7. Dirithromycin macrolide separation. Columns: A = μ Bondapak C₁₈; B = Nucleosil C₁₈; C = Spherisorb ODS-II; D = YMC ODS; E = Zorbax Rx-C₁₈; F = Supelcosil LC18; G = Supelcosil LC18-DB; H = Hypersil ODS. Peaks: a = dirithromycin, 2.5 mg/ml, degraded in mobile phase for at least 24 h to form b = erythromyclamine and c = *epi*dirithromycin, additional erythromyclamine was added to some sample solutions. Mobile phase: acetonitrile–methanol–50 mM aqueous potassium phosphate, pH 7.5 (44:19:37). Flow-rate: 2.0 ml/min. Detection: absorbance at 205 nm. Injection volume: 10 μ l. Column temperature: 40°C.

demonstrates that the groupings are only approximate and will not be valid for every separation.

β -Lactam antibiotics

Three β -lactam antibiotics, cephalexin, cefaclor and loracarbef, combined with acetaminophen as an internal standard, were investigated as another pharmaceutical compound separation. Each of these antibiotics is amphoteric, possessing carboxylic acid and primary amine groups. Results for different columns are shown in Fig. 8. The primary differences observed for columns from different groups are retention time and efficiency. Even the Zorbax ODS column, which did not group well with any columns other than the Partisil 10 ODS (2), gave a separation similar to the other columns. In this example, a simple adjustment of mobile phase strength could be used to make all the columns appear nearly identical. Therefore, the mobile phase conditions must be masking secondary retention mechanisms and stationary phase interactions that have led to differences among columns in the other examples. It is likely that this separation could be performed adequately on almost any ODS column.

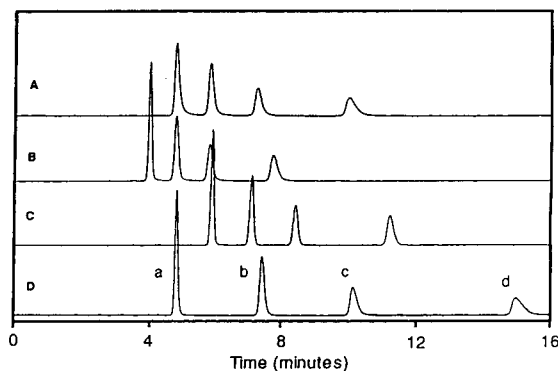


Fig. 8. Antibiotics separation. Columns: A = Zorbax ODS; B = Zorbax Rx-C₁₈; C = YMC ODS; D = Hypersil ODS. Peaks: a = 4-acetamidophenol (internal standard, 0.09 mg/ml); b = cefaclor (0.24 mg/ml); c = loracarbef (0.14 mg/ml); d = cephalexin (0.16 mg/ml). Mobile phase: acetonitrile–50 mM aqueous sodium phosphate, pH 2.5 (14:86). Flow-rate: 1.0 ml/min. Detection: absorbance at 254 nm. Injection volume: 10 μ l.

4. Conclusions

Test mixtures containing compounds chosen to accentuate the differences among ODS bonded-phase columns are useful in categorizing columns according to the similarity of chromatographic behavior. The various cluster analysis methods used to categorize the raw data set or reduced sets derived from it showed some differences in groupings, but general column categories could be discerned. The general similarity of cluster analysis results also indicated that the principal components and reduced data sets were adequate representations of the raw data.

The categories determined from the analysis were tested for validity using separations of several pharmaceutical compounds. In general, columns in the same category behaved similarly in these examples and would be likely choices as alternates for each other. Columns from different categories were more likely to exhibit differences in behavior and could be explored during method development to achieve better retention, selectivity or peak shape. Similar behavior observed for columns from different categories can be an indication of method ruggedness with respect to column characteristics for the chosen separation conditions.

The work described here has been focused on small organic molecules. The test mixtures used may not be appropriate for prediction of column similarity with regard to behavior toward polypeptides and proteins where other interactions may become important.

The utility of the categories described here would be greatly extended if additional columns could be readily classified. This could be done qualitatively by visual examination of test mixture chromatograms or by using linear discriminant analysis to categorize a column not included in the original set.

Acknowledgement

Helpful comments on the manuscript from Eugene Rickard are gratefully acknowledged.

References

- [1] B.A. Bidlingmeyer, *Practical HPLC Methodology and Applications*, Wiley, New York, 1992.
- [2] *LC·GC*, 11 (1993) 566.
- [3] A.P. Goldberg, *Anal. Chem.*, 54 (1982) 342.
- [4] K. Kimata, K. Iwaguchi, S. Onishi, K. Jinno, R. Ecksteen, K. Hosoya, M. Araki and N. Tanaka, *J. Chromatogr. Sci.*, 27 (1989) 721.
- [5] H. Engelhardt, H. Löw and W. Götzinger, *J. Chromatogr.*, 544 (1991) 371.
- [6] S.J. Schmitz, H. Zwanziger and H. Engelhardt, *J. Chromatogr.*, 544 (1991) 381.
- [7] H. Engelhardt and M. Jungheim, *Chromatographia*, 29 (1990) 59.
- [8] M.F. Delaney, A.N. Papas and M.J. Walters, *J. Chromatogr.*, 410 (1987) 31.
- [9] M.J. Walters, *J. Assoc. Off. Anal. Chem.*, 70 (1987) 465.
- [10] D.V. McCalley, *J. Chromatogr.*, 636 (1993) 213.
- [11] A. Jardine, C. Dowle, A. Martin and C. Davidson, *Anal. Proc.*, 29 (1992) 63.
- [12] M.C. Pietrogrande, M.I. Turnes Carou and F. Dondi, *Analisis*, 20 (1992) 111.
- [13] D.V. McCalley, *J. Chromatogr.*, 357 (1986) 221.
- [14] T. Daldrup and B. Kardel, *Chromatographia*, 18 (1984) 81.
- [15] P.C. Sadek and P.W. Carr, *J. Chromatogr. Sci.*, 21 (1983) 314.
- [16] L.C. Sander and S.A. Wise, *J. High Resolut. Chromatogr. Chromatogr. Commun.*, 11 (1988) 383.
- [17] M. Verzele and C. Dewaele, *Chromatographia*, 18 (1984) 84.
- [18] M.A. Stadalius, J.S. Berus and L.R. Snyder, *LC·GC*, 6 (1988) 494.
- [19] D.L. Massart and H. De Clercq, *Anal. Chem.*, 46 (1974) 1988.
- [20] D.L. Massart, P. Lenders and M. Lauwereys, *J. Chromatogr. Sci.*, 12 (1974) 617.
- [21] H. De Clercq and D.L. Massart, *J. Chromatogr.*, 115 (1975) 1.
- [22] A. Eskes, F. Dupuis, A. Dijkstra, H. De Clercq and D.L. Massart, *Anal. Chem.*, 47 (1975) 2168.
- [23] H. De Clercq, D.L. Massart and L. Dryon, *J. Pharm. Sci.*, 66 (1977) 1269.
- [24] Th. Cachet, I. Quintens, E. Roets and J. Hoogmartens, *J. Liq. Chromatogr.*, 12 (1989) 2171.
- [25] Th. Cachet, I. Quintens, J. Paesen, E. Roets and J. Hoogmartens, *J. Liq. Chromatogr.*, 14 (1991) 1203.
- [26] J.E. Jackson, *A User's Guide to Principal Components*, Wiley, New York, 1991.
- [27] D.L. Massart, B.G.M. Vandeginste, S.N. Deming, Y. Michotte and L. Kaufman, *Chemometrics: A Textbook*, Elsevier, Amsterdam, 1988, pp. 371–384.
- [28] C.H. Romesburg, *Cluster Analysis for Researchers*, Lifetime Learning Publications, Belmont, CA, 1984.
- [29] *US Pharmacopeia XXII*, United States Pharmacopeial Convention, Rockville, MD, 1990, pp. 73–74.
- [30] B.B. Hubert and R.F. Lindauer (Editors), *Chromatographic Reagents*, United States Pharmacopeial Convention, Rockville, MD, 1990, p. 7.
- [31] B.A. Olsen, J.D. Stafford and D.E. Reed, *J. Chromatogr.*, 594 (1992) 203.



ELSEVIER

Liquid chromatographic determination of the macrolide antibiotics roxithromycin and clarithromycin in plasma by automated solid-phase extraction and electrochemical detection

Maria Hedenmo, Britt-Marie Eriksson*

Bioanalytical Chemistry, Astra Hässle AB, S-431 83 Mölndal, Sweden

Abstract

A liquid chromatographic method for the determination of the macrolide antibiotics, roxithromycin and clarithromycin, in plasma is described. The method is fully automated, employing on-line solid-phase extraction for sample clean-up, using the Prospekt unit. Plasma samples, mixed with internal standard, were injected onto exchangeable CN cartridges. After washing, the compounds were eluted and transferred to a C_{18} analytical column for separation and electrochemical detection. Clarithromycin was used as internal standard when assaying roxithromycin and vice versa. The recovery of the solid-phase extraction method was 90% and higher, and the relative standard deviation was about 3%. The limit of quantitation was $0.5 \mu\text{mol/l}$ when $25 \mu\text{l}$ of plasma was injected. Comparison with a liquid-liquid extraction method for sample clean-up showed good agreement.

1. Introduction

Roxithromycin and clarithromycin are mac-

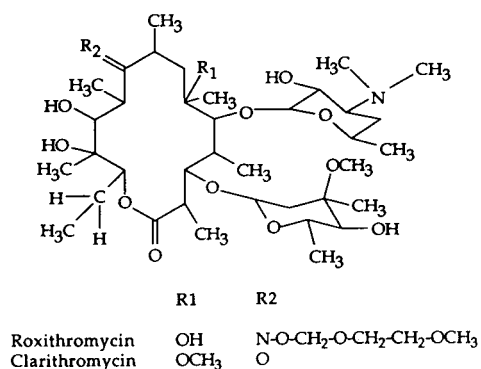


Fig. 1. Structures of roxithromycin and clarithromycin.

* Corresponding author.

rolide antibiotics (see Fig. 1 for structures) with an antibacterial spectrum similar to that of erythromycin. A limited number of papers can be found in the literature concerning the analysis of roxithromycin [1,2] and clarithromycin [3,4] in biological fluids, whereas the documentation of erythromycin is more extensive. Previously, erythromycin and its derivatives in biological fluids have been determined by microbiological assays [5,6]. These methods are, however, laborious and, in the presence of metabolites with antibacterial activity, also less selective than methods employing liquid chromatography.

Because of the poor UV absorbance of macrolides and the need for derivatization prior to liquid chromatography when using fluorescence detection, electrochemical detection seems to be the most appropriate mode for monitoring these substances [1-4,7-11]. Due to the high potential

required for oxidation of macrolides and the subsequent high background current, a Coulochem detector appears to be the most advantageous, but also other amperometric detectors have been used [7,8,11].

Sample clean-up by liquid–liquid extraction (LLE) at alkaline pH, followed by evaporation and reconstitution, has been employed in most of the previous assays. This has given recoveries for roxithromycin and clarithromycin ranging from 68 to 90% [1–3,7]. So far only one paper has been published regarding the use of solid-phase extraction (SPE) for sample preparation of erythromycin in serum and urine [9].

We have developed a fast and simple method for the determination of roxithromycin and clarithromycin in plasma for pharmacokinetic studies by using the Prospekt on-line SPE unit. This fully automated system, which has previously been described for analysis of other drugs [12–14], consists of a microprocessor, one to three six-port valves, a solvent-delivery unit and an autosampler.

2. Experimental

2.1. Chemicals

All solvents were of HPLC grade (Rathburn, Walkerburn, UK) and reagents of analytical grade (Merck, Darmstadt, Germany). Clarithromycin was provided by Abbot Labs. (Abbot Park, IL, USA) and roxithromycin by Roussel Uclaf (Romainville, France). Water was from an ELGA (Wycombe, UK) purification system.

2.2. Chromatographic system

The chromatographic system comprised a Pharmacia LKB HPLC pump 2248 (Bromma, Sweden), a CMA/200 refrigerated autosampler (CMA Microdialysis, Stockholm, Sweden), a Spark Holland (Emmen, Netherlands) Prospekt module with a microprocessor, a cartridge transport system, three six-port valves and a solvent-

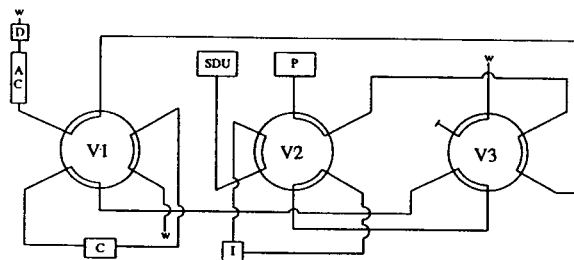


Fig. 2. Schematic disposition of the chromatographic system. V1, V2, V3 = Valves belonging to the Prospekt unit; SDU = solvent-delivery unit; P = pump; I = injector; C = cartridge; AC = analytical column; D = detector; w = waste.

delivery unit (SDU), with the capability of delivering up to six solvents. Glass vials (0.3 ml) were from Chromacol (London, UK). A schematic disposition is shown in Fig. 2.

The SPE cartridges (10 × 2 mm I.D.) contained 20 mg of Baker CN packings (30–40 μm) and were distributed by Spark Holland. The analytical column Hypersil BDS C₁₈ (3 μm, 100 × 4.6 mm I.D.) came from Shandon (Astmoor, UK) and was thermostatted at 55°C.

The mobile phase pH 7 (ionic strength $I = 0.025$) contained 4.5 mM NaH₂PO₄, 6.8 mM Na₂HPO₄ and 54% acetonitrile. The three solutions used for conditioning and washing the cartridges were (1) 100% methanol, (2) 10% methanol in water and (3) phosphate buffer pH 10.5 ($I = 0.10$) containing 29 mM Na₂HPO₄, 1.9 mM Na₃PO₄ and 10% acetonitrile. Prior to use all buffer solutions were filtered through a Millipore (Milford, MA, USA) filter (HA, 0.22 μm) and ultrasonicated for 30 min. The flow-rate over the analytical column was 1.0 ml/min and the eluent was monitored by an ESA (Bedford, MA, USA) Coulochem II electrochemical detector. A dual analytical cell Model 5011 was used with the upstream potential set at +0.65 V (cell 1) and the downstream potential at +0.85 V (cell 2). The signal was monitored at the second cell. An ESA carbon in-line filter was placed before the analytical cell to protect it. The potential applied on cell 1 was used to reduce the background current at the second cell. Data were monitored and processed by a Multichrom chromatographic

data system (VG Data Systems, Altrincham, UK).

2.3. Sample preparation

The frozen plasma samples were thawed at room temperature, mixed and centrifuged for 5 min at 1300 *g*. An aliquot of 100 μ l of the samples was pipetted into 1.5-ml glass vials and 100 μ l of the internal standard in phosphate buffer pH 10.5 ($I = 0.10$), with 10% of acetonitrile, were added. After mixing, the samples were transferred to glass vials (0.3 ml) and placed in the autosampler. A volume of 20–100 μ l of the samples was injected.

Reference plasma samples were prepared by mixing 100 μ l of drug-free plasma and 100 μ l of a solution containing both reference compound and internal standard in phosphate buffer pH 10.5 ($I = 0.10$), with 10% of acetonitrile.

2.4. Solid-phase extraction

A new extraction cartridge (connected to valve 1 in Fig. 2) was automatically inserted for each sample and conditioned with 2 ml of solvent 1 (100% methanol) followed by 2 ml of solvent 2 (10% methanol in water) and ca. 4 ml of solvent 3 (phosphate buffer pH 10.5, $I = 0.10$, with 10%

of acetonitrile) using the SDU. As described earlier [14], the CMA/200 autosampler had in the meantime prepared the sample for injection, and by a signal from the microprocessor the plasma sample was injected onto the SPE cartridge. Prior to injection the flow-rate over the cartridge was changed from 2 to 0.5 ml/min.

After 5 min of loading, when most of the plasma matrix had been washed off the cartridge, valve 1 was switched and the compounds were transferred backwards by the mobile phase onto the analytical column for separation, followed by electrochemical detection. At the same time data collection was started. Valve 1 was switched back after 3 min of elution and the SDU started to wash the capillaries with 2 ml of solvent 2 and 2 ml of solvent 1 at a flow-rate of 2 ml/min. After a total time of 15 min the procedure was repeated. The SPE procedure is summarized in Table 1.

By switching valve 2, the autosampler was directly connected to the analytical column (see Fig. 2). Injections could be made directly onto the analytical column for calculation of extraction recoveries and control of chromatographic conditions. It is also possible to use the third valve of the Prospekt unit for washing the analytical column after a completed series of plasma samples.

Table 1
Solid-phase extraction procedure

Time (min:s)	Switch valve No.	Solvent	Flow-rate (ml/min)	Comment
00:00		1	2.0	Change of cartridge; activation with 100% methanol
01:00		2		Activation with 10% methanol in water
02:00		3		Conditioning with phosphate buffer pH 10.5, $I = 0.10$, and 10% acetonitrile
03:50			0.5	Adjusting flow-rate over cartridge
04:00				Injection of sample
09:00	1			Start of elution; start of data collection
12:00	1	2	2.0	End of elution; washing of capillaries with 10% methanol in water
13:00		1		Washing with 100% methanol
14:00				End of washing

3. Results and discussion

3.1. Chromatography

The electrochemical response for the macrolides, measured as the peak areas, increased twofold by increasing pH of the phosphate buffer, used in the mobile phase, from 6 to 7. A further raise of the pH to 8 did not affect the response much and a buffer solution of pH 7 was chosen. The retention of clarithromycin and roxithromycin increased with increasing pH and the theoretical plate count was improved, but at a pH above 7 this effect was less pronounced. In order to further improve the peak shape the column was thermostatted at 55°C. When increasing the temperature from 35 to 55°C an increase of ca. 50% in the theoretical plate count was found for both clarithromycin and roxithromycin. An increase in retention was also observed.

3.2. Solid-phase extraction

We chose a pH (10.5) well above the pK_a values (ca. 9) of roxithromycin and clarithromycin in the loading buffer (solvent 3), in order to get strong retardation on the cartridge. To use a high pH at the SPE did not cause any problems, as a new cartridge was inserted for every new sample.

Two different packing materials of the cartridges were investigated, C_8 and CN. The chromatographic peaks were broader after SPE on C_8 cartridges, compared with CN cartridges. When using C_8 cartridges the theoretical plate count, N , was about 1300 for clarithromycin and roxithromycin, at a loading time of 5 min. For CN cartridges the corresponding value for N was about 5600. CN cartridges were chosen for this method.

The effects of the amount of acetonitrile in the loading buffer and of the loading time on the recovery, were investigated by experimental design [15]. A statistical full factorial design was set up with two factors: (i) the loading time, varied between 2 and 5 min and (ii) the amount of acetonitrile in solvent 3, varied between 10 and

20%. The model comprised 4 (2^2) experiments and 3 centerpoints, that is a loading time of 3.5 min and an amount of acetonitrile of 15%. The recovery was determined by comparing the peak areas after SPE with those obtained by injecting the same amount of an aqueous solution directly onto the analytical column. It was found that a combination of long loading time (5 min) and a high amount of acetonitrile (20%) gave low recoveries of clarithromycin and roxithromycin, below 50%. At the low level of acetonitrile (10%), an increase in the loading time from 2 to 5 min did not affect the recoveries. As the front peaks of the chromatograms were smaller at 5 min than at 2 min, a loading time of 5 min was chosen. The recovery and variability when using 10% of acetonitrile were further examined and are reported under *Quantitation and accuracy*.

3.3. Detection

The response of the electrochemical cell decreased during a series of analyses. It was thus important to have an internal standard that behaved similar to the analyte and compensated for the loss in sensitivity. This was the case with the couple of roxithromycin and clarithromycin. A few hours after a completed series of plasma samples the electrochemical response had regained its initial level. The cell was cleaned once a week by flushing with 6 M nitric acid followed by 1 M sodium hydroxide.

After injection of ca. 200 plasma samples a decrease in column efficiency could be seen. By adding new packing material onto the top of the column, it was possible to restore the column efficiency, at least temporarily. Washing the column with a mixture of water and methanol and changing the top frit also increased the life time. This was done once a week while the cell was cleaned.

3.4. Stability

Plasma samples containing roxithromycin and clarithromycin were stable at -20 and -70°C for at least 2 months. Plasma samples, containing phosphate buffer pH 10.5 ($I = 0.10$), with 10%

acetonitrile, were stable in a refrigerated auto-sampler for at least 24 h. Working reference solutions of roxithromycin and clarithromycin in phosphate buffer pH 10.5 ($I = 0.10$), with 10% acetonitrile, were stable for 24 h at room temperature and at least for two days in a refrigerator when kept from light.

3.5. Quantitation and accuracy

The yield of extraction was calculated by comparing the peak areas of a reference plasma sample with the peak areas of the same amount of analyte in a reference aqueous solution injected directly onto the analytical column. When comparing SPE with direct injection, area measurements were used to eliminate any difference in theoretical plate count. The yields of extraction were $89.4 \pm 5.5\%$ ($n = 11$) for roxithromycin and $99.0 \pm 5.3\%$ ($n = 11$) for clarithromycin at concentrations of 7.0 and 5.0 μM , respectively.

The ratios of the peak height of the analyte to that of the internal standard in the reference plasma samples were measured and used for calculation of plasma concentrations. The within-day variability was $\pm 3.0\%$ ($n = 10$), when assaying plasma samples containing 5.7 μM roxithromycin, and $\pm 1.9\%$ ($n = 10$) for clarithromycin at a concentration of 5.0 μM . The between-day relative standard deviation (R.S.D.) was $\pm 4.0\%$ ($n = 15$) for a plasma sample containing 3.2 μM roxithromycin and $\pm 5.8\%$ ($n = 8$) for clarithromycin at a concentration of 3.0 μM .

Both the assay of roxithromycin and that of clarithromycin was linear up to 25 μM . The limit of quantitation was 0.5 μM when injecting 25 μl of plasma with an R.S.D. of $\pm 5.7\%$ ($n = 8$) and $\pm 1.2\%$ ($n = 8$), respectively. Chromatograms of authentic human plasma samples containing roxithromycin 3.6 μM and clarithromycin 1.8 μM are shown in Figs. 3 and 4, respectively.

3.6. Comparison with an LLE method

The method was validated against a method employing LLE for sample clean-up. When measuring roxithromycin, using that work-up

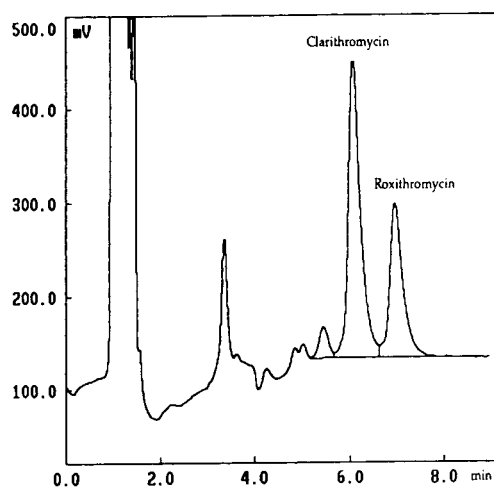


Fig. 3. Chromatogram of an authentic plasma sample containing roxithromycin (3.6 μM) and clarithromycin (internal standard, 4.8 μM). A 50- μl volume of sample was injected.

procedure, erythromycin was chosen as internal standard because of more favourable chromatographic conditions. An aliquot of 500 μl of plasma containing roxithromycin or clarithromycin and the internal standard was extracted at alkaline pH with 5 ml hexane containing 20% of isobutanol. The organic phase was separated, evaporated to dryness and reconstituted in the

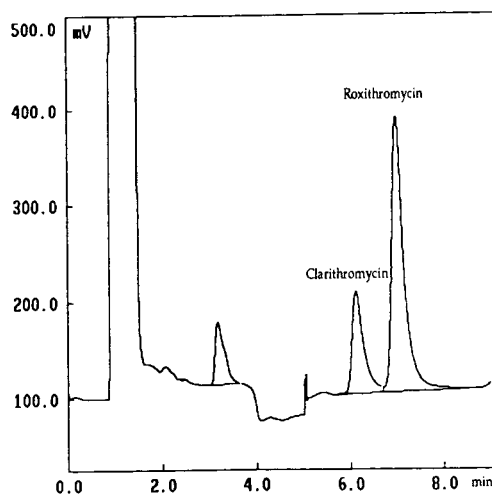


Fig. 4. Chromatogram of an authentic plasma sample containing clarithromycin (1.8 μM) and roxithromycin (internal standard, 7.0 μM). A 50- μl volume of sample was injected.

stituted in the mobile phase, which consisted of a phosphate buffer pH 7 and 45% of acetonitrile. The compounds were separated on a 3 μ m Hypersil BDS C₁₈ column (100 \times 4.6 mm I.D.) at a flow-rate of 1.2 ml/min. The column was thermostatted at 55°C and the eluent was monitored by an ESA Coulochem I electrochemical detector with a dual analytical cell Model 5011.

In order to compare the LLE method with the SPE method, results from the analysis of 32 authentic plasma samples of clarithromycin and 28 samples of roxithromycin, ranging from 360 to 15 600 nmol/l, were used. It was assumed that the logarithmic transformation of the values follow a bivariate normal distribution. The estimated ratio of the methods and the 95% confidence interval (CI) were 1.011 CI (0.977, 1.046) for clarithromycin and 1.007 CI (0.981, 1.034) for roxithromycin. Accordingly, the results from the LLE and SPE methods showed excellent agreement.

3.7. Ruggedness

The ruggedness of the method was investigated using a statistical full factorial design. The factors tested for their effect on the extraction recovery were (i) the amount of acetonitrile in solvent 3, (ii) the loading time of the SPE and (iii) the elution time. These factors were varied in small intervals, that is (i) 8 to 12%, (ii) 4 to 6 min and (iii) 2 to 4 min, respectively. For 3 factors there are 8 (2³) possible combinations of factor levels. Moreover three center points were investigated, that is, an amount of 10% acetonitrile, a loading time of 5 min and an elution time of 3 min. The levels of the center points were chosen according to the described method. A statistical analysis of variance (ANOVA) was performed to evaluate any effect of the experimental variables. No statistically significant effect on the extraction recoveries for either roxithromycin or clarithromycin was found when varying any of the factors chosen, and the method was proved rugged within the intervals studied.

4. Conclusions

The described method for determination of the macrolide antibiotics, roxithromycin and clarithromycin, in plasma samples yielded high recoveries and good precision. Validation of this automated SPE method against an LLE method gave results showing excellent agreement.

Acknowledgements

We thank Helena Toreson for assistance with the LLE method and Dr. Bengt-Arne Persson for helpful reading of the manuscript.

References

- [1] N. Grgurinovich and A. Matthews, *J. Chromatogr.*, 433 (1988) 298.
- [2] F.M. Demotes-Mainard, G.A. Vincon, C.H. Jarry and H.C. Albin, *J. Chromatogr.*, 490 (1989) 115.
- [3] S.-Y. Chu, L.T. Sennello and R.C. Sonders, *J. Chromatogr.*, 571 (1991) 199.
- [4] K. Borner, H. Hartwig and H. Lade, *Methodol. Surv. Biochem. Anal.*, 22 (1992) 137.
- [5] D.C. Grove and W.A. Randall, *Assay Methods of Antibiotics, A Laboratory Manual*, Medical Encyclopedia, New York, 1955.
- [6] A.L. Barry and R.R. Packer, *Eur. J. Clin. Microbiol.*, 5 (1986) 536.
- [7] D. Croteau, F. Vallée, M.G. Bergeron and M. LeBel, *J. Chromatogr.*, 419 (1987) 205.
- [8] L.-G. Nilsson, B. Walldorf and O. Paulsen, *J. Chromatogr.*, 423 (1987) 189.
- [9] C. Stubbs and I. Kanfer, *J. Chromatogr.*, 427 (1988) 93.
- [10] S. Laakso, M. Scheinin and M. Anttila, *J. Chromatogr.*, 526 (1990) 475.
- [11] Y. Kato, T. Yokoyama, M. Shimokawa, K. Kudo, J. Kabe and K. Mohri, *J. Liq. Chromatogr.*, 16 (1993) 661.
- [12] M.W. Nielen, A.J. Valk, R.W. Frei, U.A.Th. Brinkmann, Ph. Mussche, R. de Nijs, B. Ooms and W. Smink, *J. Chromatogr.*, 393 (1987) 69.
- [13] O.V. Olesen and B. Poulsen, *J. Chromatogr.*, 622 (1993) 39.
- [14] M. Hedenmo and B.-M. Eriksson, *J. Chromatogr. A*, 661 (1994) 153.
- [15] E. Morgan, *Chemometrics: Experimental Design*, Wiley, London, 1991.



ELSEVIER

Journal of Chromatography A, 692 (1995) 167–172

JOURNAL OF
CHROMATOGRAPHY A

Analysis of mycolic acids by high-performance liquid chromatography and fluorimetric detection Implications for the identification of mycobacteria in clinical samples

Steven R. Hagen*, Jennifer D. Thompson

Ribi ImmunoChem Research, Inc., 553 Old Corvallis Road, Hamilton, MT 59840, USA

Abstract

Mycolic acids from *Mycobacterium phlei* and *M. bovis* cell wall skeletons (CWSs) were analyzed by HPLC. After saponifying lyophilized CWSs in methanolic KOH, the mycolic acids were quantitatively extracted into chloroform. Aliquots of the CWS mycolic acid extracts were then derivatized prior to HPLC analysis with a UV reagent, *p*-bromophenacylbromide (PBPB), and three fluorescent reagents, 4-bromomethyl-6,7-dimethoxycoumarin, 4-bromomethyl-7-acetoxycoumarin and 3-bromomethyl-7-methoxy-1,4-benzoxazin-2-one. A synthetic α -branched carboxylic acid was derivatized with the same reagents and used as an internal standard along with the mycolic acids. The derivatized samples were analyzed by reversed-phase HPLC on a Waters Novapak C₁₈, 4 μ m particle size, 150 mm \times 3.9 mm stainless-steel column. Two solvent systems were used: (1) methanol and methylene chloride with the column at 30°C, and (2) methanol and isopropanol with the column at 50°C. Detection sensitivity with the fluorescent reagents was 16–50 times greater than the sensitivity observed with PBPB-derivatized samples. Unique mycolic acid elution profiles for the two mycobacterial species could be achieved with each of the solvent systems and derivatization reagents tested. Thus, the HPLC analysis of pre-column derivatized mycolic acids was useful as a means of rapidly identifying mycobacterial species. Replacement of methylene chloride with isopropanol and PBPB with a fluorescent derivatizing reagent could increase the safety and sensitivity of the assay, and make it more useful for the clinical identification of mycobacterial infections.

1. Introduction

Mycobacterial infections, especially of the *Mycobacterium tuberculosis* group, represent an increasingly serious public health risk [1]. Improvement in the clinical diagnosis of these infections is dependent upon the availability of rapid diagnostic tests [2]. To date, the types of tests employed include: biochemical and physio-

logical, genetic (DNA) probe assays, GC of cellular fatty acids and HPLC of mycolic acids (C₆₀–C₉₀ α -branched, β -hydroxy fatty acids) [2–4].

HPLC analysis of the mycolic acids has emerged as the method of choice for the diagnosis of mycobacterial infections, due to its rapid and reproducible nature [2], and because the mycolic acid elution pattern observed for each mycobacterial species has generally been found to be unique [2,5–11].

* Corresponding author.

The HPLC analysis of the mycolic acids was performed as a three-phase process. First, the acids were derivatized pre-column with a UV chromophore, *p*-bromophenacylbromide (PBPB) [12]. Next, an HPLC separation was achieved in the reversed-phase mode using methanol and methylene chloride as eluents [8]. Finally, the chromatogram can be compared to a reference library and a species identification can be made [13].

Recently, some improvements over the existing technique have been reported. Detection sensitivity was dramatically improved by utilizing 4-bromomethyl-6,7-dimethoxycoumarin (BRDC) as a pre-column derivatizing reagent [14], followed by reversed-phase HPLC with fluorescence detection [15]. Chromatographic ruggedness has been increased by employing isopropanol (in place of methylene chloride) and temperature control during chromatography [16].

This paper discusses the combination of pre-column derivatization with fluorescent reagents, followed by temperature-controlled HPLC analysis using isopropanol in place of methylene chloride. In addition to BRDC, two other fluorescent reagents were tested: 4-bromomethyl-7-acetoxycoumarin (BRAC) [17] and 3-bromomethyl-7-methoxy-1,4-benzoxazin-2-one (BRMB) [18].

2. Experimental

2.1. Reagents

HPLC-grade acetonitrile (ACN), chloroform (CHCl_3), isopropanol (IPA), methanol (MeOH), methylene chloride (MeCl_2), and reagent-grade acetone, concentrated hydrochloric acid (HCl), anhydrous magnesium sulphate (MgSO_4), potassium hydrogencarbonate (KHCO_3), potassium hydroxide (KOH) were obtained from J.T. Baker (Phillipsburg, NJ, USA). BRDC and 18:crown:6 ether were obtained from Aldrich (Milwaukee, WI, USA). PBPB crown ether solution in acetonitrile was obtained from Pierce (Rockford, IL, USA). BRAC was obtained from Regis (Morton Grove,

IL, USA). BRMB was obtained from TCI America (Portland, OR, USA). Mycobacterial cell wall skeleton (CWS) preparations and a proprietary α -branched carboxylic acid internal standard compound were obtained from Ribl ImmunoChem Research (Hamilton, MT, USA).

2.2. CWS saponification and quantitative extraction

CWS preparations from *Mycobacterium phlei* and *M. bovis* served as sources of mycolic acids. CWS samples were saponified in 25% (w/v) KOH in MeOH–water (1:1, v/v) (5 mg CWS per ml KOH solution) for 2.5 h at $102.5 \pm 2.5^\circ\text{C}$. After heating, the samples were placed in an ice bath in a fume hood, and concentrated HCl (0.076 ml per ml KOH solution) was carefully added. The resulting mixtures were extracted three times with CHCl_3 (0.8 ml CHCl_3 per ml KOH solution). Centrifugation followed each extraction, and the lower (organic) layers were collected. The combined CHCl_3 extract was dried under a stream of nitrogen, then quantitatively transferred with CHCl_3 washes into a tared tube through a luer-lok syringe fitted with a Gelman (Ann Arbor, MI, USA) 0.2- μm Acrodisc filter. Finally, the solvent was removed under a stream of nitrogen, and the tube was reweighed to obtain a known mass of CWS mycolic acid extract.

2.3. Pre-column derivatization

For each derivatization reagent test, a sample consisted of the following: 0.400 mg of mycolic acid extract (from either mycobacterial species) plus 39.4 nmol of the Ribl internal standard compound.

Derivatization with PBPB was as described previously [6], except that the samples were heated for 30 min at $85 \pm 2^\circ\text{C}$.

Coupling with BRDC was achieved in generally the same manner as previously described [15]. Briefly, 100 μl of 20 mg per ml KHCO_3 in MeOH–water (1:1, v/v) was added to each mycolic acid/internal standard sample, with subsequent drying under a stream of nitrogen. Next,

500 μ l of chloroform, 175 μ l of 2.5 mg/ml BRDC in ACN (dried over $MgSO_4$) and 25 μ l of 10.6 mg/ml 18:crown:6 in acetone (dried over $MgSO_4$) were added. The samples were then heated for 30 min at $50 \pm 2^\circ C$. Finally, the solvent was removed under a stream of nitrogen. Reaction with BRAC and BRMB was identical, except that 2.5 mg/ml BRAC in dried acetone and 2.3 mg/ml BRMB in dried ACN were used.

2.4. Chromatography

The chromatographic system was from Waters, and included two 510 pumps, a 700 WISP, a TCM (30 or $50^\circ C$) and either a 440 UV (254 nm) or a 470 fluorescence detector (16- μ l flow cell). Fluorescence excitation (ex) and emission (em) wavelengths were as follows: BRDC, ex = 345 nm, em = 425 nm; BRAC ex = 315 nm, em = 400 nm; BRMB ex = 340 nm, em = 415 nm. The system was controlled, and data were collected and processed with Waters Millennium (version 2.0) software. A Waters stainless-steel Novapak C_{18} 150 \times 3.9 mm column (preceded by a Guardpak equipped with a C_{18} insert) was used.

Prior to HPLC analysis, samples were dissolved in $CHCl_3$ -MeOH (2:1, v/v).

Depending on the reagent being tested, various linear solvent programs using MeOH and $MeCl_2$, a column temperature of $30^\circ C$ and a flow-rate of 1.5 ml/min were run (data not shown). Similarly, separations were achieved by using IPA in place of $MeCl_2$, a column temperature of $50^\circ C$ and a flow-rate of 1.5 ml/min (Table 1).

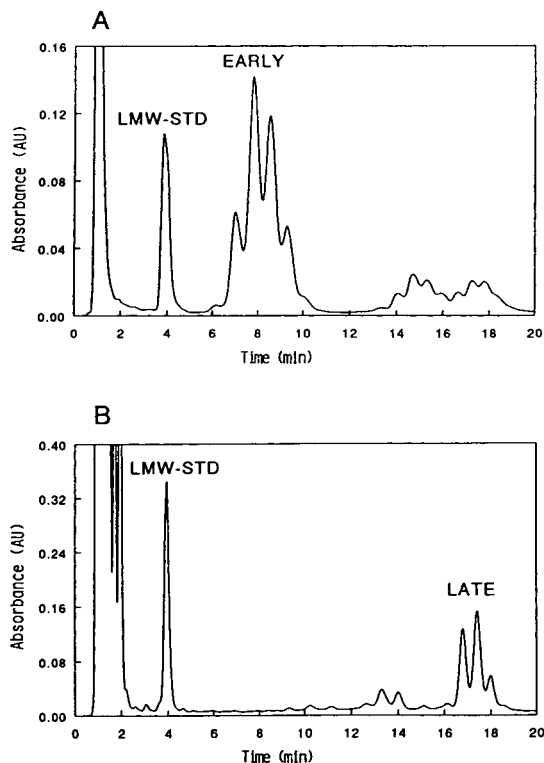


Fig. 1. Representative chromatograms of PBPB-derivatized mycolic acids from *M. phlei* (A) and *M. bovis* (B) separated with an MeOH-IPA solvent gradient (see Table 1).

3. Results and discussion

M. phlei and *M. bovis* CWS samples were used in these experiments for two reasons. First, extracts from these samples exhibited the early (*M. phlei*, see Fig. 1) and late (*M. bovis*, see Fig. 1) eluting mycolic acid groups during HPLC

Table 1
Percentages of MeOH and IPA which were used to achieve separations of mycolic acids derivatized with four reagents

Time (min)	PBPB		BRDC		BRAC		BRMB	
	MeOH	IPA	MeOH	IPA	MeOH	IPA	MeOH	IPA
0.0	60.0	40.0	80.0	20.0	85.0	15.0	72.5	27.5
18.0	6.0	94.0	10.0	90.0	10.0	90.0	10.0	90.0
18.5	60.0	40.0	80.0	20.0	85.0	15.0	72.5	27.5
25.5	60.0	40.0	80.0	20.0	85.0	15.0	72.5	27.5

analysis [16]. Thus, while only two species were tested, they yielded a complex pattern of mycolic acids which served to test the applicability of the HPLC method using elution with IPA and fluorescence detection. Second, sufficient quantities of these preparations were available for quantitative mycolic acid extraction, which was essential for the accurate determination of detection limits (discussed below).

In previous applications of the HPLC method, a “high-molecular-mass” internal standard compound (HMW-STD, Ribi ImmunoChem Research) has been used for the calculation of relative retention times (RRTs), which aid subsequent mycobacterial species identifications [2,7–11]. This compound was supplied as the PBPB ester, and has been the latest eluting peak of interest during the HPLC analysis [2,6–10].

In order to test a variety of derivatizing reagents, a lower-molecular-mass α -branched non-esterified carboxylic acid was used. This compound, identified as LMW-STD in Figs. 1–4, eluted prior to the mycolic acid peaks. Since it was available in a highly pure form, accurate determinations of the detection limits for each of the derivatizing reagents could be made (discussed below).

In general, literature protocols were followed for the preparation of the chromogenic and fluorogenic mycolic acid esters [12,14,17,18]. In order to achieve reproducible coupling of the mycolic acids and the internal standard with the fluorescent reagents, it was necessary to use $MgSO_4$ -dried acetone and ACN (data not shown). The reagent concentrations, reaction times and temperatures used for sample derivatization were found to be optimal (data not shown).

Two gradient elution solvent systems were tested for the HPLC analysis of the esterified mycolic acids: MeOH and $MeCl_2$ (data not shown), MeOH and IPA (Table 1, Figs. 1–4). Two constraints were placed on the optimization of separation with the eluents tested. First, the total run time for the analysis, including injection delay and gradient plus column re-equilibration (1 min plus 25.5 min, respectively) was arbitrarily set at 26.5 min. This represented

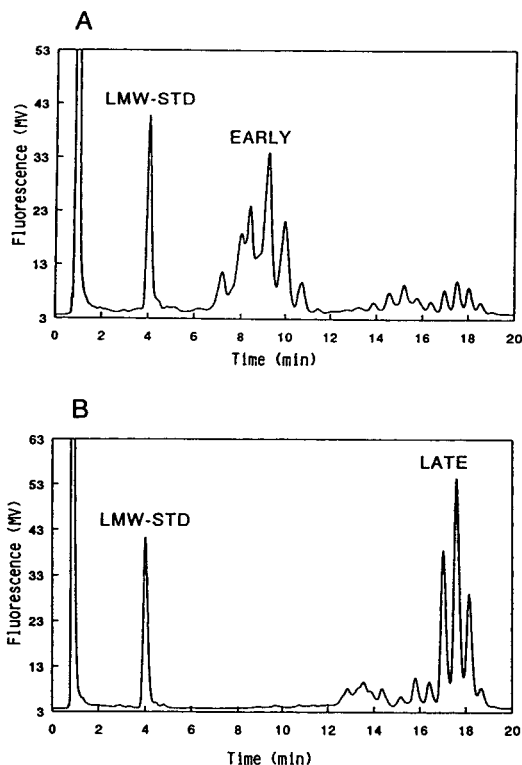


Fig. 2. Representative chromatograms of BRDC-derivatized mycolic acids from *M. phlei* (A) and *M. bovis* (B) separated with an MeOH–IPA solvent gradient (see Table 1).

a compromise between analytical speed and resolution. Second, the solvent gradient conditions were set so that the internal standard compound eluted at about 4 min for each of the reagents tested. This allowed for meaningful comparisons of the various reagents in different elution environments.

Detection limits were assessed by making HPLC analyses of serially diluted samples derivatized with PBPB and each of the fluorescent reagents. The detection limits for the internal standard are expressed as three times the average amplitude of the detector baseline noise, and ranged from 6.00 pmol for the UV reagent, PBPB to 0.12 to 0.24 pmol for the fluorescent reagents (Table 2). Detection limits for the mycolic acid extract represent the approximate minimum mass that was required for a positive species identification by the HPLC technique.

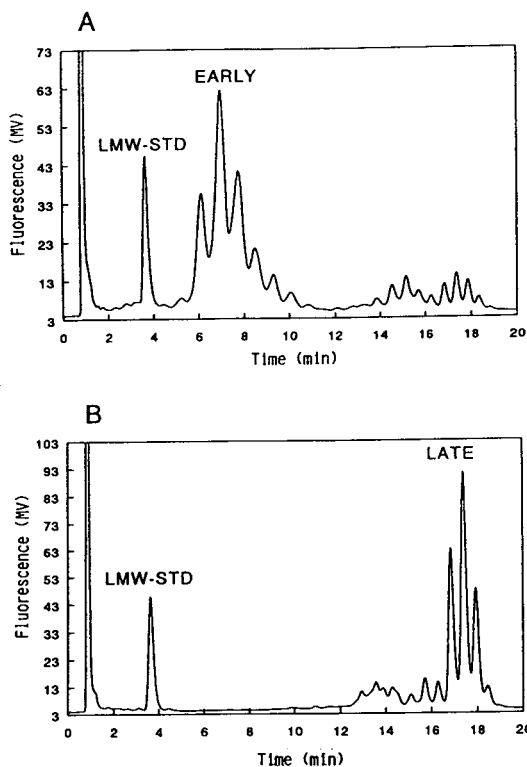


Fig. 3. Representative chromatograms of BRAC-derivatized mycolic acids from *M. phlei* (A) and *M. bovis* (B) separated with an MeOH–IPA solvent gradient (see Table 1).

These ranged from a high of 800 ng for PBPB to 30–50 ng for the fluorescent reagents (Table 2). Thus, depending on how detection limit was assessed (standard acid vs. acid extract), the fluorescent mycolic acid esters were 16–50-fold more sensitive than the PBPB esters. The results with BRDC were similar to those reported previously [15]. In light of the fact that detection limits with BRAC were enhanced about 10-fold further by employing a post-column reaction system [17], the potential exists for a 500-fold increase in sensitivity over the UV detection of PBPB esters.

While imposing the analysis and retention time constraints discussed previously, HPLC separations were optimized. Figs. 1–4 show representative chromatograms generated with MeOH–IPA for extracts from each species derivatized with PBPB and the three fluorophores. Chromato-

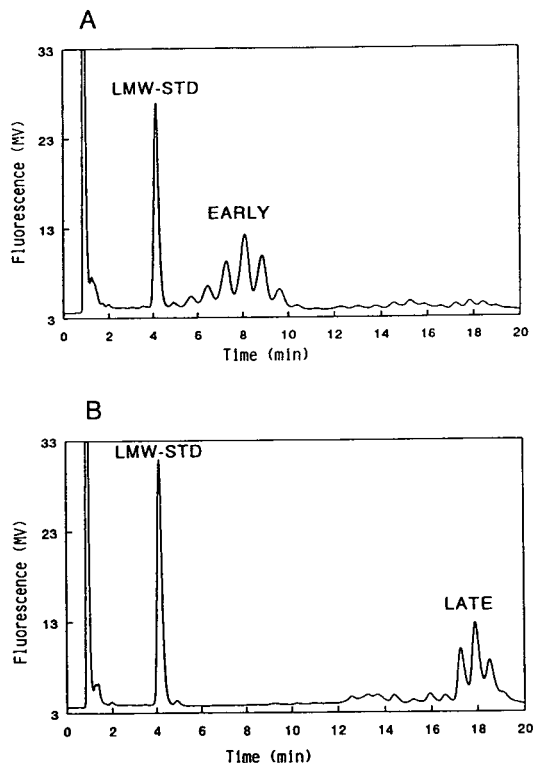


Fig. 4. Representative chromatograms of BRMB-derivatized mycolic acids from *M. phlei* (A) and *M. bovis* (B) separated with an MeOH–IPA solvent gradient (see Table 1).

grams were similarly obtained by using MeOH–MeCl₂, but are not shown.

Several observations were made as a result of these analyses. The fluorescent adducts were more polar than the PBPB derivatives, the polarity of the derivatized esters was as follows: BRAC > BRDC > BRMB > PBPB. Peak resolu-

Table 2
Detection limits (MDL, corresponding to a signal-to-noise ratio of 3) for a branched-chain carboxylic acid internal standard compound, and for representative mycolic acid extracts

Reagent	MDL acid (pmol)	MDL extract (ng)
PBPB	6.00	800
BRDC	0.19	40
BRAC	0.12	30
BRMB	0.24	50

tion was as follows in MeOH–IPA gradients: BRDC > BRAC > BRMB > PBPB. There was a selectivity (peak resolution) change when MeOH–MeCl₂ gradients were used; peak resolution was as follows: BRDC > PBPB > BRMB > BRAC (data not shown).

The results point to several improvements in the ruggedness of the current HPLC technique [2,7–11]. One improvement would be to use temperature control (above ambient conditions) and IPA in place of MeCl₂, as previously noted [16]. Chromatography using MeOH–IPA gradients and column temperature control at 50°C resulted in improved retention time reproducibility (as compared to analyses where ambient temperatures fluctuated significantly) and an approximately 25% lower column backpressure. Also, IPA is safer to use than MeCl₂, and does not cavitate in the HPLC pump heads at high operating temperatures and elevations. By using the LMW-STD in conjunction with the HMW-STD, it may be possible to bracket the mycolic acids and generate more reproducible RRTs during the process of species identification.

Finally, these experiments indicate that the clinical culture time before mycobacterial sampling could be reduced if PBPB is replaced with a more sensitive fluorescent reagent (e.g., BRDC, BRAC, BRMB). Also, the altered chromatographic selectivities of the fluorescent mycolic acid esters (shown here and previously [15]) may be useful in the optimization of HPLC for clinical mycobacterial species identification.

References

- [1] L.L. Tynes, *J. Am. Med. Assoc.*, 270 (1993) 2616.
- [2] L.S. Guthertz, S.D. Lim., Y. Jang and P.S. Duffey, *J. Clin. Microbiol.*, 31 (1993) 1876.
- [3] L.G. Wayne and G.P. Kubica, in P.H.A. Sneath (Editor), *Bergey's Manual of Systematic Bacteriology*, Vol. 2, Williams & Wilkins, Baltimore, MD, 1986, Section 16, p. 1436.
- [4] M. Garcia-Barcelo, M. Luquin, F. Belda and V. Ausina, *J. Chromatogr.*, 617 (1993) 299.
- [5] W.R. Butler, D.G. Ahearn and J.O. Kilburn, *J. Clin. Microbiol.*, 23 (1986) 182.
- [6] W.R. Butler and J.O. Kilburn, *J. Clin. Microbiol.*, 26 (1988) 50.
- [7] W.R. Butler and J.O. Kilburn, *J. Clin. Microbiol.*, 28 (1990) 2094.
- [8] W.R. Butler, K.C. Jost, Jr. and J.O. Kilburn, *J. Clin. Microbiol.*, 29 (1991) 2468.
- [9] M.M. Floyd, U.A. Silcox, W.D. Jones, Jr., W.R. Butler and J.O. Kilburn, *J. Clin. Microbiol.*, 30 (1992) 1327.
- [10] G.D. Cage, *J. Clin. Microbiol.*, 30 (1992) 2402.
- [11] W.R. Butler, L. Thibert and J.O. Kilburn, *J. Clin. Microbiol.*, 30 (1992) 2698.
- [12] H.D. Durst, M. Milano, E.J. Kikta, Jr., S.A. Connolly and E. Grushka, *Anal. Chem.*, 47 (1975) 1797.
- [13] L.S. Ramos, *Am. Biotechnology Lab.*, 10 (1992) 27.
- [14] R. Farinotti, Ph. Siard, J. Bourson, S. Kirkiacharian, B. Valeur and G. Mahuzier, *J. Chromatogr.*, 269 (1983) 81.
- [15] V.A. Simon, Y. Hale and A. Taylor, *LC·GC*, 11 (1993) 444.
- [16] S.R. Hagen, *Waters Column*, 3 (1992) 1.
- [17] H. Tsuchiya, T. Hayashi, H. Naruse and N. Takagi, *J. Chromatogr.*, 234 (1982) 121.
- [18] H. Naganuma, A. Nakanishi, J. Kondo, J. Watanabe and Y. Kawahara, *Sankyo Kenkyusho Nempa*, 40 (1988) 51.

Resolution of promethazine, ethopropazine, trimeprazine and trimipramine enantiomers on selected chiral stationary phases using high-performance liquid chromatography

Garratt W. Ponder^a, Sandra L. Butram^b, Amanda G. Adams^c,
Chandra S. Ramanathan^a, James T. Stewart^{a,*}

^aDepartment of Medicinal Chemistry, College of Pharmacy, University of Georgia, Athens, GA 30602-2352, USA

^bDepartment of Chemistry, North Georgia College, Dahlonega, GA 30597, USA

^cSolvay Pharmaceuticals, Marietta, GA 30062, USA

Abstract

The separation of the enantiomers of three phenothiazines and a dibenzazepine were investigated on several different chiral stationary phases without the use of derivatization or column switching. The phenothiazines selected were promethazine, ethopropazine and trimeprazine and the dibenzazepine was trimipramine. Three classes of columns were studied for their ability to separate the enantiomers of these compounds: brush or Pirkle, inclusionary, and affinity types. The columns studied were (α -*R*-naphthyl)ethylurea, (*S*)-*tert*-leucine-(*R*)-1-(α -naphthyl) ethylamine, dinitrobenzoylphenylglycine; β -cyclodextrin, β -acetylated cyclodextrin; γ -cyclodextrin; Chiralcel-OD; Chiralcel-OJ and Ovomuroid. Changes in mobile phase composition were studied on each column to determine the effects of solvents on the separation of the various enantiomers. Simplex calculations for mobile phase variations were not performed because they do not predict elution order reversals.

1. Introduction

Interest in this laboratory in the separation of enantiomers of phenothiazines and dibenzazepines led to an investigation of mobile phase and stationary phase interactions and their influences on enantiomeric resolution. Among the drugs of interest were promethazine, ethopropazine, trimeprazine and trimipramine. Some success has been reported for promethazine and trimipramine on the α_1 -acid glycoprotein (α_1 -AGP) protein column [1–4]. Other separations for promethazine, trimeprazine and trimipra-

mine enantiomers have been performed either by chemical derivatization of the compounds, or using cyclodextrins (CDs) as mobile phase additives [1–5].

Chiral stationary phases (CSPs) are categorized under several different types of chromatography including brush type, inclusionary and affinity. A brush-type CSP is also called a Pirkle CSP. It relies upon multiple discreet molecular interactions to discriminate between enantiomers. These interactions are dipole–dipole, π – π , steric hindrance and H bonding [6–9]. Pirkle-type columns have a wide range of physical compositions ranging from amino acids to substituted naphthyl rings and practically every com-

* Corresponding author.

mercial chromatographic supplier offers a chiral column of this type. A survey of the literature shows that Pirkle-type columns were the most successful type of CSP in the early 1980s [7–11].

CDs compose a major portion of the inclusionary type of columns. They have a toroidal geometry with a hydrophilic outer surface and a hydrophobic inner cavity. The three most common CDs are α , β and γ which are made up of 6, 7 and 8 α -D-glucopyranose units, respectively. In the reversed-phase mode, CDs separate enantiomers by a difference in energies between the two diastereomeric inclusionary complexes [8,9]. A study of the literature showed that the separation of a wide range of chiral isomers should be possible using silica-bound CD columns in the reversed-phase mode [8,9].

Other inclusionary-type CSP such as the cellulose-based CSP also utilize diastereomeric complexing energy differences to obtain separations. The Chiralcel CSPs are the most successful type of CSP since 1986 [8–12]. The free hydroxyl groups on cellulose provide an environment conducive to derivatization to form esters and carbamates; thus, allowing them to be chemically varied as much as CDs. But the cellulose-based CSP may have channels rather than the cavities of the CDs. The channels have size, capacity and structural limitations somewhat similar to those of the CDs. There is some question as to the exact nature of the cavities associated with the cellulose stationary phases. Some indicate that the cellulose material is not necessarily a channel, but an intricate crosswork of cellulose strands forming asymmetric cavities in which the chiral resolution occurs. Evidence exists in literature which argues both pro and con for these hypotheses. Analytes for which enantiomeric separations may be successful, should be aromatic, have H-bonding capacity, and not too large a structure to fit in the tubular chiral cavity. The Chiralcel-OD stationary phase, a carbamate derivative of cellulose, has been used to separate a wide variety of chiral compounds including chiral alcohols and chiral amines. The Chiralcel-OJ column is a benzoyl ester derivative of cellulose and has been used to separate compounds requiring additional π - π interactions.

The cellulose-based columns differ from CD columns in that they have severe mobile phase limitations [8,9].

Affinity chromatography utilizes the ionic formation of the amino acids in proteins to provide stereoselective regions of H bonding, hydrophobic conditions and electrostatic forces that have differing interactions between the (*R*) and (*S*) enantiomers of guest molecules [8,9]. Protein-type CSPs are versatile in their ability to work with both cationic and anionic drugs. In the past, protein-based CSPs have had functional chromatographic lifetimes of only a few months. In addition, column costs have been substantial considering their short periods of usability. However, recent modifications in protein and chromatographic technologies coupled with a better understanding of the protein stationary phase have provided some new protein stationary phases with better separating capabilities and longer lifetimes.

In this study, several CSPs were investigated for their ability to separate the enantiomers of promethazine, ethopropazine, trimeprazine and trimipramine. The CSPs investigated were (*R*)- α -naphthylethylurea, (*S*)-leucine-(*R*)- α -naphthylethylamine and dinitrobenzoylphenylglycine (Pirkle-type columns); β -CD, β -acetylated CD, γ -CD, Chiralcel-OD, Chiralcel-OJ (inclusional); and Ovomuroid (affinity). Detection of the enantiomers was performed by fluorimetric analysis using excitation at 254 nm and a 280 nm emission filter.

2. Experimental

2.1. Apparatus

The HPLC system consisted of a pump (Model 2510; Varian, Walnut Creek, CA, USA), equipped with a 100- μ l injector loop (Model 7125; Rheodyne, Cotati, CA, USA), a fluorescence detector set at excitation 254 nm with a 280 nm emission filter (Model Spectroflow 980; Kratos, Ramsey, NJ, USA), and an integrator (Model SP 4290; Spectra-Physics, San Jose, CA, USA).

2.2. Solvents and chemicals

Hexane, absolute methanol, methylene chloride, chloroform, acetonitrile, isopropanol (HPLC grade), phosphoric acid (concentrated), ethylene dichloride F.C.C. and monobasic potassium phosphate (reagent grade) were all obtained from J.T. Baker (Phillipsburg, NJ, USA). Ethanol 95% was purchased from University of Georgia Central Research Stores. Ethanol 200 proof was purchased from Midwest Grain Products (Weston, MO, USA). Triethylamine HPLC grade was purchased from Fisher (Fairlawn, NJ, USA). Trimipramine, trimeprazine, promethazine and trifluoroacetic acid (TFA) were purchased from Sigma (St. Louis, MO, USA). Ethopropazine was purchased from Aldrich (Milwaukee, WI, USA). (*R*)- and (*S*)-promethazine enantiomers used in this study were synthesized through crystallization using *D*- and *L*-dibenzoylated tartaric acid [1] and analyzed to be >99% (w/w) pure by HPLC and polarimetric analyses.

2.3. Columns

The columns used in this study were: KK-CARNU, (α -*R*-naphthyl)ethylurea (YMC, Wilmington, NC, USA), 10 cm \times 4.6 mm, 5 μ m; Sumichiral OA-4700, (*S*)-*tert*-leucine-(*R*)-1-(α -naphthyl)ethylamine (YMC), 25 cm \times 4.6 mm, 5 μ m; KK-CAPG, dinitrobenzoylphenylglycine (YMC) 10 cm \times 4.6 mm, 5 μ m; β , β -acetylated and γ -CDs (Astec, Whippany, NJ, USA), all 25 cm \times 4.6 mm, 5 μ m; Chiralcel-OD and -OJ (J.T. Baker), 25 cm \times 4.6 mm, 5 μ m and ES-OVM Ovomuroid (Mac-Mod Analytical, Chadds Ford, PA, USA), 15 cm \times 4.6 mm, 5 μ m. Equilibration of the columns was performed prior to each experiment using a minimum of 90 column volumes of mobile phase and test injections to determine chromatographic reproducibility.

2.4. Chromatographic conditions

All chromatography was performed at ambient temperature (23 \pm 1°C) and at 1 ml/min unless otherwise stated. The reversed-phase mobile

phases used were various mixtures of 0.01 *M* monobasic potassium phosphate buffers, 0.1% triethylamine, absolute methanol, isopropanol, acetonitrile and 95% ethanol with the pH adjusted to 4.0 with concentrated phosphoric acid unless otherwise indicated. All normal-phase mobile phases were various mixtures of hexane, methylene chloride, 1,2-dichloroethane, chloroform, absolute methanol, 95% ethanol, absolute ethanol, isopropanol, acetonitrile, TFA and glacial acetic acid (GAA). The mobile phases were all degassed by vacuum filtration prior to use. The concentration of solutions studied were 500 ng/ml of the racemic drug mixture dissolved in the appropriate mobile phase.

3. Results and discussion

The chemical structures of the analytes studied are shown in Fig. 1. The initial Pirkle CSPs studied were an *R*- α -naphthylethylurea (CARNU) with one chiral center and a (*S*)-*tert*-leucine-(*R*)-1-(α -naphthyl) ethylamine (OA-4700) with two chiral centers. Baseline resolution of the enantiomers of all four compounds were achieved using these two columns. As shown in Table 1, promethazine enantiomers were successfully separated on the CARNU column with a resolution of at least 1.0 (baseline $R_s = 1.50$) using a wide variety of mobile phases. (This table reports only those mobile phases that provided a R_s of at least 1.0. Other mobile phases were used but were not listed for the sole purpose to save space.) The best resolution (2.25) was achieved using a mobile phase consisting of hexane–absolute ethanol–TFA (80:15:0.2, v/v). The strengths of the mobile phases that provided enantiomeric separations ranged from 0.45 to 1.55 based on the Snyder values of the solvent selectivity triangle. Obviously, there was no distinct mobile phase strength at which the promethazine enantiomers would separate. However, a majority of the mobile phases that provided resolutions of at least 1.0 were composed of approximately 60% hexane and 13–27% methylene chloride with the remainder being an alcohol and an acidic modi-

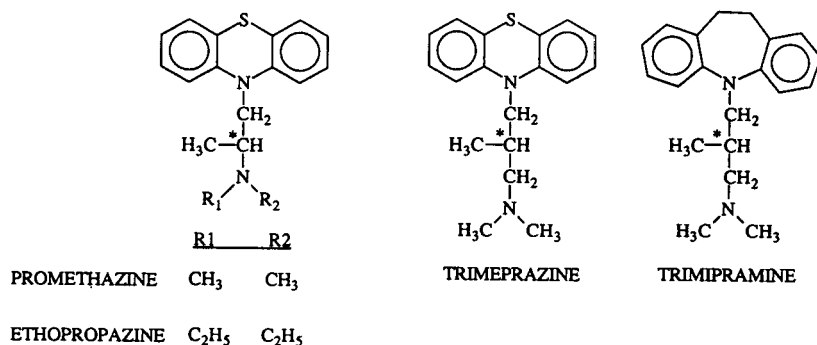


Fig. 1. Chemical structures of chiral compounds used in this study.

fier. In some cases, methylene chloride could be replaced by chloroform. This was important to enantiomeric separations on the CARNU column since methylene chloride is a dipole-interacting and chloroform a proton-donating solvent. However, chloroform was limited to no more than 25% of the total mobile phase composition. Nearly all of the mobile phases used either TFA or GAA as mobile phase modifiers to promote H bonding. Those mobile phases without either of

the two acids had at least 15–20% alcohol to assist in H bonding.

Table 2 contains resolution and mobile phase data for other enantiomeric separations achieved on the CARNU column. Separation of the ethopropazine enantiomers was similar to that found for promethazine. However, ethopropazine is more lipophilic than promethazine, therefore, its enantiomers had different chromatographic interactions with the CARNU CSP

Table 1
Resolution of promethazine enantiomers on KK-CARNU stationary phase

Mobile phase composition (v/v) ^a										R_s	k'	
A	B	C	D	E	F	G	I	J	Peak 1		Peak 2	
80					15		0.2			2.25	17.7	21.8
80		30			20		0.1			2.18	7.0	8.7
70	30			10			0.1			2.16	3.3	4.1
80	30				20		0.002			1.92	6.1	7.6
80		30			10		0.2			1.91	6.9	8.5
80			30		20		0.2			1.88	5.5	6.7
80	15	15			10		0.1			1.85	5.9	7.3
80	30				20		0.2			1.80	5.7	7.1
70	30	10					0.1			1.72	5.0	6.1
80	30				20					1.63	7.7	10.1
80			17	10			0.1			1.52	6.3	7.4
80		30			20				0.1	1.34	11.7	13.7
70	30					20				1.24	3.9	4.5
70	30			10		10				1.11	3.3	3.9
70	25					25				1.09	3.7	4.2
80	30				20				0.2	1.06	10.9	13.2
70	30					20	0.1			1.01	3.1	3.7

^a A = Hexane; B = methylene chloride; C = chloroform; D = 1,2-dichloroethane; E = absolute methanol; F = absolute ethanol; G = 95% ethanol; I = trifluoroacetic acid; J = glacial acetic acid.

Table 2
Resolution of ethopropazine and trimeprazine enantiomers on KK-CARNU stationary phase

Drug	Mobile phase composition (v/v) ^a										R_s	k'	
	A	B	C	D	E	F	G	I	J	Peak 1		Peak 2	
Ethopropazine	80					15		0.2			1.89	20.1	23.5
	70	30			10			0.1			1.86	3.6	4.1
	80		30			20		0.1			1.69	8.2	9.5
	80			30		20		0.2			1.43	6.3	7.3
	80	30				20			1		1.36	15.7	18.0
	80	30				20		0.001			1.33	6.7	7.9
	80	30				20		0.2			1.31	6.4	7.4
	80			17	10			0.1			1.26	7.1	7.9
	80	30				20			0.2		1.23	10.6	12.2
	80	15	15			10			0.1		1.22	6.7	7.7
	70	30				10			0.1		1.20	5.4	6.2
	70	30					10	0.1			1.00	3.4	3.7
	Trimeprazine	80					15		0.2		1.11	23.7	25.7

^a Solvents as in Table 1.

and the mobile phases investigated. The result was a decrease in the total number of separations with resolutions of at least 1.0 for the ethopropazine enantiomers. Trimeprazine and trimipramine enantiomers were not baseline resolved on the CARNU column. Trimeprazine had only one enantiomeric separation with a resolution value greater than 1.0 and trimipramine enantiomers did not separate under any of the mobile phase conditions tested.

Substituting 1,2-dichloroethane for methylene chloride or chloroform in the mobile phase had little effect on enantiomeric resolution or peak shape, but 1,2-dichloroethane did change retention times on the CARNU column. This would be expected since methylene chloride and 1,2-dichloroethane are in the same Snyder solvent group, while chloroform is in a different group. Fig. 2 shows the separations of ethopropazine on the CARNU column using mobile phases containing methylene chloride and 1,2-dichloroethane. Other mobile phase changes included the substitution of absolute methanol, acetonitrile, isopropanol, 95% ethanol and absolute ethanol within a given mobile phase. Acetonitrile was not useful in providing an adequate fluorimetric environment for the detection of the

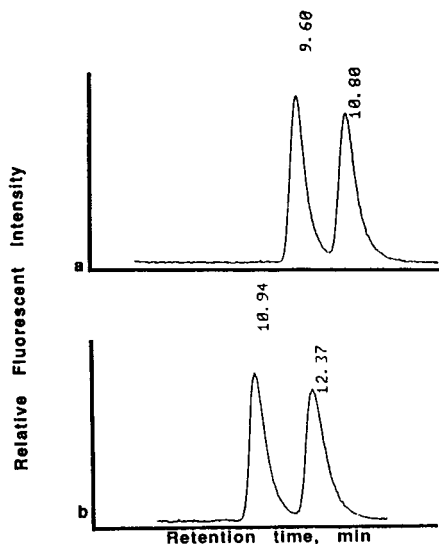


Fig. 2. (a) Typical HPLC chromatogram of the separation of ethopropazine enantiomers on CARNU column with hexane–methylene chloride–absolute ethanol–TFA (350:150:100:1, v/v) at 1 ml/min. (b) Typical HPLC chromatogram of the separation of ethopropazine enantiomers on CARNU column with hexane–1,2-dichloroethane–absolute ethanol–TFA (400:150:100:1, v/v) at 1 ml/min.

enantiomers of any of the four compounds. Isopropanol tended to decrease resolution as well as significantly reduce retention times when compared to all other solvents except methanol. For example, promethazine enantiomers were detected at 7.40 and 8.33 min ($R_s = 1.24$) using 95% ethanol on the CARNU column, but all of the resolution was lost with isopropanol and a single peak was obtained at a retention time of 5.56 min. Mobile phase additives such as TFA and GAA were tested. As a rule, TFA gave retention times approximately 50–60% that of GAA, while R_s with TFA was 1.1–1.7 times greater than GAA. The reader should take note that 0.1% of TFA has an *apparent* pH of 2.0 in a non-aqueous environment. However, the lifetimes of the Pirkle columns used in this study have been measured in years, therefore, it does not appear that the TFA does detrimental damage to the silica backbone of the stationary phase.

Results of enantiomeric separations on the OA-4700 column are shown in Table 3. Pro-

methazine enantiomers were separated with a resolution of 1.70 using a mobile phase of hexane–methylene chloride–absolute ethanol–trifluoroacetic acid (160:15:10:0.1, v/v). Other separations of promethazine enantiomers with resolutions of at least 1.0 used mobile phases containing 1,2-dichloroethane rather than methylene chloride. Absolute methanol proved to be too polar for promethazine enantiomeric separations to occur; therefore, absolute ethanol was used. Small amounts of TFA were added to enhance H bonding. However, there were few separations with resolution values of at least 1.0 for promethazine enantiomers on the OA-4700 column. No separations with a resolution value of at least 1.0 occurred when absolute methanol, chloroform, isopropanol or GAA were components in the mobile phase. Using a wide variety of mobile phases on the OA-4700 column, resolution values of ethopropazine enantiomers were 0.70–0.99. Enantiomeric separations on the OA-4700 column for both trimeprazine and trimipramine yielded resolutions of at least 1.5

Table 3
Resolution of promethazine, trimeprazine and trimipramine enantiomers on OA-4700 stationary phase

Drug	Mobile phase composition (v/v) ^a					R_s	k'	
	A	B	D	F	I		Peak 1	Peak 2
Promethazine	160	15		10	0.1	1.70	3.4	4.2
	120		15	10	0.1	1.44	2.3	2.5
	160		15	10	0.1	1.25	3.6	3.9
	90		15	10	0.1	1.17	1.4	1.6
	80		15	10	0.1	1.11	1.2	1.4
Trimeprazine	160		15	10	0.1	2.62	3.9	4.6
	120		15	10	0.1	2.50	2.4	2.8
	90		15	10	0.1	1.71	1.5	1.8
	160	15		10	0.1	1.70	3.3	3.9
	80		15	10	0.1	1.51	1.3	1.5
	80	15		10		1.25	0.8	1.0
	60		15	10	0.1	1.10	0.8	0.9
	50		15	10	0.1	1.00	0.2	0.7
Trimipramine	160	15		10	0.1	2.00	3.5	3.9
	120		15	10	0.1	1.76	2.2	2.6
	90		15	10	0.1	1.26	1.5	1.6
	160		15	10	0.1	1.25	3.6	4.0

^a Solvents as in Table 1.

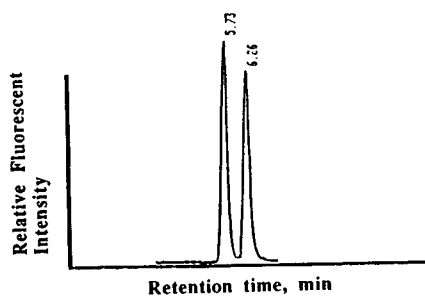


Fig. 3. Typical HPLC chromatogram of the separation of trimeprazine enantiomers on Sumichiral OA-4700 column with hexane–1,2-dichloroethane–absolute ethanol–TFA (800:150:100:1, v/v) at 1 ml/min.

with a variety of mobile phases. Figs. 3 and 4 show typical chromatograms for trimeprazine and trimipramine enantiomers on the OA-4700 column. Later calculations determined that the solvent strength of the mobile phase should be ≤ 0.90 in order for the trimeprazine and trimipramine enantiomers to separate on the OA-4700 column. In general, mobile phases with a solvent strength greater than 0.744 did not provide enantiomeric separations of promethazine, trimeprazine and trimipramine.

It was of interest that the enantiomers of promethazine and ethopropazine could easily be baseline resolved on the CARNU column with one chiral center, while trimeprazine and trimipramine enantiomers required the OA-4700 column with two chiral centers to achieve baseline separation. Both promethazine and ethopropazine have H-bonding sites α to the chiral centers; whereas trimeprazine and trimipramine

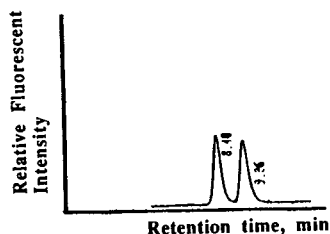


Fig. 4. Typical HPLC chromatogram of the separation of trimipramine enantiomers on Sumichiral OA-4700 column with hexane–1,2-dichloroethane–absolute ethanol–TFA (1200:150:100:1, v/v) at 1 ml/min.

have the H-bonding sites β to the chiral centers. The CARNU and OA-4700 stationary phases differ by the addition of a leucine amino acid moiety in the OA-4700 column backbone. It appears that the amino acid provides a specific spatial arrangement conducive to the separation of the enantiomers with their H-bonding centers β to the chiral center. Promethazine and ethopropazine do not require spatial rearrangement of the stationary phase's H-bonding center, therefore their enantiomers separated better on the CARNU column than on the OA-4700 column.

The energies associated with the various diastereomeric complexes for promethazine were low enough to allow the complexes to form, but the difference in diastereomeric complex energies was great enough for the enantiomers to separate. The ethopropazine enantiomers were unable to be separated on the OA-4700 column. Until modeling studies currently in progress in these laboratories are complete, this phenomenon is attributed to low complex energy differences due to increased lipophilicities associated with the N,N-diethyl groups of ethopropazine as opposed to the N,N-dimethyl groups on promethazine. Trimipramine has an ethylene bridge that replaces the sulfur bridge of a phenothiazine. The ethylene group causes the two phenyl rings of trimipramine to be almost perpendicular to each other, therefore the aromatic region of trimipramine is twisted. Trimipramine complexed with the stationary phase tended to have high Gibbs free energies with only minute differences between each one of the diastereomeric complex energies on the CARNU column. The high energies associated with the π – π interacting region were overcome on the OA-4700 column and enantiomeric resolutions occurred.

The next column studied was the KK-CAPG column operated in the reversed-phase mode. Even though this CSP is not usually run in the reversed-phase mode, there was some evidence in the literature which showed that a dinitrobenzoylphenylglycine column was used in the reversed-phase mode with positive enantioselectivity [10,11]. However, the results from this work were not adequate. Peak symmetry was poor ($a/b \geq 2.0$) with no signs of enantiomeric

separations for any of the four compounds. To convert the CSP back to the normal-phase mode, considerable time and consideration was used for the proper selection of mobile phases in order to best readjust the stationary phase. Tests were run on the column using previously reported separations to determine if the CSP was adequately restored for normal-phase use. With the column operated in the normal-phase mode, separations were achieved for the phenothiazines, but the enantiomer peaks were only separated by 0.20 min, thereby giving an $R_s \leq 0.40$. No enantiomeric separations were obtained for trimipramine using this stationary phase. This is surprising since the stationary phase is strongly π -acidic and the compounds are π -basic in nature. The CSP must not be able to hold the π - π interaction long enough for a difference in diastereomeric complex energies to occur.

Attempts to separate the enantiomers of promethazine, ethopropazine, trimeprazine and trimipramine using the three CD bonded phases were unsuccessful. Typical resolution values for the β and β -acetylated columns with a cavity opening of 7.8 Å across the wider opening were less than 0.45 and the peaks tended to be highly asymmetric ($a/b \geq 1.9$). However, the γ -CD column with a cavity opening of 9.5 Å across the wider opening did improve enantiomeric separations, but the resolution was ≤ 0.80 . The γ -CD column was the most versatile and consistent CD column for the compounds studied since many of the mobile phases gave enantiomeric resolutions near 0.80.

According to Wainer and Drayer [8], there are a few basic structural rules that a compound should meet in order for the enantiomers to be separated on cyclodextrin stationary phases. These are: (1) the compound should not be so large that it cannot at least partially enter the CD cavity; (2) the chiral center should be near the mouth of the CD cavity; (3) the compound should have an aromatic system α or β to the chiral center, but occasionally the ring can be γ to the chiral center; and finally (4) there should be the potential for H bonding at or near the center for chirality. As seen in Fig. 1, the compounds promethazine, ethopropazine, tri-

mepazine and trimipramine all fit this description. However, the β , β -acetylated and γ -CDs did not allow the baseline separation of any of the four compounds. This was probably due to the size of the inclusion cavity. When modeling promethazine and trimipramine structures with the β - and γ -CD structures, our data showed that the basic three ring structures were almost entirely in high energy states. The γ -CD column, which gave better, but not baseline separations, has a cavity diameter and volume 1.22 and 1.67 times larger, respectively, than the β -CD cavity. This meant that the analytes were allowed to enter the γ cavity more freely than the β cavity. Yet, the enantiomeric distinction was not great enough in either case to allow baseline separations to occur for any of the compounds.

The cellulose-based stationary phases, Chiralcel-OJ [cellulose tris(4-methyl benzoate)] and Chiralcel-OD [cellulose tris(3,5-dinitrophenyl carbamate)] were investigated next. These columns were severely limited in the kinds of solvents that could be used in the mobile phase. Therefore, the mobile phases were either hexane-absolute ethanol or hexane-isopropanol mixtures. No enantiomeric baseline resolutions greater than 1.12 were detected for any of the racemic pairs using isopropanol on either cellulose column. While the Chiralcel-OD column did not provide enantiomeric separations with any of the mobile phases, the Chiralcel-OJ column provided separations ($R_s \geq 1.50$) for promethazine and near-baseline enantiomeric separations for ethopropazine and trimeprazine using hexane-absolute ethanol mobile phases as seen in Table 4. Fig. 5 shows a typical chromatogram for promethazine enantiomers on the Chiralcel-OJ column. Flow-rate analysis on these columns was performed at 0.5 and 0.8 ml/min, since the stationary phase is coated and not covalently bound. As expected, 0.8 ml/min gave better peak shapes, but there was no significant difference in resolutions for the same mobile phase at the two different flow-rates.

The enantioselective separations of the phenothiazines on the polymeric cellulose Chiralcel-OJ column is interesting in that it too consists of α -D-glucopyranose moieties, but not in a cyclic

Table 4
Resolution of promethazine, ethopropazine and trimeprazine enantiomers on Chiralcel-OJ stationary phase

Drug	Mobile phase composition (v/v) ^a			Flow-rate (ml/min)	R_s	k'	
	A	F	H			Peak 1	Peak 2
Promethazine	70	30		0.5	1.94	4.8	6.0
	90	10		0.5	1.88	6.9	8.8
	80	20		0.5	1.78	5.5	6.8
	80	20		0.8	1.70	3.0	3.9
	95	5		0.5	1.37	10.6	13.3
	95	5		0.8	1.21	6.1	7.8
	95		5	0.8	1.07	9.6	13.1
	90		10	0.5	1.01	9.9	12.6
Ethopropazine	80		20	0.5	1.04	2.9	4.5
Trimeprazine	90		10	0.5	1.12	7.4	9.0
	60	40		0.8	1.06	2.2	2.6
	50	50		0.5	1.06	4.0	4.6
	70	30		0.8	1.04	2.4	2.7

^aA = Hexane; F = absolute ethanol; H = Isopropanol.

form. Detectable enantiomeric separations were obtained for promethazine ($R_s \leq 1.94$), trimeprazine ($R_s \leq 1.12$) and ethopropazine ($R_s \leq 1.04$) on the OJ column. This may be due to the planar characteristic of the phenothiazine tricyclic region versus the distorted and twisted tricyclic region of the dibenzazepine trimipramine. It is possible that the stereospecific tubes formed by the cellulose polymers are sterically

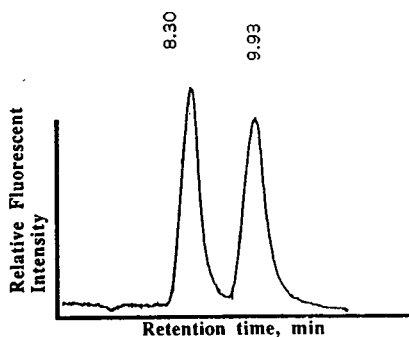


Fig. 5. Typical HPLC chromatogram of the separation of promethazine enantiomers on Chiralcel-OJ column with hexane–absolute ethanol (50:50) at 0.8 ml/min.

limited; thus, making it difficult for the trimipramine enantiomers to enter the enantiodiscriminating cavity regions [13,14].

The last column investigated was the ovomucoid column from the affinity category. The poor enantioselective results of the four compounds on the ovomucoid column were possibly a result of the high affinity of these compounds for serum proteins. Promethazine enantiomers were separated with a resolution of 0.50, but none of the other compounds showed resolution. These results were interesting since all four compounds are highly protein bound in vivo (90–95%) [15]. It is possible that the proteinaceous stationary phase made little or no distinction between the enantiomers for these compounds; therefore, enantiomeric separations for these compounds require a different chiral environment than is provided by this stationary phase.

4. Conclusions

The CARNU and OA-4700 Pirkle-type CSP tended to provide more separations for large

aromatic compounds than the CAPG CSP. Typically, the CARNU and OA-4700 CSPs gave best results with approximately 60% hexane and 5–15% of an alcohol. A strong modifier such as TFA for basic compounds will sharpen peaks and tend to improve resolution. This allowed an investigator ample opportunity to select the remaining components and component ratios of the mobile phases in order to determine if chiral separations were possible for compounds of interest on that stationary phase. The Chiralcel-OJ CSP was able to separate the three phenothiazine compounds but did not show any tendency for an enantiomeric resolution for trimipramine. This indicated the channels composing the chiral separation centers in the cellulose CSP were not as strictly size limited as the CDs; rather, they were limited in the shape of the compound presented to the stationary phase. This Chiralcel-OD cellulose stationary phase would probably work best with analytes smaller than the ones studied here. Since there was little distinction between the bioactivity of each enantiomer of the compounds used in this study, it was possible that the highly protein bound nature of these compounds in vivo meant that there would be no distinction by protein CSP. Unless one enantiomer has a known bioactivity or therapeutic index different from the other enantiomer, a protein-based CSP would probably not be the starting point in trying to determine the proper stationary phase for a chiral resolution.

Acknowledgements

G.W.P. thanks YMC for the gift of the KK-CARNU and KK-CAPG columns, Solvay Phar-

maceuticals for a Graduate Fellowship and Dr. C.D. Blanton for his guidance in synthesizing the promethazine enantiomers.

References

- [1] J. Lars, G. Nilsson, J. Hermansson, U. Hacksell and S. Sundell, *Acta Pharm. Suec.*, 21 (1984) 309.
- [2] M. Enquist and J. Hermansson, *J. Chromatogr.*, 519 (1990) 285.
- [3] D. Haupt, C. Pettersson and D. Westerlund, *Chirality*, 5 (1993) 224.
- [4] C.B. Eap, L. Koeb, E. Holsboer-Trachsler and P. Baumann, *Ther. Drug Monit.*, 14 (1992) 380.
- [5] A.D. Cooper and T.M. Jefferies, *J. Pharm. Biomed. Anal.*, 8 (1990) 847.
- [6] W.H. Pirkle, J.P. Chang and J.A. Burke III, *J. Chromatogr.*, 598 (1992) 1.
- [7] L. Siret, A. Tambute, M. Caude and R. Rosset, *J. Chromatogr.*, 540 (1991) 129.
- [8] I.W. Wainer and D.E. Drayer, *Drug Stereochemistry: Analytical Methods and Pharmacology*, Marcel Dekker, New York, 1988.
- [9] A.M. Krstulovic, *Chiral Separations By HPLC: Applications to Pharmaceutical Compounds*, Ellis Horwood, New York, 1989.
- [10] K.G. Feitsma and B.F.H. Drenth, *Pharm. Weekbl., Sci. Ed.*, 10 (1988) 1.
- [11] D.R. Taylor and K. Maher, *J. Chromatogr. Sci.*, 30 (1992) 67.
- [12] H.Y. Aboul-Enein, *Anal. Lett.*, 25 (1992) 231.
- [13] S.J. Grieb, S.A. Matlin, J.G. Phillips, A.M. Belengeur and H.J. Ritchie, *Chirality*, 6 (1994) 129.
- [14] S.A. Matlin, M.E. Tiritan, A.J. Crawford, Q.B. Cass and D.R. Boyd, *Chirality*, 6 (1994) 135.
- [15] *United States Pharmacopeia Drug Information*, Vol. I, United States Pharmacopeial Convention, Rockville, MD, 14th ed., 1994.



ELSEVIER

Journal of Chromatography A, 692 (1995) 183–193

JOURNAL OF
CHROMATOGRAPHY A

Comparison of theory-based and empirical modeling for the prediction of chromatographic behavior in the ion-pairing separation of benzodiazepine-derived pharmaceutical compounds

Larry A. Larew*, Bernard A. Olsen, John D. Stafford, Melinda V. Wilhelm

Lilly Research Laboratories, Eli Lilly and Company, P.O. Box 685, Drop Code TL12, Lafayette, IN 47902, USA

Abstract

Two approaches were examined for predicting chromatographic behavior during the reversed-phase ion-pairing separation of benzodiazepine-derived pharmaceutical compounds. The capacity factor for olanzapine and its resolution from a closely related compound, desmethylolanzapine, were studied as a function of the percentage of acetonitrile, the ion-pairing reagent concentration and the buffer pH. In the first approach, the results were analyzed using the theory-based software package DryLab I/mp. In the second approach, statistical analysis was used to derive empirical equations to predict the dependence of the chromatographic behavior on each of the experimental variables. At the lowest ion-pairing reagent concentration, DryLab I/mp was found to be a poor predictor of resolution. For this complex separation, the empirical equations derived from the statistical analysis were found to predict better the chromatographic behavior over the ranges tested. These equations were used to generate response-surface plots to evaluate the method ruggedness.

1. Introduction

The desire to speed up chromatographic method development has led to the design and implementation of computer modeling software [1]. Software packages have been described for both isocratic [2] and gradient separations [3]. Recent applications of this approach to chromatographic method development have included separations of drug substances [4] and phenolic pollutants [5]. Software designed to study multi-parameter effects (pH, temperature, percentage of organic modifier and buffer concentration) have also been described [6–8]. DryLab I/mp is a chro-

matographic simulation package capable of predicting the optimum conditions for performing multi-parameter separations, including ion-pairing assays [6].

Statistical analysis using factorial designed studies to model multi-parameter chromatographic behavior has been used as an alternative approach [9–11]. This approach has been successfully used to optimize the ion-pairing separations of alkaloids [9] and monoamine neurotransmitters [10], along with the isocratic reversed-phase separation of hormonal steroids [11].

Olanzapine, an investigational new drug for the treatment of schizophrenia, and related compounds are in the benzodiazepine class of phar-

* Corresponding author.

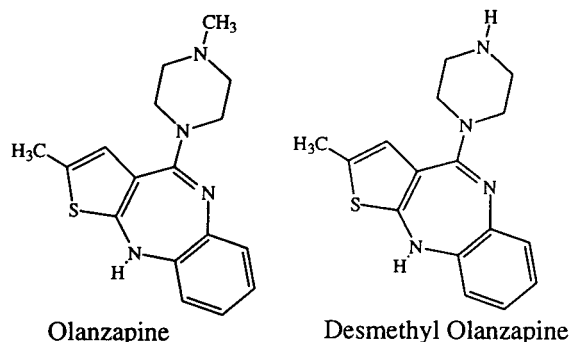


Fig. 1. Structures of olanzapine and desmethylolanzapine.

maceuticals. These compounds can be characterized as having low water solubility, high basicity and aromaticity. The structures of olanzapine and a closely related compound, desmethylolanzapine, are shown in Fig. 1. Note that the only difference between these two compounds is the presence of a methyl group on the distal nitrogen of the piperazine ring. The development of a chromatographic method capable of separating these highly basic and similar compounds was not trivial.

Despite the similarities in these compounds, a reversed-phase ion-pairing method was developed that could perform the separation. The eluent was composed of acetonitrile and sodium phosphate buffer with sodium dodecyl sulfate (SDS) as the ion-pairing reagent. During method development, accurate preparation of the mobile phase, i.e. percentage of acetonitrile, concentration of SDS and pH, was determined to be critical for method reproducibility. The purpose of this investigation was to compare the applicability of DryLab I/mp and statistical analysis for modeling this multi-parameter chromatographic separation. The models derived would be used to determine the method ruggedness.

2. Experimental

2.1. Reagents and materials

HPLC-grade acetonitrile, phosphoric acid (85%, w/w) and sodium hydroxide (50%, w/w) aqueous solutions were obtained from EM Sci-

ence (Gibbstown, NJ, USA). Electrophoresis-grade SDS was obtained from Eastman Kodak (Rochester, NY, USA). Water for mobile phases was purified with a Milli-Q system from Millipore (Milford, MA, USA). The aqueous component of each mobile phase was prepared by adding 5.0 mL of phosphoric acid per 1500 ml of water and dissolving the appropriate amount of SDS to obtain the specified concentration. The pH of each aqueous component was adjusted to the desired value by dropwise addition of sodium hydroxide solution. The appropriate volume of acetonitrile was combined with each aqueous component to yield the desired mobile phase composition. Olanzapine and desmethylolanzapine were obtained from Eli Lilly (Lafayette, IN, USA). Samples were prepared at concentrations of ca. 0.2 mg/ml (olanzapine) and 0.1 mg/ml (desmethylolanzapine) in the mobile phase. Chromatographic separations were performed using a 250 mm × 4.6 mm I.D. column of 5- μ m particle size Zorbax Rx/SB-C₈ (MacMod, Chadds Ford, PA, USA).

2.2. Apparatus

The HPLC system consisted of a Model 600E multi-solvent delivery system (Waters, Bedford, MA, USA) equipped with a column oven set at 35°C, a Model 728 autoinjector (Alcott, Norcross, GA, USA) equipped with a 20- μ L fixed-loop injection valve (Valco, Houston, TX, USA) and a Model 757 single-wavelength UV detector operated at 220 nm (Applied Biosystems, Ramsey, NJ, USA). The mobile phase flow-rate was 1.5 ml/min for all experiments. An in-house data acquisition system was used to record all chromatograms. The software packages, DryLab I/mp (LC Resources, Walnut Creek, CA, USA), JMP (SAS Institute, Cary, NC, USA) and Excel (Microsoft, Redmond, WA, USA) were operated on a Macintosh IICI computer (Apple Computer, Cupertino, CA, USA).

2.3. Procedure

Table 1 contains a summary of the experiments performed to model the chromatographic behavior. All separations were performed iso-

Table 1
Experimental design

Experiment No.	Acetonitrile (%)	SDS (mM)	Buffer pH
1	53	10	3.0
2	43	50	3.0
3	43	10	3.0
4	53	10	2.0
5	53	50	2.0
6	43	10	2.0
7	43	50	2.0
8	53	50	3.0
9	53	30	2.0
10	43	30	3.0
11	53	70	2.0
0	48	30	2.5

cratically. Experiments 1–8 represent a factorial design study using every possible combination of either 43 or 53% acetonitrile, 10 or 50 mM SDS and a pH of 2.0 or 3.0. Experiments 9–11 were performed to make additional predictions based on variations in SDS concentration. Experiment 0 was performed each day as an equipment check, using the center points of each of the variable ranges.

2.4. DryLab I/mp

DryLab I/mp required results from two or three initial runs, in which all conditions were held constant except the variable being studied to make predictions of chromatographic behavior. Results from only two initial runs were needed to make predictions for the percentage of organic component. For example, results from the paired experiments 6, 4 and 7, 5 could be used for this purpose. In both cases the ion-pairing reagent concentration and pH were held constant, but the percentage of acetonitrile was varied. Several other combinations of experiments could also be treated in this way. Results from three initial experiments were required to make predictions for ion-pairing reagent concentration. In experiments 4, 5, 9 and 11 the percentage of acetonitrile and pH were held constant and the ion-pairing reagent concentration was varied.

Use of DryLab I/mp was straightforward. For each study, the retention times and peak areas of the analytes in the respective two or three experiments were entered. DryLab I/mp then made predictions of resolution (R_s) and capacity factor (k') over a selected range of the variables being studied. Computerized plots of the predicted chromatograms could be made. The peak areas are input so that the relative peak sizes could be appropriately plotted. The experimental values for resolution or the number of theoretical plates (N) could be input for one run to fine-tune further the predictions. The actual equations used by DryLab I/mp to predict resolution and capacity factor have been described [7, 8]. The equation for resolution is based on chromatographic theory, which assumes Gaussian band broadening. DryLab I/mp uses a quadratic fit of the data to make predictions for capacity factor values.

2.5. Statistical analysis

JMP was used to perform a statistical analysis of the experimental results. Empirical equations were derived which modeled the chromatographic behaviors (capacity factor and resolution). To compare directly the magnitude of the dependences of each behavior on each of the variables, the variables had to be normalized by converting them to integer values. For example, the percentage organic values of 43, 48 and 53% were actually represented as -1, 0 and 1. The first step in using JMP was to determine the best linear fit of the experimental variables to the behavior being modeled. By considering the value of each variable and the experimental results obtained, JMP predicted which variables or combination of variables (interaction and higher order terms) were significant. JMP derives a coefficient for each term which was found to be significant, along with an intercept term. The intercept, coefficients and experimental variables comprise an equation that models each chromatographic behavior. A more detailed discussion of the operation of JMP is beyond the scope of this paper; more information can be found in the JMP operator's handbook.

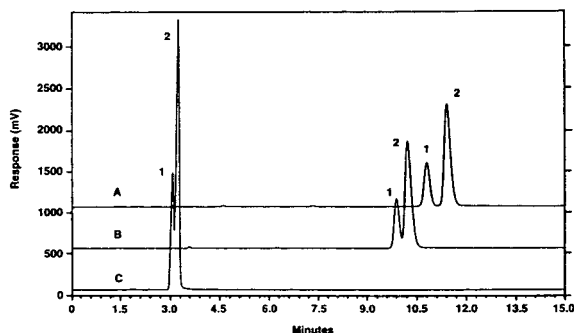


Fig. 2. Chromatograms demonstrating the effect changes in mobile phase composition on the separation of olanzapine from desmethylolanzapine. Peaks: 1 = desmethylolanzapine; 2 = olanzapine. The following mobile phase compositions are represented: (A) 43% acetonitrile–10 mM SDS–phosphate buffer (pH 2.0); (B) 48% acetonitrile–30 mM SDS–phosphate buffer (pH 2.5); (C) 53% acetonitrile–10 mM SDS–phosphate buffer (pH 2.0). All other conditions as described in the text.

3. Results

Representative chromatograms demonstrating the separation of olanzapine from desmethylolanzapine using various mobile phase conditions are shown in Figs. 2 and 3. As would be expected, the retention times and peak resolutions were dependent on the mobile phase. The

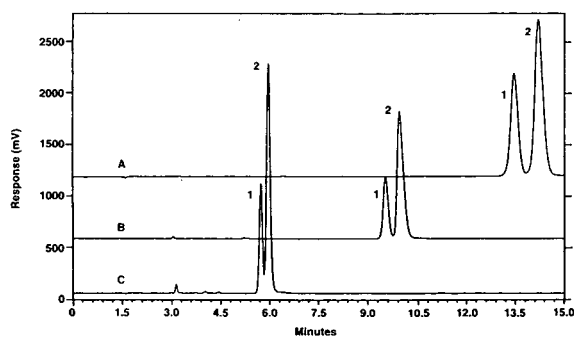


Fig. 3. Chromatograms demonstrating the effect of changes in SDS concentration on the separation of olanzapine from desmethylolanzapine. Peak identities as in Fig. 2. Each mobile phase contained 53% acetonitrile and phosphate buffer (pH 2.0). The SDS concentrations were as follows: (A) 70; (B) 50; (C) 30 mM. All other conditions as described in the text.

results obtained from each experiment for the capacity factor of the olanzapine peak and the resolution between the olanzapine and desmethylolanzapine peaks are summarized in Table 2. As shown, the capacity factor for olanzapine ranged from a minimum of 1.0 (experiment 1) to a maximum of 31.8 (experiment 7). Using the conditions chosen for experiment 1, olanzapine and desmethylolanzapine would be expected to elute with minimum retention because the percentage of acetonitrile was at a maximum and the ion-pairing reagent concentration was at a minimum. Further, the pH of the buffer used in experiment 1 (3.0) was the highest value tested. Olanzapine and desmethylolanzapine would be expected to be less protonated (less cationic) at the higher pH. Therefore, their ability to form ion pairs with SDS was diminished using the conditions of experiment 1. Conversely, these compounds would be expected to elute with maximum retention using the conditions chosen for experiment 7. Experiment 7 represented the combination of highest concentration of ion-pairing reagent and lowest percentage of acetonitrile. Further, at the pH of the buffer used in experiment 7 (2.0), these compounds would be in their most protonated, or cationic, forms. Note in Table 2 that the peak elution orders reversed during experiment 2. Desmethylolanzapine eluted later than olanzapine during experiment 2. This produced a negative value for the calculated resolution obtained for experiment 2. Also note in Table 2 that these compounds co-eluted during experiments 8 and 10.

3.1. Modeling the chromatographic behavior with DryLab I/mp

Although the variables could be examined in many different combinations, the procedure for the analysis of the data using DryLab I/mp and the success of the package may be exemplified by illustrating only two of those studies. The chromatograms generated for experiments 6 and 4 are shown in Fig. 2. Experimentally, the observed resolution changed significantly with a change in the percentage of acetonitrile. Using 43% acetonitrile (experiment 6) resulted in a

Table 2
Experimental results for olanzapine capacity factor and resolution between the olanzapine and desmethylolanzapine peaks

Experiment No.	Acetonitrile (%)	SDS (mM)	pH	Experimental k'	Experimental R_s
1	53	10	3.0	1.0	1.2
2	43	50	3.0	22.6	-0.9
3	43	10	3.0	4.9	1.3
4	53	10	2.0	1.8	1.0
5	53	50	2.0	5.6	1.3
6	43	10	2.0	6.6	1.7
7	43	50	2.0	31.8	1.6
8	53	50	3.0	3.2	0.0
9	53	30	2.0	3.0	1.1
10	43	30	3.0	14.2	0.0
11	53	70	2.0	8.5	1.7
0	48	30	2.5	6.0	1.0

resolution of 1.68. Using 53% acetonitrile (experiment 4), the resolution was 0.96. The results for retention times from these two experiments were entered into the DryLab I/mp software program. The predicted values for resolution and capacity factor are shown in Table 3.

As shown in Table 3, the resolution between olanzapine and desmethylolanzapine was predicted to change only slightly over the range of percentage acetonitrile studied when compared with the actual experimental results. A net change in resolution of 0.7 was observed experimentally. DryLab I/mp did not accurately predict the observed behavior for resolution. In fact, no change was predicted for values of 43

and 53% acetonitrile. The predictions for the olanzapine capacity factor were reasonable, however. The predictions made by DryLab I/mp for the dependence of resolution on the percentage of acetonitrile using the data from the other possible combinations of SDS concentration and pH were similar to those shown in Table 3.

The chromatograms generated for experiments 4, 5, 9 and 11 are shown in Figs. 2 and 3. Experimentally, the resolution was observed to increase with increasing SDS concentration. Using 10, 30, 50 and 70 mM SDS resulted in resolution values of 0.96, 1.11, 1.29 and 1.65, respectively. The peak retention times from these experiments were entered into the DryLab

Table 3
DryLab I/mp predictions made from results of experiments 6 and 4 (10 mM SDS, pH 2.0, percentage of acetonitrile varied)

Acetonitrile %	Predicted R_s	Predicted k'	Experimental R_s	Experimental k'
43	1.4	5.7	1.7	6.6
44	1.5	4.7		
45	1.5	3.9		
46	1.6	3.3		
47	1.6	2.7		
48	1.6	2.3		
49	1.6	1.9		
50	1.6	1.6		
51	1.6	1.3		
52	1.5	1.1		
53	1.4	0.9	1.0	1.2

Table 4
DryLab I/mp predictions made from results of experiments 4, 5, 9 and 11 (53% acetonitrile, pH 2.0, SDS concentration varied)

SDS (mM)	Predicted R_s	Predicted k'	Experimental R_s	Experimental k'
10	1.4	0.9	1.0	1.2
16	1.2	1.4		
22	1.0	1.9		
28	1.0	2.5		
30	1.0	2.7	1.1	3.0
34	1.0	3.1		
40	1.0	3.7		
46	1.0	4.4		
50	1.1	4.8	1.3	5.6
52	1.1	5.1		
58	1.2	5.8		
64	1.2	6.5		
70	1.3	7.3	1.7	8.5

I/mp software program. The predicted values for resolution and capacity factor are shown in Table 4.

As shown in Table 4, the resolution between olanzapine and desmethylolanzapine was predicted to be constant from 22 to 46 mM SDS. The resolution was predicted to increase slightly from 46 to 70 mM SDS. The resolution was also predicted to increase with decreasing SDS concentration from 22 to 10 mM. The greatest resolution was predicted to occur at 10 mM SDS. Experimentally, the trend for resolution from 30 to 70 mM SDS agreed with that which was predicted. However, the actual resolution observed at 70 mM SDS was significantly larger than the predicted value. The experimental resolution at 10 mM SDS was actually slightly less than that observed at 30 mM SDS. The predicted increase in resolution at 10 mM SDS was not observed experimentally. This prediction was opposite to the observed experimental results. The predicted capacity factors were in reasonably good agreement with those observed experimentally.

3.2. Modeling of chromatographic behavior by statistical analysis

It was apparent from the results obtained using DryLab that the experimental data did not fit the model used by the software package for

making predictions of resolution at low SDS concentration. Further, DryLab did not accurately predict the dependence of resolution on changes in percentage of acetonitrile at constant SDS concentration. Additional modeling of the data was performed using the statistical analysis software JMP. Using the coded values for each variable and the data generated from experiments 1–10 and 0, empirical equations were derived. The equations derived by JMP for capacity factor and resolution are as follows:

$$k' = 5.97 - 6.94[\text{ACN}] + 6.19[\text{SDS}] - 4.53[\text{ACN}][\text{SDS}] - 1.61(\text{pH}) + 3.43[\text{ACN}][\text{ACN}] \quad (1)$$

$$R_s = 0.92 - 0.39[\text{SDS}] + 0.17[\text{ACN}][\text{SDS}] - 0.51(\text{pH}) + 0.27[\text{ACN}](\text{pH}) - 0.46[\text{SDS}](\text{pH}) \quad (2)$$

Table 5 shows the experimental results for capacity factor and resolution, along with those values calculated using the equations derived from the statistical analysis. By comparing the experimental and calculated values, it was concluded that the resolution equation provided an excellent representation of the observed chromatographic behavior. With the exception of experiment 1, the capacity factor equation also provided a reasonably good estimate of the experimental behavior. The data from experi-

Table 5
Comparison of experiment results and those predicted by statistical analysis for capacity factor and resolution

Experiment No.	Experimental k'	Calculated k'	Experimental R_s	Calculated R_s
1	1.0	-0.8	1.2	1.4
2	22.6	25.4	-0.9	-0.9
3	4.9	4.0	1.3	1.2
4	1.8	2.4	1.0	0.9
5	5.6	5.7	1.3	1.4
6	6.6	7.2	1.7	1.8
7	31.8	28.7	1.6	1.6
8	3.2	2.5	0.0	0.0
9	3.0	4.1	1.1	1.2
10	14.2	14.7	0.0	0.1
11	8.5	7.5	1.7	1.6
0	6.0	6.0	1.0	0.9

ment 11 were not used to derive Eqs. 1 and 2. However, the equations provided an excellent prediction of the results observed from that experiment.

Discussion

4.1. Ruggedness of the separation

For our purpose, the most desirable assay conditions would produce the highest resolution between the olanzapine and desmethyl-olanzapine peaks, yet still provide reasonable capacity factors and method ruggedness. Method ruggedness is defined here as insensitivity to small variations in the mobile phase preparation and long column lifetimes. The sensitivity of the capacity factor and resolution to small changes in each variable can be estimated from the value of the coefficients (slope terms) shown in the empirical equations. The larger the value of the coefficient, the greater is the effect of small changes in the variable. This is most easily demonstrated by generating graphical presentations of each equation.

The response-surface plots for capacity factor and resolution are shown in Figs. 4–9. By comparison of Figs. 4, 6 and 8, it can be concluded that k' for olanzapine exhibits the same dependence on the percentage of acetonitrile and SDS concentration over the range of

buffer pH tested (2.0–3.0). As shown by the slopes of these plots, the sensitivity of k' to small changes in the percentage of acetonitrile was dependent on the concentration of SDS chosen. Likewise, the sensitivity of k' to small changes in SDS concentration was dependent on the percentage of acetonitrile chosen. At larger SDS concentrations and smaller percentages of acetonitrile, the slopes of the response-surface plots

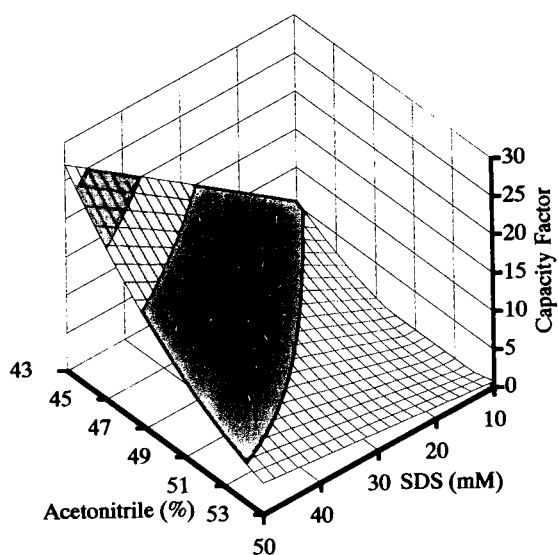


Fig. 4. k' vs. SDS concentration and percentage of acetonitrile at pH 2.5.

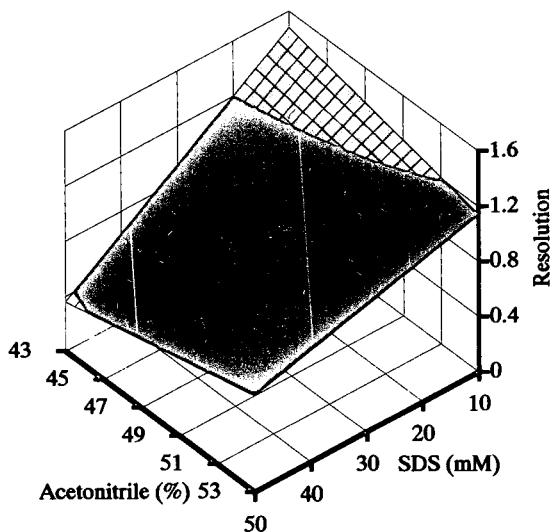


Fig. 5. Resolution vs. SDS concentration and percentage of acetonitrile at pH 2.5.

are greatest and the separation is the least rugged with respect to k' . In this same region the analysis times become excessively long. Conversely, at lower SDS concentrations and the largest percentage of acetonitrile, the slopes are not as great. However, in this region k' is too

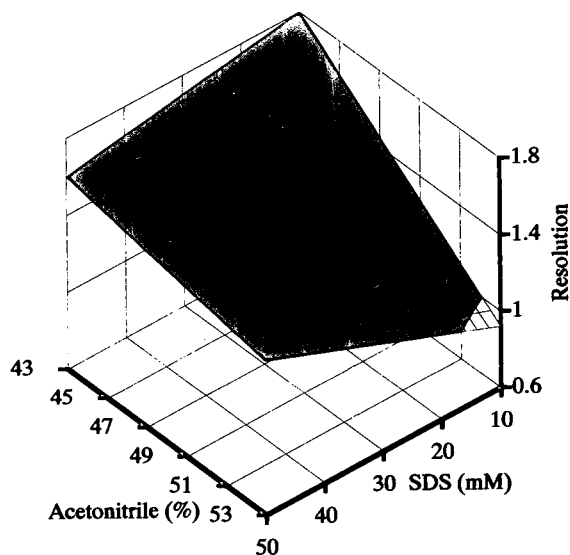


Fig. 7. Resolution vs. SDS concentration and percentage of acetonitrile at pH 2.0.

small and the separation capacity is greatly diminished. It was concluded that k' exhibits the best combination of ruggedness (relatively small slopes) and adequate compound retention around the center point regions of each plot.

By comparison of the plots shown in Figs. 5, 7

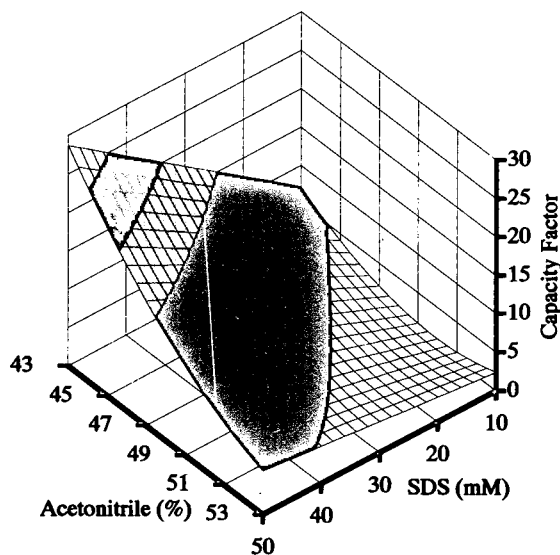


Fig. 6. k' vs. SDS concentration and percentage of acetonitrile at pH 2.0.

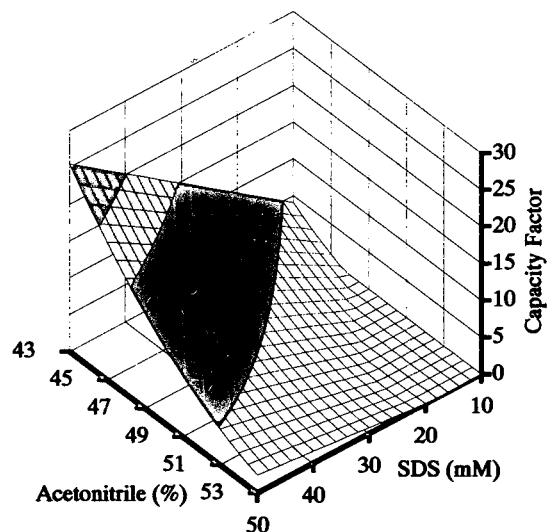


Fig. 8. k' vs. SDS concentration and percentage of acetonitrile at pH 3.0.

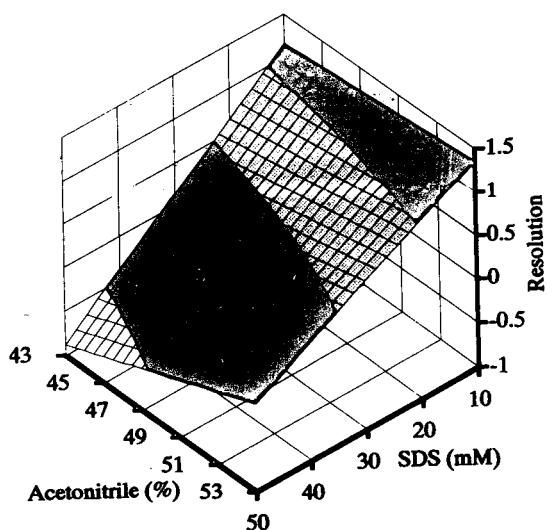


Fig. 9. Resolution vs. SDS concentration and percentage of acetonitrile at pH 3.0.

and 9, it can be concluded that the dependence of the resolution between olanzapine and desmethyloanzapine on the percentage of acetonitrile and SDS concentration is different with each buffer pH. At pH 2.0 (Fig. 7), the resolution ranges from 1.8 to 0.9, at pH 2.5 (Fig. 5) the resolution ranges from 1.5 to 0.4, and at pH 3.0 (Fig. 9), the resolution ranges from 1.4 to -0.9. The negative values for resolution observed at pH 3.0 correspond to a change in elution order between olanzapine and desmethyloanzapine. With respect to method ruggedness, at pH 2.5 (Fig. 5) the slopes are greatest at lower percentages of acetonitrile. At higher percentages of acetonitrile, the slopes are not as great. However, the combination of a low percentage of acetonitrile and a low SDS concentration resulted in the greatest resolution at pH 2.5. At pH 3.0 (Fig. 9), small changes in SDS concentration resulted in significant changes in resolution over the entire range of percentages of acetonitrile. At pH 2.0 (Fig. 7), the method is fairly rugged with respect to resolution, as evidenced by the relatively small slopes observed and the relatively large values for resolution across the entire surface.

It is apparent from the above discussion on

resolution that the pH of the buffer must be tightly controlled. Use of an improperly functioning and/or calibrated pH electrode could result in poor method ruggedness with respect to resolution. Performing the separation with a buffer pH greater than 2.5 would not be recommended owing to the relatively poor method ruggedness and decreased resolution observed. However, performing the separation with a buffer pH of less than 2.5 would not be recommended owing to the known instability of bonded phases on silica supports at low pH. A pH of 2.0 is the absolute minimum recommended for reversed-phase columns [12]. For these reasons, the center point values for percentage of acetonitrile, SDS concentration and buffer pH were concluded to be the best choice for performing the separation. Under these conditions, the desired separation will be obtained with adequate method ruggedness and column lifetimes.

4.2. Comparison of DryLab and statistical analysis

Owing to the nature of the model used by the DryLab I/mp program, it could not predict the apparent interactions between SDS, acetonitrile and pH in the resolution equation as derived by statistical analysis. Further, there is a deficiency in the DryLab software for entering ion-pair reagent information and pH while studying the effect of varying the percentage of organic component. Therefore, it is implied by DryLab that no such interactions should exist. The DryLab I/mp modeling equation for resolution does not truly consider the individual contributions to band broadening caused by the different equilibria that each analyte experiences, i.e., analyte and ion-pair reagent, analyte and stationary phase, etc. By assuming a Gaussian distribution to band broadening, DryLab predicted that the resolution would remain constant with changes in percentage of acetonitrile at constant SDS concentration and pH (see Table 3). In fact, a significant change in resolution was observed. Further, DryLab predicted that the resolution would increase with decreased SDS concentra-

Table 6

Experimental results for resolution, theoretical plates and peak asymmetry along with the resolution predicted by DryLab I/mp

Experiment No.	Theoretical plates	Peak asymmetry	Experimental R_s	Predicted R_s
4	6314	0.83	1.0	1.4
5	8485	1.56	1.3	1.2
6	12957	1.28	1.7	1.4
9	9969	1.36	1.1	1.0

tion below 20 mM (see Table 4). Behavior opposite to this prediction was observed experimentally. The capacity factor behavior was modeled reasonably well by both DryLab I/mp and statistical analysis. Therefore, the use of quadratic equations to predict chromatographic retention times during ion-pair separations are appropriate.

To understand further why the DryLab model failed to predict resolution accurately, the data from these experiments were examined more closely. The results for resolution, theoretical plates (N) and peak asymmetry obtained in experiments 4, 5, 6 and 9 along with the value of resolution predicted by DryLab are shown in Table 6. The peak shape of olanzapine was observed experimentally to change from tailing during experiments 5, 6 and 9 to fronting during experiment 4. Further, the smallest value for the number of theoretical plates was observed during experiment 4. It became apparent from examining these results that the contributions to band broadening and the retention mechanism were different during experiment 4. Perhaps the combination of low SDS concentration and high percentage of acetonitrile resulted in more interactions between the amine functional groups on these benzodiazepine-derived compounds and the silica support. If so, then the retention mechanism would no longer be strictly ion-pairing and reversed-phase in nature. Similar peak deterioration was observed by Lewis et al. [8] when modeling the effect of pH on the retention of 3,5-dimethylaniline. In that study, silanol interactions were also suggested as the cause of the observed behavior which led to erroneous predictions by DryLab.

5. Conclusions

The predictions made using theory-based software with respect to peak resolution may not be as accurate as those made from statistical analysis of factorial design studies for complex ion-pairing separations. The separation studied here did not fit the theory-based model at low SDS concentrations and high percentages of acetonitrile. The predictions made by DryLab I/mp can be obtained quickly and with a much smaller set of data than that required by factorial design studies. As part of method development, it is highly recommended that factorial design studies be considered to model the observed chromatographic behavior. This is especially true in the case of ion-pairing separations. The empirical equations derived are useful for gaining a better understanding of method ruggedness.

Acknowledgements

The authors gratefully acknowledge Dr. Michael Fogarty for his assistance with the use and operation of the computer software and Dr. Chuck Bunnell, Dr. Terry Hotten and Mr. Anh Thieu for providing authentic samples of each compound.

References

- [1] A. Drouen, J.W. Dolan, L.R. Snyder, A. Poile and P.J. Schoenmakers, *LC·GC*, 9 (1991) 714–724.
- [2] L.R. Snyder, J.W. Dolan and D.C. Lommen, *J. Chromatogr.*, 485 (1989) 65–89.

- [3] J.W. Dolan, D.C. Lommen and L.R. Snyder, *J. Chromatogr.*, 485 (1989) 91–112.
- [4] L. Wrisley, *J. Chromatogr.*, 628 (1993) 191–198.
- [5] W. Markowski, T.H. Dzido and E. Soczewinski, *J. Chromatogr.*, 523 (1990) 81–89.
- [6] J.W. Dolan, J.A. Lewis, W.D. Raddatz and L.R. Snyder, *Am. Lab.*, 24 (1992) 40D–40L.
- [7] J.A. Lewis, D.C. Lommen, W.D. Raddatz, J.W. Dolan and L.R. Snyder, *J. Chromatogr.*, 592 (1992) 183–195.
- [8] J.A. Lewis, J.W. Dolan and L.R. Snyder, *J. Chromatogr.*, 592 (1992) 197–208.
- [9] W. Lindberg, E. Johansson and K. Johansson, *J. Chromatogr.*, 211 (1981) 201–212.
- [10] P. Wester, J. Gottfries, K. Johansson, F. Klinteback and B. Winblad, *J. Chromatogr.*, 415 (1987) 261–274.
- [11] J.-Q. Wei, J.-L. Wei and X.-T. Zhou, *J. Chromatogr.*, 552 (1991) 103–111.
- [12] L.R. Snyder and J.J. Kirkland, *Introduction to Modern Liquid Chromatography*, Wiley, New York, 2nd ed., 1979, p. 281.

Simultaneous determination of granisetron and its 7-hydroxy metabolite in human plasma by reversed-phase high-performance liquid chromatography utilizing fluorescence and electrochemical detection

Venkata K. Boppana

Department of Drug Metabolism and Pharmacokinetics, SmithKline Beecham Pharmaceuticals, P.O. Box 1539,
Mail Code UW 2711, King of Prussia, PA 19406-0939, USA

Abstract

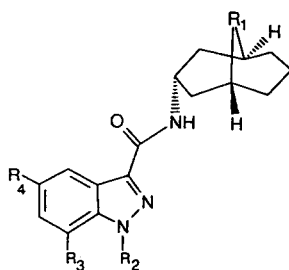
A highly sensitive and selective high-performance liquid chromatographic method was developed for the determination of granisetron and its active metabolite, 7-hydroxygranisetron (7OH-G) in human plasma. Granisetron is a selective 5-hydroxytryptamine receptor antagonist used in the treatment of cytotoxic drug-induced emesis. The method involves isolation of granisetron, 7OH-G and the internal standards from plasma by solid-phase extraction prior to reversed-phase ion-pair chromatographic separation on an octyl silica column with subsequent quantification of analytes simultaneously either with electrochemical (7OH-G) or fluorescence (granisetron) detectors which are placed in series. The recovery of granisetron and 7OH-G from human plasma was quantitative. Using 1 ml of plasma, the limits of quantification for granisetron and 7OH-G were 0.1 and 0.25 ng/ml, respectively. Linear responses in analyte/internal standard peak-area ratios were observed for analyte concentrations ranging from 0.1 to 50 ng/ml plasma. Precision and accuracy were within 13% across the calibration range for both granisetron and 7OH-G. The method was sufficiently sensitive, accurate and precise to support pharmacokinetic studies for granisetron and 7OH-G, in both normal and patient populations.

1. Introduction

Granisetron (BRL 43694, Fig. 1) {endo-1-methyl-N-(9-methyl-9-azabicyclo[3.3.1]non-3-yl)-1H-indazole-3-carboxamide} is a selective 5-hydroxytryptamine (5-HT₃) receptor antagonist which has been developed for the treatment of cytotoxic drug-induced emesis [1–3]. Initial studies in humans showed that, after intravenous and oral administration of [¹⁴C]granisetron, the drug was metabolized primarily to 7-hydroxygranisetron (7OH-G, BRL 55421), in addition to several other minor dealkylated metabolites and

hydroxy conjugates (Fig. 1). Since 7OH-G exhibited equivalent activity in both in vivo and in vitro pharmacologic models, its plasma concentrations needed to be quantitated along with granisetron in order to describe the overall pharmacokinetic and pharmacodynamic relationships following intravenous or oral administration of granisetron.

Although, an HPLC method [4] utilizing fluorescence detection was described for the quantification of granisetron in human plasma and urine, this method could not be adopted for the simultaneous quantitation of 7OH-G due to its



Compound	R ₁	R ₂	R ₃	R ₄
Granisetron	N-CH ₃	CH ₃	H	H
7OH-G	N-CH ₃	CH ₃	OH	H
Metabolite A	N-H	CH ₃	H	H
Metabolite B	N-CH ₃	H	H	H
Metabolite C	N(=O)CH ₃	CH ₃	H	H
Metabolite E	N-CH ₃	CH ₃	H	OH

Fig. 1. Structures of granisetron and its phase 1 metabolites.

weak fluorescence response. This report describes a sensitive and specific HPLC method for the simultaneous determination of granisetron and 7OH-G in human plasma. The method involves isolation of granisetron and its hydroxy metabolite by solid phase extraction prior to reversed-phase ion-pair chromatographic separation on an octyl silica column with subsequent quantification of 7OH-G and granisetron with electrochemical and fluorescence detection, respectively.

2. Materials and methods

2.1. Chemicals

Granisetron hydrochloride (G), 7OH-G hydrochloride, metabolites A (BRL 46540), B (BRL 43110), C (BRL 46541), E (BRL 48397) and internal standard A (ISA, BRL 43704, Fig. 2) were supplied by SmithKline Beecham Pharmaceuticals (Worthing, West Sussex, UK). Internal standard B (ISB, SK & F 89124; 4-[2-(N,N-dipropylamino)ethyl]-7-hydroxy-2-(3H)-indolone · HCl, Fig. 2) was supplied by Drug Substances

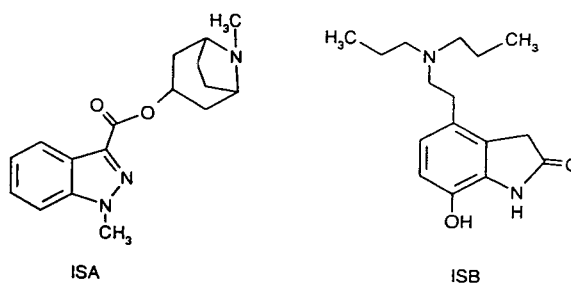


Fig. 2. Structures of internal standards.

and Products, SmithKline Beecham Pharmaceuticals (Swedeland, PA, USA). Glacial acetic acid was obtained from Mallinckrodt (Paris, KY, USA). Monobasic sodium phosphate, dibasic sodium phosphate, sodium acetate, HPLC-grade methanol and acetonitrile were obtained from J.T. Baker (Phillipsburg, NJ, USA). Disodium EDTA was obtained from EM Science (Cherry Hill, NJ, USA) and the sodium salt of hexanesulfonate was purchased from Regis (Morton Grove, IL, USA). C₂ silica solid-phase extraction (SPE) cartridges (1 ml) and the Vac-Elut manifold were purchased from Analytichem International (Harbor City, CA, USA).

2.2. Mobile phase

Sodium salt of hexanesulfonate (10 mM, 0.95 g) and 0.1 g of disodium EDTA were added to 405 ml of acetate buffer (0.1 M, pH 4.7). The solution was filtered first with a 0.5- μ m filter (type HA, Millipore). Acetonitrile (95 ml) was added to the above solution and the solution was sonicated under vacuum for 5 min.

2.3. Standard solutions

The stock standard solutions of granisetron, 7OH-G, ISA and ISB were prepared by dissolving appropriate amounts of the compounds in water to give a final solution concentration of 1 mg/ml. The solutions were stable for 4 months when stored at 4°C. Working aqueous standard solutions of granisetron and 7OH-G at concentrations of 100, 10, 1 and 0.1 μ g/ml were prepared daily by appropriate dilutions of stock

solutions with water. The working internal standard solution was prepared by appropriate dilution of the stock solutions of ISA and ISB with water to give a solution concentration of 100 ng/ml. This solution was stable for 1 month when stored at 4°C.

2.4. Extraction of granisetron and 7OH-G from plasma

The C₂ extraction column was conditioned by successive washings with 1 ml of methanol, 1 ml of water and 1 ml of 1.0 M phosphate buffer, pH 7.0. An aliquot of heparinized plasma (1 ml) was transferred to a 75 × 12 mm polypropylene tube and mixed with 50 μl of water (containing standards when preparing standard curve), 50 μl of internal standard solution (100 ng/ml of each of ISA and ISB) and 500 μl of 1.0 M phosphate buffer, pH 7.0 (the phosphate buffer should be added to plasma just prior to application of sample onto the SPE column). The sample was applied to the C₂ column under reduced pressure at 3–4 in.Hg (1 in.Hg = 3386.38 Pa). Following sample application, the column was washed successively with 1 ml water and 1 ml of acetonitrile–water (40:60, v/v). The washing solvent was completely removed from the sorbent bed prior to elution. The column was then eluted first with 1 ml of methanol and then with 1 ml of 1% trifluoroacetic acid (TFA) methanolic solution. The combined eluate was collected into a 75 × 12 mm polypropylene tube. The eluate was evaporated under a gentle stream of nitrogen at 40°C and the residue was reconstituted in 200 μl of methanol–water (10:90, v/v). The sample was vortex mixed for approximately 30 s, centrifuged at approximately 2000 g for 5 min and transferred to an autosampler vial. The vials were centrifuged at approximately 2000 g for 5 min and 10–65 μl were injected into the HPLC system for analysis.

2.5. High-performance liquid chromatography

The isocratic HPLC system consisted of a Beckman (Palo Alto, CA, USA) Model 116 pump, an electrochemical detector (ESA, Brad-

ford, MA, USA) and a fluorescence detector (Model F1000; Hitachi, Danbury, CT, USA). Chromatographic separations were carried out on a 15 cm × 2.1 mm I.D. octyl silica column (Zorbax Rx C₈ column, Mac-Mod Analytical, Chadds Ford, PA, USA) which was preceded by a 3 cm × 2.1 mm I.D. C₈ guard column (ABI Instruments, Ramsey, NJ, USA). The column was maintained at 30°C and the mobile phase eluent, 0.1 M acetate pH 4.7 with 10 mM sodium hexanesulfonate and acetonitrile (405:95, v/v), was pumped at a flow-rate of 300 μl/min. Samples were injected using an HPLC autosampler (WISP Model 710B; Waters, Milford, MA, USA). The column eluent was first directed to the electrochemical cell and then to the fluorescence detector. The potentials at the electrochemical cell were maintained at 0.15 V (*E*₁, first cell) and 0.35 V (*E*₂, second cell) and the current was measured at *E*₂. An electrochemical guard cell with an applied potential of 0.4 V was also placed before the injector in order to eliminate any oxidizable impurities in the mobile phase and thus aid in reducing background current of the analytical cell. The excitation and emission wavelengths of the fluorescence detector were set at 305 and 360 nm, respectively. The chromatographic data from each detector were collected with an automated laboratory system (Nelson Chromatography, Cupertino, CA, USA).

2.6. Validation procedures

Four pools of plasma precision samples containing 0.1 (0.25), 0.25 (0.5), 5 (5), and 50 (50) ng/ml of granisetron (7OH-G) were prepared by adding appropriate volumes of standard solutions to drug-free plasma. These plasma samples were stored at –20°C until analysis was performed. Seven replicate samples from each pool were extracted and analyzed on three separate days. Concentrations were determined by comparison with a calibration curve prepared on the day of analysis. A weighted (1/*y*) linear regression was used to construct a calibration curve for the peak area ratio of analyte to internal standard vs. analyte concentration. From the data

obtained, inter-day precision [determined as relative standard deviations (R.S.D.s) of daily means], intra-day precision (determined as mean of the daily R.S.D.s) and mean accuracy were calculated.

3. Results and discussion

Quantitative methods described earlier for granisetron and its dealkylated metabolites are primarily based on the detection of native fluorescence of these compounds. Since 7OH-G lacks any appreciable fluorescence due to the electron-withdrawing nature of its phenolic group, alternate methods of detection were explored. The phenolic group present in 7OH-G was found to be easily oxidizable at low potential and offered an alternate method of detection for this compound utilizing an electrochemical detector. Since granisetron was not electrochemically active, both fluorescence and electrochemical detectors were employed in series following chromatographic separation of granisetron and 7OH-G for simultaneous quantification in a single chromatographic run. In essence, the method involves isolation of granisetron, its active metabolite 7OH-G and the internal standards (ISA and ISB) from plasma by SPE, followed by reversed-phase ion-pair chromatographic separation of the analytes on an octyl silica column with subsequent detection of electroactive analytes (7OH-G, ISB) and fluorescent analytes (granisetron, ISA) as described above. Careful optimization of chromatographic conditions and the use of HPLC columns of reduced internal diameter (2 mm) resulted in an on-column detection limit of 20 pg for granisetron and 50 pg for 7OH-G.

Fig. 3 displays fluorescence and electrochemical chromatograms obtained simultaneously from a single injection of an aqueous standard solution of granisetron, its metabolites (7OH-G, metabolite A, metabolite B, metabolite C and metabolite E) and the internal standards (ISA and ISB). As can be seen from these figures, the electrochemical chromatogram displays signals corresponding to 7OH-G, metabolite E and ISB with no response from other analytes, which

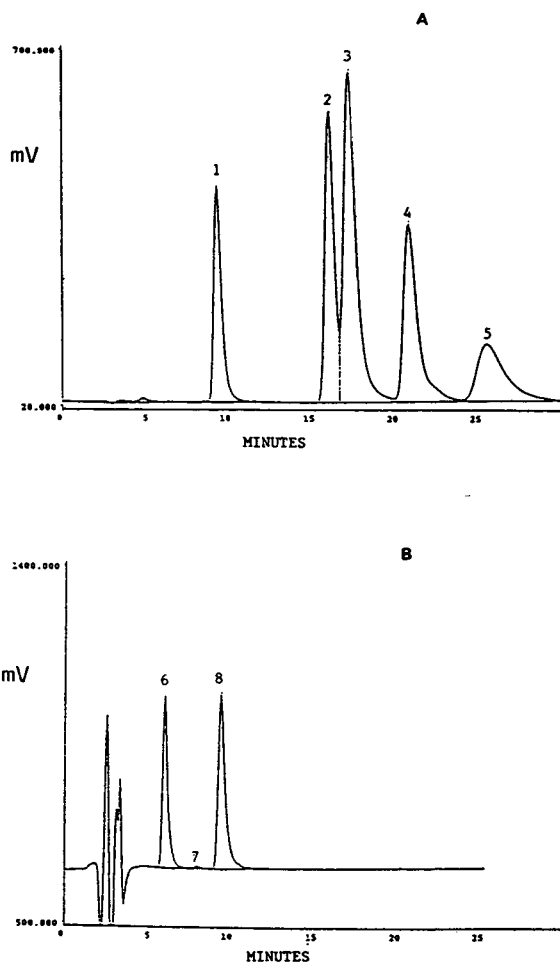


Fig. 3. Fluorescence (A) and electrochemical (B) chromatograms simultaneously obtained from a single injection of an aqueous standard solution of granisetron, its known metabolites and internal standards. Peaks: 1 = metabolite B; 2 = metabolite A; 3 = granisetron; 4 = ISA; 5 = metabolite C; 6 = ISB; 7 = metabolite E; 8 = 7OH-G.

were observed only in the fluorescence chromatogram. Although 7OH-G and metabolite B co-eluted chromatographically, 7OH-G was detected only by the electrochemical detector and metabolite B was detected only by the fluorescence detector.

3.1. Recovery and stability

The recovery of granisetron, 7OH-G and the internal standards from plasma was estimated

with seven determinations by comparing the peak areas obtained with processed samples to those obtained by direct injection of known amounts of the compounds equivalent to 100% recovery. The mean recovery of granisetron at plasma concentrations of 0.1 and 50 ng/ml was 107.9 ± 7.46 and 113.0 ± 3.16 , respectively. At plasma concentrations of 0.25 and 50 ng/ml, the mean recovery for 7OH-G was 97.7 ± 8.49 and 120.6 ± 7.11 , respectively. The mean recovery of ISA and ISB at a plasma concentration of 5 ng/ml was 123.7 ± 4.88 and 100.9 ± 5.14 , respectively.

The order in which methanol and TFA-methanol were applied to the C_2 SPE column to elute granisetron and 7OH-G greatly affected the recovery of these compounds. Quantitative recoveries of 7OH-G, granisetron, ISA and ISB were obtained when the SPE column was first eluted with methanol followed by TFA-methanol. Reversing the order of elution solvents resulted in poor recovery of 7OH-G. Granisetron, 7OH-G and the internal standards were stable in the final extracts in a sealed auto-sampler vial for at least 48 h following their isolation from plasma. However, repeat injection of the final extracts onto the HPLC system indicated marked degradation of 7OH-G with time, possibly due to oxidation of the analyte by the apparent entry of air through the septum of the vial during or after injection. Replacing the punctured septum with a new one minimized the degradation of 7OH-G and allowed the reanalysis of the samples.

3.2. Sensitivity, linearity and selectivity

Typical fluorescence and electrochemical chromatograms of plasma extracts obtained from drug-free human plasma and a plasma sample spiked with 0.1 ng/ml of granisetron and 0.25 ng/ml of 7OH-G are shown in Figs. 4 and 5, respectively. Based on the analysis of drug-free plasma samples, endogenous plasma components did not interfere with the analytes and the internal standards over the concentration range described here. In addition, none of the known metabolites of granisetron (metabolites A, B, C and E), which had been prepared synthetically,

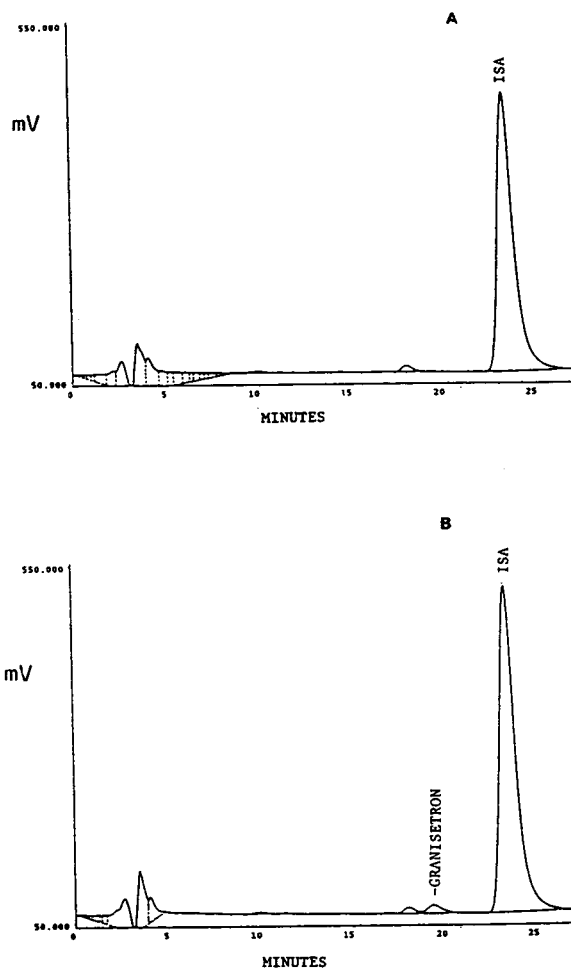


Fig. 4. Fluorescence chromatograms of extracts of drug-free human plasma spiked with ISA (A) and plasma spiked with 0.1 ng/ml of granisetron (B).

interfered with the analysis of either granisetron or 7OH-G. Fig. 6 displays fluorescence and electrochemical chromatograms obtained simultaneously from a single injection of extract obtained from a plasma sample drawn from a human volunteer 2 h after oral administration of 5 mg of granisetron. Using 1 ml of plasma, the limits of quantification for granisetron and 7OH-G were 0.1 and 0.25 ng/ml, respectively. Linear responses in analyte/internal standard peak-area ratios were observed for analyte concentrations ranging from 0.1 to 50 ng/ml plasma. Correla-

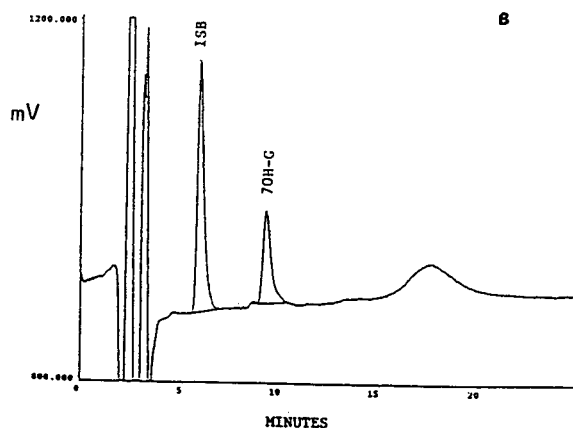
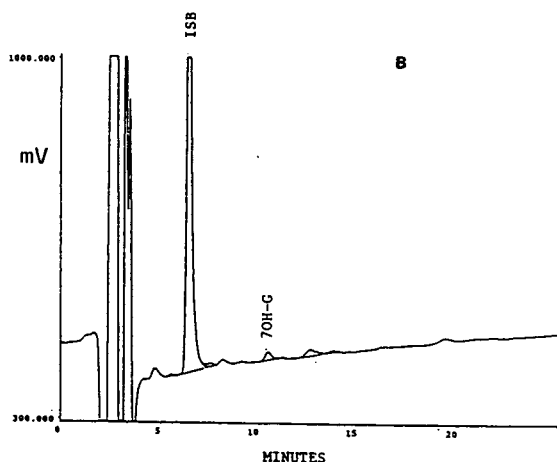
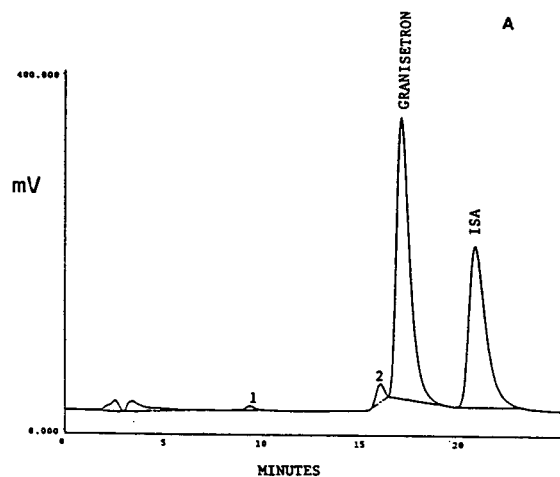
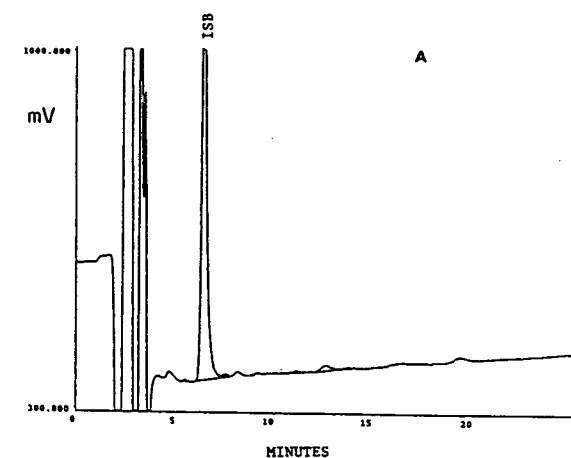


Fig. 5. Electrochemical chromatograms of extracts of drug-free human plasma spiked with ISB (A) and plasma spiked with 0.25 ng/ml of 7OH-G (B).

tion coefficients obtained using weighted ($1/y$) linear regression analysis of calibration curves were typically 0.999. The calibration curves were highly reproducible. The precision, as measured by the relative standard deviations at each of the spiked concentrations, and accuracy, evaluated by the average concentration back-calculated from the respective standard curves, are shown in Table 1 for granisetron and 7OH-G.

3.3. Accuracy and precision

Results of a three-day validation study are displayed in Table 2 for both granisetron and

Fig. 6. Fluorescence (A) and electrochemical (B) chromatograms simultaneously obtained from a single injection of plasma extract from a human subject 2 h after oral administration of 5 mg of granisetron. The plasma concentrations of granisetron and 7OH-G are 5.82 and 3.81 ng/ml, respectively.

7OH-G. The intra-day precision of the method was indicated by the mean of the daily R.S.D. The inter-day precision of the method was indicated by the R.S.D. of the daily means. The mean accuracy of the method, as indicated by the ratio of the actual to theoretical concentrations, is also shown in Table 2. The inter-day R.S.D.s of the method were also calculated by analyzing three pools of quality control plasma samples spiked with 0.5, 5.0 and 25 ng/ml of each of granisetron and 7OH-G over a period of

Table 1
Accuracy and precision data for granisetron and 7OH-G obtained from back-calculated standard curve concentrations over four days

	Nominal concentrations of granisetron and 7OH-G in plasma (ng/ml)								
	0.1	0.25	0.5	1.0	2.5	5.0	10.0	25.0	50.0
Granisetron									
Mean	0.101	0.261	0.51	1.027	2.559	5.186	10.269	24.834	49.683
S.D.	0.010	0.014	0.019	0.039	0.111	0.293	0.266	0.704	1.239
R.S.D. (%)	10.12	5.20	3.75	3.77	4.33	5.64	2.59	2.84	2.49
Accuracy (%)	101.0	104.4	102.0	102.7	102.4	103.7	102.7	99.3	99.4
7OH-G									
Mean	0.131	0.259	0.441	0.979	2.371	4.551	9.236	24.208	53.412
S.D.	0.028	0.031	0.037	0.127	0.277	0.274	0.768	1.086	2.626
R.S.D. (%)	21.02	11.969	8.37	12.97	11.68	6.02	8.31	4.49	4.92
Accuracy (%)	130.8	103.6	88.2	97.9	94.8	91.03	92.4	96.8	106.8

6 days. The inter-day R.S.D.s from the analysis of these samples, were found to be 7.32, 7.20 and 8.21% for granisetron ($n = 12$) and 12.92, 13.34 and 12.68% for 7OH-G ($n = 11$), respectively.

3.4. Application of the procedure to clinical plasma samples

The quantitative HPLC methodology described here provided for selective and sensitive

Table 2
Accuracy and precision data for granisetron and 7OH-G in plasma

Parameter	Concentrations of granisetron and 7OH-G in plasma (ng/ml)							
	Granisetron				7OH-G			
	0.1	0.25	5.0	50.0	0.25	0.5	5.0	50.0
R.S.D. (%)								
Day 1	7.03	6.59	2.20	2.74	9.10	12.49	9.22	5.13
Day 2	2.83	6.91	8.24	13.05	6.89	9.35	7.36	11.59
Day 3	7.03	2.99	0.91	9.26	9.68	9.19	6.46	1.92
Error (%)^a								
Day 1	+1.0	+2.8	+5.2	-4.2	-1.6	-1.8	-3.1	+1.4
Day 2	+2.0	+3.2	+5.2	+1.6	+4.0	-4.2	-5.6	+4.9
Day 3	0.0	-2.0	+0.3	+3.6	+9.2	-8.6	-5.0	-8.1
R.S.D. (%)								
Inter-day ^b	1.53	2.86	2.76	3.21	5.33	3.63	1.40	6.77
Intra-day ^c	5.63	5.50	3.78	8.35	8.56	10.34	7.68	6.21
Mean accuracy (%)	99.7	101.3	103.6	97.9	103.2	95.1	95.4	99.4

^a (Calculated concentration – actual concentration)/actual concentration × 100.

^b R.S.D.s of daily means.

^c Mean of the daily R.S.D.s.

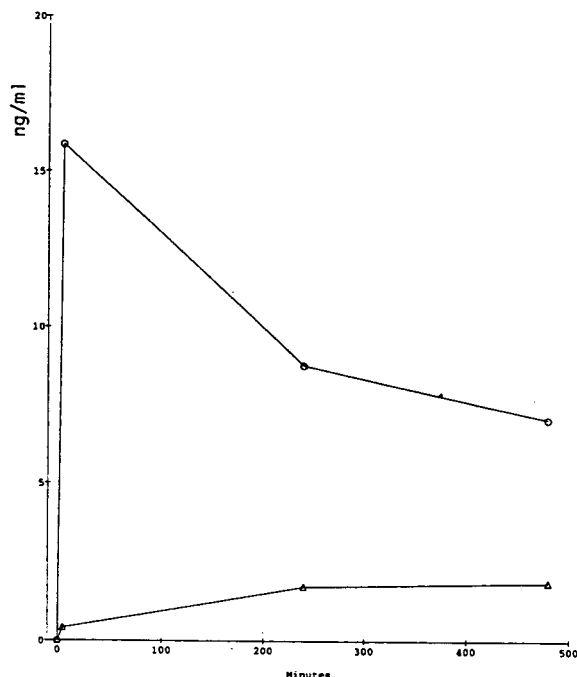


Fig. 7. Plasma concentrations of granisetron (○) and 7OH-G (△) following intravenous administration of 40 mg/kg of granisetron to a healthy volunteer.

detection of granisetron and 7OH-G in human plasma samples. Fig. 7 shows the application of this assay to a pharmacokinetic study in a human subject in which plasma concentrations of granisetron and 7OH-G were measured from serial blood samples drawn at 0, 5, 240 and 480 min following intravenous administration of 40 μ g/kg of granisetron. As can be observed from

the plasma concentration versus time curve, the methodology was sufficiently sensitive to support pharmacokinetic studies of granisetron in humans.

4. Conclusions

A sensitive HPLC method has been developed for the simultaneous determination of granisetron and its active metabolite, 7OH-G, in human plasma utilizing both fluorescence and electrochemical detection. The assay performed acceptably in a three-day validation over a concentration range of 0.1 to 50 ng/ml for granisetron and 0.25 to 50 ng/ml for 7OH-G. The method was sufficiently sensitive, accurate and precise to support pharmacokinetic studies for granisetron and 7OH-G in both normal and patient populations.

References

- [1] J. Carmichael, B.M.J. Cantwell, C.M. Edwards, W.G. Rapeport and A.L. Harris, *Br. Med. J.*, 297 (1988) 110.
- [2] J.W. Upward, B.D.C. Arnold, C. Link, D.M. Pierce, A. Allen and T.C.G. Tasker, *Eur. J. Cancer*, 26 (suppl. 1) (1990) S12.
- [3] J. Carmichael, B.M.J. Cantwell, C.M. Edwards, B.D. Zussman, S. Thompson, W.G. Rapeport and A.L. Harris, *Cancer Chemother. Pharmacol.*, 24 (1989) 45.
- [4] A. Clarkson, P.E. Coates and B.D. Zussman, *Br. J. Clin. Pharmacol.*, 25 (1988) 136P.



ELSEVIER

Journal of Chromatography A, 692 (1995) 203–205

JOURNAL OF
CHROMATOGRAPHY A

Short communication

Determination of citrate, inositol and gentisic acid in a pharmaceutical diagnostic formulation by ion-moderated partition chromatography

Russell W. Chong*, Brenda J. Moore

Mallinckrodt Medical, Inc., P.O. Box 5840, St. Louis, MO 63134, USA

Abstract

An ion-moderated partition chromatographic method has been developed for rapid determination of excipients in a pharmaceutical diagnostic formulation. Citrate, inositol, and gentisic acid (2,5-dihydroxybenzoic acid) are separated and analyzed using an 0.005 *M* sulfuric acid–acetonitrile (80:20) mobile phase with a 100 × 7.8 mm strong cation-exchange column consisting of sulfonated cross-linked styrene–divinylbenzene copolymer in the hydrogen form. Detection is by refractive index. The method has proven to be rugged for more than 100 injections over a one-year period on the same column.

1. Introduction

The separation of organic acids and carbohydrates/sugar alcohols via ion-moderated partition (strong cation-exchange resin consisting of sulfonated cross-linked styrene–divinylbenzene copolymer in the hydrogen form) using dilute sulfuric acid as a mobile phase is well known [1–5]. However, retention is excessive for aromatic acids under these conditions. The use of an organic modifier such as acetonitrile in the mobile phase allows for the analysis of aromatic acids in a reasonable amount of time. However, there is apprehension among users of this type of column in using organic modifiers because of swelling of the sulfonated divinylbenzene–styrene copolymer stationary phase. A method has been developed using an organic modifier in

the mobile phase which allows for the rapid separation and quantitation of citrate (organic acid), inositol (sugar alcohol), and gentisic acid (aromatic acid) in a formulation of OctreoScan (Mallinckrodt, St. Louis, MO, USA), a diagnostic for gastro-entero-pancreatic endocrine tumors. This method has proven to be rugged in routine use.

2. Experimental

2.1. Materials and reagents

Trisodium citrate dihydrate (analytical-reagent grade), inositol (organic-reagent grade), sulfuric acid (analytical-reagent grade), and acetonitrile (HPLC grade) were from Mallinckrodt (St. Louis, MO, USA). The gentisic acid was from

* Corresponding author.

Aldrich (Milwaukee, WI, USA). The γ -cyclodextrin was from Wacker (New Canaan, CT, USA).

2.2. High-performance liquid chromatography

Chromatographic measurements were performed at ambient temperature on a 100 mm \times 7.8 mm I.D. stainless-steel column packed with 9- μ m sulfonated divinylbenzene–styrene copolymer in the hydrogen form (Fast Acid Column, Bio-Rad, Hercules, CA, USA). The chromatograph consisted of a Waters (Milford, MA, USA) 510 pump, 712 WISP injector, and a 410 refractive index detector. Chromatograms were obtained and analyzed on a PE Nelson (Cupertino, CA, USA) Access*Chrom data system. The mobile phase was 0.005 M sulfuric acid–acetonitrile (80:20, v/v). The flow-rate was 0.8 ml/min and the injection volume was 20 μ l. The column was stored in 0.005 M sulfuric acid between analyses. Samples were dissolved in mobile phase.

3. Results and discussion

The assay was linear in the concentration ranges of 2.2 to 11.0 mg/ml for trisodium citrate (anhydrous basis), 4.0 to 20.0 mg/ml inositol, and 0.8 to 4.0 mg/ml gentisic acid (Table 1). Repeatability was typically less than or equal to 2% R.S.D. Recovery of each component in the presence of the other two ranged between 98 and 102%.

A system peak which is dependent on the

Table 1
Linearity of assay

Component	Slope	y-Intercept	Correlation coefficient
Citrate	7 423	–747	0.9999
Inositol	11 423	747	0.9999
Gentisic Acid	5 525	–95	0.9999

Slope in terms of peak height counts $\text{mg}^{-1} \text{ml}^{-1}$. Intercept in terms of peak height counts. Five data points for each component were used for the regression.

relative concentration of acetonitrile in the sample versus the mobile phase was observed between the inositol and gentisic acid peaks. However, this peak did not interfere with quantitation. The active ingredient in the formulation, a peptide, is at a concentration 200-fold lower than any of the excipients and was not detected under these chromatographic conditions so it did not interfere with the assay. The relative amount of acetonitrile in the mobile phase affects the retention time of the system peak and gentisic acid (increasing acetonitrile decreases retention time). However, very little effect was observed on the retention times for citrate and inositol. Slight changes in the molarity of the sulfuric acid in the mobile phase did not significantly affect retention times.

Generally, separations using ion-moderated partition chromatography are performed on a column length of 300 mm at elevated temperatures to improve column efficiency, lower back-pressure, and enhance reproducibility. This sepa-

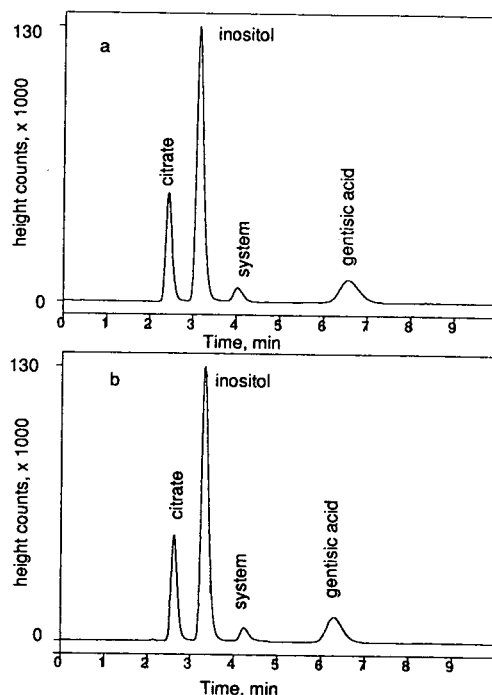


Fig. 1. Chromatograms of separation. (a) HPLC column used for one year, (b) new HPLC column.

Table 2
Capacity factors and resolution from nearest neighboring peak

Component	k'		R_s	
	New column	Used column	New column	Used column
Citrate	0.2	0.2	2.5	2.4
Inositol	0.5	0.6	2.5	2.4
Gentisic acid	1.9	2.3	3.8	4.2

t_0 determined by retention of γ -cyclodextrin.

ration was performed on a 100 mm column at ambient temperature. Column efficiency was sufficient for this separation, backpressure was well within the manufacturer's specifications, and reproducibility was not a problem. Clearly, the use of a shorter column where separation of different classes of compounds are involved may provide faster analysis without significant loss of resolution.

Fig. 1a shows a chromatogram of a mixed standard injected onto a column after more than 100 injections over a period of one year. Fig. 1b shows a chromatogram of a mixed standard injected onto a new column. Table 2 gives k' and R_s values. No noticeable deterioration of the separation was observed between the new and used columns. Only a slight increase in column backpressure was noted over the one year period.

4. Conclusions

A rapid and rugged HPLC assay has been developed for the separation and quantitation of citrate (organic acid), inositol (sugar alcohol) and gentisic acid (aromatic acid) using ion-modulated partition chromatography.

References

- [1] T. Jupille, M. Gray, B. Black and M. Gould, *Am. Lab.*, 13, No. 8 (1981) 80.
- [2] R. Pecina and G. Bonn, *J. Chromatogr.*, 287 (1984) 245.
- [3] P. Oefner, G. Bonn and G. Bartsch, *J. Liq. Chromatogr.*, 8 (1985) 1009.
- [4] J. Blake, M. Clarke and G. Richards, *J. Chromatogr.*, 398 (1987) 265.
- [5] J. Heard and K. Talmadge, *Am. Lab.*, 24, No. 8 (1992) 24.



ELSEVIER

Journal of Chromatography A, 692 (1995) 207–212

JOURNAL OF
CHROMATOGRAPHY A

Use of overlapping resolution mapping scheme for optimization of the high-performance liquid chromatographic separation of pharmaceuticals

Chye Peng Ong^a, K.K. Chow^a, Choon Lan Ng^b, Fei Min Ong^b, Hian Kee Lee^b,
Sam Fong Yau Li^{b,*}

^aAnalytical Services, Quality Department, Glaxo Development, 1 Pioneer Sector 1, Jurong, Singapore 2262, Singapore

^bDepartment of Chemistry, National University of Singapore, Kent Ridge Crescent, Singapore 0511, Singapore

Abstract

The use of overlapping resolution mapping (ORM) for the optimization of HPLC separations was examined. The ORM scheme was employed to predict the optimum conditions required for the isocratic HPLC separation of a group of basic pharmaceuticals. The ORM scheme involved first performing seven pre-planned experiments located on a triangle representing the mobile phase compositions. From these experiments, and through the use of a Basic program, the optimum conditions required for separation were established. The scheme was initially applied to establish the optimum mobile phase compositions consisting of quaternary mixtures of buffered acetonitrile, methanol and 2-propanol with a C₁₈ column. This approach was found to offer a very rapid and versatile means of determining the optimum HPLC conditions required for such a complex mobile phase system. Complete separation of all the peaks in the mixture was achieved using a mobile phase composition of acetonitrile–methanol–2-propanol–buffer (50:15:5:30, v/v) derived from the ORM scheme. The usefulness and versatility of the ORM scheme was further demonstrated through the use of the optimum mobile phase compositions with different C₁₈ columns. It was found that satisfactory separation was achieved by adopting the established optimum mobile phase composition without the need to perform any further re-optimization. In addition, the precision, selectivity and linearity of the method developed were found to be highly reproducible and reliable.

1. Introduction

High-performance liquid chromatography (HPLC) is widely used for the analysis of pharmaceuticals [1]. The many advantages of HPLC include its simplicity, accuracy, precision, versatility, reliability, reproducibility and most importantly its selectivity. With increasing complexity of pharmaceutical samples to be analysed, the demands on the use of HPLC techniques have

intensified in recent years. The development of HPLC columns with a wide variety of coatings and polarities [2] and the use of multi-modifier systems are some of the popular approaches now employed. Many systems are being developed to meet the current needs, particularly in the area of improving the separation selectivity for the determination of various components in complicated mixtures or matrices.

The use of multi-modifier mobile phase systems in HPLC has been demonstrated in many applications [3,4] and the success of such an

* Corresponding author.

approach is found to be greatly dependent on the actual determination of the optimum mobile phase compositions required for separation. The usual trial-and-error approach, although simple and easy to apply, suffers from serious drawbacks as it is laborious and contains many uncertainties. This problem is further exacerbated if the number of modifiers used increases. A way to circumvent this is to use systematic experimental designs which require few experiments to be performed and are capable of locating optimum conditions required for the separation. Palasota et al. [5] have successfully employed a sequential simplex algorithm for the separation of amino acids in a constraint simplex mixture space and Heinisch et al. [6] described the use of several prioritized criteria to search for the optimum eluent strength for HPLC separations using an interpretative approach.

In this work, the use of overlapping resolution mapping (ORM), a systematic experimental design for the optimization of HPLC separations, was examined. The scheme is an experimentally based optimization procedure. Compared with the commonly used simplex optimization approach, which tends to locate only the most favourable local optimum, the ORM is more capable of locating the global optimum. More important, in contrast to simplex procedures, which usually require a relatively large number of experiments to locate optimum separation conditions, the ORM scheme requires only a small set of preplanned experiments which are carried out systematically. The number of experiments for the ORM scheme is usually governed by the experimental design and the order of polynomial chosen to relate the resolution to the experimental parameters.

The application of the ORM scheme to predict the optimum conditions required for the isocratic HPLC separation of a group of basic pharmaceuticals was studied in this work. The scheme was initially applied to establish the optimum conditions for reversed-phase HPLC separations using a C_{18} column and a mobile phase consisting of quaternary mixtures of buffered acetonitrile, methanol and 2-propanol. This approach was found to offer a very rapid and versatile

means of determining the optimum HPLC conditions involving complex mobile phase systems such as quaternary mixtures. The usefulness and versatility of the ORM scheme is further demonstrated through the use of the optimum mobile phase compositions derived on different C_{18} columns. The aim is to demonstrate the ruggedness of the ORM scheme in which satisfactory separation can be achieved for another column by simply adopting the established optimum mobile phase compositions without the need to perform any further optimization. The precision, linearity and selectivity of the method were also evaluated.

2. Experimental

2.1. Instrumental

All chromatographic separations were performed using either a Shimadzu (Kyoto, Japan) LC-6A isocratic instrument equipped with an SPD-6A variable-wavelength UV detector or a Hewlett-Packard (HP) Model 1050 instrument equipped with a variable-wavelength UV detector. Both detectors were set at 216 nm. With the Shimadzu system, chromatographic data were collected and analysed on a Shimadzu CR6A Chromatopac integrator. The chromatographic data from the HP 1050 LC system were collected and analysed using an HP ChemStation.

The reversed-phased HPLC columns used were Phase-Sep ODS-2, 5 μm (20 cm \times 4.6 mm I.D.) (column I) and YMC-Pack ODS-A, 5 μm (25 cm \times 4.6 mm I.D.) (column II). The Phase-Sep column (column I) was first employed to determine the optimum mobile phase composition using the ORM scheme. Once the optimum mobile phase had been established, the YMC column (column II) was then used.

2.2. Reagent and materials

A basic drug substance, ondansetron (abbreviated as DS1), and its related impurities GDL1, GDL2 and GDL3 were investigated (structures are given elsewhere [7]). Standards of

DS1 and the impurities were obtained from Glaxo Development. All other chemicals used, unless stated otherwise, were of the purest grade available.

3. Results and discussion

In a previous paper [8], we reported the use of the ORM scheme for the optimization the mobile phase compositions for the separation of environmental pollutants. In this work, the ORM scheme was employed to establish the mobile phase compositions required to separate a group of basic pharmaceuticals. The need for the use of a multi-modifier system in this study

derives from the fact that binary mobile phases are unable to separate this group of compounds satisfactorily.

The ORM scheme consisted of a number of steps, shown schematically in Fig. 1. For this work the criteria for the separation were first the resolution (at least 1.5 between adjacent peaks) and second the analysis time of the separation (capacity factor not more than 20). These values were defined to ensure that separation could be achieved within a reasonable time range. As the ORM scheme is based on the Snyder selectivity triangular experimental design [9], binary mixtures of buffered methanol, buffered acetonitrile and buffered 2-propanol were chosen to represent the three vertices of the triangle. At the same time, four other experimental points were strategically chosen on the triangular resolution plot. The locations of the seven experiments in this triangular plot are shown in Fig. 2. It should be noted that the choice of the three modifiers for this work was largely based on the consideration that a wide range of selectivity can be achieved using the combination of these three modifiers [9].

In order to determine the appropriate solvent strength [10] required for the system, the proportion of methanol in the binary mixture representing the first vertex was adjusted until the retention time of the last-elution peak was within the pre-set limit (capacity factor not more than 20). It was found that a mobile phase composition of 74% (v/v) of methanol in the buffer gave

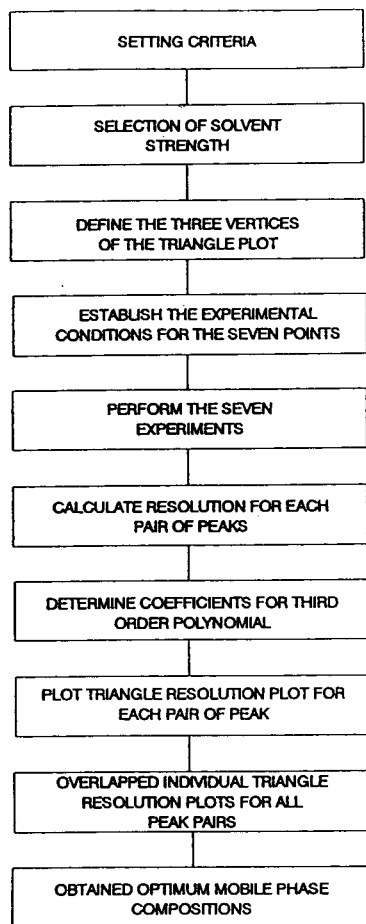


Fig. 1. Schematic diagram of the ORM scheme.

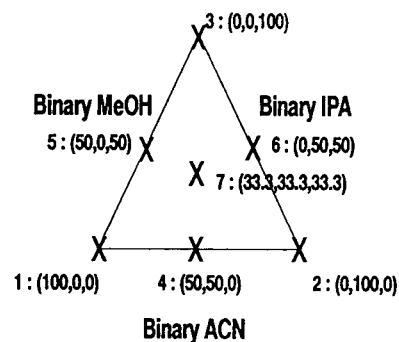


Fig. 2. Triangle plot showing composition portion of mobile phase consisting of mixtures of binary solvents (buffered methanol, buffered acetonitrile, buffered 2-propanol).

Table 1
Eluent mixtures used in the seven preliminary experiments

Experimental point No.	Methanol	Acetonitrile	2-Propanol	Buffer ^a
1	74.0	0.0	0.0	26.0
2	0.0	71.6	0.0	28.4
3	0.0	0.0	52.9	47.1
4	37.0	35.8	0.0	27.2
5	37.0	0.0	26.5	36.6
6	0.0	35.8	26.5	37.7
7	24.7	23.9	17.6	33.8

^a 0.02 M sodium dihydrogenphosphate adjusted to pH 5.4 with 50% (v/v) sodium hydroxide.

retention times which satisfied this criterion (capacity factor within the limit) and was thus chosen to represent one of the vertices. It should be emphasized that at this stage of the ORM scheme there is no requirement to ensure that solvent strength selected must meet the resolution criterion. Based on this composition, the solvent strength of the system was known. The solvent strength found was then utilized to calculate the compositions of the other two binary mixtures at the other two vertices. Similarly, the modifier compositions at the remaining four experimental points of the triangle in Fig. 2 were calculated. Table 1 shows the mobile phase compositions of the seven experimental points.

Experiments based on Table 1 were conducted and the results of these seven preliminary experiments are given in Table 2. From these results, the resolution between adjacent peaks, R , could be calculated and they are given in Table 3.

Subsequently, the R values of each pair of peaks over the seven sets of experiments were fitted into a third-order polynomial:

$$R = a_1x_1 + a_2x_2 + a_3x_3 + a_{12}x_1x_2 + a_{23}x_2x_3 + a_{13}x_1x_3 + a_{123}x_1x_2x_3$$

where a_i are constants and x_i are the proportion of binary mixture (modifier and buffer) at the respective positions on the triangular plot shown in Fig. 2.

With the aid of a modified version of the Basic program given in Ref. [10], the constants for each pair of peaks were determined. Sub-

sequently, the R values at other mobile phase compositions besides the seven experiment points were calculated using the above equation. These R values were then used to construct the triangular resolution plots. As there were three pairs of adjacent peaks, three resolution plots were obtained. A typical resolution plot for one of these pairs is shown in Fig. 3. From Fig. 3, it

Table 2
Retention times (min) using the seven eluents listed in Table 1

Experimental point No.	GDL1	GDL2	DS1	GDL3
1	3.792	8.903	4.642	26.175
2	2.918	12.628	4.308	28.557
3	3.145	5.812	5.812	43.082
4	3.357	5.873	10.573	13.408
5	3.343	6.253	4.565	32.378
6	2.892	4.142	3.267	15.475
7	3.123	4.512	3.365	14.958

Table 3
Resolution, R , between adjacent peaks

Experimental point No.	Peak pair 1–2	Peak pair 2–3	Peak pair 3–4
1	0.906	1.433	1.540
2	1.805	1.809	1.459
3	1.053	0.065	2.242
4	0.753	2.172	1.854
5	1.016	0.495	1.963
6	0.889	0.852	1.913
7	0.645	1.229	2.123

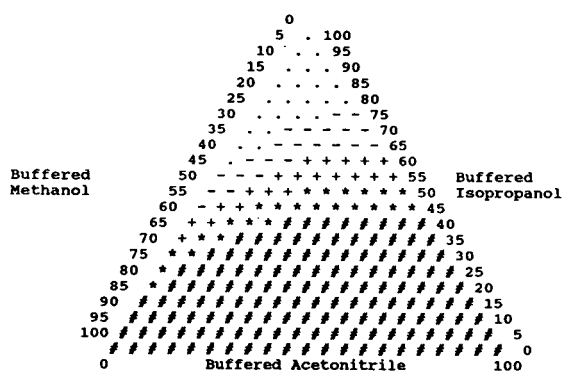


Fig. 3. Typical triangle resolution plot for a particular peak pair, where $\cdot = R \leq 0.4$; $- = 0.4 < R \leq 0.6$; $+ = 0.6 < R \leq 0.8$; $* = 0.8 < R \leq 1.0$; and $\# = R > 1.0$.

can be seen that the resolution plot is divided into regions. Each of these regions is characterized by a symbol which gives the expected resolution range/value for that particular pair of peaks at the mobile phase composition concerned. In other words, for a mobile phase composition found in the region marked #, the separation is expected to have a resolution equal to or greater than unity for that particular pair of peaks. Therefore, by overlapping all the three triangular resolution plots and retaining the minimum resolution values, the mobile phase compositions which could provide resolution equal to or greater than unity for all four peaks in the mixture could also be determined. The overlapped triangular plot is shown in Fig. 4.

To confirm the success of the ORM optimization procedure, an additional experiment using one of the mobile phase compositions in the optimum region (marked A in Fig. 4) was performed to verify that a satisfactory separation of all the peaks could be achieved. This corresponds to a mobile phase composition of acetonitrile–methanol–2-propanol–buffer (50:15:5:30, v/v). The chromatogram obtained using this mobile phase is shown in Fig. 5. A satisfactory separation was achieved and the resolution of all the peaks exceeded 1.5.

To demonstrate further the usefulness of the ORM scheme and to validate the methodology developed, a series of experiments were per-

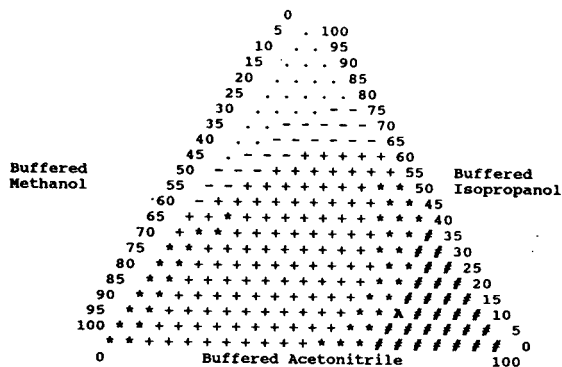


Fig. 4. Overlapped triangle resolution plot for all peak pairs, where $\cdot = R \leq 0.4$; $- = 0.4 < R \leq 0.6$; $+ = 0.6 < R \leq 0.8$; $* = 0.8 < R \leq 1.0$; and $\# = R > 1.0$.

formed. First, to demonstrate the ruggedness of the method, the same mobile phase was employed with another C_{18} column (column II). The results obtained are shown in Fig. 6. It can be seen that a satisfactory separation of all the peaks was achieved with a resolution greater than 1.5 for all the peaks. In addition, the precision, selectivity and linearity of the method were determined. The results obtained in the precision and linearity study are summarized in Table 4. It can be seen that highly reproducible results (R.S.D. not greater than 0.25%) are achievable using this method. The linearity study also yielded satisfactory results, R^2 values greater than 0.99 being obtained for all four compounds.

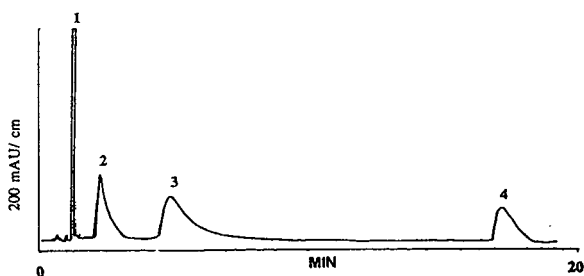


Fig. 5. Chromatogram of DS1 and its related impurities. Conditions: mobile phase, acetonitrile–methanol–2-propanol–0.02 M NaH_2PO_4 (50:15:5:30, v/v); flow-rate, 1.0 ml/min; column, I. Peak identification: 1 = GDL1; 2 = DS1; 3 = GDL2; 4 = GDL3.

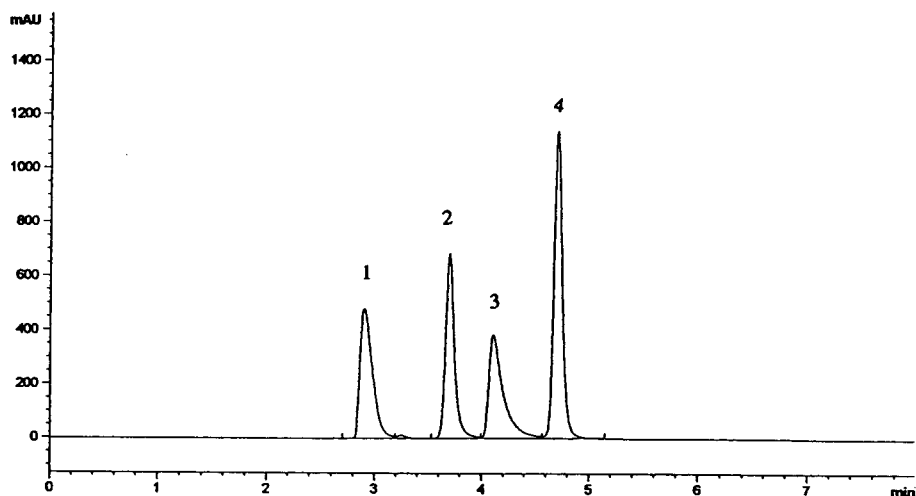


Fig. 6. Chromatogram of DS1 and its related impurities. Conditions: mobile phase, acetonitrile–methanol–2-propanol–0.02 M NaH_2PO_4 (50:15:5:30, v/v); flow-rate, 1.0 ml/min; column, II. Peak identification: 1 = GDL1; 2 = DS1; 3 = GDL2; 4 = GDL3.

4. Conclusions

The use of a systematic scheme for the optimization of the HPLC separation of a group of pharmaceuticals was demonstrated. The scheme required seven pre-planned experiments located on a triangular resolution plot. The optimization procedure was systematic, simple to use and capable of locating global optimum conditions for separations involving complex mobile phase systems. In addition, once the optimum con-

ditions had been established, satisfactory separation was also obtained even when another column with the same type of stationary phase was used.

References

- [1] A. Aszalos (Editor), *Modern Analysis of Antibiotics*, Marcel Dekker, New York, 1986, Ch. 7, p. 239.
- [2] W.T. Wahyuni and K. Jinno, *J. High Resolut. Chromatogr. Chromatogr. Commun.*, 10 (1987) 687.
- [3] G. Baier, G. Wollensak, E. Mur, B. Redl, G. Stoffler and W. Gottinger, *J. Chromatogr.*, 525 (1990) 319.
- [4] G. Werner, V. Schneider and J. Emmert, *J. Chromatogr.*, 525 (1990) 265.
- [5] J.A. Palasota, J.M. Palasota, H.L. Chang and S.N. Deming, *Anal. Chim. Acta*, 270 (1992) 101.
- [6] S. Heinisch, P. Riviere and J.L. Rocca, *Chromatographia*, 36 (1993) 157.
- [7] K.D. Altria, *Chromatographia*, 35 (1993) 177.
- [8] S.F.Y. Li, H.K. Lee and C.P. Ong, *J. Chromatogr.*, 506 (1990) 245.
- [9] L.R. Snyder, *J. Chromatogr. Sci.*, 16 (1978) 223.
- [10] J.C. Berridge, *Techniques for the Automated Optimization of HPLC Separations*, Wiley, Chichester, 1985.

Table 4
Precision and R^2 values for the four compounds

Compound	R.S.D. (%) ^a		R^2 ^b
	Retention time	Area	
GDL1	0.10	0.11	0.997
DS1	0.11	0.11	0.999
GDL2	0.15	0.14	0.999
GDL3	0.12	0.21	0.999

^a $n = 5$.

^b From 1.0 to 0.2% (w/w).



ELSEVIER

Journal of Chromatography A, 692 (1995) 213–219

JOURNAL OF
CHROMATOGRAPHY A

Preparative high-performance liquid chromatography for the purification of natural anthocyanins

Maurizio Fiorini

Istituto di Merceologia, Università di Bologna, Piazza Scaravilli 2, 40126 Bologna, Italy

Abstract

Preparative HPLC was applied to the purification of anthocyanins from raw extracts of strawberry, elderberry, eggplant and radish and from encyanin. For each separation, the chromatographic conditions were optimized to achieve an efficient purification in the shortest time. The anthocyanins isolated were compared with reference standards, whenever they were available. In addition, UV-visible characterization was carried out on all the anthocyanins purified. Determination of the complete structure of acylated anthocyanins will require further support from fast atom bombardment MS and NMR analyses, which are in progress.

1. Introduction

Anthocyanins are a widely distributed class of natural pigments, as they are found in many flowers and fruits, where they impart brilliant red and blue colours [1]. For example, the colours of berry fruits, such as strawberry, bilberry and cranberry, are due to many different anthocyanins. Having been eaten for thousands of years without any apparent adverse effects on human health, anthocyanins have attracted the interest of many food scientists and technologists when synthetic food colourants, many of the red type, have been questioned because of their adverse health effects and progressively banned from food composition. Unfortunately, anthocyanins are far less stable than synthetic dyes and undergo structural transformations which end up with loss of colour, especially under pH conditions typically found in many foods and drinks to which anthocyanins would have to be added. For this reason, they have been the subject of

many studies addressing the problem of their stability.

We have focused particularly on the study of colour changes undergone by anthocyanins [2] and from the beginning we faced the problem of the limited commercial availability of pure anthocyanins. As analytical HPLC had been proved to be very effective for the identification of anthocyanins in many natural sources [3–8], preparative HPLC seemed to be the right tool to isolate the needed anthocyanins at the high degree of purity desired. In contrast to analytical HPLC, preparative HPLC has received less attention. Teharara and co-workers [9,10] and Sen Lu et al. [11] used preparative HPLC for the purification of acylated anthocyanins from some species of flowers, while Shi and co-workers purified acylated anthocyanins from stems and leaves of *Tradescantia* [12,13] and from sweet potato [14], in the view of their potential use as food colourants.

We started by studying the simple 3-glucoside

of the most common anthocyanidins, namely delphinidin (Dp), cyanidin (Cy), pelargonidin (Pg), petunidin (Pt), peonidin (Pn) and malvidin (Mv). Enocyanin, a concentrate from red grape skins, is known to contain the 3-glucosides of Dp, Cy, Pt, Pn and Mv, while strawberry was chosen as the source of Pg-3-glucoside. Elderberry was chosen owing to its higher Cy-3-glucoside content compared with enocyanin, and because anthocyanins with two and three sugar moieties could be isolated [8].

After the first results showing the limited colour stability of simple 3-glucosides [2], the acylated anthocyanins were chosen for further investigation. For this reason, we studied the purification of pigments extracted from eggplant and radish. This paper reports the results of preparative HPLC on the above-mentioned extracts.

2. Experimental

2.1. Materials

Frozen strawberries were purchased at a local supermarket. Eggplant and radish were purchased at a local grocery. Elderberries were collected from bushes in a public garden during September 1991 and stored at -20°C until used. Enocyanin was a gift from Enocanossa (Ciano d'Enza, Italy).

Some anthocyanins were purchased in limited amounts from Extrasynthèse (Génay, France), viz., Pg-3-glucoside, Cy-3-glucoside and 3,5-diglucoside, Pr-3-glucoside and Mv-3-glucoside.

2.2. Pigment extraction

Frozen strawberries (2500 g) were thawed and mixed in a food mixer for 5 min and the pomace obtained was filtered, yielding 1500 ml of clear extract. The residue was extracted three times with 100 ml of methanol (Merck, Darmstadt, Germany) containing 0.01 mol l^{-1} hydrochloric acid (Aldrich, Milwaukee, WI, USA). The methanolic extracts were concentrated under reduced pressure, then mixed with the aqueous

extract. As a first purification step, pigments were adsorbed on a column ($20 \times 2.5 \text{ cm I.D.}$) filled with Amberlite GC-50 ion-exchange resin (Aldrich), then the column was washed with HCl at pH 2 and finally the pigments were eluted with methanol containing 0.01 mol l^{-1} HCl. The eluate was concentrated under reduced pressure and then freeze-dried, yielding 1.2 g of dried extract, to be further purified by preparative HPLC.

Elderberries (650 g) were blended in a food mixer and the pomace obtained was extracted overnight with methanol containing 0.01 mol l^{-1} HCl (300 ml). After filtration, the solution was concentrated under reduced pressure and then freeze-dried, resulting in 1.8 g of extract.

Enocyanin (50 g) was extracted with 100 ml of 0.01 mol l^{-1} HCl in methanol with magnetic stirring for several hours. The residue was filtered and extracted several times until the solvent was almost colourless. The total volume of acid methanol, 500 ml, was reduced to 100 ml by distillation under reduced pressure and pigments were precipitated with 800 ml of diethyl ether. The precipitation step was then repeated, resulting in 15 g of purified pigment mixture.

Eggplants (1120 g) were peeled, obtaining 87 g of skin, which was cut into small pieces and extracted with 250 ml of formic acid in water (5%, v/v) overnight at 4°C . After filtration, the extract was adsorbed on a Sep-Pak Vac C_{18} cartridge (Waters, Milford, MA, USA), containing 10 g of packing material. The column was washed five times with 20 ml of HCl at pH 1 and dried under vacuum and the pigments were eluted with 25 ml of methanol containing 0.025 g of HCl. After concentration and freeze-drying, 0.48 g of pigment mixture was obtained.

Radishes (900 g) were peeled, yielding 100 g of skin, which was extracted under the conditions used for eggplant; 0.42 g of mixed pigments was obtained.

Tradescantia leaves (4 g) were chopped with scissors, suspended in 50 ml of formic acid solution, treated in a Ultra-Turrax homogenizer (Janke and Kukkal, Staufen Germany) and extracted overnight at 4°C . The filtered extract was adsorbed on a Sep-Pak Vac C_{18} cartridge (2 g),

then the column was washed with 25 ml of HCl at pH 1 and then dried by suction. The pigments were eluted with 3 ml of methanol–water 80:20 (v/v). In this preliminary trial, no quantification was made on the purified extract, owing to the very limited quantity of leaves available.

2.3. Instrumentation and conditions

The chromatographic system was composed of two Model 510 pumps, a model 481 variable-wavelength UV–Vis detector, a Model 730 integrator and a Model 721 system controller (all from Waters). Injections were carried out with a Model 7725i injector (Rheodyne, Cotati, CA, USA) equipped with a 20- μ l loop for analytical HPLC and a 1-ml loop for preparative work.

The analytical column was a Spherisorb ODS-2 (250 \times 4.6 mm I.D.) (Phase Separations, Deeside, Clwyd, UK), 10 μ m, pore size 80 Å; the flow-rate was set at 1 ml min⁻¹. The preparative column (250 \times 10 mm I.D.) with the same stationary phase was used at a flow-rate of 3 ml min⁻¹. For both columns, a μ -Bondapak C₁₈ guard insert column (Waters) was used. Both columns were operated at room temperature.

The mobile phase was composed of 5% formic acid (pH 2.2 at 20°C) and methanol, in different ratios according to the separation needs. The acid concentration was chosen so that the pH of this solution obtained was a good compromise between the need to avoid too low a pH to hydrolyse silica-ODS bonds while maintaining anthocyanins in the highly coloured flavilium ion form, to enhance detection at 500–530 nm. The organic and aqueous phases were degassed by filtration through 0.45- μ m membranes (Millipore, Bedford, MA, USA) under vacuum.

The elution conditions were as follows.

Strawberry: analytical runs, 0–10 min 30% methanol, 10–20 min from 30 to 35% methanol, 20–25 min from 35 to 45%, held constant up to 30 min; preparative runs, isocratic with 35% methanol. A 5-mg amount was injected in each run.

Elderberry: analytical runs, 0–17 min 27% methanol, 17–30 min from 27 to 50% methanol;

preparative runs, isocratic with 30% methanol. An 18-mg amount was injected in each run.

Encyanin: analytical runs, 0–10 min from 30 to 35% methanol, 10–18 min from 35 to 40% methanol, held constant up to 22 min, 22–25 min from 40 to 45% methanol, held constant up to 30 min; preparative runs, 0–15 min 30% methanol, 15–25 min from 30 to 40% methanol, 25–30 min from 40 to 50% methanol. A 10-mg amount was injected in each run.

Radish: analytical runs, 0–20 min from 35 to 45% methanol, 20–25 min from 45 to 55% methanol, held constant up to 30 min; preparative runs, 0–10 min 40% methanol, 10–25 min from 40 to 50% methanol, held constant up to 30 min. A 5-mg amount was injected in each run.

Eggplant: analytical runs, 0–4 min 25% methanol, 4–25 min from 25 to 35% methanol, 25–30 min from 35 to 50% methanol, held constant up to 35 min; preparative runs, isocratic with 25% methanol. A 5-mg amount was injected in each run.

All gradient steps were linear.

UV–visible spectra were recorded on a Lambda 15 spectrophotometer (Perkin-Elmer, Norwalk, CT, USA) in 1-cm quartz cells, using 0.01% (v/v) HCl in methanol as solvent.

3. Results and discussion

Results obtained from the purification of the different raw extracts are reported in separate tables, along with the UV–visible data. Retention times reported in Tables 1–5 were obtained on the analytical column.

3.1. Strawberry

The three more abundant anthocyanins found in strawberry extract were isolated and characterized as reported in Table 1. F1 and F2 were compared with authentic samples and were identified without uncertainty as Cy-3-glucoside and Pg-3-glucoside, respectively, while the identification of F3 as Pg-3-arabioside was based on UV–Vis data, which show that the aglycone is

Table 1
Characterization of the three more abundant anthocyanins isolated from strawberry

Peak No.	Anthocyanin	t_R (min) ^a	Concentration in raw extract (%) ^b	Purity % ^b	UV-visible characterization				
					λ_{max} (nm)	E_{UV}/E_{vis} (%)	E_{acyl}/E_{vis} (%)	E_{440}/E_{vis} (%)	Shift with AlCl ₃ (nm)
F1	Cy-3-glucoside	14.15	2.2	95.0	281, 524	75	–	22	19
F2	Pg-3-glucoside	19.02	90.0	99.0	270, 508	63	–	38	None
F3	Pg-3-arabinoside ^c	23.18	4.2	95.0	270, 511	81	–	40	None

^a Retention times refer to the separation on the analytical column.

^b Calculated from the ratio of the peak area to the total area of peaks corresponding to anthocyanins.

^c Tentative identification based on spectral characterization and chromatographic behaviour.

pelargonidin, and on the later elution of 3-arabinoside with respect to 3-glucoside [4].

The maximum amount of extract that could be purified in a single run on the preparative column was 5 mg. Injections of larger amounts resulted in strong distortion of Pg-3-glucoside peak, which started to overlap with the Pg-3-arabinoside peak with a consequent loss of separation.

3.2. Encyanin

Table 2 summarizes the characterization data obtained for the fractions isolated from encyanin. The UV-Vis data are in good agreement with those reported in the literature [15,16]. The encyanin sample used in this study contained very limited amounts of diglucosides and acylated pigments which would have preceded Dp-3-glucoside (the former) and followed

Mv-3-glucoside (the latter). This observation suggests the use of *Vitis vinifera* berries as the starting material for preparing the pigment concentrate.

3.3. Elderberry

Table 3 reports the results of the purification and characterization of pigments from elderberry. The purity of Cy-3-glucoside and Cy-3-sambubioside was not as high as expected. The separation of these two anthocyanins with methanol as organic solvent is then difficult; the same problem has been reported by other workers using acetonitrile [4]. Brønnum-Hansen and Hansen [8] reported on this separation carried out with tetrahydrofuran as a substitute for methanol. It should be noted that the comparison between the composition reported by Brønnum-Hansen and Hansen [8] and that reported

Table 2
Characterization of anthocyanins isolated from encyanin

Peak No.	Anthocyanin	t_R (min) ^a	Concentration in raw extract (%) ^b	Purity % ^b	UV-visible characterization				
					λ_{max} (nm)	E_{UV}/E_{vis} (%)	E_{acyl}/E_{vis} (%)	E_{440}/E_{vis} (%)	Shift with AlCl ₃ (nm)
E1	Dp-3-glucoside	10.46	17.4	99.5	279, 540	62	–	20	45
E2	Cy-3-glucoside	13.45	3.7	96.0	281, 530	66	–	22	35
E3	Pt-3-glucoside	15.64	20.9	98.5	279, 539	63	–	20	46
E4	Pn-3-glucoside	19.15	5.8	93.5	280, 529	64	–	26	None
E5	Mv-3-glucoside	20.63	45.8	99.6	278, 540	58	–	20	None

^{a,b} See Table 1.

Table 3
Characterization of anthocyanins isolated from elderberry

Peak No.	Anthocyanin	t_R (min) ^a	Concentration in raw extract (%) ^b	Purity % ^b	UV-visible characterization				
					λ_{max} (nm)	E_{UV}/E_{vis} (%)	E_{acyl}/E_{vis} (%)	E_{440}/E_{vis} (%)	Shift with AlCl ₃ (nm)
S1	Cy-3,5-diglucoside	6.70	15.7	99.7	279, 526	56	—	14	37
S2	Cy-3-sambubioside	16.62	59.8	94.0	282, 529	58	—	22	34
S3	Cy-3-glucoside	17.83	20.4	90.7	282, 529	60	—	23	36

^{a,b} See Table 1.

here reveals a higher content of Cy-3,5-diglucoside in our sample (15.7% instead of 0.8%).

3.4. Radish

Radish extract was purified to obtain acylated anthocyanin. Fig. 1 shows the chromatograms of radish extract before and after a mild alkaline treatment by which acyl acids are selectively removed from sugars [17]. It appears clearly that the three main anthocyanin in radish extract are acylated, along with at least other four minor pigments. The preparative purification was then directed to the isolation of the three main anthocyanins and the more abundant of the four minor anthocyanins.

Table 4 gives the characterization data for the purified radish anthocyanins. The high values of E_{acyl}/E_{vis} ratios and the comparison between the chromatograms obtained before and after the

mild alkaline hydrolysis of each pigment after purification confirmed the presence of acyl acids. The UV-vis data also suggest that Pg is the aglycone in all the pigments and this was further confirmed by comparing the chromatogram of an authentic Pg sample (obtained from the acid hydrolysis of Pg-3-glucoside) with the chromatograms of purified pigments R1–R4 after the same treatment [18]. The values of the E_{440}/E_{vis} ratios compare well with those published for Pg pigments substituted at the 3- and 5-positions [19].

The identification of the different anthocyanins is made more complex by the absence of reference standards. The determination of sugar/aglycone ratios and of sugars and acyl acids is in progress but the complete structures will have to be confirmed by fast atom bombardment (FAB) MS and NMR studies, in order to determine the exact position of sugar-aglycone and acyl acid-

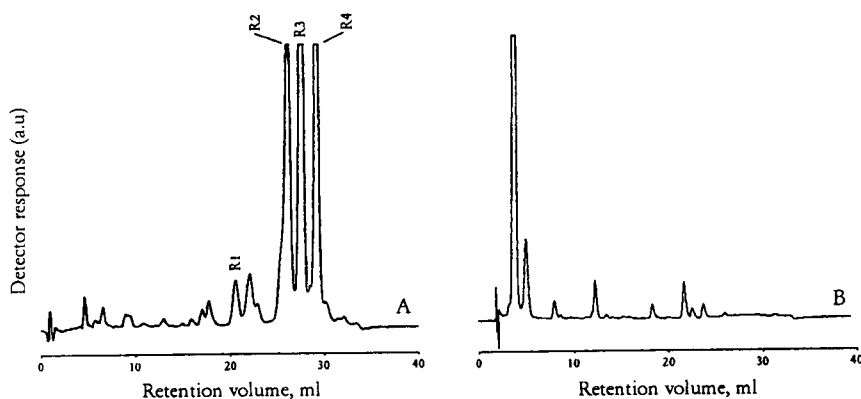


Fig. 1. Chromatograms obtained with the analytical column for radish extract. (A) Raw extract as such; (B) extract after mild alkaline hydrolysis. Peaks are labelled according to Table 4.

Table 4
Characterization of anthocyanins isolated from radish

Peak No.	Anthocyanin	t_R (min) ^a	Concentration in raw extract (%) ^b	Purity % ^b	UV-visible characterization				
					λ_{max} (nm)	E_{UV}/E_{vis} (%)	E_{acyl}/E_{vis} (%)	E_{440}/E_{vis} (%)	Shift with AlCl ₃ (nm)
R1	Pg-3,5-diglycoside, acylated ^c	20.71	3.1	92.1	279,328,509	78	68	20	None
R2	Pg-3,5-diglycoside, acylated ^c	26.30	25.3	91.4	286,317,507	77	64	20	None
R3	Pg-3,5-diglycoside, acylated ^c	27.75	38.0	94.1	286,318,508	72	58	19	None
R4	Pg-3,5-diglycoside, acylated ^c	29.36	26.0	92.0	287,318,508	72	59	19	None

^{a-c} See Table 1.

sugar linkages. At present a tentative identification based on the few literature data available [20] suggests that R2, R3 and R4 are Pg-5-glucoside-3-diglucosides acylated with caffeic, ferulic and coumaric acid, respectively.

3.5. Eggplant

Fig. 2 shows the chromatograms of a raw eggplant extract before and after mild alkaline treatment. Eggplant extract purification was also carried out to obtain acylated anthocyanins, but it turned out that they were just a minor fraction in the pigment mixture. It was known from the

literature that eggplant varieties harvested in Japan contain mainly highly acylated anthocyanins [21,22], whereas varieties from other countries contain no acylated pigments at all [23]. The variety used in this study is intermediate, but in any case it is not a good source of acylated anthocyanins.

Table 5 reports the characterization data for the two fractions isolated. The aglycone is Dp for both fractions, as suggested by UV-vis data and confirmed by comparison with a chromatogram of an authentic Dp sample obtained from Dp-3-glucoside.

The E_{440}/E_{vis} ratio for M1 is in good agree-

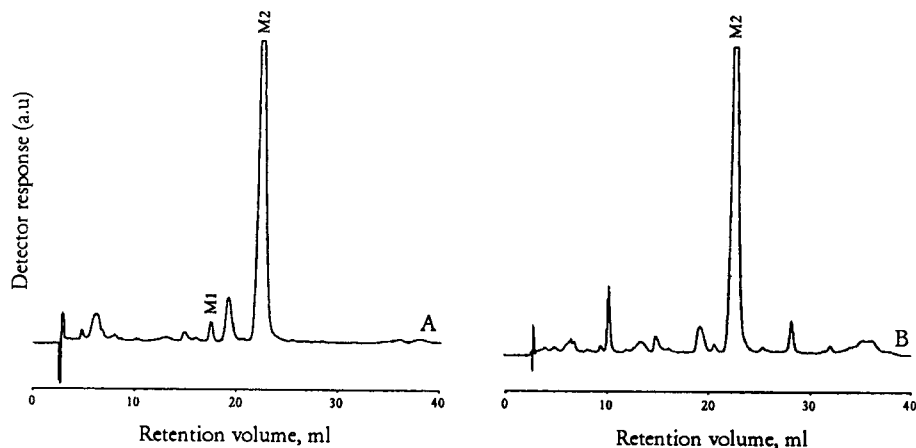


Fig. 2. Chromatograms obtained with the analytical column for eggplant extract. (A) Raw extract as such; (B) extract after mild alkaline hydrolysis. Peaks are labelled according to Table 5.

Table 5
Characterization of anthocyanins isolated from eggplant

Peak No.	Anthocyanin	t_R (min) ^a	Concentration in raw extract (%) ^b	Purity % ^b	UV-visible characterization				
					λ_{max} (nm)	E_{UV}/E_{vis} (%)	E_{acyl}/E_{vis} (%)	E_{440}/E_{vis} (%)	Shift with AlCl ₃ (nm)
M1	Dp-3,5-diglucoside, acylated ^c	17.53	7.5	97.1	281,323,540	80	80	11	48
M2	Dp-3-arabinoside ^c	22.47	87.0	95.0	283,542	75	–	17	46

^{a-c} See Table 1.

ment with the value reported for Dp-3,5-diglucoside [18], so that M1 can be an acylated derivative of such an anthocyanin, whereas the value for M2 is the same as that reported for a Dp-3-glycoside. As M2 is eluted after Dp-3-glucoside, the sugar in M2 could be arabinose, but further evidence is needed to support this suggestion.

In conclusion, it has been shown that preparative HPLC is an efficient method to isolate pure anthocyanins, either simple monoglucosides or more complex acylated di- and triglycosides, from natural sources. For these more complex types of pigments, the lack of reference standards makes identification difficult and further evidence from FAB-MS and NMR spectroscopy is needed. Such experiments are in progress, along with the identification of sugars and acyl acids.

Acknowledgement

Financial support from Regione Emilia-Romagna, Assessorato Agricoltura e Alimentazione, is gratefully acknowledged.

References

- [1] J.B. Harborne, *The Comparative Biochemistry of the Flavonoids*, Academic Press, New York, 1967.
- [2] M. Fiorini and G. Barbiroli, in A. Nemcsics and J. Schanda (Editors), *Proceedings of the 7th Congress of the International Colour Association, Budapest, June 1993*, Hungarian Colour Committee, Budapest, 1993, p. 235.
- [3] H.S. Lee and V. Hong, *J. Chromatogr.*, 624 (1992) 371.
- [4] J.P. Goiffon, M. Brun and M.J. Bourrier, *J. Chromatogr.*, 537 (1991) 101.
- [5] V. Hong and R.E. Wrolstad, *J. Agric. Food. Chem.*, 38 (1990) 708.
- [6] V. Hong and R.E. Wrolstad, *J. Agric. Food. Chem.*, 38 (1990) 698.
- [7] A. Baj, E. Bombardelli, B. Gabetta and E.M. Martinelli, *J. Chromatogr.*, 279 (1983) 365.
- [8] K. Brønnum-Hansen and J.H. Hansen, *J. Chromatogr.*, 262 (1983) 385.
- [9] N. Terahara, K. Toki and T. Honda, *Z. Naturforsch.*, C, 48 (1993) 430.
- [10] N. Terahara, K. Toki, N. Saito, T. Honda, T. Isono, H. Furumoto and Y. Kontani, *J. Chem. Soc., Perkin Trans. 1*, (1990) 3327.
- [11] T. Sen Lu, N. Saito, M. Yokoi, A. Shigihara and T. Honda, *Phytochemistry*, 31 (1992) 659.
- [12] Z. Shi, M. Lin and F.J. Francis, *J. Food Sci.*, 57 (1992) 761.
- [13] M. Lin, Z. Shi, and F.J. Francis *J. Food Sci.*, 57 (1992) 766.
- [14] Z. Shi, I.A. Bassa, S.L. Gabriel and F.J. Francis, *J. Food Sci.*, 57 (1992) 755.
- [15] J.B. Harborne, *J. Chromatogr.*, 1 (1958) 473.
- [16] J.B. Harborne, *Biochem. J.*, 74 (1958) 262.
- [17] B.V. Chandler and K.A. Harper, *Aust. J. Chem.*, 14 (1961) 586.
- [18] F.J. Francis, in P. Markakis (Editor), *Anthocyanins as Food Colors*, Academic Press, New York, 1982, Ch. 7, p. 184.
- [19] F.J. Francis, in P. Markakis (Editor), *Anthocyanins as Food Colors*, Academic Press, New York, 1982, Ch. 7, p. 187.
- [20] T. Fuleki, *J. Food Sci.*, 34 (1969) 365.
- [21] S. Sakamura, S. Watanabe and Y. Obata, *Agric. Biol. Chem.*, 27 (1963) 663.
- [22] S. Sakamura, S. Watanabe and Y. Obata, *Agric. Biol. Chem.*, 30 (1966) 420.
- [23] S.S. Tanchev, P.J. Ruskov and C.F. Timberlake, *Phytochemistry*, 9 (1970) 1681.



ELSEVIER

Journal of Chromatography A, 692 (1995) 221–232

JOURNAL OF
CHROMATOGRAPHY A

Compositional distribution characterization of poly(methyl methacrylate)–graft-polydimethylsiloxane copolymers

Timothy C. Schunk^{a,*}, Timothy E. Long^b

^a*Analytical Technology Division, Research Laboratories, Eastman Kodak Company, Rochester, NY 14650-2136, USA*

^b*Polymer Research, Eastman Chemical Company, Kingsport, TN 37662, USA*

Abstract

Graft copolymers prepared by radical polymerization of a low-molecular-mass monomer with a macromonomer display heterogeneity in both molecular mass and chemical composition. The characterization of these joint distributions by a single technique [e.g., size-exclusion chromatography (SEC)] is hindered by the effects of both variables on the separation mechanism. Separation emphasizing chemical composition heterogeneity can be efficiently performed by gradient elution high-performance liquid chromatography (HPLC) combining precipitation and adsorption retention. Comparison of Fourier transform IR and evaporative light-scattering detection indicated decreasing polydimethylsiloxane (PDMS) macromonomer incorporation corresponding to increasing retention time for a poly(methyl methacrylate) (PMMA)–graft-PDMS copolymer. More detailed information was obtained by multidetector SEC of composition fractions from gradient elution HPLC. SEC separation in an isorefractive solvent for PDMS (tetrahydrofuran) with low-angle laser-light scattering, differential viscometry, and differential refractive index detection allowed determination of the molecular mass of both the whole copolymer and that of the PMMA backbone for each HPLC fraction. Comparison with an independent SEC determination of the PDMS macromonomer molecular mass allowed estimation of the number of pendant PDMS chains per graft copolymer molecule across the HPLC chromatogram. Results indicated a relatively constant incorporation of the number of PDMS side chains with increasing PMMA backbone molecular mass, leading to a relative decrease in weight fraction PDMS incorporation with increasing molecular mass of the whole graft copolymer molecule.

1. Introduction

Graft copolymers are branched macromolecules with a backbone composed of one type of polymer and side chains (grafts) of another polymer. Several approaches have become common for the synthesis of graft copolymers with most falling into three categories: grafting-onto, grafting-from and the macromonomer technique. Grafting-onto reactions proceed by the reaction of a terminal group on the side-chain polymer

with reactive functionalities distributed along the backbone polymer. Grafting-from reactions require the growth of polymer side chains from initiating sites on a backbone polymer by the polymerization of a low-molecular-mass monomer. Finally, the macromonomer technique employs the incorporation of a terminal polymerizable group on the eventual side-chain polymer into a growing backbone polymer during the polymerization of a low-molecular-mass monomer [1].

There are several advantages to the use of the macromonomer technique over the other two

* Corresponding author.

approaches which have attracted increasing interest in recent years [2,3]. A relatively large number of different macromonomers are available with convenient polymerizable terminal groups, allowing access to a wide range of copolymer compositions [4]. Living polymerization methods can be used to provide macromonomers of well-defined chain length, molecular mass distribution, and terminal functionality [5,6]. Macromonomers allow control of the number of grafts per copolymer macromolecule through choice of the polymerization reaction mixture ratio of macromonomer to low-molecular-mass monomer [4].

The chemical and physical properties of graft copolymers can be tailored to suit various applications by choice of the different chemical compositions of the copolymer backbone and side chain. In many cases the copolymer segments are immiscible in the solid phase leading to unique thermal, mechanical, and interfacial properties similar to diblock copolymers [7]. The tailoring of these chemical and physical properties has led to the application of graft copolymers as emulsifiers, surface modifiers, thermoplastic elastomers, and polymer blend compatibilizers [8].

The performance of these tailored graft copolymers is in part dependent upon the choice of the constituent polymers and their molecular mass, but also on the distributions in molecular mass and chemical composition present in the final graft copolymer. It is common for a graft copolymer sample to contain both ungrafted backbone and side-chain homopolymers, as well as a range of copolymer compositions [9]. As with any copolymer, the molecular mass and chemical composition of graft copolymers share a joint distribution in heterogeneity. Techniques such as size-exclusion chromatography (SEC) with selective detection cannot provide complete copolymer characterization due to the dependence of polymer hydrodynamic size on chemical composition. In addition, techniques such as solvent precipitation fractionation or fractional dissolution can be unreliable with graft copolymers due to their surface-active properties that can inhibit clean phase separation behavior [9–

11]. An alternative technique has been suggested recently by Stejskal et al. [12] for the separation of a graft copolymer into fractions for subsequent analysis. This approach involves fractionation in demixing solvents, which although effective can be quite time consuming and difficult to predict the separation dependence on molecular mass and chemical composition (see Table 3 of Ref. [12]).

The focus of the current experimental investigation was to provide a chemical composition separation of a graft copolymer into fractions suitable for SEC with molecular-mass-sensitive detection. The free-radical-polymerized graft (g) copolymer poly(methyl methacrylate)-g-polydimethylsiloxane (PMMA-g-PDMS) was separated by gradient elution HPLC into a series of chemical composition fractions. Chemical composition across the HPLC and SEC separations was evaluated by use of a solvent-evaporation Fourier transform infrared (FT-IR) interface. SEC of a series of HPLC fractions in a solvent isorefractive with the PDMS side chains allowed low-angle laser-light scattering (LALLS) determination of the molecular mass of the PMMA backbone polymer. Universal calibration with differential viscometry detection allowed determination of the overall molecular mass of each narrow composition graft copolymer fraction. With these data along with the molecular mass of the narrow-dispersity PDMS macromonomer, the number of side chains grafted on the PMMA backbone polymer was determined for each HPLC fraction.

2. Experimental

2.1. Synthesis

The PDMS macromonomer was prepared by anionic polymerization of hexamethylcyclotrisiloxane (Petrarch Systems, Bristol, PA, USA) in freshly distilled cyclohexane (Eastman Kodak, Rochester, NY, USA) with *sec*-butyllithium initiator (Lithco, Division of FMC, Philadelphia, PA, USA) and distilled tetrahydrofuran (THF) promoter (Fisher Scientific, Pittsburgh, PA,

USA). The polymerizable terminal functional group was formed by termination with [3-(methacryloxy)propyl]dimethylchlorosilane (Petrarch Systems) after 48 h polymerization. The PDMS macromonomer was then precipitated in methanol (Eastman Kodak) and dried under vacuum at 60°C.

PMMA-g-PDMS copolymer was prepared by free radical polymerization at 20% solids using the above macromonomer and methyl methacrylate [freshly distilled from calcium hydride (both Eastman Kodak Company)] in chlorobenzene (Aldrich, Milwaukee, WI, USA, distilled from phosphorus pentoxide (Eastman Kodak) under nitrogen) at 60°C with 2,2'-azobisisobutyronitrile initiator (Eastman Kodak). The polymerization feed ratio was 40% weight PDMS macromonomer. The isolated copolymer was extracted with *n*-hexane (Eastman Kodak) to remove excess PDMS macromonomer and dried under vacuum at 60°C. NMR analysis of the raw copolymer yielded an average value of 40% weight PDMS which was reduced to 32% weight after *n*-hexane extraction. NMR spectra were obtained with a General Electric QE300 300 MHz spectrometer (Fremont, CA, USA).

2.2. Gradient HPLC

Semipreparative-scale high-performance liquid chromatography (HPLC) separations were performed on a Varian Analytical Instruments (San Fernando, CA, USA) Model 5060 ternary gradient chromatograph with a LiChrospher Si100 10 μm silica 250 \times 4.6 mm column (EM Separations, Gibbstown, NJ, USA). Gradient elution separations were performed at 1.0 ml/min on 100- μl sample injections from 40 to 100% (v/v) solvent B in cyclohexane linear over 50 min followed by a 10-min hold. Solvent B was 10% (v/v) ethanol in toluene. No attempt was made to optimize the gradient shape beyond linear. Column void volume was determined as 2.45 ml and gradient pumping system lag volume 3.27 ml to the column inlet. Solvents were obtained from J.T. Baker (Phillipsburg, NJ, USA) (toluene and cyclohexane, HPLC grade) and Quantum Chemical (Tuscola, IL, USA) (absolute etha-

not). The eluent flow was split 20:1 to an ISCO (Lincoln, NE, USA) Model FOXY fraction collector and an Applied Chromatography Systems (Cheshire, UK) Model 750/14 evaporative light-scattering (ELS) detector with an evaporator temperature setting of 80 and nitrogen gas flow pressure of 25 p.s.i.g. (1 p.s.i. = 6894.76 Pa).

The solubility of a PMMA narrow standard (molecular mass $M_{\text{peak}} = 185\,000$) was evaluated in the HPLC solvent system (cyclohexane-toluene-ethanol) by a method similar to that of Ref. [13]. A stock solution of 10 mg/ml PMMA was prepared in ethanol-toluene (10:90) and subsequently used to prepare a series of 1.0 mg/ml solutions varying in cyclohexane content from 40% to 90% by volume. After standing overnight, 100- μl aliquots of these solutions were injected on the LiChrospher Si100 column with a 15 min linear gradient from 40 to 100% solvent B in cyclohexane. The peak area by ELS detection was plotted as a function of sample solvent concentration and the midpoint of 40.3% (v/v) cyclohexane determined as the solubility limit of PMMA in this solvent system.

Gradient elution HPLC separation with a solvent-evaporation FT-IR interface was performed on a Perkin-Elmer (Norwalk, CT, USA) Series 4 quaternary gradient chromatograph with the same column and solvent conditions as above. The solvent-evaporation FT-IR interface was of our own design, but similar to those of Dekmezian et al. [14] and Cheung and co-workers [15,16]. Copolymer fractions of 75 s duration starting at 20 min elution time were spray deposited onto 115°C 13 \times 2 mm polished germanium disks (Spectral Systems, Hopewell Junction, NY, USA) at 50 Torr (1 Torr = 133.322 Pa) in a 75°C chamber.

2.3. Size-exclusion chromatography

Graft copolymer SEC was performed on either of two systems. For copolymer analysis with the solvent-evaporation FT-IR interface, SEC separations were performed with a Perkin-Elmer Series 4 chromatograph on a three-column set of PLgel 10 μm 300 \times 7.5 mm mixed bed columns

(Polymer Labs., Amherst, MA, USA) at 1.0 ml/min freshly distilled THF (J.T. Baker) with 200- μ l injections of 3.0 mg/ml. Differential refractive index (DRI) detection was done using a Waters–Millipore (Milford, MA, USA) Model R401. The SEC column set was calibrated with narrow polystyrene (PS) standards and the log M –retention volume data fitted with a third-order polynomial. Copolymer fractions were deposited with the solvent-evaporation FT-IR interface on 100°C disks at 50 Torr in a 65°C chamber in 30-s increments starting at 17 min elution time. SEC with molecular-mass-sensitive detection was performed on a system described previously [17] using DRI, LALLS and differential viscometry detection with three PLgel 5 μ m 300 \times 7.5 mm mixed bed columns. Universal calibration was done with narrow PS standards ranging from 0.01 to 2.5 mg/ml decreasing with increasing molecular mass at minimum detectable concentrations.

SEC of the PDMS macromonomer in toluene (J.T. Baker) was at 1.0 ml/min on a three-column set of 10 μ m 300 \times 7.5 mm PLgel mixed bed columns. Detection was with a model R401 DRI detector from 200- μ l injections of 2.0 mg/ml samples and narrow PS standard calibration. PS equivalent weight average $\bar{M}_w = 12\,300$ and number average $\bar{M}_n = 10\,600$. Conversion to PDMS equivalent values with Mark–Houwink coefficients yielded $\bar{M}_w = 13\,100$ and $\bar{M}_n = 11\,400$. Mark–Houwink coefficients in toluene were PS: $K = 1.12 \cdot 10^{-4}$ dl/g, $\alpha = 0.722$ and PDMS: $K = 1.36 \cdot 10^{-4}$ dl/g, $\alpha = 0.69$.

2.4. Fourier transform infrared spectrometry

FT-IR spectra of the deposited copolymer fractions were obtained on a Mattson Polaris FT-IR spectrometer (Madison, WI, USA) with 16 scans at 4 cm^{-1} resolution. All copolymer film fractions were solvent annealed [16] with dichloromethane (J.T. Baker) vapor prior to FT-IR analysis. Quantitative calculations of copolymer fraction composition from FT-IR spectra were performed by a PLS-2 algorithm using GRAMS 386 software (Galactic Industries, Salem, NH, USA) and FT-IR calibration spectra

of solvent-cast films of molecular mass 130 000 PMMA and 265 000 PDMS standards (American Polymer Standards).

3. Results and discussion

Considerable discussion has appeared in the literature concerning chemical composition separations of copolymers by HPLC dominated either by precipitation/redissolution or adsorption phenomena [18–20]. The general goal is to obtain copolymer resolution based on chemical composition with as little confounding molecular mass resolution as possible. It is therefore desirable to take advantage of both precipitation and adsorption retention in a synergistic manner to obtain the required separation [13].

Precipitation HPLC is performed with the use of a gradient from a non-solvent to increasing percentages of a good solvent on a stationary phase possessing weak adsorption interactions for the copolymer. In many cases the effect of copolymer molecular mass is mixed with that of chemical composition in a precipitation HPLC separation [21]. In contrast, adsorption retention controls separation when the copolymer molecules are soluble in all solvent compositions during a gradient elution HPLC separation. Strong adsorption interactions on small-pore column packings provide copolymer retention resulting in composition separations with very little molecular mass influence [22].

Usually a compromise between copolymer solubility and chromatographic solvent strength range is required to obtain copolymer separation over a broad chemical composition distribution. At best a synergistic combination may be obtained which allows initial retention of copolymer molecules by precipitation in a non-solvent-rich eluent and subsequent adsorption retention interactions after the solubility limit has been exceeded during the gradient [13]. Such a system was employed for the gradient HPLC separation of a PMMA–g-PDMS copolymer sample by chemical composition as shown in Fig. 1.

The ELS detector signal (Fig. 1) provides a convenient method of observing the elution of

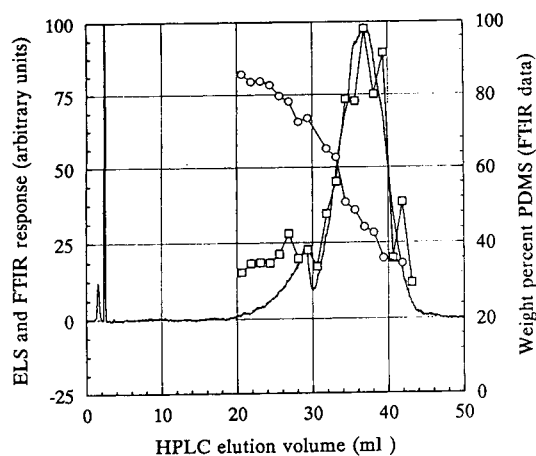


Fig. 1. Gradient elution HPLC chromatogram of a 1.0 mg injection of PMMA-g-PDMS copolymer. The evaporative light-scattering detection response (solid line) is overlaid on the total copolymer mass (□) (PMMA + PDMS) calculated from FT-IR spectra of solvent-evaporation interface deposited fractions. The weight percent PDMS incorporation values derived from the FT-IR spectra are shown as ○.

non-volatile copolymer components during a gradient HPLC separation without regard to analyte or solvent chromophores. However, the ELS response is a complex function of analyte concentration and composition and is not easily calibrated [23,24]. An additional means of detection is required to provide chemical functional group information across the chromatogram, namely FT-IR spectrometry with a solvent-evaporation interface [14–16].

Fig. 2 shows the FT-IR spectrum obtained from a dried film of a 75-s HPLC fraction of PMMA-g-PDMS near the chromatogram peak maximum of Fig. 1. Excellent signal-to-noise and spectral band shapes are obtained for this fraction corresponding to less than 90 μg of copolymer. Quantitative FT-IR analysis of seventeen deposited film fractions across the HPLC chromatogram shown in Fig. 1 indicates a monotonic decrease in PDMS incorporation in the graft copolymer exceeding a range of 50% (w/w). The ELS and FT-IR chromatograms are in good agreement. Note that the ELS response decreases more rapidly with copolymer concentration in wings of the peak than does the FT-IR

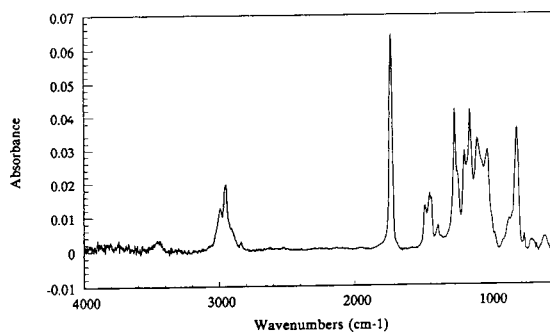


Fig. 2. FT-IR spectrum of a PMMA-g-PDMS HPLC fraction collected with the solvent-evaporation interface over 75 s elution time centered at 36.875 min (see Fig. 1). The spectrum was collected from 16 scans at 4 cm^{-1} resolution from less than 90 μg of copolymer after annealing with dichloromethane vapor.

data. This is consistent with the usual non-linear ELS concentration response.

PDMS homopolymer is completely soluble in these gradient solvents and is unretained on the silica packing. However, since the majority of the PMMA-g-PDMS sample is insoluble in the starting eluent solvent of cyclohexane-toluene-ethanol (60:36:4, v/v/v), the mode of retention is in question. PMMA homopolymer was observed to have a solubility limit of cyclohexane-toluene-ethanol (40.3:53.73:5.97, v/v/v). Taking into account the gradient lag and column void volume, this corresponds to an elution volume of 22.1 ml. Fig. 1 clearly indicates that nearly all copolymer components are retained beyond this solubility limit even though increasing PDMS incorporation only increases copolymer solubility. Indeed, the observed elution volume of PMMA is shown in Fig. 3 to be at the end of the copolymer distribution for a molecular mass 49 700 standard. Note that although the copolymer chromatogram tails out to the elution time of PMMA, no resolved PMMA homopolymer was observed to be present from the graft copolymerization reaction.

The retention process for PMMA-g-PDMS in this solvent system on silica relies on initial precipitation of the copolymer followed by adsorption retention after redissolution in the sol-

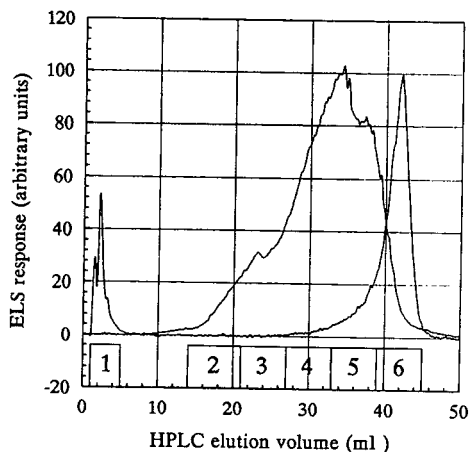


Fig. 3. Comparison of the gradient elution HPLC chromatograms of 10.0 mg of PMMA-g-PDMS and 0.5 mg of a molecular mass 49 700 PMMA. The intervals used for semi-preparative fraction collection of the graft copolymer are shown in the numbered boxes.

vent gradient. PDMS has only weak adsorption interactions on silica; however PMMA cannot be eluted with toluene as the strong solvent [13]. Therefore, a low percentage of ethanol was added as a hydrogen-bond displacer [22], despite the fact that ethanol is a non-solvent for both graft copolymer components.

The molecular mass resolution of this separation was evaluated with a series of narrow PMMA standards. The data for PMMA elution volume converted to the corresponding solvent composition at elution is shown in Fig. 4. The small pores (nominal 100 Å) of the silica column packing provide exclusion and nearly molecular mass independent elution for PMMA in excess of 48 800. The effect of low-molecular-mass resolution is shown in the fronting peak shape of the 49 700 PMMA in Fig. 3. Similar results have been observed previously for a different solvent system on this type of silica adsorbent [13]. Molecular-mass-independent separations under adsorption conditions have also been reported by Mori [22] for styrene-alkyl methacrylate copolymers. Unfortunately, a narrow-composition molecular mass series of graft copolymers was not available to determine the generality of this phenomenon for the current study.

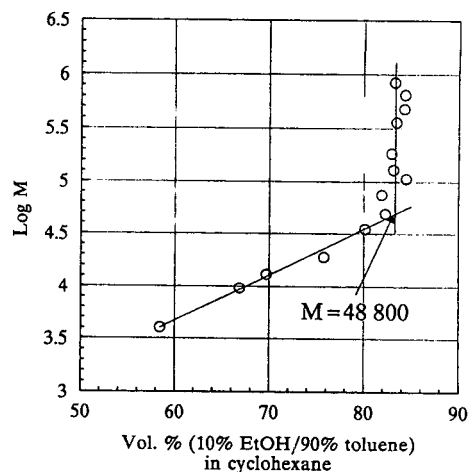


Fig. 4. Variation of solvent concentration required for PMMA elution from 100 Å pore silica as a function of polymer molecular mass.

The compositional heterogeneity observed across the SEC molecular size separation of the whole PMMA-g-PDMS sample (Fig. 5) was also determined using the solvent-evaporation FT-IR interface. Since the PDMS copolymer component is isorefractive with the THF SEC mobile phase, the molecular size distributions given by

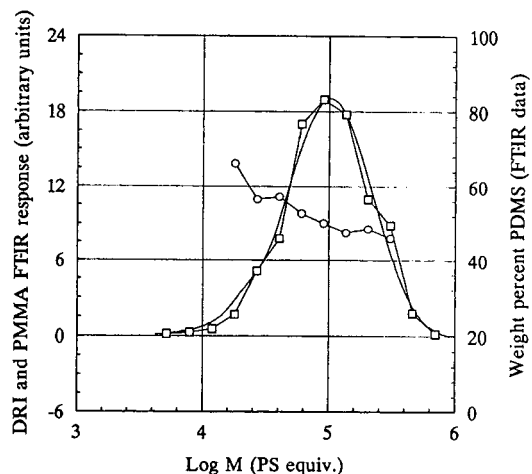


Fig. 5. Comparison of the PS equivalent molecular mass distributions from DRI response (solid line) and mass of PMMA (\square) determined from FT-IR spectra from the solvent-evaporation interface for 0.6 mg of a whole PMMA-g-PDMS sample. Variation in the FT-IR determined weight percent PDMS is shown as \circ .

the DRI detector is compared with that of the PMMA portion of the copolymer calculated from the FT-IR spectra. The agreement is quite good. Note that, although the average values of PDMS obtained from HPLC (55.0%, w/w) and SEC (52.5%, w/w) are in good agreement, the range of compositions observed across the chromatogram is dramatically reduced in SEC by the overlap of various compositions of similar molecular size. In addition, the average composition values from the FT-IR data for both HPLC and SEC appear biased toward prediction of high PDMS incorporation relative to NMR analysis. This most likely results from the use of homopolymer standards for the PLS-2 calibration set despite linear calibration results. Copolymer standards are not currently available and alternatives are being investigated.

Additional information regarding the joint composition and molecular mass distributions of graft copolymers may be obtained by orthogonal separations. Augenstein and Stickler [24] presented a detailed experimental investigation of the precipitation HPLC separation of terpolymers produced by methyl methacrylate grafting from ethylene-propene-diene copolymer. HPLC was performed on weakly adsorbing cyanopropyl-bonded silica with a THF–2,2,4-trimethylpentane gradient subsequent to SEC fractionation. ELS detection of the HPLC chromatograms clearly showed the compositional heterogeneity present in the graft copolymer as a function of molecular size, but was unable to quantify the actual copolymer composition due to the lack of ELS detector selectivity.

Further characterization of the graft copolymer structure of PMMA–g-PDMS was pursued in the current experimental study after having established that a chemical composition separation could be efficiently performed by adsorption HPLC with presumably minimal molecular mass influence. SEC with molecular-mass-sensitive detection (LALLS, differential viscometry and DRI [17]) provided an attractive approach to obtaining detailed information about both the mass of the whole copolymer molecule and that of the PMMA backbone by use of a mobile phase solvent (THF) isorefractive with the

PDMS side chains. As discussed below, the narrow composition fractions provided by HPLC separation were better suited to molecular-mass-sensitive detection methods than the whole copolymer by minimizing errors introduced by the effect of copolymer composition heterogeneity on refractive index and hydrodynamic size.

It is difficult to obtain accurate molecular mass data from SEC of a compositionally heterogeneous copolymer primarily due to the lack of accurate concentration detector response. Calculation of molecular mass by universal calibration using differential viscometry (DV) and DRI detection is performed by calculation of the local intrinsic viscosity at each retention volume according to Eq. 1 [25].

$$[\eta]_i = \frac{\eta_{sp,i}}{c_i} \quad (1)$$

The local intrinsic viscosity, $[\eta]_i$, at each elution volume data point is calculated from the specific viscosity, $\eta_{sp,i}$, measured by the DV and the local concentration, c_i . The c_i at each elution volume data point is conventionally obtained from the injected sample mass, m , with the DRI response normalized across the entire chromatogram of n data points, where W_i is the DRI response at each volume increment Δv as shown in Eq. 2.

$$c_i = \frac{W_i}{\sum_{i=1}^n W_i \Delta v} \cdot m \quad (2)$$

A fit to the universal calibration data determined for the SEC column set using narrow polymer standards then yields the molecular mass distribution plot.

$$[\eta]_1 M_1 = [\eta]_2 M_2 \quad (3)$$

If the copolymer sample is heterogeneous in composition across the SEC chromatogram, then the DRI response varies with copolymer refractive index yielding inaccurate local concentration values. In turn Eq. 1 provides inaccurate local intrinsic viscosity values and thereby Eq. 3 yields incorrect molecular masses, M_i .

The variation in PMMA–g-PDMS copolymer

composition across the SEC profile was determined from FT-IR spectra of deposited fractions and is shown in Fig. 5. Correction of the DRI response for local copolymer refractive index variation [26] using the FT-IR determined copolymer composition might yield an improved molecular mass distribution using universal calibration. However, the propagation of error through this series of data corrections is not likely to yield accurate results beyond the center of the copolymer distribution.

Despite the copolymer compositional heterogeneity overlapping the SEC molecular size separation, an alternative exists for molecular mass determination using LALLS detection. SEC in a solvent isorefractive with the PDMS side chains of the graft copolymer allows accurate molecular mass determination of the PMMA backbone [27]. Eq. 4 gives the relationship between the excess Rayleigh scattering, $\bar{R}_{\theta i}$, and M_i at each elution volume.

$$\frac{K^*c_i}{\bar{R}_{\theta i}} = \frac{1}{M_i} + 2A_{2i}c_i \quad (4)$$

The instrumental constant, K^* , is given by Eq. 5 from the solvent refractive index, n_0 , the polymer refractive index increment, $(\partial n/\partial c)$, the laser wavelength in vacuum, λ_0 , and Avogadro's number, N_A .

$$K^* = \frac{4\pi^2 \bar{n}_0^2 (\partial n/\partial c)^2}{N_A \lambda_0^4} \quad (5)$$

The second virial coefficient term, $2A_{2i}c_i$, in Eq. 4 has little contribution at the low concentrations employed in SEC and is usually ignored. For a copolymer of segregated comonomer units, such as the current graft copolymer, the refractive index increment can be accurately replaced by the average refractive index given by Eq. 6.

$$\overline{(\partial n/\partial c)} = (\partial n/\partial c)_A \bar{x}_A + (\partial n/\partial c)_B \bar{x}_B \quad (6)$$

The average refractive index increment of the copolymer, $\overline{(\partial n/\partial c)}$, is related to those of the corresponding homopolymers $[(\partial n/\partial c)_A$ and $(\partial n/\partial c)_B]$ by their respective weight fractions of

comonomer incorporation, $(\bar{x}_A$ and $\bar{x}_B)$. In THF $(\partial n/\partial c)_{\text{PDMS}} \approx 0$ and therefore $(\partial n/\partial c) = (\partial n/\partial c)_{\text{PMMA}} \bar{x}_{\text{PMMA}}$. In addition, the concentration of the PMMA backbone at each elution volume data point is accurately given by Eq. 2 provided m is replaced with the injected sample mass of PMMA in the copolymer. The molecular mass distribution of the PMMA backbone of the graft copolymer shown in Fig. 6 is thereby obtained directly from Eq. 4. This isorefractive solvent approach has also been discussed by Prud'homme and Bywater [28] for the characterization of block copolymers.

The difficulty of erroneous concentration detector (DRI) response due to compositional heterogeneity can be resolved by the prior HPLC separation of the graft copolymer into narrow composition fractions. However, application of SEC to HPLC fractions was limited by requiring sufficient mass of HPLC fractions to obtain accurate concentration solutions for SEC molecular-mass-sensitive detector calculations. The semipreparative-scale HPLC chromatogram of the PMMA-g-PDMS sample was shown in Fig. 3 in comparison to a PMMA standard of similar M to the cutoff value of Fig. 4. Overload HPLC shows only moderate peak distortion consistent with an adsorption copolymer retention mechanism [29].

The somewhat overloaded HPLC composition separation prior to SEC provides more uniform chemical composition fractions despite only moderate narrowing in molecular mass distribution. This is shown in Fig. 7 for SEC-FT-IR of a HPLC fraction collected near the peak maximum of Fig. 3. The minimal resolution loss due to HPLC overload is indicated by comparison of the average PMDS value for the two HPLC spectra covering the same elution range of Fig. 1 (39.2%, w/w) and the overall average across the entire peak of Fig. 7 (39.7%, w/w). In addition, these more narrow composition fractions allowed increased accuracy in the normalized DRI concentration response for use with differential viscometry and universal calibration molecular mass calculations.

SEC with molecular-mass-sensitive detection was applied to each HPLC composition fraction

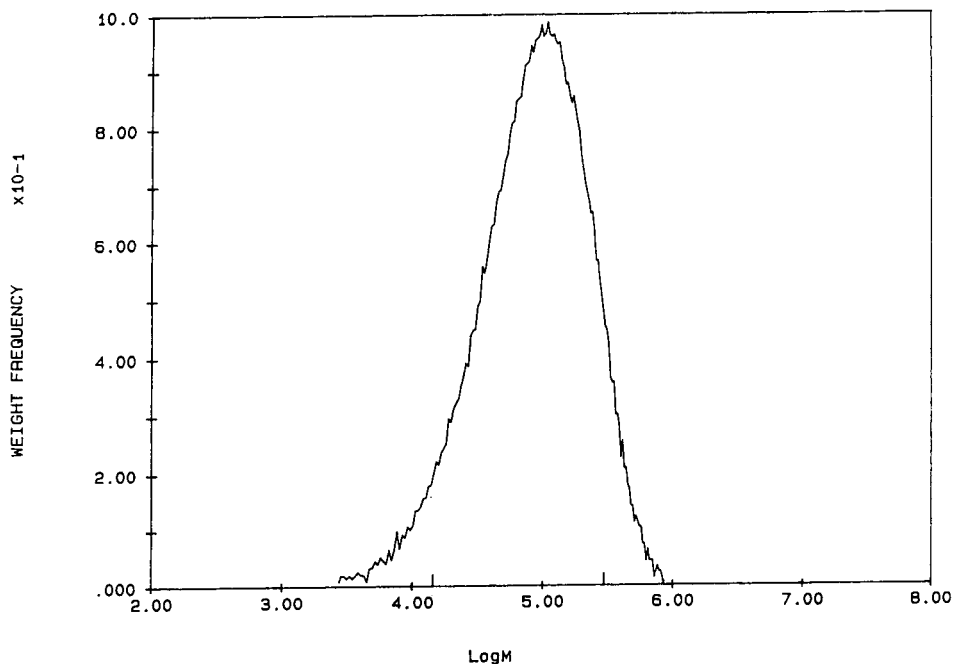


Fig. 6. Low-angle laser-light scattering molecular mass distribution of 0.4 mg PMMA-g-PDMS using the PMMA-corrected sample concentration and refractive index increment. $M_n = 43\,500$; $M_w = 125\,000$; M_z (z average molecular weight) 228 000; $M_w/M_n = 2.87$. Ticks (at 4.2 and 5.0 of the log M axis) denote extrapolation.

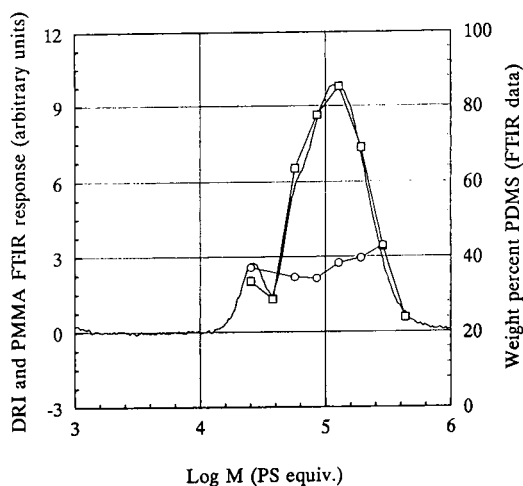


Fig. 7. SEC analysis of a 2.0-ml fraction centered at 38 min elution time for a gradient elution HPLC separation of 10.0 mg of PMMA-g-PDMS (see Fig. 3). The PS equivalent molecular mass distributions are shown for DRI response (solid line) and mass of PMMA (\square) determined from FT-IR spectra from the solvent-evaporation interface for 0.6 mg of copolymer. Variation in the FT-IR-determined weight percent PDMS is shown as \circ .

Table 1
Gradient HPLC fractions of PMMA-g-PDMS copolymer

HPLC fraction No.	Mass of fraction isolated (mg)	True SEC injected concentration (mg/ml)	DRI calculated PDMS (% w/w)
1	Insufficient mass for analysis		
2	2.67	1.60	58.6
3	6.12	1.83	43.0
4	14.60	1.64	28.1
5	17.00	1.91	27.0
6	4.12	1.85	17.9
Whole sample	—	1.77	32

Fractions combined from five repeat HPLC separations totalling 50 mg.

listed in Table 1. The calibrated DRI response was used to determine the concentration of PMMA in each sample and by difference the weight percent PDMS. The PMMA-corrected concentration and PMMA ($\partial n/\partial c$) was then used to calculate the molecular mass distribution from the LALLS response. The true concentration

Table 2
SEC results for gradient HPLC composition fractions of PMMA-g-PDMS copolymer

HPLC fraction No.	Universal calibration \bar{M}_w	LALLS \bar{M}_w of PMMA backbone	Calculated weight-average PDMS branches per copolymer molecule
2	78 500	26 800	3.95
3	90 800	47 800	3.28
4	136 000	91 000	3.44
5	202 000	144 000	4.43
6	199 000	164 000	2.67

and normalized DRI response was used with the differential viscometry detector to calculate the universal calibration molecular-mass distribution for each copolymer fraction. Thereby SEC of each HPLC fraction resulted in two molecular mass values as listed in Table 2, the molecular mass of the whole copolymer molecule and that of the PMMA backbone. The difference between these values was then divided by the molecular mass of the PDMS macromonomer

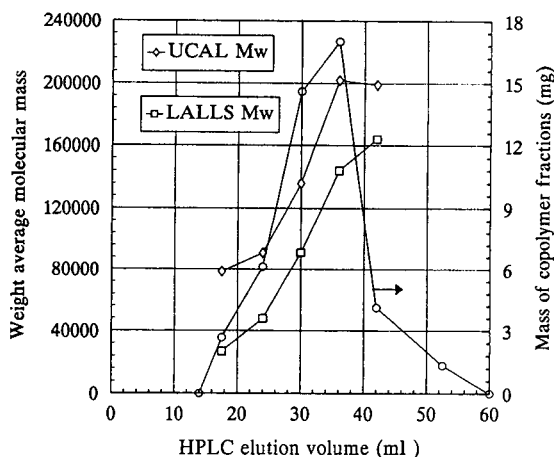


Fig. 8. Comparison of the universal calibration (UCAL, \diamond) and low-angle laser-light scattering (LALLS, \square) weight-average molecular masses determined for HPLC fractions (Fig. 3) of PMMA-g-PDMS. The mass of copolymer fractions (\circ) isolated from gradient elution HPLC indicates the composition separation profile. Data from Tables 1 and 2.

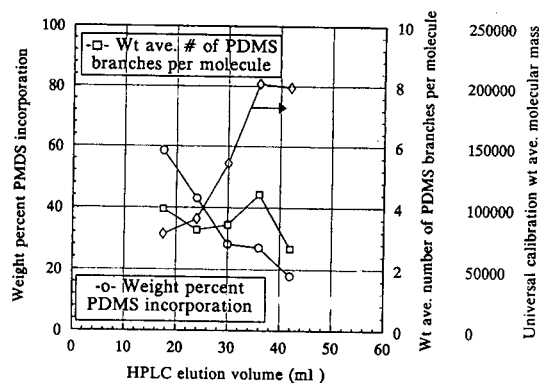


Fig. 9. Comparison of the universal calibration weight-average molecular mass (\diamond) of each HPLC composition fraction with the DRI-determined weight percent PDMS incorporation (\circ) and the estimated weight-average number of PDMS side chains per copolymer molecule (\square). Data from Tables 1 and 2.

$\bar{M}_w = 13\ 100$ to obtain an estimate of the weight-average number of PDMS side chains per copolymer molecule.

The data of Tables 1 and 2 are plotted in Figs. 8 and 9. The universal calibration molecular mass of the whole copolymer molecule and the LALLS determined molecular mass of the PMMA backbone are nearly parallel across the HPLC elution range as shown in Fig. 8. The mass of the isolated HPLC fractions gives an indication of the HPLC chromatogram consistent with Fig. 3. The DRI calculated weight percent PDMS is seen to decrease monotonically across the series of HPLC fractions in Fig. 9. In comparison with the steadily increasing molecular mass of the copolymer molecules, the estimate of the weight-average number of PDMS branches per graft copolymer molecule is relatively constant.

4. Conclusions

HPLC composition separation of PMMA-g-PDMS copolymer was achieved by adsorption

retention after initial precipitation. Relative to the observed retention behavior of PMMA, the HPLC separation was expected to be nearly independent of molecular mass for polymer molecules in excess of 48 800. FT-IR detection using a solvent-evaporation interface indicated a broad range of copolymer compositions present in a radical-polymerized PMMA-g-PMDS copolymer prepared from methyl methacrylate monomer and a 13 100 PDMS macromonomer. The same degree of compositional heterogeneity was not directly observable by SEC-FT-IR due to the coelution of a range of different copolymer compositions with similar molecular size in solution.

Semipreparative HPLC of the graft copolymer sample allowed preparation of more narrow composition fractions for subsequent SEC characterization. SEC with molecular-mass-sensitive detection (differential viscometry and LALLS) allowed estimation of both the whole copolymer molecular mass and that of the PMMA backbone in each HPLC composition fraction. Comparison of these results with the molecular mass of the starting PDMS macromonomer allowed calculation of the weight average number of PDMS branches per copolymer molecule. These results indicated a narrow range of the number of branches per molecule, but a steadily decreasing weight percent incorporation of PDMS with increasing copolymer molecular mass.

These experimental studies establish that gradient elution adsorption HPLC can be an efficient means of resolving broad composition heterogeneity in graft copolymers. Isolated narrow composition fractions from an HPLC separation can then be characterized by SEC with molecular-mass-sensitive detection to provide detailed structural information. The solvent-evaporation FT-IR interface was shown to be a powerful tool for obtaining quantitative composition information across both SEC and gradient HPLC separations. As essentially a microfraction collection device, the solvent-evaporation interface lends the possibility of performing subsequent analyses, such as SEC with molecu-

lar-mass-sensitive detection, on HPLC fractions whose composition has been quantitatively determined by FT-IR spectrometry. These approaches are under continuing investigation.

Acknowledgements

The authors would like to acknowledge the assistance of T.H. Mourey and S.M. Miller (Eastman Kodak) with performing the multi-detector SEC experiments.

References

- [1] P. Remp and P. Lutz, in G. Allen and J. Bevington (Editors), *Comprehensive Polymer Science*, Vol. 6, Pergamon, New York, 1989, pp. 404–405.
- [2] R. Milkovich and M.T. Chang, CPC International, *US Pat.*, 3 786 116 (1974); *US Pat.*, 3 842 059 (1974); *US Pat.*, 3 862 101 (1975).
- [3] S.D. Smith, G. York, D.W. Dwight, J.E. McGrath, J. Stejskal and P. Kratochvíl, *Polym. Prepr., ACS Div. Polym. Chem.*, 28 (1987) 458.
- [4] G. Meijs and E. Rizzardo, *Rev. Macromol. Chem. Phys.*, C30 (1990) 305.
- [5] R. Milkovich, in J.E. McGrath (Editor), *Anionic Polymerization—Kinetics, Mechanisms, and Synthesis (ACS Symposium Series, Vol. 166)*, American Chemical Society, Washington, DC, 1981, p. 41.
- [6] R. Young, R. Quirk and L. Fetters, *Adv. Polym. Sci.*, 56 (1984) 1.
- [7] P. Dreyfuss and R. Quirk, in J. Kroschwitz (Editor), *Encyclopedia of Polymer Science and Engineering*, Vol. 7, Wiley, New York, 1987, p. 552.
- [8] R.J. Ceresa, *Block and Graft Copolymerization*, Vol. 2, Wiley, New York, 1976.
- [9] Y. Ikada, in H.J. Cantow (Editor), *Structure and Properties of Polymers (Advances in Polymer Science, Vol. 29)*, Springer, New York, 1978, p. 47.
- [10] Z. Tuzar and P. Kratochvíl, *Adv. Colloid Interface Sci.*, 6 (1976) 201.
- [11] Z. Tuzar, A. Sikora, D. Straková, J. Podešva, J. Stejskal and P. Kratochvíl, *Collect. Czech. Chem. Commun.*, 50 (1985) 2588.
- [12] J. Stejskal, D. Straková, P. Kratochvíl, S.D. Smith and J.E. McGrath, *Macromolecules*, 22 (1989) 861.
- [13] T.C. Schunk, *J. Chromatogr. A*, 661 (1994) 215.
- [14] A.H. Dekmezian, T. Morioka and C.E. Camp, *J. Polym. Sci. Part B Polym. Phys.*, 28 (1990) 1903.

- [15] P. Cheung, S.T. Balke and T.C. Schunk, in T. Provder, H.G. Barth and M.W. Urban (Editors), *Hyphenated Techniques in Polymer Characterization (ACS Advances in Chemistry Series)*, American Chemical Society, Washington, DC, in press.
- [16] P. Cheung, S.T. Balke, T.C. Schunk and T.H. Mourey, *J. Appl. Polym. Sci.: Appl. Polym. Symp.*, 52 (1993) 105.
- [17] T.H. Mourey and S.T. Balke, in T. Provder (Editor), *Chromatography of Polymers Characterization by SEC and FFF (ACS Symposium Series, Vol. 521)*, American Chemical Society, Washington, DC, 1993, Ch. 12.
- [18] G. Glöckner, *Gradient HPLC of Copolymers and Chromatographic Cross-Fractionation*, Springer, New York, 1991.
- [19] T.H. Mourey and T.C. Schunk, in E. Heftmann (Editor), *Chromatography (Journal of Chromatography Library, Vol. 51B)*, Elsevier, Amsterdam, 1992, Ch. 22.
- [20] T.C. Schunk, *J. Chromatogr. A.*, 656 (1993) 591.
- [21] G. Glöckner, M. Stickler and W. Wunderlich, *Fresenius' Z. Anal. Chem.*, 330 (1988) 46.
- [22] S. Mori, *Polymer*, 32 (1991) 2230.
- [23] T.H. Mourey and L.H. Oppenheimer, *Anal. Chem.*, 56 (1984) 2427.
- [24] M. Augenstein and M. Stickler, *Makromol. Chem.*, 191 (1990) 415.
- [25] R. Lew, P. Cheung, S.T. Balke and T.H. Mourey, *J. Appl. Polym. Sci.*, 47 (1993) 1685.
- [26] D.-C. Lee, T.A. Speckhard, A.D. Sorensen and S.L. Cooper, *Macromolecules*, 19 (1986) 2383.
- [27] J.S. Lindner and S.S. Huang, in H.G. Barth and J.W. Mays (Editors), *Modern Methods of Polymer Characterization*, Wiley, New York, 1991, Ch. 9.
- [28] J. Prud'homme and S. Bywater, *Macromolecules*, 4 (1971) 543.
- [29] H. Engelhardt, M. Czok, R. Schultz and E. Schweinheim, *J. Chromatogr.*, 458 (1988) 79.



ELSEVIER

Journal of Chromatography A, 692 (1995) 233–238

JOURNAL OF
CHROMATOGRAPHY A

Short communication

Rapid scaleable chromatographic purification of nucleic acids from proteinaceous mixtures

Yana L. Hofman^{a,*}, Kelly L. Petrillo^b, Helen C. Greenblatt^a, Robert Lehrer^a,
Mark S. Payne^b

^a*BTR-Separations, CPU Quillen, 3521 Silverside Road, Wilmington, DE 19810, USA*

^b*DuPont Central Science and Engineering, Glasgow Site 301, Newark, DE 19714, USA*

Abstract

The present studies describe a unique HPLC method for the purification of nucleic acids from proteins, scaleable to a preparative or process level, using a Zorbax PRO-10/DN 300 Å silica packing. Columns of this material have an extremely high affinity for proteinaceous materials, and a very low affinity for nucleic acids. We demonstrate this by separating salmon DNA from bovine serum albumin; and describe use of the PRO-10/D-N column to separate plasmid DNA from bacterial lysates. The method is quick and, unlike phenol–chloroform extraction, utilizes physiological buffers to minimize hazardous operations. This LC method is faster than classical non-LC methods, is less labor intensive, and uses no organic solvents, thereby eliminating the need for post-separation recovery operations. The high recovery of DNA purified by Zorbax PRO-10/D-N provides DNA material suitable for many common molecular manipulations including restriction enzyme cleavage, ligation, and amplification.

1. Introduction

Nucleic acids for cloning purposes and for use in a variety of hybridization-based diagnostic assays generally must be highly purified and free of a broad range of impurities such as proteins and organic solvents. Traditionally, the removal of proteins from nucleic acids has been achieved by phenol–chloroform extraction [1]. The toxicity of these organic solvents requires that specialized and costly handling and disposal procedures be used [2]. An alternative method for separating proteins from nucleic acids, the McCormick process [3], involves contacting the protein–nucleic acid mixture with siliceous-based particulates that have been specially prepared to en-

hance their affinity for proteins and substantially decrease their affinity for nucleic acids. This solid-phase extraction protocol is characterized by single use of the silica product. Scale-up of either of these extraction procedures to produce larger quantities of a given nucleic acid is, at the very least, impractical. Saburov and co-workers [4,5] suggested the use of fluorinated polymers for the separation of nucleic acids from proteins using reversed-phase chromatography. They describe separation by chromatographic sorbent on the basis of controlled pore glasses and polytetrafluoroethylene.

We have developed an HPLC method for separation of proteins from nucleic acids by utilizing a Zorbax PRO-10/D-N column with packing prepared using the McCormick process. With this method, polyanions such as nucleic

* Corresponding author.

acids will pass through the column in a controlled fashion, to be collected at the end of the packed column, while the protein from the original mix becomes bound to the silica surface. The procedure is rapid, requiring only 15–20 min to complete; and we have demonstrated that the column may be re-used at least 200 times before regeneration is required. This chromatographic purification procedure has advantages over other techniques, particularly at the preparative or process level. We have demonstrated the utility of a commercial Zorbax PRO-10/D-N column by using it to purify (1) salmon DNA from bovine serum albumin and (2) plasmid DNA from bacterial lysates.

2. Experimental

2.1. D-N Chromatography

Zorbax PRO-10/D-N 300 Å packing material consists of uniform 10- μ m spherical particles of totally porous silica. Proprietary steps yield a particle with a low surface concentration of polyvalent cations, and an enhanced concentration of mildly acidic hydroxyl groups. A standard HPLC column (25 cm \times 4.6 mm I.D.) packed with PRO-10/D-N (BTR-Separations) was used for chromatography. The column was run at ambient temperature using a Rainin HPLC method manager with a Dynamax SD-1 delivery system, a Dynamax UV-1 detector, and a Macintosh LC system (Rainin, Richfield, NJ, USA). Mobile phase was 5 mM 2-(N-morpholino)ethanesulfonic acid (MES, Sigma, St. Louis, MO, USA), injection volume was 50 μ l, and flow-rate was 0.4 ml/min.

2.2. Preparation of bacterial lysates

Escherichia coli strain XL1-Blue [6] harboring the plasmid pUC18 [7] was grown in LB media [1] supplemented with 50 μ g/ml ampicillin (Sigma) with vigorous shaking at 37°C until saturation (14–20 h). Bacterial cells were harvested by centrifugation, alkaline-lysed, and neutralized as described [1] resulting in a cleared

lysate consisting primarily of plasmid DNA and soluble protein.

2.3. Purification of plasmid DNA by organic extraction

Plasmid DNA was purified from cleared lysates by phenol and chloroform extraction, followed by ethanol precipitation as described [1].

2.4. Transformation assay

E. coli strain XL1-Blue was transformed by the calcium chloride procedure as described [1] and selected on LB plates supplemented with 50 μ g/ml ampicillin.

2.5. Restriction and ligation analysis

Restriction enzymes and DNA ligase were purchased from New England Biolabs. (Beverly, MA, USA) and used according to the manufacturer's recommendations.

2.6. Polymerase chain reaction (PCR) analysis

A PCR kit (Perkin-Elmer Cetus, Norwalk, CT, USA) was used according to the manufacturer's recommendations. The 5' primer is a synthetic oligomer with the sequence 5'-GCCGATATCCACCCAGAAACGCTGGTGA-3', and the 3' primer is a synthetic oligomer with the sequence 5'-CGCGATATCCCAA-TGCTTAATTCAGTGAG-3'. Thermal cycling parameters were 1' at 94°C, 1' at 55°C, 1' at 72°C, 40 cycles.

2.7. Miscellaneous

Bovine serum albumin (BSA), salmon DNA, and MES were obtained from Sigma. Water was used after passing through a Milli-Q purification system (Millipore, Bedford, MA, USA).

3. Results and discussion

3.1. Separation of salmon DNA from BSA by D-N chromatography

Solutions of salmon DNA and BSA were used to optimize mobile phase and pH conditions, and to characterize chromatographic performance of the D-N HPLC column. The mobile phase of choice was found to be MES. The desired results could not be achieved with the use of a variety of phosphate buffers. Salmon DNA and BSA solutions were prepared in MES buffers ranging in pH from 4.3 to 7.1 and analyzed by D-N chromatography. The optimal pH for BSA removal (adsorption to the column) and minimal loss of DNA occurred at pH 7.0 (data not shown). The

pH of the mobile phase was determined to be between 5.0 and 5.4. Effective separation of DNA from BSA under these conditions was demonstrated by passing the following three samples through a D-N column: (1) salmon DNA at 0.02 mg/ml in MES buffer pH 7.0, (2) BSA at 2.6 mg/ml in MES buffer pH 7.0 and (3) a mixture of salmon DNA at 0.02 mg/ml and BSA at 2.6 mg/ml in MES buffer pH 7.0. The chromatograms obtained indicate high recovery and high purification of salmon DNA from BSA using this procedure (Fig. 1).

Calculations by others indicate that an analytical column (25 cm × 0.46 cm) has a capacity of approximately 40 mg of protein, whereas a preparative column (25 cm × 1 in.; 1 in. = 2.54 cm) has a capacity of approximately 1.0 g of

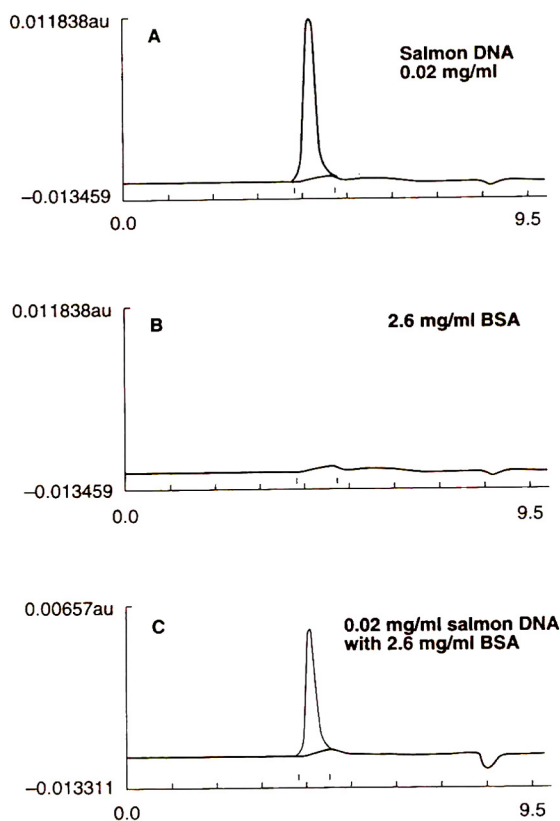


Fig. 1. Separation of salmon DNA from BSA by D-N chromatography. HPLC chromatograms (A_{260}) obtained from Zorbax PRO-10/D-N columns loaded with (A) 50 μ l of salmon DNA at 0.02 mg/ml in MES buffer pH 7.0, (B) 50 μ l of BSA at 2.6 mg/ml in MES buffer pH 7.0 and (C) 50 μ l of a mixture of salmon DNA at 0.02 mg/ml and BSA at 2.6 mg/ml in MES buffer pH 7.0. Protein is adsorbed to the column. Time scale on the x-axis in minutes.

protein [8]. Thus 50- μ l injections of BSA at 2.6 mg/ml suggests that the analytical column may be re-used approximately 300 times before regeneration is required. A column may be regenerated by contact with acetonitrile for 2–3 h followed by 0.1 % trifluoroacetic acid for 2 h and 5 mM MES for 1 h.

3.2. Separation of plasmid DNA from bacterial lysate by D-N chromatography

A cleared bacterial lysate was prepared from a saturated culture of *E. coli* harboring the plasmid pUC18 as described (Experimental). The lysate was divided equally and plasmid DNA was recovered from one half by phenol and chloroform extraction, and from the other half by D-N chromatography. Recovery of plasmid DNA was determined by transformation of competent *E. coli* and selection on ampicillin plates. The elution profile of plasmid DNA from the D-N column coincides with a major peak in the chromatogram which is well separated from peaks corresponding to other lysate or buffer components (Fig. 2). Fractions (minutes) 5–7

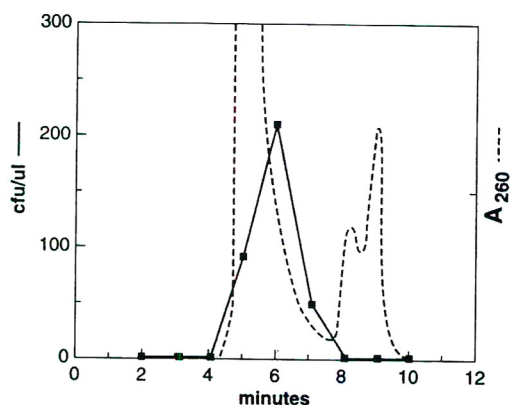


Fig. 2. Elution profile of plasmid DNA from D-N column. Cleared lysate (50 μ l) prepared from *E. coli* harboring pUC18 was loaded onto a Zorbax PRO-10/D-N column and fractions collected were analyzed for plasmid DNA by transformation assay (solid line). The corresponding A_{260} HPLC chromatogram tracing (dashed line) indicates various peaks representing plasmid DNA (minutes 4–7), and non-plasmid nucleic acids or other lysate components (minutes 8–10). cfu/ul = colony-forming units per μ l of column fraction.

were pooled and the yield of plasmid DNA was compared to that obtained by organic extraction. After adjusting for different final volumes, the relative recovery of plasmid DNA from D-N separation was determined to be statistically equivalent to that from organic extraction (Fig. 3). No attempt was made to determine the fate of RNA present in the crude lysate.

3.3. Molecular manipulation of plasmid DNA purified by D-N chromatography

Restriction cleavage and re-ligation tests were performed as general functional assays for plasmid DNA purified from bacterial lysates (Table 1). Plasmid DNA samples prepared by organic extraction or by D-N chromatography were subjected to cleavage by the restriction enzymes HindIII or KpnI. Each of these enzymes has one recognition site in the plasmid pUC18, and cleavage results in a linear DNA molecule which is incapable of transforming competent *E. coli* cells. Results indicate that plasmid DNA prepared by D-N chromatography is efficiently cleaved by restriction enzymes.

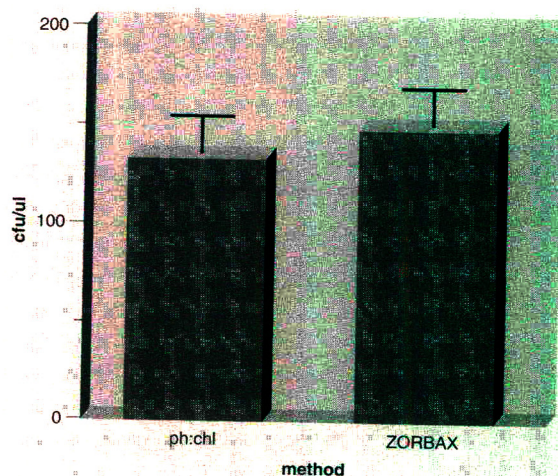


Fig. 3. Recovery of plasmid DNA from cleared bacterial lysates. Yield of plasmid pUC18 from *E. coli* lysate by Zorbax PRO-10/D-N column is compared to yield by phenol–chloroform extraction (ph:chl), as determined by transformation assay. cfu/ul = Colony-forming units per μ l of final sample, after adjusting volumes for the two different methods.

Table 1
Restriction digest and re-ligation analysis of plasmid pUC18 prepared by phenol–chloroform (ph:chl) extraction and Zorbax-PRO/D-N methods

Treatment	Colony-forming units	
	ph:chl	Zorbax
None	569	701
HindIII restriction ^a	6 (99%)	13 (98%)
Re-ligation ^b	245 (43%)	287 (41%)
KpnI restriction	1 (100%)	0 (100%)
Re-ligation	245 (43%)	295 (42%)

^a Efficiency of digestion is shown in parentheses.

^b Efficiency of re-ligation is shown in parentheses.

Restricted plasmid DNA was also subjected to re-ligation by DNA ligase, resulting in circular plasmids which are capable of transforming competent *E. coli* cells. The termini of HindIII cleaved DNA have 5' overhangs, while the

termini of KpnI cleaved DNA have 3' overhangs. In both cases a re-ligation efficiency of approximately 40% was obtained, which is equivalent to that obtained from re-ligated plasmid DNA prepared by organic extraction.

Amplification by PCR was also performed as a general functional assay for plasmid DNA purified from bacterial lysates (Fig. 4). The β -lactamase gene of the plasmid pUC18 was used as the target for PCR, and plasmid DNA samples prepared by organic extraction or by D-N chromatography were the starting material. Results indicate that plasmid DNA prepared by D-N chromatography is efficiently amplified by PCR.

4. Conclusions

We have described an HPLC method for the separation of nucleic acids from proteins based on Zorbax PRO-10/D-N silica. The process is simple, quick, effective, and uses only aqueous buffers. We demonstrated that plasmid DNA purified by this method from a complex mixture of proteins (bacterial lysates) is of equivalent yield and quality compared to preparation by organic extraction. In addition, the method is easily scaleable to a preparative or process level. The method described here could find application for the purification of nucleic acids from a variety of sources, including bacteria, plants, animals and environmental samples.

References

- [1] T. Maniatis, E.F. Fritsch and J. Sambrook, *Molecular Cloning: A Laboratory Manual*, Cold Spring Harbor Laboratory, New York, 1989.
- [2] *Prudent Practices for Handling Hazardous Chemicals in Laboratories*, National Academy Press, Washington, DC, 1981.
- [3] R.M. McCormick, *Anal. Biochem.*, 181 (1989) 66.
- [4] V.V. Saburov, S.I. Turkin, M.R. Muydinov, S.V. Ivanov and V.P. Zubov, *Proceedings of Chromatography in Biology and Medicine*, International Symposium, Moscow, 1986, p. 200.

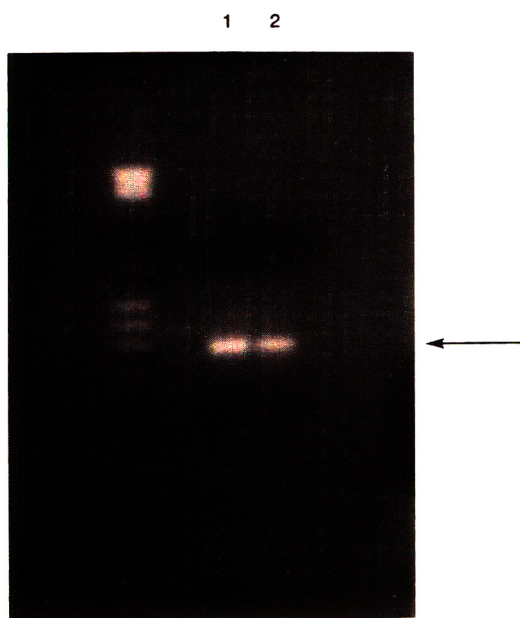


Fig. 4. Amplification of plasmid DNA. Ethidium bromide agarose gel electrophoresis of PCR amplification of the β -lactamase gene from pUC18 prepared by D-N column chromatography (lane 1) or by phenol–chloroform extraction (lane 2). Arrow indicates expected PCR product. Molecular mass size markers are at the left.

- [5] V.V. Saburov, T.I. Vener, S.D. Gilyarevsky and S.V. Ivanov, *14th International Congress of Biochemistry*, Vol. 1, Prague, 1988, p. 235.
- [6] W.O. Bullock, J.M. Fernandez and J.M. Short, *Biotechniques*, 5 (1987) 376.
- [7] C. Yanisch-Perron, J. Vieira and J. Messing, *Gene*, 33 (1985) 103.
- [8] J. Cline, K. Lundberg, K. Nielson, A. Sorge, J. Short and E. Mathur, *Strategies in Molecular Biology, Stratagene Cloning*, La Jolla, CA, Vol. 4, No. 4, 1990, p. 49.

Separation of photosynthetic pigments and their precursors by reversed-phase high-performance liquid chromatography using a photodiode-array detector

Benoît Schoefs^{a,*}, Martine Bertrand^b, Yves Lemoine^a

^aPlant Cytophysiology and Phycology Laboratory (SN2), University of Lille 1, 59655 Villeneuve d'Ascq, France

^bNational Institute for Techniques and Sciences of the Sea, Digue de Collignon, 50110 Tourlaville, France

Abstract

A reversed-phase HPLC method is described for the separation of photosynthetic pigments, allowing the rapid and efficient separation of protochlorophyll(ide)s, chlorophyll(ide)s and *cis*- and *trans*-carotenoid isomers. The pigment contents of non-illuminated and illuminated bean leaves were determined and compared. Both sample types present the same carotenoid pattern. The main carotenoids are always *trans*-violaxanthin, *trans*-lutein and β -carotene. The tetrapyrrole pigment contents are very different. Non-illuminated leaves mainly contain protochlorophyllide and protochlorophyll esters whereas illuminated leaves contain mainly chlorophylls.

1. Introduction

Tswett, who discovered liquid chromatography, was also the first to analyse plant pigments [1]. Since these pioneer assays, the number of papers dealing with this technique has increased dramatically. The Association of Official Analytical Chemists [2] recommends the use of silica gel as the major adsorbent to separate carotenoids and chlorophylls (Chls) on a thin-layer chromatographic plate or by open-column chromatography. Both methods are lengthy and losses, degradations or modifications of the pigments could occur [3,4]. Moreover these techniques cannot separate compounds with very similar structures.

During the 1980s, the technique of HPLC was introduced for the separation and determination of plant pigments (for reviews, see [5–7]). The introduction of photodiode-array detection systems has increased the analytical power of HPLC because such detectors allow the simultaneous recording of chromatograms at various wavelengths during a single run and real-time identification and determination of the pigments. General advantages of such a detector have been reviewed [5,8]. The C₁₈ reversed-phase column is particularly suitable for the separation of complex mixtures containing tetrapyrrole rings and hydrocarbon molecules [9–11]. Moreover, the bound phase is very inert and there is no risk of decomposition or structural modification of (proto)chlorophyll(ide)s and carotenoids when these molecules are in contact with the bound phase [12]. The utilization of a ternary system of non-aqueous solvents, rather than a solvent system containing water or buffer, avoids partial

* Corresponding author. Present address: Photobiology Laboratory, Department of Botany (B22), University of Liège, 4000 Liège, Belgium.

precipitation or crystallization of the solutes on the solid phase, optimizes sample solubilization, gives a better peak shape and prolongs the column lifetime [12]. HPLC represents the best method for pigment separation owing to advantages such as speed, high resolution and sensitivity (for a review, see [5]). Several methods for the separation of either protochlorophyllides (Pchl_{id}) or protochlorophylls (Pchl) [13,14], Chls [15–17], carotenoids [18–20], or both Chls and carotenoids [9,19–22] have been described. To our knowledge, the only method exhibiting a good separation of Pchl_{id}(s), chlorophyllide (Chl_{id}), Chls and carotenoids in the same run was that of Eskins and Harris [23]. However, this method does not achieve the separation of carotenoid isomers or of Pchl_{id} esters.

Pigments of green plants are generally known as carotenoids and Chls. Carotenoids consist of carotenes and xanthophylls and can be found in vivo as *cis/trans*-(*Z/E*)-isomers (for reviews, see [5,24,25]). In addition to Chl *a* and *b*, it has been shown that pheophytin *a* and Chl *a* epimers (i.e., Chl *a'*) play an important role in photosynthesis [26,27] and not only occur as degradation products of Chl *a*. Chl precursors are particularly abundant in dark-grown plants [28–30]. As soon as such plants are illuminated, Pchl_{id}s are enzymatically transformed to Chl_{id}s [31], which are subsequently esterified in several steps to Chl *a* [32–34]. Pchl_{id}s and their esters have also been detected spectroscopically in greening and in green material [35,36].

The HPLC–photodiode-array detection system described in this paper allows in one step a simple, reproducible and rapid separation and identification of over twenty plant pigments including the different Pchl_{id} esters and the *cis/trans*-carotenoid isomers. Such a resolution is not achieved by the method of Eskins and Harris [23].

2. Experimental

2.1. Plant material and culture conditions

Seeds of *Phaseolus vulgaris* cv. Red Kidney were cultivated in the dark at 298 K for 10 days

as described by Schoefs et al. [37]. In order to obtain their greening, the seedlings were placed under fluorescent (Sylvania, Natural Super, 36 W) for different time periods between 0 and 16 h.

Wheat seeds (*Triticum aestivum* var. Castran) were grown for 6 days in the dark on a perlite–vermiculite (50:50) bed at 298 K.

Cucumber seeds (*Cucumis sativus* var. Marketer, Le Paysan, Avignon, France) were grown in the dark for 3 days on a perlite–vermiculite (50:50) bed at 298 K. The cotyledons were immersed in a 1.82 mM solution of δ -aminolevulinic acid (ALA) (Sigma, St. Louis, MO, USA) in order to increase the content of divinyl- (DV) Pchl_{id} [38].

A green safe light was used while harvesting.

2.2. Preparation of authentic references

Monovinyl- (MV) Pchl_{id} was prepared from etiolated wheat and bean leaves. The leaves were cut into small segments and immersed in diethyl ether for 24 h in the dark at 253 K. The extract was filtered through a Whatman (Maidstone, UK) ashless filter [39]. The filtrate essentially contains MV-Pchl_{id}. DV-Pchl_{id} was prepared from δ -ALA-fed cucumber cotyledons as described by Wellburn [38].

The carotenoids were separated on silica gel thin-layer plates (5513, Merck, Darmstadt, Germany) using the method described by Eichenberger and Grob [40]. The coloured bands were scraped off and the pigments were eluted with methanol. The pigments were characterized by their fluorescence properties using a Hitachi (Tokyo, Japan) F 1301 spectrofluorimeter and/or by absorption spectra recorded with a Uvikon 940 double-beam spectrophotometer (Kontron, Milan, Italy). The identification was done by comparison of the absorbance maxima obtained here with those in the literature [24]. The pigments were injected or dried under vacuum using a Heito Rotavapor. The pigments were stored in amber-coloured bottles with screw-caps at 243 K under nitrogen. Under these conditions, they remain stable for at least 1 month without any damage. Differentiation of *cis*- and *trans*-

carotenoid isomers can be done on the basis of the “*cis*-peak” in the near-UV region [24].

All the manipulations were performed under a green safe light at 277 K.

2.3. Preparation of samples

Dark-grown bean leaves were harvested using a weak green light in order to avoid any photo-transformation of pigments [5]. Just after the harvest, the leaves were hand-ground in methanol. The extracts were clarified by centrifugation at 50 000 *g* for 10 min at 277 K. The supernatant was filtered through a 0.45- μ m PTFE filter membrane (Millipore, Bedford, MA, USA) and vacuum-dried using the Rotavapor and again solubilized in 0.5 ml of methanol. The sample was either dried again under nitrogen and stored in the dark at 253 K or immediately used for HPLC analysis.

2.4. Instrumentation and HPLC analysis

The chromatographic separation of pigments was carried out on an HPLC system that consists of one pump and its solvent-delivery system (SP 8700; Spectra-Physics, Darmstadt, Germany) and a Model 991-25 UV-Vis photodiode-array detector (Waters, Milford, MA, USA). The acquisition and treatment of data were performed using the Waters 991 software. The time and wavelength resolution were 1.1 ± 0.1 s and 2 nm, respectively. The pigment extract was injected with a Rheodyne (Cotati, CA, USA) Model 7125 sample valve equipped with a 100- μ l loop. Up to 100 μ l of methanolic extracts were injected. Separations were carried out with a Zorbax (DuPont, Wilmington, DE, USA) reversed-phase column (particle size of the packing 4.65 nm; 25 cm \times 4.6 mm I.D.).

The solvents used as the mobile phase were as suggested by Foyer et al. [10], but their proportions and the type of gradient were modified to obtain an adequate separation and detection of the different pigments (i.e., esters of Pchlide). The solvents were degassed prior use by bubbling helium (Quality U; Air Liquide, Paris, France) through them. Solvent A [acetonitrile-methanol (70:30, v/v)] was mixed with increas-

ing proportions of solvent B (dichloromethane) during all the runs. The programme was as follows: solvent A was delivered isocratically from 0 to 7 min followed by a 2-min linear gradient to 20% solvent B. This solvent mixture was run isocratically until 30 min. The column was re-equilibrated between two sample analyses for a minimum of 20 min with solvent A. All runs were performed at 293 K. The flow-rate was 1 ml min⁻¹.

Methanol (pro analysi) was purchased from Merck (Darmstadt, Germany), diethyl ether (Normapur) from Prolabo (Paris, France) and dichloromethane and acetonitrile (both HiPer-Solv) from BDH (Poole, UK).

3. Results and discussion

Fig. 1 presents a typical chromatogram obtained at 437 nm for pigments extracted from dark-grown 10-day-old bean leaves. Well resolved and clear peak shapes are obtained, even for the first peaks. The absorbance properties of the eluted pigments and their identification are reported in Table 1. It is important to note that the pigment absorbance maxima are blue-shifted when they are eluted in the presence of dichloromethane [41].

On such a non-polar column, the pigments are approximately eluted according to decreasing

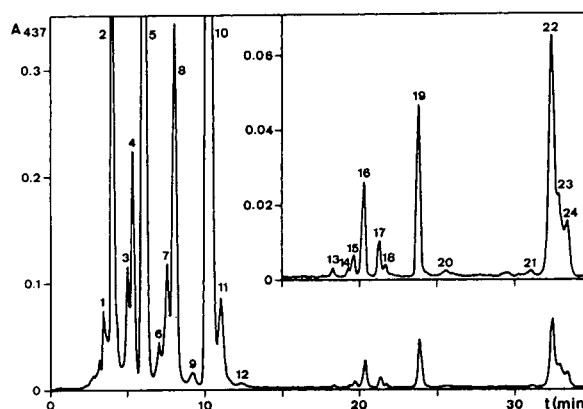


Fig. 1. Reversed-phase HPLC at 437 nm of the pigments extracted from 10-day-old dark-grown bean leaves. For identification of the peaks, see Table 1.

Table 1

Identification and absorbance maxima in the elution mixture of the pigments presented in Fig. 1.

Peak No.	Pigment	Absorbance maxima in the eluent (nm) (± 1.4 nm)	Log k' \pm S.D. ($n = 3$)
1	MV-protochlorophyllide	430,580,634	-0.40 ± 0.02
2	MV-protochlorophyllide	430,580,634	-0.28 ± 0.02
3	<i>trans</i> -Neoxanthin	413,439,469	0.00 ± 0.02
4	<i>cis</i> -Neoxanthin	317,409,434,465	0.06 ± 0.01
5	<i>trans</i> -Violaxanthin	412,437,469	0.18 ± 0.01
6	<i>cis</i> -Violaxanthin	319,408,433,464	0.20 ± 0.01
7	Lutein-5,6-epoxide	412,437,469	0.34 ± 0.02
8	<i>trans</i> -Antheraxanthin	423,444,474	0.47 ± 0.02
9	<i>cis</i> -Antheraxanthin	323,413,439,465	0.50 ± 0.02
10	<i>trans</i> -Lutein	427,444,474	0.54 ± 0.01
11	<i>cis</i> -Lutein	321,406,440,468	0.58 ± 0.01
12	<i>cis</i> -Lutein	320,402,442,468	0.60 ± 0.02
13	Chlide <i>a</i> geranylgeraniol	432,665	0.74 ± 0.01
14	Unidentified carotenoid	440,470	0.75 ± 0.01
15	PChlide geranylgeraniol	434,634	0.79 ± 0.02
16	<i>cis</i> - β -Cryptoxanthin	324,446,474	0.85 ± 0.01
17	PChlide phytatrienol	430,634	0.88 ± 0.01
18	PChlide phytadienol	430,636	0.90 ± 0.01
19	PChlide phytol	430,634	0.93 ± 0.01
20	<i>cis</i> - β -Carotene-5,6-epoxide	316,410,434,470	0.94 ± 0.02
21	α -Carotene	416,446,474	1.05 ± 0.01
22	<i>trans</i> - β -Carotene	420,454,482	1.06 ± 0.02
23	<i>cis</i> - β -Carotene	334,415,418,448,472	1.08 ± 0.02
24	<i>cis</i> - β -Carotene	334,415,418,446,474	1.08 ± 0.02

polarities; for instance, the α -carotene derivatives lutein-5,6-epoxide (two hydroxy and one epoxy group) and lutein (two epoxy groups) are eluted successively, whereas α -carotene (devoid of oxygen) is eluted later (see Table 1; for the structures, see Ref. [5]).

The polar molecules such as MV-Pchlide (Mg-2-vinylpheoporphyrin a_5 monomethyl ester, peaks 1 and 2) and the various xanthophylls, neoxanthine [(3*S*,5*R*,6*R*,3'*S*,5'*R*,6'*S*) - 5',6' - epoxy - 6,7 - didehydro - 5,6,5',6' - tetrahydro - β , β - carotene - 3,5,3' - triol, peaks 3 and 4], violaxanthine [(3*S*,5*R*,6*S*,3'*S*,5'*S*,6'*S*) - 5,6,5',6' - diepoxy - 5,6,5',6' - tetrahydro - β , β -carotene - 3,3' - diol, peaks 5 and 6], taraxanthine (5,6-epoxylutein, peak 7), antheraxanthine (5,6-epoxy - 5,6 - didehydro- β , β -carotene-3,3'-diol, peaks 8 and 9), lutein [(3*R*,3'*R*,6'*R*) - β , ϵ - carotene - 3,3' - diol, peaks 10 and 11] are eluted early. Then come the different esterified Pchlides (peaks 15 and 17–19). The non-polar α - and

β -carotene [(6'*R*)- β , ϵ -carotene and β , β -carotene, peaks 21–23] and the carotenoid precursors (i.e., phytoene and phytofluene), which are more saturated, are eluted at the longest retention times (Tables 1 and 2).

Peak 2 was identified as Mg-2-vinyl-4-ethylpheoporphyrin a_5 monomethyl ester (MV-Pchlide) owing to its absorbance and fluorescence properties and to its co-migration with the authentic standard (data not shown). This result is in agreement with the literature as it has been demonstrated that bean belongs in the dark-

Table 2
Carotenoid precursors found in 20-day-old dark-grown or greening bean leaves

Pigment	log k' \pm S.D. ($n = 3$)	Absorbance maxima (nm)
Phytofluene	1.12 ± 0.01	336,354,374
Phytoene	1.16 ± 0.01	275,288,302

grown monovinyl plant group [42]. Recently, Shioi and Takamiya [39] confirmed this result and indicated that bean leaves also contain minute amounts of Mg-2,4-divinylpheoporphyrin a_5 monomethyl ester (DV-Pchlde [29]). Our assays of cucumber extracts have shown that DV-Pchlde is unfortunately not separated from MV-Pchlde by this method. It must be added that a polyethylene column is generally used for the separation of MV- and DV-Pchlde [39]. The resolution of both pigments using a reversed-phase column has been reported only once but with retention times around 100 min [13]. From its absorbance spectral properties, peak 1 is also identified as MV-Pchlde. It is possible that it corresponds to an epimer of Pchlde or an "X-Pchlde" as proposed by Mukaida et al. [43]. Pheophorbide and/or pheophytins, the well known degradation products of protochlorophyllide and protochlorophyllide esters, were never detected among the pigments of non-illuminated samples, indicating that the extraction and conservation of the sample were satisfactory.

Despite the dark-growth conditions, traces of Chlide *a* geranylgeraniol ester are observed (peak 13). Eskins and Harris [23] also found Chl *a* in dark-grown leaf pigment extracts; they considered it as an artifact due to the green safe light (see Experimental). If we cannot exclude this hypothesis, it is worth noting that the presence of Chl *a* traces has already been reported in dark-grown plants [30,44,45].

Four Pchlde esters are detected (peaks 15, 17, 18 and 19). By comparison with the peaks found for *Cucurbita maxima* Pchl [43,46], we identified them as Mg-2-vinylpheoporphyrin a_5 geranylgeraniol ester (peak 15), Mg-2-vinylpheoporphyrin a_5 phytatrienol ester (peak 17), Mg-2-vinylpheoporphyrin a_5 phytadienol ester (peak 18) and Mg-2-vinylpheoporphyrin a_5 phytol ester (peak 19). This sequence is identical with that of pheophytins [52].

Usually, carotenoid precursors are not observed in wild plants (see Table 1) [5]. In order to accumulate these pigments, one uses chemicals (e.g., norflurazon) which block carotenoid synthesis from the precursors [47,48], but it is time consuming to prepare a sample with both

carotenoids and precursors. We found that very old dark-grown leaves contain carotenoids and two precursors, namely phytoene (7,8,11,12,7',8',11', 12'-octahydro- ψ,ψ -carotene) and phytofluene (7,8,11,12,7',8'-hexahydro- ψ,ψ -carotene) (Table 2). The stereochemistry could not be determined because the elution solvents do not transmit UV-radiation in the range where the *cis* peak absorbs. By comparison between Tables 1 and 2, it appears that *trans*- β -carotene is partially co-eluted with phytofluene. The two pigments are easily differentiated and quantified, however, using a photodiode-array detector because they have no common absorbance band.

All the xanthophylls are well resolved into their *cis*- and *trans*-isomers (Fig. 1, Table 1). Carotene isomers are poorly separated in the present system, however, and this analysis would need, for instance, the use of a calcium hydroxide column [49,50]. However, good absorption spectra can be obtained from the data for the different carotene isomers (Fig. 2). It should be noted that the relative height of the *cis* peak depends on the *cis*-double-bound position, the more central giving the highest absorbance [24].

The two main tetrapyrrole pigments are Pchlde and Pchlde phytol ester. The main xanthophyll peaks correspond to *trans*-violaxan-

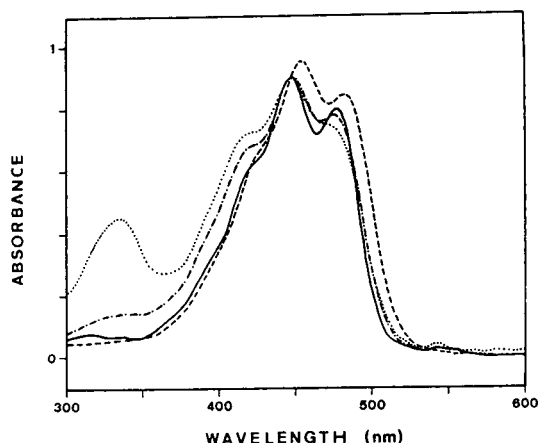


Fig. 2. Absorbance spectra in the elution mixture of (—) α -carotene, (---) all-*trans*- β -carotene, (-·-·) *cis*- β -carotene and (·····) *cis*- β -carotene. The spectra of *cis*- β -carotene do not correspond with that of pure molecules as elution peaks 23–24 overlap.

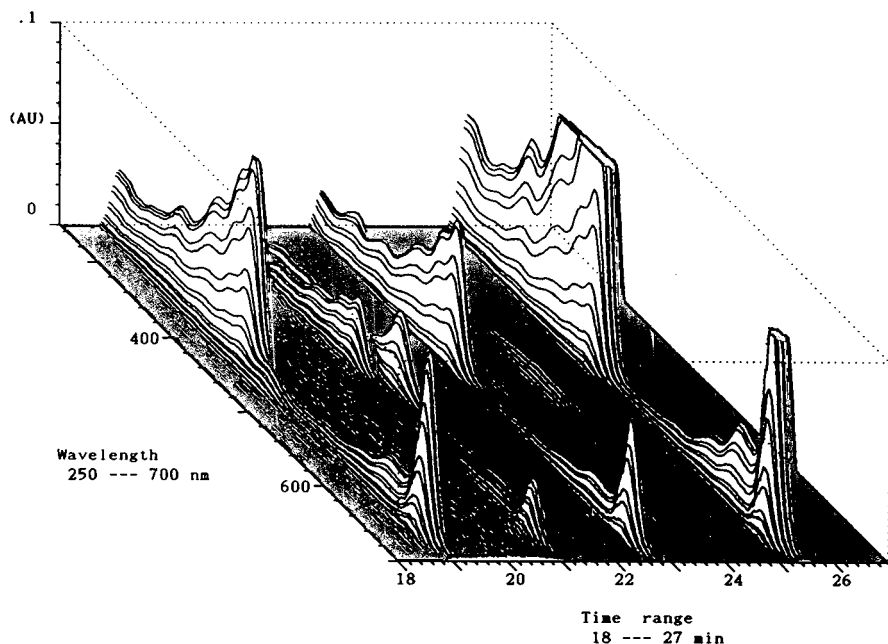


Fig. 3. Three-dimensional plot of the different Chlide *a* esters and chlorophyll *b* from a greening bean leaf. From the left, one can distinguish Chlide *a* geranylgeraniol, Chlide *a* phytatrienol, Chl *b*, Chlide *a* phytadienol and Chlide *a* phytol (Chl *a*).

thin and *trans*-lutein. These results are in agreement with those of Barry et al. [51]. Although the sequence of the peaks presented in Fig. 1 is similar to that of Eskins and Harris [23] for bean leaves, our method gives a better separation and resolution of the pigments, especially for the *cis/trans*-isomers of xanthophylls and for the different Pchlade ester forms.

The method was also applied to pigments from several greening higher plants and green algae. The carotenoid pattern is identical with that found for non-illuminated leaves. In illuminated leaves, the Pchlade esters are replaced by Chl(ide) esters. The four Chlide *a* esters, described by Schoch et al. [52], namely Chlide *a* geranylgeraniol, Chlide *a* phytatrienol, Chlide *a* phytadienol and Chlide *a* phytol (chlorophyll *a*) are well separated from Chl *b* (Fig. 3). In green leaves and algae, the main pigments are *trans*-violaxanthine, *trans*-lutein, β -carotene, Chl *a* and Chl *b* (Table 3). The method presented here appears to be very suitable for the separation of photosynthetic pigments and their precursors from a wide range of organisms.

Table 3

Additional pigments found during greening of a 10-day-old bean leaf

Pigment	$\log k' \pm \text{S.D.}$ ($n = 3$)	Absorbance maxima (nm)
Chlide <i>a</i>	0.65 ± 0.01	432,665
Chlide <i>a</i> geranylgeraniol	0.82 ± 0.02	432,665
Chlide <i>a</i> phytatrienol	0.86 ± 0.01	432,665
Chl <i>b</i>	0.88 ± 0.01	458,658
Chlide <i>a</i> phytadienol	0.90 ± 0.01	432,665
Chlide <i>a</i> phytol	0.95 ± 0.02	432,665
Chlide <i>a'</i>	0.97 ± 0.01	432,665
Pheophytin <i>a</i>	1.08 ± 0.02	409,674

Acknowledgements

This work was supported by a Travel Grant (BV A90/76) from the Belgian French Community Education Ministry and by a grant from the French Embassy in Belgium to B. Schoefs. The presentation of these results at the HPLC'94 Congress by B.S. was supported by the Lefranc Foundation of the University of Liège and the

Agathon de Potter Foundation of the Belgian Royal Academy of Sciences, the Education Department of the French Community of Belgium and by the Organizing Committee.

References

- [1] M. Tswett, *Ber. Dtsch. Bot. Ges.*, 24 (1906) 384.
- [2] Association of Official Analytical Chemists, *Official Methods of Analysis of the Association of Official Analytical Chemists*, AOAC, Washington, DC, 14th ed., 1984.
- [3] H.H. Strain, J. Sherma and M. Grandolfo, *Anal. Chem.*, 38 (1967) 926.
- [4] M. Senge, D. Dörnemann and H. Senger, *FEBS Lett.*, 234 (1988) 215.
- [5] T.W. Goodwin and G. Britton, in T.W. Goodwin (Editor), *Chemistry and Biochemistry of Plant Pigments*, Academic Press, London, 1988, p. 61.
- [6] S.J. Schwartz and I.H. von Elbe, *J. Liq. Chromatogr.*, 5, Suppl. 1 (1982) 43.
- [7] K.S. Rowan, *Photosynthetic Pigments of Algae*, Cambridge University Press, Cambridge, 1988.
- [8] R. Taulmer and D. Barcelo, *Trends Anal. Chem.*, 12 (1993) 319.
- [9] Y. Lemoine, J.P. Dubacq, G. Zabulon and J.M. Ducruet, *Can. J. Bot.*, 64 (1986) 2959.
- [10] C.H. Foyer, M. Dujardin and Y. Lemoine, *Plant Physiol. Biochem.*, 27 (1989) 751.
- [11] A.M.M. Gilmore and H.Y. Yamamoto, *J. Chromatogr.*, 543 (1991) 137.
- [12] H.J.C.F. Nelis and A.P. De Leenheer, *Anal. Chem.*, 55 (1983) 270.
- [13] C.M. Hanamoto and P.A. Castelfranco, *Plant Physiol.*, 73 (1983) 79.
- [14] G.A. Peschek, B. Hinterstoisser, M. Wsatyn, O. Kunter, B. Pineau, A. Missbichler and J. Lang, *J. Biol. Chem.*, 264 (1989) 11827.
- [15] S. Burke and S. Aronoff, *Chromatographia*, 12 (1979) 808.
- [16] S. Shioi and S.I. Beale, *Anal. Biochem.*, 162 (1987) 493.
- [17] E. Forni, M. Ghezzi and A. Polesello, *Chromatographia*, 26 (1988) 120.
- [18] R.J. Brushway, *J. Agric. Food Chem.*, 35 (1987) 849.
- [19] G.K. Gregory, T.-S. Chen and T. Philip, *J. Food Sci.*, 52 (1987) 1071.
- [20] B. Stancher, F. Zonta and P. Bogoni, *J. Micronutr. Anal.*, 3 (1977) 97.
- [21] T. Baumann and L.H. Grimme, *Biochim. Biophys. Acta*, 637 (1981) 8.
- [22] S. Scalia and G.W. Francis, *Chromatographia*, 28 (1989) 129.
- [23] K. Eskins and L. Harris, *Photochem. Photobiol.*, 33 (1981) 131.
- [24] B.H. Davis, in T.W. Goodwin (Editor), *Chemistry and Biochemistry of Plant Pigments*, Academic Press, London, 1976, p. 38.
- [25] Y. Koyama, *J. Photochem. Photobiol. B*, 9 (1991) 265.
- [26] H. Michel and J. Deisenhofer, *Biochemistry*, 27 (1988) 1.
- [27] H. Maeda, T. Watanabe, M. Kobayashi and I. Ikegami, *Biochim. Biophys. Acta*, 1099 (1992) 74.
- [28] M. Bertrand, B. Bereza and E. Dujardin, *Z. Naturforsch., Teil C*, 43 (1988) 443.
- [29] B. Schoefs and F. Franck, *J. Exp. Bot.*, 44 (1993) 1053.
- [30] A.D.J. Meeuse and E.C.J. Ott, *Acta Bot. Neerl.*, 11 (1962) 227.
- [31] B. Schoefs and F. Franck, in M. Baltscheffsky (Editor), *Progress in Photosynthesis Research*, Vol. III, Kluwer, Dordrecht, 1990, p. 755.
- [32] A.R. Wellburn, *Phytochemistry*, 9 (1970) 2311.
- [33] A.R. Wellburn, *Biochem. Physiol. Pflanz.*, 169 (1976) 265.
- [34] S. Schoch, *Z. Naturforsch., Teil C*, 33 (1978) 712.
- [35] B. Schoefs and F. Franck, *C.R. Acad. Sci., Ser. III*, 313 (1991) 441.
- [36] F. Franck and K. Strzalka, *FEBS Lett.*, 309 (1992) 73.
- [37] B. Schoefs, M. Bertrand and F. Franck, *Photosynthetica*, 27 (1992b) 497.
- [38] F.C. Belanger and C.A. Rebeiz, *J. Biol. Chem.*, 255 (1980) 1266.
- [39] Y. Shioi and K. Takamiya, *Plant Physiol.*, 100 (1992) 1291.
- [40] W. Eichenberger and E.C. Grob, *Helv. Chim. Acta*, 45 (1962) 974.
- [41] G. Britton, in Y. Dei (Editor), *Methods in Plant Biochemistry*, Vol. 7, Academic Press, New York, 1991, p. 473.
- [42] E.E. Carey and C.A. Rebeiz, *Plant Physiol.*, 79 (1985) 1.
- [43] N. Mukaida, N. Kawai, Y. Onoue and Y. Nishikawska, *Anal. Sci.*, 9 (1993) 625.
- [44] H. Adamson, M. Lennon, K.-L. Ou, N. Packer and J. Walmsley, in M. Baltscheffsky (Editor), *Progress in Photosynthesis Research*, Vol. III, Kluwer, Dordrecht, 1990, p. 687.
- [45] H. Durchan, E.V. Pakshina and N.N. Lebedev, *Photosynthetica*, 28 (1993) 567.
- [46] N. Mukaida and Y. Nishikawa, *Nippon Kagaku Kaishi*, 11 (1990) 1244.
- [47] S. Frosch, M. Jabben, R. Bergfeld and H. Mohr, *Planta*, 145 (1979) 497.
- [48] H.W. Kümmel and L.H. Grimme, *Z. Naturforsch.*, 30 (1975) 333.
- [49] M. Fujiwara, M. Hayashi, M. Tasumi, K. Kanaji, Y. Koyama and K. Satoh, *Chem. Lett.*, (1987) 2005.
- [50] Y. Lemoine, G. Zabulon and S.S. Brody, in N. Murata (Editor), *Research in Photosynthesis*, Vol. I, Kluwer, Dordrecht, 1992, p. 331.
- [51] P. Barry, A.J. Young and G. Britton, *J. Exp. Bot.*, 42 (1991) 229.
- [52] S. Schoch, U. Lempert and W. Rüdiger, *Z. Pflanzenphysiol.*, 83 (1977) 427.

Short communication

Analysis of nerve agent degradation products using capillary ion electrophoresis

Stuart A. Oehrle^{a,*}, Paul C. Bossle^b

^a*Waters Corporation, 34 Maple Street, Milford, MA 01757, USA*

^b*Research and Technology Directorate, US Army Edgewood Research, Development and Engineering Center, Aberdeen Proving Ground, MD 21010-5423, USA*

Abstract

A method has been developed for the analysis of nerve agent degradation products using capillary ion electrophoresis. Analysis of the primary degradation products isopropyl methylphosphonic acid, ethyl methylphosphonic acid, pinacolyl methylphosphonic acid and methylphosphonic acid was accomplished with run times of less than 5 min. Detection of low mg/l levels of degradation products in spiked water samples was possible. Little sample preparation was required for the analysis of the alkyl methylphosphonic acids.

1. Introduction

With the end of the cold war military bases throughout the USA and elsewhere are being closed. Those bases that contained or stored chemical nerve agents must be identified, monitored and, if necessary, remediated. Those bases that currently store or destroy chemical munitions must also be monitored for possible contamination. Once exposed to the environment most chemical nerve agents readily degrade by hydrolysis to form alkyl methylphosphonic acids. Fig. 1 shows the breakdown process of each nerve agent [1]. The first hydrolysis is rapid and each particular alkyl methylphosphonic acid formed is particular to each originating nerve agent. While there are no current US Environmental Protection Agency regulations for these nerve agent degradation products, there are several military methods which describe the

analysis of these compounds [1,2]. Most of these methods describe the use on ion chromatography for analysis. Using ion chromatography, low mg/l to mid ng/l levels of detection can be easily obtained [1,2]. Some of these methods require the use of a silver resin for chloride removal prior to analysis. This is because several of the compounds of interest elute near the chloride peak thus making identification and quantitation difficult if the chloride is not removed. Typical analysis times by ion chromatography for these alkyl methylphosphonic acids is 14 min or longer. Capillary ion electrophoresis (CIE) has been previously shown to be a fast and reliable technique for ion analysis [3–8]. CIE was applied to the analysis of these acids since the separation technique is different from ion chromatography and may provide better resolution or selectivity than ion chromatography. A chromate, high-mobility, electrolyte with an osmotic flow modifier (OFM) was used to separate the alkyl phosphonic acids. OFM is added to the elec-

* Corresponding author.

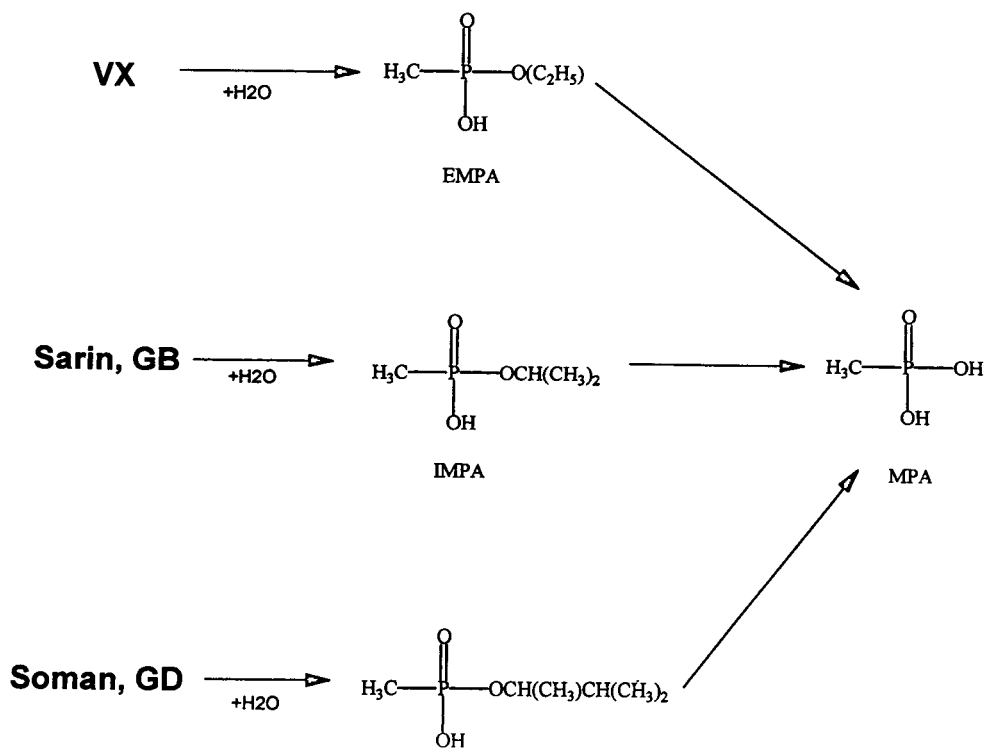


Fig. 1. Nerve agent degradation pathway for the three main alkyl methylphosphonic acids studied.

tolyte as an additive that reverses the normally cathodic direction of the electroosmotic flow (EOF) that is found in fused-silica capillaries. This creates a co-electroosmotic condition that augments the mobility of the analytes. To reduce excess carbonate typically found in the water samples, a Milli-Trap H⁺ cartridge was used to reduce the carbonate. Analysis of the four main phosphonic acids was done in a spiked ground-water sample.

2. Experimental

2.1. Instrumentation

The capillary electrophoresis (CE) system employed was the Quanta 4000E CIA (Waters, Milford, MA, USA). A Hg lamp was used for

indirect UV detection at 254 nm. AccuSep polyimide fused-silica capillaries of 60 cm × 75 μm I.D. were used throughout.

Data acquisition was carried out with a Waters Millennium 2010 Chromatography Manager with a SAT/IN module connecting the CE system to the data station with the signal polarity inverted from the CE system. Detector time constant for the CE was set at 0.1 s for anion analysis. The data rate for the CE was 20 points/s. Collection of electropherographic data was initiated by a signal connection between the CE system and the SAT/IN module.

2.2. Chemicals and sample treatment

The chromate electrolyte was prepared from a concentrate containing 100 mM Na₂CrO₄ (Fisher Scientific, Pittsburgh, PA, USA) and

0.017 mM H₂SO₄ (Fisher Scientific Ultrex Grade). Milli-Q reagent-grade water (Millipore, Bedford, MA, USA) was used for all rinsing, dilution and preparation. OFM was obtained in the Br form as a 20 mM concentrate from Waters [9]. Milli-Trap H⁺ cartridges (Waters) were used for sample pretreatment of the ground- and tapwater samples. H⁺ resin was obtained from Bio-Rad (Hercules, CA, USA) and converted to the Ag⁺ form by soaking the resin for 24 h in a concentrated solution of AgNO₃. The resulting resin was packed in 3–5-ml slurries onto 10-ml syringes with disposable filters on the end of them and rinsed several times with high-purity water. Water samples were then passed through the resin and the effluent collected as well as a water blank. Standards of isopropyl methylphosphonic acid (IMPA), ethyl methylphosphonic acid (EMPA), pinacolyl methylphosphonic acid (PMPA) and methylphosphonic acid (MPA) were supplied by the US Army Environmental

Center (USAEC). All other chemicals used were of ACS grade or better.

3. Results and discussion

Fig. 2 is an electropherogram of all four compounds of interest. The advantage of CIE is that these peaks elute after the main anions (i.e. chloride, sulfate, nitrate, etc.) that are found in most water samples and the analysis time is less than 5 min. The main peak prior to MPA at 2.7 min in Fig. 2 is carbonate. Prior to carbonate in the electropherogram fluoride and phosphate would migrate as well. These two peaks were found to almost coelute since the electrolyte pH had been raised, to allow for MPA to be resolved from carbonate, from the normal pH of 8 to a higher pH of approximately 9.2. Fig. 3A is an electropherogram of a spiked groundwater sample. The migration of MPA with carbonate is still

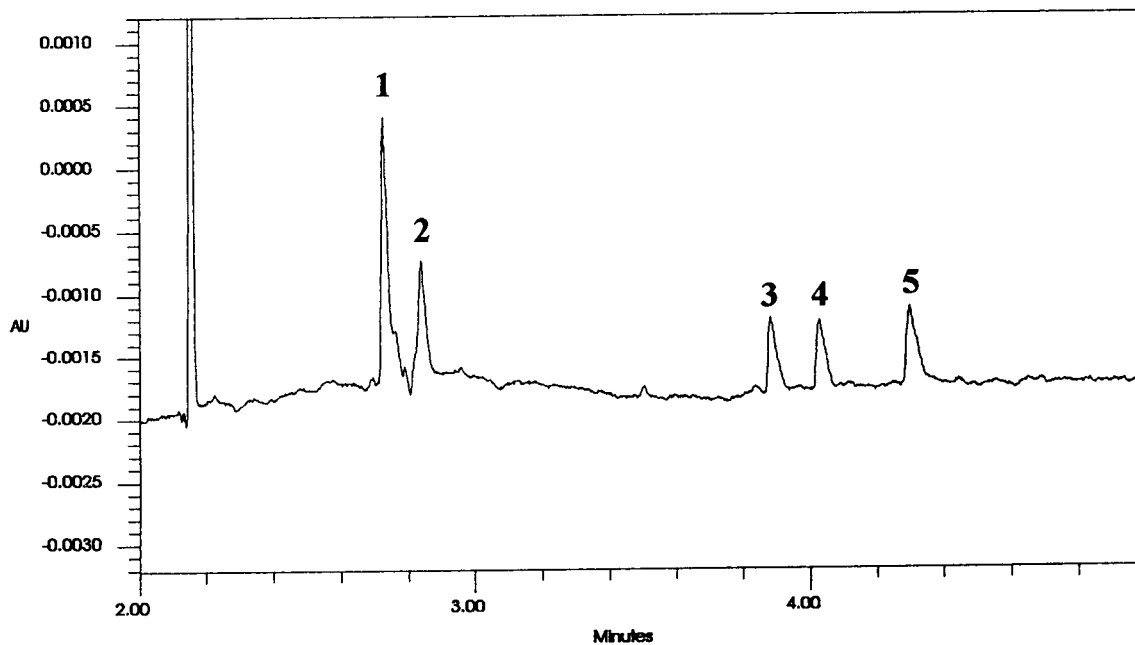


Fig. 2. Electropherogram of a standard. CIE conditions: fused-silica 60 cm × 75 μm I.D. capillary; voltage: 18 kV (negative); electrolyte: 4.5 mM chromate–0.5 mM OFM–1.0 mM NaHCO₃; indirect UV detection at 254 nm; hydrostatic injecton (10 cm for 30 s). Peaks: 1 = carbonate (8.0 mg/l); 2 = MPA (7.0 mg/l); 3 = EMPA (3.1 mg/l); 4 = IMPA (3.3 mg/l); 5 = PMPA (3.3 mg/l).

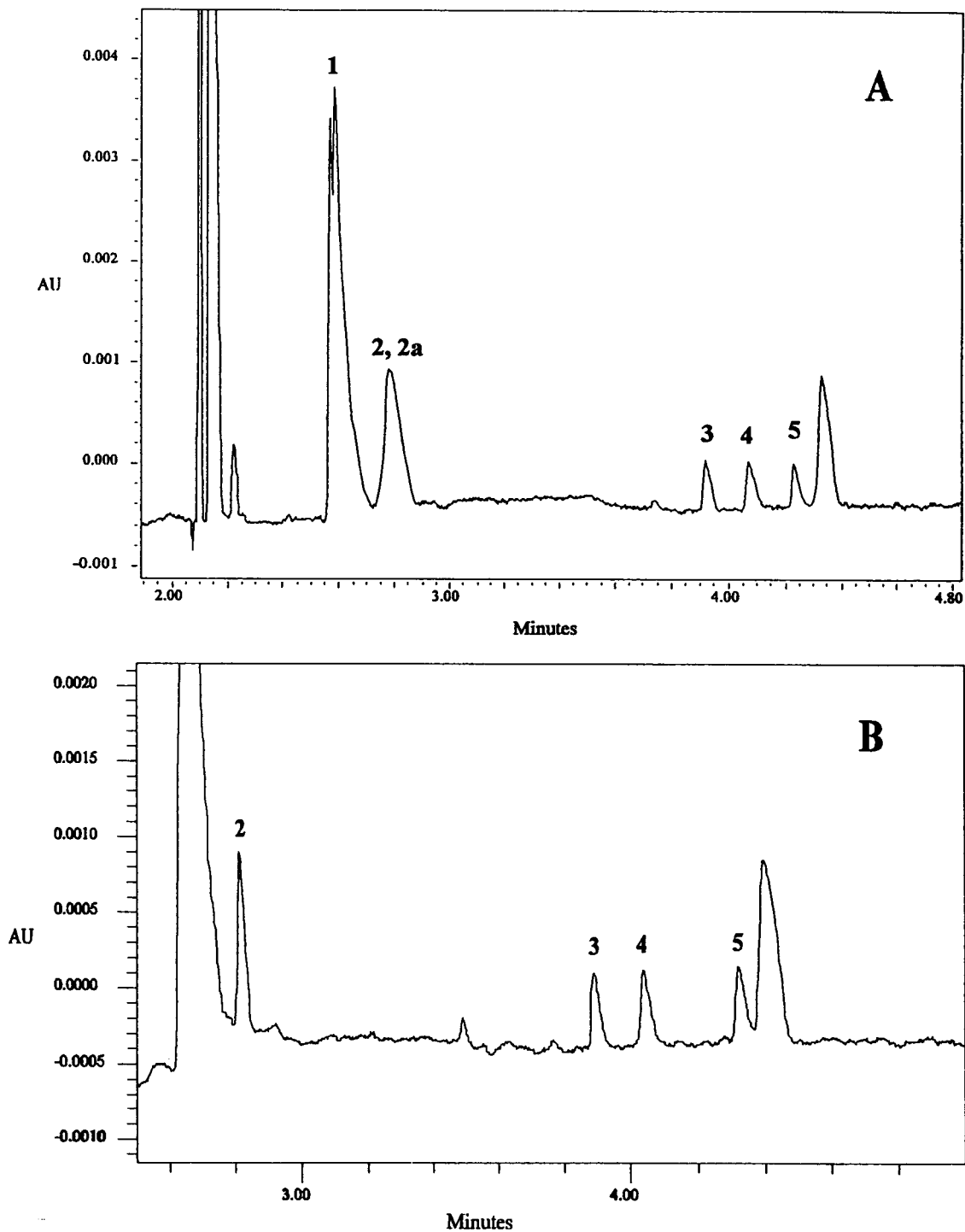


Fig. 3. Electropherogram of spiked groundwater sample without (A) and with (B) passing it through a Milli-Trap H⁺ cartridge. Peaks: 1 = fluoride and hydrogen phosphate; 2 = MPA (7.1 mg/l); 2a = carbonate (natural levels); 3 = EMPA (3.1 mg/l); 4 = IMPA (3.3 mg/l); 5 = PMPA (3.3 mg/l). Conditions as in Fig. 1.

an issue, especially in groundwater samples that contain high carbonate levels as is the case with the sample in Fig. 3. One solution was to run the samples through a Milli-Trap H⁺ cartridge which removes any excess carbonate from the sample without effecting the remaining ions. Milli-Trap H⁺ cartridges have been described and used previously for carbonate removal from groundwater samples prior to ion chromatographic

analysis [10,11]. Fig. 3B is the same spiked groundwater sample except that it had been passed through a Milli-Trap cartridge. MPA is now resolved (Fig. 3B) and the peak just prior to it is fluoride and hydrogenphosphate.

In the case of samples containing very high chloride levels sample pretreatment by passing the water through an Ag⁺ resin, just like for ion chromatographic analysis, can be done as well.

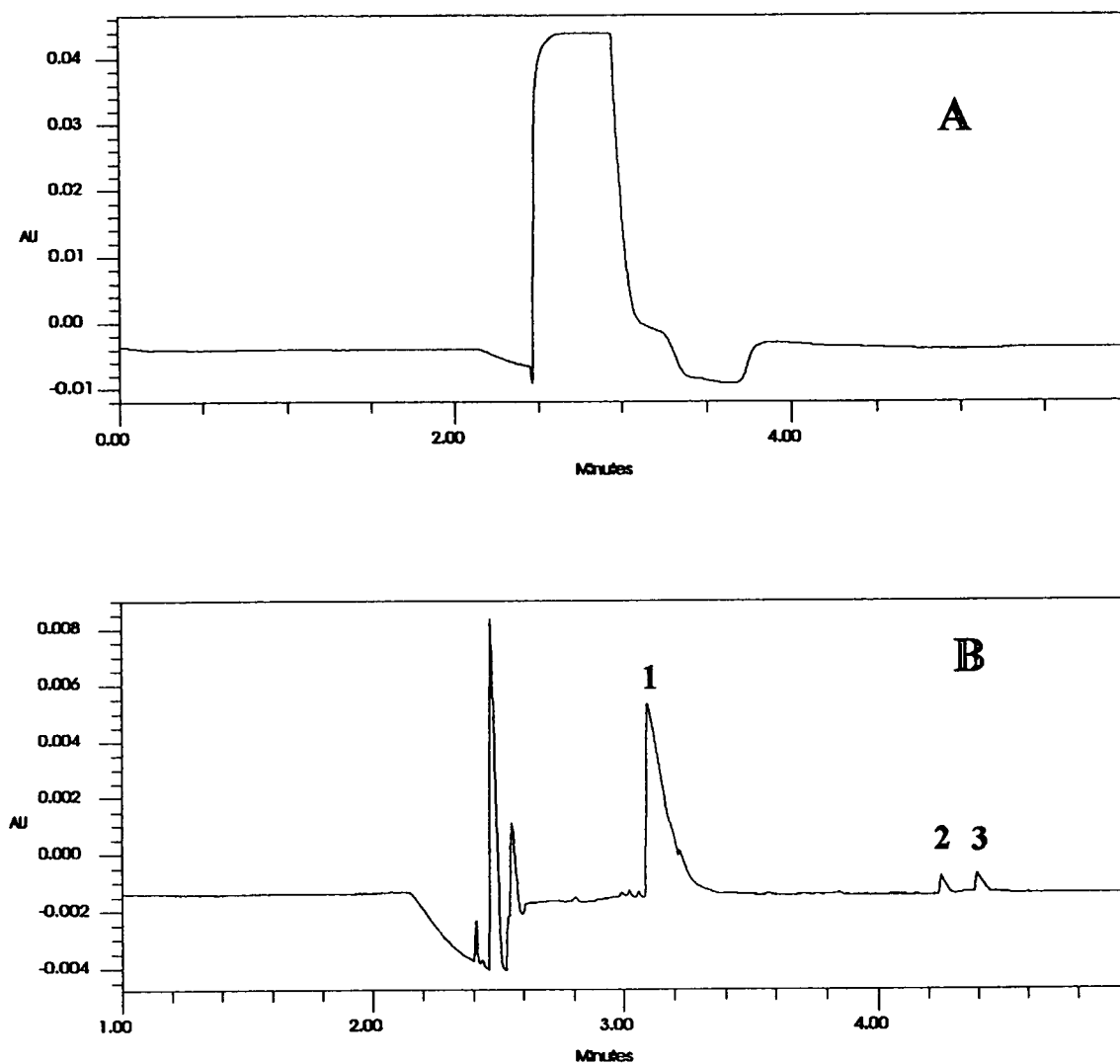


Fig. 4. Electropherogram of the spiked water sample containing a high level of chloride (approximately 4000 mg/l) before (A) and after (B) pretreatment with the Ag⁺ resin. Peaks: 1 = fluoride/phosphate and carbonate (natural levels); 2 = EMPA; 3 = IMPA. Conditions as in Fig. 1.

Fig. 4A is an example of a spiked water sample containing over 4000 mg/l of chloride with IMPA and EMPA spiked in at levels of approximately 7.0 mg/l. Fig. 4A is the spiked groundwater sample without any pretreatment, and Fig. 4B is the same sample after passing the water sample through the Ag^+ resin. As can be seen in Fig. 4B the high chloride level has been reduced now allowing for EMPA and IMPA to be resolved.

CIE offers the potential for analysis of these main alkyl methylphosphonic acids with analysis times of less than 5 min. Further, the use of a silver resin and the Milli-Trap cartridge for sample pretreatment offers the potential for reducing interfering ions from the sample prior to analysis.

4. Further work

Further work on improving this method will continue, especially in the area of MPA detection. One area of interest is in using electromigration as an injection technique. This offers the ability to preconcentrate ions on the head of

the capillary. Another area of interest is in other electrolytes which may mask the carbonate completely allowing for easier MPA identification and quantitation.

References

- [1] A. Kingery and H. Allen, *Anal. Chem.*, 66 (1994) 155.
- [2] P. Bossle, D. Reutter and E. Sarver, *J. Chromatogr.*, 407 (1987) 397.
- [3] G. Bondoux, P. Jandik and W.R. Jones, *J. Chromatogr.*, 602 (1992) 79.
- [4] W.R. Jones and P. Jandik, *J. Chromatogr.*, 546 (1991) 445.
- [5] J.P. Romano and J. Krol, *J. Chromatogr.*, 640 (1993) 403.
- [6] P.E. Jackson and P.R. Haddad, *J. Chromatogr.*, 640 (1993) 481.
- [8] P. Jandik and W.R. Jones, *J. Chromatogr.*, 546 (1991) 431.
- [9] Waters Chromatography Division of Millipore, *US Pat.*, 5 104 506, 5 128 055 and 5 156 728 (1992).
- [10] W. Jones and P. Jandik, *Am. Lab.*, June (1990) 24.
- [11] W. Jones and P. Jandik, *J. Chromatogr. Sci.*, 27 (1990) 449.

Extending the scope of chiral separation of basic compounds by cyclodextrin-mediated capillary zone electrophoresis

Changyu Quang¹, Morteza G. Khaledi*

Department of Chemistry, North Carolina State University, P.O. Box 8204, Raleigh, NC 27695, USA

Abstract

In a previous paper on cyclodextrin-mediated capillary zone electrophoresis, it was shown that the use of short-chain tetraalkylammonium cations leads to a reversal in the direction of the electroosmotic flow without an adverse effect on enantioselectivity. As a result, enantiomeric resolution of basic (cationic) compounds can be improved as the electroosmotic flow counteracts the migration of solute enantiomers. It is demonstrated in this report that the scope of chiral separation of basic compounds can be further extended by a combination of reversing the electroosmotic flow and enhancing enantioselectivity through the chemical modifications of β -cyclodextrin. Therefore, β -cyclodextrin and its derivatives were evaluated as chiral recognition agents for the chiral separations of 22 basic compounds with rather complex molecular structures. The differences in enantioselectivity displayed by β -cyclodextrin and derivatives are discussed in order to achieve a better understanding of the chiral interactions involved in the discrimination of solute enantiomers.

1. Introduction

Cyclodextrin (CD)-mediated capillary zone electrophoresis (CZE) has been successful, versatile, and inexpensive for separation of chiral compounds [1–18]. Chiral separation of dansylated amino acids, catecholamines, and other chiral amines have been reported where CDs have either been incorporated into a gel matrix [5,6], mixed with a micellar phase [7,8], or used in the free buffer solutions. Although chiral separation by CD-mediated CZE has been quite successful, individual separation problems frequently require different types of derivatized CDs (e.g., dimethylated-, trimethylated- β -CD

and others). At this time, selections of the appropriate chiral selectors for a given chiral compound are not straightforward since predictions of the enantioselectivity of CDs based on the molecular structures of guest molecules are often difficult. Therefore, it is necessary to evaluate the different enantioselectivity of CDs for a wide range of chiral compounds in order to better understand the chiral interactions involved in the discrimination of solute enantiomers and to effectively utilize them in chiral separations.

In a previous work on CD-mediated CZE, it was shown that the use of short-chain tetraalkylammonium (TAA) cations in the buffer solution leads to a reversal in the direction of the electroosmotic flow (EOF) at the acidic condition of pH 2.5 [1]. As a result, enantiomeric resolution of basic (cationic) compounds can be improved as the EOF counteracts the migration

* Corresponding author.

¹ Present address: Battelle Pacific Northwest Laboratory, M.S. P7-07, P.O. Box 999, Richland, WA 99352, USA.

of solute enantiomers [1,2]. The advantage of the short-chain TAA cations as compared to the long-chain cationic surfactants is that the formers do not interact strongly with CDs, leaving the chiral recognition sites more accessible for solute enantiomers. On the other hands, the short-chain TAA cations effectively cover the fused-silica capillary surface, leading to a reversal of the EOF at the acidic condition of pH 2.5. It is demonstrated in this report that the scope of chiral separation of basic compounds by CD-mediated CZE can be further extended by a combination of reversing the EOF with enhancing enantioselectivity through the chemical modifications of β -CD.

2. Experimental

2.1. Apparatus

Experiments were carried out on a laboratory-built CZE unit, consisting of a ± 30 kV high-voltage power supply (Series EH; Glassman High Voltage, Whitehouse, NJ, USA), a UV-Vis detector (Model 200; Linear Instruments, Reno, NV, USA) and a Spectra-Physics integrator (Model SP4200; Spectra-Physics, San Jose, CA, USA). Untreated fused-silica capillary tubes (Polymicro Technologies, Phoenix, AZ, USA) of $52 \mu\text{m}$ I.D. \times $360 \mu\text{m}$ O.D. were used as the separation columns. The total length of the capillary was 62 cm, and 50 cm to the detector. The capillary temperature was maintained at 40°C by jacketing it in light mineral oil using a constant-temperature circulator (Type K2-R; Lauda, Germany). The injection samples were dissolved in water-methanol mixture and introduced into the capillary by gravity, 10 cm height for 5 s. The applied voltage was 20 kV for all the electrophoretic separations.

2.2. Chemicals

Tetramethylammonium (TMA) hydroxide (40% in water) and tetrabutylammonium (TBA) hydroxide (40% in water) were obtained from Aldrich (Milwaukee, WI, USA). Heptakis(2,3,6-

tri-O-methyl)- β -cyclodextrin (TM- β -CD) was purchased from Sigma (St. Louis, MO, USA). β -CD, dimethyl- β -cyclodextrin (DM- β -CD) and hydroxypropyl- β -cyclodextrin (HP- β -CD) were gifts from American Maize-Products Co. (Hammond, IN, USA). All racemic samples were commercially available from Sigma, and their chemical structures are listed in Table 1.

2.3. Procedures

A computer program, MIXBUF (a program developed in this laboratory in Turbo Vision), was used to calculate the buffer composition with a given ionic strength at pH 2.50. The appropriate amount of CD was dissolved in the buffer electrolyte, then the solution was filtered with a $0.45\text{-}\mu\text{m}$ filter before use.

3. Results and discussion

3.1. Theoretical considerations

With a buffer electrolyte containing CD, the relationship between the electrophoretic mobility (in short mobility, μ) of a solute and CD inclusion complexation can be expressed as [5]

$$\mu = \frac{\mu^f + K_{\text{CD}}[\text{CD}]\mu^c}{1 + K_{\text{CD}}[\text{CD}]} \quad (1)$$

where μ^f and μ^c are the mobilities of the solute in the free and complexed forms, respectively. K_{CD} is the formation constant of inclusion complex. $[\text{CD}]$ represents the concentration of CD in the buffer electrolyte.

Resolution, R_s , between two enantiomers in CZE in the presence of electroosmosis can be expressed as [19,20]

$$R_s = \frac{\sqrt{N}}{4} \cdot \frac{\Delta\mu}{\mu_{\text{av}} + \mu_{\text{eo}}} \quad (2)$$

where N is the number of theoretical plates, μ_{eo} is the electroosmotic mobility, μ_{av} is the average electrophoretic mobility and $\Delta\mu$ is the mobility difference for a pair of enantiomers. By using Eq. 1, $\Delta\mu$ can be derived as

$$\Delta\mu = \frac{(\mu^f - \mu^c)\Delta K[\text{CD}]}{(1 + K_{\text{CD}1}[\text{CD}])(1 + K_{\text{CD}2}[\text{CD}])} \quad (3)$$

where ΔK is the difference in formation constants for the two enantiomers (e.g., $K_{\text{CD}2} - K_{\text{CD}1}$).

Substituting Eq. 3 into Eq. 2 gives

$$R_s = \frac{(\mu^f - \mu^c)\Delta K[\text{CD}]}{(1 + K_{\text{CD}1}[\text{CD}])(1 + K_{\text{CD}2}[\text{CD}])} \cdot \frac{\sqrt{N}}{4(\mu_{\text{av}} + \mu_{\text{eo}})} \quad (4)$$

As theoretically indicated by Eq. 4, there are several methods for improving enantiomeric resolution, R_s :

Enhancing enantioselectivity (ΔK)

This approach involves selecting a suitable chiral recognition agent. The selection of chiral selector, however, requires an understanding of the chiral interactions between the chiral selector and solute molecules. For this reason, it is necessary to evaluate the differences in enantioselectivity displayed by β -CD and its derivatives for a wide range of chiral compounds.

Controlling electroosmosis

The term of $\mu_{\text{av}} + \mu_{\text{eo}}$ in Eq. 4 indicates that both the magnitude and direction (sign) of μ_{eo} relative to those of the mobility of solutes will affect R_s . Maximum R_s could be obtained when $\mu_{\text{eo}} = -\mu_{\text{av}}$ at the expense of analysis time approaching infinity. Methods of incorporating β -CD into a gel matrix [5], and using coated capillary columns at low-pH conditions [10,11] are intended to eliminate or considerably reduce the EOF. In a bare fused-silica capillary, the migration of basic (cationic) compounds is in the same direction of the EOF. Therefore, it is possible to increase enantiomeric resolution by reversing the EOF to counteract the migration of the basic enantiomers. One limitation of such an approach, however, is the loss of efficiency due to longitudinal diffusion as the migration times of solutes are prolonged.

Optimizing [CD]

For a given chiral compound, as reported by Wren and Row [15,16], R_s can be improved by optimizing the concentration of CD since R_s is a function of [CD]. However, since R_s depends on $K_{\text{CD}1}$ and $K_{\text{CD}2}$, the optimum CD concentration may be different from one pair of chiral compounds to another.

Using charged CDs

The term of $(\mu^f - \mu^c)$ in Eq. 4 can be increased by using CDs with the electric charges opposite to that of guest enantiomers, such that the chiral recognition agents and solute enantiomers will move in the opposite directions. Such an example has been reported by Otsuka and Terabe [7] who used a positively charged β -CD for the separation of anionic enantiomers. However, there exists a chance that the introduction of electrostatic interactions would adversely influence the enantioselectivity of β -CDs.

3.2. Effect of short-chain TAA cations

The role of sodium, TMA and TBA cations were compared as the buffer cations in the absence of CD for the non-chiral separation of a mixture of aromatic amines. As shown in Fig. 1, the use of short-chain TAA cations extended the migration range, and obviously the overall resolution was improved at the expense of analysis times. The μ_{eo} values were measured as 1.1, -1.2, and -0.9 ($\cdot 10^{-4}$ cm²/V s) for the buffer conditions in Fig. 1A (sodium), B (TMA) and C (TBA), respectively. The reversed EOF was determined by reversing the polarity of the applied voltage and injecting neutral solutes. Note that although the EOF was reversed under the buffer conditions in Fig. 1B and C, the magnitude of μ_{eo} values was still smaller than that of the mobility of all the test solutes. Therefore, the aromatic amines still migrate towards and are detected at the negative electrode.

The separations in Fig. 1 also illustrate the effect of the buffer cations on separation selectivity. A baseline separation of isoproterenol and

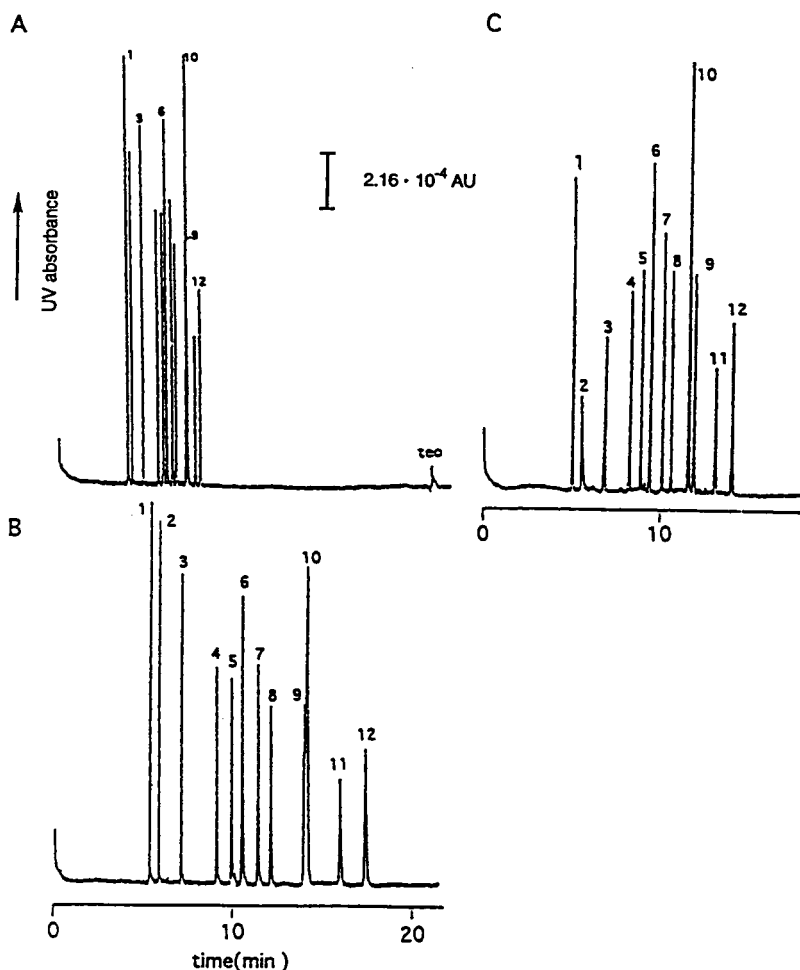


Fig. 1. Effect of the buffer cations on the separation of 12 organic amines. Buffer electrolytes: (A) 50 mM sodium phosphate (pH 2.50), (B) 50 mM TMA phosphate (pH 2.50) and (C) 50 mM TBA phosphate (pH 2.50). Peaks: 1 = imidazole; 2 = nicotine; 3 = doxylamine; 4 = 2-methylphenethylamine; 5 = 1-methylphenylpropylamine; 6 = pseudoephedrine; 7 = norepinephrine; 8 = epinephrine; 9 = isoproterenol; 10 = propranolol; 11 = metoprolol; 12 = nadolol. Capillary: 62 cm (50 cm to the detector) \times 52 μ m I.D. \times 360 μ m O.D. The applied voltage is 20 kV, and the current is 37 μ A for (A), 34 μ A for (B) and 29 μ A for (C).

propranolol (peaks 9 and 10) was obtained only with the TBA phosphate buffer (Fig. 1C).

Fig. 2 shows chiral separation of norephedrine, pseudoephedrine and ephedrine. As predicted by the chiral recognition model proposed earlier [1], norephedrine, which can not be resolved by β -CD because of the lack of an alkyl group on the N atom, can be resolved by DM- β -CD that introduces a steric effect between the N atom of the guest molecule and the C-2 positions of β -CD. Again, a selectivity difference was

observed between using TMA and TBA as buffer cations as shown in Fig. 2. In the TMA phosphate buffer, (1*S*,2*R*)-norephedrine co-eluted with (1*R*,2*R*)-ephedrine; a better overall separation was provided with the TBA phosphate buffer. The migration order in the above separations can be explained by the proposed model [1] and was confirmed by injecting pure enantiomeric samples.

Fig. 3 shows another example of the effect of buffer cations on chiral separation. Interestingly,

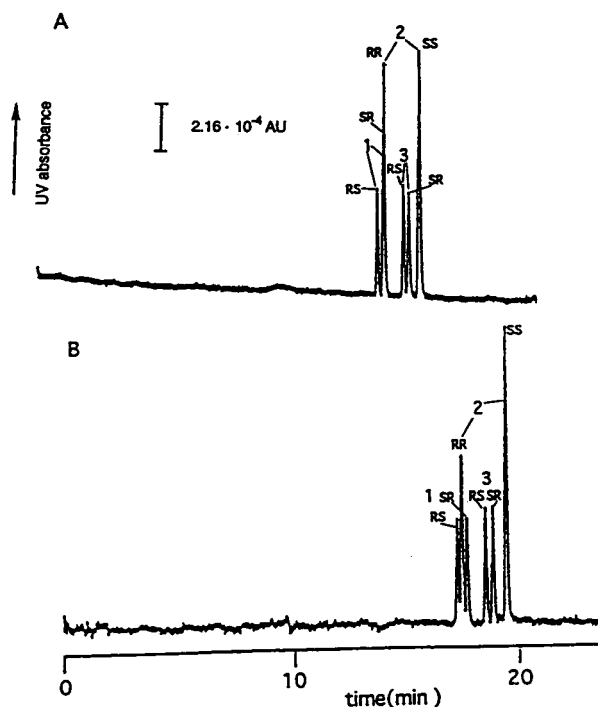


Fig. 2. Chiral separation of (1) norephedrine, (2) pseudoephedrine and (3) ephedrine. Buffer electrolytes: 20 mM DM- β -CD in (A) 50 mM TMA phosphate (pH 2.50) and (B) 100 mM TBA phosphate (pH 2.50). Other conditions as in Fig. 1.

a complete chiral separation of trimipramine, an antidepressant drug, was obtained only by using a buffer of 100 mM TBA phosphate (pH 2.50) containing 20 mM HP- β -CD.

As compared to the TMA cations, the TBA cations have many significant features such as providing a different separation selectivity, increasing the solubility of β -CD [1]; and having low conductivity. However, it was found that the TBA cations compete with analytes to some extent for the hydrophobic cavity of β -CDs, which reduces the enantiomeric resolution of some compounds. In this regard, the TMA cations are less competitive due to a shorter alkyl chain, and generally more suitable for chiral separation of basic compounds.

3.3. Effect of chemical modifications of β -CD

Fig. 4 shows chiral separation of norepinephrine, epinephrine, isoproterenol and propranolol with different types of β -CDs. It can be seen that increasing the size of the substituent on the N atom of guest molecule [e.g., H-, CH₃- and (CH₃)₂CH-, for norepinephrine, epinephrine and isoproterenol] and alkylating the hydroxyl groups at the C-2 positions of β -CD (e.g., DM- β -CD) leads to higher enantioselectivity (see Fig. 4A and B). Note that the more retained enantiomers have the same stereochemical arrangement, having the *S* absolute configuration, except propranolol, for which this configuration is defined as *R* [10,11].

Using the proposed chiral recognition model [1], it is conceivable that the steric interaction between the substituent on the N atom of guest molecules and the functional groups at the C-2 positions of β -CD generally decrease the stability of inclusion complexes (comparing DM- β -CD with β -CD), but it destabilize the complexes formed by the *S*-enantiomers to a lesser extent as compared to those of *R*-enantiomers. In other words, the steric effect increases the differences in stability of complexes formed by *S*- and *R*-enantiomers, leading to an increase in enantiomeric resolution. A chiral recognition mechanism for propranolol on β -CD stationary phase in HPLC has been described by Armstrong et al. [21].

It is important to note that since β -CD contains 21 hydroxyl groups, the products obtained from chemical modifications are always a mixture of the derivatized β -CD with various degree of substitution [22]. It is known that the partial alkylation of β -CD is more likely to occur at the hydroxyl groups at C-2 and C-6 positions [23,24]. Since DM- β -CD and HP- β -CD are partially alkylated products of β -CD, they may possess similar molecular structures, leading to their similarity in enantioselectivity (see Fig. 4B and D).

We have evaluated β -CD and its derivatives for chiral separation of 22 basic compounds with rather complex molecular structures, including β -blockers, calcium-channel blockers, antihis-

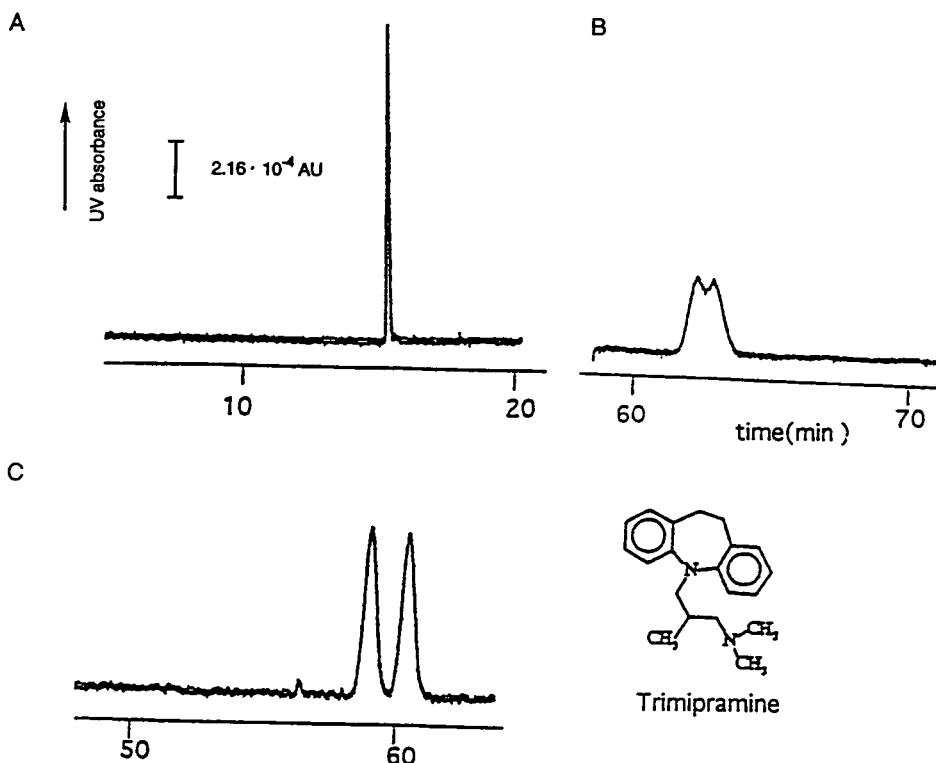


Fig. 3. Chiral separation of trimipramine. Buffer electrolytes: 20 mM HP- β -CD in (A) 50 mM sodium phosphate (pH 2.5), (B) 50 mM TMA phosphate (pH 2.5) and (C) 100 mM TBA phosphate (pH 2.5). Other conditions as in Fig. 1.

tamines, catecholamines, and other chiral amines. Their chemical structures are listed and separation data are summarized in Table 1. For each racemate, separation factor, α , was calculated by [5]

$$\alpha = \mu_1 / \mu_2 \quad (5)$$

μ_1 and μ_2 are the mobilities of two enantiomers (note: $\mu = \mu_{\text{obs}} - \mu_{\text{eo}}$). R_s was calculated according to Eq. 2 by assuming N equal to 100 000. Baseline separation is generally obtained when R_s exceeds 1.5.

From the data in Table 1, it appears that HP- β -CD shows a similarity in enantioselectivity to both DM- β -CD and β -CD. This is indicated by the fact that HP- β -CD resolve the same group of the basic compounds as DM- β -CD, and it also resolves compounds such as doxylamine, chlorpheniramine and labetalol that are well

resolved by β -CD, which, apparently, is related to its unique molecular structures. According to the manufacture, there are 6–7 mol of hydroxypropyl ($\text{HOCH}_2\text{CH}_2\text{CH}_2-$) per mol of β -CD. In other words, two thirds of the hydroxyl groups remain unreacted on the rim of β -CD. It can be expected that HP- β -CD resembles DM- β -CD by having some of the C-2 and C-6 hydroxyl groups substituted, and differs with DM- β -CD by having longer and polar substituents and by having lesser degree of substitution. The unreacted hydroxyl groups on the D-(+)-glucopyranose units provide HP- β -CD with the characteristics of native β -CD. Consequently, HP- β -CD is generally more selective for basic compounds with a chiral center located at a distance from the hydrophobic moiety such as trimipramine and some of the β -blockers. On the other hand, DM- β -CD is more suitable for compounds with a chiral center close to the aromatic ring such as

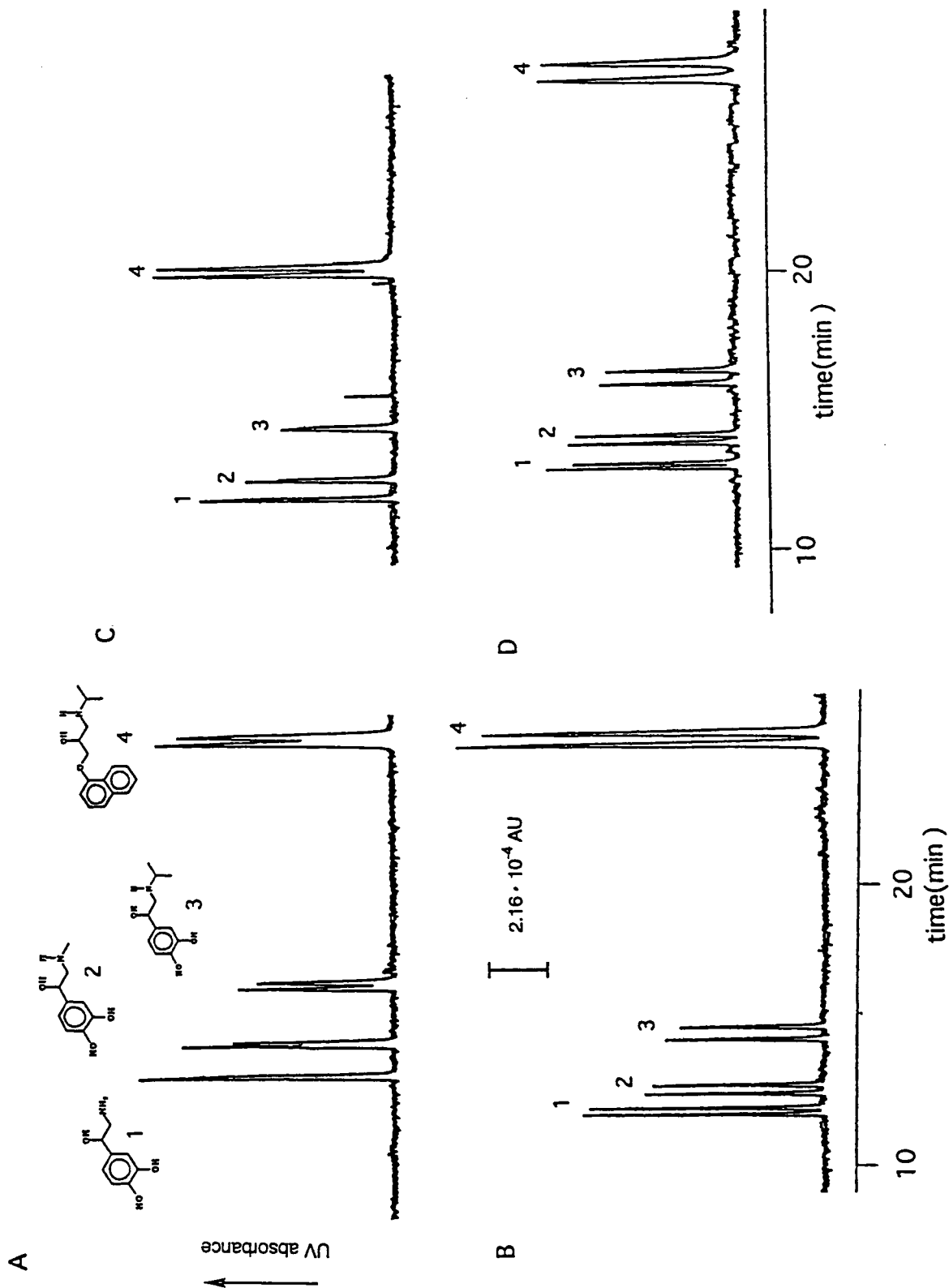
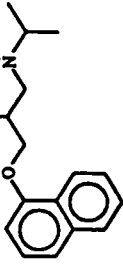
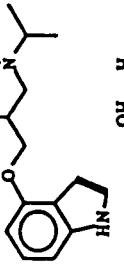
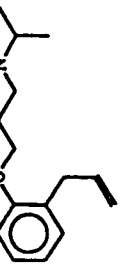
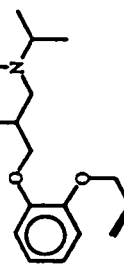
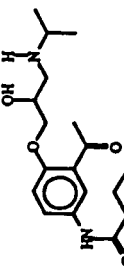
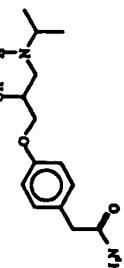
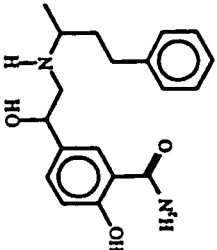
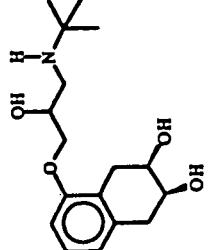
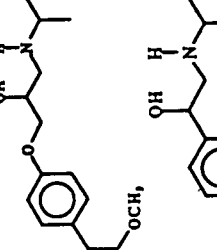
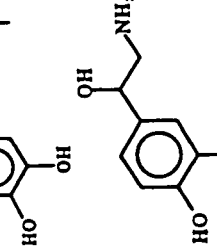
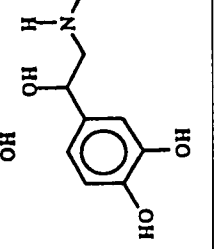



Fig. 4. Effect of the type of β -CDs on chiral separation of (1) norepinephrine, (2) epinephrine, (3) isoproterenol and (4) propranolol. Buffer electrolytes: 50 mM TMA phosphate (pH 2.50) containing: (A) 20 mM β -CD, (B) 20 mM DM- β -CD, (C) 20 mM TM- β -CD and (D) 20 mM HP- β -CD. Other conditions as in Fig. 1.

Table 1
Separation data for basic (cationic) compounds

Name	Structure	β -CD			TM- β -CD			DM- β -CD			HP- β -CD		
		t_R	α	R_s	t_R	α	R_s	t_R	α	R_s	t_R	α	R_s
Propranolol		24.83	1.005	0.79	20.06	1.007	1.10	25.19	1.008	1.34	26.83	1.010	1.75
		25.08			20.34			25.62				27.43	
Pindolol		18.40	1.005	0.68	15.32	N.S.	N.S.	17.43	1.009	1.26	17.61	1.007	0.94
		18.56						17.71			17.82		
Alprenolol		33.30	1.004	0.78	17.54	N.S.	N.S.	24.68	1.006	1.02	24.95	1.008	1.38
		30.60						25.00			25.39		
Oxprenolol		19.42	N.S.	N.S.	16.00	N.S.	N.S.	18.14	1.005	0.74	17.90	1.006	0.84
								18.31			18.09		
Acebutolol		23.41	N.S.	N.S.	19.85	N.S.	N.S.	19.49	N.S.	N.S.	20.45	N.S.	N.S.
Atenolol		27.80	N.S.	N.S.	16.34	N.S.	N.S.	16.95	1.004	0.56	18.68	1.004	0.59
								17.07			18.82		

Labetalol ^a		29.50 29.96	1.007	1.22	22.33	N.S.	27.45 27.52	1.001	0.20	28.67 29.10	1.006	1.18
Nadolol ^a		19.16	N.S.	17.92	N.S.	N.S.	17.24	N.S.	N.S.	17.89 18.08	1.006	0.84
Metoprolol		33.20	N.S.	18.13	N.S.	N.S.	26.36 26.56	1.003	0.60	29.84	N.S.	
Isoproterenol		15.94 16.15	1.008	1.04	14.68	N.S.	14.46 14.90	1.018	2.37	15.64 16.12	1.018	2.39
Norepinephrine		12.76	N.S.	11.88	N.S.	N.S.	11.80 12.01	1.011	1.40	12.62 12.79	1.008	1.06
Epinephrine		13.89 14.02	1.007	0.85	12.57	N.S.	12.53 12.82	1.015	1.81	13.51 13.80	1.013	1.68

(Continued on p. 262)

Table 1 (continued)

Name	Structure	β-CD		TM-β-CD		DM-β-CD		HP-β-CD	
		<i>t_R</i>	α	<i>t_R</i>	α	<i>t_R</i>	α	<i>t_R</i>	α
Normetanephrine		11.64	N.S.	11.65	N.S.	10.75	N.S.	11.78	N.S.
Metanephrine		12.38	N.S.	12.32	N.S.	11.33	N.S.	12.42	N.S.
Norephedrine		14.16	N.S.	11.04	N.S.	12.16 12.45	1.015	12.92	N.S.
Ephedrine		15.37 15.63	1.010	11.51	N.S.	12.97 13.16	1.009	13.91 14.03	1.005 0.68
Pseudoephedrine		15.28 16.43	1.043	11.21 11.42	1.012	11.18 12.73	1.049	12.83 14.32	1.070 8.68
Doxylamine		9.52 9.75	1.017	7.59	N.S.	7.85	N.S.	7.70 7.77	1.007 0.72

Chlorpheniramine		13.60	1.015	1.90	9.29	1.005	0.51	11.48	1.006	0.75	10.20	1.011	1.31
		13.93			9.35				11.59			10.37	
Trimipramine		50.70	N.S.	N.S.	21.74	N.S.	N.S.	32.32	N.S.	N.S.	34.01	1.004	0.83
											34.37		
Verapamil		49.98	N.S.	N.S.	23.19	1.022	3.70	32.32	N.S.	N.S.	40.20	1.003	0.78
					24.30							40.60	
Hydroxyzine		54.80	N.S.	N.S.	29.30	N.S.	N.S.	33.42	N.S.	N.S.	43.60	N.S.	

Buffer: 50 mM TMA phosphate at pH 2.50 containing 20 mM chiral recognition agent. Migration times (t_R) are in minutes; $\alpha = \mu_1/\mu_2$ ($\mu = \mu_{\text{obs}} - \mu_{\text{e0}}$; $\mu_{\text{e0}} = -1.2 \cdot 10^{-4} \text{ cm}^2/\text{V s}$); R_s was calculated by using Eq. 2, and by assuming $N = 100\,000$. N.S. = No separation.

^a Diastereomers.

norephedrine, ephedrine, norepinephrine and epinephrine with the exception of pseudoephedrine. Finally, it is important to note that although β -CD and TM- β -CD are less selective for the basic compounds listed in Table 1, they showed remarkable high enantioselectivity for certain groups of compounds, e.g., β -CD for doxylamine, chlorpheniramine and labetalol, and TM- β -CD for verapamil and propranolol, for which the mechanism is not known.

Fig. 5 shows two electropherograms of the separation of 12 chiral amines using (A) 20 mM DM- β -CD and (B) 20 mM HP- β -CD. Clearly, the separation capability of CZE is extended by using the TMA cations to reverse the EOF, and at the same time by incorporating selective interaction into the solute migration. Not only many of the chiral amines were resolved, but also all the amines were separated from each other. Comparing the above two separations, it is clear that HP- β -CD is a better chiral selector for doxylamine (pair 1) and labetalol (pair 12) for the reasons mentioned earlier, but not for pindolol and oxprenolol (pairs 7 and 8) which co-eluted.

Fig. 6 shows a separation of the same group of chiral amines with a TBA phosphate buffer solution containing 20 mM HP- β -CD. In comparison with the separation in Fig. 5B, a better separation was obtained for pindolol and oxprenolol (pairs 7 and 8). However, the presence of TBA cations causes a decrease in the enantiomeric resolution for the early-eluted amines such as doxylamine and norepinephrine due to the competing effect of the TBA cations. Finally, for some partially resolved enantiomers such as those of atenolol, oxprenolol, pindolol (in the case of HP- β -CD), enantiomeric resolution of these compounds can be further improved by lowering the separation temperature and by using higher concentrations of the TMA cations [2].

It is not surprising that the enantiomers of acebutolol could not be resolved. It seems that the presence of a long-chain substituent at the *para* position (see Table 1) prevents the aromatic moiety from penetrating deeply into the β -CD cavity, leaving the chiral center of the guest

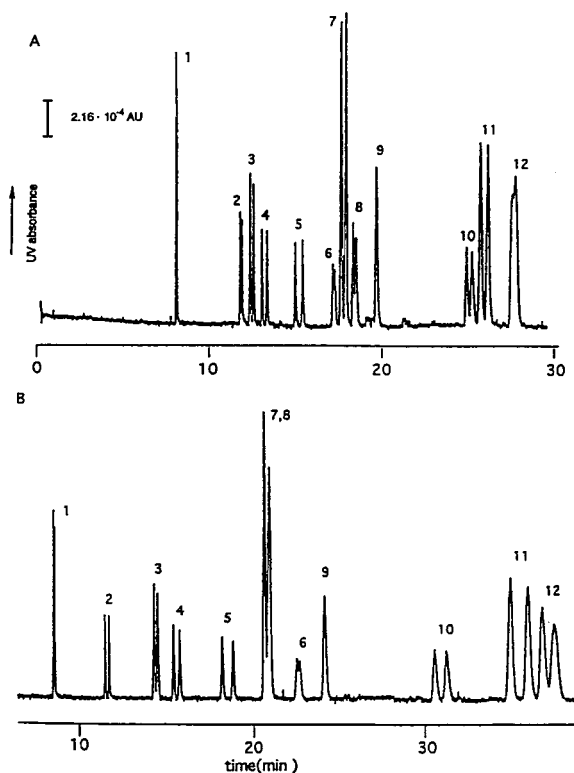


Fig. 5. A comparison of separations of 12 chiral amines using two different chiral selectors. Buffer electrolytes: 50 mM TMA phosphate (pH 2.50) containing (A) 20 mM DM- β -CD and (B) 20 mM HP- β -CD. Peaks: 1 = doxylamine; 2 = chlorpheniramine; 3 = norepinephrine; 4 = epinephrine; 5 = isoproterenol; 6 = atenolol; 7 = pindolol; 8 = oxprenolol; 9 = acebutolol; 10 = alprenolol; 11 = propranolol; 12 = labetalol. Other conditions as in Fig. 1.

molecule beyond the reach of the functional groups on the rim of β -CD cavity. Similarly, no chiral separation for normetaphrine and metamphetamine was achieved by using any of the β -CDs. This might also be due to the steric effect at the *meta* position of the aromatic moiety, which prevented the functional groups of the guest molecules from interacting with the functional groups on the rim of β -CD. Therefore, it is suggested that the usefulness of β -CD derivatives with longer substituents or other kinds of chiral selectors (e.g., helical amylose oligomers [25]), be explored for the separation of the enantiomers of these compounds.

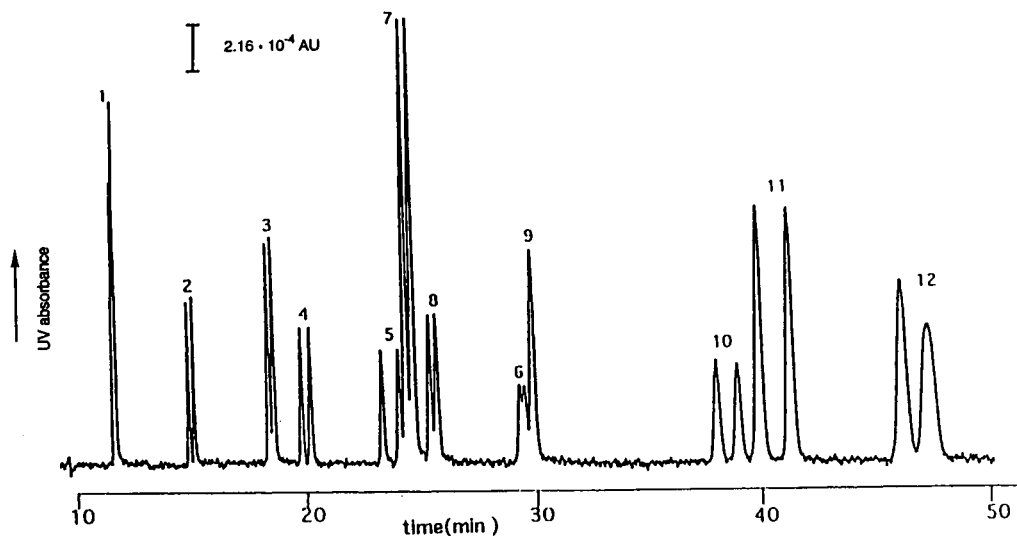


Fig. 6. Effect of TBA cations on the separation of the chiral amines. Buffer electrolyte: 20 mM HP- β -CD in 100 mM TBA phosphate (pH 2.50). Peak numbers as in Fig. 5, and other conditions as in Fig. 1.

Acknowledgements

The authors acknowledge research grants from the National Institutes of Health (GM 38738). We thank American Maize-Products Company for providing β -cyclodextrin and its derivatives in this study.

References

- [1] C. Quang and M.G. Khaledi, *Anal. Chem.*, 65 (1993) 3354.
- [2] C. Quang and M.G. Khaledi, *J. High Resolut. Chromatogr.*, 17 (1994) 99.
- [3] J. Snopek, I. Jelinek and E. Smolkova-Keulemansova, *J. Chromatogr.*, 452 (1988) 571.
- [4] R. Kuhn and S.H. Kuhn, *Chromatographia*, 34 (1992) 505.
- [5] A. Guttman, A. Paulus, A.S. Cohen, N. Grinberg and B.L. Karger, *J. Chromatogr.*, 448 (1988) 41.
- [6] I.D. Cruzado and G. Vigh, *J. Chromatogr.*, 608 (1992) 421.
- [7] K. Otsuka and S. Terabe, in N.A. Guzman (Editor), *Capillary Electrophoresis Technology*, Marcel Dekker, New York, 1993, p. 627.
- [8] H. Nishi, T. Fukuyama and S. Terabe, *J. Chromatogr.*, 553 (1991) 503.
- [9] M.J. Sepaniak, R.O. Cole and B.K. Clark, *J. Liq. Chromatogr.* 15 (1992) 1023.
- [10] S. Fanali, *J. Chromatogr.*, 474 (1988) 441.
- [11] S. Fanali, *J. Chromatogr.*, 545 (1991) 437.
- [12] J. Snopek, H. Soini, M. Novotny, E. Smolkova-Keulemansova and I. Jelinek, *J. Chromatogr.*, 559 (1991) 215.
- [13] H. Soini, M.-J. Riekkola and M.V. Novotny, *J. Chromatogr.* 608 (1992) 265.
- [14] R. Kuhn, F. Stoecklin and F. Erni, *Chromatographia*, 33 (1992) 32.
- [15] S.A.C. Wren and R.C. Rowe, *J. Chromatogr.*, 603 (1992) 274.
- [16] S.A.C. Wren and R.C. Rowe, *J. Chromatogr.*, 609 (1992) 363.
- [17] M.W.F. Nielen, *Anal. Chem.*, 65 (1993) 885.
- [18] K. Otsuka and S. Terabe, *J. Liq. Chromatogr.*, 16 (1993) 945.
- [19] J.C. Giddings, *Sep. Sci.*, 4 (1969) 181.
- [20] J.W. Jorgenson and K.D. Lukacs, *Anal. Chem.*, 53 (1981) 1298.
- [21] D.W. Armstrong, T.J. Word, R.D. Armstrong and T.E. Beesley, *Science*, 232 (1986) 1132.
- [22] R.P. Frankewich, K.N. Thimmaiah and W.L. Hinze, *Anal. Chem.*, 63 (1991) 2924.
- [23] W.A. Konig, *Carbohydr. Res.*, 192 (1989) 51.
- [24] V. Schurig and H.-P. Nowotny, *Angew. Chem., Int. Ed. Engl.*, 29 (1990) 939.
- [25] C. Quang and M.G. Khaledi, *J. High Resolut. Chromatogr.*, 17 (1994) 609.



ELSEVIER

Journal of Chromatography A, 692 (1995) 267-274

JOURNAL OF
CHROMATOGRAPHY A

Determination of polycarboxylic acids by capillary electrophoresis with copper complexation

Jean P. Wiley

Unilever Research US, 45 River Road, Edgewater, NJ 07020, USA

Abstract

Reversed-polarity CE on unmodified silica, making use of copper sulfate as a combination complexation agent/electrolyte and myristyltrimethylammonium bromide as an electroosmotic flow modifier, has been shown to be a reliable and rapid method of analysis for polycarboxylic acid builders. Since separation is governed by a combination of charge and charge density, a number of similar polycarboxylic acids can be identified by unique retention times. Baseline resolution and symmetrical peak shapes are observed for a mixture of polycarboxylic acids including oxydisuccinic, ethylenediaminetetraacetic, nitrilotriacetic and diethylenetriaminepentaacetic acids. Using direct detection at 254 nm, the limit of detection for these acids approaches 100 ppb (ng/ml), making the technique viable for trace analysis.

CE results for nitrilotriacetic and citric acids in formulated products are comparable to results obtained by LC-UV detection. The CE method has been shown to be as sensitive as LC with amperometric detection, but less selective and easier to stabilize.

Other compounds which complex with copper(II) salts, such as ethylhydroxydiphosphonate can be determined at low levels in formulated products using this method.

1. Introduction

A rapid and sensitive method is required to analyze formulated detergent and personal care products for polycarboxylic acids (Fig. 1). Capillary electrophoresis (CE), utilizing copper complexation, has been identified as a technique that can sensitively separate and detect polycarboxylic acids in raw materials and finished products. Polycarboxylic acids act as builders in these formulations by complexing calcium ions in hard water. Builders enable surfactants to do the job of cleaning, rather than being complexed with calcium.

Early detergent formulations consisted of soap, which acted as both surfactant and builder.

The introduction of sodium carbonate and sodium silicate to these formulations resulted in a "built" product at lower cost. Phosphate-built detergents enjoyed popularity up until the early 1970s, when environmental concerns resulted in a number of states banning their usage. Phosphates had been shown to cause the eutrophication of stagnant bodies of water.

Since 1970 much effort has been dedicated to finding a builder that is at once effective, biodegradable and affordable. Sodium citrate has been shown to be safe, effective and biodegradable, but is rather expensive. Nitrilotriacetate (NTA) seemed to be a viable replacement for the phosphates until 1971, when the US Surgeon General declared it to be unsafe on the basis of

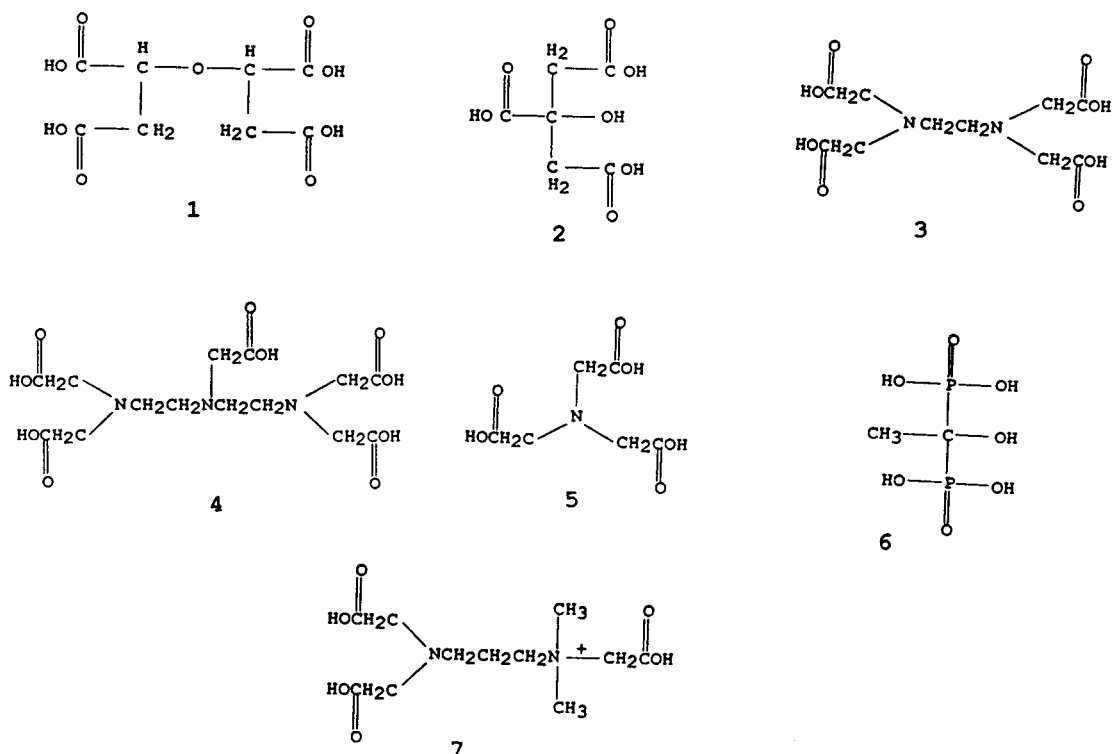


Fig. 1. Structures of compounds discussed in this paper. 1 = Oxydisuccinic acid; 2 = citric acid; 3 = ethylenediaminetetraacetic acid; 4 = diethylenetriaminepentaacetic acid; 5 = nitrilotriacetic acid; 6 = ethylhydroxydiphosphonate; 7 = aminopropyl-dimethylaminetriacetic acid.

suspected teratogenicity. NTA is used throughout Canada as a builder [1]. A number of other polycarboxylic builders have been studied over the years, including ethylenediaminetetraacetic acid (EDTA), oxydisuccinic acid (ODS) and diethylenetriaminepentaacetic acid (DTPA).

Many polycarboxylic acids do not have substantial UV absorptivities outside the low UV (200–220 nm). Even at these wavelengths, sensitivity is limited. This has been overcome for aminocarboxylic acids, using a liquid chromatographic method with pulsed amperometric detection (PAD) [2]. However, PAD detectors are highly selective and can be slow to equilibrate. Not all polycarboxylic acids will respond to PAD. Polycarboxylic acids, when complexed with copper, exhibit strong UV absorption and can be easily detected at low ppm levels at 254 nm.

The use of a negative power source, along

with an electroosmotic flow (EOF) modifier, for anion analysis is referred to as “reversed-polarity CE” simply because the polarity is reverse to the traditional polarity. At low pH, an unmodified electroosmotic flow would carry anions to the negative electrode. When the electroosmotic flow is controlled, the bulk flow of electrolyte allows the anions to travel to the positive electrode. Varghese and Cole [3] demonstrated the use of cetyltrimethylammonium chloride as an EOF modifier in reversed-polarity CE. In our work we used a similar EOF modifier, myristyltrimethylammonium bromide.

The idea to use copper sulfate as the electrolyte in our CE method originated from the copper complexation (ligand-exchange) chiral LC technique utilized by Phenomenex in their Chirex CSP 3126 D-penicillamine bonded column [4]. The penicillamine column proved useful for

the separation of *R,R* and *S,S* isomers of oxydisuccinic acid. Analytical work on the penicillamine column conducted here at Unilever demonstrated that the ODS–copper complex absorbs so strongly in the UV that the limit of detection is in the low $\mu\text{g/ml}$ range. A reversed-polarity CE method was then devised using copper sulfate as a combination complexation agent/electrolyte with detection by direct UV at 254 nm. The copper complexation CE method generated two peaks for oxydisuccinic acid. One was a combination of *R,R* and *S,S*, while the other was a separate peak for *meso*-ODS. The limit of detection was in the range of a fraction of a $\mu\text{g/ml}$. This low limit of detection makes the technique suitable for biodegradation studies which require the measurement of trace levels.

2. Experimental

All analyses were performed on the Millipore/

Waters (Milford, MA, USA) Quanta 4000 CE instrument. The capillary was an uncoated silica from Polymicro Technologies (Phoenix, AZ, USA). It was $60\text{ cm} \times 360\ \mu\text{m O.D.} \times 75\ \mu\text{m I.D.}$ Data were collected on a Waters 746 data module.

The cupric sulfate used in preparing the electrolyte solution was certified anhydrous from Fisher Scientific (Fairlawn, NJ, USA). The myristyltrimethylammonium bromide was 99%, obtained from Aldrich (Milwaukee, WI, USA). The sodium citrate dihydrate used as a standard was certified from Fisher Scientific. The EDTA was diluted from a certified 0.1 M solution from Fisher Scientific. The DTPA standard was 98% pure from Aldrich. Oxydisuccinic acid was generated internally (E. Gutierrez and D. Wu); aminopropyltrimethylaminetriacetic acid was custom synthesized by Goldschmidt Chemical Co. (Hopewell, VA, USA).

Formulated products were dissolved in water and passed through a conditioned (methanol,

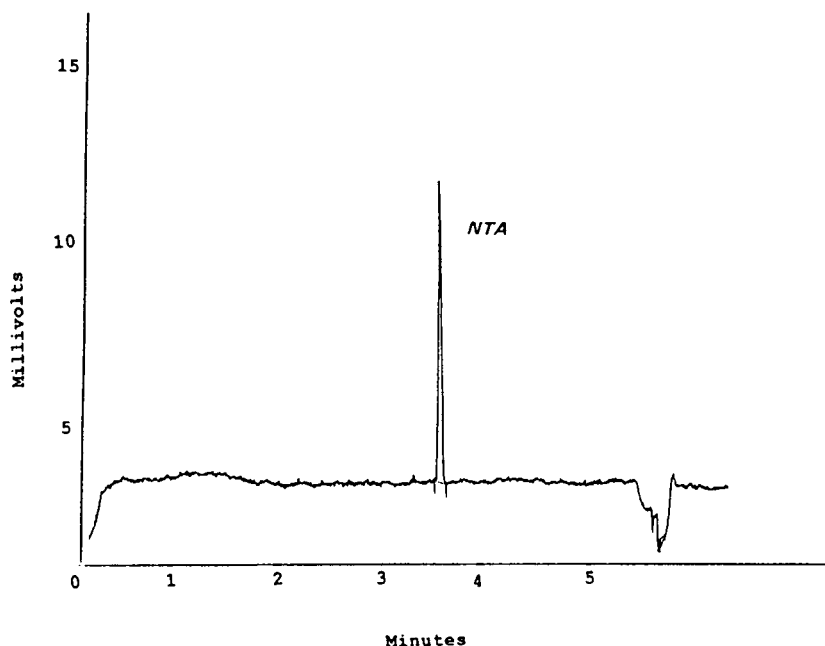


Fig. 2. Analysis of nitrilotriacetate (NTA) in formulated product by CE. Silica capillary: $60\text{ cm} \times 75\ \mu\text{m}$. Electrolyte: 5 mM cupric sulfate, 1 mM myristyltrimethylammonium bromide. Negative power supply: 20 kV. Injection: hydrostatic, 20 s. Detection: 254 nm, direct. Sample: Canadian hard surface cleaner: 0.035 g/100 ml water; NTA content 7.9%. Sample filtered prior to injection.

water) Waters C₁₈ Sep-Pak prior to analysis. Individual experimental conditions are described in the captions to the figures.

3. Discussion

Reversed-polarity CE on unmodified silica, making use of copper sulfate as a combination complexation agent/electrolyte and myristyltrimethylammonium bromide as an EOF modifier, has been shown to be a reliable and rapid method of analysis for polycarboxylic acid builders. Since separation is governed by a combination of charge and charge density, a number of

similar polycarboxylic acids can be identified by unique retention times. For the series of polycarboxylic acids examined in this paper, the elution time is before the "water dip", indicating a net negative charge on the acid. In the case of EDTA, for example, the molecules must not be totally complexed with copper, or they would behave like neutral species and elute along with the water peak.

The copper complexes are readily detected by direct UV at 254 nm, with a limit of determination near 0.1 $\mu\text{g/ml}$. The limit of detection may well be an order of magnitude lower (0.01 $\mu\text{g/ml}$), particularly if the sampling time is extended in the hydrostatic injection mode. External standard quantitation was employed in all cases. The CE approach can obtain limits of detection comparable to the pulsed amperometric detector. CE analysis of a solution of 100 ng/ml ODS resulted in peaks with a signal-to-noise level > 10. The CE method has the added advantage over PAD that it can be used for polycarboxylic acids not containing an amine functionality, such as ODS and citrate. PAD systems can be difficult to stabilize; CE with direct UV detection is quite rugged. The response curve for hydrostatic injection appears linear over a wider range of concentration than for electromigration.

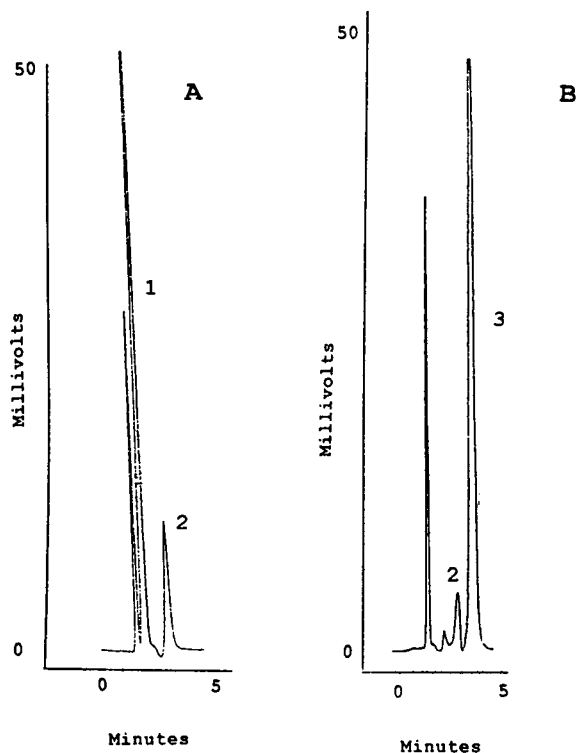


Fig. 3. Analysis of NTA and citrate in formulated products by liquid chromatography. Column: Hamilton PRP-1 (25 cm \times 4.6 mm). Mobile phase: 0.1% (v/v) trifluoroacetic acid in water. Flow-rate: 1 ml/min. Injection volume: 50 μl . Detection: direct UV at 230 nm. (A) Canadian liquid hard surface cleaner. (B) Liquid laundry detergent. Peaks: 1 = NTA; 2 = trifluoroacetic acid; 3 = citrate.

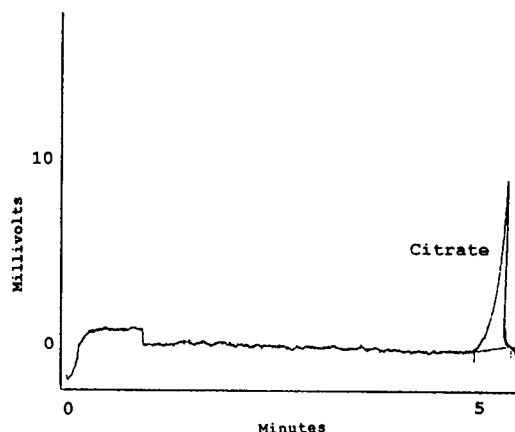


Fig. 4. Analysis of citrate in formulated product by CE. Conditions of analysis as in Fig. 2. Sample: liquid laundry detergent, 0.037 g/100 ml water; citrate content 8.8%. Sample filtered prior to injection.

3.1. Nitrilotriacetate and citrate

Nitrilotriacetate, used in Canada as a builder, can be easily quantitated in formulated products by the new complexation CE technique (Fig. 2). Results have been shown to be comparable to those obtained using a modified literature LC method [2] (Fig. 3) which calls for a polymeric reversed-phase column and trifluoroacetic acid as mobile phase modifier. The level of NTA in the hard surface cleaner in Figs. 2 and 3 is 7.9% (w/w). The literature reference for the LC method requires PAD to achieve a 100 ng/ml detection limit for aminopolycarboxylic acids. Our

modified procedure takes advantage of UV detection as a more stable detection system for higher levels of analyte.

Citrate in formulated products can be quantitated by CE (Fig. 4), with results comparable to those found for liquid chromatography. The level of citrate in the liquid laundry detergent in Figs. 3 and 4 is 8.8% (w/w), expressed as disodium citrate dihydrate. By CE, the peak shape for citrate exhibits a good deal of fronting. Mikkers et al. [5] have explained that fronting can be predicted when the mobility of the analyte is greater than the main co-ion in the electrolyte. However, peak deformations gener-

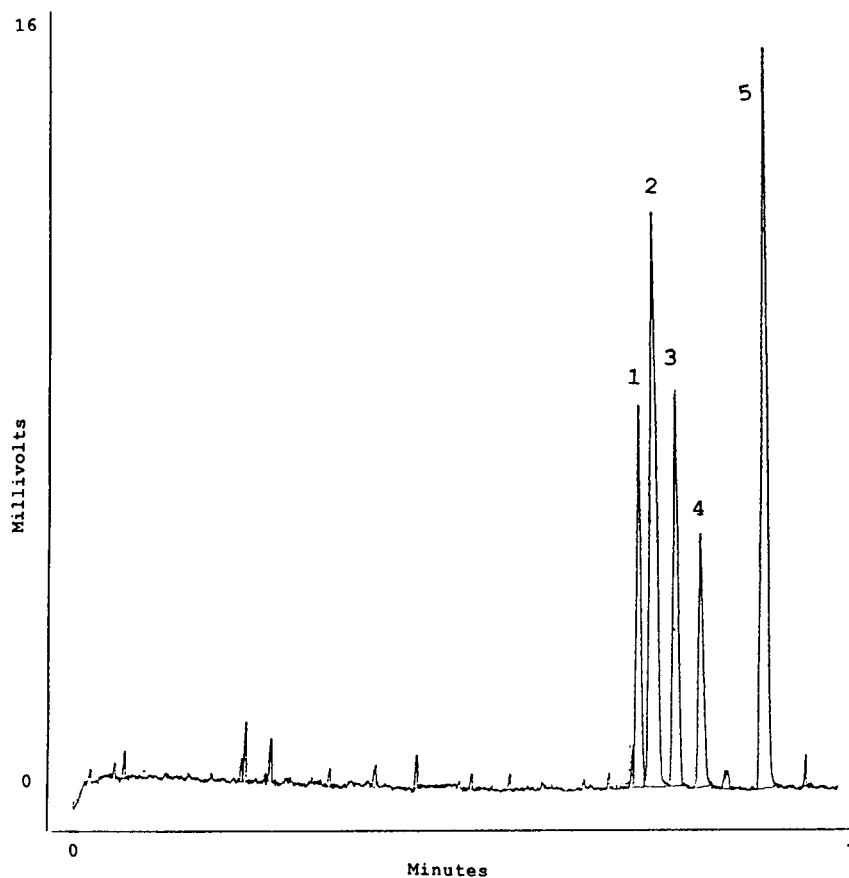


Fig. 5. Analysis of a mixture of polycarboxylic acids by CE. Silica column and electrolyte as in Fig. 2. Negative power supply: 13 kV. Injection: hydrostatic, 30 s. Peaks: 1 = ODS, *R,R* and *S,S*, 12.5 ppm; 2 = EDTA, 33.6 ppm; 3 = NTA, 20.6 ppm; 4 = ODS, *meso*, 8.9 ppm; 5 = DTPA, 21.2 ppm.

ally have more than one cause. At low pH, weak acids can demonstrate fronting. The pH of the electrolyte solution in Fig. 4 is 5.3. As long as a considerable amount of acid is in the protonated form, a high concentration of hydronium ions can result in the conductivity of the sample zone being higher than that of the electrolyte.

3.2. Mixture of polycarboxylic acids

Unique retention times and baseline resolution were demonstrated for a series of polycarboxylic acids analyzed using the complexation CE meth-

od. They include ODS, EDTA, NTA and DTPA (Fig. 5). Dilutions of this series were first introduced onto the capillary by hydrostatic injection. Then the entire series was run using the electrokinetic mode of injection. The range of linearity using hydrostatic injection was greater than electrokinetic injection (Fig. 6). Using hydrostatic injection, the area responses of the builders were linear between approximately 2 and 30 $\mu\text{g}/\text{ml}$; using electrokinetic injection, non-linear responses were obtained for this concentration range. However, the electrokinetic injection mode may be advantageous for trace

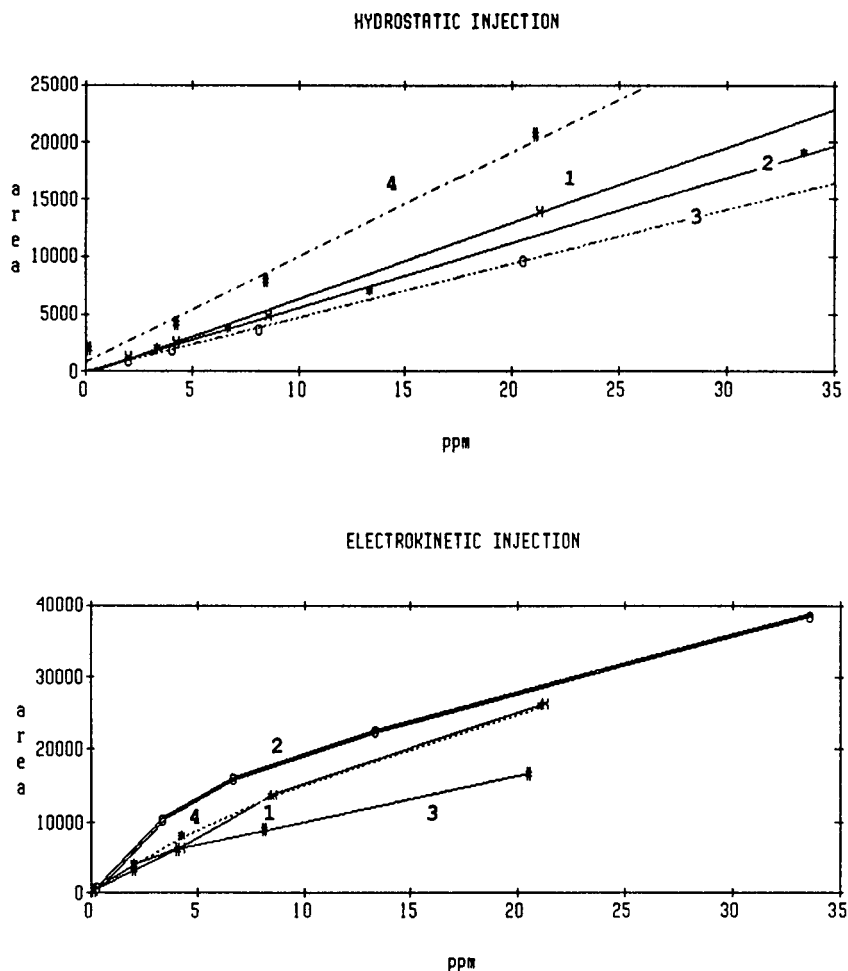


Fig. 6. Comparison of area responses based upon injection mode. Curves: 1 = ODS; 2 = EDTA; 3 = NTA; 4 = DTPA.

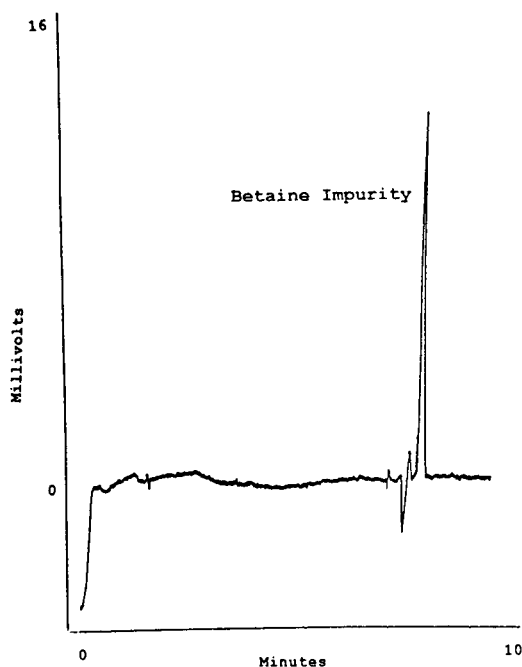


Fig. 7. Electropherogram of aminopropyltrimethylammoniumacetate, a potential by-product in the commercial synthesis of cocoamidopropylbetaine surfactants. Conditions as in Fig. 2.

analysis as it allows for concentration of the anions in the sample at the head of the capillary [6].

3.3. Aminopropyltrimethylammoniumacetate

Aminopropyltrimethylammoniumacetate is a possible non-surfactant byproduct of the commercial synthesis of cocoamidopropylbetaine surfactants. This tricarboxylic acid could potentially result from the addition of 3 mol of chloroacetic acid to residual dimethylaminopropylamine. We asked Goldschmidt Chemical Co. to synthesize it as a standard for analysis. We were unsuccessful in developing an ion chromatography method which would permit its detection, yet it is easily determined by the new CE copper complexation technique (Fig. 7). The figure is illustrative of the analysis of a 20 $\mu\text{g/ml}$ aqueous solution of the standard. The compound elutes just after the “water dip”, suggesting a slightly positive net charge under the conditions of analysis. This elution behavior is consistent with the mechanism postulated for polycarboxylic acids using the copper complexation CE approach.

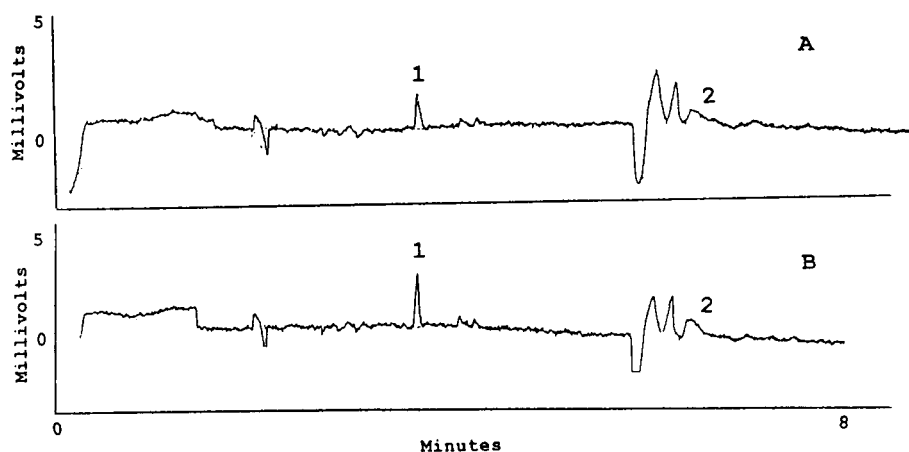


Fig. 8. Analysis of EDTA and EHDP in liquid hand soap by CE. (A) Liquid hand soap, 4% (w/v) in water. (B) Liquid hand soap (4%, w/v) spiked with additional EDTA and EHDP. Peaks: 1 = EDTA; 2 = EHDP. Analysis conditions as in Fig. 2 except for mode of injection: electrokinetic, 20 s, 5 kV.

3.4. Additional applications

Preliminary CE work with EDTA and ethylhydroxydiphosphonate (EHDP), which can be present in liquid soaps as preservatives, indicates that this technique may also be viable for phosphonates (Fig. 8) and other species which complex copper(II) salts.

4. Conclusions

CE analysis of polycarboxylic acids on untreated silica, with copper complexation and electroosmotic flow modification, can be a useful technique to monitor these ingredients in formulated products as well as in studies which require trace ($\mu\text{g/ml}$) levels of detection. Both amine-containing carboxylic acids, such as EDTA and NTA, and non-amine-containing carboxylic acids, such as citric acid and ODS, can be analyzed by this procedure. Hydrostatic injection of these acids results in a greater linear response range than electromigration. Other species which complex copper(II), such as EHDP, may also be detected by this procedure.

Modifications of the electrolyte composition may be necessary to enhance the peak shape for the phosphonates.

Acknowledgements

The author acknowledges Unilever Research US for supporting the research described in this paper. The author also thanks Ms. Betty Bautista, Dr. Henry Kalinoski and Dr. Richard Montgomery of Unilever Research US for their technical assistance.

References

- [1] A. Cahn, *Inform*, 5 (1994) 70–74.
- [2] J. Dai and G. Heiz, *Anal. Chem.*, 60 (1988) 301–306.
- [3] J. Varghese and R. Cole, *J. Chromatogr. A*, 652 (1993) 369–376.
- [4] *Product Literature: Chiral Separations*, Phenomenex, Torrance, CA, 1993.
- [5] F.E.P. Mikkers, F.M. Everaerts and T.P.E.M. Verheggen, *J. Chromatogr.*, 169 (1979) 11–20.
- [6] X. Huang, M. Gordon and R. Zare, *Anal. Chem.*, 60 (1988) 375–377.

Review

Mass spectrometric detectors for samples separated by planar electrophoresis

Kenneth L. Busch

School of Chemistry and Biochemistry, Georgia Institute of Technology, Atlanta, GA 30332-0400, USA

Abstract

Mass spectrometric detection for samples separated by planar chromatography (high-performance thin-layer chromatography and planar electrophoresis) has evolved over the past 10 years from concept to feasibility and to commercial availability. This review concentrates on the interface between planar electrophoresis and mass spectrometry. Although hardware aspects of the interface have been developed and refined over the past few years, and there are impressive demonstrations of feasibility, we are only beginning to exploit new methods in sample storage, preparation and reaction in conjunction with planar chromatographic separation, and new uses of complex multi-dimensional imaging data.

Contents

1. Introduction	275
2. Experimental	277
3. Evaluation of results	278
3.1. Chromatographic resolution	279
3.2. Spectroscopic resolution	281
3.3. Sample preparation	284
3.4. Sample reactions and derivatization	286
3.5. Data handling	287
4. Conclusions	288
Acknowledgements	288
References	288

1. Introduction

Complex mixture analysis is a proving ground for analytical methods that combine high-resolution separation techniques with equally powerful detection systems. Mass spectrometry (MS) has been used as the detection system for gas chromatography (GC) and liquid chromatog-

raphy (LC), and GC-MS and LC-MS are now optimized, ubiquitous tools for complex mixture analysis. Growing needs for separations of biological mixtures have catalyzed advances in high-performance liquid chromatography, capillary electrophoresis, affinity chromatography and planar forms of electrophoresis, including agarose and polyacrylamide gel electrophoresis (PAGE).

In devising the interface between the chromatograph and the mass spectrometer, the instrument designer is concerned with the sample flux available to the mass spectrometer. From this perspective, separation methods can be divided into “sequential-in-time” and “sequential-in-space” techniques.

Column methods (sequential-in-time) such as gas chromatography, liquid chromatography and capillary electrophoresis introduce fractions of the sample mixtures sequentially to the source of the mass spectrometer, and separation resolution is related to the difference in retention times that can be achieved. Coupling to the mass spectrometer can be on-line or off-line, although the on-line combination (despite the limitations placed on the operation of the mass spectrometric detector) is more popular. In planar chromatography (sequential-in-space), sample mixture components are distributed in x and y dimensions. The detector is focused randomly in time to any specified (x, y, z) coordinate for data measurement. Although the combination of planar chromatography with mass spectrometry can be on-line (and mass spectrometry can be used to monitor the progress of the spatial development), the most popular combination of mass spectrometry with planar chromatography has been in an off-line configuration.

Although the analytical attributes of planar chromatography have been ably reviewed [1–3], relatively few have advocated any expanded use beyond the applications areas in which these particular advantages were overwhelming. For thin-layer chromatography, early exposure of most scientists to a “low-tech” and “low-performance” version provided initial impressions at odds with current instrumentally based, higher performance versions of planar chromatography now available. However, planar forms of electrophoresis such as agarose gel electrophoresis and polyacrylamide gel electrophoresis were adopted readily by biochemists with the need to separate complex mixtures of biomolecules, and these methods have evolved into sophisticated separations systems with complex imaging detectors. Insulated within the biochemical community, the planar electrophoretic methods became isolated

from the mainstream of the analytical separations community, which focused instead on column-based methods of separations with great success. A fair proportion of that success was derived from the ease with which mass spectrometric detection could be enlisted to support the need to identify hundreds and sometimes thousands of separated components. Conversely, the lower respect afforded planar chromatography was also a function of the simple detector systems in common use. Although a number of sophisticated activation, derivatization and color development schemes have been developed, often with extraordinary sensitivity and excellent selectivity, the determination of the location of the spot on a planar chromatogram was usually based on visual observation of the spot on the uniform silica gel background. Although derivatization chemistry involved in detection methods evolved rapidly in sophistication, essential aspects of the instrumental spectrophotometric detection did not. Even with the development of multiple-wavelength measurements and instrumental UV–Vis scanners, the amount of analytical information was not substantially increased.

The predominant attraction of mass spectrometry with column chromatographic separations was that the detection was over-determined. This means that there is more information potentially available in the mass spectrum than is generally needed to identify the sample component at a particular retention time. The analyst could therefore be assured that almost any analysis could be successfully completed. If the chromatographic separation was insufficient, then the detector could provide needed independent information.

In planar chromatography, the need for an over-determined detection method is even more cogent. In planar chromatographic separations, the sample molecules are by definition present in a matrix of chromatographic support material, whether the matrix is silica gel in HPTLC or polyacrylamide or agarose gel in electrophoresis. Differential interfaces in GC–MS or LC–MS preferentially transport sample molecules to the source of the mass spectrometer, providing a

substantial sample enrichment. This is not possible in planar chromatography. The detection method must function *in situ* to provide a measurement related to the sample independently of the matrix. Spectrophotometric methods can accomplish this discrimination with relative ease, but do not provide enough information to identify the sample unambiguously. Mass spectrometry provides specific analytical information necessary to identify the compound, but must do so with the constraint that the sample and matrix contribute to the observed mass spectrum.

Some early work in planar electrophoresis (PE)–MS used procedures in which the individual sample bands were removed and the sample solution derived from those bands examined individually. In considering PE–MS, it is more appropriate to review the analytical aspects of planar chromatography. In planar chromatography, compounds are separated by their differential migration along the development axis or axes. The time domain in which the mass spectrometer must operate is independent of chromatographic development. Rather than have each component available in the mass spectrometer source only within the elution window, as in separation-in-time, a planar chromatographic detector can integrate the signal for any sample spot for as long as necessary. Analogously, shorter data acquisition intervals can be assigned to higher level components, or components of lesser interest. Samples cannot be “lost” in a planar chromatogram. Components of a mixture that will not separate under the chosen conditions are lost on the column in GC or LC, but can be easily retrieved from the point of initial sample deposition in planar chromatography, and may be eluted and detected using other analytical methods. Alternatively, the system can be viewed as a chromatographic cleanup of the non-partitioning material in which none of the matrix is discarded. As the chromatographic development time is not a factor in detector operation, any component in the chromatogram can be investigated in any order. This independence of access order is an advantage in complex mixture analysis when targeted components are sought, or when a priority ranking to

the compounds present can be assigned. A related advantage is the fact that the chromatogram can be rescanned many times in order to establish the required level of analytical accuracy in spatial profile and sample identification. Finally, the data measured in an off-line detection system for planar chromatography can not only be used to identify the components separated within the chromatogram, but can also be interpreted to provide on-line control for measurement of additional data, as in TLC–MS [4,5].

As PE–MS develops, its conceptual origin in TLC–MS becomes more clear. Many of the hardware approaches are similar. Yet there are some differences that are emphasized in the coupling. An agarose or a PAGE gel contains a great deal of water that must be (1) removed before the gel itself can be placed inside the vacuum system for sampling or (2) the sample molecules must be removed or transferred from the gel matrix. Both of these methods have been pursued in PE–MS, although the latter is preferred. The biomolecules typically separated in planar electrophoresis are high-mass molecules, and will require use of a mass spectrometer that can operate in the appropriate mass range. These biomolecules may also require special handling to preserve their integrity or higher order structures. Finally, the complexity of the mixtures separated by two-dimensional planar electrophoretic methods may be high, exceeding even the hundreds of components separated in a capillary GC–MS run. The sample preparation and handling and the data collection and handling systems must be adequate for this task.

2. Experimental

Experiments in PE–MS and TLC–MS have used several different instruments [6–10] described briefly here; this paper reviews concepts and does not repeat previously published results. In brief, gel disruption methods used mechanical or ultrasonic homogenizers, and continuous-flow fast atom bombardment (FAB) with a VG-70SEQ double-focusing hybrid mass spectrometer. For matrix-assisted laser desorption ioniza-

tion (MALDI) mass spectra recorded with a Fourier transform (FT) mass spectrometer, a Nicolet FTMS-2000 instrument interfaced with a Quanta-Ray DCR-11 Nd:YAG laser was used [11]. Using the 266-nm line (frequency-quadrupled), the laser can fire only in the *Q*-switched mode (10-ns pulse width), and energies range from 2 to 20 mJ per pulse. With the 355-nm line (frequency-tripled) in the *Q*-switched mode, laser energies range from 20 to 60 mJ per pulse. In all instances, the laser beam diameter at the substrate surface was approximately 0.2 mm. For MS–MS experiments with the FT-MS, collision-induced dissociation (CID) was accomplished by isolating an ion of interest and then accelerating that ion into argon collision gas, which was maintained at a static pressure of approximately 3×10^{-6} Torr. Translational collision energies were in the range 50–100 eV (laboratory). For MALDI experiments with a time-of-flight (TOF) mass spectrometer, mass spectra were acquired on a custom-built instrument that can be operated in both the linear and reflected ion modes [12]. The TOF mass spectrometer consists of a 1.4-m long drift tube that houses a custom-built ion source and a Chevron microchannel plate detector. A Laser Science VSL-337ND nitrogen laser provides 3-ns pulses of 337-nm light, which are steered and focused so that the 3×8 mm beam is reduced to approximately 0.126 mm^2 in area. Power densities of 10 MW/cm^2 are typically used for MALDI mass spectra. Typically, the ion output from 20–30 laser shots are summed using an oscilloscope, and then transferred to a computer for further data analysis. Instruments used in other researchers' work are usually commercial instruments described in the appropriate references.

3. Evaluation of results

The coupling of chromatography with mass spectrometry is driven by the ability of an integrated system to provide more information than is necessary to solve most analytical problems. Ideally, one measures only enough information (with the minimum necessary resolu-

tion, the maximum possible speed, the highest possible sensitivity, the lowest possible cost and with accuracy, precision and reliability) to solve the problem at hand. However, the ideal problem answered with the ideal solution process is an imaginary construct. We accept less than exemplary separation and less than exemplary detection only because we use the synergistic nature of the combined information to derive a solution. Specifically, in PE–MS, the information that we want is sample band location, sample band homogeneity and sample mass. Further, we often know a great deal about the sample to begin with. We use the mass information from the mass spectrum to support our initial suspicions, and we can use sample reactions and derivatizations to provide further circumstantial evidence for sample identity. We shall therefore concentrate on the various aspects of the PE–MS coupling, following the order (1) chromatographic and spectroscopic resolution, (2) sample preparation, (3) sample reactions and derivatizations and (4) data handling.

3.1. Chromatographic resolution

How can mass spectrometry be used to increase the "resolution" of the chromatography? Can we use the information present in the mass spectrum to discern the presence of unresolved spots in a chromatographic spot or band? As in TLC–MS, use of the mass-resolved information in PE–MS allows unresolved spots on a planar electropherogram to be identified. The practice of using mass spectral data to establish the homogeneity of a sample band in PE–MS is shown in Fig. 1, redrawn from the data of Fenselau and Vestling [13]. The right-hand side shows the more general expectation that ions from samples in spot A and spot B will trace different *xy* profiles. The MALDI data shows a simple measurement of the molecular ions of two different proteins in a single electrophoretic band, showing the presence of unresolved sample components. In general, the presence of *n* different components is shown by the presence of *n* separate molecular ion masses. Fragment ions of common masses or background ions

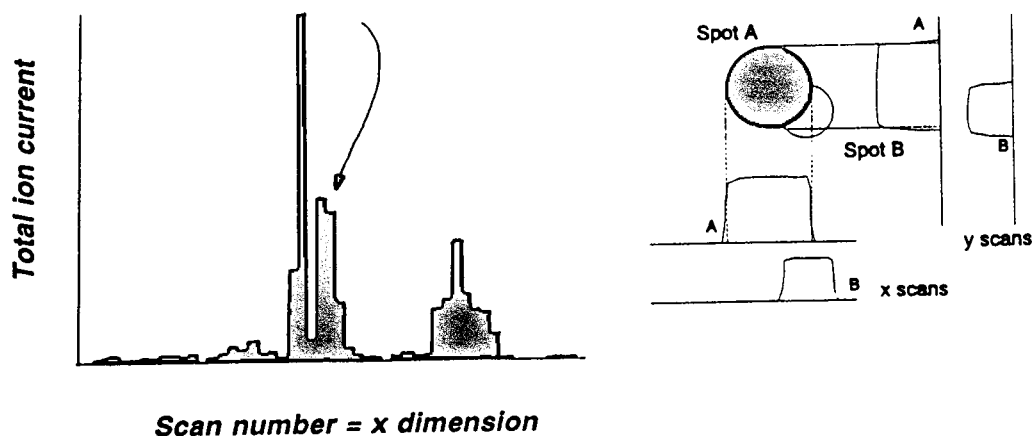


Fig. 1. Expected variations in mass-selected ions from samples A and B with x and y dimensions are shown on the right. The left portion shows PE-MS data with MALDI ionization (adapted from Ref. [13]); total ion current is plotted against scan number in the x -dimension. The presence of two concurrent masses (indicated by arrow; M_r 10 026 and 11 001), representing two different molecular species, at a given band signifies unresolved components.

cannot be used to deconvolute overlapped spots. The same conceptual experiment is carried out in GC-MS and LC-MS when time-resolved traces of mass-selected ions are reconstructed from the full data set measured. This deconvolution helps to identify all of the ions that belong together in the mass spectrum of a single component (they should exhibit identical time traces) and helps to emphasize unresolved peaks or background ions (distinctive and different time behaviors). In planar chromatography, the conceptual basis of the experiment is exactly the same, although the time base is replaced by a linear spatial dimension. Two such spatial dimensions (x and y) can be used independently to increase the effective resolution of the chromatographic separation and to establish sample-band homogeneity. The PE-MS data shown consist only of data measured along one linear dimension.

In PE-MS, the spatial dimensions of the area from which ions are generated should be much smaller than the size of the sample spot or the sample band. In particle-induced desorption ionization [FAB and liquid secondary ion mass spectrometry (LSIMS)], which has been used in TLC-MS, the diameter of the probe beam is limited to a diameter of 0.1–1 mm. The larger size is appropriately used for sputtering sample molecules from single excised spots, while the

smaller size is used for imaging across sample spots with xy dimensions of 1 mm or more. With microprobe mass spectrometers, image fields of 100–200 μm have been used to examine samples in TLC spots [14,15]. In PE-MS, sample bands are of approximately the same size, and similar FAB and LSIMS ion sources can be used. For MALDI (see below), the diameter of the laser beam should also be about 0.1–0.3 mm, and this spot size is readily achieved with commercial MALDI instruments.

3.2. Spectroscopic resolution

What about mass resolution in the mass spectrometer used for PE-MS? Mass resolution is closely related to the accessible mass range of the instrument, and we shall consider these issues together. The sieving properties of an electrophoretic gel provide separation (and some crude molecular mass information) for sample molecules with molecular masses from 5000 to over 200 000. The mass spectrometric detector must be able to deal with molecules within this mass range. For singly charged ions, the TOF mass spectrometer is the sole viable instrumental option. We therefore briefly review the capabilities of this spectrometer with respect to resolution and mass range. In a TOF mass

spectrometer, ions should be created at the same time, in the same place and with the same amount of kinetic energy. A pulsed ionization source such as a laser is conventionally used. The ions are extracted from the source and sent down the flight tube of the instrument. Ions of different mass but with the same kinetic energy will travel at different velocities, and the time of their arrival at the detector at the end of the flight tube will correlate with their masses. Although very high-mass ions will be traveling slowly, they will eventually reach the detector. Therefore, if a detector signal can be generated that heralds their arrival, even very high-mass ions can be analyzed in a TOF mass spectrometer. The mass resolution is limited by the ideality of the initial constraints of ion formation at the same time, the same place and with the same energy. In general, the mass resolution of the TOF mass spectrometer is relatively low (under 1000) and the mass peaks are very wide.

We consider if the relatively low mass resolution of a TOF instrument is an impediment in biomolecular analysis. For higher mass biomolecules, such as proteins, the ability to determine molecular mass within even 10–15 u is sufficient to establish the congruence between the expected mass and the observed mass, or to determine a mass difference from the expected mass that corresponds to any of the common biotransformations such as acetylation or phosphorylation. As the MALDI ionization process [16,17] produces molecular ions almost exclusively, an ion in the high-mass end of the mass spectrum is almost certainly a molecular ion. Further, if there are two signals present, there are most likely two compounds present in the interrogated band (and then we know that the spot is not homogeneous, as described above), as the lower mass ion is seldom a fragment of the higher mass ion. Proteins often analyzed by MALDI TOF dissociate primarily by loss of complete amino acid residues, and the mass shifts that this loss encumbers is easily discerned by the TOF mass analyzer. For most situations, the relatively low resolution of the TOF mass analysis is not debilitating.

Higher mass resolution can be achieved if

another method of mass analysis is used. The FT ion cyclotron resonance mass spectrometer can measure the masses of stored ions with extraordinary accuracy. Dunphy [11] has described the coupling of MALDI with FT-MS in the analysis of samples in planar electropherograms. Moderate mass resolutions of 5000–10 000 were achieved in these analyses, but the masses that could be stored in the cell were restricted to below 2000 u because of the strength of the magnet in the instrument. Several workers have described the use of ion re-measurement techniques that make it possible to store mass-selected ions for extended periods of time, generating mass resolutions of several hundred thousand [18–20]. The ability to perform this experiment with ions generated from sample molecules separated in a planar chromatogram is particularly attractive as the separation is complete, and either a few or many of the ions can be so examined at the leisure of the investigator. The ability to store ions of very high mass is problematic at this point. For a singly charged ion, the limit on the magnetic field strength of even a 7 T superconducting magnet restricts the mass of the ion that can be stored in a cell of reasonable dimensions to perhaps 10 000 u (this will vary from instrument to instrument). The future contribution of FT-MS will be in its ability to provide accurate mass measurements rather than extremely high mass ranges, and in the ability to pursue multiple stages of collision-induced dissociation for mass-selected parent ions. Exact mass differences for ions of high masses, if they can be determined with sufficient accuracy, can unambiguously indicate the nature of the loss, and therefore provide specific structural information. The exact mass measurement is not used to derive the empirical formula of an ion. Rather, the exact mass difference between two high-mass ions is used to define the atomic composition of the group involved in the dissociation or fragmentation. As large-mass biomolecules such as proteins often dissociate in regular patterns involving sequential losses of single amino acid residues, the exact mass difference resolution required is actually fairly modest.

If electrospray ionization [21,22] is used, multiply charged ions (usually $[M + nH]^{n+}$) can be generated, and the effective mass range of the analyzer is increased proportionately by a factor of n . PE-MS using electrospray ionization has been reported [23], and with multiple reports of electrospray ionization coupled with FT-MS, PE-MS with electrospray will be a popular avenue for near future applications (see the next section).

3.3. Sample preparation

There are two aspects of the preparation of the sample considered. The first is the manipulation of the electropherogram itself into a form compatible with the mass spectrometer's requirements, and the second is the incorporation of the matrix that allows the ionization process to succeed. A distinction is drawn here between methods that attempt to analyze the gel in x or xy dimensions, and those that elute the sample components from the gel and then present a discrete sample solution to the mass spectrometer for analysis. There are ample examples of the latter sort [24–30], including the work of Camilleri et al. and other early workers. More recent work that also involves the preparation of discrete sample solutions includes the investigation [11] of the “freeze-squeeze” method [31,32], originally described for the rapid recovery of long DNA strands from agarose gels, gel disruption and homogenization methods [33,34] used in conjunction with flow-FAB ionization.

A water-rich gel can be placed under vacuum, but as the gel shrinks with dehydration, the spatial separation of sample components is adversely affected, and analysis of whatever is left is unlikely to provide interpretable mass spectra. The very first attempts at PE-MS [35] used plasma desorption ionization (very fast and very heavy ions derived from a tandem accelerator, or present as fission fragments of a radioactive nuclide, are used to sputter molecules and ions from a thin sample surface) to determine mass spectra for protein mixtures separated by gel electrophoresis and then transferred to a nitrocellulose membrane with an electroblotting pro-

cedure. The use of nitrocellulose membranes and electroblotting procedures is well known within the bioanalytical community. The next foray into PE-MS used secondary ion mass spectrometry (SIMS) to analyze samples separated in paper and cellulose acetate electropherograms, and in these instances no transfer or blotting procedure was necessary [36]. With agarose gel electrophoresis and PAGE, the standard blotting procedures using capillary blots, vacuum blots and electroblots were further developed [37,38]. Within the limits of the SIMS ionization and the mass range of the quadrupole mass filter (below 2000 u), the experiment was successful in first demonstrating the spatial fidelity of the transferred material, the two-dimensional imaging capabilities of the PE-MS combination and the use of mass spectral information to deconvolute overlapped compounds in a single electrophoretic band. Additional work studied various quantitative aspects of sample sputtering from paper and cellulose acetate electrophoretic membranes, and the use of digestion reactions of larger peptides on the transfer membrane [39].

Limitations of Southern and Western blots for PE-MS soon became apparent, and extensive experience suggested that electroblots were preferred for reasons of transfer efficiency and preservation of spatial fidelity. Reports of the electroblotting technique in PE-MS appeared almost simultaneously from a number of research groups [11,40–44]. The electroblot procedure is still being developed for PE-MS [45], now with plasma desorption ionization and samples in the mass range up to 14 000 u. Experience suggests that the transfer efficiency with electroblotting techniques is in the range 60–90%, and that the spatial fidelity can be preserved for scanning and imaging experiments. Heating of the gel during transfer must be carefully monitored, but standard electrotransfer cells control this potential problem. PE-MS routinely uses electrotransfer methods, in contrast to the dot blot and capillary blot methods developed earlier [39,46]. Fig. 2A shows the general method used in small gel electrotransfers, illustrating the spatial fidelity that is maintained in the xy plane.

The nature of the membrane to which the

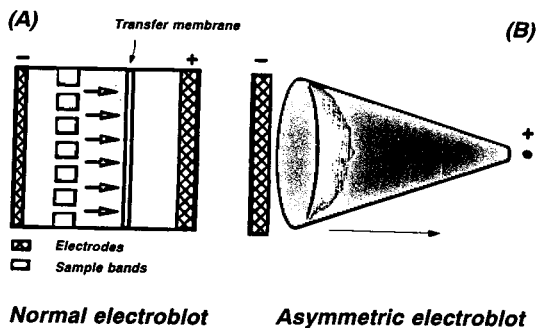


Fig. 2. (A) Normal electroblot procedure. (B) Asymmetric electroblot used to generate a variation in matrix-to-sample ratio along the dimension indicated by the arrow.

sample is transferred is important. Early work used nitrocellulose membranes, following standard biochemical protocols, and the early observation that ion signals for high-mass biomolecules from such surfaces were of greater intensity than other surfaces such as metals. Recently, a number of other membrane surfaces have been used in PE-MS, including nylon and poly(vinylidene difluoride) (PVDF) [47–50]. Although these materials are new to mass spectrometrists using MALDI, these and a host of other materials are well known in biological applications. The membrane or modified membrane material must be able to blot the sample compound, and it must also be compatible with the matrix molecules used in MALDI. The matrix-to-sample ratio may often be 1000:1 to 10 000:1. Methods for application of the MALDI matrix, an integral part of sample preparation, are considered next.

Selection of the appropriate MALDI matrix is discussed in detail elsewhere [51–54], and only a brief summary is provided here. There is more than sufficient energy in the incident laser beam to degrade a biological molecule. In simple terms, the role of the matrix is to act as an energy buffer, absorbing most of the energy from the laser beam and converting it into an appropriate mix of thermal energy that leads to vaporization of the matrix and encapsulated sample molecules, and electronic or photo-excitation that leads to ionization of the sample molecules. Useful matrix materials therefore

exhibit a high molar absorptivity at the wavelength chosen, an intermediate volatility and photoexcitation or charge-transfer properties in a useful energy range. In addition, as discussed in detail in the original literature in this area, the matrix and the sample molecules should co-crystallize on the surface so that an efficient energy coupling can occur. Empirically, researchers find matrices that work and continue to use them while searching for others that may work better. Predictions based on a detailed understanding of the mechanisms in the laser-energized micro-volume are beyond our current understanding of the process, echoing a situation that developed in FAB-MS some 15 years ago.

Of relevance to PE-MS and the transfer of materials to a blotting membrane is the question of when and how the matrix is to be applied to the membrane. Strupat et al. [50] have recently completed a study of the mass spectra that result from different methods for application of the MALDI matrix, including whether the matrix solution is applied to a dried or a partially dry membrane. They also studied the use of membranes of different types, including five PVDF membranes differing in pore sizes and surface areas. Superior results in terms of widths of the signals measured are found for PVDF membranes with higher specific areas, and better signal intensity is found when the matrix solution is applied to a membrane that is only partially dried. In each case, the solution in which the matrix compound is dissolved must be able to wet the membrane and distribute the matrix so that enhancing crystallization can occur. Scanning electron micrographs of membranes so prepared emphasize the importance of homogeneous, ultra-fine crystal formation. Of course, it is not possible to examine each membrane individually before mass spectrometric analysis, and a standard protocol is established and then followed with expectations of success. As a number of other membrane materials are investigated for use in MALDI [17,55], it can be expected that they will be used for PE-MS applications also.

Some of the vagaries of this procedure can be removed if the transfer medium is designed

ahead of time to enhance the desorption. Hutchens and Yip [56] have described surfaces in which energy-absorber molecules are “tethered” to the surface, leading to an enhancement in the laser-induced desorption of subsequently adsorbed sample molecules. In addition, these surfaces can also be used as part of the sample clean-up itself, using well known methods of affinity chromatography. These developments are adaptations of the practice of using modified adsorbent materials in thin-layer chromatography [57,58]. In almost all instances, the high level of background signal at lower masses in MALDI mass spectra (derived primarily from the matrix itself and its degradation products) can be limiting when use is made of reactions that generate fragment or product ions that lie within the same mass region. Changes in the matrix-to-sample ratios may make this problem more tractable, and MS–MS can potentially isolate the collision-induced dissociations of a mass-selected parent ion from such background noise in the mass spectrum.

In practice, the mass spectrum is modified most simply by changing the matrix-to-sample ratio, and this has led to the proposal for transfer described here. In the usual procedures, the sample molecules are transferred to the membrane, and then a matrix solution is syringed on to the surface of the membrane. If the initial selection of matrix-to-sample molecule ratio is unsatisfactory, then the sample membrane can be withdrawn from the mass spectrometer and additional matrix can be applied prior to a second analysis. Matrix molecules can be placed ahead of time in the transfer membrane material at a known and homogeneous concentration. With the matrix already present, the problem of finding the appropriate matrix-to-sample ratio can be simplified by use of an asymmetric electroblot procedure, as illustrated in Fig. 2B. As before, the concept for this transfer has its origins in earlier work on transfer procedures developed for TLC–MS. The band shown on the left in Fig. 2B is induced to move under the influence of a potential gradient established between a planar or curved electrode and a point electrode, as shown. The potential gradient

causes a movement of the charged sample molecules towards the point electrode in an asymmetric fashion, and clearly there has to be a dimensional asymmetry in the physical set-up also. The transfer generates an analogous concentration gradient. The darker shading shown represents a higher sample concentration nearer the point electrode achieved at some point during the transfer. Note that transfer is not carried through to completion. If the matrix is homogeneously distributed in the transfer medium, then the matrix-to-sample ratio decreases along the linear path to the point electrode. As the matrix-to-sample ratio is critical in generating a high-quality MALDI mass spectrum, the ability to acquire rapidly a series of mass spectra (at different matrix-to-sample ratios) with focusing of the incident laser beam at different points along that gradation line can be advantageous. The range of matrix-to-sample ratios that can be accommodated depends both on the time allocated for the transfer and the dimensions and spacing of the electrodes, but a factor of 10–100 should be readily achieved.

Use of the matrix in MALDI allows the mass spectra of high mass biomolecules to be recorded, but the addition of the matrix is not without complicating consequences. In particular, the lower mass region of the mass spectrum is congested, filled with ions arising from the matrix molecules, and from degradation of the matrix molecules on interaction with the incident laser beam. Fig. 3 illustrates this characteristic for the positive-ion MALDI mass spectrum of cytochrome *c* recorded from a matrix of α -cyano-4-hydroxycinnamic acid. The high-mass region of the mass spectrum is unobscured, containing singly, double and triple charged forms of the molecular ion for this sample. The region below m/z 1000 is uninterpretable; the range of mass obscured varies with the matrix and with the conditions of laser ionization. The consequence is that spectral interpretation must occur exclusively in the high-mass range, and that derivatizations or sample reactions (see the next section) should preferably lead to higher mass product ions. An alternative approach is to isolate the ion of interest in an MS–MS experi-

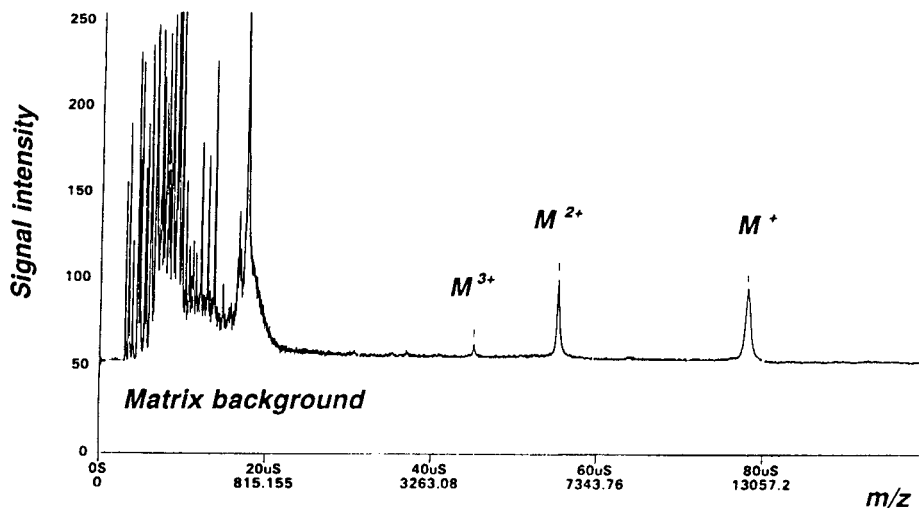


Fig. 3. Positive-ion MALDI mass spectrum of cytochrome *c* showing the spectral background generated from the use of the energy-absorbing matrix (cinnamic acid).

ment, and then to create lower mass ions in collision-induced dissociations or surface-induced dissociations. The FT-MS instrument described earlier is easily used for these MS–MS experiments.

The emphasis so far has been on MALDI. The earliest work on PE–MS used FAB and LSIMS, and the choice of solvent matrix was not as critical. The solvent did have to dissolve the sample from the transfer membrane, or from the electrophoretic gel itself, but most of the standard solvent matrices used in FAB and LSIMS were adequate. For the plasma desorption ionization work reported, the passage of the fast incident particle through the sample solution placed on a nitrocellulose support often provided an interpretable signal. As the direction of the incoming beam was not specified in these experiments, the scanning and imaging experiments could not be completed except through excision of the sample band and examination of discrete individual samples.

3.4. Sample reactions and derivatization

The heritage of TLC–MS in the development of PE–MS is seen again in the use of surface derivatization reactions [59] that can be used to

enhance ion signals, to highlight the presence of certain structural features within the target molecule or to degrade the sample molecule controllably, as in the digestion of larger proteins into smaller peptide fragments. A number of functional-group-specific reactions have been developed for use in mass spectrometry; many of the reactions used in FAB and electrospray also work [60] in MALDI. Derivatization labels used make known and predictable changes in the mass spectrum and, in fact, also within the MS–MS spectrum. The expected mass changes are generally below 100 u per reaction. If several sites react, then the expected mass change is multiplied accordingly. An exemplary reaction is that of the amino groups in peptides with 2-iminothiolane [61]. The mass shift is easily discernible with even lower resolution TOF mass analyzers. Cohen and Chait [62] have described a clever application of this derivatization reaction that documents the accessibility of lysine residues in a globular protein to derivatization. Reagents that introduce small, recognizable cleavages can also be useful in establishing the presence or absence of certain functional groups in sample molecules held at the surface of a planar chromatogram. A match between an expected and an observed mass shift is a necessary but not a sufficient condition for establishing structure. An exact

mass match between the expected and the observed change is, in contrast, a very specific indication for the proposed structural feature.

A number of reactions are already in place that can be used as probes of biomolecular structure, including enzymatic and non-enzymatic protein digestion reactions, sequencing chemistry such as the Edman reaction and various oxidation and reduction reactions, especially those that involve the sulfur-containing amino acids [63]. Of special interest to PE-MS is the fact that these reactions can be carried out sequentially, and under conditions independent of the chromatographic separation itself. The gel or the transfer membrane can be removed from the mass spectrometer and incubated with a digestion enzyme; the products can then be analyzed by mass spectrometry [13,47]. Cytochrome *c* supported on a PVDF membrane was incubated with trypsin [47] to yield a distribution of tryptic peptides that can be used to map the primary sequence. A much wider variety of such derivatization/digestion reactions can be expected to be exploited in the near future with growing research in PE-MS. Of particular interest will be the ability to analyze a sample held on

a membrane, then expose it to a specific substrate or co-factor and subsequently to identify differences in the mass spectrum that correspond to expected interactions.

The repetitive withdrawal and reinsertion of sample membranes into the source of the mass spectrometer is not an elegant way of completing these surface reaction experiments. A surface tracking probe has been devised for use in TLC-MS [64,65]. Derivatization reagents are delivered to the surface of the planar chromatogram in a flow-injection mode, and real-time continuous analysis of the surface by mass spectrometry provides direct spectral evidence for the new products expected of the derivatization. Also demonstrated, and of particular importance in PE-MS of complex biomolecules, is the ability to follow reactions that are reversible either with time or with the addition of a second reagent. The conceptual design for this surface capillary is shown in Fig. 4.

Although preliminary results show that normal staining procedures are not compatible with mass spectrometric detection, staining with colloidal gold particles can be used, although the quality of the measured mass spectrum suffers, and the

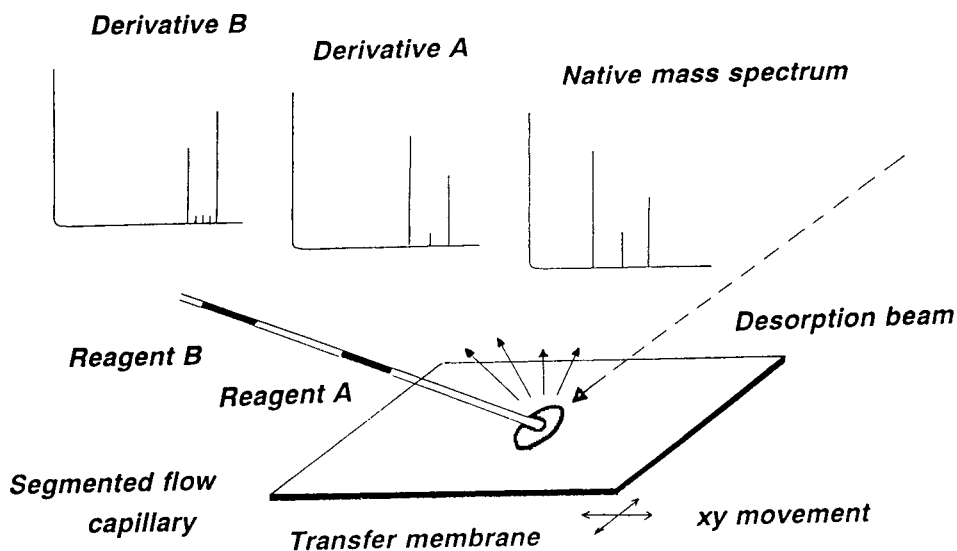


Fig. 4. A segmented flow capillary can bring reagents to the surface to a transfer membrane for in situ derivatization/digestion reactions monitored in real time as the sample is analyzed. The native mass spectrum should change to the spectrum of derivative A, and then to the mass spectrum of derivative B, with the mass differences reflecting the expected structural changes.

potential exists for the formation of adduct ions between the dye and the sample molecules [50]. The use of mass spectrometry may help to provide insight into the interaction between such dyes and biological sample molecules on the membrane.

3.5. Data handling

Most modern data systems deal easily with data sets modelled in three dimensions. GC–MS data sets contain m/z information and relative intensity information as a function of time or scan number, and clever graphical displays make it straightforward to discern information. One-dimensional mass spectral scanning in planar chromatography similarly leads to three-dimensional data sets in which the time dimension is replaced by a linear dimension of sample movement. Data manipulation and display are accomplished with the same processing routines already in widespread use. True imaging requires treatment of data in four dimensions, viz., m/z , relative intensity and x and y dimensions. Ion microprobes and ion microscopes are integrated with data handling systems that deal with this higher level of data. Concerns of additional storage capability within the data system and multi-dimensional data displays have already been satisfactorily addressed. To catalyze the development of commercial PE–MS systems, it only remains for the manufacturers to import this already developed technology base into their present data systems.

There is a larger problem at hand than the higher order or sheer bulk of the data generated in PE–MS. In off-line PE–MS, the separation is completed before detection of the bands is pursued. Mass spectrometry is only one of a number of methods that can be used for spot location and sample band detection. The list of analytical methods that can be used includes visual analysis, UV–Vis spectrophotometry, spectrofluorimetry, optical microscopy techniques, electron microscopy techniques, electron spectroscopy for chemical analysis (ESCA), Auger spectroscopy, reflectance infrared spectroscopy, radioimaging methods, near-infrared analyses and mass spectrometry in several forms,

including secondary ion mass spectrometry, fast atom bombardment, and laser desorption ionization. Coordinated sample positioning and manipulation are central to each of these methods. Detection of sample bands in planar electrophoresis has traditionally been accomplished with optical detectors. Detection schemes range in complexity from simple visible staining procedures and hand-held ultraviolet lamps to sophisticated scanning densitometers and image analysis systems. These optical methods have proved themselves reliable and indispensable, with typical detection limits in the low nanogram range. New optical technologies, including solid-state multi-channel optical devices and charge-coupled detectors, provide even higher performance. In PE–MS, the goal is to afford priority to the sample, and to bring a number of independent analytical methods to the problem. As optical detection methods are among the most sensitive, and are non-destructive, it is logical to begin with such methods, and then to use the mass spectrometry when sample identity must be confirmed with more specific information. There is a substantial increase in the certainty of detection as more independent analytical methods are used. However, the optical image can also be used to guide the mass spectrometric analysis. In discrete analyses, this is already the case; the sample spots are independently located by color development or quenching, and that particular sample area is examined with mass spectrometry. More sophisticated control and analysis are possible when the optical detector and the mass spectrometric detector operate in unison. This combination has been demonstrated in TLC–MS [15] and application to PE–MS will certainly occur in the near future.

A global coordinate system describes the distribution of sample molecules in the xy plane of chromatographic separation, and may also expand to include the z -dimension of depth as well. As detection methods for planar electrophoresis evolve into integrated systems that include optical spectroscopy in addition to mass spectrometry, several aspects of the global coordinate system will increase in importance. The first is the ability to calibrate in space across multiple separations as well as we can presently calibrate

in time. With automated injection systems and very reproducible flow and temperature profiles, a retention time reproducibility of less than 1% can be readily achieved. It is fair to say that the same level of reproducibility has not yet been achieved in planar separations. However, automated methods for sample application and chromatogram development will ultimately have the same effect in planar chromatography as in column chromatography, and incorporation of cross-axis bar codes into the electropherogram itself will allow for both sample identification and *xy* axis calibration. The bar code calibrant/identification is also important in the development of parallel detection systems that operate simultaneously (as in optical detection concurrent with mass spectrometric analysis), and repetitive analyses in which the sample chromatogram surface is sequentially treated with reagents, and re-analyzed, or when the time evolution of the sample signal is followed in kinetic or degradation studies.

The use of chemometrics in the processing of imaging data has grown in direct proportion to increases in computing power, and we can also reasonably expect that these methods will be used to extract information from electrophoretic images. Graphical overlays of optical with mass spectroscopic data may provide new insights into electrophoretic separations, even as the physical scale with which mass spectra data can be measured are reduced; this has been the case with high spatial resolution TLC-MS. It is probable that the usual display of mass spectral information on an *xy* plot of *m/z* value and relative intensity will be displaced by more useful graphical constructs (consider the many means with which multi-dimensional NMR data are displayed). The need for enlightenment in explaining mass spectrometry to biochemists and vice versa will proliferate accordingly.

4. Conclusions

The development of mass spectrometric detectors for planar electrophoresis has followed a course charted previously for the development of the interface between thin-layer chromatography

and mass spectrometry. Despite false starts and more than a fair share of misleading claims in the early literature of PE-MS, one can reliably foresee the specific developments in PE-MS in parallel analogy to TLC-MS. A list of significant developments is given in Table 1. The scanning capabilities just now becoming evident in PE-MS will be supplanted by imaging capabilities that allow a full two-dimensional characterization of the separated bands. Experimental methods for sample preparation, reaction and manipulation will become noticeably more sophisticated as users realize that the separation matrix itself can be used innovatively as a support and as a tool. The widespread consensus that small amounts of sample are difficult to manage is an outdated holdover from our insistence on trying to handle those samples in liquid form and in liquid streams. We shall most certainly develop methods that fully use the chemistry that has been developed for sample digestions and derivatizations, and in so doing we shall take advantage of the ability inherent in planar chromatography to carry out these reactions repetitively, simultaneously and sequentially. In so doing, we shall uncover experimental protocols that can lead to extraordinary specificity at very high sensitivity. Operations at the picomole to femtomole level will become the normal and expected level of analysis for targeted analyses. In proving the validity of these measurements, we shall be forced on the other hand to develop data systems, imaging systems and analysis systems that can manage 1000 times as much information as we confront today. As is the case of TLC-MS today, we shall seek to integrate many different types of spectroscopic data and analytical measurement in one global coordinate system, and then to search for correlations and patterns in those data. Time, removed from consideration in the "off-line" nature of the planar chromatographic separation itself, will reassert an impact as multi-dimensional data are also searched repetitively for relevant changes. Distinctions between TLC-MS and PE-MS will eventually disappear as we construct a seamless, automated analytical approach that takes full advantage of the particular advantages of planar chromatography for analytical measurements.

Table 1
Relevant developments in planar electrophoresis–mass spectrometry

Year	Transfer method ^a	Ionization ^a	Ref.
1986	Capillary, electroblot	PD	35
1987	Capillary blot	Imaging SIMS	37
1988	Southern, Northern	Imaging SIMS	38
1989	(Diffusion)	(FAB)	24,25
1990	Disruption	Flow FAB	26
	Disruption	FAB	27
	Electroelution	MALDI (FT-MS)	11
	Capillary blot	MALDI	46
1991	Electroelution	MALDI (FT-MS)	41
	Freeze–squeeze	FAB	40
	(Electroelution)	(HPLC–LSIMS)	28
1992	Electroblot (PVDF)	MALDI (IR, TOF)	43
	–	MALDI (UV)	53
	–	(MALDI)	30
1993	Electroblot (PVDF)	Scanning MALDI	13
	Nitrocellulose	PD	45
	Electroelution	Electrospray	23
1994	Electroblot (PVDF)	Scanning MALDI	47

^a Terms in parentheses indicate that the samples were analyzed individually after removal from the electropherogram.

Most important, we shall finally take advantage of our expertise in materials science and nanofabrication to reduce the scale of our separation technology to the scale at which the analytical methodology already operates. Planar chip electrophoresis is seductively feasible. The growth curve for PE–MS is in the exponential stage; the pathway is marked, and the games are open.

Acknowledgements

The National Science Foundation and the National Institutes of Health provided early support for our work in TLC–MS and PE–MS. I would especially like to thank Unilever Research and Monsanto for their support in this work, and the Georgia Institute of Technology for supporting patent applications. Several graduate students (past and present) have worked on these projects over the years, including Michele Stan-

ley-Schilling, Steve Brown, Jocelyn Dunphy (working through Oak Ridge Associated Universities) and Michael Bartlett. Kevin Schey and Dan Knapp at the Medical University of South Carolina have graciously provided access to MALDI–TOF instrumentation.

References

- [1] C.F. Poole and S.K. Poole, *Anal. Chem.*, 66 (1994) 27A.
- [2] C.F. Poole and S.K. Poole, *Anal. Chem.*, 61 (1989) 1257A.
- [3] D.C. Fenimore and C.M. Davis, *Anal. Chem.*, 53 (1981) 252A.
- [4] J.C. Dunphy and K.L. Busch, *Biomed. Environ. Mass Spectrom.*, 17 (1988) 405.
- [5] S.J. Doherty and K.L. Busch, *J. Planar Chromatogr.*, 2 (1989) 149.
- [6] K.L. Busch, S.M. Brown, S.J. Doherty, J.C. Dunphy and M.V. Buchanan, *J. Liq. Chromatogr.*, 13 (1990) 2841.

- [7] Y. Nakagawa and K. Iwatani, *J. Chromatogr.*, 562 (1991) 99.
- [8] P. Martin, W. Moden, P. Wall and I.D. Wilson, *J. Planar Chromatogr.*, 5 (1992) 255.
- [9] K.L. Busch, *Trends Anal. Chem.*, 11 (1992) 314.
- [10] F.P. Novak and D.M. Hercules, *Anal. Lett.*, 18, No. A4 (1985) 503.
- [11] J.C. Dunphy, *Ph.D. Dissertation*, Indiana University, 1990.
- [12] J.W. Finch and K.L. Schey, presented at the 40th ASMS Conference on Mass Spectrometry and Allied Topics, Washington, DC, 31 May–5 June 1994, Symposium book, p. 352.
- [13] C. Fenselau and M.M. Vestling, *Am. Lab.*, 25, No. 16 (1993) 74.
- [14] S.J. Doherty and K.L. Busch, *Anal. Chim. Acta*, 218 (1989) 217.
- [15] J.O. Mullis, K.L. Busch and J.A. Chakel, *J. Planar Chromatogr.*, 5 (1992) 9.
- [16] M. Karas and F. Hillenkamp, *Anal. Chem.*, 60 (1988) 2299.
- [17] M.C. Fitzgerald, G.R. Parr and L.M. Smith, *Anal. Chem.*, 65 (1993) 3204.
- [18] J.P. Speir, G.S. Gorman, C.C. Pitsenberger, C.A. Turner, P.P. Wang and I.J. Amster, *Anal. Chem.*, 65 (1993) 1746.
- [19] E. Williams and F.W. McLafferty, *J. Am. Soc. Mass Spectrom.*, 1 (1990) 427.
- [20] Z. Guan, S.A. Hofstadler and D.A. Laude, Jr., *Anal. Chem.*, 65 (1993) 1588.
- [21] P. Kebarle and L. Tang, *Anal. Chem.*, 65 (1993) 972A.
- [22] J.B. Fenn, M. Mann, C.K. Meng, S.F. Wong and C.M. Whitehouse, *Science*, 246 (1989) 64.
- [23] M. le Maire, S. Deschamps, J.V. Moller, J.P. Le Caer and J. Rossier, *Anal. Biochem.*, 214 (1993) 50.
- [24] P. Camilleri, N.J. Haskins and A.J. Hill, *Rapid Commun. Mass Spectrom.*, 3 (1989) 346.
- [25] P. Camilleri, N.J. Haskins and A.J. Hill, *Rapid Commun. Mass Spectrom.*, 3 (1989) 440.
- [26] S.M. Brown and K.L. Busch, presented at the 38th ASMS Conference on Mass Spectrometry and Allied Topics, Tucson, AZ, 3–8 June 1990, Symposium book, p. 1325.
- [27] K. Duffin, J.J. Shieh, R. Leimgruber, E. Kolodziej and P. Toren, presented at the 38th ASMS Conference on Mass Spectrometry and Allied Topics, Tucson, AZ, 3–8 June 1990, Symposium book, p. 293.
- [28] S.C. Hall, D.M. Smith, F.R. Masiarz, V.W. Soo, H.M. Tran, L.B. Epstein and A.L. Burlingame, *Proc. Natl. Acad. Sci. U.S.A.*, 90 (1993) 1927.
- [29] R.C. Beavis and B.T. Chait, *Proc. Natl. Acad. Sci. U.S.A.*, 87 (1990) 673.
- [30] W. Zhang, R. Aebersold, D. Hess and B.T. Chait, presented at the 40th ASMS Conference on Mass Spectrometry and Allied Topics, Washington, DC, 31 May–5 June 1992, Symposium book, p. 1951.
- [31] R.W.J. Thuring, J.P.M. Sanders and P. Borst, *Anal. Biochem.*, 66 (1975) 213.
- [32] L. Wieslander, *Anal. Biochem.*, 98 (1979) 305.
- [33] S.M. Brown and K.L. Busch, *Spectrosc. Lett.*, 24 (1991) 1275.
- [34] K.L. Busch and S.M. Brown, *US Pat.*, 5 208 458 (1993).
- [35] G.P. Jonsson, A.B. Hedin, P.L. Hakansson, B.U. Sunquist, B.J. Save, P.F. Nielson, P. Roepstorff, K.E. Johansson, I. Kamensky and M.S. Linberg, *Anal. Chem.*, 58 (1986) 1084.
- [36] M.S. Stanley and K.L. Busch, *Adv. Mass Spectrom.*, 11 (1989) 432.
- [37] M.S. Stanley, K.L. Duffin, S.J. Doherty and K.L. Busch, *Anal. Chim. Acta*, 200 (1987) 447.
- [38] M.S. Stanley and K.L. Busch, *J. Planar Chromatogr.*, 1 (1988) 135.
- [39] M.S. Stanley, *Ph.D. Dissertation*, Indiana University, Bloomington, IN, 1989.
- [40] Y. Cao, J. Yin, K.L. Busch and L.A. Bottomley, presented at the 39th ASMS Conference on Mass Spectrometry and Allied Topics, Nashville, TN, 19–24 May 1991, Symposium book, p. 390.
- [41] J.C. Dunphy, R.L. Hettich, M.V. Buchanan and K.L. Busch, presented at the 39th ASMS Conference on Mass Spectrometry and Allied Topics, Nashville, TN, 19–24 May 1991, Symposium book, p. 13.
- [42] M.P. Lacey, T. Keough, R. Takiguku, R.E. Schneider, T.N. Asquith, M.P. Purdon, R.A. Sanders, J.D. Pinkston and R.D. Hentschel, presented at the 39th ASMS Conference on Mass Spectrometry and Allied Topics, Nashville, TN, 19–24 May 1991, Symposium book, p. 358.
- [43] C. Eckerskorn, K. Strupat, M. Karas, F. Hillenkamp and F. Lottspeich, *Electrophoresis*, 13 (1992) 664.
- [44] K.L. Busch and J.C. Dunphy, *US Pat.*, 5 245 185 (1993).
- [45] K. Klarksov and P. Roepstorff, *Biol. Mass Spectrom.*, 22 (1993) 433.
- [46] M. Karas, U. Bahr, A.I. Imgedoh, E. Nordhoff, B. Stahl, K. Strupat and F. Hillenkamp, *Anal. Chim. Acta*, 241 (1990) 175.
- [47] M.M. Vestling and C. Fenselau, *Anal. Chem.*, 66 (1994) 471.
- [48] R.M. Aebersold, D.B. Teplow, L.E. Hood and S.B. Kent, *J. Biol. Chem.*, 261 (1986) 4229.
- [49] M.P. Lacey and T. Keough, *Anal. Chem.*, 63 (1991) 1482.
- [50] K. Strupat, M. Karas, F. Hillenkamp, C. Eckerskorn and F. Lottspeich, *Anal. Chem.*, 66 (1994) 464.
- [51] B. Stahl, M. Steup, M. Karas and F. Hillenkamp, *Anal. Chem.*, 63 (1991) 1463.
- [52] D.J. Harvey, *J. Am. Soc. Mass Spectrom.*, 7 (1993) 614.
- [53] K.K. Mock, C.W. Sutton and J.S. Cottrell, *Rapid Commun. Mass Spectrom.*, 6 (1992) 233.
- [54] N. Medina, T. Huth-Fehre, A. Westman and B.U.R. Sundqvist, *Org. Mass Spectrom.*, 29 (1994) 207.
- [55] E.J. Zaluzec, D.A. Gage, J. Allison and J.T. Watson, *J. Am. Soc. Mass Spectrom.*, 5 (1994) 230.
- [56] T.W. Hutchens and T.-T. Yip, *Rapid Commun. Mass Spectrom.*, 7 (1993) 576.

- [57] J.D. Harper, P.A. Martel and C.M. O'Donnel, *J. Liq. Chromatogr.*, 13 (1989) 31.
- [58] W.P.N. Fernando, M.L. Larrivee and C.F. Poole, *Anal. Chem.*, 65 (1993) 588.
- [59] H. Jork, W. Funk, W. Fischer and H. Wimmer, *Thin-Layer Chromatography: Reagents and Detection Methods*, VCH, Weinheim, 1994.
- [60] J.M.E. Quirke, C.L. Adams and G.J. Van Berkel, *Anal. Chem.*, 66 (1994) 1302.
- [61] M.G. Bartlett and K.L. Busch, *Biol. Mass Spectrom.*, 23 (1994) 353.
- [62] S.L. Cohen and B.T. Chait, presented at the 41st ASMS Conference on Mass Spectrometry and Allied Topics, San Francisco, CA, 30 May–4 June 1993, Symposium book, p. 414a.
- [63] E.J. Zaluzec, D.A. Gage and J.T. Watson, *J. Am. Soc. Mass Spectrom.*, 5 (1994) 359.
- [64] K.L. Busch, presented at the 1994 Pittsburgh Conference on Analytical Chemistry and Applied Spectroscopy, March 1994, paper 020.
- [65] S.M. Brown, H. Schurz and K.L. Busch, *J. Planar Chromatogr.*, 3 (1990) 222.



ELSEVIER

Journal of Chromatography A, 692 (1995) 291–300

JOURNAL OF
CHROMATOGRAPHY A

Selectivity control in micellar electrokinetic chromatography of small peptides using mixed fluorocarbon–hydrocarbon anionic surfactants

Bing Ye, Mohammadreza Hadjmohammadi¹, Morteza G. Khaledi*

Department of Chemistry, North Carolina State University, Box 8204, Raleigh, NC 27695, USA

Abstract

Electrophoretic mobilities and capacity factors for a group of Trp-containing small peptides were determined by micellar electrokinetic chromatography (MEKC) using mixtures of a fluorocarbon anionic surfactant, lithium perfluorooctane sulfonate, and a hydrocarbon anionic surfactant, lithium dodecyl sulfate. Upon mixing these two surfactants, which have different microenvironments and interactive characteristics, greater control over migration of solutes is achieved. The changes in the composition of mixed micelles such as the mole fraction of the surfactants result in different solute–micelle binding as well as migration times of the micelles (t_{mc}). Consequently, capacity factor, selectivity and elution window (t_{mc}/t_0) change with the composition of the mixed micellar system. Another characteristic of the mixtures of fluorocarbon–hydrocarbon surfactants is the possibility of forming two different types of micelles which offers an additional partitioning process for each solute in the MEKC system. Such a unique phenomenon offers a higher degree of selectivity control. This mixed MEKC system is quite effective for the separation of small peptides. It provides an alternative to the free-solution capillary zone electrophoresis system for the separation of charged solutes with nearly identical electrophoretic mobility.

1. Introduction

The rapid development of capillary zone electrophoresis (CZE) during the past decade has shown that it is one of the most powerful separation techniques. As one of the early demonstrations of the analytical power of CZE [1], peptide separation will continue to be among the most common applications of this technique. Since CZE is a method strongly dependent on charge differences between analyte species, it has been considered as a complementary method to RP-HPLC for peptide mapping. The primary

factor for manipulation of selectivity of CZE separations is the buffer pH which alters the analytes' charges and, thus, their mobilities [2]. However, for the separation of peptides with high structural similarities, optimization of pH may not be adequate due to the nearly identical mobilities over the entire pH range.

Meanwhile, by introducing micelle-forming surfactants to the buffer medium, a dynamic partition mechanism of solutes into the micellar pseudo-stationary phase is established to supplement the differences in the electrophoretic mobilities of ionic analytes such as peptides [3]. Micellar electrokinetic chromatography (MEKC) incorporates both aspects of electrophoretic and chromatographic separations, so that subtle dif-

* Corresponding author.

¹ On sabbatical leave.

ferences in the hydrophobicity, charge, size, and shape of analytes can be effectively utilized to enhance separation [4–7].

Since the first description by Terabe et al. [3], considerable attention has been paid to the effects of the composition of the micellar solutions on MEKC separations [8]. Greater control of migration behavior and selectivity has been achieved through manipulating several compositional parameters such as type and concentration of surfactants, addition of modifiers such as cyclodextrins, urea, or organic solvents, as well as pH and temperature. Among these approaches which have often resulted in the enhancement of resolution in MEKC separations, the type of surfactants generally influences migration patterns and exhibits great selectivity effects in MEKC. Partition coefficients of analytes into micelles and mobility of micelles depend upon the nature of the hydrophobic moiety, the charged head group, and perhaps even the counterion of the micelle-forming surfactants. Thus, one can tailor the structure of surfactants in MEKC in order to solve different separation problems.

One alternative to tailoring micellar microenvironments is to mix surfactants with different structural properties in order to manipulate solute–micelle interactions. By mixing two surfactants with different microenvironments and interactive characteristics, such as hydrocarbon and fluorocarbon functional groups, one can achieve a greater control over migration of solutes in electrokinetic chromatography (EKC). We refer to this mode as mixed micellar electrokinetic chromatography (MMEKC). The changes in the composition of mixed micelles (e.g. mole fraction of surfactants) would result in different solute–micelle partitioning. The use of mixed surfactants has attracted attention only recently. The majority of the reported use of mixed surfactants in MEKC, however, has involved addition of a non-ionic surfactant (such as Brij 35) to an ionic surfactant [9–11]. An extensive study has been initiated in this laboratory in exploring the usefulness of a wide variety of mixed micellar systems in EKC. Several mixed micellar systems such as the mixture of a fluoro-

carbon and a hydrocarbon micelles, the ternary mixture of these two micelles with Brij 35, mixed bile salt surfactants, and the binary, ternary, and even quaternary mixtures of a hydrocarbon [sodium dodecyl sulfate (SDS)] and different bile salts have already been explored [12–14].

The aim of this study was to evaluate a MMEKC system using mixtures of a fluorocarbon surfactant, lithium perfluorooctane sulfonate (LiPFOS) and a hydrocarbon surfactant, lithium dodecyl sulfate (LiDS), for the separation of charged solutes such as small peptides. Liu et al. have demonstrated successful separation of structurally similar small peptides and tryptic digests by using anionic (SDS) and cationic [dodecyltrimethylammonium bromide (DTAB), hexadecyltrimethylammonium bromide (HTAB)] surfactants as well as cyclodextrins [15]. Another interesting example of selectivity in MEKC separation of small peptides is the use of an anionic surfactant taurodeoxycholic acid (TDC) [16]. For large peptides, on the other hand, their interactions with micelles become too strong and the separation cannot be readily achieved. Using non-ionic surfactant (Tween 20) [17] as well as combining organic solvent with the cationic surfactant cetyltrimethylammonium bromide (CTAB) [18] were two successful approaches which reduced such interactions between peptides and micelles and led to the separations of angiotensins and motilins.

Liquid mixtures of fluorocarbon and hydrocarbon solvents exhibit large positive deviations from ideal solutions described by Raoult's Law. The abnormal interactions of fluorocarbon and hydrocarbon surfactants in micellar systems were first pointed out by Mukerjee et al. [19]. In addition to the intra-hydrophobic interactions between hydrocarbon–hydrocarbon, and fluorocarbon–fluorocarbon functional groups, there exists a hydrocarbon–fluorocarbon mutual phobia effect. This often results in the coexistence of two types of micelles (demixing) in the range of the mole fraction where the critical micelle concentration (CMC) goes through a maximum (so called azeotropic point): one type of micelle is fluorocarbon-rich and the other one is rich in hydrocarbon surfactant. Some evi-

dences for demicellization in the mixture of LiPFOS and LiDS were reported by Asakawa et al. [20]. If such a condition exists under the operating conditions of MMEKC, higher degrees of selectivity control are expected to yield because of the presence of an additional partitioning process for each solute [12].

2. Experimental

2.1. Apparatus

All experiments were carried out on a laboratory-built CE system. It consisted of a 0–30 kV high-voltage power supply (Series EH; Glassman High Voltage, Whitehouse Station, NJ, USA), a variable-wavelength UV–Vis detector (Model 200; Linear Instruments, Reno, NV, USA) operating at 214 nm, and 52 μm I.D. \times 375 μm O.D. fused-silica capillary tubing (Polymicro Technologies, Phoenix, AZ, USA). The total length of the capillary was 55.7 cm, and the polyimide coating was burned off 42.3 cm from the injection end to form the detection window. The capillary temperature was maintained at 40°C by jacketing in light mineral oil using a constant-temperature circulator (Type K2-R; Lauda, Germany). Electropherograms were recorded with an electronic integrator (HP3394A; Hewlett-Packard, Avondale, PA, USA).

2.2. Materials

Nine test peptides (from Sigma, St. Louis, MO, USA), listed in Table 1, were used as received. LiDS was also purchased from Sigma and LiPFOS was a gift from 3M (St. Paul, MN, USA).

2.3. Procedure

In order to maintain relatively low electrical current (especially at high surfactant concentrations), a pH 8 borate buffer with an ionic strength of only 5 mM was used in all MEKC

Table 1
Peptides separated

Peak	Peptide
1	Ala-Trp (AW)
2	Trp-Ala (WA)
3	Trp-Tyr (WY)
4	Glu-Trp (EW)
5	Trp-Gly-Gly (WGG)
6	Trp-Leu (WL)
7	Leu-Trp (LW)
8	Trp-Phe (WF)
9	Trp-Trp (WW)

experiments. The total surfactant concentration was varied from 75 to 150 mM and mixtures of LiDS and LiPFOS were prepared from stock solutions at different mole fractions. The sample injection end was raised manually to 3 cm high for hydrodynamic injection from the anode end of the capillary for 5 s.

A new capillary was flushed with 1 M LiOH for 1 h, 1 M HCl for 15 min and water for 15 min before the running buffer was introduced into the tube. The capillary was rinsed with the running buffers for 3 min and then with power applied for another 3 min between each run.

2.4. Determination of t_0 and t_{mc}

The micellar migration time (t_{mc}) and the migration time of the electroosmotic flow marker, i.e. “unretained” solute, (t_0) were obtained through an indirect method using homologous series of alkylphenones [21].

The electrophoretic mobility μ was determined by measurement of the migration times (t) relative to that of the electroosmotic flow marker (t_0) according to the following equation [1]:

$$\mu = \frac{L}{E} \cdot \left(\frac{1}{t} - \frac{1}{t_0} \right) \quad (1)$$

where L is the length of the capillary to the detector and E is the electric field strength.

3. Results and discussion

The high resolving power of CZE facilitates the separation of peptides that differ slightly in their mobilities. Depending on a particular peptide mixture, pH can be adjusted to control the net charge, and consequently the quality of separation as well as the analysis time. In Fig. 1a, the amino groups of the N-terminal of the nine Trp-containing small peptides are completely deprotonated at pH 12.4 while the carboxyl groups bear an identical negative charge, thus separation is mainly based on their size. As the pH of the buffer is decreased to 8.0, the net charges on the molecules are close to zero, so most peptides migrate near t_0 and the separation deteriorates. When the pH is further decreased to 2.5 (Fig. 1b), which is close to the pK_a values of the carboxyl group of C-terminal, the resolution is improved at the expense of the longer analysis time as compared to the previous two conditions. However, EW (peak 4) and WY (peak 3) co-migrate as well as peaks of WF (peak 8) and WW (peak 9) overlap. One benefit from choosing a low or a high pH is that the unwanted coulombic interaction between the peptides and the capillary wall is reduced. At low pH, the silanol groups on the capillary surface are protonated and there is little interaction between the positively charged peptides and the silica wall [22]. At high pH, on the other hand, peptides are negatively charged which results in an electrostatic repulsion between wall and analyte [23].

Fig. 2 shows the separations of peptides by MMEKC carried out at pH 8.0 at different LiPFOS mole fractions in a mixed micellar system of LiPFOS and LiDS at a constant total micelle concentration of 125 mM. Much better separation, reasonable peak shape, and analysis time are observed in the MMEKC system as compared to that obtained in the CZE mode (Fig. 1a and b). Interestingly large variations in selectivity are achieved as a result of changing the composition of the mixed micellar solution as evidenced by changes in the relative retention of the peaks and the frequent changes in the migration order of the bands. For example, EW

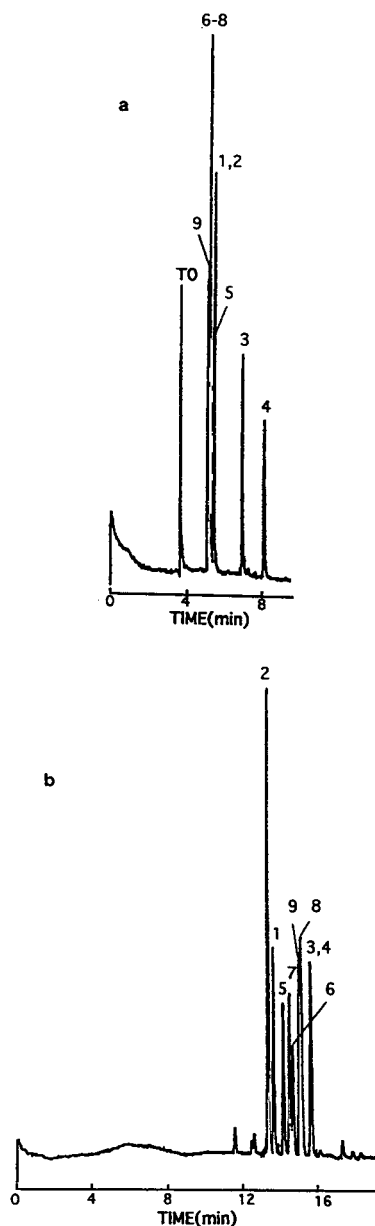


Fig. 1. CZE of peptides. Separation buffers and operating voltages are: (a) 100 mM phosphate-borate buffer (pH 12.4), 9 kV; (b) 100 mM phosphate buffer (pH 2.5), 15 kV. Peak numbers correspond to Table 1.

(peak 4), which migrates in the middle of chromatogram in a mixture of 100 mM LiDS–25 mM LiPFOS (Fig. 2a) is the last compound in 25 mM LiDS–100 mM LiPFOS mixed micelles (Fig. 2c).

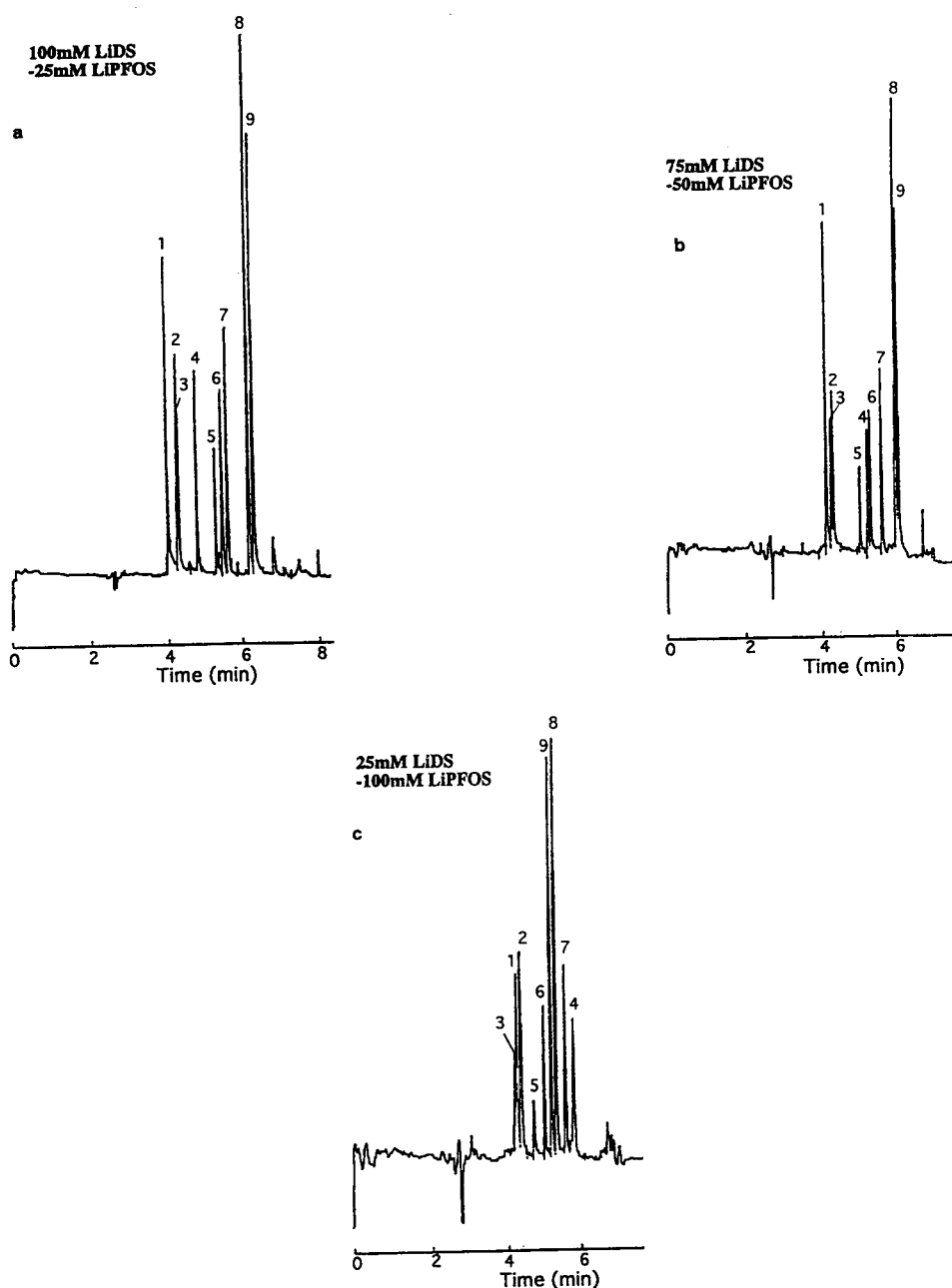


Fig. 2. MMEKC separation of peptides at 125 mM total micelle concentration. Mole fraction of LiPFOS: (a) 0.2, (b) 0.4 and (c) 0.8. Peak numbers correspond to Table 1. Operating voltage: 20 kV.

Capacity factor k' is an important migration parameter for both neutral and charged solutes in MEKC. It is defined as the ratio of the

number of moles of solute associated with micelles to that in the aqueous phase. In other words, k' is the parameter that directly reflects

solute–micelle interactions. For charged solutes, it can be calculated from Eq. 2 [5,6]:

$$k' = \frac{\mu - \mu_0}{\mu_m - \mu} \quad (2)$$

where μ_m is the mobility of the micelles and μ_0 is the mobility of the charged solute in the absence of micelles. Fig. 3 illustrates the effect of the mole fraction of the LiPFOS surfactant in the LiDS–LiPFOS mixed micelles on the capacity factor at 125 mM total micelle concentration. A similar trend was observed at other micelle concentrations. The overall k' values of these peptides in the fluorocarbon system are smaller than that in the hydrocarbon system which means that the solutes interact less with the LiPFOS micelles. This agrees with the phobia effect between the hydrocarbon and the fluorocarbon functional groups. Thus, the capacity factors of the majority of the peptides decrease upon increasing the mole fraction of the fluorocarbon surfactants. Among these peptides, capacity factors of the most hydrophobic compounds like WW, WF decrease to a larger extent with the increase in the LiPFOS mole fraction $[X(\text{LiPFOS})]$. On the other hand, the capacity factors of the polar ones such as EW, AW, WA and WY change slightly over the entire mole fraction range because the k' values are less than

1 which indicates these peptides prefer the aqueous over the micellar phase. For LW, WL and WGG with intermediate hydrophobic characteristics, the extents of reduction in k' are smaller than those for the hydrophobic peptides but larger than those for the polar ones.

Note that the capacity factors for most of the peptides (except hydrophobic WW and WF) either increase or remain constant in the region of $X(\text{LiPFOS}) = 0\text{--}0.2$. The exact reason for this behavior which has also been observed for uncharged aromatic compounds [12] is not known. However, this can be attributed to the dual nature of solutes interactions with the fluorocarbon micelles: first is the favorable hydrogen bonding interactions between the polar functional groups with the fluorocarbons and the second is the unfavorable phobia effect between the hydrocarbon moieties of the solutes and the fluorocarbon groups of micelles [24]. Apparently, the second effect is predominant at $X(\text{LiPFOS}) > 0.20$ for all solutes. This turning point as well as $X(\text{LiPFOS}) = 0.4$ separates the entire mole fraction range to three regions of A, B and C as shown in Fig. 3. In the region A, where the mole fraction of fluorocarbon surfactants varies from 0 to 0.2, WW and WF, which are very hydrophobic, interact less with the micellar phase of increasing fluorocarbon content, i.e., k' decreases with $X(\text{LiPFOS})$. On the other hand, polar compounds such as EW, AW and WA apparently favor the interaction with the fluorocarbon containing mixed micelles. When $X(\text{LiPFOS})$ further increases from 0.2 to 0.4 (region B), the phobia interaction between hydrocarbon and fluorocarbon functional groups becomes dominant and thus capacity factors of all peptides decrease. When the mole fraction of the fluorocarbon surfactant reaches 0.4, the capacity factors, k' , of all peptides are below 2. Consequently the effect of changing composition by increasing fluorocarbon surfactants in micellar phases becomes less significant. The extent of reduction in k' upon increasing $X(\text{LiPFOS})$ in the region C becomes smaller than that in the region B.

It is important to note, however, that using k' as the migration parameter might be associated

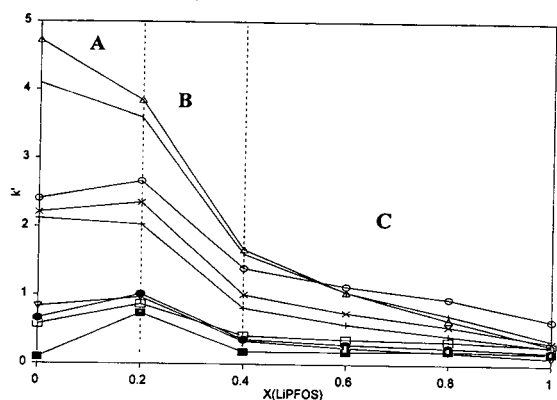


Fig. 3. Effect of changing micellar phase composition on capacity factor, k' , of peptides. Total micelle concentration: 125 mM. pH 8.0. Experimental conditions as in Fig. 2. \blacksquare = EW; \square = AW; \bullet = WA; ∇ = WY; \circ = LW; $+$ = WGG; \times = WL; $|$ = WF; \triangle = WW; --- = micelle.

with some uncertainties. One source of such uncertainties comes from the accuracy of determination of t_{mc} which is essential on obtaining k' values (Eq. 2). The problem of accurate measurement of t_{mc} in MEKC due to the lack of a reliable method is even more complicated in the MMEKC systems. This is especially true for the situation where there might be two distinctive types of micelles formed. Intuitively, one can conclude that net mobility is a more reliable parameter than capacity factor in MMEKC systems.

The net electrophoretic mobility μ of a charged solute in MEKC is the weighted sum of two mobility terms and can be expressed as [6]:

$$\mu = \frac{k'}{k'+1} \cdot \mu_m + \frac{1}{k'+1} \cdot \mu_0 \quad (3)$$

In Eq. 3, the ratio $k'/(k'+1)$ represents the fraction of the solute that associates with the micelles and migrate at μ_m while $1/(k'+1)$ is the fraction of the charged solute in the aqueous phase and moving at μ_0 . Therefore, the first term on the right side of the Eq. 3 can be regarded as an electrokinetic term and the second one an electrophoretic term. Fig. 4 illustrates the effect of mixed micellar composition on these two terms. The electrokinetic terms decrease for the peptides (except EW) upon increasing the concentration of the fluorocarbon surfactant after $X(\text{LiPFOS}) = 0.20$ (Fig. 4a), which indicates that these solutes interact more with the hydrocarbon surfactants than the fluorocarbon surfactants. The electrophoretic term, on the other hand, remained nearly unchanged or even increased (Fig. 4b). Obviously, upon the reduction of peptide–micelle interactions (i.e., decrease of the electrokinetic term) with an increase in $X(\text{LiPFOS})$, the electrophoretic effect plays a larger role at higher $X(\text{LiPFOS})$. The contribution from the electrokinetic term to overall mobility, however, is predominant as compared with that from the electrophoretic term.

The variations in peptides net mobilities as a function of the mole fraction of LiPFOS are nearly linear (Fig. 5). In spite of the increase in the mobility of the mixed micellar phase with the $X(\text{LiPFOS})$, the net mobilities for all peptides

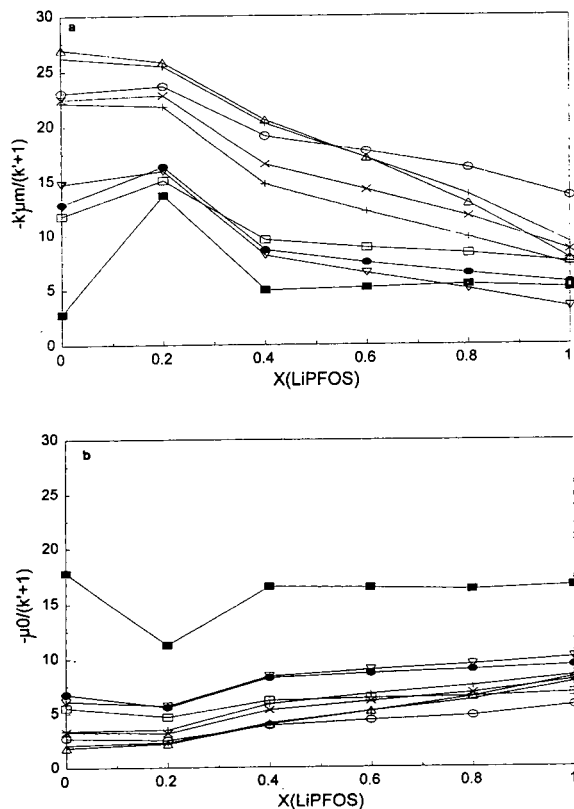


Fig. 4. Effect of changing micellar phase composition on (a) $-[k'/(k'+1)]\mu_m$ term and (b) $-[1/(k'+1)]\mu_0$ term in Eq. 3. Other conditions as in Fig. 3.

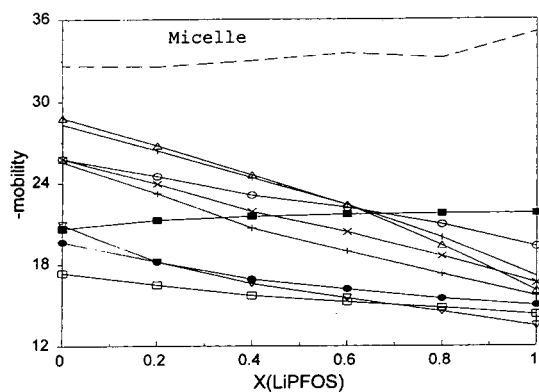


Fig. 5. Effect of changing micellar phase composition on the net mobility of peptides. Other conditions as in Fig. 3.

(except EW) decrease. At pH 8, these solutes carry net negative charges and move with the anionic micelles towards the anode, therefore, more negative values indicate larger mobilities. Meanwhile, the electroosmotic mobility μ_{EOF} is larger than the mobilities of both micelles and the peptides which results in their net migration towards the cathode where the detector is located. EW which apparently has the largest negative charge among these peptides is probably electrostatically repelled from the anionic micelles and is almost insensitive to the changes of the micellar composition.

Elution window defined as the ratio of t_{mc} and t_0 is an important factor that influences resolution and depends on the composition of the mixed micelle in MMEKC. Since the LiPFOS micelle has a larger negative mobility than the LiDS micelle, the t_{mc}/t_0 ratio increases with $X(\text{LiPFOS})$ (Fig. 6). Note that μ_{EOF} is little affected by the compositional variations. Consequently, the resolution can be enhanced without an adverse effect of longer analysis times. This demonstrates another advantage of this approach over adding other modifiers such as organic solvent where the resolution is improved at the expense of longer analysis times.

One other important factor that influences mobility variations with the mixed micellar composition in MMEKC is the micelle-induced $\text{p}K_{\text{a}}$ shift. The extent of ionization of ionizable solutes in the MMEKC system depends on the apparent ionization constant in micellar solution, $K_{\text{a,app}}$, which is different from the aqueous ionization constant, K_{a} , and can be expressed as [25]:

$$K_{\text{a,app}} = K_{\text{a}} \cdot \frac{K_{\text{A}^-}^{\text{m}}[\text{M}] + 1}{K_{\text{HA}}^{\text{m}}[\text{M}] + 1} \quad (4)$$

where K^{m} values are the respective binding constants of the acid, HA, and its conjugated base, A^- , to the micelle. Because the electrostatic repulsion between the A^- and the head group of anionic micelles such as LiPFOS and LiDS greatly reduces solute–micelle interactions, the term $K_{\text{A}^-}^{\text{m}}[\text{M}]$ is negligible as compared to 1. So $K_{\text{a,app}}$ is a function of the binding constant of the fully protonated acid to micelle K_{HA}^{m} , micelle concentration $[\text{M}]$, and aqueous K_{a} . In fluorocarbon–hydrocarbon mixed micellar system, the extent of $\text{p}K_{\text{a}}$ shift caused by the compositional variation of the micellar phase is dependent on the difference in binding constants of the acid,

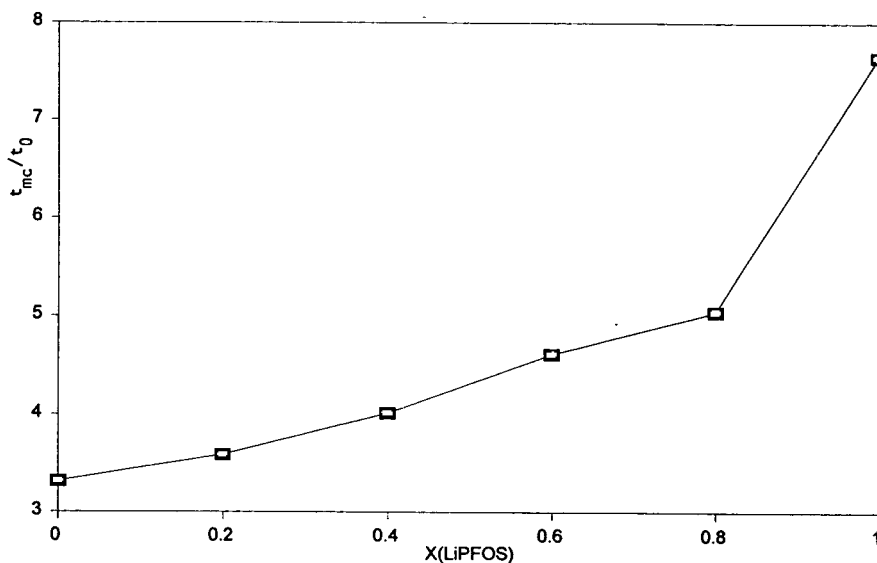


Fig. 6. Effect of changing micellar phase composition on elution window (t_{mc}/t_0) at 125 mM total micelle concentration.

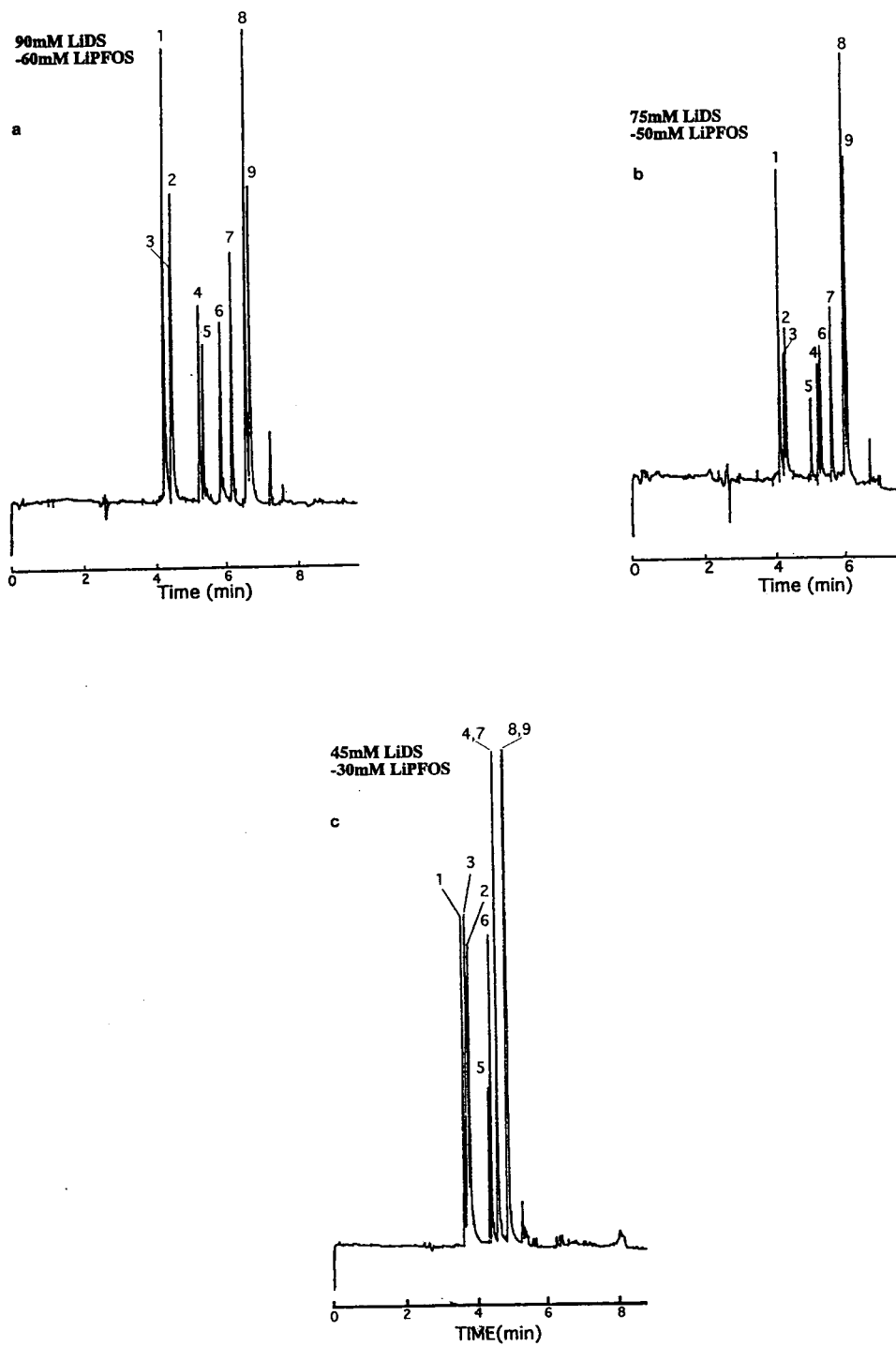


Fig. 7. MMEKC separation of peptides at $X(\text{LiPFOS}) = 0.4$. Total micelle concentration: (a) 150 mM, (b) 125 mM and (c) 75 mM. Peak numbers correspond to Table 1. Other conditions as in Fig. 2.

HA, to the hydrocarbon micelle (HC) and the fluorocarbon micelle (FC) and can be derived from Eq. 4 as:

$$pK_{a,app}^{HC} - pK_{a,app}^{FC} = \log (K_{HA}^{HC}[M] + 1) - \log (K_{HA}^{FC}[M] + 1) \quad (5)$$

According to Eq. 5, at a constant $[M]$, the larger the difference between K_{HA}^{HC} and K_{HA}^{FC} , the larger the difference in $pK_{a,app}^{HC}$ and $pK_{a,app}^{FC}$. Therefore hydrophobic peptides such as WW and WF that have a larger difference in their binding to the hydrocarbon micelles and the fluorocarbon micelles are expected to have larger pK_a shifts with the mixed micellar composition. Consequently, the degree of variation of their electrophoretic terms with $X(\text{LiPFOS})$ for these compounds is greater (Fig. 4b).

Fig. 7 shows the effect of the total micelle concentration on the separation of the peptide mixture at $X(\text{LiPFOS}) = 0.4$. Except EW (peak 4), changes in the overall migration patterns are relatively small compared to the previous set of separation (Fig. 2). For uncharged solutes, total micelle concentration only affects k' and elution window (t_{mc}/t_0) with little or no impact on selectivity. For charged molecules such as peptides, the effect of total surfactant concentration on selectivity can take place through the different magnitude of the micelle-induced pK_a shift (Eqs. 4 and 5). Apparently, this phenomenon is not much pronounced for the mixtures at the operating conditions.

Acknowledgement

We gratefully acknowledge a research grant from the National Institutes of Health (GM 38738).

References

- [1] J.W. Jorgenson and K.D. Lukacs, *Anal. Chem.*, 53 (1981) 1298.
- [2] S.C. Smith and M.G. Khaledi, *Anal. Chem.*, 65 (1993) 193.
- [3] S. Terabe, K. Otsuka, K. Ichikawa, A. Tsuchiya and T. Ando, *Anal. Chem.*, 56 (1984) 111.
- [4] S.C. Smith and M.G. Khaledi, *J. Chromatogr.*, 632 (1993) 177.
- [5] J.K. Strasters and M.G. Khaledi, *Anal. Chem.*, 63 (1991) 2503.
- [6] M.G. Khaledi, S.C. Smith and J.K. Strasters, *Anal. Chem.*, 63 (1991) 1820.
- [7] C. Quang, J.K. Strasters and M.G. Khaledi, *Anal. Chem.*, 66 (1994) 1646.
- [8] M.G. Khaledi, in J. Landers (Editor), *Handbook of Capillary Electrophoresis: A Practical Approach*, CRC Press, Boca Raton, FL, 1993, p. 43.
- [9] E.L. Little and J.P. Foley, *J. Microcol. Sep.*, 4 (1992) 145.
- [10] H.T. Rasmussen, L.K. Goebel and H.M. McNair, *J. Chromatogr.*, 517 (1990) 549.
- [11] B.R. Thomas and S. Ghodbane, *J. Liq. Chromatogr.*, 16 (1993) 1983.
- [12] M.G. Khaledi and M.R. Hadjmohammadi, in preparation.
- [13] J.G. Bumgarner and M.G. Khaledi, *Electrophoresis*, 15 (1994) 1260.
- [14] M.G. Khaledi, R.S. Sahota, C. Quang, J.K. Strasters and S.C. Smith, in N. Guzman (Editor), *Capillary Electrophoresis Technology*, Marcel Dekker, New York, 1993, p. 185.
- [15] J. Liu, K.A. Cobb and M. Novotny, *J. Chromatogr.*, 519 (1990) 189.
- [16] I. Beijersten and D. Westerlund, *Anal. Chem.*, 65 (1993) 3484.
- [17] N. Matsubara and S. Terabe, *Chromatographia*, 34 (1992) 493.
- [18] T. Yashima, A. Tsuchiya, O. Morita and S. Terabe, *Anal. Chem.*, 64 (1992) 2981.
- [19] P. Mukerjee and A.Y.S. Yang, *J. Phys. Chem.*, 80 (1976) 1388.
- [20] T. Asakawa, K. Johten, S. Miyagishi and M. Nishida, *Langmuir*, 4 (1988) 136.
- [21] D.M. Smith, J.K. Strasters and M.G. Khaledi, unpublished results.
- [22] R.M. McCormick, *Anal. Chem.*, 60 (1988) 2322.
- [23] H.H. Lauer and D. McManigill, *Anal. Chem.*, 58 (1986) 166.
- [24] S. Yang and M.G. Khaledi, *Anal. Chem.*, in press.
- [25] M.G. Khaledi and A.H. Rodgers, *Anal. Chim. Acta*, 239 (1990) 121.



Linear solvation energy relationships in micellar liquid chromatography and micellar electrokinetic capillary chromatography

Shenyuan Yang, Morteza G. Khaledi*

Department of Chemistry, North Carolina State University, P.O. Box 8204, Raleigh, NC 27695-8204, USA

Abstract

Linear solvation energy relationships (LSERs) were used to evaluate and characterize chemical interactions that influence retention behavior in micellar liquid chromatography (MLC) and micellar electrokinetic capillary chromatography (MEKC). High correlations were found between solutes' capacity factors in MLC and in MEKC, as well as binding constants to micelles and their solvatochromic parameters using two anionic surfactants, sodium dodecyl sulfate (SDS) and sodium cholate (SC), and one cationic surfactant, tetradecyltrimethylammonium bromide (C_{14} TAB). Surprisingly, in the C_{14} TAB MLC system capacity factor (k') vs. solvatochromic parameters gives better correlation than $\log k'$ vs. solvatochromic parameters, which is an opposite behavior to that observed in the SDS MLC system. The capacity factors in the C_{14} TAB MLC system were characterized using LSERs with and without organic modifiers. It was found that the addition of a small amount of short-chain alcohols (e.g., 7% 2-propanol or 5% butanol) does not significantly change the high correlations between k' vs. solvatochromic parameters. The changes in the coefficients with the volume fraction of organic solvents were explained by comparing the differences in chemical natures between mobile phase and stationary phase. Stationary phase shows a significant effect on the chemical interactions in MLC through LSER study using a diphenyl column and a C_8 column.

LSERs were also used to characterize retention behavior in MEKC. High correlations between the logarithm of solutes' capacity factors and their solvatochromic parameters were observed for a group of 25 uncharged substituted aromatic compounds and polycyclic aromatic hydrocarbons with SDS and SC micelles. It was found that solutes' size and basicity are the two dominant factors that influence the migration behavior in MEKC.

1. Introduction

In micellar liquid chromatography (MLC) and micellar electrokinetic capillary chromatography

(MEKC), the amphiphilic nature of micelles provides both hydrophobic and polar (or electrostatic) sites of interactions with solutes. In MLC [1-4], solutes partition from the bulk mobile phase into micelles and into the stationary phases. Solutes' retention behavior depends on various chemical interactions (e.g., hydrophobic, dipolar, and hydrogen bonding) in these parti-

* Corresponding author.

tioning processes. The exact nature of these interactions depends upon the chemical nature of solutes as well as the compositions of the mobile phase, and the stationary phase. MEKC is a mode of capillary electrophoresis (CE) for the separation of uncharged compounds [5–7]. In MEKC, separation of uncharged molecules is solely due to the extent and differences of their interactions with the micelles. In other words, chemical interactions in the partitioning processes control the separations of solutes in these two micellar-mediated chromatographic techniques. A study of the chemical interactions in these systems should provide a better understanding of solutes' retention behavior and selectivity pattern in MLC and MEKC.

Attempts to achieve a better understanding of the retention process in MLC have been mostly qualitative in nature and have been based on the observed changes in retention behavior as a function of the composition of the micellar eluents, the stationary phase, as well as solutes structural properties [8–11]. Quantitative structure–retention relationships (QSRRs) can play an important role in achieving a better understanding of the role of different factors that influence retention behavior in MLC and MEKC. Recently, linear solvation energy relationships (LSERs) [12–18] have been successfully applied for the evaluation of retention behaviors in RPLC with hydro–organic eluents, stationary phase effect in RPLC and for the characterization of partitioning process between *n*-octanol and water for non-electrolytes. In LSERs, solvent-related properties of solutes, SP, can be described in terms of the solvatochromic parameters in the following general form:

$$SP = SP_0 + mV/100 + s\pi^* + b\beta + a\alpha \quad (1)$$

where SP is the solutes' property that depends on solute–solvent interactions, SP_0 is the regression constant, V is the molar volume of solutes, π^* is a measure of solutes' ability to engage in dipolarity/polarizability interactions with the solvent, β is the solutes' basicity and α is the solutes' acidity. Coefficients (m , s , b and a) are related to the chemical nature of the solvent systems.

The term $mV/100$ represents the unfavorable endoergic cavity formation process of separating the solvent molecules in order to provide a suitably sized cavity for solutes; $V/100$ instead of V is used to adjust the magnitude of the cavity term within a same range as the other independent variables in Eq. 1. The term $s\pi^*$ represents the dipolarity/polarizability term that measures the favorable exoergic effects of solute–solvent, dipole–dipole and dipole–induced dipole interactions. Exoergic hydrogen bonding terms, $b\beta$ and $a\alpha$, measure the effects of specific associations involving hydrogen bond acceptor (HBA) basic solutes and hydrogen bond donor (HBD) acidic solvents ($b\beta$ term) as well as the interactions between HBA basic solvents and HBD acidic solutes ($a\alpha$ term).

In order to express the net interactive properties of the aqueous and organic phases in different partitioning processes (e.g., micelle–water or *n*-octanol–water), the following relationships can be written [13,18]:

$$m = M(\delta_A^2 - \delta_B^2) \quad (2)$$

$$s = S(\pi_B^* - \pi_A^*) \quad (3)$$

$$b = C(\alpha_B - \alpha_A) \quad (4)$$

$$a = D(\beta_B - \beta_A) \quad (5)$$

where M , S , C and D are constants, δ is the Hildebrand solubility parameter (which is a measure of the cohesiveness of a phase). π^* , β and α in Eqs. 3–5 are the solvent's dipolarity/polarizability, basicity and acidity. The subscript B corresponds to *n*-octanol, micelle or stationary phase and the subscript A denotes the bulk aqueous phase or HPLC mobile phase. The significance of the chemical interactions in MLC and MEKC can be evaluated through a comparative study of the coefficients obtained from the different terms in the LSER models.

In this work, capacity factors in MLC and in MEKC as well as solute–micelle binding constants are quantitatively evaluated by LSER modeling and compared to the LSER models involving capacity factors in RPLC with hydro–

organic eluents and *n*-octanol–water partition coefficients.

2. Experimental

2.1. Chromatographic system

The MLC data were obtained from Ref. [19]. The MLC system has been described previously [11]. In MEKC, all the experiments were carried out on a laboratory-built CE system, which comprised a 0–30-kV high-voltage power supply (Series EH; Glassman High Voltage, Whitehouse Station, NJ, USA) and a 50 μm I.D. \times 375 μm o.d. fused-silica capillary tubing (Polymicro Technologies, Phoenix, AZ, USA). The total length of the capillary was 62 cm and detection was performed at 50 cm downstream. The samples were introduced into the anodic end of the capillary by gravity, 10 cm height for 8 s. Positive voltage of 20 kV was applied throughout the experiment. A variable-wavelength UV detector (Model 200; Linear Instruments, Reno, NV, USA) was used with the wavelength at 210 nm for sodium dodecyl sulfate (SDS) buffers and 254 nm for sodium cholate (SC) buffer. The

electropherograms were recorded using an integrator (Model SP 4200; Spectra-Physics, San Jose, CA, USA).

2.2. Reagents

The stock solutions of SDS (Sigma, St. Louis, MO, USA), and SC (Aldrich, Milwaukee, WI, USA) were prepared by dissolving the required amount of surfactant in doubly distilled deionized water and were filtered through a 0.45 μm nylon-66 membrane filter (Rainin, Woburn, MA, USA). All the test solutes were purchased from Aldrich. Test solutes in MLC and their solvatochromic parameters are listed in Table 1. The reported solvatochromic parameters values have been at room temperature [14], while the operating temperature for the MLC was 38°C. It has been found that temperature effect on these values is negligible [18]. In MEKC, buffer solutions were kept at pH 7.00 and 0.05 *M* phosphate (ionic strength) for both SDS and SC. Room temperature was maintained throughout the experiment. The void time (i.e., t_{e0}) of the system was measured from the time of injection of methanol to the first deviation from the baseline. Dodecaphenone was used to determine

Table 1
Test solutes in MLC and their solvatochromic parameters

Compound	$V/100$	π^*	β	α
(1) Benzylamine	0.665	0.35	0.59	0.06
(2) Benzyl alcohol	0.634	0.99	0.52	0.39
(3) Acetanilide	0.776	0.86	0.90	0.56
(4) Phenol	0.536	0.72	0.33	0.61
(5) Benzaldehyde	0.606	0.92	0.44	0
(6) Benzotrile	0.590	0.90	0.37	0
(7) Acetophenone	0.690	0.90	0.49	0.04
(8) Nitrobenzene	0.631	1.01	0.30	0
(9) Benzoic acid	0.650	0.74	0.40	0.59
(10) Anisol	0.639	0.73	0.32	0
(11) Benzene	0.491	0.59	0.10	0
(12) Propiophenone	0.788	0.88	0.49	0
(13) Butyropenone	0.886	0.86	0.49	0
(14) Chlorobenzene	0.581	0.71	0.07	0
(15) Naphthalene	0.753	0.70	0.15	0
(16) Anthracene	1.015	0.80	0.20	0

Solvatochromic data are from Ref. [14].

t_{mc} , the migration time of micelles in both SDS and SC buffer systems.

3. Results and discussion

3.1. Retention behavior in MLC

In this study, the effects of organic solvent type and concentration as well as stationary phase on the retention behavior in MLC are examined. Capacity factors in MLC and solute–micelle binding constants are evaluated using LSER.

The results of the LSER models between capacity factor (k' and $\log k'$) in MLC, solute–micelle binding constant (K_{mw}), as well as

capacity factor ($\log k'$) in RPLC with hydro–organic eluents and the solvatochromic parameters for a group of 16 aromatic compounds are shown in Table 2. The LSER modeling was originally developed for non-electrolytes and the solvatochromic polarity parameters have been measured for a wide range of solutes under non-ionizable conditions [12,16]. Apparently, the presence of a partially charged solute (e.g., benzoic acid) among the 16 test solutes in this study does not have a significant impact on the LSER models.

One common factor among all of the LSER models in Table 2 is that the cavity term is the most important factor. In all of the reported LSER studies [12–18], the SP term in Eq. 1 represents the logarithm of a solvent related

Table 2
LSER regression for retention behavior in MLC and solute–micelle binding

SP	SP ₀	<i>m</i>	<i>s</i>	<i>b</i>	<i>a</i>	$-b/m$	<i>n</i>	<i>r</i>	S.E.
<i>Solute–micelle binding constant</i>									
Log K_{mw} (C ₁₄ TAB + 3% 2-PrOH)	0.97	2.67 (0.14) ^a	−0.88 (0.10)	−1.44 (0.10)	0.32 (0.08)	0.54	16	0.9703	0.118
Log K_{mw} (SDS + 3% 2-PrOH)	0.34	2.81 (0.18)	−0.29 (0.14)	−1.36 (0.13)	−0.35 (0.11)	0.48	16	0.9585	0.160
<i>Retention in MLC</i>									
Log k' (0.08 M SDS + 3% 2-PrOH)	1.27	1.52 (0.14)	−0.92 (0.11)	−0.78 (0.10)	−0.92 (0.08)	0.51	16	0.9702	0.120
k' (0.08 M SDS + 3% 2-PrOH)	−5.52	121.90 (9.04)	−40.42 (6.93)	−59.94 (6.40)	−8.63 ^b (5.36)	0.49	16	0.9485	7.81
Log k' (0.08 M C ₁₄ TAB + 3% 2-PrOH)	1.02	1.01 (0.09)	−0.23 ^b (0.13)	−0.76 (0.06)	−0.02 ^b (0.01)	0.75	16	0.9434	0.078
k' (0.08 M C ₁₄ TAB + 3% 2-PrOH)	0.53	53.89 (2.67)	−8.22 (2.04)	−32.46 (1.89)	1.36 ^b (1.58)	0.60	16	0.9746	2.304
<i>Retention in RPLC with hydro–organic eluents</i>									
Log k' (40% MeOH)	−0.33	3.22 (0.08)	−0.32 (0.06)	−1.73 (0.06)	−0.23 (0.05)	0.54	16	0.9938	0.068
Log k' (40% 2-PrOH)	−0.16	1.84 (0.11)	−0.31 (0.09)	−1.43 (0.08)	−0.22 (0.07)	0.78	16	0.9764	0.097

n = Number of test solutes; *r* = correlation coefficient of linear regression; S.E. = standard error of the *y* estimate.

^a 95% confidence level of the coefficient.

^b Values are not statistically significant at the 95% confidence level.

property such as capacity factor ($\log k'$) in RPLC with hydro-organic eluents, *n*-octanol-water partition coefficient ($\log P_{ow}$), or aqueous solubility ($\log S_w$). This is because the logarithms of these solvent related properties represent the free energy of transfer of solutes from one phase (e.g., mobile phase or aqueous phase) to another phase (e.g., stationary phase or *n*-octanol phase). Surprisingly, in the C_{14} TAB MLC system k' vs. solvatochromic parameters gives a better correlation ($r = 0.9746$) than $\log k'$ vs. solvatochromic parameters ($r = 0.9434$) as shown in Fig. 1. A similar observation has been previously reported for the relationship between k' in MLC and $\log P_{ow}$ for the same group of compounds [11] as well as for the relation between k' and the carbon number of homologous series [9,20]. A clear curvature has been observed in the $\log k'$ vs. $\log P_{ow}$ and $\log k'$ vs. number of carbons in homologous series (N_c) plots. However, an opposite behavior is observed for the LSER model in SDS MLC system, i.e., $\log k'$ vs. solvatochromic parameters gives better correlation than k' vs. solvatochromic parameters. In the conventional RPLC with hydro-organic solvents and *n*-octanol-water partitioning process, solutes' size ($V/100$) and basicity (β) are the two predominant terms [14–16]. However, this was not the case for the retention ($\log k'$) in MLC with SDS micelles. It was also seen that the significance of the chemical interactions is quite different for the solute-micelle binding constant ($\log K_{mw}$) in these two micellar systems (SDS and C_{14} TAB), which is evident from the different regression coefficients (m , s , b and a). For example, the $a\alpha$ term is a positive value for the solutes binding to C_{14} TAB micelles while it is a negative value for the SDS system. This result suggests that the C_{14} TAB micellar phase provides more basic environment for the binding of acidic solutes than the SDS micellar phase. It was also found that C_{14} TAB micelles have less dipolar environment (more negative s value) for solutes than SDS micelles (less negative s value). This indicates that the type of surfactant has a significant impact on the chemical interactions in the partitioning processes in MLC, which in turn affects the retention behavior dramatically. Fur-

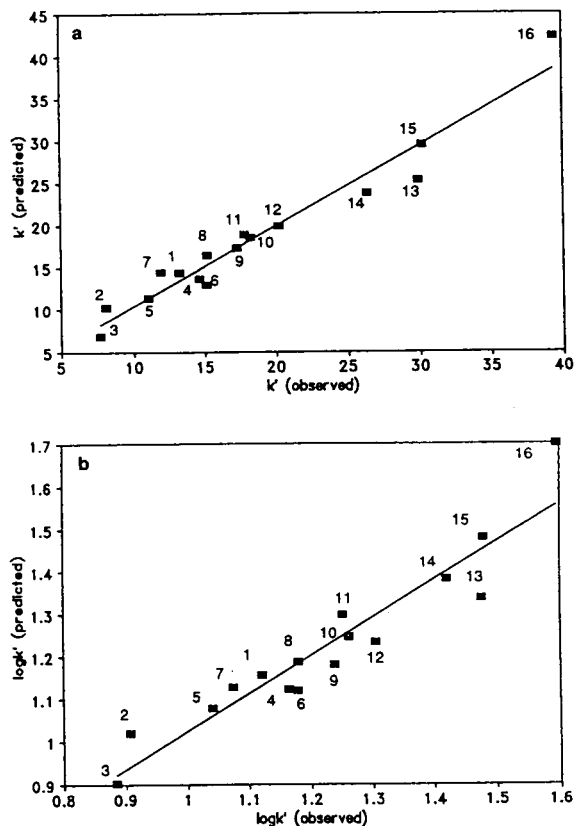


Fig. 1. (a) The plot of the capacity factors predicted by LSER vs. the capacity factors observed in MLC with 0.08 M C_{14} TAB and 3% 2-propanol. The LSER model is $k' = 0.53 + 53.89V/100 - 8.22\pi^* - 32.46\beta + 1.36\alpha$ ($n = 16$, $r = 0.9746$, S.E. = 2.304). (b) The plot of the logarithm of capacity factors predicted by LSER vs. the logarithm of capacity factors observed in MLC with 0.08 M C_{14} TAB and 3% 2-propanol. The LSER model is $\log k' = 1.02 + 1.01V/100 - 0.23\pi^* - 0.76\beta - 0.02\alpha$ ($n = 16$, $r = 0.9434$, S.E. = 0.078).

ther study is needed to explain the remarkable differences in these two micellar systems.

3.2. Effect of organic solvents on retention behavior in MLC

Organic solvents (mainly short-chain alcohols) have been widely used in MLC systems to enhance column efficiency [21], to influence eluents' strength, and to improve the overall separations [8,22–25]. The addition of organic solvents in micellar eluents may change the

micelle structure and the extent of adsorption of surfactant monomers on the stationary phase, thus influencing the retention behavior and selectivity in MLC [8,20,22–24]. The results of the LSER study in a C₁₄TAB MLC system with and without organic solvents are shown in Table 3. The magnitude of coefficient *m* reflects the difference in the solubility parameters between the stationary phase and the micellar mobile phase as shown in Eq. 2. Solubility parameter value of the mobile phase (δ_A) decreases with the increase of volume fraction of organic solvents because they are less cohesive (e.g., $\delta = 11.5$ for 2-propanol) than water ($\delta = 23.4$). However, solubility parameter value of the stationary phase (δ_B) increases with the increase of volume fraction of organic solvents. The combined effect of mobile phase and stationary phase is that *m* values decrease with an increase in volume fraction of organic solvents. The solvent property complementary to solutes' dipolarity/polarizability (π^*) is solvent's dipolarity/polarizability (π_1^*) as shown in Eq. 3. Alcohols are less dipolar (e.g., $\pi_1^* = 0.48$ for 2-propanol) than water ($\pi_1^* = 1.09$), therefore, the dipolarity of the

mobile phase (π_A^*) decreases with the increase of volume fraction of short-chain alcohols. The dipolarity of the stationary phase (π_B^*) increases with the increase of volume fraction of short-chain alcohols. The overall effect contributed from the mobile phase and the stationary phase makes the coefficient *s* become less negative with the increase of volume fraction of short-chain alcohols. Coefficient *b* denotes the difference in hydrogen bond donor ability (α_1) between the stationary phase and the mobile phase. As shown in Table 3, the *b* values increase (less negative) with the increase of volume fraction of short-chain alcohols. Alcohols are less acidic (e.g., $\alpha_1 = 0.76$ for 2-propanol) than water ($\alpha_1 = 1.17$), therefore, the acidity of the mobile phase (α_A) decreases with the increase of volume fraction of short-chain alcohols, while the acidity of the stationary phase (α_B) may increase with the increase of volume fraction of short-chain alcohols. However, the *a*-coefficient value that represents solvent's basicity (β_1) decreases with the increase of volume fraction of short-chain alcohols because alcohols are stronger base (e.g., $\beta_1 = 0.68$ for 2-propanol) than water ($\beta_1 = 0.18$)

Table 3
Effect of organic solvent on retention behavior in MLC

Condition ^a (<i>k'</i>)	SP ₀	<i>m</i>	<i>s</i>	<i>b</i>	<i>a</i>	$-b/m$	<i>n</i>	<i>r</i>	S.E.
0% 2-PrOH (or butanol)	-41.43	238.90 (8.04)	-22.33 (6.16)	-136.09 (5.69)	26.59 (4.77)	0.57	16	0.9858	6.945
1% 2-PrOH	-24.16	141.23 (5.22)	-14.21 (4.00)	-79.15 (3.69)	11.47 (3.10)	0.56	16	0.9833	4.409
3% 2-PrOH	-14.72	108.54 (4.32)	-13.06 (3.31)	-64.53 (3.06)	9.11 (2.56)	0.59	16	0.9817	3.731
5% 2-PrOH	-14.68	100.91 (3.98)	-12.01 (3.05)	-59.63 (2.82)	7.21 (2.36)	0.59	16	0.9822	3.437
7% 2-PrOH	-13.80	94.47 (3.70)	-10.76 (2.84)	-57.63 (2.62)	7.27 (2.20)	0.61	16	0.9828	3.202
2% butanol	-7.55	81.36 (4.20)	-11.13 (3.22)	-51.69 (2.97)	5.50 (2.49)	0.64	16	0.9723	3.629
3% butanol	-4.38	67.65 (3.95)	-9.90 (3.01)	-45.76 (2.78)	6.25 (2.33)	0.68	16	0.9666	3.394
5% butanol	-3.33	56.72 (3.51)	-9.22 (2.69)	-38.81 (2.48)	4.83 (2.08)	0.68	16	0.9633	3.032

See Table 2 for the definitions of *n*, *r* and S.E.

^a With 0.04 M C₁₄TAB.

(with two exceptions). The basicities of both the mobile phase (β_A) and the stationary phase (β_B) increase with the increase in volume fraction of short-chain alcohols. The same strategy can also be used to explain the different results at the same volume fraction of 2-propanol and butanol. For example, butanol is less cohesive and less acidic solvent than 2-propanol, the combined effect of the mobile phase and the stationary phase makes the m value in the butanol MLC system smaller than that in the 2-propanol MLC system and the b value less negative in the butanol MLC system than in the 2-propanol MLC system. A similar trend was observed for the retention behavior ($\log k'$) with the change of volume fraction of methanol in the conventional RPLC [15].

It was also found that the addition of a small amount of short-chain alcohols (up to 7% 2-propanol or 5% butanol) does not significantly change the ratio of $-b/m$ and the high correlations between k' and solvatochromic parameters. Carr et al. [18] have reported that the ratio of $-b/m$ is quite consistent from column to column as the amount of mobile phase modifier is varied and it is about +1.3 to +1.4 in acetonitrile–water mixtures, +1.3 for methanol–water and +1.75 for tetrahydrofuran (THF)–water. Kamlet et al. [15] obtained different $-b/m$ values (0.65–0.92) for a group of substituted aromatic compounds in the methanol–water RPLC system which are more similar to the $-b/m$ value observed in this work [0.54 for methanol–water (40:60)] as shown in Table 2. The high correlation for k' vs. solvatochromic parameters is a unique situation in the C_{14} TAB MLC system, however, the exact reason is not known yet.

3.3. Stationary phase effect in MLC

Not surprisingly, the stationary phase is an important factor in retention behavior and separation as well as for the determination of $\log P_{ow}$ by MLC [11,20,25]. Table 4 shows the regression results for the same group of 16 compounds on a C_8 column and a diphenyl column in MLC at the same mobile phase conditions (0.040 M C_{14} TAB, 3% 2-propanol, pH 7.0). The different LSER models (as represented by the coefficients in Table 4) indicate the large differences in chemical interactions in the two MLC systems with different stationary phases. For instance, on the diphenyl bonded stationary phase the dipolar/polarizability interactions between solutes and the surroundings (mobile and stationary phase) favor solutes' partition into the stationary phase because s has a positive value (+5.18), which is in contrast to all of the other LSER reports [12–18]. In addition, the larger m value for the C_8 phase indicates that it is less cohesive (smaller δ_B) than the diphenyl stationary phase (larger δ_B).

3.4. Migration behavior in MEKC

In MEKC, migration behaviors of uncharged solutes are primarily dependent upon their interactions with micelles and water. The type of surfactant in MEKC has a major effect on separation of uncharged solutes. The partitioning process of various solutes can be affected by the chemical property (e.g., hydrophobic moiety/chain length, ionic head group/charge) of a surfactant. In this study, two micelles were investigated; they are (1) SDS (an anionic hydro-

Table 4
Stationary phase effect on retention behavior in MLC (diphenyl vs. C_8)

SP	SP ₀	m	s	b	a	$-b/m$	n	r	S.E.
k' (C_8)	-14.72	108.54 (4.32)	-13.06 (3.31)	-64.53 (3.06)	9.11 (2.56)	0.59	16	0.9817	3.73
k' (diphenyl)	-23.34	82.55 (3.15)	5.18 (2.42)	-51.33 (2.23)	8.65 (1.87)	0.62	16	0.9832	2.72

See Table 2 for the definitions of n , r and S.E. Mobile phase conditions: 0.04 M C_{14} TAB, 3% 2-PrOH.

carbon surfactant) and (2) SC (an anionic bile salt surfactant). The test solutes and their solvatochromic parameters for the LSER study in MEKC are listed in Table 5. The set includes substituted aromatic compounds and polycyclic aromatic hydrocarbons (PAHs).

The results of the LSER models for MEKC using two different micellar pseudo-phases (SDS and SC) are listed in Table 6 and compared with that of *n*-octanol–water partitioning process. The correlation coefficients (*r*) of the regression were quite high for both SDS and SC systems, which suggests that migration behavior in MEKC can be characterized by LSER. Figs. 2 and 3 show high correlations between the experimentally observed $\log k'$ and the predicted $\log k'$ by LSER for both SDS and SC micellar systems. Concentration of surfactant has a significant effect on migration factors in MEKC, which is due to the change in the phase ratio, however,

coefficients (*m*, *s*, *b* and *a*) are only slightly varied with the change of SDS concentration from 0.020 to 0.040 *M* as shown in Table 6. It was also found that coefficients (*m*, *s*, *b* and *a*) in the LSER model for $\log K_{mw}$ with SDS micelles are very similar to those obtained in the LSER models using $\log k'$ at different concentrations of SDS (0.02 or 0.04 *M*) as shown in Table 6. This is because *k'* in MEKC is directly related to K_{mw} as [6,7,26]:

$$k' = K_{mw}([S] - \text{CMC}) \quad (6)$$

where [S] is the surfactant concentration and CMC is the critical micelle concentration of the surfactant.

The above-mentioned results suggest that $\log k'$ in MEKC can be used for the characterization of chemical interactions in the micelle–water partitioning process. Therefore, in this work \log

Table 5
Test solutes in MEKC and their solvatochromic parameters

Compound	<i>V</i> /100	π^*	β	α
(1) Benzene	0.491	0.59	0.10	0
(2) Toluene	0.592	0.55	0.11	0
(3) Ethylbenzene	0.668	0.53	0.12	0
(4) Acetophenone	0.690	0.90	0.49	0.04
(5) Propiophenone	0.788	0.88	0.49	0
(6) Benzylaldehyde	0.606	0.92	0.44	0
(7) Benzonitrile	0.590	0.90	0.37	0
(8) Nitrobenzene	0.631	1.01	0.30	0
(9) Anisol	0.639	0.73	0.32	0
(10) Methyl benzoate	0.736	0.75	0.39	0
(11) Fluorobenzene	0.520	0.62	0.07	0
(12) Chlorobenzene	0.581	0.71	0.07	0
(13) Bromobenzene	0.624	0.79	0.06	0
(14) Iodobenzene	0.671	0.81	0.05	0
(15) <i>p</i> -Dichlorobenzene	0.671	0.70	0.03	0
(16) <i>o</i> -Dichlorobenzene	0.671	0.80	0.03	0
(17) 4-Chlorotoluene	0.679	0.67	0.08	0
(18) 4-Chloroanisole	0.720	0.73	0.22	0
(19) Phenol	0.536	0.72	0.33	0.61
(20) 4-Chlorophenol	0.626	0.72	0.23	0.67
(21) 4-Chlorobenzyl alcohol	0.724	1.11	0.42	0.40
(22) 4-Chloroaniline	0.653	0.73	0.40	0.31
(23) Naphthalene	0.753	0.70	0.15	0
(24) 1-Naphthalene	0.851	0.66	0.16	0
(25) Biphenyl	0.920	1.18	0.20	0

Solvatochromic data are from Ref. [14].

Table 6
Effect of micelles on migration behavior in MEKC

SP	SP ₀	<i>m</i>	<i>s</i>	<i>b</i>	<i>a</i>	$-b/m$	<i>n</i>	<i>r</i>	S.E.
Log <i>k'</i> (0.02 M SDS)	-2.21	4.53 (0.09)	-0.19 (0.06)	-1.84 (0.06)	-0.05 ^a (0.04)	0.41	25	0.9869	0.087
Log <i>k'</i> (0.04 M SDS)	-1.88	4.42 (0.05)	-0.15 (0.05)	-1.88 (0.05)	-0.07 ^a (0.07)	0.43	25	0.9885	0.081
Log <i>k'</i> (0.06 M SC)	2.07	4.56 (0.09)	-0.24 (0.06)	-2.84 (0.06)	0.26 (0.04)	0.62	25	0.9903	0.084
Log <i>K_{mw}</i> ^b (0.02–0.04 M SDS)	-0.41	4.33 (0.08)	-0.11 (0.05)	-1.92 (0.05)	-0.09 (0.04)	0.44	25	0.9890	0.079
Log <i>P_{ow}</i>	0.11	5.49 (0.08)	-0.43 (0.05)	-3.88 (0.05)	0.02 ^a (0.04)	0.71 ^a	25	0.9952	0.080

See Table 2 for the definitions of *n*, *r* and S.E.

^a Values are not statistically significant at the 95% confidence level.

^b *K_{mw}* values are estimated according to Eq. 6 with the two SDS concentrations (0.02 and 0.04 M).

k' values in MEKC were used to build the LSER models for the comparison of chemical interactions in micelle–water and *n*-octanol–water partitioning processes.

It was also seen that migration behavior of solutes in MEKC with SDS and SC micelles are mainly influenced by their size (*V*/100) and hydrogen bond basicity (β) because the absolute values of *m* and *b* are relatively large. However, solutes' dipolarity/polarizability (π^*) and acidity (α) cause smaller changes in the capacity factor than the other two parameters (e.g., size and

basicity). This is a similar behavior to the *n*-octanol–water partitioning process [14] and to the retention behavior in RPLC with hydro-organic solvent [15]. It is, however, different from the retention behavior ($\log k'$) in the SDS MLC system as shown in Table 2. The coefficient *m* reflects the effect of solvents' cohesiveness on solutes' capacity factor or partition constant. It is a large positive value because water is a very cohesive solvent and is not easy to create a cavity for the solute as compared to *n*-octanol and micelles. Water has a high hydrogen bonding

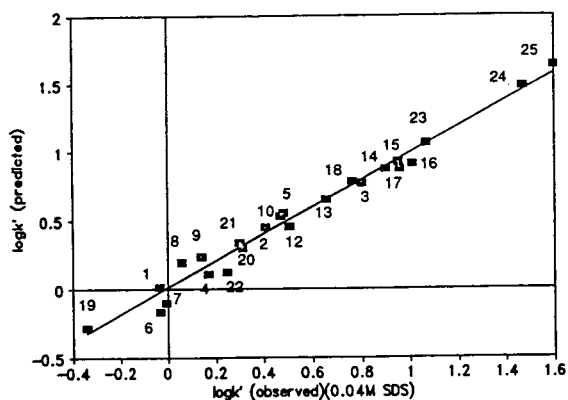


Fig. 2. The plot of the logarithm of capacity factors predicted by LSER vs. the logarithm of capacity factors observed in MEKC with 0.040 M SDS; 20 kV, pH 7.0, 0.050 M phosphate buffer.

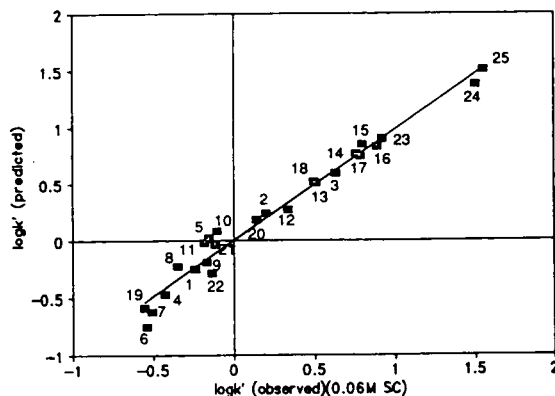


Fig. 3. The plot of the logarithm of capacity factors predicted by LSER vs. the logarithm of capacity factors observed in MEKC with 0.060 M SC; 20 kV, pH 7.0, 0.050 M phosphate buffer.

donor ability ($\alpha = 1.17$), therefore, one can anticipate that solutes' basicity would have a significant impact on the migration behavior in MEKC and in micelle–water partitioning process.

It was found that SC micelles are slightly less cohesive than SDS micelles, but more cohesive than *n*-octanol, which is reflected by the *m* values as shown in Table 6. It was also seen that SC micelles are less acidic than SDS micelles, but are more acidic than *n*-octanol by comparing the *b* values of the different LSER models. The *m* and *b* values as well as the ratio $-b/m$ using SC micelles in MEKC are more similar to those obtained in *n*-octanol–water system and are different from those observed using SDS micelles in MEKC. The reason behind this may be the similarity in environment between *n*-octanol and SC micelles. However, the dissimilarity between *n*-octanol and SC micelles results in the obviously different solute–solvent dipolar interactions and hydrogen bond interaction with solutes playing the role of HBD acids and solvents as HBA bases (the $s\pi^*$ and $a\alpha$ terms). It is also obvious that the difference in chemical selectivity for this group of test solutes with SDS and SC micelles is mainly due to different hydrogen bonding interactions. An extensive study of LSER of migration behavior in MEKC is underway and the results will be reported elsewhere [27].

Acknowledgements

We gratefully thank Dr. E.D. Breyer for the MLC data. A research grant from the US National Institutes of Health (GM 38738) is also acknowledged.

References

- [1] D.W. Armstrong and S.J. Henry, *J. Liq. Chromatogr.*, 3 (1980) 657.
- [2] L.J. Cline Love, J.G. Habarta and J.G. Dorsey, *Anal. Chem.*, 56 (1984) 1132A.
- [3] J.G. Dorsey, *Adv. Chromatogr.*, 27 (1987) 167.
- [4] M.G. Khaledi, *Trends Anal. Chem.*, 7 (1988) 293.
- [5] S. Terabe, K. Otsuka and T. Ando, *Anal. Chem.*, 57 (1985) 834.
- [6] S. Terabe, in N.A. Guzman (Editor), *Capillary Electrophoresis Technology*, Part I, Marcel Dekker, New York, 1993, p. 65.
- [7] M.G. Khaledi, in J.P. Landers (Editor), *Handbook of Capillary Electrophoresis*, CRC Press, Ann Arbor, MI, 1993, Ch. 3, p. 43.
- [8] M.G. Khaledi, J.K. Strasters, A.H. Rodgers and E.D. Breyer, *Anal. Chem.*, 62 (1990) 17.
- [9] M.G. Khaledi, E. Peuler and J. Ngeh-Ngwainhi, *Anal. Chem.*, 59 (1987) 2738.
- [10] M.G. Khaledi, *Anal. Chem.*, 60 (1988) 876.
- [11] M.G. Khaledi and E.D. Breyer, *Anal. Chem.*, 61 (1989) 1040.
- [12] R.W. Taft, J.M. Abboud, M.J. Kamlet and M.H. Abraham, *J. Solution Chem.*, 14 (1985) 153.
- [13] R.W. Taft, M.H. Abraham, G.R. Famini, R.M. Doherty, J.M. Abboud and M.J. Kamlet, *J. Pharm. Sci.*, 74 (1985) 807.
- [14] M.J. Kamlet, R.M. Doherty, M.H. Abraham, Y. Marcus and R.W. Taft, *J. Phys. Chem.*, 92 (1988) 5244.
- [15] M.J. Kamlet, M.H. Abraham, P.W. Carr, R.M. Doherty and R.W. Taft, *J. Chem. Soc., Perkin Trans. II*, (1988) 2087.
- [16] P.W. Carr, *Microchem. J.*, 48 (1993) 4.
- [17] R.S. Helburn, S.C. Rutan, J. Pompano, D. Mitchem and W.T. Patterson, *Anal. Chem.*, 66 (1994) 610.
- [18] P.W. Carr, R.M. Doherty, M.J. Kamlet, R.W. Taft, W. Melander and Cs. Horváth, *Anal. Chem.*, 58 (1986) 2674.
- [19] E.D. Breyer, *Ph.D. Dissertation*, University of New Orleans, New Orleans, LA, 1990.
- [20] S. Yang, L. Kruk and M.G. Khaledi, *J. Chromatogr. A*, 664 (1994) 1.
- [21] J.G. Dorsey, M. DeEchegaray and J.S. Landy, *Anal. Chem.*, 55 (1983) 924.
- [22] J.K. Strasters, E.D. Breyer, A.H. Rodgers and M.G. Khaledi, *J. Chromatogr.*, 511 (1990) 17.
- [23] A.S. Kord and M.G. Khaledi, *Anal. Chem.*, 64 (1992) 1894.
- [24] A.S. Kord and M.G. Khaledi, *J. Chromatogr.*, 631 (1993) 125.
- [25] S. Yang and M.G. Khaledi, *Anal. Chim. Acta.*, 294 (1994) 135.
- [26] S. Smith and M.G. Khaledi, *J. Chromatogr.*, 632 (1993) 177.
- [27] S. Yang and M.G. Khaledi, *Anal. Chem.*, (1995) in press.

Micellar liquid chromatographic separation of sulfonamides in physiological samples using direct on-column injection

Shenyuan Yang, Morteza G. Khaledi*

Department of Chemistry, North Carolina State University, P.O. Box 8204, Raleigh, NC 27695-8204, USA

Abstract

A mixture of twelve sulfonamides was separated by micellar liquid chromatography (MLC) using sodium dodecyl sulfate (SDS) micelles and a hydrophilic endcapped C_{18} column. Retention behavior and selectivity pattern of sulfonamides in MLC were examined with the change of SDS concentration and volume fraction of an organic modifier (1-propanol). The suitable condition was found to be 0.070 M SDS and 6.0% 1-propanol for the separation of these twelve sulfonamides. Under this condition, the isocratic separation of the sulfonamides was achieved within 15 min with a relatively high column efficiency for MLC (ca. 7000 plates/25 cm column). Retention times of these twelve sulfonamides were found to be very repeatable, which is due to the highly reproducible retention behavior in MLC. The same twelve sulfonamides were successfully separated in the spiked physiological fluids (human urine and cow milk) through direct on-column injection by MLC.

1. Introduction

Micellar liquid chromatography (MLC) has been regarded as a powerful alternative to both conventional reversed-phase LC (RPLC) with hydro-organic eluents and ion-pair chromatography (IPC) for the analysis of biosamples [1–3]. Due to the existence of micelles, MLC has several unique advantages such as capability of simultaneous separation of ionic and non-ionic compounds, possibility of simultaneous enhancement of solvent strength and separation selectivity, reproducible and predictable retention behavior, possibility of direct on-column injection of physiological samples, enhanced luminescence detectability, safety and cost [4–7]. The possibility of direct on-column injection of physiological samples is one of the important merits of

MLC for bioanalysis as compared to conventional RPLC and IPC. This is due to the fact that the protein matrix of a biological sample can be solubilized by micelles [e.g., sodium dodecyl sulfate (SDS) micelles] and eluted with the solvent front. This obviates the need for the time consuming and tedious sample preparation step, thus making direct, on-column injections of physiological fluids possible. This method has been used for the analysis of therapeutic drugs [8], nucleosides and bases [9], illegal drugs [10], cephalosporins [11], anticancer 6-thiopurine compounds [12] and steroids [13] in biological fluids.

Sulfonamides are a group of antibacterial compounds commonly used for the prevention and the treatment of diseases in livestock products. The sulfonamides residues in treated animals may pose a health threat to consumers through allergic or toxic reactions, or through

* Corresponding author.

induction of antibiotic resistance in pathogenic organisms [14,15]. Separation of these drugs by RPLC, GC, and capillary electrophoresis (CE) has already been reported [14–19]. Protein precipitation and extraction processes are often used to remove the protein matrix from physiological fluid samples in RPLC [14,16]. These processes are tedious, time consuming and may result in the loss of the analytes.

In this work, the retention behavior of sulfonamides in MLC is examined. A mixture of twelve sulfonamides in physiological fluids was separated under isocratic conditions in MLC and by direct on-column injection.

2. Experimental

2.1. Chromatographic system

An HPLC pump (Model 400; Applied Biosystems, Foster City, CA, USA) and a variable-wavelength absorbance detector (Model 783A, Applied Biosystems) set at 254 nm and a VIGI injector (Valco, Houston, TX, USA) were utilized in this work. The HPLC system was controlled by the Chemresearch chromatographic

data management system controller software (ISCO, Lincoln, NE, USA) running on a PC-88 Turbo personal computer (IDS, Paramount, CA, USA). A 5- μ m particle size, 250 \times 4.6 mm YMC-Pack ODS-AQ column (YMC, Wilmington, NC, USA) was used as the analytical column. The column was thermostated at 40°C by a water circulator bath (Lauda Model MT-6; Brinkmann Instruments, Westbury, NY, USA). A silica precolumn was used to saturate the mobile phase with silicates and protect the analytical column.

2.2. Reagents

All the sulfonamides were obtained from Sigma (St. Louis, MO, USA) and are identified in Table 1. The structures of these sulfonamides are shown in Fig. 1. The sample solutions were prepared by diluting the stock solutions (5 mg/ml in methanol) with the mobile phase. The stock solution of SDS (Sigma) was prepared by dissolving the required amount of surfactant in doubly distilled, deionized water and was filtered through a 0.45- μ m nylon-66 membrane filter (Rainin Instruments, Woburn, MA, USA). The ionic strength of the mobile phase was adjusted

Table 1
Retention and efficiency of sulfonamides in MLC

Compound	t_R (min)	k'	N (plates/25 cm column) ^a	h^b
(1) Sulfacetamide	3.43	0.87	7988	6.26
(2) Sulfadiazine	3.77	1.06	9027	5.54
(3) Sulfamerazine	4.56	1.49	7297	6.85
(4) Sulfathiazole	5.17	1.82	8450	5.92
(5) Sulfamethazine	5.56	2.03	8223	6.08
(6) Sulfamethoxy pyridazine	6.46	2.52	7814	6.40
(7) Sulfachloropyridazine	6.81	2.71	8696	5.75
(8) Sulfamonomethoxine	7.24	2.94	6894	7.25
(9) Sulfabenzamide	8.56	3.67	6886	7.26
(10) Sulfadimethoxine	10.78	4.88	6153	8.13
(11) Sulfaquinoxaline	13.09	6.14	6335	7.89
(12) Sulfisomidine	15.00	7.18	6710	7.45
Average			7012	7.13

Mobile phase: 0.070 M SDS, 6.0% 1-propanol, 0.020 M NaH₂PO₄, pH 3.0, YMC-Pack ODS-AQ column.

^a Calculated by using Foley-Dorsey equation [23].

^b Reduced plate height.

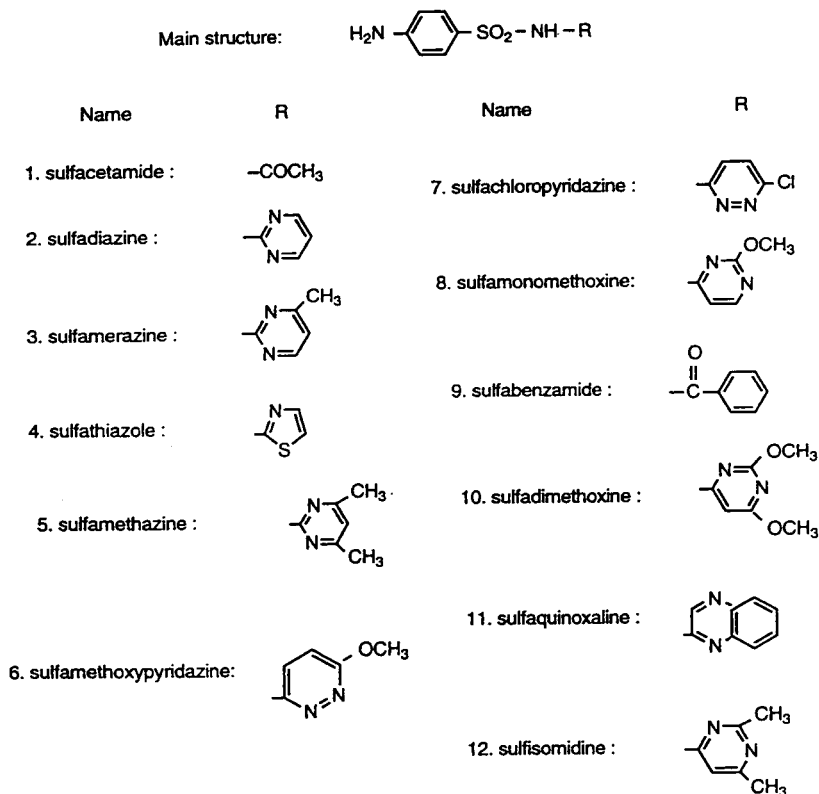


Fig. 1. The structures of sulfonamides.

by adding phosphate buffer so that the total buffer concentration of the final solution was 0.020 M. After adding the required amount of 1-propanol the pH was adjusted to 3.0. The urine matrix was from a healthy volunteer and filtered through a 10-mm glass microfiber filter (Rainin Instruments) and a 0.45- μ m nylon-66 filter (Rainin Instruments) prior to on-column injection. The milk matrix was obtained from a local grocery store and was also filtered through a 10-mm glass microfiber filter (Rainin Instruments) before use. Due to the high viscosity of the milk sample, its filtration through a 0.45- μ m filter paper under vacuum was not successful.

3. Results and discussion

MLC separations can be influenced by the types/concentrations of both surfactant and or-

ganic modifier, pH, ionic strength and temperature [3,4,6]. In this work, the effects of SDS concentration and volume fraction of 1-propanol on the retention behavior and separation of sulfonamides were investigated.

3.1. Effect of mobile phase composition on the separation of sulfonamides

The dependence of retention factor on volume fraction of organic modifier and micelle concentration in the MLC system can be described by Eqs. 1 and 2 [5,20].

$$\ln k' = -S\varphi_{\text{org}} + \ln k'_0 \quad (1)$$

$$1/k' = (K_{\text{mw}}[M] + 1)/(P_{\text{sw}}\phi) \quad (2)$$

where k' is the retention factor of a solute, φ_{org} is the volume fraction of organic modifier (1-propanol), k'_0 is the retention factor in a purely

aqueous micellar mobile phase, S is the solvent strength parameter, $[M]$ is the micelle (SDS) concentration, ϕ is the phase ratio, K_{mw} is the binding constant of solute to micelles and P_{sw} is the partition coefficient of a compound from mobile phase into stationary phase. Fig. 2 shows the retention behavior of sulfonamides as a function of volume fraction of 1-propanol and concentration of SDS.

The dependence of selectivity ($\alpha = k'_2/k'_1$) in MLC systems on the volume fraction of organic solvent and micelle concentration can be described by Eqs. 3 and 4 [5,20].

$$\ln \alpha = -(S_2 - S_1)\phi_{org} + (\ln k'_{0,2} - \ln k'_{0,1}) \quad (3)$$

$$\alpha = \frac{(\alpha_{sw})([M] + 1/K_{mw,1})}{(\alpha_{mw})([M] + 1/K_{mw,2})} \quad (4)$$

where α_{sw} is the stationary phase partitioning selectivity ($P_{sw,2}/P_{sw,1}$) and α_{mw} is the selectivity of binding to (or partitioning into) micelles ($K_{mw,2}/K_{mw,1}$). This is shown in Fig. 3 for sulfonamides with the changes of volume fraction of 1-propanol and concentration of SDS.

Micelle concentration is equal to the difference of the concentration of surfactant and its

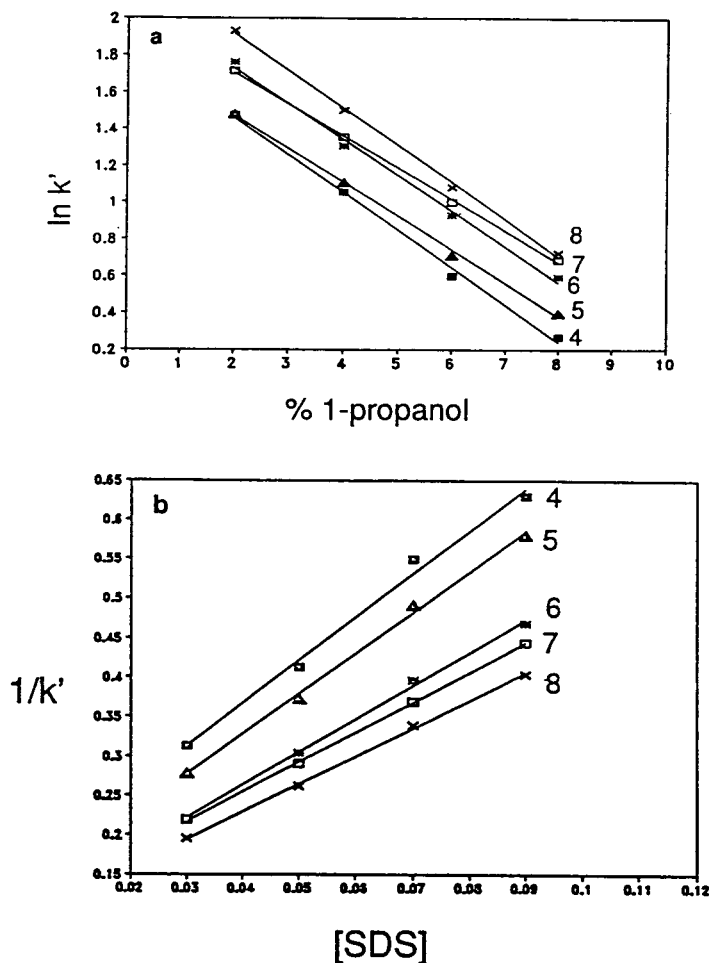


Fig. 2. The effect of (a) the volume fraction of 1-propanol (0.070 M SDS) and (b) the SDS micelle concentration (6.0% 1-propanol) on the retention behavior of sulfonamides.

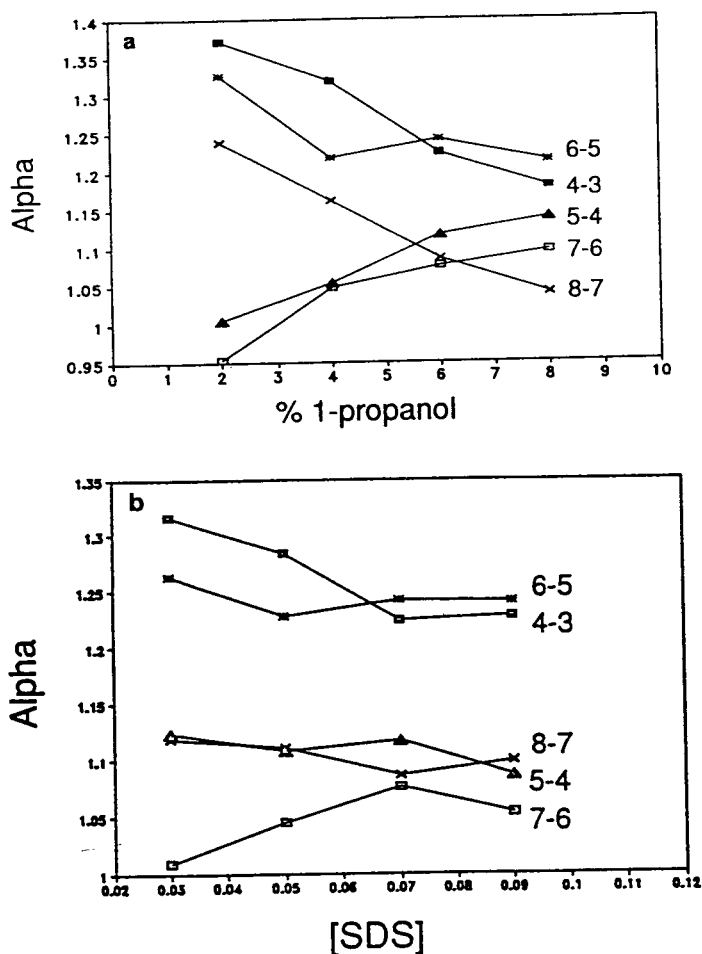


Fig. 3. The effect of (a) the volume fraction of 1-propanol (0.070 M SDS) and (b) the SDS micelle concentration (6.0% 1-propanol) on the selectivity of sulfonamides.

critical micelle concentration (CMC) (i.e., $[M] = C_{sf} - \text{CMC}$). The CMC value of a surfactant depends on many solution conditions. For example, the CMC value for SDS was found to be ca. 8 mM in aqueous solution at 25°C [4]. However, the CMC values for SDS were not available at our experimental conditions (i.e., 40°C, 2–8% 1-propanol, 0.020 M phosphate buffer and pH 3.0). Eq. 2 describes the relationship between retention factor and micelle concentration. At a constant volume fraction of organic modifier (e.g., 6% 1-propanol), $1/k'$ is linearly dependent on the concentration of SDS as shown in Fig. 2b assuming that CMC is a constant ($R^2 > 0.99$ for

all of the sulfonamides). Therefore, we assume that the concentration of SDS, instead of SDS micelles concentration, can be used to find a suitable mobile phase condition without changing the results significantly.

Based on the experimental results in Figs. 2 and 3, the suitable mobile phase condition was found to be 0.070 M SDS, 6.0% 1-propanol for the separation of compounds 4–8. The mobile phase conditions did not have as much effect on the separation of the early-eluting peaks (1–3) and late-eluting peaks (9–12). In other words, compounds 4–8 were the “critical” pairs, and their separation was crucial. Therefore, the suit-

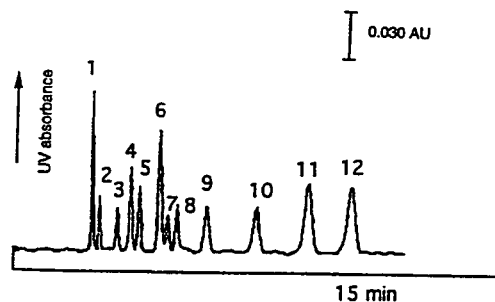


Fig. 4. The isocratic separation of 12 sulfonamides. The suitable mobile phase conditions: 0.070 M SDS, 6.0% 1-propanol, 0.020 M NaH_2PO_4 , pH 3.0.

able mobile phase condition for the separation of compounds 4–8 was also suitable for the whole mixture containing twelve sulfonamides. Fig. 4 shows the good separation of these 12 sulfonamides in 15 min under this mobile phase conditions. High column efficiencies ($N \approx 7000$ plates/25 cm column) were achieved using the hydrophilic endcapped YMC ODS-AQ column for the sulfonamides as shown in Table 1. The achieved column efficiency using the ODS-AQ column is much higher than that typically obtained in MLC using the conventional C_{18} columns [20,21] and is slightly higher than that using a Flurooctyl (FO) column [21]. This results further confirm the belief that the stationary

phase effect is significant in MLC and deserves more attention [21,22]. Column efficiencies were calculated by using Foley and Dorsey's equation [23].

$$N = \frac{41.7 \cdot \left(\frac{t_R}{W_{0.1}}\right)^2}{\frac{B}{A} + 1.25} \quad (5)$$

where N is the column efficiency, t_R is the retention time of a solute, $W_{0.1}$ is the width at the 10% peak height, and B/A is the asymmetric factor of the peak.

Retention behavior of sulfonamides was repeatable with high precision using micellar eluent as shown in Table 2, which is due to the highly reproducible retention behavior in MLC separations [5,7,20,21].

3.2. Direct on-column separation of sulfonamides in physiological fluids

Physiological fluid samples initially used in this work were human urine and cow milk. There were no pretreatments for these samples except filtration and dilution. The chromatograms of urine and milk blanks are shown in Figs. 5 and 6, respectively. As shown in Fig. 5, there are some unidentified components in the urine matrix, but

Table 2
Repeatability of sulfonamides' retention in MLC

Compound	t_R (min)	Average	S.D.
1	3.40, 3.43, 3.43, 3.43, 3.43, 3.43, 3.43, 3.43, 3.43	3.43	0.01061
2	3.76, 3.77, 3.77, 3.77, 3.77, 3.77	3.77	0.00408
3	4.56, 4.56, 4.57, 4.56, 4.57, 4.56	4.56	0.00516
4	5.16, 5.17, 5.17, 5.17, 5.17, 5.17	5.17	0.00408
5	5.56, 5.56, 5.55, 5.56, 5.55	5.56	0.00548
6	6.46, 6.46, 6.46, 6.46	6.46	0
7	6.82, 6.82, 6.81, 6.82, 6.82, 6.82, 6.81	6.82	0.00488
8	7.24, 7.23, 7.24, 7.24, 7.23, 7.23	7.24	0.00548
9	8.58, 8.57, 8.57, 8.57, 8.57, 8.56	8.57	0.00632
10	10.81, 10.81, 10.76, 10.76, 10.76	10.78	0.02739
11	13.13, 13.06, 13.09	13.09	0.03512
12	15.00, 15.00, 15.01, 15.01, 15.00	15.00	0.00548

Retention times of sulfonamides were randomly collected in one day.

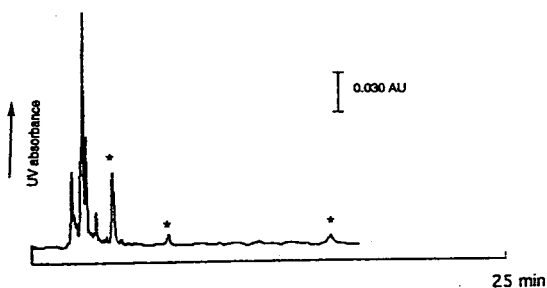


Fig. 5. Urine blank. Mobile phase conditions as in Fig. 4. Full scale of detection is 0.250. * = Unidentified components in urine matrix.

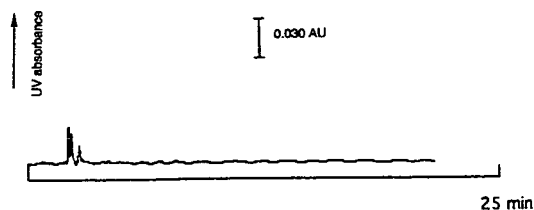


Fig. 6. Milk blank (1% milk–water–mobile phase, 1:1:1) under the mobile phase conditions given in Fig. 4. Full scale of detection is 0.250.

they did not interfere with the separation of these twelve sulfonamides. The separation of sulfonamides in spiked urine and milk are demonstrated in Figs. 7 and 8, respectively. Good separations of these twelve sulfonamides were

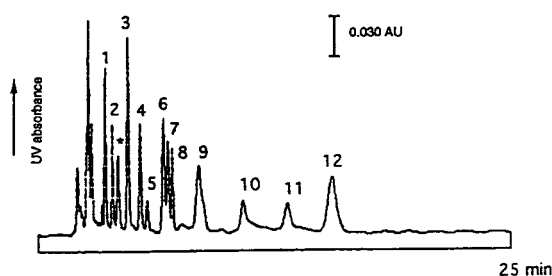


Fig. 7. Separation of sulfonamides in urine sample under the mobile phase conditions given in Fig. 4. Urine sample was spiked by 2.5 μg of compounds 8 and 10, 1 μg of compound 12 and about 0.5 μg of any other sulfonamides in 1 ml urine matrix. Full scale of detection is 0.250. * = Unidentified component in urine matrix.

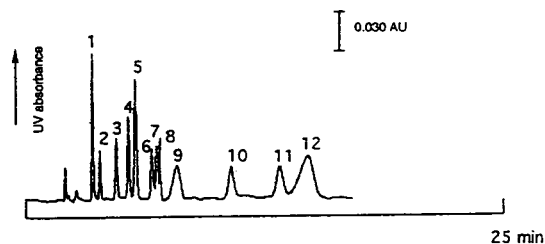


Fig. 8. Separation of sulfonamides in milk sample. Mobile phase conditions as in Fig. 4. Milk sample was prepared by spiking 2.5 μg of compounds 8 and 10, 1 μg of compound 12 and about 0.5 μg of any other sulfonamides in 1 ml milk blank. Full scale of detection is 0.250.

achieved in these two physiological fluid samples, which suggests that MLC is a suitable technique for the rapid analysis of sulfonamides in physiological fluids. The retention time of sulfisomidine (compound 12) in the milk sample (Fig. 8) was relatively lower than those in the urine sample (Fig. 7) or without sample matrix (Fig. 4). This might be due to sample matrix effects. As mentioned in the experimental section, filtration of the milk sample through a 0.45- μm filter paper under vacuum was not successful due to its high viscosity. The infiltrated milk matrix may have caused some damages to the packing materials of the column that lead to deterioration of peak shapes and reduction of retention times. Further studies will concentrate on the separation of different pharmaceutical drugs in various physiological fluid samples.

Acknowledgements

We thank YMC Inc. for the donation of a YMC-Pack ODS-AQ column and a research grant from the US National Institutes of Health (GM 38738).

References

- [1] D.W. Armstrong and S.J. Henry, *J. Liq. Chromatogr.*, 3 (1980) 657.

- [2] L.J. Cline Love, J.G. Habarta and J.G. Dorsey, *Anal. Chem.*, 56 (1984) 1132A.
- [3] M.G. Khaledi, *Trends Anal. Chem.*, 7 (1988) 293.
- [4] J.G. Dorsey, *Adv. Chromatogr.*, 27 (1987) 167.
- [5] M.G. Khaledi, J.K. Strasters, A.H. Rodgers and E.D. Breyer, *Anal. Chem.*, 62 (1990) 130.
- [6] W.L. Hinze, in W.L. Hinze and D.W. Armstrong (Editors), *Ordered Media in Chemical Separation (ACS Symposium Series, No. 324)*, American Chemical Society, Washington, DC, 1987, Ch. 1, p. 2.
- [7] J.K. Strasters, E.D. Breyer, A.H. Rodgers and M.G. Khaledi, *J. Chromatogr.*, 511 (1990) 17.
- [8] F.J. Deluccia, M. Arunyanart, L.J. Cline Love, *Anal. Chem.*, 57 (1985) 1564.
- [9] Y.-N. Kim and P.R. Brown, *J. Chromatogr.*, 384 (1987) 209.
- [10] A. Berthod, J.M. Asensio and J.J. Laserna, *J. Liq. Chromatogr.*, 12 (1989) 2621.
- [11] J. Haginaka, J. Wakai, H. Yasuda and T. Nakagawa, *Anal. Chem.*, 59 (1987) 2732.
- [12] P.M. Fraga, E.B. Gonzalez and A. Sanz-Medel, *Anal. Chim. Acta*, 212 (1988) 181.
- [13] M. Amin, K. Harrington and R. von Wandruszka, *Anal. Chem.*, 65 (1993) 2346.
- [14] V.K. Agarwal, *J. Chromatogr.*, 624 (1992) 411.
- [15] D. Guggisberg, A.E. Mooser and H. Koch, *J. Chromatogr.*, 624 (1992) 425.
- [16] J. Abian, M.I. Churchwell and W.A. Korfmacher, *J. Chromatogr.*, 629 (1993) 267.
- [17] Q.-X. Dang, Z.-P. Sun and D.-K. Ling, *J. Chromatogr.*, 603 (1992) 259.
- [18] C.L. Ng, H.K. Lee and S.F. Li, *J. Chromatogr.*, 632 (1993) 165.
- [19] S.C. Su, A.V. Hartkopf and B.L. Karger, *J. Chromatogr.*, 119 (1976) 523.
- [20] A.S. Kord and M.G. Khaledi, *Anal. Chem.*, 64 (1992) 1901.
- [21] S. Yang, L. Kruk and M.G. Khaledi, *J. Chromatogr. A*, 664 (1994) 1.
- [22] S. Yang and M.G. Khaledi, *Anal. Chim. Acta*, 294 (1994) 135.
- [23] J.P. Foley and J.G. Dorsey, *Anal. Chem.*, 55 (1983) 730.

Experimental evidence for the existence of duoselective (Type III) enantiomer separations in the capillary electrophoretic analysis of chiral weak acids

Mary E. Biggin¹, Robert L. Williams, Gyula Vigh*

Chemistry Department, Texas A&M University, College Station, TX 77843-3255, USA

Abstract

Experimental evidence has been found for the existence of the theoretically predicted *duoselective* (Type III) enantiomer separations in the capillary electrophoretic (CE) analysis of chiral weak acids. The mobilities of the enantiomers of 3,5-dinitrobenzamido phenylalanine were determined in the pH 3–6 range using constant ionic strength ϵ -amino-*n*-caproic acid background electrolytes and β -cyclodextrin as resolving agent. The complex formation constants and ionic mobilities of the free and complexed enantiomers were determined using the multiple equilibria-based electrophoretic mobility model. The extended peak resolution equation of CE was then used to calculate the peak resolution surfaces as a function of the pH and the β -cyclodextrin concentration of the background electrolyte, the dimensionless electroosmotic flow coefficient, and the effective portion of the applied potential. Though the observed peak resolution values were lower than predicted by the theory due to the presence of electromigration dispersion, the predicted and observed loci of the extrema of the resolution surface agreed well. The desionoselective/ionoselective/duoselective (DID) separation selectivity model and the peak resolution model permit the rational optimization of the CE separation of weak acid enantiomers.

1. Introduction

Capillary electrophoretic (CE) enantiomer separations have developed rapidly over the past few years, as demonstrated by a number of excellent, recent reviews [1,2]. Following an equilibrium model which rationalized such separations at constant pH as a function of the resolving agent concentration [3–5], an extended model was introduced to describe the effective mobilities (electroosmotic flow-corrected actual

mobilities) of the enantiomers of weak electrolyte solutes as a function of both the pH and the chiral resolving agent concentration of the background electrolyte [6,7]. Specifically, the effective mobility of the *R*-enantiomer of a weak acid, μ_R^{eff} , was expressed as:

$$\mu_R^{\text{eff}} = \frac{\mu_-^0 + \mu_{\text{RCD}}^0 - K_{\text{RCD}}[\text{CD}]}{1 + K_{\text{RCD}}[\text{CD}] + \frac{[\text{H}_3\text{O}^+]}{K_a} (1 + K_{\text{HRCD}}[\text{CD}])} \quad (1)$$

where μ_-^0 is the ionic mobility of the fully

* Corresponding author.

¹ Present address: Clarke College, Dubuque, IA 52002, USA.

dissociated free enantiomer, $\mu_{\text{RCD}^-}^0$ is the ionic mobility of the fully dissociated complexed enantiomer, K_a is the acid dissociation constant of the enantiomer, K_{RCD^-} and K_{HRCD} are the formation constants for the complexes of the dissociated and non-dissociated forms of the enantiomer and the chiral resolving agent, cyclodextrin (CD), and $[\text{H}_3\text{O}^+]$ and $[\text{CD}]$ are the hydronium and cyclodextrin concentrations, respectively. A similar expression was derived for the *S*-enantiomer. With these, separation selectivity, α , which was defined as the ratio of the effective mobilities of the two enantiomers:

$$\alpha = \frac{\mu_{\text{R}}^{\text{eff}}}{\mu_{\text{S}}^{\text{eff}}} \quad (2)$$

became:

$$\alpha = \frac{\mu_{-}^0 + \mu_{\text{RCD}^-}^0 - K_{\text{RCD}^-}[\text{CD}]}{\mu_{-}^0 + \mu_{\text{SCD}^-}^0 - K_{\text{SCD}^-}[\text{CD}]} \times \frac{1 + K_{\text{SCD}^-}[\text{CD}] + \frac{[\text{H}_3\text{O}^+]}{K_a} (1 + K_{\text{HSCD}}[\text{CD}])}{1 + K_{\text{RCD}^-}[\text{CD}] + \frac{[\text{H}_3\text{O}^+]}{K_a} (1 + K_{\text{HRCD}}[\text{CD}])} \quad (3)$$

Depending on the magnitude of the μ^0 and K values, three kinds of enantiomer separations were predicted [6,7]. In a *desionoselective* separation (previously called *Type I* separation [6,7]), $K_{\text{RCD}^-} = K_{\text{SCD}^-}$, $\mu_{\text{RCD}^-}^0 = \mu_{\text{SCD}^-}^0$ and $K_{\text{HRCD}} \neq K_{\text{HSCD}}$, i.e. only the non-dissociated forms of the solutes complex selectively. This reduces the first term in Eq. 3 to unity and simplifies Eq. 3; in a *desionoselective* separation selectivity increases monotonously toward a limiting high value at low pH (below the $\text{p}K_a$) and high CD concentration.

In an *ionoselective* separation (previously called *Type II* separation [6,7]), $\mu_{\text{RCD}^-}^0 \neq \mu_{\text{SCD}^-}^0$, $K_{\text{RCD}^-} \neq K_{\text{SCD}^-}$ and $K_{\text{HRCD}} = K_{\text{HSCD}}$, i.e. only the dissociated forms of the enantiomers complex selectively. The first and second terms in Eqn. 3 oppose each other, and $\alpha < 1$, $\alpha = 1$, and $\alpha > 1$ are all possible depending on the values of the parameters (μ^0 and K values) and the composition of the background electrolyte ($[\text{H}_3\text{O}^+]$ and $[\text{CD}]$ values), allowing for — if so

desired — the reversal of the migration order of the enantiomers.

In a *duoselective* separation (previously called *Type III* separation [6,7]), $\mu_{\text{RCD}^-}^0 \neq \mu_{\text{SCD}^-}^0$, $K_{\text{RCD}^-} \neq K_{\text{SCD}^-}$ and $K_{\text{HRCD}} \neq K_{\text{HSCD}}$, i.e. both the dissociated and the non-dissociated forms of the enantiomers complex differently and $\alpha < 1$, $\alpha = 1$, and $\alpha > 1$ are again possible depending on the values of the parameters (μ^0 and K values) and the background electrolyte composition variables ($[\text{H}_3\text{O}^+]$ and $[\text{CD}]$). Thus, in a *duoselective* separation the migration order of the enantiomers can be once again reversed if so desired.

In subsequent papers [8–10] an equation was derived for peak resolution as a function of separation selectivity, the effective charge of the enantiomers and the dimensionless electroosmotic flow:

$$R_s = \sqrt{\frac{E l e_0}{8 k T}} \times \frac{\text{abs}(\alpha - 1) \sqrt{\text{abs}(\alpha + \beta)} \sqrt{\text{abs}(1 + \beta)} \sqrt{z_{\text{R}}^{\text{eff}}} \sqrt{z_{\text{S}}^{\text{eff}}}}{\sqrt{\text{abs}[(\alpha + \beta)^3] z_{\text{R}}^{\text{eff}}} + \sqrt{\alpha \text{abs}[(1 + \beta)^3] z_{\text{S}}^{\text{eff}}}} \quad (4)$$

where E is the field strength, l the length of the capillary from injector to detector, e_0 the electric charge, k the Boltzman constant, and T the absolute temperature, $z_{\text{R}}^{\text{eff}}$, $z_{\text{S}}^{\text{eff}}$ the effective charge of the enantiomers, and β the dimensionless electroosmotic flow coefficient defined as:

$$\beta = \frac{\mu_{\text{eo}}}{\mu_{\text{S}}^{\text{eff}}} \quad (5)$$

with

$$\mu_{\text{S}}^{\text{obs}} = \mu_{\text{S}}^{\text{eff}} + \mu_{\text{eo}} \quad (6)$$

where $\mu_{\text{S}}^{\text{obs}}$ is the observed mobility of the *S*-enantiomer, and μ_{eo} is the coefficient of the electroosmotic flow. This equation encompasses, as a limiting case, the R_s expression derived by Kennedler et al. in the absence of electroosmotic flow [11].

The effective charge of the *R*-enantiomer, $z_{\text{R}}^{\text{eff}}$, was expressed [8] as:

$$z_{\text{R}}^{\text{eff}} = \frac{z_{-}^0 + z_{\text{RCD-}}^0 - K_{\text{RCD-}}[\text{CD}]}{1 + K_{\text{RCD-}}[\text{CD}] + \frac{[\text{H}_3\text{O}^+]}{K_{\text{a}}}(1 + K_{\text{HRCD}}[\text{CD}])} \quad (7)$$

with z_{-}^0 and $z_{\text{RCD-}}^0$ as the ionic charges of the fully dissociated enantiomer, non-complexed and complexed, respectively.

Since different selectivity surfaces belong to the different separation types, and since R_s depends on α and z^{eff} , there will be a unique peak resolution surface for each separation type [9,10]. *Desionoselective* separations will have a single lobe, while *ionoselective* separations and *duoselective* separations will have two lobes on their $R_s([\text{H}_3\text{O}^+], [\text{CD}])$ surfaces. Knowledge of the general shape of these surfaces is important for the rational optimization of the CE separation of the enantiomers of weak electrolytes.

Though three different enantiomer separation types were predicted theoretically, only *desionoselective* separations have been observed experimentally for chiral weak acids, either with β -cyclodextrin [6] or hydroxypropyl β -cyclodextrin [8], as resolving agent. The objective of this paper is to provide the first experimental evidence for the existence of *duoselective* separations in the CE analysis of monoprotic chiral weak acids.

2. Experimental

A P/ACE 2100 system (Beckman Instruments, Fullerton, CA, USA), operated at 210 nm and at a thermostating liquid bath temperature of 37°C was used for the mobility measurements. The injector electrode was kept at ground potential, the detector electrode at high positive potential. The field strength was varied between 190 and 260 V/cm to keep the power dissipation around 100 mW. The 0.1–0.2 mM samples were injected electrokinetically. Benzyl alcohol, simultaneously injected at the detector end of the capillary, was used as electroosmotic flow marker. Untreated, 25 μm I.D., 150 μm O.D. (40.0 cm from injector to detector, 46.4 cm total length)

fused-silica capillaries (Polymicro Technologies, Phoenix, AZ, USA) were used for the separations.

The background electrolytes (BGE) contained 0–15 mM β -cyclodextrin (American Maize Products, Hammond, IN, USA) as chiral resolving agent, 100 mM ϵ -amino-*n*-caproic acid, EACA, (Sigma, St. Louis, MO, USA) as buffer component, 100 mM methanesulfonic acid, MSA, (Aldrich, Milwaukee, WI, USA) as ionic strength adjusting agent and 250MHR PA hydroxyethyl cellulose, HEC, (Aqualon Company, Wilmington, DE, USA) as electroosmotic flow-controlling agent. The buffer pH was adjusted by a concentrated LiOH (Aldrich) solution. The test solute, 3,5-dinitrobenzamido phenylalanine (DPA), was synthesized according to a modified Schotten-Bauman procedure [12] from both racemic and enantiomerically pure phenylalanine (Aldrich) and 3,5-dinitrobenzoyl chloride (Fluka, Ronkonkoma, NY, USA). In order to monitor the ionic strength-related mobility changes, a strong electrolyte, *p*-toluenesulfonic acid, PTSA (Aldrich), was added to each sample. All BGEs were freshly prepared using deionized water from a Millipore Q unit (Millipore, Milford, MA, USA). Irrespective of the pH of the BGE, the cation concentration was maintained constant at 100 mM (cation-concentration balanced background electrolytes [8–10]).

The parameters in Eqs. 1 and 4 and the three-dimensional selectivity and resolution surfaces were calculated from the measured, electroosmotic flow-corrected effective mobilities using the Origin Ver. 3.0 software package (MicroCal, Northampton, MA, USA) running on a 486DX2 66 MHz 16M RAM personal computer (Computer Access, College Station, TX, USA), as described in Refs. [8–10].

3. Results and discussions

3.1. Determination of the model parameters for 3,5-dinitrobenzamido phenylalanine

The K_{a} and μ_{-}^0 values of the weak acid test solute, DPA, were determined using the counterion concentration-balanced BGEs in the pH 3–6

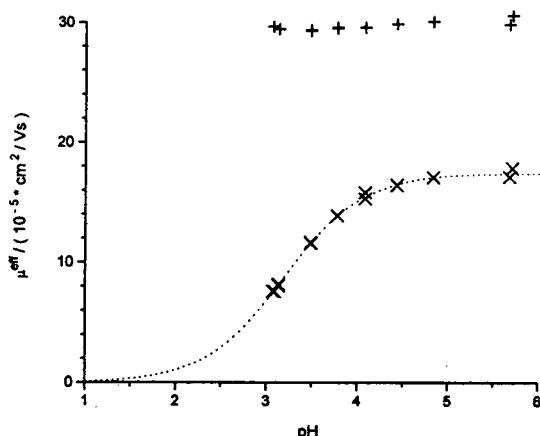


Fig. 1. Effective mobility of PTSA⁻ (symbol +) and DPA⁻ (symbol ×) in 100 mM ϵ -amino-*n*-caproic acid, 100 mM methanesulfonic acid buffers as a function of the BGE pH value, adjusted by lithium hydroxide.

range. The effective mobilities of DPA (symbol ×) and PTSA (symbol +) are plotted in Fig. 1 as a function of pH. The mobilities of the permanent anion, PTSA⁻, are indeed constant — within experimental scatter — in the counter-ion concentration balanced BGEs indicating that the μ^{eff} values of the enantiomers are suitable for the $\text{p}K_{\text{a}}$ and μ_{-}^0 determinations [8]. The calculated K_{a} and μ_{-}^0 values of DPA are listed in Table 1.

In order to determine the $\mu_{\text{RCD}^{-}}^0$, $\mu_{\text{SCD}^{-}}^0$, $K_{\text{RCD}^{-}}$ and $K_{\text{SCD}^{-}}$ values, listed in Table 1, the concentration of β -cyclodextrin was varied between 0 and 15 mM in pH = 5.68 BGEs where DPA is almost completely dissociated, and the effective mobilities as a function of c_{CD} were measured (Fig. 2). Next, the K_{HRCD} and K_{HSCD}

Table 1
Estimated model parameter values for DPA

μ_{-}^0 (10^{-5} cm ² /Vs)	17.49 ± 0.09
$10^4 K_{\text{a}}$	6.4 ± 0.1
$\text{p}K_{\text{a}}$	3.19
$\mu_{\text{RCD}^{-}}^0$ (10^{-5} cm ² /Vs)	6.5 ± 0.4
$\mu_{\text{SCD}^{-}}^0$ (10^{-5} cm ² /Vs)	5.8 ± 0.8
$K_{\text{RCD}^{-}}^0$	100 ± 7
$K_{\text{SCD}^{-}}^0$	62 ± 7
K_{HRCD}	81.1 ± 0.8
K_{HSCD}	62.7 ± 0.5

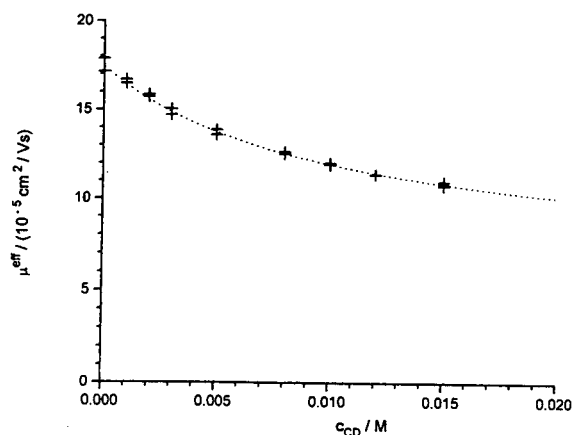


Fig. 2. Effective mobility of the less mobile enantiomer of DPA⁻ (symbol +) as a function of the β -cyclodextrin concentration in pH 5.68 counter-ion concentration balanced 100 mM EACA BGEs.

values were determined from the effective mobilities measured in pH = 3.08 BGEs (where DPA is less than 50% dissociated) as c_{CD} was varied between 0 and 15 mM (Fig. 3). The calculated constant values are listed in Table 1.

Since $\mu_{\text{RCD}^{-}}^0 = 5.82 \cdot 10^{-5}$ cm²/Vs and $\mu_{\text{SCD}^{-}}^0 = 6.53 \cdot 10^{-5}$ cm²/Vs, $K_{\text{RCD}^{-}} = 62$ and $K_{\text{SCD}^{-}} = 100$, and $K_{\text{HRCD}} = 62.7$ and $K_{\text{HSCD}} = 81.1$, the separation of the enantiomers of DPA represents a *duoselective* separation. To the best of our

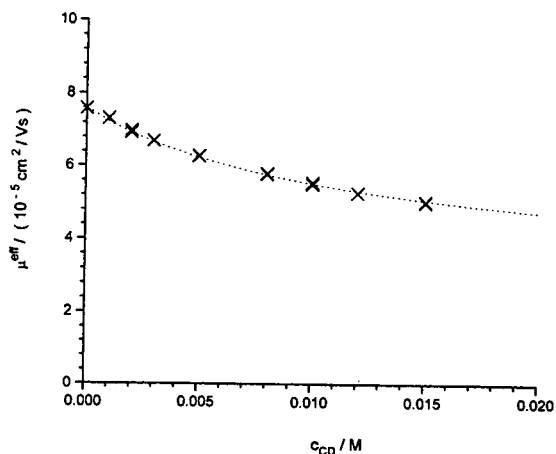


Fig. 3. Effective mobility of the less mobile enantiomer of DPA⁻ (symbol ×) as a function of the β -cyclodextrin concentration in pH 3.08 counter-ion concentration balanced 100 mM EACA BGEs.

knowledge, this is the first, experimentally demonstrated example of a *duoselective* CE separation of a chiral weak acid.

3.2. Separation selectivity and peak resolution surfaces

Once the model parameters are known, the selectivity and resolution surfaces can be calculated and studied to understand the behavior of a *duoselective* weak acid separation and to find the conditions which lead to optimum peak resolution. The selectivity surface is shown in Fig. 4 as a function of c_{CD} and pH. At high pH ($\text{pH} > \text{p}K_a + 1$), selectivity passes a maximum value as c_{CD} is varied: the maximum is located at 15 mM. Fortunately, the surface is sufficiently flat in the $10 < c_{CD} < 20 \text{ mM}$ range, which leads to rugged separations. If one keeps the CD concentration constant at $c_{CD} = 15 \text{ mM}$ and begins to decrease the pH from 6, α first remains constant, then begins to decrease in the vicinity of the $\text{p}K_a$. Upon further decrease of the pH, α becomes less than unity, indicating that the migration order of the enantiomers is reversed. Simultaneously, as the pH is decreased, the locus of α_{max} shifts

toward lower cyclodextrin concentrations. This follows the predicted typical behavior of a *duoselective* separation [6].

The calculated peak resolution surface is shown in Fig. 5. Since resolution depends on the magnitude of the electroosmotic flow as well (expressed here as β), its value has to be fixed for the calculations. With uncoated fused-silica capillaries, the electroosmotic flow works against the migration of the anionic solutes. However, in these measurements, its magnitude was kept low by the addition of HEC. Therefore, the surface in Fig. 5 was calculated with $\beta = 0$. There are two lobes on the resolution surface: the primary lobe is at high pH, and the migration order of the enantiomers is D first, L second. The secondary lobe is at low pH, and there the migration order of the enantiomers is L first, D second. The two lobes are separated by a valley, where the resolution is zero. At high pH, on the primary lobe, resolution is high and the resolution maximum on the fortunately flat R_s surface is in the $12 < c_{CD} < 18 \text{ mM}$ range. If one keeps the CD concentration constant at 15 mM and moves toward lower pH values, R_s drops precipitously around the $\text{p}K_a$ value. There are

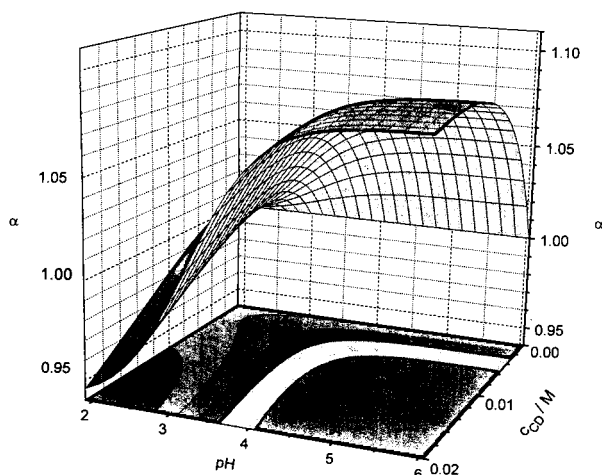


Fig. 4. Selectivity surface for the separation of the enantiomers of DPA^- (duoselective separation) as a function of the β -cyclodextrin concentration and the pH in counter-ion concentration balanced 100 mM EACA BGEs. The surface was calculated with Eq. 3 and the constants in Table 1.

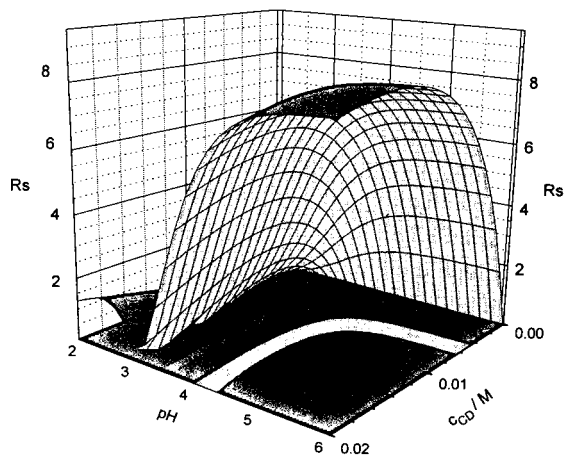


Fig. 5. Peak resolution surface for the separation of the enantiomers of DPA^- (duoselective separation) as a function of the β -cyclodextrin concentration and the pH in counter-ion concentration balanced 100 mM EACA BGEs. The surface was calculated with Eq. 4 and the constants in Table I for $\beta = 0$ and $E = 215 \text{ V/cm}$, $T = 298 \text{ K}$ and $l = 38.65 \text{ cm}$.

two factors which cause this rapid loss of resolution: the loss of selectivity shown in Fig. 4, and the accompanying loss in effective solute charge (cf. Eq. 3). As pH is decreased further, resolution is increased again, albeit with a reversed peak migration order. Even though selectivity keeps increasing as pH is lowered further (cf. Fig. 4), R_s goes through a maximum, because the loss of effective charge overcompensates the selectivity gain. This surface agrees with what was predicted theoretically as typical for a *duoselective* separation and indicates that reasonably rugged separations can be achieved as long as the pH is kept at least one pH unit above the pK_a . Above this limit, the pH can be selected freely to accommodate other considerations.

In order to demonstrate how closely the predicted values agree with the measured ones, another series of experiments was carried out in which the pH of the counter-ion concentration-balanced 100 mM EACA BGE was varied between 3 and 5.8, and the β -cyclodextrin concentration was kept at 15 mM. The selectivity values are plotted in Fig. 6 (symbol \times measured values, solid line, calculated values), indicating that the agreement is excellent. The predicted (symbol \times) and measured (symbol $+$) R_s values for the same set of experiments are shown in Fig.

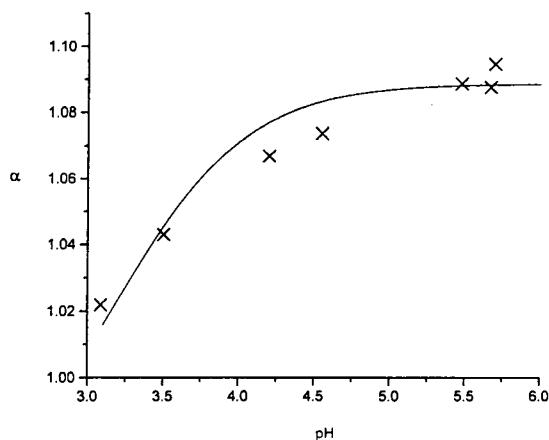


Fig. 6. Comparison of the predicted (solid line) and measured (symbol \times) selectivity values for DPA^- as a function of pH in counter-ion concentration balanced 100 mM EACA, 15 mM β -cyclodextrin BGEs.

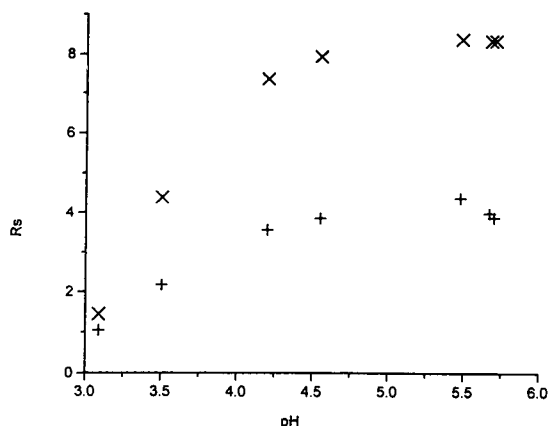


Fig. 7. Comparison of the predicted (symbol \times) and measured (symbol $+$) R_s values for DPA^- as a function of pH in counter-ion concentration balanced 100 mM EACA, 15 mM β -cyclodextrin BGEs. The measured values were obtained using $E = 215$ V/cm, with electroosmotic flows varying in the $(0.2\text{--}0.4) \cdot 10^{-5}$ cm²/Vs range.

7. Though the measured values are about 50% smaller than the theoretically predicted ones (indicating the presence of additional peak broadening mechanisms in excess of longitudinal diffusion considered in the derivation of Eq. 4), the loci of the experimental and theoretical peak resolution maxima agree well, indicating that the model is suitable for the selection of the operating conditions which lead to maximum resolution of the enantiomers. As an example, the electropherogram of a DPA sample is shown in Fig. 8.

4. Conclusions

The multiple equilibria-based mobility model of CE was used to determine the complex formation constants and ionic mobilities in the CE separation of the enantiomers of a weak acid, DPA. The numeric values of the constants indicate that this separation represents a *duoselective* separation, and serves as the first experimental evidence for the existence of this theoretically predicted separation possibility. The model parameters and the extended peak resolution equation were used to calculate the

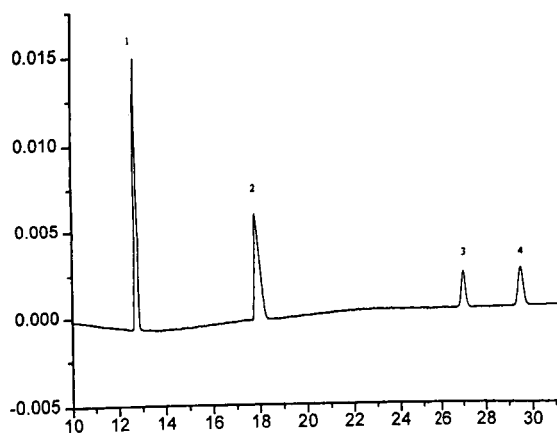


Fig. 8. Electropherogram of a DPA^- sample, obtained in a counter-ion concentration balanced 100 mM EACA, pH = 5.69, 15 mM β -cyclodextrin BGE. $E = 215$ V/cm at $T = 310$ K. Peak identity: 1 = PTSA^- , 2 = 3,5-dinitrobenzoic acid, 3 and 4 = DPA enantiomers. x-axis: time (min); y-axis: absorbance (mAU).

predicted peak resolution surface for the enantiomers, which was then compared to the experimentally determined values. Though the actual peak resolution values were lower than the theoretically predicted ones due to the presence of additional peak broadening mechanisms other than longitudinal diffusion, the loci of the peak resolution extrema agreed with the theoretical predictions, indicating that the model can be used for the selection of the operating conditions which lead to maximum resolution of the enantiomers.

Acknowledgements

Partial financial support by the National Science Foundation (CHE-8919151 and an NSF-

REU fellowship to M.E.B.), the Texas Coordination Board of Higher Education Advanced Research Program (Project Number 010366-016), Beckman Instruments (Fullerton, CA, USA), the WR Johnson Pharmaceutical Research Institute (Springfield, PA, USA), and the Dow Chemical Company (Midland, MI, USA) is gratefully acknowledged. American Maize Products Corporation (Hammond, IN, USA) and the Aqualon Corporation (Wilmington, DE, USA), respectively, are acknowledged for the donation of the β -cyclodextrin and hydroxyethyl cellulose samples.

References

- [1] R. Kuhn and S. Hoffstetter-Kuhn, *Chromatographia*, 34 (1992) 505.
- [2] J. Snopek, I. Jelinek and E. Smolkova-Keulemansova, *J. Chromatogr.*, 609 (1992) 1.
- [3] S.A.C. Wren and R.C. Rowe, *J. Chromatogr.*, 603 (1992) 235.
- [4] S.A.C. Wren and R.C. Rowe, *J. Chromatogr.*, 609 (1992) 363.
- [5] S.A.C. Wren and R.C. Rowe, *J. Chromatogr.*, 635 (1993) 113.
- [6] Y.Y. Rawjee, D.U. Staerk and Gy. Vigh, *J. Chromatogr. A.*, 635 (1993) 291.
- [7] Y.Y. Rawjee, R.L. Williams and Gy. Vigh, *J. Chromatogr. A.*, 652 (1993) 233.
- [8] Y.Y. Rawjee and Gy. Vigh, *Anal. Chem.*, 66 (1994) 619.
- [9] Y.Y. Rawjee, R.L. Williams and Gy. Vigh, *J. Chromatogr. A.*, 680 (1994) 599.
- [10] Y.Y. Rawjee, R.L. Williams, L. Buckingham and Gy. Vigh, *J. Chromatogr. A.*, 688 (1994) 273.
- [11] W. Friedl and E. Kenndler, *Anal. Chem.*, 65 (1993) 2003.
- [12] P.L. Camacho, Gy. Vigh and D.H. Thompson, *J. Chromatogr.*, 641 (1993) 31.

Author Index Vols. 691 and 692

- Abbas, A.A. and Shelly, D.C.
Optical properties of axial-illumination flow cells for simultaneous absorbance-fluorescence detection in micro liquid chromatography 691(1995)37
- Adams, A.G., see Ponder, G.W. 692(1995)173
- Agnellini, D., see Pace, M. 691(1995)331
- Aguilar, M.-I., see Xie, J. 691(1995)263
- Anegayama, M., see Moriyama, H. 691(1995)81
- Archer, J., see Jinno, K. 691(1995)91
- Au, T., see Woolf, E. 692(1995)45
- Baker, T.R., see Hayes, F.J. 692(1995)73
- Banks, Jr., J.F.
Separation and analysis of proteins by perfusion liquid chromatography and electrospray ionization mass spectrometry 691(1995)325
- Bayer, E., see Schmeer, K. 691(1995)285
- Begum, B., see Hardcastle, J.E. 691(1995)225
- Bertrand, M., see Schoefs, B. 692(1995)239
- Biggin, M.E., Williams, R.L. and Vigh, G.
Experimental evidence for the existence of duoselective (Type III) enantiomer separations in the capillary electrophoretic analysis of chiral weak acids 692(1995)319
- Blackwell, J.A., see Whitman, D.A. 691(1995)205
- Bonetti, A., see Galletti, G.C. 692(1995)27
- Boppana, V.K.
Simultaneous determination of granisetron and its 7-hydroxy metabolite in human plasma by reversed-phase high-performance liquid chromatography utilizing fluorescence and electrochemical detection 692(1995)195
- Bossle, P.C., see Oehrle, S.A. 692(1995)247
- Bowers, L.D.
Foreword 691(1995)1
- Boyes, B.E. and Walker, D.G.
Selectivity optimization of reversed-phase high-performance liquid chromatographic peptide and protein separations by varying bonded-phase functionality 691(1995)337
- Breier, J., see Freitag, R. 691(1995)101
- Brennan, J.J., see Pullen, R.H. 691(1995)187
- Buciński, A., see Nasal, A. 692(1995)83
- Busch, K.L.
Mass spectrometric detectors for samples separated by planar electrophoresis (Review) 692(1995)275
- Buszewski, B., see Czajkowska, T. 691(1995)217
- Butram, S.L., see Ponder, G.W. 692(1995)173
- Camacho-Torralba, P.L. and Vigh, Gy.
High-performance chiral displacement chromatographic separations in the normal-phase mode. III. Separation of the enantiomers of 5-vinylpyrrolidin-2-one using the Chiralcel-OD stationary phase 691(1995)213
- Capparella, M., Foster III, W., Larrousse, M., Phillips, D.J., Pomfret, A. and Tuvim, Y.
Characteristics and applications of a new high-performance liquid chromatography guard column 691(1995)141
- Carlson, I.H., see Lensmeyer, G.L. 691(1995)239
- Chen, A. and Lunte, C.E.
Microdialysis sampling coupled on-line to fast microbore liquid chromatography 691(1995)29
- Chen, J.-G., Woltman, S.J. and Weber, S.G.
Sensitivity and selectivity of the electrochemical detection of the copper(II) complexes of bioactive peptides, and comparison to model studies by rotating ring-disc electrode 691(1995)301
- Chen, Y.-L., see Jinno, K. 691(1995)91
- Cho, Y.J., see Hyun, M.H. 692(1995)91
- Chong, R.W. and Moore, B.J.
Determination of citrate, inositol and gentisic acid in a pharmaceutical diagnostic formulation by ion-moderated partition chromatography 692(1995)203
- Chow, K.K., see Ong, C.P. 692(1995)207
- Chung, H.-C., see Hsu, M.-C. 692(1995)67
- Claessens, H.A., see Kirkland, J.J. 691(1995)3
- Clerc, J.-T., see Grogg-Sulser, K. 692(1995)121
- Császár, J., see Schmeer, K. 691(1995)285
- Cui, Y. and Olesik, S.V.
Reversed-phase high-performance liquid chromatography using enhanced-fluidity mobile phases 691(1995)151
- Czajkowska, T., Hrabovsky, I., Buszewski, B., Gilpin, R.K. and Jaroniec, M.
Comparison of the retention of organic acids on alkyl and alkylamide chemically bonded phases 691(1995)217
- De Vos, F. and Slegers, G.
High-performance liquid chromatographic determination of (4-[¹¹C]methoxyphenyl)-(5-fluoro-2-hydroxyphenyl)-methylethylaminebutyric acid and its benzophenone metabolite 692(1995)97
- Dinelli, G., see Galletti, G.C. 692(1995)27
- Dobson, R.L.M., see Hayes, F.J. 692(1995)73
- Dumont, P.J. and Fritz, J.S.
Effect of resin sulfonation on the retention of polar organic compounds in solid-phase extraction 691(1995)123
- Dumont, P.J., see Fritz, J.S. 691(1995)133
- Eriksson, B.-M., see Hedenmo, M. 692(1995)161
- Fang, X., see Rosenfeld, J.M. 691(1995)231
- Farkas, G., see Schmeer, K. 691(1995)285
- Fiorini, M.
Preparative high-performance liquid chromatography for the purification of natural anthocyanins 692(1995)213
- Fladung, N.C.
Optimization of automated solid-phase extraction for quantitation of polycyclic aromatic hydrocarbons in aqueous media by high-performance liquid chromatography-UV detection 692(1995)21
- Forsmann, W.-G., see Schepky, A.G. 691(1995)255
- Foster III, W., see Capparella, M. 691(1995)141
- Freitag, R. and Breier, J.
Displacement chromatography in biotechnological downstream processing 691(1995)101

- Fritz, J.S., Dumont, P.J. and Schmidt, L.W.
Methods and materials for solid-phase extraction
691(1995)133
- Fritz, J.S., see Dumont, P.J. 691(1995)123
- Galletti, G.C., Bonetti, A. and Dinelli, G.
High-performance liquid chromatographic
determination of sulfonyleureas in soil and water
692(1995)27
- Gardana, C., see Pace, M. 691(1995)331
- Geiser, F.O., see Ricker, R.D. 691(1995)67
- Gilpin, R.K., see Czajkowska, T. 691(1995)217
- Greenblatt, H.C., see Hofman, Y.L. 692(1995)233
- Grogg-Sulser, K., Helmlin, H.-J. and Clerc, J.-T.
Qualitative and quantitative determination of illicit
heroin street samples by reversed-phase high-
performance liquid chromatography: method
development by CARTAGO-S 692(1995)121
- Grushka, E., see Mizrotsky, N. 691(1995)21
- Haddix, H., see Woolf, E. 692(1995)45
- Hadjmohammadi, M., see Ye, B. 692(1995)291
- Hagen, S.R. and Thompson, J.D.
Analysis of mycolic acids by high-performance liquid
chromatography and fluorimetric detection.
Implications for the identification of mycobacteria in
clinical samples 692(1995)167
- Hardcastle, J.E., He, M., Begum, B. and Vermillion-
Salsbury, R.
Use of secondary chemical equilibria in liquid
chromatography to determine dissociation constants of
leukotriene B₄ and prostaglandin B₂ 691(1995)225
- Hayes, F.J., Baker, T.R., Dobson, R.L.M. and Tsueda,
M.S.
Rapid liquid chromatographic-mass spectrometric
assay for oxymetazoline in whole rat blood
692(1995)73
- He, M., see Hardcastle, J.E. 691(1995)225
- Hearn, M.T.W., see Mao, Q.-M. 691(1995)273
- Hearn, M.T.W., see Xie, J. 691(1995)263
- Hedenmo, M. and Eriksson, B.-M.
Liquid chromatographic determination of the macrolide
antibiotics roxithromycin and clarithromycin in plasma
by automated solid-phase extraction and
electrochemical detection 692(1995)161
- Helmlin, H.-J., see Grogg-Sulser, K. 692(1995)121
- Hermanson, G.T., Mattson, G.R. and Krohn, R.I.
Preparation and use of immunoglobulin-binding affinity
supports on Emphaze beads 691(1995)113
- Hofman, Y.L., Petrillo, K.L., Greenblatt, H.C., Lehrer,
R. and Payne, M.S.
Rapid scaleable chromatographic purification of nucleic
acids from proteinaceous mixtures 692(1995)233
- Hrabovsky, I., see Czajkowska, T. 691(1995)217
- Hsu, M.-C., Lin, Y.-S. and Chung, H.-C.
High-performance liquid chromatographic method for
potency determination of cephalixin in commercial
preparations and for stability studies 692(1995)67
- Huang, C.-Y., see Lee, Y.-C. 692(1995)137
- Hyun, M.H., Ryoo, J.-J., Cho, Y.J. and Jin, J.S.
Unusual examples of the liquid chromatographic
resolution of racemates. Resolution of π -donor
analytes on a π -donor chiral stationary phase
692(1995)91
- Itoh, K., see Jinno, K. 691(1995)91
- Jaroniec, M., see Czajkowska, T. 691(1995)217
- Jin, J.S., see Hyun, M.H. 692(1995)91
- Jinno, K., Nakagawa, K., Saito, Y., Ohta, H., Nagashima,
H., Itoh, K., Archer, J. and Chen, Y.-L.
Nano-scale design of novel stationary phases to
enhance selectivity for molecular shape and size in
liquid chromatography 691(1995)91
- Johansen, S.S., see Rastogi, S.C. 692(1995)53
- Justice, J.D., see Ricker, R.D. 691(1995)67
- Kaliszan, R., see Nasal, A. 692(1995)83
- Kato, Y., see Moriyama, H. 691(1995)81
- Kempe, M. and Mosbach, K.
Separation of amino acids, peptides and proteins on
molecularly imprinted stationary phases 691(1995)317
- Khaledi, M.G., see Quang, C. 692(1995)253
- Khaledi, M.G., see Yang, S. 692(1995)301
- Khaledi, M.G., see Yang, S. 692(1995)311
- Khaledi, M.G., see Ye, B. 692(1995)291
- Khalifa, M., see Schmeer, K. 691(1995)285
- Kirkland, J.J., Van Straten, M.A. and Claessens, H.A.
High pH mobile phase effects on silica-based reversed-
phase high-performance liquid chromatographic
columns 691(1995)3
- Komiya, K., see Moriyama, H. 691(1995)81
- Koves, E.M.
Use of high-performance liquid chromatography-diode
array detection in forensic toxicology 692(1995)103
- Kristol, L., see Mizrotsky, N. 691(1995)21
- Krohn, R.I., see Hermanson, G.T. 691(1995)113
- Lai, F. and White, L.
Automated precolumn concentration and high-
performance liquid chromatographic analysis of
polynuclear aromatic hydrocarbons in water using a
single pump and a single valve 692(1995)11
- Larew, L.A., Olsen, B.A., Stafford, J.D. and Wilhelm,
M.V.
Comparison of theory-based and empirical modeling
for the prediction of chromatographic behavior in the
ion-pairing separation of benzodiazepine-derived
pharmaceutical compounds 692(1995)183
- Larrousse, M., see Capparella, M. 691(1995)141
- Lee, H.K., see Ong, C.P. 692(1995)207
- Lee, Y.-C., Huang, C.-Y., Wen, K.-C. and Suen, T.-T.
Determination of liquiritin, glycyrrhizin, hesperidin,
cinnamic acid, cinnamaldehyde, honokiol and
magnolol in the traditional Chinese medicinal
preparation Wu-Ji-San by high-performance liquid
chromatography 692(1995)137
- Lehrer, R., see Hofman, Y.L. 692(1995)233
- Lemoine, Y., see Schoefs, B. 692(1995)239
- Lensmeyer, G.L., Onsager, C., Carlson, I.H. and Wiebe,
D.A.
Use of particle-loaded membranes to extract steroids
for high-performance liquid chromatographic analyses.
Improved analyte stability and detection 691(1995)239
- Li, S.F.Y., see Ong, C.P. 692(1995)207
- Lima III, L.R. and Synovec, R.E.
Laser-based dynamic surface tension detection for
liquid chromatography by probing a repeating drop
radius 691(1995)195
- Lin, Y.-S., see Hsu, M.-C. 692(1995)67

- Long, T.E., see Schunk, T.C. 692(1995)221
- Lukulay, P.H. and McGuffin, V.L.
Solvent modulation in liquid chromatography:
extension to serially coupled columns 691(1995)171
- Lunte, C.E., see Chen, A. 691(1995)29
- Mao, Q.-M., Prince, I.G. and Hearn, M.T.W.
High-performance liquid chromatography of amino
acids, peptides and proteins. CXXXIX. Impact of
operating parameters in large-scale chromatography of
proteins 691(1995)273
- Mattson, G.R., see Hermanson, G.T. 691(1995)113
- Matuszewski, B., see Woolf, E. 692(1995)45
- Mauri, P.L., see Pace, M. 691(1995)331
- McGuffin, V.L., see Lukulay, P.H. 691(1995)171
- Metzger, W., see Reif, K. 692(1995)131
- Mizrotsky, N., Kristol, L. and Grushka, E.
Use of chromatographic system peaks for continuous
quantitative analysis 691(1995)21
- Molnár-Perl, I., see Schmeer, K. 691(1995)285
- Moore, B.J., see Chong, R.W. 692(1995)203
- Moriyama, H., Anegayama, M., Komiya, K. and Kato, Y.
Characterization of a new reversed-phase
chromatographic column on a 2- μ m porous
microspherical silica gel 691(1995)81
- Mosbach, K., see Kempe, M. 691(1995)317
- Mosbach, K., see Nicholls, I.A. 691(1995)349
- Nagashima, H., see Jinno, K. 691(1995)91
- Nakagawa, K., see Jinno, K. 691(1995)91
- Nasal, A., Sznitowska, M., Buciniński, A. and Kaliszan, R.
Hydrophobicity parameter from high-performance
liquid chromatography on an immobilized artificial
membrane column and its relationship to bioactivity
692(1995)83
- Ng, C.L., see Ong, C.P. 692(1995)207
- Nicholls, I.A., Ramström, O. and Mosbach, K.
Insights into the role of the hydrogen bond and
hydrophobic effect on recognition in molecularly
imprinted polymer synthetic peptide receptor mimics
691(1995)349
- Oehrle, S.A. and Bossle, P.C.
Analysis of nerve agent degradation products using
capillary ion electrophoresis 692(1995)247
- Ohta, H., see Jinno, K. 691(1995)91
- Olesik, S.V., see Cui, Y. 691(1995)151
- Olsen, B.A. and Sullivan, G.R.
Chemometric categorization of octadecylsilyl bonded-
phase silica columns using test mixtures and
confirmation of results with pharmaceutical compound
separations 692(1995)147
- Olsen, B.A., see Larew, L.A. 692(1995)183
- Ong, C.P., Chow, K.K., Ng, C.L., Ong, F.M., Lee, H.K.
and Li, S.F.Y.
Use of overlapping resolution mapping scheme for
optimization of the high-performance liquid
chromatographic separation of pharmaceuticals
692(1995)207
- Ong, F.M., see Ong, C.P. 692(1995)207
- Onsager, C., see Lensmeyer, G.L. 691(1995)239
- Pace, M., Agnellini, D., Gardana, C., Mauri, P.L. and
Pietta, P.G.
High-performance liquid chromatographic assay of
glycosyltransferases using flavonoids as substrate
691(1995)331
- Patonay, G., see Pullen, R.H. 691(1995)187
- Payne, M.S., see Hofman, Y.L. 692(1995)233
- Petrillo, K.L., see Hofman, Y.L. 692(1995)233
- Phillips, D.J., see Capparella, M. 691(1995)141
- Pietta, P.G., see Pace, M. 691(1995)331
- Pomfret, A., see Capparella, M. 691(1995)141
- Ponder, G.W., Butram, S.L., Adams, A.G., Ramanathan,
C.S. and Stewart, J.T.
Resolution of promethazine, ethopropazine,
trimeprazine and trimipramine enantiomers on selected
chiral stationary phases using high-performance liquid
chromatography 692(1995)173
- Prince, I.G., see Mao, Q.-M. 691(1995)273
- Pullen, R.H., Brennan, J.J. and Patonay, G.
Chiral separation retention mechanisms in high-
performance liquid chromatography using bare silica
stationary phase and β -cyclodextrin as a mobile phase
additive 691(1995)187
- Quang, C. and Khaledi, M.G.
Extending the scope of chiral separation of basic
compounds by cyclodextrin-mediated capillary zone
electrophoresis 692(1995)253
- Ramanathan, C.S., see Ponder, G.W. 692(1995)173
- Ramström, O., see Nicholls, I.A. 691(1995)349
- Rastogi, S.C. and Johansen, S.S.
Comparison of high-performance liquid
chromatographic methods for the determination of 1,2-
dibromo-2,4-dicyanobutane in cosmetic products
692(1995)53
- Ravindranath, Y., see Stout, M.L. 692(1995)59
- Reif, K. and Metzger, W.
Determination of aflatoxins in medicinal herbs and
plant extracts 692(1995)131
- Ricker, R.D., Sandoval, L.A., Justice, J.D. and Geiser,
F.O.
Multivariate visualization in the size-exclusion
chromatography and pattern recognition of biological
samples 691(1995)67
- Rosenfeld, J.M. and Fang, X.
Simultaneous sorption and analytical derivatization on
a polystyrene-divinylbenzene polymer. Preparation of
chromophoric and fluorophoric derivatives of the
prostaglandins 691(1995)231
- Ryoo, J.-J., see Hyun, M.H. 692(1995)91
- Saito, Y., see Jinno, K. 691(1995)91
- Sandoval, L.A., see Ricker, R.D. 691(1995)67
- Schepky, A.G., Schulz-Knappe, P. and Forssmann, W.-G.
High-performance liquid chromatographic
determination of sulfated peptides in human
hemofiltrate using a radioactivity monitor
691(1995)255
- Schmeer, K., Khalifa, M., Császár, J., Farkas, G., Bayer,
E. and Molnár-Perl, I.
Compositional analysis of the phenylthiocarbamyl
amino acids by liquid chromatography-atmospheric
pressure ionization mass spectrometry with particular
attention to the cyst(e)ine derivatives 691(1995)285
- Schmidt, L.W., see Fritz, J.S. 691(1995)133
- Schoefs, B., Bertrand, M. and Lemoine, Y.
Separation of photosynthetic pigments and their
precursors by reversed-phase high-performance liquid
chromatography using a photodiode-array detector
692(1995)239

- Schulz-Knappe, P., see Schepky, A.G. 691(1995)255
- Schunk, T.C. and Long, T.E.
Compositional distribution characterization of poly(methyl methacrylate)-graft-polydimethylsiloxane copolymers 692(1995)221
- Shelly, D.C., see Abbas, A.A. 691(1995)37
- Shelly, D.C., see Siddiqui, A. 691(1995)55
- Shephard, G.S., Thiel, P.G. and Sydenham, E.W.
Liquid chromatographic determination of the mycotoxin fumonisin B₂ in physiological samples 692(1995)39
- Siddiqui, A. and Shelly, D.C.
Amperostatic-potentiometric detection for micro high-performance liquid chromatography 691(1995)55
- Simpson, R.C.
Modification of a conventional high-performance liquid chromatography autoinjector for use with capillary liquid chromatography 691(1995)163
- Slegers, G., see De Vos, F. 692(1995)97
- Smith, L.L., see Teng, J.I. 691(1995)247
- Stafford, J.D., see Larew, L.A. 692(1995)183
- Stewart, J.T., see Ponder, G.W. 692(1995)173
- Stout, M.L. and Ravindranath, Y.
Alkylsulphonic acid ion pairing with radial compression columns for determining plasma or cerebrospinal fluid 1-β-D-arabinofuranosylcytosine in pediatric pharmacokinetic analysis 692(1995)59
- Suen, T.-T., see Lee, Y.-C. 692(1995)137
- Sullivan, G.R., see Olsen, B.A. 692(1995)147
- Sydenham, E.W., see Shephard, G.S. 692(1995)39
- Synovec, R.E., see Lima III, L.R. 691(1995)195
- Sznitowska, M., see Nasal, A. 692(1995)83
- Teng, J.I. and Smith, L.L.
High-performance liquid chromatographic analysis of human erythrocyte oxysterols as Δ⁴-3-ketone derivatives 691(1995)247
- Thiel, P.G., see Shephard, G.S. 692(1995)39
- Thompson, J.D., see Hagen, S.R. 692(1995)167
- Tsueda, M.S., see Hayes, F.J. 692(1995)73
- Tuvim, Y., see Capparella, M. 691(1995)141
- Van Straten, M.A., see Kirkland, J.J. 691(1995)3
- Vermillion-Salsbury, R., see Hardcastle, J.E. 691(1995)225
- Vigh, Gy., see Biggin, M.E. 692(1995)319
- Vigh, Gy., see Camacho-Torralba, P.L. 691(1995)213
- Walker, D.G., see Boyes, B.E. 691(1995)337
- Weber, S.G., see Chen, J.-G. 691(1995)301
- Weber, T.P., see Whitman, D.A. 691(1995)205
- Wen, K.-C., see Lee, Y.-C. 692(1995)137
- White, L.B., see Wu, R. 692(1995)1
- White, L., see Lai, F. 692(1995)11
- Whitman, D.A., Weber, T.P. and Blackwell, J.A.
Chemometric characterization of Lewis base-modified zirconia for normal phase chromatography 691(1995)205
- Wiebe, D.A., see Lensmeyer, G.L. 691(1995)239
- Wiley, J.P.
Determination of polycarboxylic acids by capillary electrophoresis with copper complexation 692(1995)267
- Wilhelm, M.V., see Larew, L.A. 692(1995)183
- Williams, R.L., see Biggin, M.E. 692(1995)319
- Woltman, S.J., see Chen, J.-G. 691(1995)301
- Woolf, E., Au, T., Haddix, H. and Matuszewski, B.
Determination of L-735 524, an human immunodeficiency virus protease inhibitor, in human plasma and urine via high-performance liquid chromatography with column switching 692(1995)45
- Wu, R. and White, L.B.
Automated procedure for determination of trace amounts of aldehydes in drinking water 692(1995)1
- Xie, J., Aguilar, M.-I. and Hearn, M.T.W.
High-performance liquid chromatography of amino acids, peptides and proteins. CXXXVIII. Adsorption of horse heart cytochrome c onto a tentacle-type cation exchanger 691(1995)263
- Yang, S. and Khaledi, M.G.
Linear solvation energy relationships in micellar liquid chromatography and micellar electrokinetic capillary chromatography 692(1995)301
- Yang, S. and Khaledi, M.G.
Micellar liquid chromatographic separation of sulfonamides in physiological samples using direct on-column injection 692(1995)311
- Ye, B., Hadjmohammadi, M. and Khaledi, M.G.
Selectivity control in micellar electrokinetic chromatography of small peptides using mixed fluorocarbon-hydrocarbon anionic surfactants 692(1995)291

PUBLICATION SCHEDULE FOR THE 1995 SUBSCRIPTION

Journal of Chromatography A and *Journal of Chromatography B: Biomedical Applications*

MONTH	1994	J 1995	F 1995	M 1995	
Journal of Chromatography A	Vols. 683–688	689/1 689/2 690/1 690/2	691/1 + 2 692/1 + 2 693/1 693/2	694/1 694/2	The publication schedule for further issues will be published later.
Bibliography Section				713/1	
Journal of Chromatography B: Biomedical Applications		663/1 663/2	664/1 664/2	665/1 665/2	

INFORMATION FOR AUTHORS

(Detailed *Instructions to Authors* were published in *J. Chromatogr. A*, Vol. 657, pp. 463–469. A free reprint can be obtained by application to the publisher, Elsevier Science B.V., P.O. Box 330, 1000 AH Amsterdam, Netherlands.)

Types of Contributions. The following types of papers are published: Regular research papers (full-length papers), Review articles, Short Communications and Discussions. Short Communications are usually descriptions of short investigations, or they can report minor technical improvements of previously published procedures; they reflect the same quality of research as full-length papers, but should preferably not exceed five printed pages. Discussions (one or two pages) should explain, amplify, correct or otherwise comment substantively upon an article recently published in the journal. For Review articles, see inside front cover under Submission of Papers.

Submission. Every paper must be accompanied by a letter from the senior author, stating that he/she is submitting the paper for publication in the *Journal of Chromatography A* or *B*.

Manuscripts. Manuscripts should be typed in **double spacing** on consecutively numbered pages of uniform size. The manuscript should be preceded by a sheet of manuscript paper carrying the title of the paper and the name and full postal address of the person to whom the proofs are to be sent. As a rule, papers should be divided into sections, headed by a caption (*e.g.*, Abstract, Introduction, Experimental, Results, Discussion, etc.). All illustrations, photographs, tables, etc., should be on separate sheets.

Abstract. All articles should have an abstract of 50–100 words which clearly and briefly indicates what is new, different and significant. No references should be given.

Introduction. Every paper must have a concise introduction mentioning what has been done before on the topic described, and stating clearly what is new in the paper now submitted.

Experimental conditions should preferably be given on a *separate* sheet, headed "Conditions". These conditions will, if appropriate, be printed in a block, directly following the heading "Experimental".

Illustrations. The figures should be submitted in a form suitable for reproduction, drawn in Indian ink on drawing or tracing paper. Each illustration should have a caption, all the *captions* being typed (with double spacing) together on a *separate sheet*. If structures are given in the text, the original drawings should be provided. Coloured illustrations are reproduced at the author's expense, the cost being determined by the number of pages and by the number of colours needed. The written permission of the author and publisher must be obtained for the use of any figure already published. Its source must be indicated in the legend.

References. References should be numbered in the order in which they are cited in the text, and listed in numerical sequence on a separate sheet at the end of the article. Please check a recent issue for the layout of the reference list. Abbreviations for the titles of journals should follow the system used by *Chemical Abstracts*. Articles not yet published should be given as "in press" (journal should be specified), "submitted for publication" (journal should be specified), "in preparation" or "personal communication".

Vols. 1–651 of the *Journal of Chromatography*; *Journal of Chromatography, Biomedical Applications* and *Journal of Chromatography, Symposium Volumes* should be cited as *J. Chromatogr.* From Vol. 652 on, *Journal of Chromatography A* (incl. Symposium Volumes) should be cited as *J. Chromatogr. A* and *Journal of Chromatography B: Biomedical Applications* as *J. Chromatogr. B*.

Dispatch. Before sending the manuscript to the Editor please check that the envelope contains four copies of the paper complete with references, captions and figures. One of the sets of figures must be the originals suitable for direct reproduction. Please also ensure that permission to publish has been obtained from your institute.

Proofs. One set of proofs will be sent to the author to be carefully checked for printer's errors. Corrections must be restricted to instances in which the proof is at variance with the manuscript.

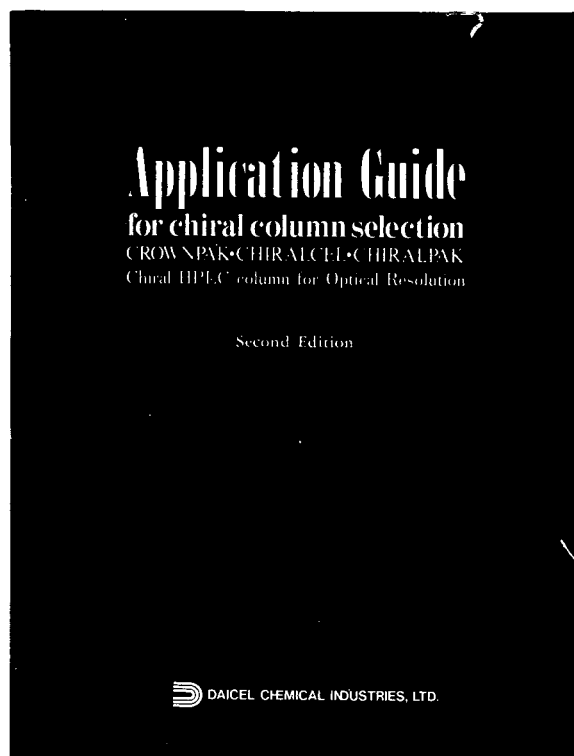
Reprints. Fifty reprints will be supplied free of charge. Additional reprints can be ordered by the authors. An order form containing price quotations will be sent to the authors together with the proofs of their article.

Advertisements. The Editors of the journal accept no responsibility for the contents of the advertisements. Advertisement rates are available on request. Advertising orders and enquiries can be sent to the Advertising Manager, Elsevier Science B.V., Advertising Department, P.O. Box 211, 1000 AE Amsterdam, Netherlands; Tel: 31 (20) 485 379; Fax: 31 (20) 485 3810. Courier shipments to street address: Molenwerf 1, 1014 AG Amsterdam, Netherlands. UK: T.G. Scott & Son Ltd., Tim Blake, Portland House, 21 Narborough Road, Cosby, Leics. LE9 5TA, UK; Tel: (0116) 2750 521/2753 333; Fax: (0116) 2750 522. USA and Canada: Weston Media Associates, Daniel S. Lipner, P.O. Box 1110, Greens Farms, CT 06436-1110, USA; Tel: (203) 261 2500; Fax: (203) 261 0101.

Chiral HPLC Column

Application Guide for Chiral HPLC Column Selection **SECOND EDITION!**

FREE OF CHARGE



The 112-page green book contains chromatographic resolutions of over 350 chiral separations, cross-indexed by chemical compound class, structure, and the type of chiral column respectively. This book also lists chromatographic data together with analytical conditions and structural information. A quick reference guide for column selection from a wide range of DAICEL chiral HPLC columns is included.

To request this book, please let us know by fax or mail.

 **DAICEL CHEMICAL INDUSTRIES, LTD.**

AMERICA

CHIRAL TECHNOLOGIES, INC.

730 Springdale Drive, P.O. Box 564
Exton, PA 19341
Phone: 800-624-4725
Facsimile: 610-594-2325

EUROPE

DAICEL (EUROPA) GmbH

Oststr. 22
D-40211 Düsseldorf, Germany
Phone: +49-211-369848
Facsimile: +49-211-364429

ASIA/OCEANIA

DAICEL CHEMICAL INDUSTRIES, LTD.

CHIRAL CHEMICALS NDD
8-1, Kasumigaseki 3-chome,
Chiyoda-ku, Tokyo 100, JAPAN
Phone: +81-3-3507-3151
Facsimile: +81-3-3507-3193